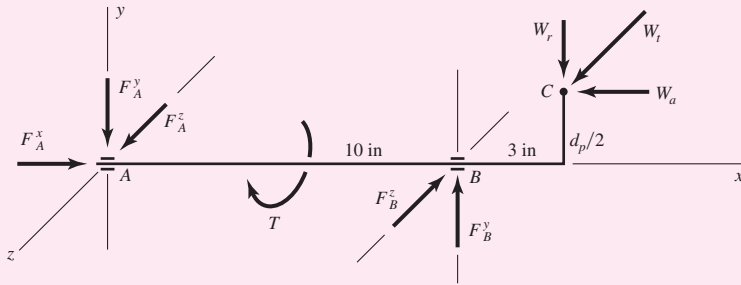


**Figure 13-39**

Free-body diagram of motor shaft of Ex. 13-9.



These three forces,  $W_r$  in the  $-y$  direction,  $W_a$  in the  $-x$  direction, and  $W_t$  in the  $+z$  direction, are shown acting at point C in Fig. 13-39. We assume bearing reactions at A and B as shown. Then  $F_A^x = W_a = 23.3$  lbf. Taking moments about the  $z$  axis,

$$-(17.0)(13) + (23.3) \left( \frac{1.732}{2} \right) + 10F_B^y = 0$$

or  $F_B^y = 20.1$  lbf. Summing forces in the  $y$  direction then gives  $F_A^y = 3.1$  lbf. Taking moments about the  $y$  axis, next

$$10F_B^z - (40.4)(13) = 0$$

or  $F_B^z = 52.5$  lbf. Summing forces in the  $z$  direction and solving gives  $F_A^z = 12.1$  lbf. Also, the torque is  $T = W_t d_p/2 = (40.4)(1.732/2) = 35$  lbf · in.

For comparison, solve the problem again using vectors. The force at C is

$$\mathbf{W} = -23.3\mathbf{i} - 17.0\mathbf{j} + 40.4\mathbf{k} \text{ lbf}$$

Position vectors to B and C from origin A are

$$\mathbf{R}_B = 10\mathbf{i} \quad \mathbf{R}_C = 13\mathbf{i} + 0.866\mathbf{j}$$

Taking moments about A, we have

$$\mathbf{R}_B \times \mathbf{F}_B + \mathbf{T} + \mathbf{R}_C \times \mathbf{W} = \mathbf{0}$$

Using the directions assumed in Fig. 13-39 and substituting values gives

$$10\mathbf{i} \times (F_B^y\mathbf{j} - F_B^z\mathbf{k}) - T\mathbf{i} + (13\mathbf{i} + 0.866\mathbf{j}) \times (-23.3\mathbf{i} - 17.0\mathbf{j} + 40.4\mathbf{k}) = \mathbf{0}$$

When the cross products are formed, we get

$$(10F_B^y\mathbf{k} + 10F_B^z\mathbf{j}) - T\mathbf{i} + (35\mathbf{i} - 525\mathbf{j} - 201\mathbf{k}) = \mathbf{0}$$

whence  $T = 35$  lbf · in,  $F_B^y = 20.1$  lbf, and  $F_B^z = 52.5$  lbf.

Next,

$$\mathbf{F}_A = -\mathbf{F}_B - \mathbf{W}, \text{ and so } \mathbf{F}_A = 23.3\mathbf{i} - 3.1\mathbf{j} + 12.1\mathbf{k} \text{ lbf.}$$

## 13-17 Force Analysis—Worm Gearing

If friction is neglected, then the only force exerted by the gear will be the force  $W$ , shown in Fig. 13-40, having the three orthogonal components  $W^x$ ,  $W^y$ , and  $W^z$ . From the geometry of the figure, we see that

$$\begin{aligned} W^x &= W \cos \phi_n \sin \lambda \\ W^y &= W \sin \phi_n \\ W^z &= W \cos \phi_n \cos \lambda \end{aligned} \quad (13-41)$$

We now use the subscripts  $W$  and  $G$  to indicate forces acting against the worm and gear, respectively. We note that  $W^y$  is the separating, or radial, force for both the worm and the gear. The tangential force on the worm is  $W^x$  and is  $W^z$  on the gear, assuming a  $90^\circ$  shaft angle. The axial force on the worm is  $W^z$ , and on the gear,  $W^x$ . Since the gear forces are opposite to the worm forces, we can summarize these relations by writing

$$\begin{aligned} W_{Wt} &= -W_{Ga} = W^x \\ W_{Wr} &= -W_{Gr} = W^y \\ W_{Wa} &= -W_{Gt} = W^z \end{aligned} \quad (13-42)$$

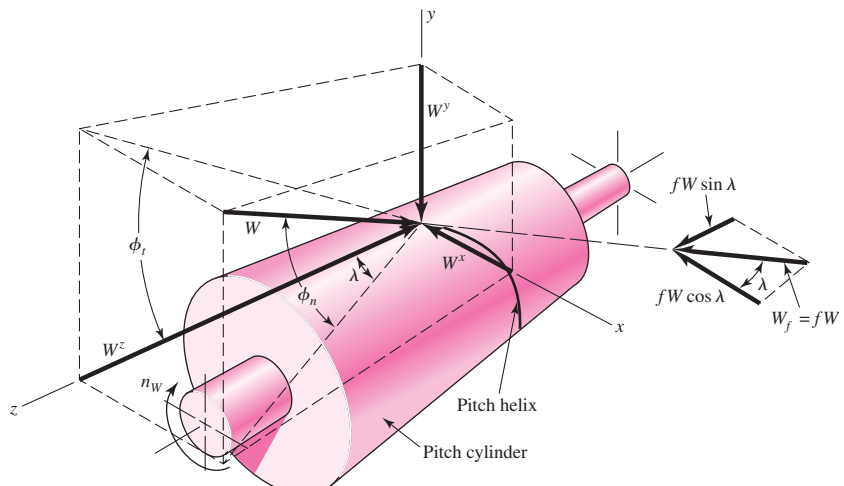
It is helpful in using Eq. (13-41) and also Eq. (13-42) to observe that *the gear axis is parallel to the  $x$  direction and the worm axis is parallel to the  $z$  direction* and that we are employing a right-handed coordinate system.

In our study of spur-gear teeth we have learned that the motion of one tooth relative to the mating tooth is primarily a rolling motion; in fact, when contact occurs at the pitch point, the motion is pure rolling. In contrast, the relative motion between worm and worm-gear teeth is pure sliding, and so we must expect that friction plays an important role in the performance of worm gearing. By introducing a coefficient of friction  $f$ , we can develop another set of relations similar to those of Eq. (13-41). In Fig. 13-40 we see that the force  $W$  acting normal to the worm-tooth profile produces a frictional force  $W_f = fW$ , having a component  $fW \cos \lambda$  in the negative  $x$  direction and another component  $fW \sin \lambda$  in the positive  $z$  direction. Equation (13-41) therefore becomes

$$\begin{aligned} W^x &= W(\cos \phi_n \sin \lambda + f \cos \lambda) \\ W^y &= W \sin \phi_n \\ W^z &= W(\cos \phi_n \cos \lambda - f \sin \lambda) \end{aligned} \quad (13-43)$$

**Figure 13-40**

Drawing of the pitch cylinder of a worm, showing the forces exerted upon it by the worm gear.



Equation (13–42), of course, still applies.

Inserting  $-W_{Gt}$  from Eq. (13–42) for  $W^z$  in Eq. (13–43) and multiplying both sides by  $f$ , we find the frictional force  $W_f$  to be

$$W_f = fW = \frac{fW_{Gt}}{f \sin \lambda - \cos \phi_n \cos \lambda} \quad (13-44)$$

A useful relation between the two tangential forces,  $W_{Wt}$  and  $W_{Gt}$ , can be obtained by equating the first and third parts of Eqs. (13–42) and (13–43) and eliminating  $W$ . The result is

$$W_{Wt} = W_{Gt} \frac{\cos \phi_n \sin \lambda + f \cos \lambda}{f \sin \lambda - \cos \phi_n \cos \lambda} \quad (13-45)$$

*Efficiency*  $\eta$  can be defined by using the equation

$$\eta = \frac{W_{Wt}(\text{without friction})}{W_{Wt}(\text{with friction})} \quad (a)$$

Substitute Eq. (13–45) with  $f = 0$  in the numerator of Eq. (a) and the same equation in the denominator. After some rearranging, you will find the efficiency to be

$$\eta = \frac{\cos \phi_n - f \tan \lambda}{\cos \phi_n + f \cot \lambda} \quad (13-46)$$

Selecting a typical value of the coefficient of friction, say  $f = 0.05$ , and the pressure angles shown in Table 13–6, we can use Eq. (13–46) to get some useful design information. Solving this equation for helix angles from 1 to  $30^\circ$  gives the interesting results shown in Table 13–6.

Many experiments have shown that the coefficient of friction is dependent on the relative or sliding velocity. In Fig. 13–41,  $V_G$  is the pitch-line velocity of the gear and  $V_W$  the pitch-line velocity of the worm. Vectorially,  $\mathbf{V}_W = \mathbf{V}_G + \mathbf{V}_S$ ; consequently, the sliding velocity is

$$V_S = \frac{V_W}{\cos \lambda} \quad (13-47)$$

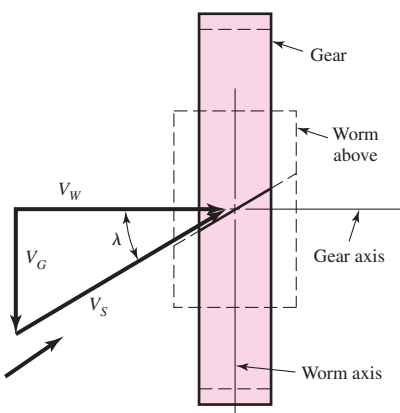
**Table 13–6**

Efficiency of Worm Gearsets for  $f = 0.05$

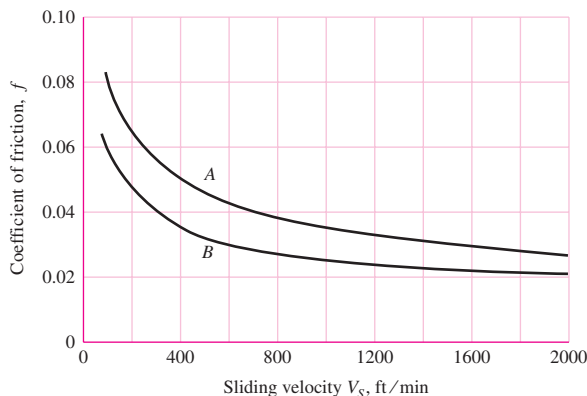
Helix Angle $\psi$ , deg	Efficiency $\eta$ , %
1.0	25.2
2.5	45.7
5.0	62.0
7.5	71.3
10.0	76.6
15.0	82.7
20.0	85.9
30.0	89.1

**Figure 13–41**

Velocity components in worm gearing.

**Figure 13–42**

Representative values of the coefficient of friction for worm gearing. These values are based on good lubrication. Use curve *B* for high-quality materials, such as a case-hardened steel worm mating with a phosphor-bronze gear. Use curve *A* when more friction is expected, as with a cast-iron worm mating with a cast-iron worm gear.



Published values of the coefficient of friction vary as much as 20 percent, undoubtedly because of the differences in surface finish, materials, and lubrication. The values on the chart of Fig. 13–42 are representative and indicate the general trend.

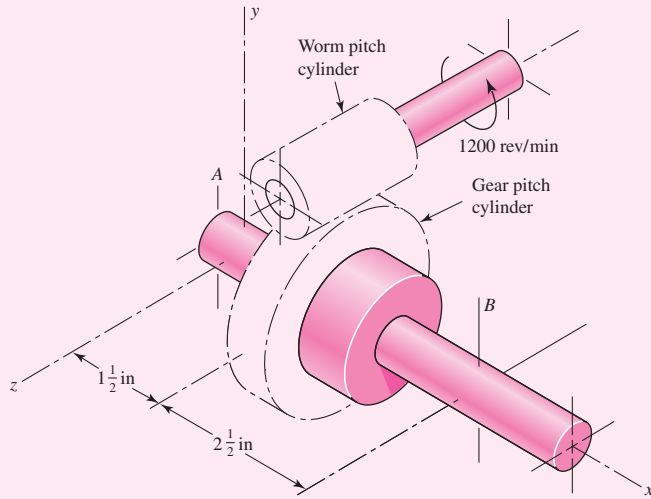
### EXAMPLE 13–10

A 2-tooth right-hand worm transmits 1 hp at 1200 rev/min to a 30-tooth worm gear. The gear has a transverse diametral pitch of 6 teeth/in and a face width of 1 in. The worm has a pitch diameter of 2 in and a face width of  $2\frac{1}{2}$  in. The normal pressure angle is  $14\frac{1}{2}^\circ$ . The materials and quality of work needed are such that curve *B* of Fig. 13–42 should be used to obtain the coefficient of friction.

- (a) Find the axial pitch, the center distance, the lead, and the lead angle.
- (b) Figure 13–43 is a drawing of the worm gear oriented with respect to the coordinate system described earlier in this section; the gear is supported by bearings *A* and *B*. Find the forces exerted by the bearings against the worm-gear shaft, and the output torque.

**Figure 13–43**

The pitch cylinders of the worm gear train of Ex. 13–10.



**Solution** (a) The axial pitch is the same as the transverse circular pitch of the gear, which is

**Answer**

$$p_x = p_t = \frac{\pi}{P} = \frac{\pi}{6} = 0.5236 \text{ in}$$

The pitch diameter of the gear is  $d_G = N_G/P = 30/6 = 5$  in. Therefore, the center distance is

**Answer**

$$C = \frac{d_W + d_G}{2} = \frac{2 + 5}{2} = 3.5 \text{ in}$$

From Eq. (13–27), the lead is

$$L = p_x N_W = (0.5236)(2) = 1.0472 \text{ in}$$

**Answer**

Also using Eq. (13–28), find

**Answer**

$$\lambda = \tan^{-1} \frac{L}{\pi d_W} = \tan^{-1} \frac{1.0472}{\pi(2)} = 9.46^\circ$$

(b) Using the right-hand rule for the rotation of the worm, you will see that your thumb points in the positive  $z$  direction. Now use the bolt-and-nut analogy (the worm is right-handed, as is the screw thread of a bolt), and turn the bolt clockwise with the right hand while preventing nut rotation with the left. The nut will move axially along the bolt toward your right hand. Therefore the surface of the gear (Fig. 13–43) in contact with the worm will move in the negative  $z$  direction. Thus, the gear rotates clockwise about  $x$ , with your right thumb pointing in the negative  $x$  direction.

The pitch-line velocity of the worm is

$$V_W = \frac{\pi d_W n_W}{12} = \frac{\pi(2)(1200)}{12} = 628 \text{ ft/min}$$

The speed of the gear is  $n_G = (\frac{2}{30})(1200) = 80$  rev/min. Therefore the pitch-line velocity of the gear is

$$V_G = \frac{\pi d_G n_G}{12} = \frac{\pi(5)(80)}{12} = 105 \text{ ft/min}$$

Then, from Eq. (13–47), the sliding velocity  $V_S$  is found to be

$$V_S = \frac{V_W}{\cos \lambda} = \frac{628}{\cos 9.46^\circ} = 637 \text{ ft/min}$$

Getting to the forces now, we begin with the horsepower formula

$$W_{Wt} = \frac{33\,000H}{V_W} = \frac{(33\,000)(1)}{628} = 52.5 \text{ lbf}$$

This force acts in the negative  $x$  direction, the same as in Fig. 13–40. Using Fig. 13–42, we find  $f = 0.03$ . Then, the first equation of group (13–42) and (13–43) gives

$$\begin{aligned} W &= \frac{W^x}{\cos \phi_n \sin \lambda + f \cos \lambda} \\ &= \frac{52.5}{\cos 14.5^\circ \sin 9.46^\circ + 0.03 \cos 9.46^\circ} = 278 \text{ lbf} \end{aligned}$$

Also, from Eq. (13–43),

$$\begin{aligned} W^y &= W \sin \phi_n = 278 \sin 14.5^\circ = 69.6 \text{ lbf} \\ W^z &= W(\cos \phi_n \cos \lambda - f \sin \lambda) \\ &= 278(\cos 14.5^\circ \cos 9.46^\circ - 0.03 \sin 9.46^\circ) = 264 \text{ lbf} \end{aligned}$$

We now identify the components acting on the gear as

$$\begin{aligned} W_{Ga} &= -W^x = 52.5 \text{ lbf} \\ W_{Gr} &= -W^y = -69.6 \text{ lbf} \\ W_{Gt} &= -W^z = -264 \text{ lbf} \end{aligned}$$

At this point a three-dimensional line drawing should be made in order to simplify the work to follow. An isometric sketch, such as the one of Fig. 13–44, is easy to make and will help you to avoid errors.

We shall make  $B$  a thrust bearing in order to place the gearshaft in compression. Thus, summing forces in the  $x$  direction gives

**Answer**

$$F_B^x = -52.5 \text{ lbf}$$

Taking moments about the  $z$  axis, we have

**Answer**

$$-(52.5)(2.5) - (69.6)(1.5) + 4F_B^y = 0 \quad F_B^y = 58.9 \text{ lbf}$$

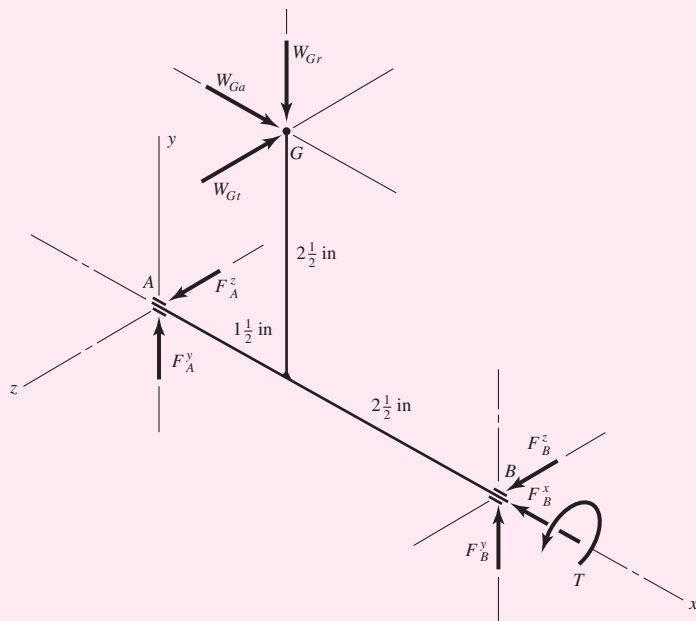
Taking moments about the  $y$  axis,

**Answer**

$$(264)(1.5) - 4F_B^z = 0 \quad F_B^z = 99 \text{ lbf}$$

**Figure 13-44**

An isometric sketch used in Ex. 13-10.



These three components are now inserted on the sketch as shown at *B* in Fig. 13-44. Summing forces in the *y* direction,

$$\text{Answer} \quad -69.6 + 58.9 + F_A^y = 0 \quad F_A^y = 10.7 \text{ lbf}$$

Similarly, summing forces in the *z* direction,

$$\text{Answer} \quad -264 + 99 + F_A^z = 0 \quad F_A^z = 165 \text{ lbf}$$

These two components can now be placed at *A* on the sketch. We still have one more equation to write. Summing moments about *x*,

$$\text{Answer} \quad -(264)(2.5) + T = 0 \quad T = 660 \text{ lbf} \cdot \text{in}$$

It is because of the frictional loss that this output torque is less than the product of the gear ratio and the input torque.

## PROBLEMS

Problems marked with an asterisk (\*) are linked to problems in other chapters, as summarized in Table 1-1 of Sec. 1-16, p. 24.

### 13-1

A 17-tooth spur pinion has a diametral pitch of 8 teeth/in, runs at 1120 rev/min, and drives a gear at a speed of 544 rev/min. Find the number of teeth on the gear and the theoretical center-to-center distance.

### 13-2

A 15-tooth spur pinion has a module of 3 mm and runs at a speed of 1600 rev/min. The driven gear has 60 teeth. Find the speed of the driven gear, the circular pitch, and the theoretical center-to-center distance.

- 13-3** A spur gearset has a module of 6 mm and a velocity ratio of 4. The pinion has 16 teeth. Find the number of teeth on the driven gear, the pitch diameters, and the theoretical center-to-center distance.
- 13-4** A 21-tooth spur pinion mates with a 28-tooth gear. The diametral pitch is 3 teeth/in and the pressure angle is  $20^\circ$ . Make a drawing of the gears showing one tooth on each gear. Find and tabulate the following results: the addendum, dedendum, clearance, circular pitch, tooth thickness, and base-circle diameters; the lengths of the arc of approach, recess, and action; and the base pitch and contact ratio.
- 13-5** A  $20^\circ$  straight-tooth bevel pinion having 14 teeth and a diametral pitch of 6 teeth/in drives a 32-tooth gear. The two shafts are at right angles and in the same plane. Find:  
(a) The cone distance  
(b) The pitch angles  
(c) The pitch diameters  
(d) The face width
- 13-6** A parallel helical gearset uses a 20-tooth pinion driving a 36-tooth gear. The pinion has a right-hand helix angle of  $30^\circ$ , a normal pressure angle of  $25^\circ$ , and a normal diametral pitch of 4 teeth/in. Find:  
(a) The normal, transverse, and axial circular pitches  
(b) The normal base circular pitch  
(c) The transverse diametral pitch and the transverse pressure angle  
(d) The addendum, dedendum, and pitch diameter of each gear
- 13-7** A parallel helical gearset consists of a 19-tooth pinion driving a 57-tooth gear. The pinion has a left-hand helix angle of  $30^\circ$ , a normal pressure angle of  $20^\circ$ , and a normal module of 2.5 mm. Find:  
(a) The normal, transverse, and axial circular pitches  
(b) The transverse diametral pitch and the transverse pressure angle  
(c) The addendum, dedendum, and pitch diameter of each gear
- 13-8** To avoid the problem of interference in a pair of spur gears using a  $20^\circ$  pressure angle, specify the minimum number of teeth allowed on the pinion for each of the following gear ratios.  
(a) 2 to 1  
(b) 3 to 1  
(c) 4 to 1  
(d) 5 to 1
- 13-9** Repeat Prob. 13-8 with a  $25^\circ$  pressure angle.
- 13-10** For a spur gearset with  $\phi = 20^\circ$ , while avoiding interference, find:  
(a) The smallest pinion tooth count that will run with itself  
(b) The smallest pinion tooth count at a ratio  $m_G = 2.5$ , and the largest gear tooth count possible with this pinion  
(c) The smallest pinion that will run with a rack
- 13-11** Repeat problem 13-10 for a helical gearset with  $\phi_n = 20^\circ$  and  $\psi = 30^\circ$ .
- 13-12** The decision has been made to use  $\phi_n = 20^\circ$ ,  $P_t = 6$  teeth/in, and  $\psi = 30^\circ$  for a 2:1 reduction. Choose a suitable pinion and gear tooth count to avoid interference.
- 13-13** Repeat Problem 13-12 with  $\psi = 45^\circ$ .
- 13-14** By employing a pressure angle larger than standard, it is possible to use fewer pinion teeth, and hence obtain smaller gears without undercutting during machining. If the gears are spur gears, what is the smallest possible pressure angle  $\phi_t$  that can be obtained without undercutting for a 9-tooth pinion to mesh with a rack?

**13-15**

A parallel-shaft gearset consists of an 18-tooth helical pinion driving a 32-tooth gear. The pinion has a left-hand helix angle of  $25^\circ$ , a normal pressure angle of  $20^\circ$ , and a normal module of 3 mm. Find:

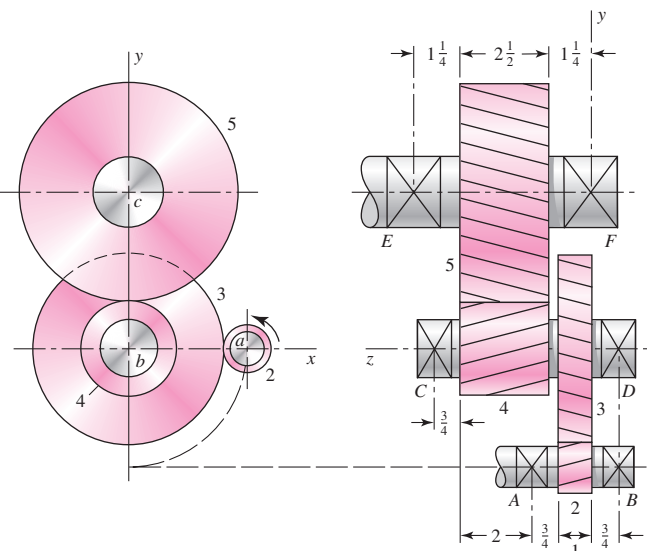
- The normal, transverse, and axial circular pitches
- The transverse module and the transverse pressure angle
- The pitch diameters of the two gears

**13-16**

The double-reduction helical gearset shown in the figure is driven through shaft *a* at a speed of 700 rev/min. Gears 2 and 3 have a normal diametral pitch of 12 teeth/in., a  $30^\circ$  helix angle, and a normal pressure angle of  $20^\circ$ . The second pair of gears in the train, gears 4 and 5, have a normal diametral pitch of 8 teeth/in., a  $25^\circ$  helix angle, and a normal pressure angle of  $20^\circ$ . The tooth numbers are:  $N_2 = 12$ ,  $N_3 = 48$ ,  $N_4 = 16$ ,  $N_5 = 36$ . Find:

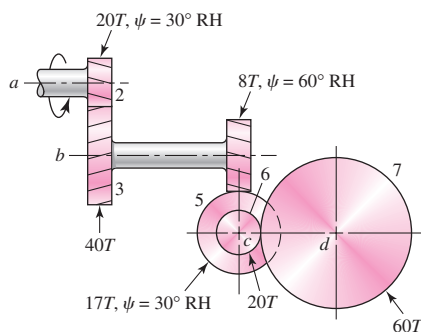
- The directions of the thrust force exerted by each gear upon its shaft
- The speed and direction of shaft *c*
- The center distance between shafts

*Problem 13-16*  
Dimensions in inches.

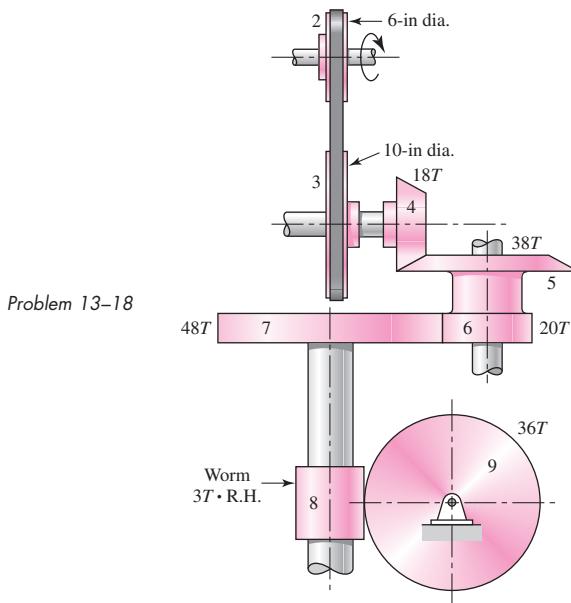
**13-17**

Shaft *a* in the figure rotates at 600 rev/min in the direction shown. Find the speed and direction of rotation of shaft *d*.

*Problem 13-17*

**13-18**

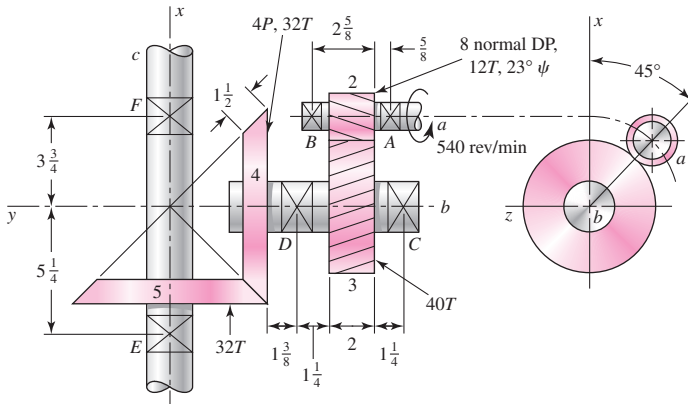
The mechanism train shown consists of an assortment of gears and pulleys to drive gear 9. Pulley 2 rotates at 1200 rev/min in the direction shown. Determine the speed and direction of rotation of gear 9.

**13-19**

The figure shows a gear train consisting of a pair of helical gears and a pair of miter gears. The helical gears have a  $17\frac{1}{2}^\circ$  normal pressure angle and a helix angle as shown. Find:

- The speed of shaft *c*
- The distance between shafts *a* and *b*
- The diameter of the miter gears

Problem 13-19  
Dimensions in inches.

**13-20**

A compound reverted gear train is to be designed as a speed increaser to provide a total increase of speed of exactly 45 to 1. With a  $20^\circ$  pressure angle, specify appropriate numbers of teeth to minimize the gearbox size while avoiding the interference problem in the teeth.

**13-21**

Repeat Prob. 13-20 with a  $25^\circ$  pressure angle.

**13-22**

Repeat Prob. 13-20 for a gear ratio of exactly 30 to 1.

**13-23**

Repeat Prob. 13-20 for a gear ratio of approximately 45 to 1.

**13-24**

A gearbox is to be designed with a compound reverted gear train that transmits 25 horsepower with an input speed of 2500 rev/min. The output should deliver the power at a rotational speed in the range of 280 to 300 rev/min. Spur gears with  $20^\circ$  pressure angle are to be used. Determine

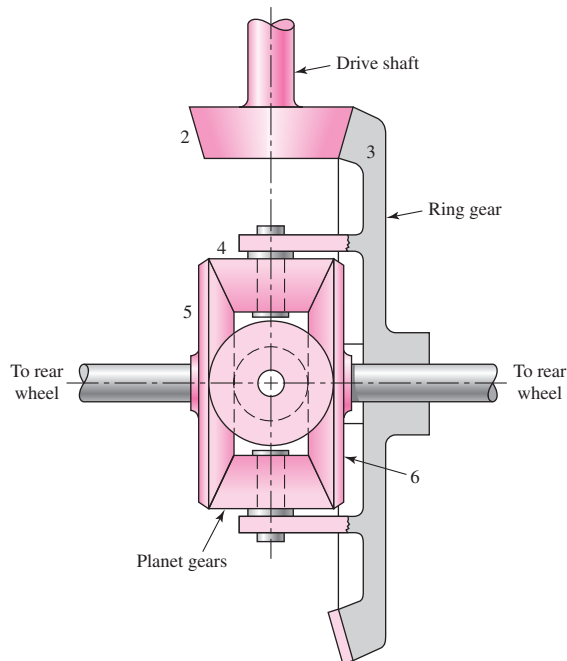
suitable numbers of teeth for each gear, to minimize the gearbox size while providing an output speed within the specified range. Be sure to avoid an interference problem in the teeth.

### 13-25

The tooth numbers for the automotive differential shown in the figure are  $N_2 = 16$ ,  $N_3 = 48$ ,  $N_4 = 14$ ,  $N_5 = N_6 = 20$ . The drive shaft turns at 900 rev/min.

- What are the wheel speeds if the car is traveling in a straight line on a good road surface?
- Suppose the right wheel is jacked up and the left wheel resting on a good road surface. What is the speed of the right wheel?
- Suppose, with a rear-wheel drive vehicle, the auto is parked with the right wheel resting on a wet icy surface. Does the answer to part (b) give you any hint as to what would happen if you started the car and attempted to drive on?

Problem 13-25



### 13-26

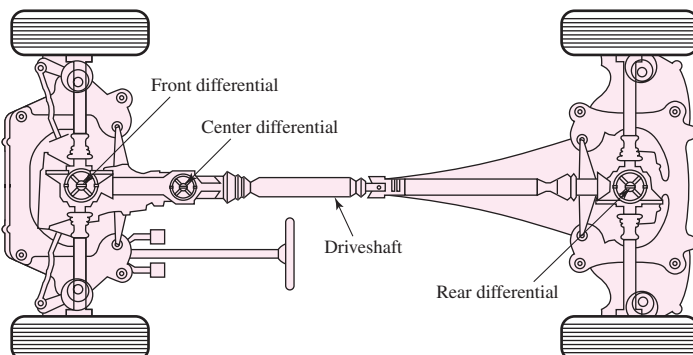
The figure illustrates an all-wheel drive concept using three differentials, one for the front axle, another for the rear, and the third connected to the drive shaft.

- Explain why this concept may allow greater acceleration.
- Suppose either the center of the rear differential, or both, can be locked for certain road conditions. Would either or both of these actions provide greater traction? Why?

Problem 13-26

The Audi "Quattro concept," showing the three differentials that provide permanent all-wheel drive.

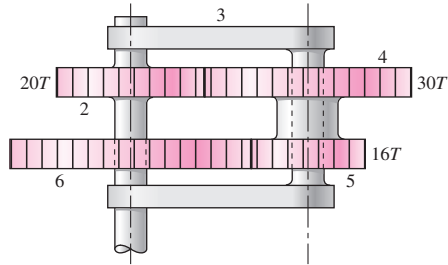
(Reprinted by permission of Audi of America, Inc.)



**13-27**

In the reverted planetary train illustrated, find the speed and direction of rotation of the arm if gear 2 is unable to rotate and gear 6 is driven at 12 rev/min in the clockwise direction.

Problem 13-27

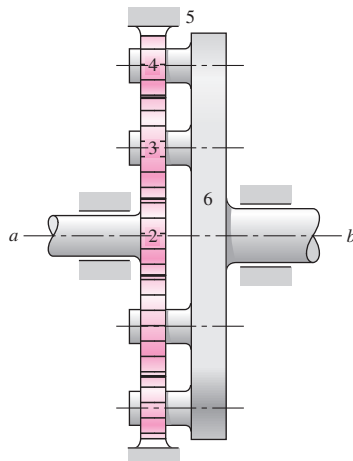
**13-28**

In the gear train of Prob. 13-27, let gear 6 be driven at 85 rev/min counterclockwise while gear 2 is held stationary. What is the speed and direction of rotation of the arm?

**13-29**

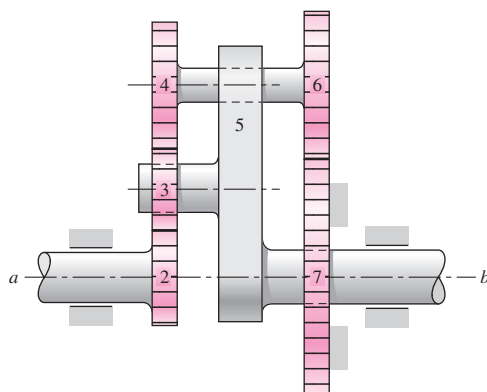
Tooth numbers for the gear train shown in the figure are  $N_2 = 12$ ,  $N_3 = 16$ , and  $N_4 = 12$ . How many teeth must internal gear 5 have? Suppose gear 5 is fixed. What is the speed of the arm if shaft *a* rotates counterclockwise at 320 rev/min?

Problem 13-29

**13-30**

The tooth numbers for the gear train illustrated are  $N_2 = 20$ ,  $N_3 = 16$ ,  $N_4 = 30$ ,  $N_6 = 36$ , and  $N_7 = 46$ . Gear 7 is fixed. If shaft *a* is turned through 10 revolutions, how many turns will shaft *b* make?

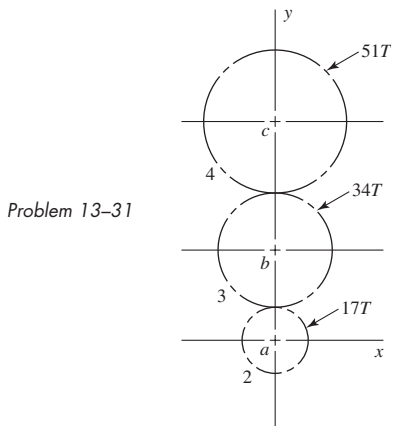
Problem 13-30



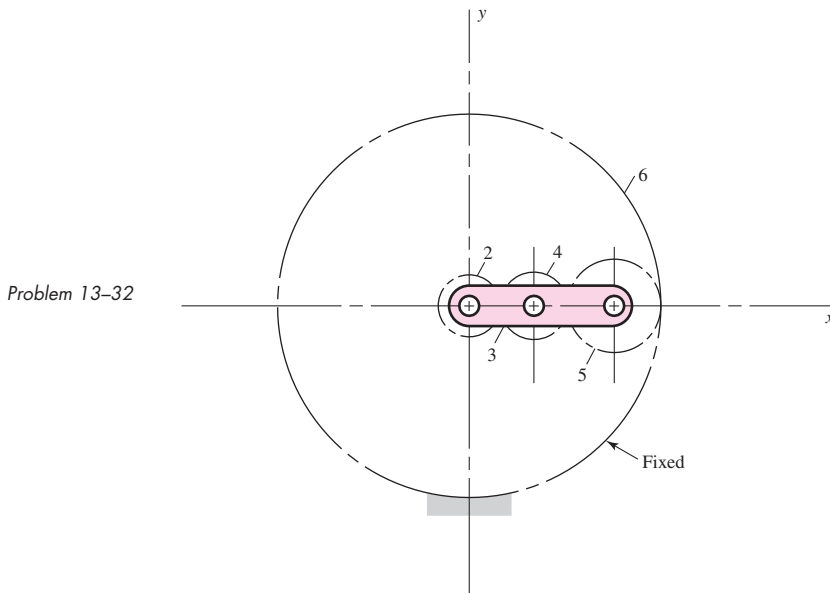
**13-31**

Shaft *a* in the figure has a power input of 75 kW at a speed of 1000 rev/min in the counter-clockwise direction. The gears have a module of 5 mm and a  $20^\circ$  pressure angle. Gear 3 is an idler.

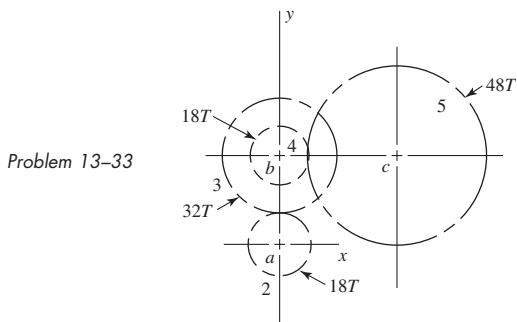
- Find the force  $F_{3b}$  that gear 3 exerts against shaft *b*.
- Find the torque  $T_{4c}$  that gear 4 exerts on shaft *c*.

**13-32**

The 24T 6-pitch  $20^\circ$  pinion 2 shown in the figure rotates clockwise at 1000 rev/min and is driven at a power of 25 hp. Gears 4, 5, and 6 have 24, 36, and 144 teeth, respectively. What torque can arm 3 deliver to its output shaft? Draw free-body diagrams of the arm and of each gear and show all forces that act upon them.

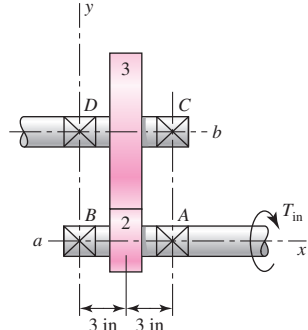
**13-33**

The gears shown in the figure have a module of 12 mm and a  $20^\circ$  pressure angle. The pinion rotates at 1800 rev/min clockwise and transmits 150 kW through the idler pair to gear 5 on shaft *c*. What forces do gears 3 and 4 transmit to the idler shaft?

**13-34**

The figure shows a pair of shaft-mounted spur gears having a diametral pitch of 5 teeth/in with an 18-tooth  $20^\circ$  pinion driving a 45-tooth gear. The horsepower input is 32 maximum at 1800 rev/min. Find the direction and magnitude of the maximum forces acting on bearings A, B, C, and D.

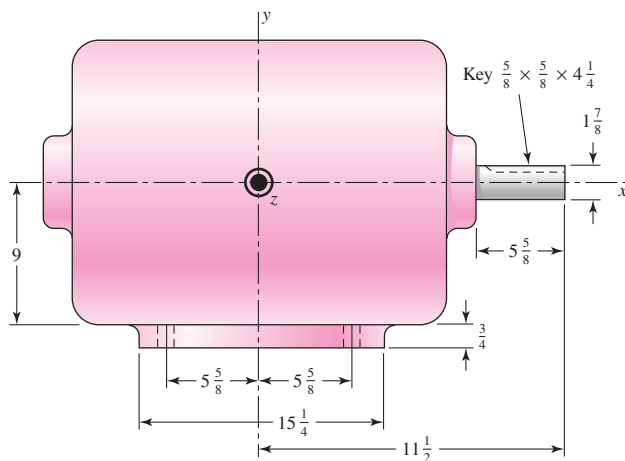
Problem 13-34

**13-35**

The figure shows the electric-motor frame dimensions for a 30-hp 900 rev/min motor. The frame is bolted to its support using four  $\frac{3}{4}$ -in bolts spaced  $11\frac{1}{4}$  in apart in the view shown and 14 in apart when viewed from the end of the motor. A 4 diametral pitch  $20^\circ$  spur pinion having 20 teeth and a face width of 2 in is keyed to the motor shaft. This pinion drives another gear whose axis is in the same  $xz$  plane. Determine the maximum shear and tensile forces on the mounting bolts based on 200 percent overload torque. Does the direction of rotation matter?

Problem 13-35

NEMA No. 364 frame; dimensions in inches. The  $z$  axis is directed out of the paper.



**13-36**

Continue Prob. 13-24 by finding the following information, assuming a diametral pitch of 6 teeth/in.

- (a) Determine pitch diameters for each of the gears.
- (b) Determine the pitch line velocities (in ft/min) for each set of gears.
- (c) Determine the magnitudes of the tangential, radial, and total forces transmitted between each set of gears.
- (d) Determine the input torque.
- (e) Determine the output torque, neglecting frictional losses.

**13-37**

A speed-reducer gearbox containing a compound reverted gear train transmits 35 horsepower with an input speed of 1200 rev/min. Spur gears with  $20^\circ$  pressure angle are used, with 16 teeth on each of the small gears and 48 teeth on each of the larger gears. A diametral pitch of 10 teeth/in is proposed.

- (a) Determine the speeds of the intermediate and output shafts.
- (b) Determine the pitch line velocities (in ft/min) for each set of gears.
- (c) Determine the magnitudes of the tangential, radial, and total forces transmitted between each set of gears.
- (d) Determine the input torque.
- (e) Determine the output torque, neglecting frictional losses.

**13-38\***

For the countershaft in Prob. 3-72, p. 138, assume the gear ratio from gear *B* to its mating gear is 2 to 1.

- (a) Determine the minimum number of teeth that can be used on gear *B* without an interference problem in the teeth.
- (b) Using the number of teeth from part (a), what diametral pitch is required to also achieve the given 8-in pitch diameter?
- (c) Suppose the  $20^\circ$  pressure angle gears are exchanged for gears with  $25^\circ$  pressure angle, while maintaining the same pitch diameters and diametral pitch. Determine the new forces  $F_A$  and  $F_B$  if the same power is to be transmitted.

**13-39\***

For the countershaft in Prob. 3-73, p. 138, assume the gear ratio from gear *B* to its mating gear is 5 to 1.

- (a) Determine the minimum number of teeth that can be used on gear *B* without an interference problem in the teeth.
- (b) Using the number of teeth from part (a), what module is required to also achieve the given 300-mm pitch diameter?
- (c) Suppose the  $20^\circ$  pressure angle for gear *A* is exchanged for a gear with  $25^\circ$  pressure angle, while maintaining the same pitch diameters and module. Determine the new forces  $F_A$  and  $F_B$  if the same power is to be transmitted.

**13-40\***

For the gear and sprocket assembly analyzed in Prob. 3-77, p. 139, information for the gear sizes and the forces transmitted through the gears was provided in the problem statement. In this problem, we will perform the preceding design steps necessary to acquire the information for the analysis. A motor providing 2 kW is to operate at 191 rev/min. A gear unit is needed to reduce the motor speed by half to drive a chain sprocket.

- (a) Specify appropriate numbers of teeth on gears *F* and *C* to minimize the size while avoiding the interference problem in the teeth.
- (b) Assuming an initial guess of 125-mm pitch diameter for gear *F*, what is the module that should be used for the stress analysis of the gear teeth?

- (c) Calculate the input torque applied to shaft *EFG*.  
 (d) Calculate the magnitudes of the radial, tangential, and total forces transmitted between gears *F* and *C*.

**13-41\***

For the gear and sprocket assembly analyzed in Prob. 3–79, p. 139, information for the gear sizes and the forces transmitted through the gears was provided in the problem statement. In this problem, we will perform the preceding design steps necessary to acquire the information for the analysis. A motor providing 1 hp is to operate at 70 rev/min. A gear unit is needed to double the motor speed to drive a chain sprocket.

- (a) Specify appropriate numbers of teeth on gears *F* and *C* to minimize the size while avoiding the interference problem in the teeth.  
 (b) Assuming an initial guess of 10-in pitch diameter for gear *F*, what is the diametral pitch that should be used for the stress analysis of the gear teeth?  
 (c) Calculate the input torque applied to shaft *EFG*.  
 (d) Calculate the magnitudes of the radial, tangential, and total forces transmitted between gears *F* and *C*.

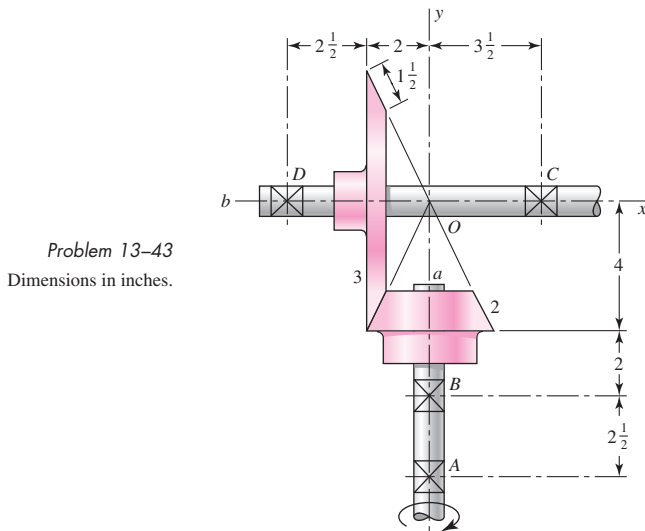
**13-42\***

For the bevel gearset in Probs. 3–74 and 3–76, pp. 138 and 139 respectively, shaft *AB* is rotating at 600 rev/min and transmits 10 hp. The gears have a  $20^\circ$  pressure angle.

- (a) Determine the bevel angle  $\gamma$  for the gear on shaft *AB*.  
 (b) Determine the pitch-line velocity.  
 (c) Determine the tangential, radial, and axial forces transmitted through the gears. Were the forces given in Prob. 3–74 correct?

**13-43**

The figure shows a 16T  $20^\circ$  straight bevel pinion driving a 32T gear, and the location of the bearing centerlines. Pinion shaft *a* receives 2.5 hp at 240 rev/min. Determine the bearing reactions at *A* and *B* if *A* is to take both radial and thrust loads.

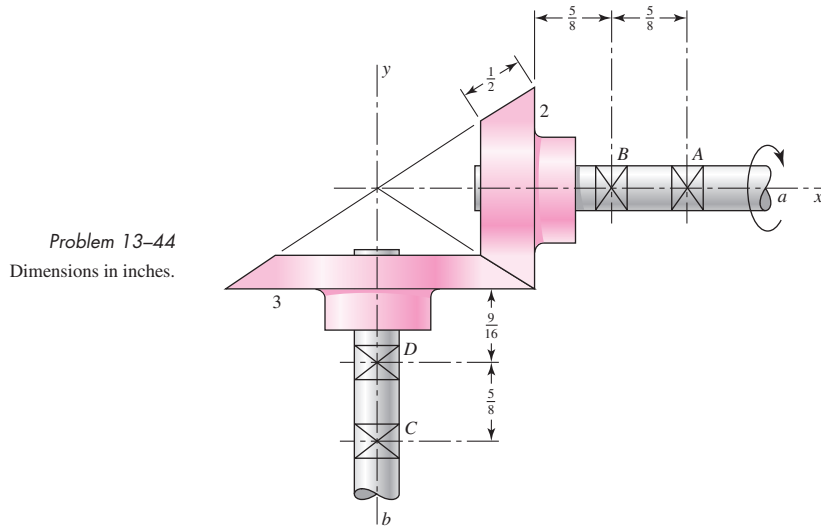


Problem 13-43

Dimensions in inches.

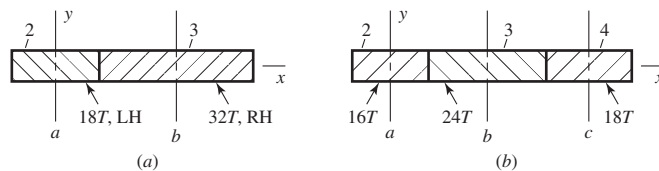
**13-44**

The figure shows a 10 diametral pitch 18-tooth  $20^\circ$  straight bevel pinion driving a 30-tooth gear. The transmitted load is 25 lbf. Find the bearing reactions at *C* and *D* on the output shaft if *D* is to take both radial and thrust loads.

**13-45**

The gears in the two trains shown in the figure have a normal diametral pitch of 5 teeth/in, a normal pressure angle of  $20^\circ$ , and a  $30^\circ$  helix angle. For both gear trains the transmitted load is 800 lbf. In part *a* the pinion rotates counterclockwise about the *y* axis. Find the force exerted by each gear in part *a* on its shaft.

**Problem 13-45**

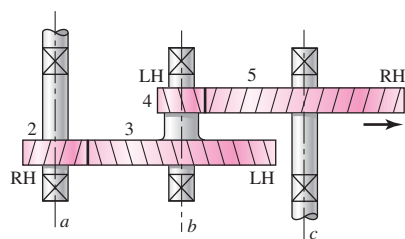
**13-46**

This is a continuation of Prob. 13-45. Here, you are asked to find the forces exerted by gears 2 and 3 on their shafts as shown in part *b*. Gear 2 rotates clockwise about the *y* axis. Gear 3 is an idler.

**13-47**

A gear train is composed of four helical gears with the three shaft axes in a single plane, as shown in the figure. The gears have a normal pressure angle of  $20^\circ$  and a  $30^\circ$  helix angle. Shaft *b* is an idler and the transmitted load acting on gear 3 is 500 lbf. The gears on shaft *b* both have a normal diametral pitch of 7 teeth/in and have 54 and 14 teeth, respectively. Find the forces exerted by gears 3 and 4 on shaft *b*.

**Problem 13-47**



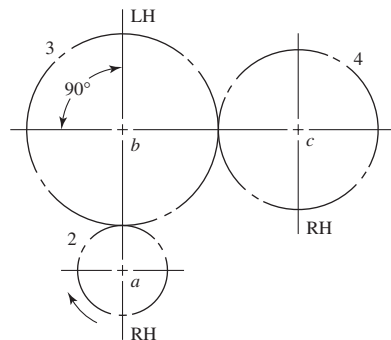
**13-48**

In the figure for Prob. 13-34, pinion 2 is to be a right-hand helical gear having a helix angle of  $30^\circ$ , a normal pressure angle of  $20^\circ$ , 16 teeth, and a normal diametral pitch of 6 teeth/in. A 25-hp motor drives shaft *a* at a speed of 1720 rev/min clockwise about the *x* axis. Gear 3 has 42 teeth. Find the reaction exerted by bearings *C* and *D* on shaft *b*. One of these bearings is to take both radial and thrust loads. This bearing should be selected so as to place the shaft in compression.

**13-49**

Gear 2, in the figure, has 16 teeth, a  $20^\circ$  transverse angle, a  $15^\circ$  helix angle, and a module of 4 mm. Gear 2 drives the idler on shaft *b*, which has 36 teeth. The driven gear on shaft *c* has 28 teeth. If the driver rotates at 1600 rev/min and transmits 6 kW, find the radial and thrust load on each shaft.

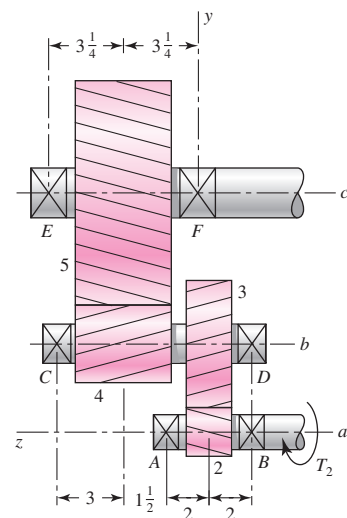
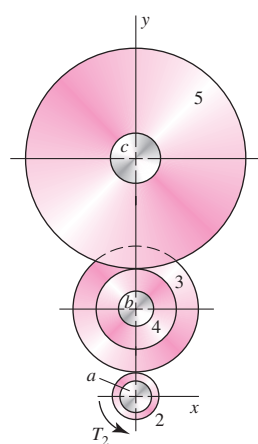
Problem 13-49

**13-50**

The figure shows a double-reduction helical gearset. Pinion 2 is the driver, and it receives a torque of 1200 lbf · in from its shaft in the direction shown. Pinion 2 has a normal diametral pitch of 8 teeth/in, 14 teeth, and a normal pressure angle of  $20^\circ$  and is cut right-handed with a helix angle of  $30^\circ$ . The mating gear 3 on shaft *b* has 36 teeth. Gear 4, which is the driver for the second pair of gears in the train, has a normal diametral pitch of 5 teeth/in, 15 teeth, and a normal pressure angle of  $20^\circ$  and is cut left-handed with a helix angle of  $15^\circ$ . Mating gear 5 has 45 teeth. Find the magnitude and direction of the force exerted by the bearings *C* and *D* on shaft *b* if bearing *C* can take only radial load while bearing *D* is mounted to take both radial and thrust load.

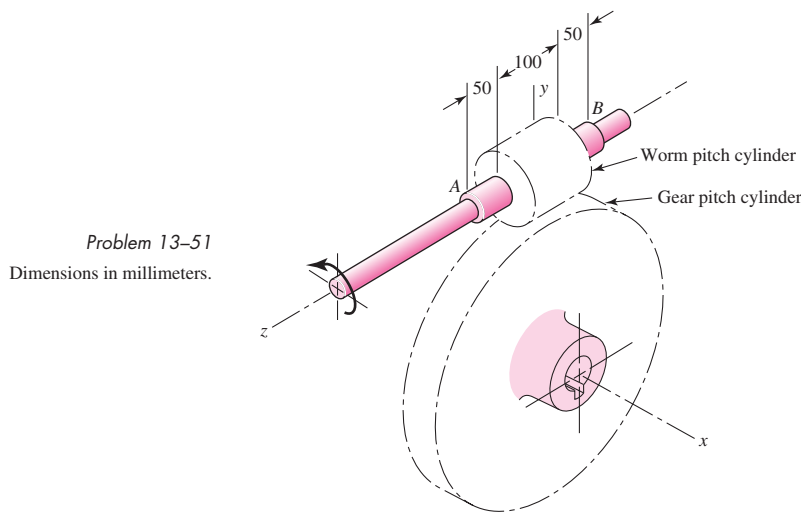
Problem 13-50

Dimensions in inches.



**13-51**

A right-hand single-tooth hardened-steel (hardness not specified) worm has a catalog rating of 2000 W at 600 rev/min when meshed with a 48-tooth cast-iron gear. The axial pitch of the worm is 25 mm, the normal pressure angle is  $14\frac{1}{2}^\circ$ , the pitch diameter of the worm is 100 mm, and the face widths of the worm and gear are, respectively, 100 mm and 50 mm. The figure shows bearings *A* and *B* on the worm shaft symmetrically located with respect to the worm and 200 mm apart. Determine which should be the thrust bearing, and find the magnitudes and directions of the forces exerted by both bearings.



Problem 13-51

Dimensions in millimeters.

**13-52**

The hub diameter and projection for the gear of Prob. 13-51 are 100 and 37.5 mm, respectively. The face width of the gear is 50 mm. Locate bearings *C* and *D* on opposite sides, spacing *C* 10 mm from the gear on the hidden face (see figure) and *D* 10 mm from the hub face. Find the output torque and the magnitudes and directions of the forces exerted by the bearings on the gearshaft.

**13-53**

A 2-tooth left-hand worm transmits  $\frac{3}{4}$  hp at 600 rev/min to a 36-tooth gear having a transverse diametral pitch of 8 teeth/in. The worm has a normal pressure angle of  $20^\circ$ , a pitch diameter of  $1\frac{1}{2}$  in, and a face width of  $1\frac{1}{2}$  in. Use a coefficient of friction of 0.05 and find the force exerted by the gear on the worm and the torque input. For the same geometry as shown for Prob. 13-51, the worm velocity is clockwise about the *z* axis.

**13-54**

Write a computer program that will analyze a spur gear or helical-mesh gear, accepting  $\phi_n$ ,  $\psi$ ,  $P_t$ ,  $N_P$ , and  $N_G$ ; compute  $m_G$ ,  $d_P$ ,  $d_G$ ,  $p_t$ ,  $p_n$ ,  $p_x$ , and  $\phi_t$ ; and give advice as to the smallest tooth count that will allow a pinion to run with itself without interference, run with its gear, and run with a rack. Also have it give the largest tooth count possible with the intended pinion.

# 14

## Spur and Helical Gears

### Chapter Outline

- 14-1** The Lewis Bending Equation **734**
- 14-2** Surface Durability **743**
- 14-3** AGMA Stress Equations **745**
- 14-4** AGMA Strength Equations **747**
- 14-5** Geometry Factors  $I$  and  $J$  ( $Z_I$  and  $Y_J$ ) **751**
- 14-6** The Elastic Coefficient  $C_p$  ( $Z_E$ ) **756**
- 14-7** Dynamic Factor  $K_v$  **756**
- 14-8** Overload Factor  $K_o$  **758**
- 14-9** Surface Condition Factor  $C_f$  ( $Z_R$ ) **758**
- 14-10** Size Factor  $K_s$  **759**
- 14-11** Load-Distribution Factor  $K_m$  ( $K_H$ ) **759**
- 14-12** Hardness-Ratio Factor  $C_H$  **761**
- 14-13** Stress Cycle Life Factors  $Y_N$  and  $Z_N$  **762**
- 14-14** Reliability Factor  $K_R$  ( $Y_Z$ ) **763**
- 14-15** Temperature Factor  $K_T$  ( $Y_\theta$ ) **764**
- 14-16** Rim-Thickness Factor  $K_B$  **764**
- 14-17** Safety Factors  $S_F$  and  $S_H$  **765**
- 14-18** Analysis **765**
- 14-19** Design of a Gear Mesh **775**

This chapter is devoted primarily to analysis and design of spur and helical gears to resist bending failure of the teeth as well as pitting failure of tooth surfaces. Failure by bending will occur when the significant tooth stress equals or exceeds either the yield strength or the bending endurance strength. A surface failure occurs when the significant contact stress equals or exceeds the surface endurance strength. The first two sections present a little of the history of the analyses from which current methodology developed.

The American Gear Manufacturers Association<sup>1</sup> (AGMA) has for many years been the responsible authority for the dissemination of knowledge pertaining to the design and analysis of gearing. The methods this organization presents are in general use in the United States when strength and wear are primary considerations. In view of this fact it is important that the AGMA approach to the subject be presented here.

The general AGMA approach requires a great many charts and graphs—too many for a single chapter in this book. We have omitted many of these here by choosing a single pressure angle and by using only full-depth teeth. This simplification reduces the complexity but does not prevent the development of a basic understanding of the approach. Furthermore, the simplification makes possible a better development of the fundamentals and hence should constitute an ideal introduction to the use of the general AGMA method.<sup>2</sup> Sections 14–1 and 14–2 are elementary and serve as an examination of the foundations of the AGMA method. Table 14–1 is largely AGMA nomenclature.

## 14–1 The Lewis Bending Equation

Wilfred Lewis introduced an equation for estimating the bending stress in gear teeth in which the tooth form entered into the formulation. The equation, announced in 1892, still remains the basis for most gear design today.

To derive the basic Lewis equation, refer to Fig. 14–1a, which shows a cantilever of cross-sectional dimensions  $F$  and  $t$ , having a length  $l$  and a load  $W^t$ , uniformly distributed across the face width  $F$ . The section modulus  $I/c$  is  $Ft^2/6$ , and therefore the bending stress is

$$\sigma = \frac{M}{I/c} = \frac{6W^t l}{Ft^2} \quad (a)$$

Gear designers denote the components of gear-tooth forces as  $W_t$ ,  $W_r$ ,  $W_a$  or  $W^t$ ,  $W^r$ ,  $W^a$  interchangeably. The latter notation leaves room for post-subscripts essential to free-body diagrams. For instance, for gears 2 and 3 in mesh,  $W_{23}^t$  is the transmitted force of

---

<sup>1</sup>500 Montgomery Street, Suite 350, Alexandria, VA 22314-1560.

<sup>2</sup>The standards ANSI/AGMA 2001-D04 (revised AGMA 2001-C95) and ANSI/AGMA 2101-D04 (metric edition of ANSI/AGMA 2001-D04), *Fundamental Rating Factors and Calculation Methods for Involute Spur and Helical Gear Teeth*, are used in this chapter. The use of American National Standards is completely voluntary; their existence does not in any respect preclude people, whether they have approved the standards or not, from manufacturing, marketing, purchasing, or using products, processes, or procedures not conforming to the standards.

The American National Standards Institute does not develop standards and will in no circumstances give an interpretation of any American National Standard. Requests for interpretation of these standards should be addressed to the American Gear Manufacturers Association. [Tables or other self-supporting sections may be quoted or extracted in their entirety. Credit line should read: "Extracted from ANSI/AGMA Standard 2001-D04 or 2101-D04 *Fundamental Rating Factors and Calculation Methods for Involute Spur and Helical Gear Teeth*" with the permission of the publisher, American Gear Manufacturers Association, 500 Montgomery Street, Suite 350, Alexandria, Virginia 22314-1560.] The foregoing is adapted in part from the ANSI foreword to these standards.

**Table 14-1**

Symbols, Their Names,  
and Locations\*

<b>Symbol</b>	<b>Name</b>	<b>Where Found</b>
$b$	Net width of face of narrowest member	Eq. (14-16)
$C_e$	Mesh alignment correction factor	Eq. (14-35)
$C_f$	Surface condition factor	Eq. (14-16)
$C_H$	Hardness-ratio factor	Eq. (14-18)
$C_{ma}$	Mesh alignment factor	Eq. (14-34)
$C_{mc}$	Load correction factor	Eq. (14-31)
$C_{mf}$	Face load-distribution factor	Eq. (14-30)
$C_p$	Elastic coefficient	Eq. (14-13)
$C_{pf}$	Pinion proportion factor	Eq. (14-32)
$C_{pm}$	Pinion proportion modifier	Eq. (14-33)
$d$	Operating pitch diameter of pinion	Ex. (14-1)
$d_P$	Pitch diameter, pinion	Eq. (14-22)
$d_G$	Pitch diameter, gear	Eq. (14-22)
$E$	Modulus of elasticity	Eq. (14-10)
$F$	Net face width of narrowest member	Eq. (14-15)
$f_P$	Pinion surface finish	Fig. 14-13
$H$	Power	Fig. 14-17
$H_B$	Brinell hardness	Ex. 14-3
$H_{BG}$	Brinell hardness of gear	Sec. 14-12
$H_{BP}$	Brinell hardness of pinion	Sec. 14-12
$hp$	Horsepower	Ex. 14-1
$h_t$	Gear-tooth whole depth	Sec. 14-16
$I$	Geometry factor of pitting resistance	Eq. (14-16)
$J$	Geometry factor for bending strength	Eq. (14-15)
$K$	Contact load factor for pitting resistance	Eq. (6-65)
$K_B$	Rim-thickness factor	Eq. (14-40)
$K_f$	Fatigue stress-concentration factor	Eq. (14-9)
$K_m$	Load-distribution factor	Eq. (14-30)
$K_o$	Overload factor	Eq. (14-15)
$K_R$	Reliability factor	Eq. (14-17)
$K_s$	Size factor	Sec. 14-10
$K_T$	Temperature factor	Eq. (14-17)
$K_v$	Dynamic factor	Eq. (14-27)
$m$	Metric module	Eq. (14-15)
$m_B$	Backup ratio	Eq. (14-39)
$m_G$	Gear ratio (never less than 1)	Eq. (14-22)
$m_N$	Load-sharing ratio	Eq. (14-21)
$N$	Number of stress cycles	Fig. 14-14
$N_G$	Number of teeth on gear	Eq. (14-22)
$N_P$	Number of teeth on pinion	Eq. (14-22)
$n$	Speed	Ex. 14-1

(Continued)

**Table 14-1**

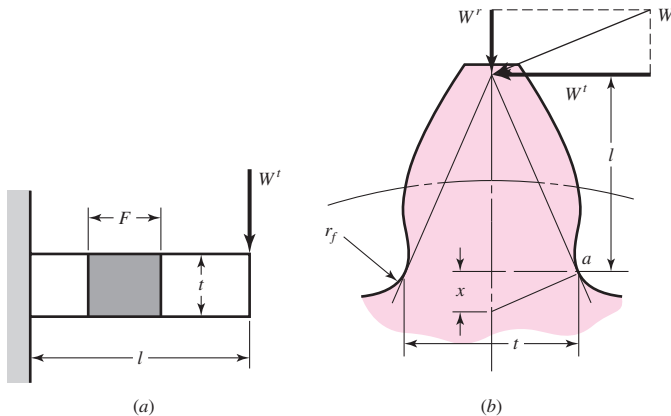
Symbols, Their Names, and Locations*	Symbol	Name	Where Found
(Continued)			
	$n_p$	Pinion speed	Ex. 14-4
	$P$	Diametral pitch	Eq. (14-2)
	$P_d$	Diametral pitch of pinion	Eq. (14-15)
	$p_N$	Normal base pitch	Eq. (14-24)
	$p_n$	Normal circular pitch	Eq. (14-24)
	$p_x$	Axial pitch	Eq. (14-19)
	$Q_v$	Transmission accuracy level number	Eq. (14-29)
	$R$	Reliability	Eq. (14-38)
	$R_a$	Root-mean-squared roughness	Fig. 14-13
	$r_f$	Tooth fillet radius	Fig. 14-1
	$r_G$	Pitch-circle radius, gear	In standard
	$r_P$	Pitch-circle radius, pinion	In standard
	$r_{bP}$	Pinion base-circle radius	Eq. (14-25)
	$r_{bG}$	Gear base-circle radius	Eq. (14-25)
	$S_C$	Buckingham surface endurance strength	Ex. 14-3
	$S_c$	AGMA surface endurance strength	Eq. (14-18)
	$S_t$	AGMA bending strength	Eq. (14-17)
	$S$	Bearing span	Fig. 14-10
	$S_I$	Pinion offset from center span	Fig. 14-10
	$S_F$	Safety factor—bending	Eq. (14-41)
	$S_H$	Safety factor—pitting	Eq. (14-42)
	$W^t$ or $W_t^\dagger$	Transmitted load	Fig. 14-1
	$Y_N$	Stress cycle factor for bending strength	Fig. 14-14
	$Z_N$	Stress cycle factor for pitting resistance	Fig. 14-15
	$\beta$	Exponent	Eq. (14-44)
	$\sigma$	Bending stress	Eq. (14-2)
	$\sigma_C$	Contact stress from Hertzian relationships	Eq. (14-14)
	$\sigma_c$	Contact stress from AGMA relationships	Eq. (14-16)
	$\sigma_{all}$	Allowable bending stress	Eq. (14-17)
	$\sigma_{c,all}$	Allowable contact stress, AGMA	Eq. (14-18)
	$\phi$	Pressure angle	Eq. (14-12)
	$\phi_t$	Transverse pressure angle	Eq. (14-23)
	$\psi$	Helix angle at standard pitch diameter	Ex. 14-5

\*Because ANSI/AGMA 2001-C95 introduced a significant amount of new nomenclature, and continued in ANSI/AGMA 2001-D04, this summary and references are provided for use until the reader's vocabulary has grown.

<sup>†</sup>See preference rationale following Eq. (a), Sec. 14-1.

body 2 on body 3, and  $W_{32}^t$  is the transmitted force of body 3 on body 2. When working with double- or triple-reduction speed reducers, this notation is compact and essential to clear thinking. Since gear-force components rarely take exponents, this causes no complication. Pythagorean combinations, if necessary, can be treated with parentheses or avoided by expressing the relations trigonometrically.

| Figure 14-1



Referring now to Fig. 14-1b, we assume that the maximum stress in a gear tooth occurs at point *a*. By similar triangles, you can write

$$\frac{t/2}{x} = \frac{l}{t/2} \quad \text{or} \quad x = \frac{t^2}{4l} \quad (b)$$

By rearranging Eq. (a),

$$\sigma = \frac{6W^tl}{Ft^2} = \frac{W^t}{F} \frac{1}{t^2/6l} = \frac{W^t}{F} \frac{1}{t^2/4l} \frac{4}{6} \quad (c)$$

If we now substitute the value of *x* from Eq. (b) in Eq. (c) and multiply the numerator and denominator by the circular pitch *p*, we find

$$\sigma = \frac{W^t p}{F \left(\frac{2}{3}\right) xp} \quad (d)$$

Letting  $y = 2x/3p$ , we have

$$\sigma = \frac{W^t}{Fpy} \quad (14-1)$$

This completes the development of the original Lewis equation. The factor *y* is called the *Lewis form factor*, and it may be obtained by a graphical layout of the gear tooth or by digital computation.

In using this equation, most engineers prefer to employ the diametral pitch in determining the stresses. This is done by substituting  $P = \pi/p$  and  $Y = \pi y$  in Eq. (14-1). This gives

$$\sigma = \frac{W^t P}{FY} \quad (14-2)$$

where

$$Y = \frac{2xP}{3} \quad (14-3)$$

The use of this equation for *Y* means that only the bending of the tooth is considered and that the compression due to the radial component of the force is neglected. Values of *Y* obtained from this equation are tabulated in Table 14-2.

**Table 14-2**

Values of the Lewis Form Factor $Y$ (These Values Are for a Normal Pressure Angle of $20^\circ$ , Full-Depth Teeth, and a Diametral Pitch of Unity in the Plane of Rotation)	Number of Teeth	$Y$	Number of Teeth	$Y$
	12	0.245	28	0.353
	13	0.261	30	0.359
	14	0.277	34	0.371
	15	0.290	38	0.384
	16	0.296	43	0.397
	17	0.303	50	0.409
	18	0.309	60	0.422
	19	0.314	75	0.435
	20	0.322	100	0.447
	21	0.328	150	0.460
	22	0.331	300	0.472
	24	0.337	400	0.480
	26	0.346	Rack	0.485

The use of Eq. (14-3) also implies that the teeth do not share the load and that the greatest force is exerted at the tip of the tooth. But we have already learned that the contact ratio should be somewhat greater than unity, say about 1.5, to achieve a quality gearset. If, in fact, the gears are cut with sufficient accuracy, the tip-load condition is not the worst, because another pair of teeth will be in contact when this condition occurs. Examination of run-in teeth will show that the heaviest loads occur near the middle of the tooth. Therefore the maximum stress probably occurs while a single pair of teeth is carrying the full load, at a point where another pair of teeth is just on the verge of coming into contact.

### **Dynamic Effects**

When a pair of gears is driven at moderate or high speed and noise is generated, it is certain that dynamic effects are present. One of the earliest efforts to account for an increase in the load due to velocity employed a number of gears of the same size, material, and strength. Several of these gears were tested to destruction by meshing and loading them at zero velocity. The remaining gears were tested to destruction at various pitch-line velocities. For example, if a pair of gears failed at 500 lbf tangential load at zero velocity and at 250 lbf at velocity  $V_1$ , then a *velocity factor*, designated  $K_v$ , of 2 was specified for the gears at velocity  $V_1$ . Then another, identical, pair of gears running at a pitch-line velocity  $V_1$  could be assumed to have a load equal to twice the tangential or transmitted load.

Note that the definition of dynamic factor  $K_v$  has been altered. AGMA standards ANSI/AGMA 2001-D04 and 2101-D04 contain this caution:

Dynamic factor  $K_v$  has been redefined as the reciprocal of that used in previous AGMA standards. It is now greater than 1.0. In earlier AGMA standards it was less than 1.0.

Care must be taken in referring to work done prior to this change in the standards.

In the nineteenth century, Carl G. Barth first expressed the velocity factor, and in terms of the current AGMA standards, they are represented as

$$K_v = \frac{600 + V}{600} \quad (\text{cast iron, cast profile}) \quad (14-4a)$$

$$K_v = \frac{1200 + V}{1200} \quad (\text{cut or milled profile}) \quad (14-4b)$$

where  $V$  is the pitch-line velocity in feet per minute. It is also quite probable, because of the date that the tests were made, that the tests were conducted on teeth having a cycloidal profile instead of an involute profile. Cycloidal teeth were in general use in the nineteenth century because they were easier to cast than involute teeth. Equation (14-4a) is called the *Barth equation*. The Barth equation is often modified into Eq. (14-4b), for cut or milled teeth. Later AGMA added

$$K_v = \frac{50 + \sqrt{V}}{50} \quad (\text{hobbed or shaped profile}) \quad (14-5a)$$

$$K_v = \sqrt{\frac{78 + \sqrt{V}}{78}} \quad (\text{shaved or ground profile}) \quad (14-5b)$$

In SI units, Eqs. (14-4a) through (14-5b) become

$$K_v = \frac{3.05 + V}{3.05} \quad (\text{cast iron, cast profile}) \quad (14-6a)$$

$$K_v = \frac{6.1 + V}{6.1} \quad (\text{cut or milled profile}) \quad (14-6b)$$

$$K_v = \frac{3.56 + \sqrt{V}}{3.56} \quad (\text{hobbed or shaped profile}) \quad (14-6c)$$

$$K_v = \sqrt{\frac{5.56 + \sqrt{V}}{5.56}} \quad (\text{shaved or ground profile}) \quad (14-6d)$$

where  $V$  is in meters per second (m/s).

Introducing the velocity factor into Eq. (14-2) gives

$$\sigma = \frac{K_v W^t P}{F Y} \quad (14-7)$$

The metric version of this equation is

$$\sigma = \frac{K_v W^t}{F m Y} \quad (14-8)$$

where the face width  $F$  and the module  $m$  are both in millimeters (mm). Expressing the tangential component of load  $W^t$  in newtons (N) then results in stress units of megapascals (MPa).

As a general rule, spur gears should have a face width  $F$  from 3 to 5 times the circular pitch  $p$ .

Equations (14-7) and (14-8) are important because they form the basis for the AGMA approach to the bending strength of gear teeth. They are in general use for

estimating the capacity of gear drives when life and reliability are not important considerations. The equations can be useful in obtaining a preliminary estimate of gear sizes needed for various applications.

### EXAMPLE 14-1

A stock spur gear is available having a diametral pitch of 8 teeth/in, a  $1\frac{1}{2}$ -in face, 16 teeth, and a pressure angle of  $20^\circ$  with full-depth teeth. The material is AISI 1020 steel in as-rolled condition. Use a design factor of  $n_d = 3$  to rate the horsepower output of the gear corresponding to a speed of 1200 rev/m and moderate applications.

#### Solution

The term *moderate applications* seems to imply that the gear can be rated by using the yield strength as a criterion of failure. From Table A-20, we find  $S_{ut} = 55$  kpsi and  $S_y = 30$  kpsi. A design factor of 3 means that the allowable bending stress is  $30/3 = 10$  kpsi. The pitch diameter is  $N/P = 16/8 = 2$  in, so the pitch-line velocity is

$$V = \frac{\pi d n}{12} = \frac{\pi(2)1200}{12} = 628 \text{ ft/min}$$

The velocity factor from Eq. (14-4b) is found to be

$$K_v = \frac{1200 + V}{1200} = \frac{1200 + 628}{1200} = 1.52$$

Table 14-2 gives the form factor as  $Y = 0.296$  for 16 teeth. We now arrange and substitute in Eq. (14-7) as follows:

$$W^t = \frac{FY\sigma_{all}}{K_v P} = \frac{1.5(0.296)10\,000}{1.52(8)} = 365 \text{ lbf}$$

The horsepower that can be transmitted is

$$\text{Answer} \quad hp = \frac{W^t V}{33\,000} = \frac{365(628)}{33\,000} = 6.95 \text{ hp}$$

It is important to emphasize that this is a rough estimate, and that this approach must not be used for important applications. The example is intended to help you understand some of the fundamentals that will be involved in the AGMA approach.

### EXAMPLE 14-2

Estimate the horsepower rating of the gear in the previous example based on obtaining an infinite life in bending.

#### Solution

The rotating-beam endurance limit is estimated from Eq. (6-8)

$$S'_e = 0.5S_{ut} = 0.5(55) = 27.5 \text{ kpsi}$$

To obtain the surface finish Marin factor  $k_a$  we refer to Table 6-3 for machined surface, finding  $a = 2.70$  and  $b = -0.265$ . Then Eq. (6-19) gives the surface finish Marin factor  $k_a$  as

$$k_a = aS_{ut}^b = 2.70(55)^{-0.265} = 0.934$$

The next step is to estimate the size factor  $k_b$ . From Table 13–1, the sum of the addendum and dedendum is

$$l = \frac{1}{P} + \frac{1.25}{P} = \frac{1}{8} + \frac{1.25}{8} = 0.281 \text{ in}$$

The tooth thickness  $t$  in Fig. 14–1b is given in Sec. 14–1 [Eq. (b)] as  $t = (4lx)^{1/2}$  when  $x = 3Y/(2P)$  from Eq. (14–3). Therefore, since from Ex. 14–1  $Y = 0.296$  and  $P = 8$ ,

$$x = \frac{3Y}{2P} = \frac{3(0.296)}{2(8)} = 0.0555 \text{ in}$$

then

$$t = (4lx)^{1/2} = [4(0.281)0.0555]^{1/2} = 0.250 \text{ in}$$

We have recognized the tooth as a cantilever beam of rectangular cross section, so the equivalent rotating-beam diameter must be obtained from Eq. (6–25):

$$d_e = 0.808(hb)^{1/2} = 0.808(Ft)^{1/2} = 0.808[1.5(0.250)]^{1/2} = 0.495 \text{ in}$$

Then, Eq. (6–20) gives  $k_b$  as

$$k_b = \left( \frac{d_e}{0.30} \right)^{-0.107} = \left( \frac{0.495}{0.30} \right)^{-0.107} = 0.948$$

The load factor  $k_c$  from Eq. (6–26) is unity. With no information given concerning temperature and reliability we will set  $k_d = k_e = 1$ .

In general, a gear tooth is subjected only to one-way bending. Exceptions include idler gears and gears used in reversing mechanisms. We will account for one-way bending by establishing a miscellaneous-effects Marin factor  $k_f$ .

For one-way bending the steady and alternating stress components are  $\sigma_a = \sigma_m = \sigma/2$  where  $\sigma$  is the largest repeatedly applied bending stress as given in Eq. (14–7). If a material exhibited a Goodman failure locus,

$$\frac{S_a}{S'_e} + \frac{S_m}{S_{ut}} = 1$$

Since  $S_a$  and  $S_m$  are equal for one-way bending, we substitute  $S_a$  for  $S_m$  and solve the preceding equation for  $S_a$ , giving

$$S_a = \frac{S'_e S_{ut}}{S'_e + S_{ut}}$$

Now replace  $S_a$  with  $\sigma/2$ , and in the denominator replace  $S'_e$  with  $0.5S_{ut}$  to obtain

$$\sigma = \frac{2S'_e S_{ut}}{0.5S_{ut} + S_{ut}} = \frac{2S'_e}{0.5 + 1} = 1.33S'_e$$

Now  $k_f = \sigma/S'_e = 1.33S'_e/S'_e = 1.33$ . However, a Gerber fatigue locus gives mean values of

$$\frac{S_a}{S'_e} + \left( \frac{S_m}{S_{ut}} \right)^2 = 1$$

Setting  $S_a = S_m$  and solving the quadratic in  $S_a$  gives

$$S_a = \frac{S_{ut}^2}{2S'_e} \left( -1 + \sqrt{1 + \frac{4S'^2_e}{S_{ut}^2}} \right)$$

Setting  $S_a = \sigma/2$ ,  $S_{ut} = S'_e/0.5$  gives

$$\sigma = \frac{S'_e}{0.5^2} \left[ -1 + \sqrt{1 + 4(0.5)^2} \right] = 1.66S'_e$$

and  $k_f = \sigma/S'_e = 1.66$ . Since a Gerber locus runs in and among fatigue data and Goodman does not, we will use  $k_f = 1.66$ . The Marin equation for the fully corrected endurance strength is

$$\begin{aligned} S_e &= k_a k_b k_c k_d k_e k_f S'_e \\ &= 0.934(0.948)(1)(1)(1)1.66(27.5) = 40.4 \text{ kpsi} \end{aligned}$$

For stress, we will first determine the fatigue stress-concentration factor  $K_f$ . For a 20° full-depth tooth the radius of the root fillet is denoted  $r_f$ , where

$$r_f = \frac{0.300}{P} = \frac{0.300}{8} = 0.0375 \text{ in}$$

From Fig. A-15-6

$$\frac{r}{d} = \frac{r_f}{t} = \frac{0.0375}{0.250} = 0.15$$

Since  $D/d = \infty$ , we approximate with  $D/d = 3$ , giving  $K_t = 1.68$ . From Fig. 6-20,  $q = 0.62$ . From Eq. (6-32)

$$K_f = 1 + (0.62)(1.68 - 1) = 1.42$$

For a design factor of  $n_d = 3$ , as used in Ex. 14-1, applied to the load or strength, the maximum bending stress is

$$\begin{aligned} \sigma_{\max} &= K_f \sigma_{\text{all}} = \frac{S_e}{n_d} \\ \sigma_{\text{all}} &= \frac{S_e}{K_f n_d} = \frac{40.4}{1.42(3)} = 9.5 \text{ kpsi} \end{aligned}$$

The transmitted load  $W^t$  is

$$W^t = \frac{FY\sigma_{\text{all}}}{K_v P} = \frac{1.5(0.296)9500}{1.52(8)} = 347 \text{ lbf}$$

and the power is, with  $V = 628$  ft/min from Ex. 14-1,

$$hp = \frac{W^t V}{33000} = \frac{347(628)}{33000} = 6.6 \text{ hp}$$

Again, it should be emphasized that these results should be accepted *only* as preliminary estimates to alert you to the nature of bending in gear teeth.

In Ex. 14–2 our resources (Fig. A–15–6) did not directly address stress concentration in gear teeth. A photoelastic investigation by Dolan and Broghamer reported in 1942 constitutes a primary source of information on stress concentration.<sup>3</sup> Mitchiner and Mabie<sup>4</sup> interpret the results in term of fatigue stress-concentration factor  $K_f$  as

$$K_f = H + \left(\frac{t}{r}\right)^L \left(\frac{t}{l}\right)^M \quad (14-9)$$

where  $H = 0.34 - 0.458 \cdot 366 \cdot 2\phi$

$$L = 0.316 - 0.458 \cdot 366 \cdot 2\phi$$

$$M = 0.290 + 0.458 \cdot 366 \cdot 2\phi$$

$$r = \frac{(b - r_f)^2}{(d/2) + b - r_f}$$

In these equations  $l$  and  $t$  are from the layout in Fig. 14–1,  $\phi$  is the pressure angle,  $r_f$  is the fillet radius,  $b$  is the dedendum, and  $d$  is the pitch diameter. It is left as an exercise for the reader to compare  $K_f$  from Eq. (14–9) with the results of using the approximation of Fig. A–15–6 in Ex. 14–2.

## 14–2

### Surface Durability

In this section we are interested in the failure of the surfaces of gear teeth, which is generally called *wear*. *Pitting*, as explained in Sec. 6–16, is a surface fatigue failure due to many repetitions of high contact stresses. Other surface failures are *scoring*, which is a lubrication failure, and *abrasion*, which is wear due to the presence of foreign material.

To obtain an expression for the surface-contact stress, we shall employ the Hertz theory. In Eq. (3–74) it was shown that the contact stress between two cylinders may be computed from the equation

$$p_{\max} = \frac{2F}{\pi bl} \quad (a)$$

where  $p_{\max}$  = largest surface pressure

$F$  = force pressing the two cylinders together

$l$  = length of cylinders

and half-width  $b$  is obtained from Eq. (3–73):

$$b = \sqrt{\frac{2F}{\pi l} \frac{\left[(1 - v_1^2)/E_1\right] + \left[(1 - v_2^2)/E_2\right]}{(1/d_1) + (1/d_2)}} \quad (14-10)$$

where  $v_1$ ,  $v_2$ ,  $E_1$ , and  $E_2$  are the elastic constants and  $d_1$  and  $d_2$  are the diameters, respectively, of the two contacting cylinders.

To adapt these relations to the notation used in gearing, we replace  $F$  by  $W^t/\cos \phi$ ,  $d$  by  $2r$ , and  $l$  by the face width  $F$ . With these changes, we can substitute the value of  $b$

---

<sup>3</sup>T. J. Dolan and E. I. Broghamer, *A Photoelastic Study of the Stresses in Gear Tooth Fillets*, Bulletin 335, Univ. Ill. Exp. Sta., March 1942. See also W. D. Pilkey, *Peterson's Stress-Concentration Factors*, 2nd ed., John Wiley & Sons, New York, 1997, pp. 383–385, 412–415.

<sup>4</sup>R. G. Mitchiner and H. H. Mabie, "Determination of the Lewis Form Factor and the AGMA Geometry Factor J of External Spur Gear Teeth," *J. Mech. Des.*, Vol. 104, No. 1, Jan. 1982, pp. 148–158.

as given by Eq. (14–10) in Eq. (a). Replacing  $p_{\max}$  by  $\sigma_C$ , the *surface compressive stress (Hertzian stress)* is found from the equation

$$\sigma_C^2 = \frac{W^t}{\pi F \cos \phi} \frac{(1/r_1) + (1/r_2)}{\left[ (1 - v_1^2)/E_1 \right] + \left[ (1 - v_2^2)/E_2 \right]} \quad (14-11)$$

where  $r_1$  and  $r_2$  are the instantaneous values of the radii of curvature on the pinion- and gear-tooth profiles, respectively, at the point of contact. By accounting for load sharing in the value of  $W^t$  used, Eq. (14–11) can be solved for the Hertzian stress for any or all points from the beginning to the end of tooth contact. Of course, pure rolling exists only at the pitch point. Elsewhere the motion is a mixture of rolling and sliding. Equation (14–11) does not account for any sliding action in the evaluation of stress. We note that AGMA uses  $\mu$  for Poisson's ratio instead of  $v$  as is used here.

We have already noted that the first evidence of wear occurs near the pitch line. The radii of curvature of the tooth profiles at the pitch point are

$$r_1 = \frac{d_P \sin \phi}{2} \quad r_2 = \frac{d_G \sin \phi}{2} \quad (14-12)$$

where  $\phi$  is the pressure angle and  $d_P$  and  $d_G$  are the pitch diameters of the pinion and gear, respectively.

Note, in Eq. (14–11), that the denominator of the second group of terms contains four elastic constants, two for the pinion and two for the gear. As a simple means of combining and tabulating the results for various combinations of pinion and gear materials, AGMA defines an *elastic coefficient*  $C_p$  by the equation

$$C_p = \left[ \frac{1}{\pi \left( \frac{1 - v_P^2}{E_P} + \frac{1 - v_G^2}{E_G} \right)} \right]^{1/2} \quad (14-13)$$

With this simplification, and the addition of a velocity factor  $K_v$ , Eq. (14–11) can be written as

$$\sigma_C = -C_p \left[ \frac{K_v W^t}{F \cos \phi} \left( \frac{1}{r_1} + \frac{1}{r_2} \right) \right]^{1/2} \quad (14-14)$$

where the sign is negative because  $\sigma_C$  is a compressive stress.

### EXAMPLE 14–3

The pinion of Examples 14–1 and 14–2 is to be mated with a 50-tooth gear manufactured of ASTM No. 50 cast iron. Using the tangential load of 382 lbf, estimate the factor of safety of the drive based on the possibility of a surface fatigue failure.

#### Solution

From Table A–5 we find the elastic constants to be  $E_P = 30$  Mpsi,  $v_P = 0.292$ ,  $E_G = 14.5$  Mpsi,  $v_G = 0.211$ . We substitute these in Eq. (14–13) to get the elastic coefficient as

$$C_p = \left\{ \frac{1}{\pi \left[ \frac{1 - (0.292)^2}{30(10^6)} + \frac{1 - (0.211)^2}{14.5(10^6)} \right]} \right\}^{1/2} = 1817$$

From Example 14–1, the pinion pitch diameter is  $d_P = 2$  in. The value for the gear is  $d_G = 50/8 = 6.25$  in. Then Eq. (14–12) is used to obtain the radii of curvature at the pitch points. Thus

$$r_1 = \frac{2 \sin 20^\circ}{2} = 0.342 \text{ in} \quad r_2 = \frac{6.25 \sin 20^\circ}{2} = 1.069 \text{ in}$$

The face width is given as  $F = 1.5$  in. Use  $K_v = 1.52$  from Example 14–1. Substituting all these values in Eq. (14–14) with  $\phi = 20^\circ$  gives the contact stress as

$$\sigma_C = -1817 \left[ \frac{1.52(380)}{1.5 \cos 20^\circ} \left( \frac{1}{0.342} + \frac{1}{1.069} \right) \right]^{1/2} = -72\,400 \text{ psi}$$

The surface endurance strength of cast iron can be estimated from

$$S_C = 0.32H_B \text{ kpsi}$$

for  $10^8$  cycles, where  $S_C$  is in kpsi. Table A–24 gives  $H_B = 262$  for ASTM No. 50 cast iron. Therefore  $S_C = 0.32(262) = 83.8$  kpsi. Contact stress is not linear with transmitted load [see Eq. (14–14)]. If the factor of safety is defined as the loss-of-function load divided by the imposed load, then the ratio of loads is the ratio of stresses squared. In other words,

$$n = \frac{\text{loss-of-function load}}{\text{imposed load}} = \frac{S_C^2}{\sigma_C^2} = \left( \frac{83.8}{72.4} \right)^2 = 1.34$$

One is free to define factor of safety as  $S_C/\sigma_C$ . Awkwardness comes when one compares the factor of safety in bending fatigue with the factor of safety in surface fatigue for a particular gear. Suppose the factor of safety of this gear in bending fatigue is 1.20 and the factor of safety in surface fatigue is 1.34 as above. The threat, since 1.34 is greater than 1.20, is in bending fatigue since both numbers are based on load ratios. If the factor of safety in surface fatigue is based on  $S_C/\sigma_C = \sqrt{1.34} = 1.16$ , then 1.20 is greater than 1.16, but the threat is not from surface fatigue. The surface fatigue factor of safety can be defined either way. One way has the burden of requiring a squared number before numbers that instinctively seem comparable can be compared.

In addition to the dynamic factor  $K_v$  already introduced, there are transmitted load excursions, nonuniform distribution of the transmitted load over the tooth contact, and the influence of rim thickness on bending stress. Tabulated strength values can be means, ASTM minimums, or of unknown heritage. In surface fatigue there are no endurance limits. Endurance strengths have to be qualified as to corresponding cycle count, and the slope of the S-N curve needs to be known. In bending fatigue there is a definite change in slope of the S-N curve near  $10^6$  cycles, but some evidence indicates that an endurance limit does not exist. Gearing experience leads to cycle counts of  $10^{11}$  or more. Evidence of diminishing endurance strengths in bending have been included in AGMA methodology.

### 14–3 AGMA Stress Equations

Two fundamental stress equations are used in the AGMA methodology, one for bending stress and another for pitting resistance (contact stress). In AGMA terminology, these are called *stress numbers*, as contrasted with actual applied stresses, and are

designated by a lowercase letter  $s$  instead of the Greek lower case  $\sigma$  we have used in this book (and shall continue to use). The fundamental equations are

$$\sigma = \begin{cases} W^t K_o K_v K_s \frac{P_d}{F} \frac{K_m K_B}{J} & \text{(U.S. customary units)} \\ W^t K_o K_v K_s \frac{1}{bm_t} \frac{K_H K_B}{Y_J} & \text{(SI units)} \end{cases} \quad (14-15)$$

where for U.S. customary units (SI units),

- $W^t$  is the tangential transmitted load, lbf (N)
- $K_o$  is the overload factor
- $K_v$  is the dynamic factor
- $K_s$  is the size factor
- $P_d$  is the transverse diametral pitch
- $F(b)$  is the face width of the narrower member, in (mm)
- $K_m$  ( $K_H$ ) is the load-distribution factor
- $K_B$  is the rim-thickness factor
- $J(Y_J)$  is the geometry factor for bending strength (which includes root fillet stress-concentration factor  $K_f$ )
- ( $m_t$ ) is the transverse metric module

Before you try to digest the meaning of all these terms in Eq. (14-15), view them as advice concerning items the designer should consider *whether he or she follows the voluntary standard or not*. These items include issues such as

- Transmitted load magnitude
- Overload
- Dynamic augmentation of transmitted load
- Size
- Geometry: pitch and face width
- Distribution of load across the teeth
- Rim support of the tooth
- Lewis form factor and root fillet stress concentration

The fundamental equation for pitting resistance (contact stress) is

$$\sigma_c = \begin{cases} C_p \sqrt{W^t K_o K_v K_s \frac{K_m}{d_P F} \frac{C_f}{I}} & \text{(U.S. customary units)} \\ Z_E \sqrt{W^t K_o K_v K_s \frac{K_H}{d_{w1} b} \frac{Z_R}{Z_I}} & \text{(SI units)} \end{cases} \quad (14-16)$$

where  $W^t$ ,  $K_o$ ,  $K_v$ ,  $K_s$ ,  $K_m$ ,  $F$ , and  $b$  are the same terms as defined for Eq. (14-15). For U.S. customary units (SI units), the additional terms are

- $C_p$  ( $Z_E$ ) is an elastic coefficient,  $\sqrt{\text{lbf/in}^2}$  ( $\sqrt{\text{N/mm}^2}$ )
- $C_f$  ( $Z_R$ ) is the surface condition factor
- $d_P$  ( $d_{w1}$ ) is the pitch diameter of the *pinion*, in (mm)
- $I$  ( $Z_I$ ) is the geometry factor for pitting resistance

The evaluation of all these factors is explained in the sections that follow. The development of Eq. (14-16) is clarified in the second part of Sec. 14-5.

## 14-4 AGMA Strength Equations

Instead of using the term *strength*, AGMA uses data termed *allowable stress numbers* and designates these by the symbols  $s_{at}$  and  $s_{ac}$ . It will be less confusing here if we continue the practice in this book of using the uppercase letter  $S$  to designate strength and the lowercase Greek letters  $\sigma$  and  $\tau$  for stress. To make it perfectly clear we shall use the term *gear strength* as a replacement for the phrase *allowable stress numbers* as used by AGMA.

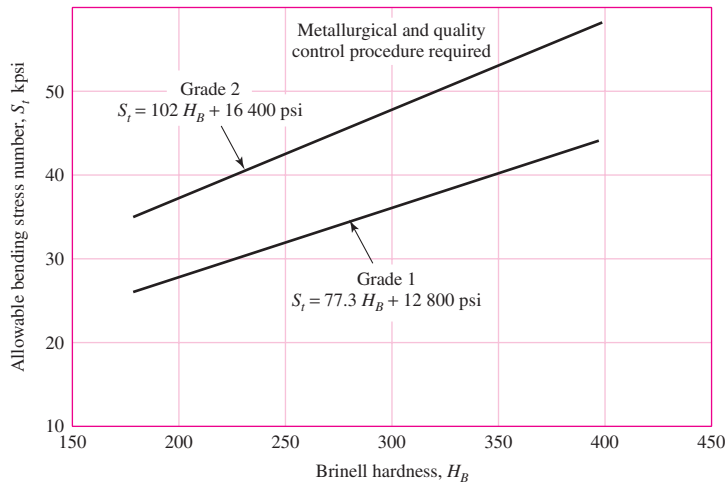
Following this convention, values for *gear bending strength*, designated here as  $S_t$ , are to be found in Figs. 14-2, 14-3, and 14-4, and in Tables 14-3 and 14-4. Since gear strengths are not identified with other strengths such as  $S_{ut}$ ,  $S_e$ , or  $S_y$  as used elsewhere in this book, their use should be restricted to gear problems.

In this approach the strengths are modified by various factors that produce limiting values of the bending stress and the contact stress.

**Figure 14-2**

Allowable bending stress number for through-hardened steels. The SI equations are  $S_t = 0.533H_B + 88.3$  MPa, grade 1, and  $S_t = 0.703H_B + 113$  MPa, grade 2.

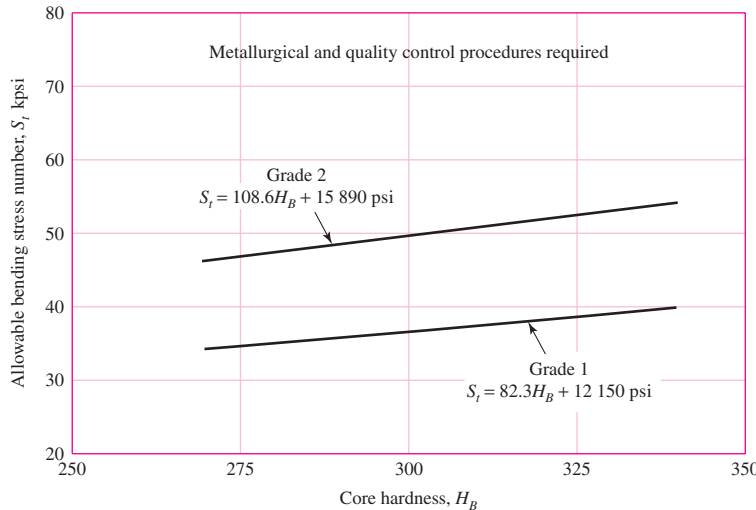
(Source: ANSI/AGMA 2001-D04 and 2101-D04.)



**Figure 14-3**

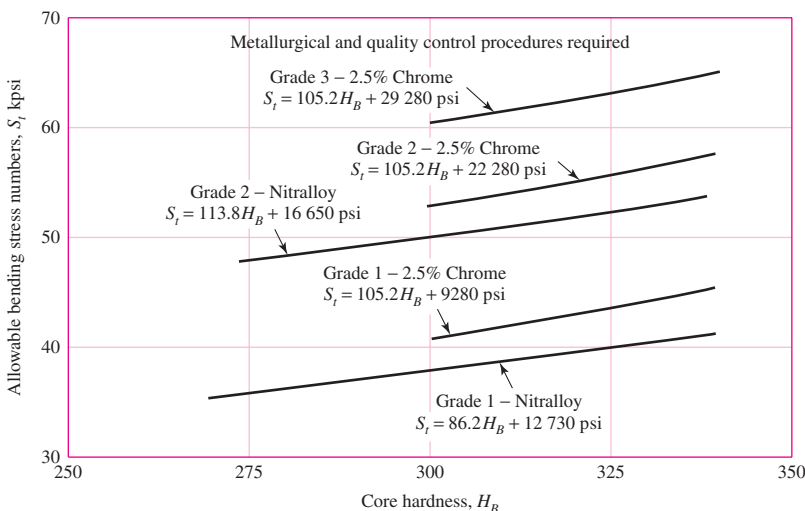
Allowable bending stress number for nitrided through-hardened steel gears (i.e., AISI 4140, 4340),  $S_t$ . The SI equations are  $S_t = 0.568H_B + 83.8$  MPa, grade 1, and  $S_t = 0.749H_B + 110$  MPa, grade 2.

(Source: ANSI/AGMA 2001-D04 and 2101-D04.)



**Figure 14-4**

Allowable bending stress numbers for nitriding steel gears  $S_t$ . The SI equations are  $S_t = 0.594H_B + 87.76$  MPa  
 Nitralloy grade 1  $S_t = 0.784H_B + 114.81$  MPa  
 Nitralloy grade 2  $S_t = 0.7255H_B + 63.89$  MPa  
 2.5% chrome, grade 1  $S_t = 0.7255H_B + 153.63$  MPa  
 2.5% chrome, grade 2  $S_t = 0.7255H_B + 201.91$  MPa  
 2.5% chrome, grade 3  
 (Source: ANSI/AGMA 2001-D04, 2101-D04.)

**Table 14-3**

Repeatedly Applied Bending Strength  $S_t$  at  $10^7$  Cycles and 0.99 Reliability for Steel Gears

Source: ANSI/AGMA 2001-D04.

Material Designation	Heat Treatment	Minimum Surface Hardness <sup>1</sup>	Allowable Bending Stress Number $S_t$ , <sup>2</sup> psi		
			Grade 1	Grade 2	Grade 3
Steel <sup>3</sup>	Through-hardened Flame <sup>4</sup> or induction hardened <sup>4</sup> with type A pattern <sup>5</sup>	See Fig. 14-2 See Table 8*	See Fig. 14-2 45 000	See Fig. 14-2 55 000	—
	Flame <sup>4</sup> or induction hardened <sup>4</sup> with type B pattern <sup>5</sup>	See Table 8*	22 000	22 000	—
	Carburized and hardened	See Table 9*	55 000	65 000 or 70 000 <sup>6</sup>	75 000
	Nitrided <sup>4,7</sup> (through-hardened steels)	83.5 HR15N	See Fig. 14-3	See Fig. 14-3	—
Nitralloy 135M, Nitralloy N, and 2.5% chrome (no aluminum)	Nitrided <sup>4,7</sup>	87.5 HR15N	See Fig. 14-4	See Fig. 14-4	See Fig. 14-4

Notes: See ANSI/AGMA 2001-D04 for references cited in notes 1–7.

<sup>1</sup>Hardness to be equivalent to that at the root diameter in the center of the tooth space and face width.

<sup>2</sup>See tables 7 through 10 for major metallurgical factors for each stress grade of steel gears.

<sup>3</sup>The steel selected must be compatible with the heat treatment process selected and hardness required.

<sup>4</sup>The allowable stress numbers indicated may be used with the case depths prescribed in 16.1.

<sup>5</sup>See figure 12 for type A and type B hardness patterns.

<sup>6</sup>If bainite and microcracks are limited to grade 3 levels, 70 000 psi may be used.

<sup>7</sup>The overload capacity of nitrided gears is low. Since the shape of the effective S-N curve is flat, the sensitivity to shock should be investigated before proceeding with the design. [7]

\*Tables 8 and 9 of ANSI/AGMA 2001-D04 are comprehensive tabulations of the major metallurgical factors affecting  $S_t$  and  $S_c$  of flame-hardened and induction-hardened (Table 8) and carburized and hardened (Table 9) steel gears.

**Table 14-4**

Repeatedly Applied Bending Strength  $S_t$  for Iron and Bronze Gears at  $10^7$  Cycles and 0.99 Reliability

Source: ANSI/AGMA 2001-D04.

Material	Material Designation <sup>1</sup>	Heat Treatment	Typical Minimum Surface Hardness <sup>2</sup>	Allowable Bending Stress Number, $S_t$ , <sup>3</sup> psi
ASTM A48 gray cast iron	Class 20	As cast	—	5000
	Class 30	As cast	174 HB	8500
	Class 40	As cast	201 HB	13 000
ASTM A536 ductile (nodular) Iron	Grade 60-40-18	Annealed	140 HB	22 000–33 000
	Grade 80-55-06	Quenched and tempered	179 HB	22 000–33 000
	Grade 100-70-03	Quenched and tempered	229 HB	27 000–40 000
	Grade 120-90-02	Quenched and tempered	269 HB	31 000–44 000
Bronze		Sand cast	Minimum tensile strength 40 000 psi	5700
	ASTM B-148 Alloy 954	Heat treated	Minimum tensile strength 90 000 psi	23 600

Notes:

<sup>1</sup>See ANSI/AGMA 2004-B89, *Gear Materials and Heat Treatment Manual*.

<sup>2</sup>Measured hardness to be equivalent to that which would be measured at the root diameter in the center of the tooth space and face width.

<sup>3</sup>The lower values should be used for general design purposes. The upper values may be used when:

High quality material is used.

Section size and design allow maximum response to heat treatment.

Proper quality control is effected by adequate inspection.

Operating experience justifies their use.

The equation for the allowable bending stress is

$$\sigma_{\text{all}} = \begin{cases} \frac{S_t}{S_F} \frac{Y_N}{K_T K_R} & \text{(U.S. customary units)} \\ \frac{S_t}{S_F} \frac{Y_N}{Y_\theta Y_Z} & \text{(SI units)} \end{cases} \quad (14-17)$$

where for U.S. customary units (SI units),

$S_t$  is the allowable bending stress, lbf/in<sup>2</sup> (N/mm<sup>2</sup>)

$Y_N$  is the stress cycle factor for bending stress

$K_T$  ( $Y_\theta$ ) are the temperature factors

$K_R$  ( $Y_Z$ ) are the reliability factors

$S_F$  is the AGMA factor of safety, a stress ratio

The equation for the allowable contact stress  $\sigma_{c,\text{all}}$  is

$$\sigma_{c,\text{all}} = \begin{cases} \frac{S_c}{S_H} \frac{Z_N C_H}{K_T K_R} & \text{(U.S. customary units)} \\ \frac{S_c}{S_H} \frac{Z_N Z_W}{Y_\theta Y_Z} & \text{(SI units)} \end{cases} \quad (14-18)$$

where the upper equation is in U.S. customary units and the lower equation is in SI units. Also,

$S_c$  is the allowable contact stress, lbf/in<sup>2</sup> (N/mm<sup>2</sup>)

$Z_N$  is the stress cycle life factor

$C_H$  ( $Z_W$ ) are the hardness ratio factors for pitting resistance

$K_T$  ( $Y_\theta$ ) are the temperature factors

$K_R$  ( $Y_Z$ ) are the reliability factors

$S_H$  is the AGMA factor of safety, a stress ratio

The values for the allowable contact stress, designated here as  $S_c$ , are to be found in Fig. 14–5 and Tables 14–5, 14–6, and 14–7.

AGMA allowable stress numbers (strengths) for bending and contact stress are for

- Unidirectional loading
- 10 million stress cycles
- 99 percent reliability

**Figure 14–5**

Contact-fatigue strength  $S_c$  at  $10^7$  cycles and 0.99 reliability for through-hardened steel gears. The SI equations are  $S_c = 2.22H_B + 200$  MPa, grade 1, and  $S_c = 2.41H_B + 237$  MPa, grade 2. (Source: ANSI/AGMA 2001-D04 and 2101-D04.)

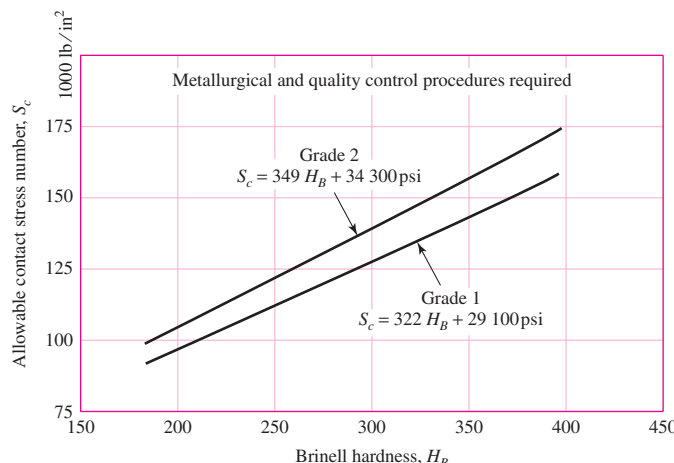


**Table 14–5**

Nominal Temperature Used in Nitriding and Hardnesses Obtained

Source: Darle W. Dudley, *Handbook of Practical Gear Design*, rev. ed., McGraw-Hill, New York, 1984.

Steel	Temperature Before Nitriding, °F	Nitriding, °F	Hardness, Rockwell C Scale Case	Hardness, Rockwell C Scale Core
Nitralloy 135*	1150	975	62–65	30–35
Nitralloy 135M	1150	975	62–65	32–36
Nitralloy N	1000	975	62–65	40–44
AISI 4340	1100	975	48–53	27–35
AISI 4140	1100	975	49–54	27–35
31 Cr Mo V 9	1100	975	58–62	27–33

\*Nitralloy is a trademark of the Nitralloy Corp., New York.

**Table 14-6**

Repeatedly Applied Contact Strength  $S_c$  at  $10^7$  Cycles and 0.99 Reliability for Steel Gears

Source: ANSI/AGMA 2001-D04.

<b>Material Designation</b>	<b>Heat Treatment</b>	<b>Minimum Surface Hardness<sup>1</sup></b>	<b>Allowable Contact Stress Number,<sup>2</sup> <math>S_c</math>, psi</b>		
			<b>Grade 1</b>	<b>Grade 2</b>	<b>Grade 3</b>
Steel <sup>3</sup>	Through hardened <sup>4</sup>	See Fig. 14-5	See Fig. 14-5	See Fig. 14-5	—
	Flame <sup>5</sup> or induction hardened <sup>5</sup>	50 HRC	170 000	190 000	—
		54 HRC	175 000	195 000	—
	Carburized and hardened <sup>5</sup>	See Table 9*	180 000	225 000	275 000
	Nitrided <sup>5</sup> (through hardened steels)	83.5 HR15N 84.5 HR15N	150 000 155 000	163 000 168 000	175 000 180 000
2.5% chrome (no aluminum)	Nitrided <sup>5</sup>	87.5 HR15N	155 000	172 000	189 000
Nitr alloy 135M	Nitrided <sup>5</sup>	90.0 HR15N	170 000	183 000	195 000
Nitr alloy N	Nitrided <sup>5</sup>	90.0 HR15N	172 000	188 000	205 000
2.5% chrome (no aluminum)	Nitrided <sup>5</sup>	90.0 HR15N	176 000	196 000	216 000

Notes: See ANSI/AGMA 2001-D04 for references cited in notes 1–5.

<sup>1</sup>Hardness to be equivalent to that at the start of active profile in the center of the face width.

<sup>2</sup>See Tables 7 through 10 for major metallurgical factors for each stress grade of steel gears.

<sup>3</sup>The steel selected must be compatible with the heat treatment process selected and hardness required.

<sup>4</sup>These materials must be annealed or normalized as a minimum.

<sup>5</sup>The allowable stress numbers indicated may be used with the case depths prescribed in 16.1.

\*Table 9 of ANSI/AGMA 2001-D04 is a comprehensive tabulation of the major metallurgical factors affecting  $S_t$  and  $S_c$  of carburized and hardened steel gears.

The factors in this section, too, will be evaluated in subsequent sections.

When two-way (reversed) loading occurs, as with idler gears, AGMA recommends using 70 percent of  $S_t$  values. This is equivalent to  $1/0.70 = 1.43$  as a value of  $k_e$  in Ex. 14-2. The recommendation falls between the value of  $k_e = 1.33$  for a Goodman failure locus and  $k_e = 1.66$  for a Gerber failure locus.

## 14-5 Geometry Factors $I$ and $J$ ( $Z_I$ and $Y_J$ )

We have seen how the factor  $Y$  is used in the Lewis equation to introduce the effect of tooth form into the stress equation. The AGMA factors<sup>5</sup>  $I$  and  $J$  are intended to accomplish the same purpose in a more involved manner.

The determination of  $I$  and  $J$  depends upon the *face-contact ratio*  $m_F$ . This is defined as

$$m_F = \frac{F}{p_x} \quad (14-19)$$

where  $p_x$  is the axial pitch and  $F$  is the face width. For spur gears,  $m_F = 0$ .

<sup>5</sup>A useful reference is AGMA 908-B89, *Geometry Factors for Determining Pitting Resistance and Bending Strength of Spur, Helical and Herringbone Gear Teeth*.

**Table 14-7**

Repeatedly Applied Contact Strength  $S_c$  10<sup>7</sup> Cycles and 0.99 Reliability for Iron and Bronze Gears

Source: ANSI/AGMA 2001-D04.

<b>Material</b>	<b>Material Designation<sup>1</sup></b>	<b>Heat Treatment</b>	<b>Typical Minimum Surface Hardness<sup>2</sup></b>	<b>Allowable Contact Stress Number,<sup>3</sup> <math>S_c</math>, psi</b>
ASTM A48 gray cast iron	Class 20	As cast	—	50 000–60 000
	Class 30	As cast	174 HB	65 000–75 000
	Class 40	As cast	201 HB	75 000–85 000
ASTM A536 ductile (nodular) iron	Grade 60–40–18	Annealed	140 HB	77 000–92 000
	Grade 80–55–06	Quenched and tempered	179 HB	77 000–92 000
	Grade 100–70–03	Quenched and tempered	229 HB	92 000–112 000
	Grade 120–90–02	Quenched and tempered	269 HB	103 000–126 000
Bronze	—	Sand cast	Minimum tensile strength 40 000 psi	30 000
	ASTM B-148 Alloy 954	Heat treated	Minimum tensile strength 90 000 psi	65 000

Notes:

<sup>1</sup>See ANSI/AGMA 2004-B89, *Gear Materials and Heat Treatment Manual*.

<sup>2</sup>Hardness to be equivalent to that at the start of active profile in the center of the face width.

<sup>3</sup>The lower values should be used for general design purposes. The upper values may be used when:

High-quality material is used.

Section size and design allow maximum response to heat treatment.

Proper quality control is effected by adequate inspection.

Operating experience justifies their use.

Low-contact-ratio (LCR) helical gears having a small helix angle or a thin face width, or both, have face-contact ratios less than unity ( $m_F \leq 1$ ), and will not be considered here. Such gears have a noise level not too different from that for spur gears. Consequently we shall consider here only spur gears with  $m_F = 0$  and conventional helical gears with  $m_F > 1$ .

### Bending-Strength Geometry Factor $J$ ( $Y_J$ )

The AGMA factor  $J$  employs a modified value of the Lewis form factor, also denoted by  $Y$ ; a fatigue stress-concentration factor  $K_f$ ; and a tooth load-sharing ratio  $m_N$ . The resulting equation for  $J$  for spur and helical gears is

$$J = \frac{Y}{K_f m_N} \quad (14-20)$$

It is important to note that the form factor  $Y$  in Eq. (14-20) is *not* the Lewis factor at all. The value of  $Y$  here is obtained from calculations within AGMA 908-B89, and is often based on the highest point of single-tooth contact.

The factor  $K_f$  in Eq. (14–20) is called a *stress-correction factor* by AGMA. It is based on a formula deduced from a photoelastic investigation of stress concentration in gear teeth over 50 years ago.

The load-sharing ratio  $m_N$  is equal to the face width divided by the minimum total length of the lines of contact. This factor depends on the transverse contact ratio  $m_p$ , the face-contact ratio  $m_F$ , the effects of any profile modifications, and the tooth deflection. For spur gears,  $m_N = 1.0$ . For helical gears having a face-contact ratio  $m_F > 2.0$ , a conservative approximation is given by the equation

$$m_N = \frac{p_N}{0.95Z} \quad (14-21)$$

where  $p_N$  is the normal base pitch and  $Z$  is the length of the line of action in the transverse plane (distance  $L_{ab}$  in Fig. 13–15).

Use Fig. 14–6 to obtain the geometry factor  $J$  for spur gears having a  $20^\circ$  pressure angle and full-depth teeth. Use Figs. 14–7 and 14–8 for helical gears having a  $20^\circ$  normal pressure angle and face-contact ratios of  $m_F = 2$  or greater. For other gears, consult the AGMA standard.

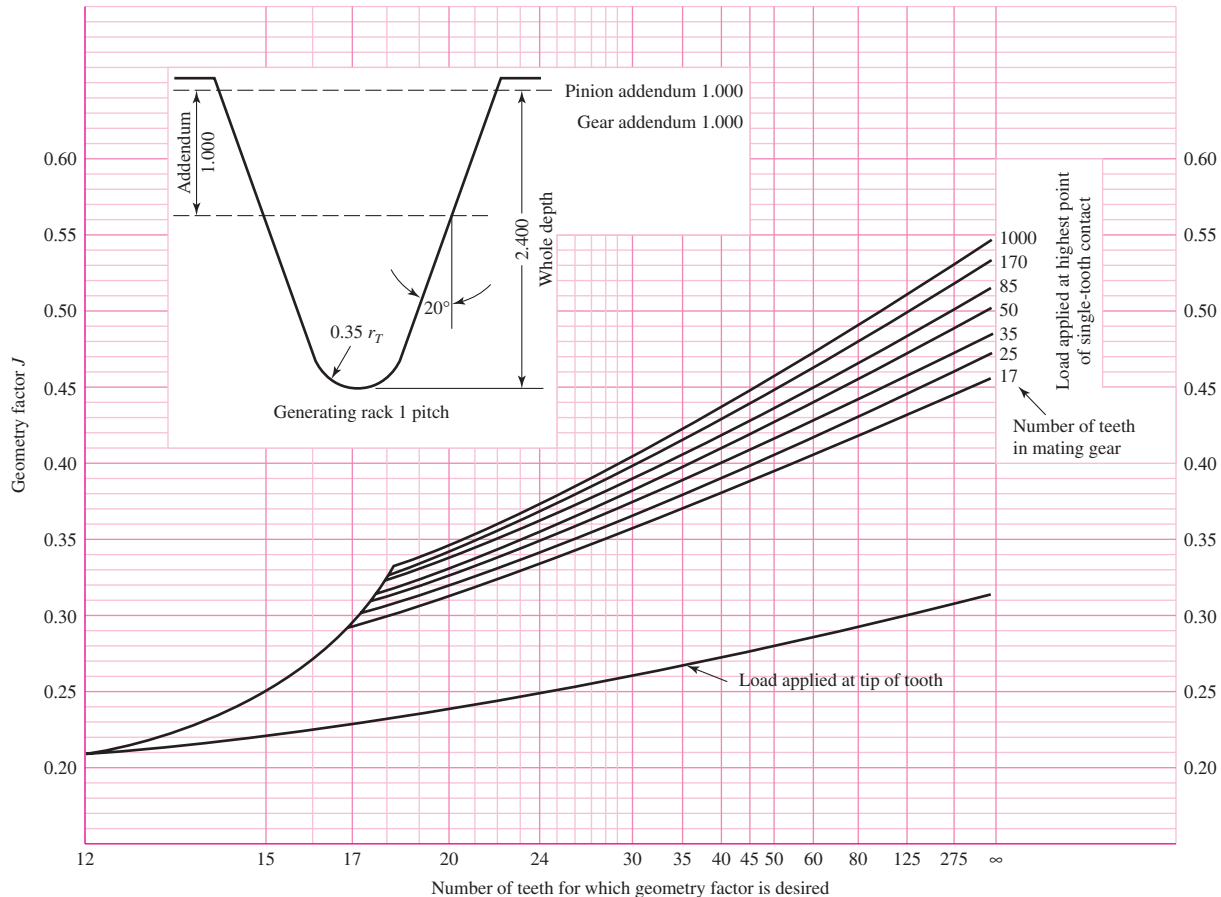
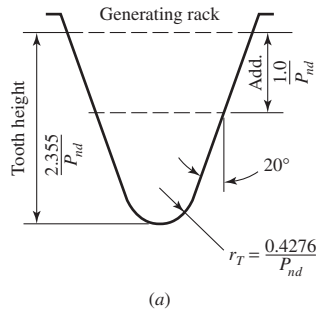


**Figure 14–6**

Spur-gear geometry factors  $J$ . Source: The graph is from AGMA 218.01, which is consistent with tabular data from the current AGMA 908-B89. The graph is convenient for design purposes.



$$m_N = \frac{P_N}{0.95Z}$$

Value for  $Z$  is for an element of indicated numbers of teeth and a 75-tooth mate

Normal tooth thickness of pinion and gear tooth each reduced 0.024 in to provide 0.048 in total backlash for one normal diametral pitch



**Figure 14-7**

Helical-gear geometry factors  $J'$ . Source: The graph is from AGMA 218.01, which is consistent with tabular data from the current AGMA 908-B89. The graph is convenient for design purposes.

### Surface-Strength Geometry Factor I ( $Z_I$ )

The factor  $I$  is also called the *pitting-resistance geometry factor* by AGMA. We will develop an expression for  $I$  by noting that the sum of the reciprocals of Eq. (14-14), from Eq. (14-12), can be expressed as

$$\frac{1}{r_1} + \frac{1}{r_2} = \frac{2}{\sin \phi_t} \left( \frac{1}{d_P} + \frac{1}{d_G} \right) \quad (14-21)$$

where we have replaced  $\phi$  by  $\phi_t$ , the transverse pressure angle, so that the relation will apply to helical gears too. Now define *speed ratio*  $m_G$  as

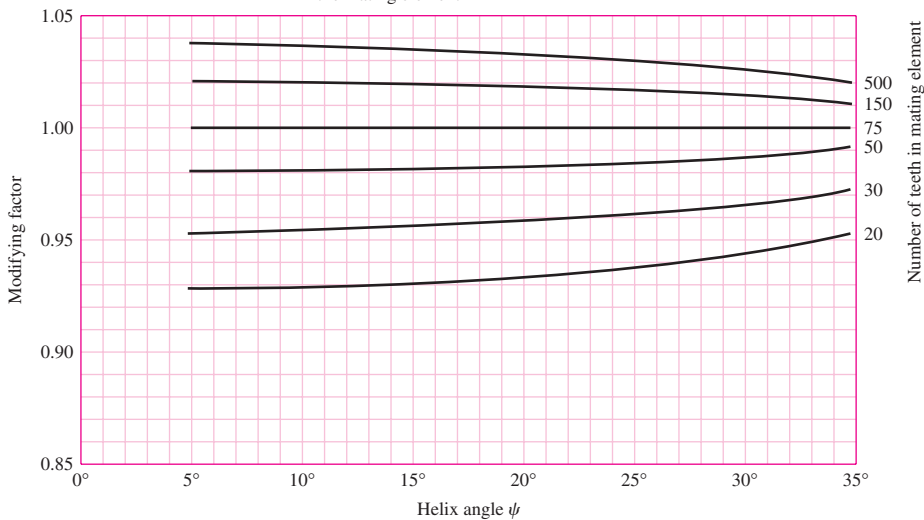
$$m_G = \frac{N_G}{N_P} = \frac{d_G}{d_P} \quad (14-22)$$

**Figure 14–8**

$J'$ -factor multipliers for use with Fig. 14–7 to find  $J$ .

Source: The graph is from AGMA 218.01, which is consistent with tabular data from the current AGMA 908-B89. The graph is convenient for design purposes.

The modifying factor can be applied to the  $J$  factor when other than 75 teeth are used in the mating element



Equation (a) can now be written

$$\frac{1}{r_1} + \frac{1}{r_2} = \frac{2}{d_P \sin \phi_t} \frac{m_G + 1}{m_G} \quad (b)$$

Now substitute Eq. (b) for the sum of the reciprocals in Eq. (14–14). The result is found to be

$$\sigma_c = -\sigma_C = C_p \left[ \frac{K_V W^t}{d_P F} \frac{1}{\frac{\cos \phi_t \sin \phi_t}{2} \frac{m_G}{m_G + 1}} \right]^{1/2} \quad (c)$$

The geometry factor  $I$  for external spur and helical gears is the denominator of the second term in the brackets in Eq. (c). By adding the load-sharing ratio  $m_N$ , we obtain a factor valid for both spur and helical gears. The equation is then written as

$$I = \begin{cases} \frac{\cos \phi_t \sin \phi_t}{2m_N} \frac{m_G}{m_G + 1} & \text{external gears} \\ \frac{\cos \phi_t \sin \phi_t}{2m_N} \frac{m_G}{m_G - 1} & \text{internal gears} \end{cases} \quad (14-23)$$

where  $m_N = 1$  for spur gears. In solving Eq. (14–21) for  $m_N$ , note that

$$p_N = p_n \cos \phi_n \quad (14-24)$$

where  $p_n$  is the normal circular pitch. The quantity  $Z$ , for use in Eq. (14–21), can be obtained from the equation

$$Z = [(r_P + a)^2 - r_{bP}^2]^{1/2} + [(r_G + a)^2 - r_{bG}^2]^{1/2} - (r_P + r_G) \sin \phi_t \quad (14-25)$$

where  $r_P$  and  $r_G$  are the pitch radii and  $r_{bP}$  and  $r_{bG}$  the base-circle radii of the pinion and gear, respectively.<sup>6</sup> Recall from Eq. (13–6), the radius of the base circle is

$$r_b = r \cos \phi_t \quad (14-26)$$

<sup>6</sup>For a development, see Joseph E. Shigley and John J. Uicker Jr., *Theory of Machines and Mechanisms*, McGraw-Hill, New York, 1980, p. 262.

Certain precautions must be taken in using Eq. (14–25). The tooth profiles are not conjugate below the base circle, and consequently, if either one or the other of the first two terms in brackets is larger than the third term, then it should be replaced by the third term. In addition, the effective outside radius is sometimes less than  $r + a$ , owing to removal of burrs or rounding of the tips of the teeth. When this is the case, always use the effective outside radius instead of  $r + a$ .

## 14–6 The Elastic Coefficient $C_p$ ( $Z_E$ )

Values of  $C_p$  may be computed directly from Eq. (14–13) or obtained from Table 14–8.

## 14–7 Dynamic Factor $K_v$

As noted earlier, dynamic factors are used to account for inaccuracies in the manufacture and meshing of gear teeth in action. *Transmission error* is defined as the departure from uniform angular velocity of the gear pair. Some of the effects that produce transmission error are:

- Inaccuracies produced in the generation of the tooth profile; these include errors in tooth spacing, profile lead, and runout
- Vibration of the tooth during meshing due to the tooth stiffness
- Magnitude of the pitch-line velocity
- Dynamic unbalance of the rotating members
- Wear and permanent deformation of contacting portions of the teeth
- Gearshaft misalignment and the linear and angular deflection of the shaft
- Tooth friction

In an attempt to account for these effects, AGMA has defined a set of *quality numbers*.<sup>7</sup> These numbers define the tolerances for gears of various sizes manufactured to a specified accuracy. Quality numbers 3 to 7 will include most commercial-quality gears. Quality numbers 8 to 12 are of precision quality. The AGMA *transmission accuracy-level number*  $Q_v$  could be taken as the same as the quality number. The following equations for the dynamic factor are based on these  $Q_v$  numbers:

$$K_v = \begin{cases} \left( \frac{A + \sqrt{V}}{A} \right)^B & V \text{ in ft/min} \\ \left( \frac{A + \sqrt{200V}}{A} \right)^B & V \text{ in m/s} \end{cases} \quad (14-27)$$

where

$$\begin{aligned} A &= 50 + 56(1 - B) \\ B &= 0.25(12 - Q_v)^{2/3} \end{aligned} \quad (14-28)$$

and the maximum velocity, representing the end point of the  $Q_v$  curve, is given by

$$(V_t)_{\max} = \begin{cases} [A + (Q_v - 3)]^2 & \text{ft/min} \\ \frac{[A + (Q_v - 3)]^2}{200} & \text{m/s} \end{cases} \quad (14-29)$$

<sup>7</sup>AGMA 2000-A88. ANSI/AGMA 2001-D04, adopted in 2004, replaced  $Q_v$  with  $A_v$  and incorporated ANSI/AGMA 2015-1-A01.  $A_v$  ranges from 6 to 12, with lower numbers representing greater accuracy. The  $Q_v$  approach was maintained as an alternate approach, and resulting  $K_v$  values are comparable.

**Table 14-8**Elastic Coefficient  $C_p$  ( $Z_E$ ),  $\sqrt{\text{psi}}$  ( $\sqrt{\text{MPa}}$ )    Source: AGMA 218.01

Pinion Material	Pinion Modulus of Elasticity $E_p$ psi (MPa)*	Gear Material and Modulus of Elasticity $E_G$ , lbf/in <sup>2</sup> (MPa)*					
		Steel $30 \times 10^6$ ( $2 \times 10^5$ )	Malleable Iron $25 \times 10^6$ ( $1.7 \times 10^5$ )	Nodular Iron $24 \times 10^6$ ( $1.7 \times 10^5$ )	Cast Iron $22 \times 10^6$ ( $1.5 \times 10^5$ )	Aluminum Bronze $17.5 \times 10^6$ ( $1.2 \times 10^5$ )	Tin Bronze $16 \times 10^6$ ( $1.1 \times 10^5$ )
Steel	$30 \times 10^6$ ( $2 \times 10^5$ )	2300 (191)	2180 (181)	2160 (179)	2100 (174)	1950 (162)	1900 (158)
Malleable iron	$25 \times 10^6$ ( $1.7 \times 10^5$ )	2180 (181)	2090 (174)	2070 (172)	2020 (168)	1900 (158)	1850 (154)
Nodular iron	$24 \times 10^6$ ( $1.7 \times 10^5$ )	2160 (179)	2070 (172)	2050 (170)	2000 (166)	1880 (156)	1830 (152)
Cast iron	$22 \times 10^6$ ( $1.5 \times 10^5$ )	2100 (174)	2020 (168)	2000 (166)	1960 (163)	1850 (154)	1800 (149)
Aluminum bronze	$17.5 \times 10^6$ ( $1.2 \times 10^5$ )	1950 (162)	1900 (158)	1880 (156)	1850 (154)	1750 (145)	1700 (141)
Tin bronze	$16 \times 10^6$ ( $1.1 \times 10^5$ )	1900 (158)	1850 (154)	1830 (152)	1800 (149)	1700 (141)	1650 (137)

Poisson's ratio = 0.30.

\*When more exact values for modulus of elasticity are obtained from roller contact tests, they may be used.

**Figure 14–9**

Dynamic factor  $K_v$ . The equations to these curves are given by Eq. (14–27) and the end points by Eq. (14–29). (ANSI/AGMA 2001-D04, Annex A)

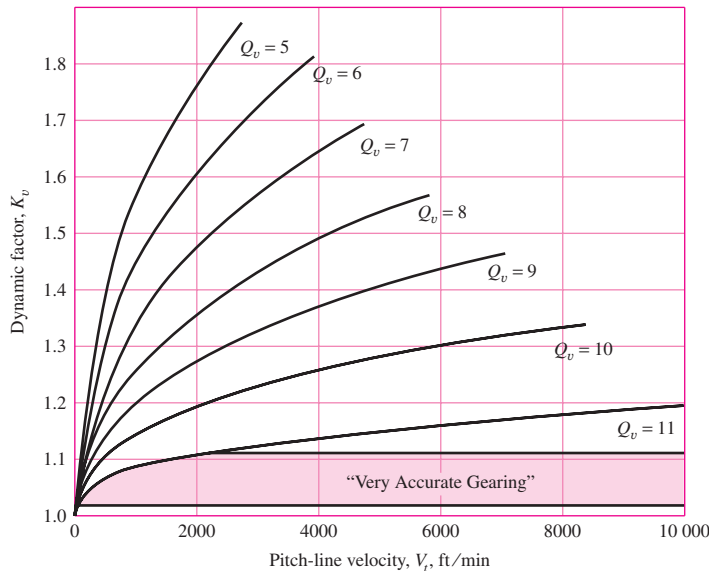


Figure 14–9 is a graph of  $K_v$ , the dynamic factor, as a function of pitch-line speed for graphical estimates of  $K_v$ .

## 14–8

### Overload Factor $K_o$

The overload factor  $K_o$  is intended to make allowance for all externally applied loads in excess of the nominal tangential load  $W^t$  in a particular application (see Figs. 14–17 and 14–18). Examples include variations in torque from the mean value due to firing of cylinders in an internal combustion engine or reaction to torque variations in a piston pump drive. There are other similar factors such as application factor or service factor. These factors are established after considerable field experience in a particular application.<sup>8</sup>

## 14–9

### Surface Condition Factor $C_f$ ( $Z_R$ )

The surface condition factor  $C_f$  or  $Z_R$  is used only in the pitting resistance equation, Eq. (14–16). It depends on

- Surface finish as affected by, but not limited to, cutting, shaving, lapping, grinding, shotpeening
- Residual stress
- Plastic effects (work hardening)

Standard surface conditions for gear teeth have not yet been established. When a detrimental surface finish effect is known to exist, AGMA specifies a value of  $C_f$  greater than unity.

<sup>8</sup>An extensive list of service factors appears in Howard B. Schwerdin, "Couplings," Chap. 16 in Joseph E. Shigley, Charles R. Mischke, and Thomas H. Brown, Jr. (eds.), *Standard Handbook of Machine Design*, 3rd ed., McGraw-Hill, New York, 2004.

## 14-10 Size Factor $K_s$

The size factor reflects nonuniformity of material properties due to size. It depends upon

- Tooth size
- Diameter of part
- Ratio of tooth size to diameter of part
- Face width
- Area of stress pattern
- Ratio of case depth to tooth size
- Hardenability and heat treatment

Standard size factors for gear teeth have not yet been established for cases where there is a detrimental size effect. In such cases AGMA recommends a size factor greater than unity. If there is no detrimental size effect, use unity.

AGMA has identified and provided a symbol for size factor. Also, AGMA suggests  $K_s = 1$ , which makes  $K_s$  a placeholder in Eqs. (14–15) and (14–16) until more information is gathered. Following the standard in this manner is a failure to apply all of your knowledge. From Table 13–1,  $l = a + b = 2.25/P$ . The tooth thickness  $t$  in Fig. 14–6 is given in Sec. 14–1, Eq. (b), as  $t = \sqrt{4lx}$  where  $x = 3Y/(2P)$  from Eq. (14–3). From Eq. (6–25) the equivalent diameter  $d_e$  of a rectangular section in bending is  $d_e = 0.808\sqrt{Ft}$ . From Eq. (6–20)  $k_b = (d_e/0.3)^{-0.107}$ . Noting that  $K_s$  is the reciprocal of  $k_b$ , we find the result of all the algebraic substitution is

$$K_s = \frac{1}{k_b} = 1.192 \left( \frac{F\sqrt{Y}}{P} \right)^{0.0535} \quad (a)$$

$K_s$  can be viewed as Lewis's geometry incorporated into the Marin size factor in fatigue. You may set  $K_s = 1$ , or you may elect to use the preceding Eq. (a). This is a point to discuss with your instructor. We will use Eq. (a) to remind you that you have a choice. If  $K_s$  in Eq. (a) is less than 1, use  $K_s = 1$ .

## 14-11 Load-Distribution Factor $K_m$ ( $K_H$ )

The load-distribution factor modified the stress equations to reflect nonuniform distribution of load across the line of contact. The ideal is to locate the gear "midspan" between two bearings at the zero slope place when the load is applied. However, this is not always possible. The following procedure is applicable to

- Net face width to pinion pitch diameter ratio  $F/d \leq 2$
- Gear elements mounted between the bearings
- Face widths up to 40 in
- Contact, when loaded, across the full width of the narrowest member

The load-distribution factor under these conditions is currently given by the *face load distribution factor*,  $C_{mf}$ , where

$$K_m = C_{mf} = 1 + C_{mc}(C_{pf}C_{pm} + C_{ma}C_e) \quad (14-30)$$

where

$$C_{mc} = \begin{cases} 1 & \text{for uncrowned teeth} \\ 0.8 & \text{for crowned teeth} \end{cases} \quad (14-31)$$

$$C_{pf} = \begin{cases} \frac{F}{10d} - 0.025 & F \leq 1 \text{ in} \\ \frac{F}{10d} - 0.0375 + 0.0125F & 1 < F \leq 17 \text{ in} \\ \frac{F}{10d} - 0.1109 + 0.0207F - 0.000228F^2 & 17 < F \leq 40 \text{ in} \end{cases} \quad (14-32)$$

Note that for values of  $F/(10d) < 0.05$ ,  $F/(10d) = 0.05$  is used.

$$C_{pm} = \begin{cases} 1 & \text{for straddle-mounted pinion with } S_1/S < 0.175 \\ 1.1 & \text{for straddle-mounted pinion with } S_1/S \geq 0.175 \end{cases} \quad (14-33)$$

$$C_{ma} = A + BF + CF^2 \quad (\text{see Table 14-9 for values of } A, B, \text{ and } C) \quad (14-34)$$

$$C_e = \begin{cases} 0.8 & \text{for gearing adjusted at assembly, or compatibility} \\ & \text{is improved by lapping, or both} \\ 1 & \text{for all other conditions} \end{cases} \quad (14-35)$$

See Fig. 14–10 for definitions of  $S$  and  $S_1$  for use with Eq. (14–33), and see Fig. 14–11 for graph of  $C_{ma}$ .

**Table 14-9**

Empirical Constants  
 $A$ ,  $B$ , and  $C$  for  
 Eq. (14–34), Face  
 Width  $F$  in Inches\*

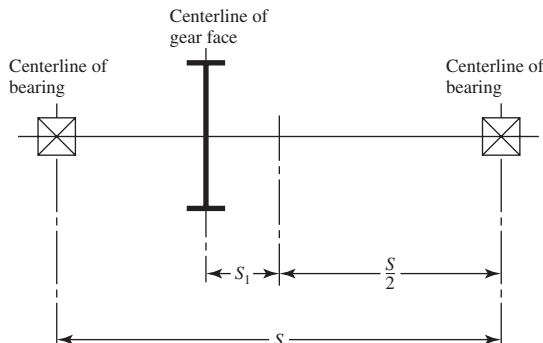
Source: ANSI/AGMA  
 2001-D04.

Condition	A	B	C
Open gearing	0.247	0.0167	$-0.765(10^{-4})$
Commercial, enclosed units	0.127	0.0158	$-0.930(10^{-4})$
Precision, enclosed units	0.0675	0.0128	$-0.926(10^{-4})$
Extraprecision enclosed gear units	0.00360	0.0102	$-0.822(10^{-4})$

\*See ANSI/AGMA 2101-D04, pp. 20–22, for SI formulation.

**Figure 14-10**

Definition of distances  $S$  and  $S_1$  used in evaluating  $C_{pm}$ , Eq. (14–33). (ANSI/AGMA 2001-D04.)



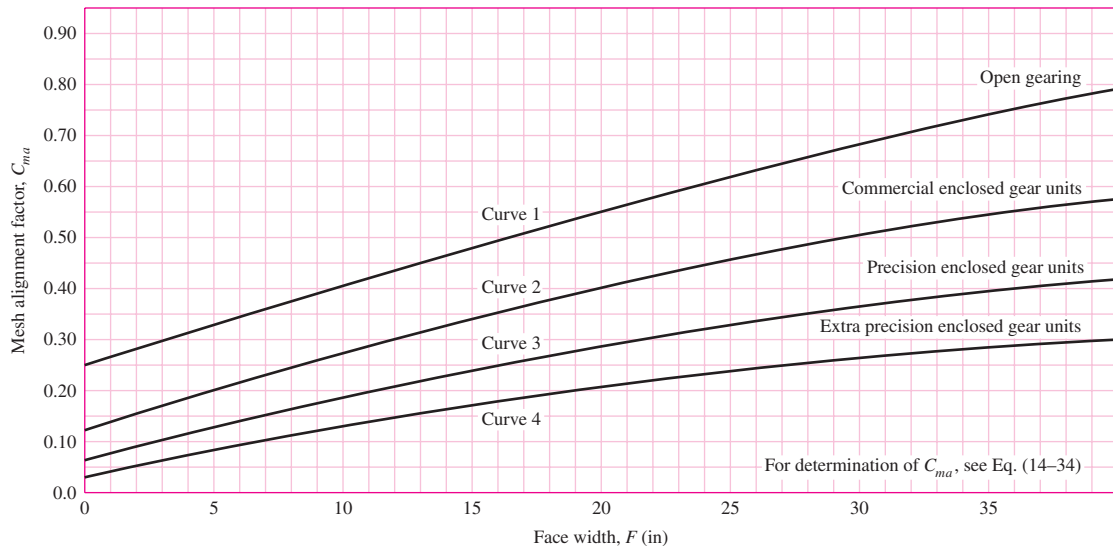


**Figure 14-11**

Mesh alignment factor  $C_{ma}$ . Curve-fit equations in Table 14-9. (ANSI/AGMA 2001-D04.)

## 14-12 Hardness-Ratio Factor $C_H$

The pinion generally has a smaller number of teeth than the gear and consequently is subjected to more cycles of contact stress. If both the pinion and the gear are through-hardened, then a uniform surface strength can be obtained by making the pinion harder than the gear. A similar effect can be obtained when a surface-hardened pinion is mated with a through-hardened gear. The hardness-ratio factor  $C_H$  is used *only for the gear*. Its purpose is to adjust the surface strengths for this effect. The values of  $C_H$  are obtained from the equation

$$C_H = 1.0 + A'(m_G - 1.0) \quad (14-36)$$

where

$$A' = 8.98(10^{-3}) \left( \frac{H_{BP}}{H_{BG}} \right) - 8.29(10^{-3}) \quad 1.2 \leq \frac{H_{BP}}{H_{BG}} \leq 1.7$$

The terms  $H_{BP}$  and  $H_{BG}$  are the Brinell hardness (10-mm ball at 3000-kg load) of the pinion and gear, respectively. The term  $m_G$  is the speed ratio and is given by Eq. (14-22). See Fig. 14-12 for a graph of Eq. (14-36). For

$$\frac{H_{BP}}{H_{BG}} < 1.2, \quad A' = 0$$

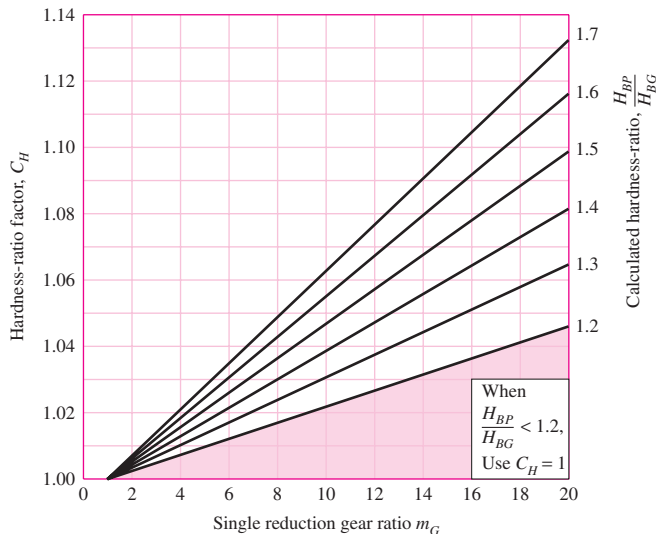
$$\frac{H_{BP}}{H_{BG}} > 1.7, \quad A' = 0.00698$$

When surface-hardened pinions with hardnesses of 48 Rockwell C scale (Rockwell C48) or harder are run with through-hardened gears (180–400 Brinell), a work hardening occurs. The  $C_H$  factor is a function of pinion surface finish  $f_P$  and the mating gear hardness. Figure 14-13 displays the relationships:

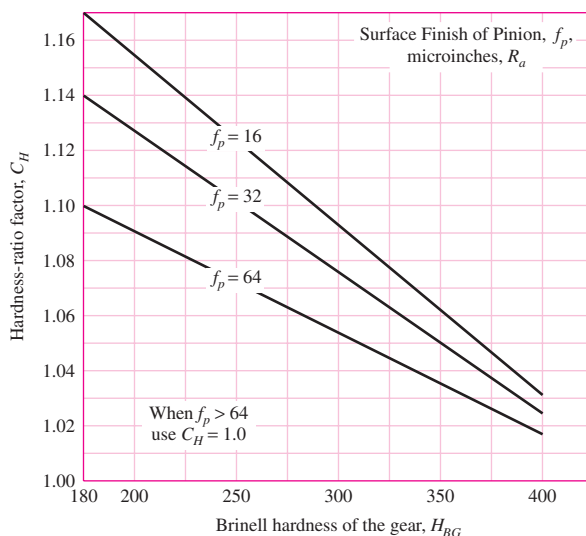
$$C_H = 1 + B'(450 - H_{BG}) \quad (14-37)$$

**Figure 14-12**

Hardness-ratio factor  $C_H$   
(through-hardened steel).  
(ANSI/AGMA 2001-D04.)

**Figure 14-13**

Hardness-ratio factor  $C_H$   
(surface-hardened steel pinion).  
(ANSI/AGMA 2001-D04.)



where  $B' = 0.000\ 75 \exp[-0.0112f_p]$  and  $f_p$  is the surface finish of the pinion expressed as root-mean-square roughness  $R_a$  in  $\mu$  in.

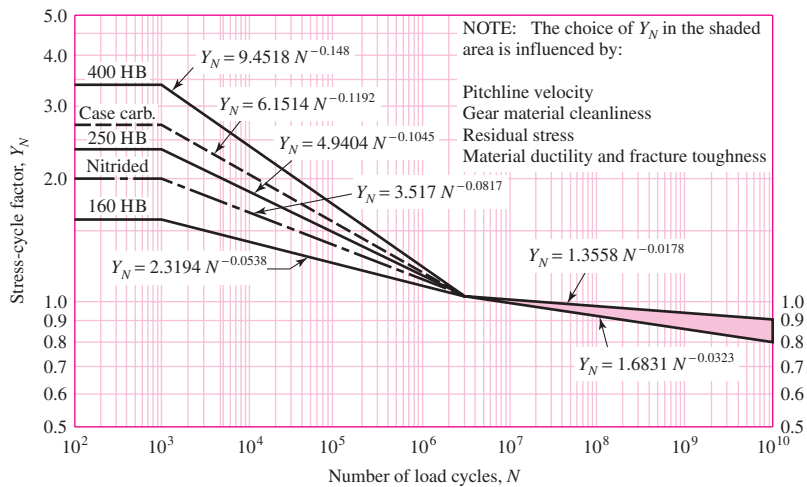
## 14-13

### Stress-Cycle Factors $Y_N$ and $Z_N$

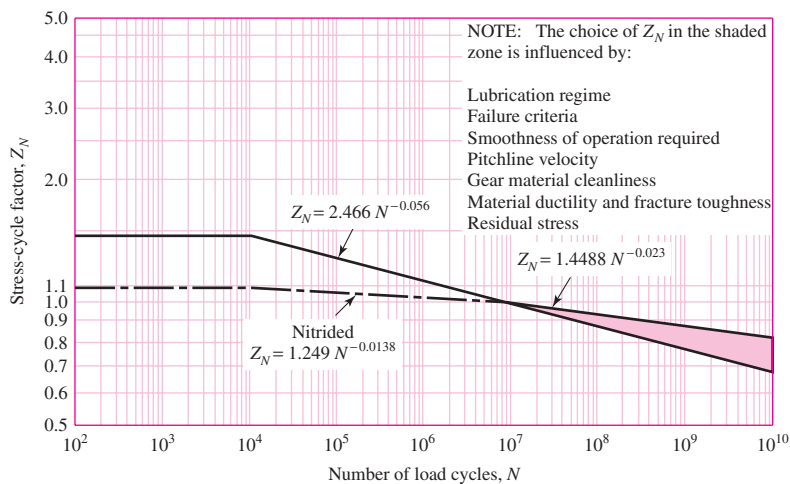
The AGMA strengths as given in Figs. 14-2 through 14-4, in Tables 14-3 and 14-4 for bending fatigue, and in Fig. 14-5 and Tables 14-5 and 14-6 for contact-stress fatigue are based on  $10^7$  load cycles applied. The purpose of the load cycle factors  $Y_N$  and  $Z_N$  is to modify the gear strength for lives other than  $10^7$  cycles. Values for these factors are given in Figs. 14-14 and 14-15. Note that for  $10^7$  cycles  $Y_N = Z_N = 1$  on each graph. Note also that the equations for  $Y_N$  and  $Z_N$  change on either side of  $10^7$  cycles. For life goals slightly higher than  $10^7$  cycles, the mating gear may be experiencing fewer than  $10^7$  cycles and the equations for  $(Y_N)_P$  and  $(Y_N)_G$  can be different. The same comment applies to  $(Z_N)_P$  and  $(Z_N)_G$ .

**Figure 14-14**

Repeatedly applied bending strength stress-cycle factor  $Y_N$ . (ANSI/AGMA 2001-D04.)

**Figure 14-15**

Pitting resistance stress-cycle factor  $Z_N$ . (ANSI/AGMA 2001-D04.)



## 14-14 Reliability Factor $K_R$ ( $Y_R$ )

The reliability factor accounts for the effect of the statistical distributions of material fatigue failures. Load variation is not addressed here. The gear strengths  $S_t$  and  $S_c$  are based on a reliability of 99 percent. Table 14-10 is based on data developed by the U.S. Navy for bending and contact-stress fatigue failures.

The functional relationship between  $K_R$  and reliability is highly nonlinear. When interpolation is required, linear interpolation is too crude. A log transformation to each quantity produces a linear string. A least-squares regression fit is

$$K_R = \begin{cases} 0.658 - 0.0759 \ln(1 - R) & 0.5 < R < 0.99 \\ 0.50 - 0.109 \ln(1 - R) & 0.99 \leq R \leq 0.9999 \end{cases} \quad (14-38)$$

For cardinal values of  $R$ , take  $K_R$  from the table. Otherwise use the logarithmic interpolation afforded by Eqs. (14-38).

**Table 14-10**

	<b>Reliability</b>	<b><math>K_R (Y_Z)</math></b>
Reliability Factors $K_R (Y_Z)$	0.9999	1.50
<i>Source: ANSI/AGMA 2001-D04.</i>	0.999	1.25
	0.99	1.00
	0.90	0.85
	0.50	0.70

**14-15****Temperature Factor  $K_T (Y_\theta)$** 

For oil or gear-blank temperatures up to 250°F (120°C), use  $K_T = Y_\theta = 1.0$ . For higher temperatures, the factor should be greater than unity. Heat exchangers may be used to ensure that operating temperatures are considerably below this value, as is desirable for the lubricant.

**14-16****Rim-Thickness Factor  $K_B$** 

When the rim thickness is not sufficient to provide full support for the tooth root, the location of bending fatigue failure may be through the gear rim rather than at the tooth fillet. In such cases, the use of a stress-modifying factor  $K_B$  or ( $t_R$ ) is recommended. This factor, the *rim-thickness factor*  $K_B$ , adjusts the estimated bending stress for the thin-rimmed gear. It is a function of the backup ratio  $m_B$ ,

$$m_B = \frac{t_R}{h_t} \quad (14-39)$$

where  $t_R$  = rim thickness below the tooth, in, and  $h_t$  = the tooth height. The geometry is depicted in Fig. 14-16. The rim-thickness factor  $K_B$  is given by

$$K_B = \begin{cases} 1.6 \ln \frac{2.242}{m_B} & m_B < 1.2 \\ 1 & m_B \geq 1.2 \end{cases} \quad (14-40)$$

**Figure 14-16**

Rim-thickness factor  $K_B$ .  
(ANSI/AGMA 2001-D04.)

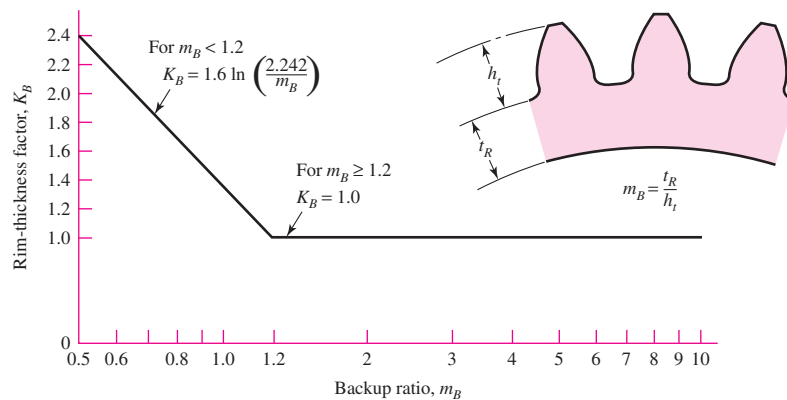


Figure 14–16 also gives the value of  $K_B$  graphically. The rim-thickness factor  $K_B$  is applied in addition to the 0.70 reverse-loading factor when applicable.

## 14-17 Safety Factors $S_F$ and $S_H$

The ANSI/AGMA standards 2001-D04 and 2101-D04 contain a safety factor  $S_F$  guarding against bending fatigue failure and safety factor  $S_H$  guarding against pitting failure.

The definition of  $S_F$ , from Eq. (14–17), is

$$S_F = \frac{S_t Y_N / (K_T K_R)}{\sigma} = \frac{\text{fully corrected bending strength}}{\text{bending stress}} \quad (14-41)$$

where  $\sigma$  is estimated from Eq. (14–15). It is a strength-over-stress definition in a case where the stress is linear with the transmitted load.

The definition of  $S_H$ , from Eq. (14–18), is

$$S_H = \frac{S_c Z_N C_H / (K_T K_R)}{\sigma_c} = \frac{\text{fully corrected contact strength}}{\text{contact stress}} \quad (14-42)$$

when  $\sigma_c$  is estimated from Eq. (14–16). This, too, is a strength-over-stress definition but in a case where the stress is *not* linear with the transmitted load  $W^t$ .

While the definition of  $S_H$  does not interfere with its intended function, a caution is required when comparing  $S_F$  with  $S_H$  in an analysis in order to ascertain the nature and severity of the threat to loss of function. To render  $S_H$  linear with the transmitted load,  $W^t$  it could have been defined as

$$S_H = \left( \frac{\text{fully corrected contact strength}}{\text{contact stress imposed}} \right)^2 \quad (14-43)$$

with the exponent 2 for linear or helical contact, or an exponent of 3 for crowned teeth (spherical contact). With the definition, Eq. (14–42), compare  $S_F$  with  $S_H^2$  (or  $S_H^3$  for crowned teeth) when trying to identify the threat to loss of function with confidence.

The role of the overload factor  $K_o$  is to include predictable excursions of load beyond  $W^t$  based on experience. A safety factor is intended to account for unquantifiable elements in addition to  $K_o$ . When designing a gear mesh, the quantity  $S_F$  becomes a design factor ( $S_F$ )<sub>d</sub> within the meanings used in this book. The quantity  $S_F$  evaluated as part of a design assessment is a factor of safety. This applies equally well to the quantity  $S_H$ .

## 14-18 Analysis

Description of the procedure based on the AGMA standard is highly detailed. The best review is a “road map” for bending fatigue and contact-stress fatigue. Figure 14–17 identifies the bending stress equation, the endurance strength in bending equation, and the factor of safety  $S_F$ . Figure 14–18 displays the contact-stress equation, the contact fatigue endurance strength equation, and the factor of safety  $S_H$ . When analyzing a gear problem, this figure is a useful reference.

The following example of a gear mesh analysis is intended to make all the details presented concerning the AGMA method more familiar.

**SPUR GEAR BENDING**  
Based on ANSI/AGMA 2001-D04

$$d_p = \frac{N_p}{P_d}$$

$$V = \frac{\pi d n}{12}$$

$$W^t = \frac{33\,000 \text{ H}}{V}$$

$$\sigma = W^t K_o K_v K_s \frac{P_d}{F} \frac{K_m K_B}{J}$$

Table below

1 [or Eq. (a), Sec. 14–10]; p. 759  
 Eq. (14–30); p. 759  
 Eq. (14–40); p. 764  
 Fig. 14–6; p. 753  
 Eq. (14–27); p. 756

Gear bending stress equation  
Eq. (14–15)

0.99( $S_t$ )<sub>10<sup>7</sup></sub> Tables 14–3, 14–4; pp. 748, 749

Gear bending endurance strength equation  
Eq. (14–17)

$$\sigma_{all} = \frac{S_t}{S_F} \frac{Y_N}{K_T K_R}$$

Fig. 14–14; p. 763  
 Table 14–10, Eq. (14–38); pp. 763, 764  
 1 if  $T < 250^\circ\text{F}$

Bending factor of safety  
Eq. (14–41)

$$S_F = \frac{S_t Y_N / (K_T K_R)}{\sigma}$$

Remember to compare  $S_F$  with  $S_H^2$  when deciding whether bending or wear is the threat to function. For crowned gears compare  $S_F$  with  $S_H^3$ .

Table of Overload Factors,  $K_o$

Driven Machine				
Power source	Uniform	Moderate shock	Heavy shock	
Uniform	1.00	1.25	1.75	
Light shock	1.25	1.50	2.00	
Medium shock	1.50	1.75	2.25	

**Figure 14–17**

Roadmap of gear bending equations based on AGMA standards. (ANSI/AGMA 2001-D04.)

### SPUR GEAR WEAR

Based on ANSI/AGMA 2001-D04

$$d_P = \frac{N_p}{P_d}$$

$$V = \frac{\pi d n}{12}$$

$$W^t = \frac{33\,000 \text{ H}}{V}$$

$$\sigma_c = C_p \left( W^t K_o K_v K_s \frac{K_m}{d_P F} \frac{C_f}{I} \right)^{1/2}$$

1 [or Eq. (a), Sec. 14–10]; p. 759  
Eq. (14–30); p. 759  
1  
Eq. (14–23); p. 755  
Eq. (14–27); p. 756  
Table below

Gear contact stress equation  
Eq. (14–16)

Eq. (14–13), Table 14–8; pp. 744, 757

Gear contact endurance strength  
Eq. (14–18)

Wear factor of safety  
Eq. (14–42)

0.99( $S_c$ )<sub>10<sup>7</sup></sub> Tables 14–6, 14–7; pp. 751, 752

Fig. 14–15; p. 763

$\sigma_{c,\text{all}} = \frac{S_c Z_N C_H}{S_H K_T K_R}$  Section 14–12, gear only; pp. 761, 762

Table 14–10, Eq. (14–38); pp. 763, 764

1 if  $T < 250^\circ\text{F}$

$$S_H = \frac{S_c Z_N C_H / (K_T K_R)}{\sigma_c}$$

Gear only

Remember to compare  $S_F$  with  $S_H^2$  when deciding whether bending or wear is the threat to function. For crowned gears compare  $S_F$  with  $S_H^3$ .

Table of Overload Factors,  $K_o$

Driven Machine				
Power source	Uniform	Moderate shock	Heavy shock	
Uniform	1.00	1.25	1.75	
Light shock	1.25	1.50	2.00	
Medium shock	1.50	1.75	2.25	

**Figure 14–18**

Roadmap of gear wear equations based on AGMA standards. (ANSI/AGMA 2001-D04.)

**EXAMPLE 14-4**

A 17-tooth  $20^\circ$  pressure angle spur pinion rotates at 1800 rev/min and transmits 4 hp to a 52-tooth disk gear. The diametral pitch is 10 teeth/in, the face width 1.5 in, and the quality standard is No. 6. The gears are straddle-mounted with bearings immediately adjacent. The pinion is a grade 1 steel with a hardness of 240 Brinell tooth surface and through-hardened core. The gear is steel, through-hardened also, grade 1 material, with a Brinell hardness of 200, tooth surface and core. Poisson's ratio is 0.30,  $J_P = 0.30$ ,  $J_G = 0.40$ , and Young's modulus is  $30(10^6)$  psi. The loading is smooth because of motor and load. Assume a pinion life of  $10^8$  cycles and a reliability of 0.90, and use  $Y_N = 1.3558N^{-0.0178}$ ,  $Z_N = 1.4488N^{-0.023}$ . The tooth profile is uncrowned. This is a commercial enclosed gear unit.

- (a) Find the factor of safety of the gears in bending.
- (b) Find the factor of safety of the gears in wear.
- (c) By examining the factors of safety, identify the threat to each gear and to the mesh.

**Solution**

There will be many terms to obtain so use Figs. 14-17 and 14-18 as guides to what is needed.

$$d_P = N_P/P_d = 17/10 = 1.7 \text{ in} \quad d_G = 52/10 = 5.2 \text{ in}$$

$$V = \frac{\pi d_P n_P}{12} = \frac{\pi(1.7)1800}{12} = 801.1 \text{ ft/min}$$

$$W^t = \frac{33\,000 \cdot H}{V} = \frac{33\,000(4)}{801.1} = 164.8 \text{ lbf}$$

Assuming uniform loading,  $K_o = 1$ . To evaluate  $K_v$ , from Eq. (14-28) with a quality number  $Q_v = 6$ ,

$$B = 0.25(12 - 6)^{2/3} = 0.8255$$

$$A = 50 + 56(1 - 0.8255) = 59.77$$

Then from Eq. (14-27) the dynamic factor is

$$K_v = \left( \frac{59.77 + \sqrt{801.1}}{59.77} \right)^{0.8255} = 1.377$$

To determine the size factor,  $K_s$ , the Lewis form factor is needed. From Table 14-2, with  $N_P = 17$  teeth,  $Y_P = 0.303$ . Interpolation for the gear with  $N_G = 52$  teeth yields  $Y_G = 0.412$ . Thus from Eq. (a) of Sec. 14-10, with  $F = 1.5$  in,

$$(K_s)_P = 1.192 \left( \frac{1.5\sqrt{0.303}}{10} \right)^{0.0535} = 1.043$$

$$(K_s)_G = 1.192 \left( \frac{1.5\sqrt{0.412}}{10} \right)^{0.0535} = 1.052$$

The load distribution factor  $K_m$  is determined from Eq. (14–30), where five terms are needed. They are, where  $F = 1.5$  in when needed:

- Uncrowned, Eq. (14–30):  $C_{mc} = 1$ ,
- Eq. (14–32):  $C_{pf} = 1.5/[10(1.7)] - 0.0375 + 0.0125(1.5) = 0.0695$
- Bearings immediately adjacent, Eq. (14–33):  $C_{pm} = 1$
- Commercial enclosed gear units (Fig. 14–11):  $C_{ma} = 0.15$
- Eq. (14–35):  $C_e = 1$

Thus,

$$K_m = 1 + C_{mc}(C_{pf}C_{pm} + C_{ma}C_e) = 1 + (1)[0.0695(1) + 0.15(1)] = 1.22$$

Assuming constant thickness gears, the rim-thickness factor  $K_B = 1$ . The speed ratio is  $m_G = N_G/N_P = 52/17 = 3.059$ . The load cycle factors given in the problem statement, with  $N(\text{pinion}) = 10^8$  cycles and  $N(\text{gear}) = 10^8/m_G = 10^8/3.059$  cycles, are

$$(Y_N)_P = 1.3558(10^8)^{-0.0178} = 0.977$$

$$(Y_N)_G = 1.3558(10^8/3.059)^{-0.0178} = 0.996$$

From Table 14.10, with a reliability of 0.9,  $K_R = 0.85$ . From Fig. 14–18, the temperature and surface condition factors are  $K_T = 1$  and  $C_f = 1$ . From Eq. (14–23), with  $m_N = 1$  for spur gears,

$$I = \frac{\cos 20^\circ \sin 20^\circ}{2} \frac{3.059}{3.059 + 1} = 0.121$$

From Table 14–8,  $C_p = 2300\sqrt{\text{psi}}$ .

Next, we need the terms for the gear endurance strength equations. From Table 14–3, for grade 1 steel with  $H_{BP} = 240$  and  $H_{BG} = 200$ , we use Fig. 14–2, which gives

$$(S_t)_P = 77.3(240) + 12\ 800 = 31\ 350 \text{ psi}$$

$$(S_t)_G = 77.3(200) + 12\ 800 = 28\ 260 \text{ psi}$$

Similarly, from Table 14–6, we use Fig. 14–5, which gives

$$(S_c)_P = 322(240) + 29\ 100 = 106\ 400 \text{ psi}$$

$$(S_c)_G = 322(200) + 29\ 100 = 93\ 500 \text{ psi}$$

From Fig. 14–15,

$$(Z_N)_P = 1.4488(10^8)^{-0.023} = 0.948$$

$$(Z_N)_G = 1.4488(10^8/3.059)^{-0.023} = 0.973$$

For the hardness ratio factor  $C_H$ , the hardness ratio is  $H_{BP}/H_{BG} = 240/200 = 1.2$ . Then, from Sec. 14–12,

$$\begin{aligned} A' &= 8.98(10^{-3})(H_{BP}/H_{BG}) - 8.29(10^{-3}) \\ &= 8.98(10^{-3})(1.2) - 8.29(10^{-3}) = 0.002\ 49 \end{aligned}$$

Thus, from Eq. (14–36),

$$C_H = 1 + 0.002\ 49(3.059 - 1) = 1.005$$

(a) **Pinion tooth bending.** Substituting the appropriate terms for the pinion into Eq. (14–15) gives

$$\begin{aligned} (\sigma)_P &= \left( W^t K_o K_v K_s \frac{P_d}{F} \frac{K_m K_B}{J} \right)_P = 164.8(1)1.377(1.043) \frac{10}{1.5} \frac{1.22(1)}{0.30} \\ &= 6417 \text{ psi} \end{aligned}$$

Substituting the appropriate terms for the pinion into Eq. (14–41) gives

**Answer** 
$$(S_F)_P = \left( \frac{S_t Y_N / (K_T K_R)}{\sigma} \right)_P = \frac{31\ 350(0.977) / [1(0.85)]}{6417} = 5.62$$

**Gear tooth bending.** Substituting the appropriate terms for the gear into Eq. (14–15) gives

$$(\sigma)_G = 164.8(1)1.377(1.052) \frac{10}{1.5} \frac{1.22(1)}{0.40} = 4854 \text{ psi}$$

Substituting the appropriate terms for the gear into Eq. (14–41) gives

**Answer** 
$$(S_F)_G = \frac{28\ 260(0.996) / [1(0.85)]}{4854} = 6.82$$

(b) **Pinion tooth wear.** Substituting the appropriate terms for the pinion into Eq. (14–16) gives

$$\begin{aligned} (\sigma_c)_P &= C_p \left( W^t K_o K_v K_s \frac{K_m}{d_P F} \frac{C_f}{I} \right)_P^{1/2} \\ &= 2300 \left[ 164.8(1)1.377(1.043) \frac{1.22}{1.7(1.5)} \frac{1}{0.121} \right]^{1/2} = 70\ 360 \text{ psi} \end{aligned}$$

Substituting the appropriate terms for the pinion into Eq. (14–42) gives

**Answer** 
$$(S_H)_P = \left[ \frac{S_c Z_N / (K_T K_R)}{\sigma_c} \right]_P = \frac{106\ 400(0.948) / [1(0.85)]}{70\ 360} = 1.69$$

**Gear tooth wear.** The only term in Eq. (14–16) that changes for the gear is  $K_s$ . Thus,

$$(\sigma_c)_G = \left[ \frac{(K_s)_G}{(K_s)_P} \right]^{1/2} (\sigma_c)_P = \left( \frac{1.052}{1.043} \right)^{1/2} 70\ 360 = 70\ 660 \text{ psi}$$

Substituting the appropriate terms for the gear into Eq. (14–42) with  $C_H = 1.005$  gives

**Answer** 
$$(S_H)_G = \frac{93\ 500(0.973)1.005 / [1(0.85)]}{70\ 660} = 1.52$$

(c) For the pinion, we compare  $(S_F)_P$  with  $(S_H)_P^2$ , or 5.73 with  $1.69^2 = 2.86$ , so the threat in the pinion is from wear. For the gear, we compare  $(S_F)_G$  with  $(S_H)_G^2$ , or 6.96 with  $1.52^2 = 2.31$ , so the threat in the gear is also from wear.

There are perspectives to be gained from Ex. 14–4. First, the pinion is overly strong in bending compared to wear. The performance in wear can be improved by surface-hardening techniques, such as flame or induction hardening, nitriding, or carburizing and case hardening, as well as shot peening. This in turn permits the gearset to be made

smaller. Second, in bending, the gear is stronger than the pinion, indicating that both the gear core hardness and tooth size could be reduced; that is, we may increase  $P$  and reduce diameter of the gears, or perhaps allow a cheaper material. Third, in wear, surface strength equations have the ratio  $(Z_N)/K_R$ . The values of  $(Z_N)_P$  and  $(Z_N)_G$  are affected by gear ratio  $m_G$ . The designer can control strength by specifying surface hardness. This point will be elaborated later.

Having followed a spur-gear analysis in detail in Ex. 14–4, it is timely to analyze a helical gearset under similar circumstances to observe similarities and differences.

### EXAMPLE 14–5

A 17-tooth  $20^\circ$  normal pitch-angle helical pinion with a right-hand helix angle of  $30^\circ$  rotates at 1800 rev/min when transmitting 4 hp to a 52-tooth helical gear. The normal diametral pitch is 10 teeth/in, the face width is 1.5 in, and the set has a quality number of 6. The gears are straddle-mounted with bearings immediately adjacent. The pinion and gear are made from a through-hardened steel with surface and core hardesses of 240 Brinell on the pinion and surface and core hardesses of 200 Brinell on the gear. The transmission is smooth, connecting an electric motor and a centrifugal pump. Assume a pinion life of  $10^8$  cycles and a reliability of 0.9 and use the upper curves in Figs. 14–14 and 14–15.

- (a) Find the factors of safety of the gears in bending.
- (b) Find the factors of safety of the gears in wear.
- (c) By examining the factors of safety identify the threat to each gear and to the mesh.

#### Solution

All of the parameters in this example are the same as in Ex. 14–4 with the exception that we are using helical gears. Thus, several terms will be the same as Ex. 14–4. The reader should verify that the following terms remain unchanged:  $K_o = 1$ ,  $Y_P = 0.303$ ,  $Y_G = 0.412$ ,  $m_G = 3.059$ ,  $(K_s)_P = 1.043$ ,  $(K_s)_G = 1.052$ ,  $(Y_N)_P = 0.977$ ,  $(Y_N)_G = 0.996$ ,  $K_R = 0.85$ ,  $K_T = 1$ ,  $C_f = 1$ ,  $C_p = 2300 \sqrt{\text{psi}}$ ,  $(S_t)_P = 31\,350 \text{ psi}$ ,  $(S_t)_G = 28\,260 \text{ psi}$ ,  $(S_c)_P = 106\,380 \text{ psi}$ ,  $(S_c)_G = 93\,500 \text{ psi}$ ,  $(Z_N)_P = 0.948$ ,  $(Z_N)_G = 0.973$ , and  $C_H = 1.005$ .

For helical gears, the transverse diametral pitch, given by Eq. (13–18), is

$$P_t = P_n \cos \psi = 10 \cos 30^\circ = 8.660 \text{ teeth/in}$$

Thus, the pitch diameters are  $d_P = N_P/P_t = 17/8.660 = 1.963 \text{ in}$  and  $d_G = 52/8.660 = 6.005 \text{ in}$ . The pitch-line velocity and transmitted force are

$$V = \frac{\pi d_P n_P}{12} = \frac{\pi(1.963)1800}{12} = 925 \text{ ft/min}$$

$$W^t = \frac{33\,000 H}{V} = \frac{33\,000(4)}{925} = 142.7 \text{ lbf}$$

As in Ex. 14–4, for the dynamic factor,  $B = 0.8255$  and  $A = 59.77$ . Thus, Eq. (14–27) gives

$$K_v = \left( \frac{59.77 + \sqrt{925}}{59.77} \right)^{0.8255} = 1.404$$

The geometry factor  $I$  for helical gears requires a little work. First, the transverse pressure angle is given by Eq. (13–19)

$$\phi_t = \tan^{-1} \left( \frac{\tan \phi_n}{\cos \psi} \right) = \tan^{-1} \left( \frac{\tan 20^\circ}{\cos 30^\circ} \right) = 22.80^\circ$$

The radii of the pinion and gear are  $r_P = 1.963/2 = 0.9815$  in and  $r_G = 6.004/2 = 3.002$  in, respectively. The addendum is  $a = 1/P_n = 1/10 = 0.1$ , and the base-circle radii of the pinion and gear are given by Eq. (13–6) with  $\phi = \phi_t$ :

$$(r_b)_P = r_P \cos \phi_t = 0.9815 \cos 22.80^\circ = 0.9048 \text{ in}$$

$$(r_b)_G = 3.002 \cos 22.80^\circ = 2.767 \text{ in}$$

From Eq. (14–25), the surface strength geometry factor

$$\begin{aligned} Z &= \sqrt{(0.9815 + 0.1)^2 - 0.9048^2} + \sqrt{(3.004 + 0.1)^2 - 2.769^2} \\ &\quad - (0.9815 + 3.004) \sin 22.80^\circ \\ &= 0.5924 + 1.4027 - 1.5444 = 0.4507 \text{ in} \end{aligned}$$

Since the first two terms are less than 1.5444, the equation for  $Z$  stands. From Eq. (14–24) the normal circular pitch  $p_N$  is

$$p_N = p_n \cos \phi_n = \frac{\pi}{P_n} \cos 20^\circ = \frac{\pi}{10} \cos 20^\circ = 0.2952 \text{ in}$$

From Eq. (14–21), the load sharing ratio

$$m_N = \frac{p_N}{0.95Z} = \frac{0.2952}{0.95(0.4507)} = 0.6895$$

Substituting in Eq. (14–23), the geometry factor  $I$  is

$$I = \frac{\sin 22.80^\circ \cos 22.80^\circ}{2(0.6895)} \frac{3.06}{3.06 + 1} = 0.195$$

From Fig. 14–7, geometry factors  $J'_P = 0.45$  and  $J'_G = 0.54$ . Also from Fig. 14–8 the  $J$ -factor multipliers are 0.94 and 0.98, correcting  $J'_P$  and  $J'_G$  to

$$J_P = 0.45(0.94) = 0.423$$

$$J_G = 0.54(0.98) = 0.529$$

The load-distribution factor  $K_m$  is estimated from Eq. (14–32):

$$C_{pf} = \frac{1.5}{10(1.963)} - 0.0375 + 0.0125(1.5) = 0.0577$$

with  $C_{mc} = 1$ ,  $C_{pm} = 1$ ,  $C_{ma} = 0.15$  from Fig. 14–11, and  $C_e = 1$ . Therefore, from Eq. (14–30),

$$K_m = 1 + (1)[0.0577(1) + 0.15(1)] = 1.208$$

(a) **Pinion tooth bending.** Substituting the appropriate terms into Eq. (14–15) using  $P_t$  gives

$$\begin{aligned} (\sigma)_P &= \left( W' K_o K_v K_s \frac{P_t}{F} \frac{K_m K_B}{J} \right)_P = 142.7(1)1.404(1.043) \frac{8.66}{1.5} \frac{1.208(1)}{0.423} \\ &= 3445 \text{ psi} \end{aligned}$$

Substituting the appropriate terms for the pinion into Eq. (14–41) gives

$$\text{Answer} \quad (S_F)_P = \left( \frac{S_t Y_N / (K_T K_R)}{\sigma} \right)_P = \frac{31\,350(0.977)/[1(0.85)]}{3445} = 10.5$$

**Gear tooth bending.** Substituting the appropriate terms for the gear into Eq. (14–15) gives

$$(\sigma)_G = 142.7(1)1.404(1.052) \frac{8.66}{1.5} \frac{1.208(1)}{0.529} = 2779 \text{ psi}$$

Substituting the appropriate terms for the gear into Eq. (14–41) gives

$$\text{Answer} \quad (S_F)_G = \frac{28\,260(0.996)/[1(0.85)]}{2779} = 11.9$$

(b) **Pinion tooth wear.** Substituting the appropriate terms for the pinion into Eq. (14–16) gives

$$\begin{aligned} (\sigma_c)_P &= C_p \left( W^t K_o K_v K_s \frac{K_m}{d_P F} \frac{C_f}{I} \right)_P^{1/2} \\ &= 2300 \left[ 142.7(1)1.404(1.043) \frac{1.208}{1.963(1.5)} \frac{1}{0.195} \right]^{1/2} = 48\,230 \text{ psi} \end{aligned}$$

Substituting the appropriate terms for the pinion into Eq. (14–42) gives

$$\text{Answer} \quad (S_H)_P = \left( \frac{S_c Z_N / (K_T K_R)}{\sigma_c} \right)_P = \frac{106\,400(0.948)/[1(0.85)]}{48\,230} = 2.46$$

**Gear tooth wear.** The only term in Eq. (14–16) that changes for the gear is  $K_s$ . Thus,

$$(\sigma_c)_G = \left[ \frac{(K_s)_G}{(K_s)_P} \right]^{1/2} (\sigma_c)_P = \left( \frac{1.052}{1.043} \right)^{1/2} 48\,230 = 48\,440 \text{ psi}$$

Substituting the appropriate terms for the gear into Eq. (14–42) with  $C_H = 1.005$  gives

$$\text{Answer} \quad (S_H)_G = \frac{93\,500(0.973)1.005/[1(0.85)]}{48\,440} = 2.22$$

(c) For the pinion we compare  $S_F$  with  $S_H^2$ , or 10.5 with  $2.46^2 = 6.05$ , so the threat in the pinion is from wear. For the gear we compare  $S_F$  with  $S_H^2$ , or 11.9 with  $2.22^2 = 4.93$ , so the threat is also from wear in the gear. For the meshing gearset wear controls.

It is worthwhile to compare Ex. 14–4 with Ex. 14–5. The spur and helical gearsets were placed in nearly identical circumstances. The helical gear teeth are of greater length because of the helix and identical face widths. The pitch diameters of the helical gears are larger. The  $J$  factors and the  $I$  factor are larger, thereby reducing stresses. The result is larger factors of safety. In the design phase the gearsets in Ex. 14–4 and Ex. 14–5 can be made smaller with control of materials and relative hardnesses.

Now that examples have given the AGMA parameters substance, it is time to examine some desirable (and necessary) relationships between material properties of spur gears in mesh. In bending, the AGMA equations are displayed side by side:

$$\sigma_P = \left( W^t K_o K_v K_s \frac{P_d}{F} \frac{K_m K_B}{J} \right)_P \quad \sigma_G = \left( W^t K_o K_v K_s \frac{P_d}{F} \frac{K_m K_B}{J} \right)_G$$

$$(S_F)_P = \left( \frac{S_t Y_N / (K_T K_R)}{\sigma} \right)_P \quad (S_F)_G = \left( \frac{S_t Y_N / (K_T K_R)}{\sigma} \right)_G$$

Equating the factors of safety, substituting for stress and strength, canceling identical terms ( $K_s$  virtually equal or exactly equal), and solving for  $(S_t)_G$  gives

$$(S_t)_G = (S_t)_P \frac{(Y_N)_P}{(Y_N)_G} \frac{J_P}{J_G} \quad (a)$$

The stress-cycle factor  $Y_N$  comes from Fig. 14–14, where for a particular hardness,  $Y_N = \alpha N^\beta$ . For the pinion,  $(Y_N)_P = \alpha N_P^\beta$ , and for the gear,  $(Y_N)_G = \alpha (N_P/m_G)^\beta$ . Substituting these into Eq. (a) and simplifying gives

$$(S_t)_G = (S_t)_P m_G^\beta \frac{J_P}{J_G} \quad (14-44)$$

Normally,  $m_G > 1$  and  $J_G > J_P$ , so equation (14–44) shows that the gear can be less strong (lower Brinell hardness) than the pinion for the same safety factor.

### EXAMPLE 14–6

In a set of spur gears, a 300-Brinell 18-tooth 16-pitch  $20^\circ$  full-depth pinion meshes with a 64-tooth gear. Both gear and pinion are of grade 1 through-hardened steel. Using  $\beta = -0.023$ , what hardness can the gear have for the same factor of safety?

#### Solution

For through-hardened grade 1 steel the pinion strength  $(S_t)_P$  is given in Fig. 14–2:

$$(S_t)_P = 77.3(300) + 12\,800 = 35\,990 \text{ psi}$$

From Fig. 14–6 the form factors are  $J_P = 0.32$  and  $J_G = 0.41$ . Equation (14–44) gives

$$(S_t)_G = 35\,990 \left( \frac{64}{18} \right)^{-0.023} \frac{0.32}{0.41} = 27\,280 \text{ psi}$$

Use the equation in Fig. 14–2 again.

#### Answer

$$(H_B)_G = \frac{27\,280 - 12\,800}{77.3} = 187 \text{ Brinell}$$

The AGMA contact-stress equations also are displayed side by side:

$$(\sigma_c)_P = C_p \left( W^t K_o K_v K_s \frac{K_m}{d_P F} \frac{C_f}{I} \right)_P^{1/2} \quad (\sigma_c)_G = C_p \left( W^t K_o K_v K_s \frac{K_m}{d_P F} \frac{C_f}{I} \right)_G^{1/2}$$

$$(S_H)_P = \left( \frac{S_c Z_N / (K_T K_R)}{\sigma_c} \right)_P \quad (S_H)_G = \left( \frac{S_c Z_N C_H / (K_T K_R)}{\sigma_c} \right)_G$$

Equating the factors of safety, substituting the stress relations, and canceling identical terms including  $K_s$  gives, after solving for  $(S_c)_G$ ,

$$(S_c)_G = (S_c)_P \frac{(Z_N)_P}{(Z_N)_G} \left( \frac{1}{C_H} \right)_G = (S_c)_P m_G^\beta \left( \frac{1}{C_H} \right)_G$$

where, as in the development of Eq. (14–44),  $(Z_N)_P/(Z_N)_G = m_G^\beta$  and the value of  $\beta$  for wear comes from Fig. 14–15. Since  $C_H$  is so close to unity, it is usually neglected; therefore

$$(S_c)_G = (S_c)_P m_G^\beta \quad (14-45)$$

### EXAMPLE 14-7

For  $\beta = -0.056$  for a through-hardened steel, grade 1, continue Ex. 14–6 for wear.

#### Solution

From Fig. 14–5,

$$(S_c)_P = 322(300) + 29\,100 = 125\,700 \text{ psi}$$

From Eq. (14–45),

$$(S_c)_G = (S_c)_P \left( \frac{64}{18} \right)^{-0.056} = 125\,700 \left( \frac{64}{18} \right)^{-0.056} = 117\,100 \text{ psi}$$

#### Answer

$$(H_B)_G = \frac{117\,100 - 29\,200}{322} = 273 \text{ Brinell}$$

which is slightly less than the pinion hardness of 300 Brinell.

Equations (14–44) and (14–45) apply as well to helical gears.

## 14-19

### Design of a Gear Mesh

A useful decision set for spur and helical gears includes

- Function: load, speed, reliability, life,  $K_o$
- Unquantifiable risk: design factor  $n_d$
- Tooth system:  $\phi$ ,  $\psi$ , addendum, dedendum, root fillet radius
- Gear ratio  $m_G$ ,  $N_p$ ,  $N_G$
- Quality number  $Q_v$
- Diametral pitch  $P_d$
- Face width  $F$
- Pinion material, core hardness, case hardness
- Gear material, core hardness, case hardness

} a priori decisions  
} design decisions

The first item to notice is the dimensionality of the decision set. There are four design decision categories, eight different decisions if you count them separately. This is a larger number than we have encountered before. It is important to use a design strategy that is convenient in either longhand execution or computer implementation. The design decisions

have been placed in order of importance (impact on the amount of work to be redone in iterations). The steps, after the a priori decisions have been made are

- Choose a diametral pitch.
- Examine implications on face width, pitch diameters, and material properties. If not satisfactory, return to pitch decision for change.
- Choose a pinion material and examine core and case hardness requirements. If not satisfactory, return to pitch decision and iterate until no decisions are changed.
- Choose a gear material and examine core and case hardness requirements. If not satisfactory, return to pitch decision and iterate until no decisions are changed.

With these plan steps in mind, we can consider them in more detail.

First select a trial diametral pitch.

*Pinion bending:*

- Select a median face width for this pitch,  $4\pi/P$
- Find the range of necessary ultimate strengths
- Choose a material and a core hardness
- Find face width to meet factor of safety in bending
- Choose face width
- Check factor of safety in bending

*Gear bending:*

- Find necessary companion core hardness
- Choose a material and core hardness
- Check factor of safety in bending

*Pinion wear:*

- Find necessary  $S_c$  and attendant case hardness
- Choose a case hardness
- Check factor of safety in wear

*Gear wear:*

- Find companion case hardness
- Choose a case hardness
- Check factor of safety in wear

Completing this set of steps will yield a satisfactory design. Additional designs with diametral pitches adjacent to the first satisfactory design will produce several among which to choose. A figure of merit is necessary in order to choose the best. Unfortunately, a figure of merit in gear design is complex in an academic environment because material and processing cost vary. The possibility of using a process depends on the manufacturing facility if gears are made in house.

After examining Ex. 14–4 and Ex. 14–5 and seeing the wide range of factors of safety, one might entertain the notion of setting all factors of safety equal.<sup>9</sup> In steel

---

<sup>9</sup>In designing gears it makes sense to define the factor of safety in wear as  $(S)^2_H$  for uncrowned teeth, so that there is no mix-up. ANSI, in the preface to ANSI/AGMA 2001-D04 and 2101-D04, states “the use is completely voluntary... does not preclude anyone from using... procedures... not conforming to the standards.”

gears, wear is usually controlling and  $(S_H)_P$  and  $(S_H)_G$  can be brought close to equality. The use of softer cores can bring down  $(S_F)_P$  and  $(S_F)_G$ , but there is value in keeping them higher. A tooth broken by bending fatigue not only can destroy the gear set, but can bend shafts, damage bearings, and produce inertial stresses up- and downstream in the power train, causing damage elsewhere if the gear box locks.

### EXAMPLE 14-8

Design a 4:1 spur-gear reduction for a 100-hp, three-phase squirrel-cage induction motor running at 1120 rev/min. The load is smooth, providing a reliability of 0.95 at  $10^9$  revolutions of the pinion. Gearing space is meager. Use Nitralloy 135M, grade 1 material to keep the gear size small. The gears are heat-treated first then nitrided.

#### Solution

Make the a priori decisions:

- Function: 100 hp, 1120 rev/min,  $R = 0.95$ ,  $N = 10^9$  cycles,  $K_o = 1$
- Design factor for unquantifiable exigencies:  $n_d = 2$
- Tooth system:  $\phi_n = 20^\circ$
- Tooth count:  $N_P = 18$  teeth,  $N_G = 72$  teeth (no interference)
- Quality number:  $Q_v = 6$ , use grade 1 material
- Assume  $m_B \geq 1.2$  in Eq. (14-40),  $K_B = 1$

*Pitch:* Select a trial diametral pitch of  $P_d = 4$  teeth/in. Thus,  $d_P = 18/4 = 4.5$  in and  $d_G = 72/4 = 18$  in. From Table 14-2,  $Y_P = 0.309$ ,  $Y_G = 0.4324$  (interpolated). From Fig. 14-6,  $J_P = 0.32$ ,  $J_G = 0.415$ .

$$V = \frac{\pi d_P n_P}{12} = \frac{\pi(4.5)1120}{12} = 1319 \text{ ft/min}$$

$$W^t = \frac{33\,000H}{V} = \frac{33\,000(100)}{1319} = 2502 \text{ lbf}$$

From Eqs. (14-28) and (14-27),

$$B = 0.25(12 - Q_v)^{2/3} = 0.25(12 - 6)^{2/3} = 0.8255$$

$$A = 50 + 56(1 - 0.8255) = 59.77$$

$$K_v = \left( \frac{59.77 + \sqrt{1319}}{59.77} \right)^{0.8255} = 1.480$$

From Eq. (14-38),  $K_R = 0.658 - 0.0759 \ln(1 - 0.95) = 0.885$ . From Fig. 14-14,

$$(Y_N)_P = 1.3558(10^9)^{-0.0178} = 0.938$$

$$(Y_N)_G = 1.3558(10^9/4)^{-0.0178} = 0.961$$

From Fig. 14-15,

$$(Z_N)_P = 1.4488(10^9)^{-0.023} = 0.900$$

$$(Z_N)_G = 1.4488(10^9/4)^{-0.023} = 0.929$$

From the recommendation after Eq. (14–8),  $3p \leq F \leq 5p$ . Try  $F = 4p = 4\pi/P = 4\pi/4 = 3.14$  in. From Eq. (a), Sec. 14–10,

$$K_s = 1.192 \left( \frac{F\sqrt{Y}}{P} \right)^{0.0535} = 1.192 \left( \frac{3.14\sqrt{0.309}}{4} \right)^{0.0535} = 1.140$$

From Eqs. (14–31), (14–33) and (14–35),  $C_{mc} = C_{pm} = C_e = 1$ . From Fig. 14–11,  $C_{ma} = 0.175$  for commercial enclosed gear units. From Eq. (14–32),  $F/(10d_P) = 3.14/[10(4.5)] = 0.0698$ . Thus,

$$C_{pf} = 0.0698 - 0.0375 + 0.0125(3.14) = 0.0715$$

From Eq. (14–30),

$$K_m = 1 + (1)[0.0715(1) + 0.175(1)] = 1.247$$

From Table 14–8, for steel gears,  $C_p = 2300\sqrt{\text{psi}}$ . From Eq. (14–23), with  $m_G = 4$  and  $m_N = 1$ ,

$$I = \frac{\cos 20^\circ \sin 20^\circ}{2} \frac{4}{4+1} = 0.1286$$

**Pinion tooth bending.** With the above estimates of  $K_s$  and  $K_m$  from the trial diametral pitch, we check to see if the mesh width  $F$  is controlled by bending or wear considerations. Equating Eqs. (14–15) and (14–17), substituting  $n_d W^t$  for  $W^t$ , and solving for the face width  $(F)_{\text{bend}}$  necessary to resist bending fatigue, we obtain

$$(F)_{\text{bend}} = n_d W^t K_o K_v K_s P_d \frac{K_m K_B}{J_P} \frac{K_T K_R}{S_t Y_N} \quad (1)$$

Equating Eqs. (14–16) and (14–18), substituting  $n_d W^t$  for  $W^t$ , and solving for the face width  $(F)_{\text{wear}}$  necessary to resist wear fatigue, we obtain

$$(F)_{\text{wear}} = \left( \frac{C_p Z_N}{S_c K_T K_R} \right)^2 n_d W^t K_o K_v K_s \frac{K_m C_f}{d_P I} \quad (2)$$

From Table 14–5 the hardness range of Nitr alloy 135M is Rockwell C32–36 (302–335 Brinell). Choosing a midrange hardness as attainable, using 320 Brinell. From Fig. 14–4,

$$S_t = 86.2(320) + 12\ 730 = 40\ 310 \text{ psi}$$

Inserting the numerical value of  $S_t$  in Eq. (1) to estimate the face width gives

$$(F)_{\text{bend}} = 2(2502)(1)1.48(1.14)4 \frac{1.247(1)(1)0.885}{0.32(40\ 310)0.938} = 3.08 \text{ in}$$

From Table 14–6 for Nitr alloy 135M,  $S_c = 170\ 000$  psi. Inserting this in Eq. (2), we find

$$(F)_{\text{wear}} = \left( \frac{2300(0.900)}{170\ 000(1)0.885} \right)^2 2(2502)1(1.48)1.14 \frac{1.247(1)}{4.5(0.1286)} = 3.44 \text{ in}$$

**Decision** Make face width 3.50 in. Correct  $K_s$  and  $K_m$ :

$$K_s = 1.192 \left( \frac{3.50\sqrt{0.309}}{4} \right)^{0.0535} = 1.147$$

$$\frac{F}{10d_P} = \frac{3.50}{10(4.5)} = 0.0778$$

$$C_{pf} = 0.0778 - 0.0375 + 0.0125(3.50) = 0.0841$$

$$K_m = 1 + (1)[0.0841(1) + 0.175(1)] = 1.259$$

The bending stress induced by  $W^t$  in bending, from Eq. (14–15), is

$$(\sigma)_P = 2502(1)1.48(1.147) \frac{4}{3.50} \frac{1.259(1)}{0.32} = 19\ 100 \text{ psi}$$

The AGMA factor of safety in bending of the pinion, from Eq. (14–41), is

$$(S_F)_P = \frac{40\ 310(0.938)/[1(0.885)]}{19\ 100} = 2.24$$

**Decision**

**Gear tooth bending.** Use cast gear blank because of the 18-in pitch diameter. Use the same material, heat treatment, and nitriding. The load-induced bending stress is in the ratio of  $J_P/J_G$ . Then

$$(\sigma)_G = 19\ 100 \frac{0.32}{0.415} = 14\ 730 \text{ psi}$$

The factor of safety of the gear in bending is

$$(S_F)_G = \frac{40\ 310(0.961)/[1(0.885)]}{14\ 730} = 2.97$$

**Pinion tooth wear.** The contact stress, given by Eq. (14–16), is

$$(\sigma_c)_P = 2300 \left[ 2502(1)1.48(1.147) \frac{1.259}{4.5(3.5)} \frac{1}{0.129} \right]^{1/2} = 118\ 000 \text{ psi}$$

The factor of safety from Eq. (14–42), is

$$(S_H)_P = \frac{170\ 000(0.900)/[1(0.885)]}{118\ 000} = 1.465$$

By our definition of factor of safety, pinion bending is  $(S_F)_P = 2.24$ , and wear is  $(S_H)_P^2 = (1.465)^2 = 2.15$ .

**Gear tooth wear.** The hardness of the gear and pinion are the same. Thus, from Fig. 14–12,  $C_H = 1$ , the contact stress on the gear is the same as the pinion,  $(\sigma_c)_G = 118\ 000 \text{ psi}$ . The wear strength is also the same,  $S_c = 170\ 000 \text{ psi}$ . The factor of safety of the gear in wear is

$$(S_H)_G = \frac{170\ 000(0.929)/[1(0.885)]}{118\ 000} = 1.51$$

So, for the gear in bending,  $(S_F)_G = 2.97$ , and wear  $(S_H)_G^2 = (1.51)^2 = 2.29$ .

**Rim.** Keep  $m_B \geq 1.2$ . The whole depth is  $h_t = \text{addendum} + \text{dedendum} = 1/P_d + 1.25/P_d = 2.25/P_d = 2.25/4 = 0.5625$  in. The rim thickness  $t_R$  is

$$t_R \geq m_B h_t = 1.2(0.5625) = 0.675 \text{ in}$$

In the design of the gear blank, be sure the rim thickness exceeds 0.675 in; if it does not, review and modify this mesh design.

This design example showed a satisfactory design for a four-pitch spur-gear mesh. Material could be changed, as could pitch. There are a number of other satisfactory designs, thus a figure of merit is needed to identify the best.

One can appreciate that gear design was one of the early applications of the digital computer to mechanical engineering. A design program should be interactive, presenting results of calculations, pausing for a decision by the designer, and showing the consequences of the decision, with a loop back to change a decision for the better. The program can be structured in totem-pole fashion, with the most influential decision at the top, then tumbling down, decision after decision, ending with the ability to change the current decision or to begin again. Such a program would make a fine class project. Troubleshooting the coding will reinforce your knowledge, adding flexibility as well as bells and whistles in subsequent terms.

Standard gears may not be the most economical design that meets the functional requirements, because no application is standard in all respects.<sup>10</sup> Methods of designing custom gears are well understood and frequently used in mobile equipment to provide good weight-to-performance index. The required calculations including optimizations are within the capability of a personal computer.

## PROBLEMS

Problems marked with an asterisk (\*) are linked to problems in other chapters, as summarized in Table 1–1 of Sec. 1–16, p. 24.

Because gearing problems can be difficult, the problems are presented by section.

### Section 14-1

- 14-1** A steel spur pinion has a pitch of 6 teeth/in, 22 full-depth teeth, and a  $20^\circ$  pressure angle. The pinion runs at a speed of 1200 rev/min and transmits 15 hp to a 60-tooth gear. If the face width is 2 in, estimate the bending stress.
- 14-2** A steel spur pinion has a diametral pitch of 10 teeth/in, 18 teeth cut full-depth with a  $20^\circ$  pressure angle, and a face width of 1 in. This pinion is expected to transmit 2 hp at a speed of 600 rev/min. Determine the bending stress.
- 14-3** A steel spur pinion has a module of 1.25 mm, 18 teeth cut on the  $20^\circ$  full-depth system, and a face width of 12 mm. At a speed of 1800 rev/min, this pinion is expected to carry a steady load of 0.5 kW. Determine the resulting bending stress.
- 14-4** A steel spur pinion has 16 teeth cut on the  $20^\circ$  full-depth system with a module of 8 mm and a face width of 90 mm. The pinion rotates at 150 rev/min and transmits 6 kW to the mating steel gear. What is the resulting bending stress?

---

<sup>10</sup>See H. W. Van Gerpen, C. K. Reece, and J. K. Jensen, *Computer Aided Design of Custom Gears*, Van Gerpen-Reece Engineering, Cedar Falls, Iowa, 1996.

- 14-5** A steel spur pinion has a module of 1 mm and 16 teeth cut on the  $20^\circ$  full-depth system and is to carry 0.15 kW at 400 rev/min. Determine a suitable face width based on an allowable bending stress of 150 MPa.
- 14-6** A  $20^\circ$  full-depth steel spur pinion has 20 teeth and a module of 2 mm and is to transmit 0.5 kW at a speed of 200 rev/min. Find an appropriate face width if the bending stress is not to exceed 75 MPa.
- 14-7** A  $20^\circ$  full-depth steel spur pinion has a diametral pitch of 5 teeth/in and 24 teeth and transmits 6 hp at a speed of 50 rev/min. Find an appropriate face width if the allowable bending stress is 20 kpsi.
- 14-8** A steel spur pinion is to transmit 20 hp at a speed of 400 rev/min. The pinion is cut on the  $20^\circ$  full-depth system and has a diametral pitch of 4 teeth/in and 16 teeth. Find a suitable face width based on an allowable stress of 12 kpsi.
- 14-9** A  $20^\circ$  full-depth steel spur pinion with 18 teeth is to transmit 2.5 hp at a speed of 600 rev/min. Determine appropriate values for the face width and diametral pitch based on an allowable bending stress of 10 kpsi.
- 14-10** A  $20^\circ$  full-depth steel spur pinion is to transmit 1.5 kW hp at a speed of 900 rev/min. If the pinion has 18 teeth, determine suitable values for the module and face width. The bending stress should not exceed 75 MPa.

### Section 14-2

- 14-11** A speed reducer has  $20^\circ$  full-depth teeth and consists of a 20-tooth steel spur pinion driving a 50-tooth cast-iron gear. The horsepower transmitted is 12 at a pinion speed of 1200 rev/min. For a diametral pitch of 8 teeth/in and a face width of 1.5 in, find the contact stress.
- 14-12** A gear drive consists of a 16-tooth  $20^\circ$  steel spur pinion and a 48-tooth cast-iron gear having a pitch of 12 teeth/in. For a power input of 1.5 hp at a pinion speed of 700 rev/min, select a face width based on an allowable contact stress of 100 kpsi.
- 14-13** A gearset has a module of 5 mm, a  $20^\circ$  pressure angle, and a 24-tooth cast-iron spur pinion driving a 48-tooth cast-iron gear. The pinion is to rotate at 50 rev/min. What horsepower input can be used with this gearset if the contact stress is limited to 690 MPa and  $F = 60$  mm?
- 14-14** A  $20^\circ$  20-tooth cast-iron spur pinion having a module of 4 mm drives a 32-tooth cast-iron gear. Find the contact stress if the pinion speed is 1000 rev/min, the face width is 50 mm, and 10 kW of power is transmitted.
- 14-15** A steel spur pinion and gear have a diametral pitch of 12 teeth/in, milled teeth, 17 and 30 teeth, respectively, a  $20^\circ$  pressure angle, and a pinion speed of 525 rev/min. The tooth properties are  $S_{ut} = 76$  kpsi,  $S_y = 42$  kpsi and the Brinell hardness is 149. For a design factor of 2.25, a face width of  $\frac{7}{8}$  in, what is the power rating of the gearset?
- 14-16** A milled-teeth steel pinion and gear pair have  $S_{ut} = 113$  kpsi,  $S_y = 86$  kpsi and a hardness at the involute surface of 262 Brinell. The diametral pitch is 3 teeth/in, the face width is 2.5 in, and the pinion speed is 870 rev/min. The tooth counts are 20 and 100. For a design factor of 1.5, rate the gearset for power considering both bending and wear.
- 14-17** A  $20^\circ$  full-depth steel spur pinion rotates at 1145 rev/min. It has a module of 6 mm, a face width of 75 mm, and 16 milled teeth. The ultimate tensile strength at the involute is 900 MPa exhibiting a Brinell hardness of 260. The gear is steel with 30 teeth and has identical material strengths. For a design factor of 1.3 find the power rating of the gearset based on the pinion and the gear resisting bending and wear fatigue.

**14-18**

A steel spur pinion has a pitch of 6 teeth/in, 17 full-depth milled teeth, and a pressure angle of  $20^\circ$ . The pinion has an ultimate tensile strength at the involute surface of 116 kpsi, a Brinell hardness of 232, and a yield strength of 90 kpsi. Its shaft speed is 1120 rev/min, its face width is 2 in, and its mating gear has 51 teeth. Rate the pinion for power transmission if the design factor is 2.

- (a) Pinion bending fatigue imposes what power limitation?
- (b) Pinion surface fatigue imposes what power limitation? The gear has identical strengths to the pinion with regard to material properties.
- (c) Consider power limitations due to gear bending and wear.
- (d) Rate the gearset.

**Section 14-3 to 14-19****14-19**

A commercial enclosed gear drive consists of a  $20^\circ$  spur pinion having 16 teeth driving a 48-tooth gear. The pinion speed is 300 rev/min, the face width 2 in, and the diametral pitch 6 teeth/in. The gears are grade 1 steel, through-hardened at 200 Brinell, made to No. 6 quality standards, uncrowned, and are to be accurately and rigidly mounted. Assume a pinion life of  $10^8$  cycles and a reliability of 0.90. Determine the AGMA bending and contact stresses and the corresponding factors of safety if 5 hp is to be transmitted.

**14-20**

A  $20^\circ$  spur pinion with 20 teeth and a module of 2.5 mm transmits 120 W to a 36-tooth gear. The pinion speed is 100 rev/min, and the gears are grade 1, 18-mm face width, through-hardened steel at 200 Brinell, uncrowned, manufactured to a No. 6 quality standard, and considered to be of open gearing quality installation. Find the AGMA bending and contact stresses and the corresponding factors of safety for a pinion life of  $10^8$  cycles and a reliability of 0.95.

**14-21**

Repeat Prob. 14-19 using helical gears each with a  $20^\circ$  normal pitch angle and a helix angle of  $30^\circ$  and a normal diametral pitch of 6 teeth/in.

**14-22**

A spur gearset has 17 teeth on the pinion and 51 teeth on the gear. The pressure angle is  $20^\circ$  and the overload factor  $K_o = 1$ . The diametral pitch is 6 teeth/in and the face width is 2 in. The pinion speed is 1120 rev/min and its cycle life is to be  $10^8$  revolutions at a reliability  $R = 0.99$ . The quality number is 5. The material is a through-hardened steel, grade 1, with Brinell hardnesses of 232 core and case of both gears. For a design factor of 2, rate the gearset for these conditions using the AGMA method.

**14-23**

In Sec. 14-10, Eq. (a) is given for  $K_s$  based on the procedure in Ex. 14-2. Derive this equation.

**14-24**

A speed-reducer has  $20^\circ$  full-depth teeth, and the single-reduction spur-gear gearset has 22 and 60 teeth. The diametral pitch is 4 teeth/in and the face width is  $3\frac{1}{4}$  in. The pinion shaft speed is 1145 rev/min. The life goal of 5-year 24-hour-per-day service is about  $3(10^9)$  pinion revolutions. The absolute value of the pitch variation is such that the transmission accuracy level number is 6. The materials are 4340 through-hardened grade 1 steels, heat-treated to 250 Brinell, core and case, both gears. The load is moderate shock and the power is smooth. For a reliability of 0.99, rate the speed reducer for power.

**14-25**

The speed reducer of Prob. 14-24 is to be used for an application requiring 40 hp at 1145 rev/min. Estimate the stresses of pinion bending, gear bending, pinion wear, and gear wear and the attendant AGMA factors of safety  $(S_F)_P$ ,  $(S_F)_G$ ,  $(S_H)_P$ , and  $(S_H)_G$ . For the reducer, what is the factor of safety for unquantifiable exigencies in  $W'$ ? What mode of failure is the most threatening?

**14-26**

The gearset of Prob. 14-24 needs improvement of wear capacity. Toward this end the gears are nitrided so that the grade 1 materials have hardnesses as follows: The pinion core is 250 and the

pinion case hardness is 390 Brinell, and the gear core hardness is 250 core and 390 case. Estimate the power rating for the new gearset.

- 14-27** The gearset of Prob. 14-24 has had its gear specification changed to 9310 for carburizing and surface hardening with the result that the pinion Brinell hardnesses are 285 core and 580–600 case, and the gear hardnesses are 285 core and 580–600 case. Estimate the power rating for the new gearset.
- 14-28** The gearset of Prob. 14-27 is going to be upgraded in material to a quality of grade 2 (9310) steel. Estimate the power rating for the new gearset.
- 14-29** Matters of scale always improve insight and perspective. Reduce the physical size of the gearset in Prob. 14-24 by one-half and note the result on the estimates of transmitted load  $W^t$  and power.
- 14-30** AGMA procedures with cast-iron gear pairs differ from those with steels because life predictions are difficult; consequently  $(Y_N)_P$ ,  $(Y_N)_G$ ,  $(Z_N)_P$ , and  $(Z_N)_G$  are set to unity. The consequence of this is that the fatigue strengths of the pinion and gear materials are the same. The reliability is 0.99 and the life is  $10^7$  revolution of the pinion ( $K_R = 1$ ). For longer lives the reducer is derated in power. For the pinion and gear set of Prob. 14-24, use grade 40 cast iron for both gears ( $H_B = 201$  Brinell). Rate the reducer for power with  $S_F$  and  $S_H$  equal to unity.
- 14-31** Spur-gear teeth have rolling and slipping contact (often about 8 percent slip). Spur gears tested to wear failure are reported at  $10^8$  cycles as Buckingham's surface fatigue load-stress factor  $K$ . This factor is related to Hertzian contact strength  $S_C$  by
- $$S_C = \sqrt{\frac{1.4K}{(1/E_1 + 1/E_2) \sin \phi}}$$
- where  $\phi$  is the normal pressure angle. Cast iron grade 20 gears with  $\phi = 14\frac{1}{2}^\circ$  and  $20^\circ$  pressure angle exhibit a minimum  $K$  of 81 and 112 psi, respectively. How does this compare with  $S_C = 0.32H_B$  ksi?
- 14-32** You've probably noticed that although the AGMA method is based on two equations, the details of assembling all the factors is computationally intensive. To reduce error and omissions, a computer program would be useful. Write a program to perform a power rating of an existing gearset, then use Prob. 14-24, 14-26, 14-27, 14-28, and 14-29 to test your program by comparing the results to your longhand solutions.
- 14-33** In Ex. 14-5 use nitrided grade 1 steel (4140) which produces Brinell hardnesses of 250 core and 500 at the surface (case). Use the upper fatigue curves on Figs. 14-14 and 14-15. Estimate the power capacity of the mesh with factors of safety of  $S_F = S_H = 1$ .
- 14-34** In Ex. 14-5 use carburized and case-hardened gears of grade 1. Carburizing and case-hardening can produce a 550 Brinell case. The core hardnesses are 200 Brinell. Estimate the power capacity of the mesh with factors of safety of  $S_F = S_H = 1$ , using the lower fatigue curves in Figs. 14-14 and 14-15.
- 14-35** In Ex. 14-5, use carburized and case-hardened gears of grade 2 steel. The core hardnesses are 200, and surface hardnesses are 600 Brinell. Use the lower fatigue curves of Figs. 14-14 and 14-15. Estimate the power capacity of the mesh using  $S_F = S_H = 1$ . Compare the power capacity with the results of Prob. 14-34.
- 14-36\*** The countershaft in Prob. 3-72, p. 138, is part of a speed reducing compound gear train using 20° spur gears. A gear on the input shaft drives gear A. Gear B drives a gear on the output shaft. The input shaft runs at 2400 rev/min. Each gear reduces the speed (and thus increases the torque) by

a 2 to 1 ratio. All gears are to be of the same material. Since gear *B* is the smallest gear, transmitting the largest load, it will likely be critical, so a preliminary analysis is to be performed on it. Use a diametral pitch of 2 teeth/in, a face-width of 4 times the circular pitch, a Grade 2 steel through-hardened to a Brinell hardness of 300, and a desired life of 15 kh with a 95 percent reliability. Determine factors of safety for bending and wear.

**14-37\***

The countershaft in Prob. 3-73, p. 138, is part of a speed reducing compound gear train using 20° spur gears. A gear on the input shaft drives gear *A* with a 2 to 1 speed reduction. Gear *B* drives a gear on the output shaft with a 5 to 1 speed reduction. The input shaft runs at 1800 rev/min. All gears are to be of the same material. Since gear *B* is the smallest gear, transmitting the largest load, it will likely be critical, so a preliminary analysis is to be performed on it. Use a module of 18.75 mm/tooth, a face-width of 4 times the circular pitch, a Grade 2 steel through-hardened to a Brinell hardness of 300, and a desired life of 12 kh with a 98 percent reliability. Determine factors of safety for bending and wear.

**14-38\***

Build on the results of Prob. 13-40, p. 728, to find factors of safety for bending and wear for gear *F*. Both gears are made from Grade 2 carburized and hardened steel. Use a face-width of 4 times the circular pitch. The desired life is 12 kh with a 95 percent reliability.

**14-39\***

Build on the results of Prob. 13-41, p. 729, to find factors of safety for bending and wear for gear *C*. Both gears are made from Grade 2 carburized and hardened steel. Use a face-width of 4 times the circular pitch. The desired life is 14 kh with a 98 percent reliability.

# 15

## Bevel and Worm Gears

### Chapter Outline

<b>15-1</b>	Bevel Gearing—General	<b>786</b>
<b>15-2</b>	Bevel-Gear Stresses and Strengths	<b>788</b>
<b>15-3</b>	AGMA Equation Factors	<b>791</b>
<b>15-4</b>	Straight-Bevel Gear Analysis	<b>803</b>
<b>15-5</b>	Design of a Straight-Bevel Gear Mesh	<b>806</b>
<b>15-6</b>	Worm Gearing—AGMA Equation	<b>809</b>
<b>15-7</b>	Worm-Gear Analysis	<b>813</b>
<b>15-8</b>	Designing a Worm-Gear Mesh	<b>817</b>
<b>15-9</b>	Buckingham Wear Load	<b>820</b>

The American Gear Manufacturers Association (AGMA) has established standards for the analysis and design of the various kinds of bevel and worm gears. Chapter 14 was an introduction to the AGMA methods for spur and helical gears. AGMA has established similar methods for other types of gearing, which all follow the same general approach.

## 15-1

### Bevel Gearing—General

Bevel gears may be classified as follows:

- Straight bevel gears
- Spiral bevel gears
- Zerol bevel gears
- Hypoid gears
- Spiroid gears

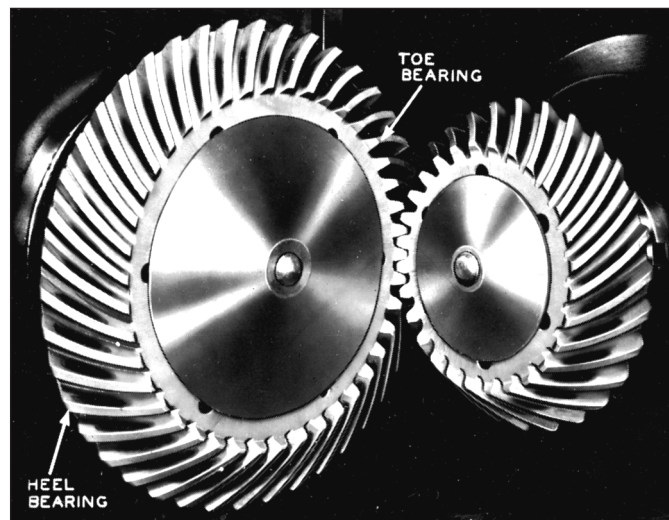
A straight bevel gear was illustrated in Fig. 13–35. These gears are usually used for pitch-line velocities up to 1000 ft/min (5 m/s) when the noise level is not an important consideration. They are available in many stock sizes and are less expensive to produce than other bevel gears, especially in small quantities.

A *spiral bevel gear* is shown in Fig. 15–1; the definition of the *spiral angle* is illustrated in Fig. 15–2. These gears are recommended for higher speeds and where the noise level is an important consideration. Spiral bevel gears are the bevel counterpart of the helical gear; it can be seen in Fig. 15–1 that the pitch surfaces and the nature of contact are the same as for straight bevel gears except for the differences brought about by the spiral-shaped teeth.

The *Zerol bevel gear* is a patented gear having curved teeth but with a zero spiral angle. The axial thrust loads permissible for Zerol bevel gears are not as large as those for the spiral bevel gear, and so they are often used instead of straight bevel gears. The Zerol bevel gear is generated by the same tool used for regular spiral bevel gears. For design purposes, use the same procedure as for straight bevel gears and then simply substitute a Zerol bevel gear.

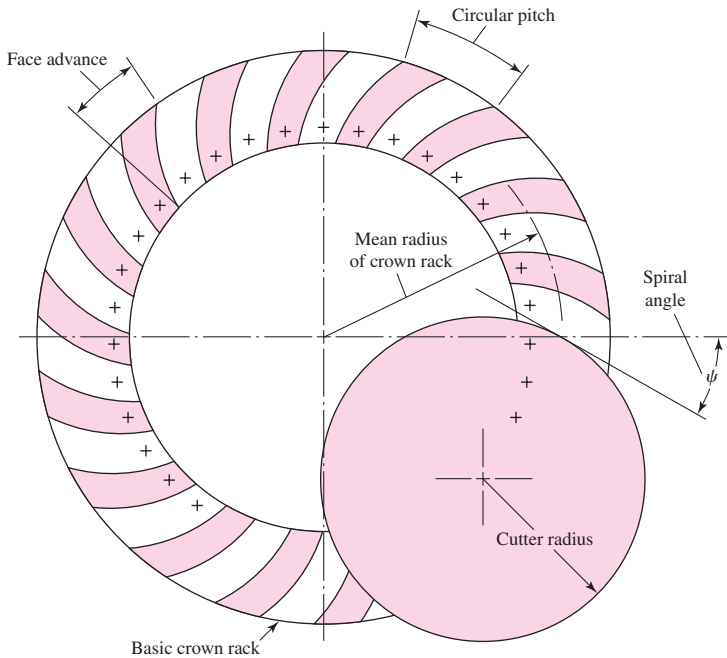
**Figure 15-1**

Spiral bevel gears. (Courtesy of Gleason Works, Rochester, N.Y.)

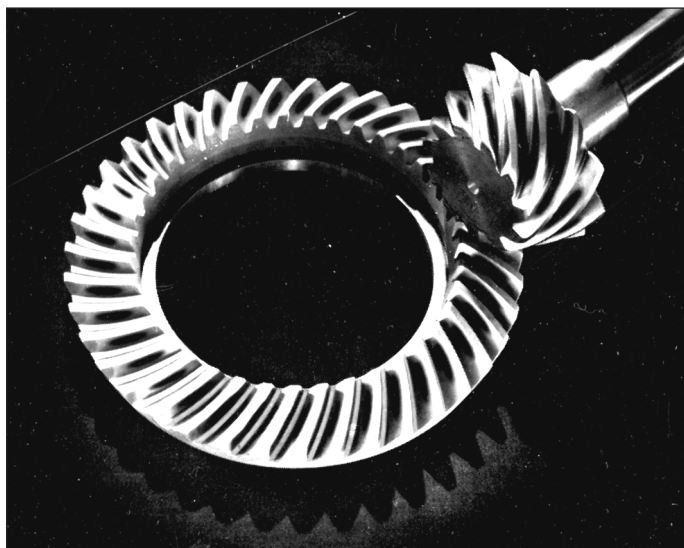


**Figure 15–2**

Cutting spiral-gear teeth on the basic crown rack.

**Figure 15–3**

Hypoid gears. (Courtesy of Gleason Works, Rochester, N.Y.)

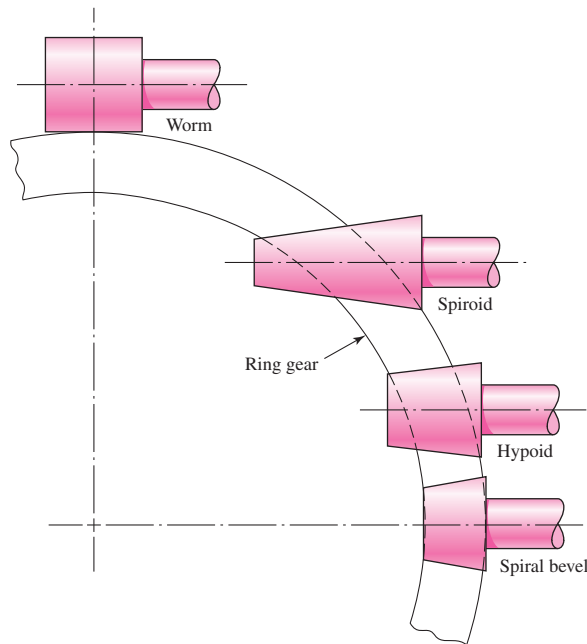


It is frequently desirable, as in the case of automotive differential applications, to have gearing similar to bevel gears but with the shafts offset. Such gears are called *hypoid gears*, because their pitch surfaces are hyperboloids of revolution. The tooth action between such gears is a combination of rolling and sliding along a straight line and has much in common with that of worm gears. Figure 15–3 shows a pair of hypoid gears in mesh.

Figure 15–4 is included to assist in the classification of spiral bevel gearing. It is seen that the hypoid gear has a relatively small shaft offset. For larger offsets, the pinion begins to resemble a tapered worm and the set is then called *spiroid gearing*.

**Figure 15-4**

Comparison of intersecting- and offset-shaft bevel-type gearings. (From Gear Handbook by Darle W. Dudley, 1962, pp. 2-24.)



## 15-2 Bevel-Gear Stresses and Strengths

In a typical bevel-gear mounting, Fig. 13-36, for example, one of the gears is often mounted outboard of the bearings. This means that the shaft deflections can be more pronounced and can have a greater effect on the nature of the tooth contact. Another difficulty that occurs in predicting the stress in bevel-gear teeth is the fact that the teeth are tapered. Thus, to achieve perfect line contact passing through the cone center, the teeth ought to bend more at the large end than at the small end. To obtain this condition requires that the load be proportionately greater at the large end. Because of this varying load across the face of the tooth, it is desirable to have a fairly short face width.

Because of the complexity of bevel, spiral bevel, Zerol bevel, hypoid, and spiroid gears, as well as the limitations of space, only a portion of the applicable standards that refer to straight-bevel gears is presented here.<sup>1</sup> Table 15-1 gives the symbols used in ANSI/AGMA 2003-B97.

### Fundamental Contact Stress Equation

$$s_c = \sigma_c = C_p \left( \frac{W^t}{F d_p I} K_o K_v K_m C_s C_{xc} \right)^{1/2} \quad (\text{U.S. customary units}) \quad (15-1)$$

$$\sigma_H = Z_E \left( \frac{1000 W^t}{bd Z_1} K_A K_v K_{H\beta} Z_x Z_{xc} \right)^{1/2} \quad (\text{SI units})$$

The first term in each equation is the AGMA symbol, whereas;  $\sigma_c$ , our normal notation, is directly equivalent.

<sup>1</sup>Figures 15-5 to 15-13 and Tables 15-1 to 15-7 have been extracted from ANSI/AGMA 2003-B97, *Rating the Pitting Resistance and Bending Strength of Generated Straight Bevel, Zerol Bevel and Spiral Bevel Gear Teeth* with the permission of the publisher, the American Gear Manufacturers Association, 500 Montgomery Street, Suite 350, Alexandria, VA, 22314-1560.

**Table 15-1**

Symbols Used in Bevel Gear Rating Equations, ANSI/AGMA 2003-B97 Standard    Source: ANSI/AGMA 2003-B97.

<b>AGMA Symbol</b>	<b>ISO Symbol</b>	<b>Description</b>	<b>Units</b>
$A_m$	$R_m$	Mean cone distance	in (mm)
$A_0$	$R_e$	Outer cone distance	in (mm)
$C_H$	$Z_W$	Hardness ratio factor for pitting resistance	
$C_i$	$Z_i$	Inertia factor for pitting resistance	
$C_L$	$Z_{NT}$	Stress cycle factor for pitting resistance	
$C_p$	$Z_E$	Elastic coefficient	$[\text{lbf/in}^2]^{0.5}$ $(\text{N/mm}^2)^{0.5}$
$C_R$	$Z_Z$	Reliability factor for pitting	
$C_{SF}$		Service factor for pitting resistance	
$C_S$	$Z_x$	Size factor for pitting resistance	
$C_{xc}$	$Z_{xc}$	Crowning factor for pitting resistance	
$D, d$	$d_{e2}, d_{e1}$	Outer pitch diameters of gear and pinion, respectively	in (mm)
$E_G, E_P$	$E_2, E_1$	Young's modulus of elasticity for materials of gear and pinion, respectively	$\text{lbf/in}^2$ $(\text{N/mm}^2)$
$e$	$e$	Base of natural (Napierian) logarithms	
$F$	$b$	Net face width	in (mm)
$F_{eG}, F_{eP}$	$b'_2, b'_1$	Effective face widths of gear and pinion, respectively	in (mm)
$f_P$	$R_{a1}$	Pinion surface roughness	$\mu\text{in } (\mu\text{m})$
$H_{BG}$	$H_{B2}$	Minimum Brinell hardness number for gear material	HB
$H_{BP}$	$H_{B1}$	Minimum Brinell hardness number for pinion material	HB
$h_c$	$E_{ht \text{ min}}$	Minimum total case depth at tooth middepth	in (mm)
$h_e$	$h'_c$	Minimum effective case depth	in (mm)
$h_{e \text{ lim}}$	$h'_{c \text{ lim}}$	Suggested maximum effective case depth limit at tooth middepth	in (mm)
$I$	$Z_I$	Geometry factor for pitting resistance	
$J$	$Y_J$	Geometry factor for bending strength	
$J_G, J_P$	$Y_{J2}, Y_{J1}$	Geometry factor for bending strength for gear and pinion, respectively	
$K_F$	$Y_F$	Stress correction and concentration factor	
$K_i$	$Y_i$	Inertia factor for bending strength	
$K_L$	$Y_{NT}$	Stress cycle factor for bending strength	
$K_m$	$K_{H\beta}$	Load distribution factor	
$K_o$	$K_A$	Overload factor	
$K_R$	$Y_z$	Reliability factor for bending strength	
$K_S$	$Y_X$	Size factor for bending strength	
$K_{SF}$		Service factor for bending strength	
$K_T$	$K_\theta$	Temperature factor	
$K_v$	$K_v$	Dynamic factor	
$K_x$	$Y_\beta$	Lengthwise curvature factor for bending strength	
	$m_{et}$	Outer transverse module	(mm)
	$m_{mt}$	Mean transverse module	(mm)
	$m_{mn}$	Mean normal module	(mm)
$m_{NI}$	$\varepsilon_{NI}$	Load sharing ratio, pitting	
$m_{NJ}$	$\varepsilon_{NJ}$	Load sharing ratio, bending	
$N$	$z_2$	Number of gear teeth	
$N_L$	$n_L$	Number of load cycles	
$n$	$z_1$	Number of pinion teeth	
$n_P$	$n_1$	Pinion speed	rev/min

(Continued)

**Table 15-1**Symbols Used in Gear Rating Equations, ANSI/AGMA 2003-B97 Standard (*Continued*)

<b>AGMA Symbol</b>	<b>ISO Symbol</b>	<b>Description</b>	<b>Units</b>
$P$	$P$	Design power through gear pair	hp (kW)
$P_a$	$P_a$	Allowable transmitted power	hp (kW)
$P_{ac}$	$P_{az}$	Allowable transmitted power for pitting resistance	hp (kW)
$P_{acu}$	$P_{azu}$	Allowable transmitted power for pitting resistance at unity service factor	hp (kW)
$P_{at}$	$P_{ay}$	Allowable transmitted power for bending strength	hp (kW)
$P_{atu}$	$P_{ayu}$	Allowable transmitted power for bending strength at unity service factor	hp (kW)
$P_d$		Outer transverse diametral pitch	teeth/in
$P_m$		Mean transverse diametral pitch	teeth/in
$P_{mn}$		Mean normal diametral pitch	teeth/in
$Q_v$	$Q_v$	Transmission accuracy number	
$q$	$q$	Exponent used in formula for lengthwise curvature factor	
$R, r$	$r_{mpt2}, r_{mpt1}$	Mean transverse pitch radii for gear and pinion, respectively	in (mm)
$R_t, r_t$	$r_{myo2}, r_{myo1}$	Mean transverse radii to point of load application for gear and pinion, respectively	in (mm)
$r_c$	$r_{c0}$	Cutter radius used for producing Zerol bevel and spiral bevel gears	in (mm)
$s$	$g_c$	Length of the instantaneous line of contact between mating tooth surfaces	in (mm)
$s_{ac}$	$\sigma_H \text{ lim}$	Allowable contact stress number	lbf/in <sup>2</sup> (N/mm <sup>2</sup> )
$s_{at}$	$\sigma_F \text{ lim}$	Bending stress number (allowable)	lbf/in <sup>2</sup> (N/mm <sup>2</sup> )
$s_c$	$\sigma_H$	Calculated contact stress number	lbf/in <sup>2</sup> (N/mm <sup>2</sup> )
$s_F$	$s_F$	Bending safety factor	
$s_H$	$s_H$	Contact safety factor	
$s_I$	$\sigma_F$	Calculated bending stress number	lbf/in <sup>2</sup> (N/mm <sup>2</sup> )
$s_{wc}$	$\sigma_{HP}$	Permissible contact stress number	lbf/in <sup>2</sup> (N/mm <sup>2</sup> )
$s_{wt}$	$\sigma_{FP}$	Permissible bending stress number	lbf/in <sup>2</sup> (N/mm <sup>2</sup> )
$T_P$	$T_1$	Operating pinion torque	lbf in (Nm)
$T_T$	$\theta_T$	Operating gear blank temperature	°F(°C)
$t_0$	$s_{ai}$	Normal tooth top land thickness at narrowest point	in (mm)
$U_c$	$U_c$	Core hardness coefficient for nitrided gear	lbf/in <sup>2</sup> (N/mm <sup>2</sup> )
$U_H$	$U_H$	Hardening process factor for steel	lbf/in <sup>2</sup> (N/mm <sup>2</sup> )
$v_t$	$v_{et}$	Pitch-line velocity at outer pitch circle	ft/min (m/s)
$Y_{KG}, Y_{KP}$	$Y_{K2}, Y_{K1}$	Tooth form factors including stress-concentration factor for gear and pinion, respectively	
$\mu_G, \mu_p$	$\nu_2, \nu_1$	Poisson's ratio for materials of gear and pinion, respectively	
$\rho_0$	$\rho y_o$	Relative radius of profile curvature at point of maximum contact stress between mating tooth surfaces	in (mm)
$\phi$	$\alpha_n$	Normal pressure angle at pitch surface	
$\phi_t$	$\alpha_{wt}$	Transverse pressure angle at pitch point	
$\psi$	$\beta_m$	Mean spiral angle at pitch surface	
$\psi_b$	$\beta_{mb}$	Mean base spiral angle	

### Permissible Contact Stress Number (Strength) Equation

$$s_{wc} = (\sigma_c)_{\text{all}} = \frac{s_{ac} C_L C_H}{S_H K_T C_R} \quad (\text{U.S. customary units}) \quad (15-2)$$

$$\sigma_{HP} = \frac{\sigma_H \lim Z_{NT} Z_W}{S_H K_\theta Z_Z} \quad (\text{SI units})$$

### Bending Stress

$$s_t = \frac{W^t}{F} P_d K_o K_v \frac{K_s K_m}{K_x J} \quad (\text{U.S. customary units}) \quad (15-3)$$

$$\sigma_F = \frac{1000 W^t}{b} \frac{K_A K_v}{m_{et}} \frac{Y_x K_{H\beta}}{Y_\beta Y_J} \quad (\text{SI units})$$

### Permissible Bending Stress Equation

$$s_{wt} = \frac{s_{at} K_L}{S_F K_T K_R} \quad (\text{U.S. customary units}) \quad (15-4)$$

$$\sigma_{FP} = \frac{\sigma_F \lim Y_{NT}}{S_F K_\theta Y_z} \quad (\text{SI units})$$

## 15-3 AGMA Equation Factors

### Overload Factor $K_o$ ( $K_A$ )

The overload factor makes allowance for any externally applied loads in excess of the nominal transmitted load. Table 15-2, from Appendix A of 2003-B97, is included for your guidance.

### Safety Factors $S_H$ and $S_F$

The factors of safety  $S_H$  and  $S_F$  as defined in 2003-B97 are adjustments to strength, not load, and consequently cannot be used as is to assess (by comparison) whether the threat is from wear fatigue or bending fatigue. Since  $W^t$  is the same for the pinion and gear, the comparison of  $\sqrt{S_H}$  to  $S_F$  allows direct comparison.

### Dynamic Factor $K_v$

In 2003-C87 AGMA changed the definition of  $K_v$  to its reciprocal but used the same symbol. Other standards have yet to follow this move. The dynamic factor  $K_v$  makes

**Table 15-2**

Overload Factors  $K_o$  ( $K_A$ )

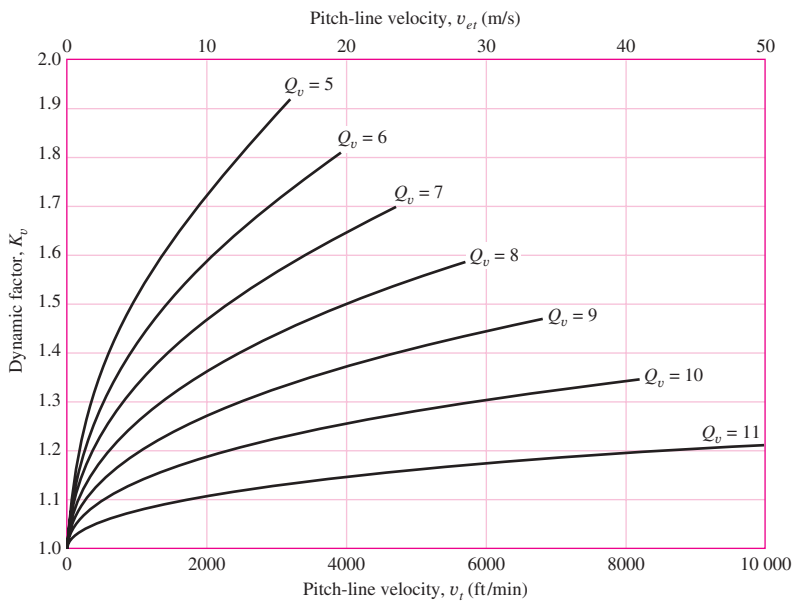
Source: ANSI/AGMA  
2003-B97.

Character of Prime Mover	Character of Load on Driven Machine			
	Uniform	Light Shock	Medium Shock	Heavy Shock
Uniform	1.00	1.25	1.50	1.75 or higher
Light shock	1.10	1.35	1.60	1.85 or higher
Medium shock	1.25	1.50	1.75	2.00 or higher
Heavy shock	1.50	1.75	2.00	2.25 or higher

Note: This table is for speed-decreasing drives. For speed-increasing drives, add  $0.01(N/n)^2$  or  $0.01(z_2/z_1)^2$  to the above factors.

**Figure 15–5**

Dynamic factor  $K_v$ .  
(Source: ANSI/AGMA 2003-B97.)



allowance for the effect of gear-tooth quality related to speed and load, and the increase in stress that follows. AGMA uses a *transmission accuracy number*  $Q_v$  to describe the precision with which tooth profiles are spaced along the pitch circle. Figure 15–5 shows graphically how pitch-line velocity and transmission accuracy number are related to the dynamic factor  $K_v$ . Curve fits are

$$K_v = \left( \frac{A + \sqrt{v_t}}{A} \right)^B \quad (\text{U.S. customary units}) \quad (15-5)$$

$$K_v = \left( \frac{A + \sqrt{200v_{et}}}{A} \right)^B \quad (\text{SI units})$$

where

$$A = 50 + 56(1 - B) \quad (15-6)$$

$$B = 0.25(12 - Q_v)^{2/3}$$

and  $v_t(v_{et})$  is the pitch-line velocity at outside pitch diameter, expressed in ft/min (m/s):

$$v_t = \pi d_P n_P / 12 \quad (\text{U.S. customary units}) \quad (15-7)$$

$$v_{et} = 5.236(10^{-5})d_1 n_1 \quad (\text{SI units})$$

The maximum recommended pitch-line velocity is associated with the abscissa of the terminal points of the curve in Fig. 15–5:

$$v_{t \max} = [A + (Q_v - 3)]^2 \quad (\text{U.S. customary units}) \quad (15-8)$$

$$v_{et \max} = \frac{[A + (Q_v - 3)]^2}{200} \quad (\text{SI units})$$

where  $v_{t \max}$  and  $v_{et \max}$  are in ft/min and m/s, respectively.

### Size Factor for Pitting Resistance $C_s$ ( $Z_x$ )

$$C_s = \begin{cases} 0.5 & F < 0.5 \text{ in} \\ 0.125F + 0.4375 & 0.5 \leq F \leq 4.5 \text{ in} \\ 1 & F > 4.5 \text{ in} \end{cases} \quad (\text{U.S. customary units}) \quad (15-9)$$

$$Z_x = \begin{cases} 0.5 & b < 12.7 \text{ mm} \\ 0.00492b + 0.4375 & 12.7 \leq b \leq 114.3 \text{ mm} \\ 1 & b > 114.3 \text{ mm} \end{cases} \quad (\text{SI units})$$

### Size Factor for Bending $K_s$ ( $Y_x$ )

$$K_s = \begin{cases} 0.4867 + 0.2132/P_d & 0.5 \leq P_d \leq 16 \text{ teeth/in} \\ 0.5 & P_d > 16 \text{ teeth/in} \end{cases} \quad (\text{U.S. customary units}) \quad (15-10)$$

$$Y_x = \begin{cases} 0.5 & m_{et} < 1.6 \text{ mm} \\ 0.4867 + 0.008339m_{et} & 1.6 \leq m_{et} \leq 50 \text{ mm} \end{cases} \quad (\text{SI units})$$

### Load-Distribution Factor $K_m$ ( $K_{H\beta}$ )

$$K_m = K_{mb} + 0.0036F^2 \quad (\text{U.S. customary units}) \quad (15-11)$$

$$K_{H\beta} = K_{mb} + 5.6(10^{-6})b^2 \quad (\text{SI units})$$

where

$$K_{mb} = \begin{cases} 1.00 & \text{both members straddle-mounted} \\ 1.10 & \text{one member straddle-mounted} \\ 1.25 & \text{neither member straddle-mounted} \end{cases}$$

### Crowning Factor for Pitting $C_{xc}$ ( $Z_{xc}$ )

The teeth of most bevel gears are crowned in the lengthwise direction during manufacture to accommodate to the deflection of the mountings.

$$C_{xc} = Z_{xc} = \begin{cases} 1.5 & \text{properly crowned teeth} \\ 2.0 & \text{or larger uncrowned teeth} \end{cases} \quad (15-12)$$

### Lengthwise Curvature Factor for Bending Strength $K_x$ ( $Y_\beta$ )

For straight-bevel gears,

$$K_x = Y_\beta = 1 \quad (15-13)$$

### Pitting Resistance Geometry Factor $I$ ( $Z_I$ )

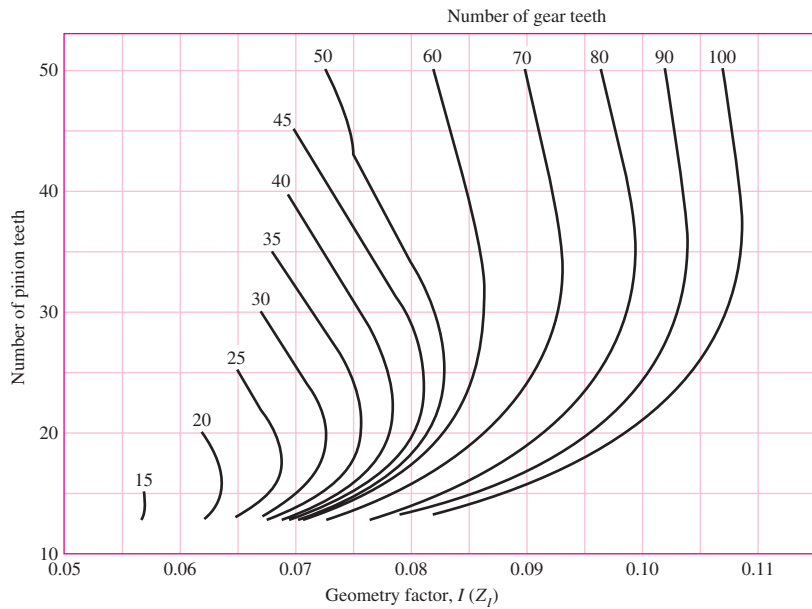
Figure 15–6 shows the geometry factor  $I$  ( $Z_I$ ) for straight-bevel gears with a  $20^\circ$  pressure angle and  $90^\circ$  shaft angle. Enter the figure ordinate with the number of pinion teeth, move to the number of gear-teeth contour, and read from the abscissa.

### Bending Strength Geometry Factor $J$ ( $Y_J$ )

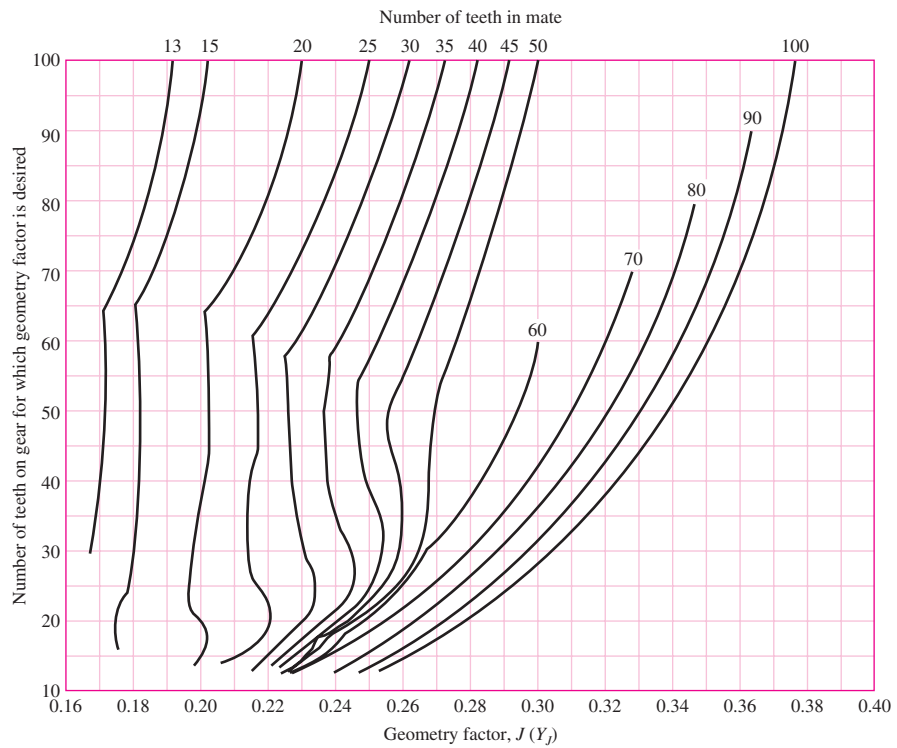
Figure 15–7 shows the geometry factor  $J$  for straight-bevel gears with a  $20^\circ$  pressure angle and  $90^\circ$  shaft angle.

**Figure 15–6**

Contact geometry factor  $I (Z_I)$  for coniflex straight-bevel gears with a  $20^\circ$  normal pressure angle and a  $90^\circ$  shaft angle.  
 (Source: ANSI/AGMA 2003-B97.)

**Figure 15–7**

Bending factor  $J (Y_J)$  for coniflex straight-bevel gears with a  $20^\circ$  normal pressure angle and  $90^\circ$  shaft angle.  
 (Source: ANSI/AGMA 2003-B97.)



### Stress-Cycle Factor for Pitting Resistance $C_L$ ( $Z_{NT}$ )

$$C_L = \begin{cases} 2 & 10^3 \leq N_L < 10^4 \\ 3.4822 N_L^{-0.0602} & 10^4 \leq N_L \leq 10^{10} \end{cases} \quad (15-14)$$

$$Z_{NT} = \begin{cases} 2 & 10^3 \leq n_L < 10^4 \\ 3.4822 n_L^{-0.0602} & 10^4 \leq n_L \leq 10^{10} \end{cases}$$

See Fig. 15–8 for a graphical presentation of Eqs. (15–14).

### Stress-Cycle Factor for Bending Strength $K_L$ ( $Y_{NT}$ )

$$K_L = \begin{cases} 2.7 & 10^2 \leq N_L < 10^3 \\ 6.1514 N_L^{-0.1182} & 10^3 \leq N_L < 3(10^6) \\ 1.6831 N_L^{-0.0323} & 3(10^6) \leq N_L \leq 10^{10} \\ 1.3558 N_L^{-0.0178} & 3(10^6) \leq N_L \leq 10^{10} \end{cases} \quad \begin{matrix} \text{general} \\ \text{critical} \end{matrix} \quad (15-15)$$

$$Y_{NT} = \begin{cases} 2.7 & 10^2 \leq n_L < 10^3 \\ 6.1514 n_L^{-0.1182} & 10^3 \leq n_L < 3(10^6) \\ 1.6831 n_L^{-0.0323} & 3(10^6) \leq n_L \leq 10^{10} \\ 1.3558 n_L^{-0.0323} & 3(10^6) \leq n_L \leq 10^{10} \end{cases} \quad \begin{matrix} \text{general} \\ \text{critical} \end{matrix}$$

See Fig. 15–9 for a plot of Eqs. (15–15).

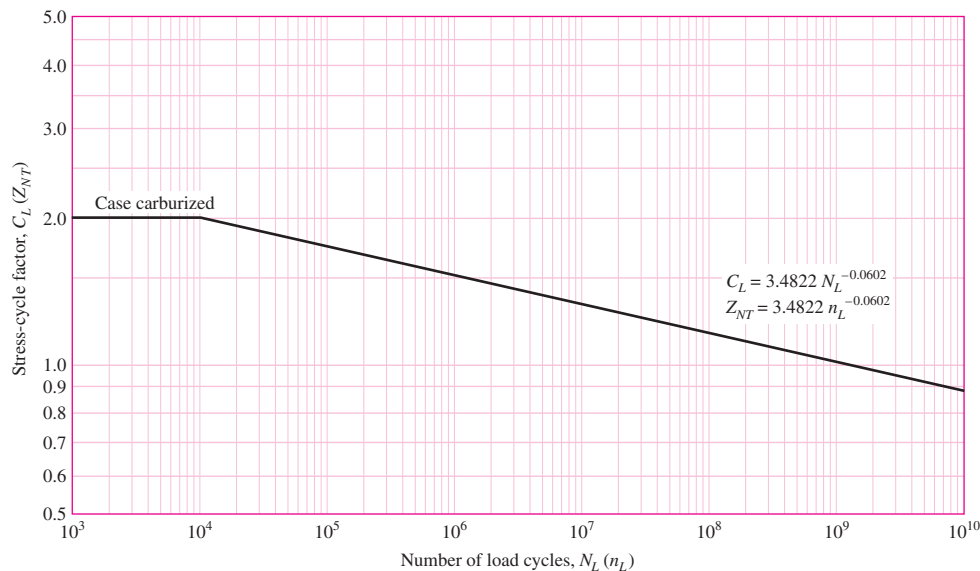


**Figure 15–8**

Contact stress-cycle factor for pitting resistance  $C_L$  ( $Z_{NT}$ ) for carburized case-hardened steel bevel gears.

(Source: ANSI/AGMA 2003-B97.)

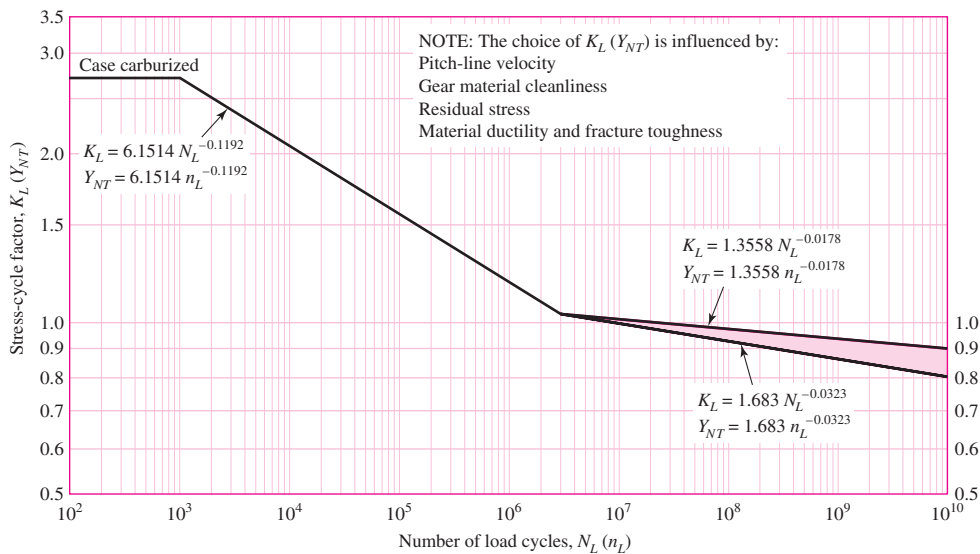


**Figure 15–9**

Stress-cycle factor for bending strength  $K_L$  ( $Y_{NT}$ ) for carburized case-hardened steel bevel gears.

(Source: ANSI/AGMA 2003-B97.)

### Hardness-Ratio Factor $C_H$ ( $Z_W$ )

$$\begin{aligned} C_H &= 1 + B_1(N/n - 1) & B_1 &= 0.008\ 98(H_{BP}/H_{BG}) - 0.008\ 29 \\ Z_W &= 1 + B_1(z_1/z_2 - 1) & B_1 &= 0.008\ 98(H_{B1}/H_{B2}) - 0.008\ 29 \end{aligned} \quad (15-16)$$

The preceding equations are valid when  $1.2 \leq H_{BP}/H_{BG} \leq 1.7$  ( $1.2 \leq H_{B1}/H_{B2} \leq 1.7$ ). Figure 15–10 graphically displays Eqs. (15–16). When a surface-hardened pinion (48 HRC or harder) is run with a through-hardened gear (180  $\leq H_B \leq 400$ ), a work-hardening effect occurs. The  $C_H(Z_W)$  factor varies with pinion surface roughness  $f_P(R_{a1})$  and the mating-gear hardness:

$$\begin{aligned} C_H &= 1 + B_2(450 - H_{BG}) & B_2 &= 0.000\ 75 \exp(-0.0122 f_P) \\ Z_W &= 1 + B_2(450 - H_{B2}) & B_2 &= 0.000\ 75 \exp(-0.52 f_P) \end{aligned} \quad (15-17)$$

where  $f_P(R_{a1})$  = pinion surface hardness  $\mu$ in ( $\mu\text{m}$ )

$H_{BG}(H_{B2})$  = minimum Brinell hardness

See Fig. 15–11 for carburized steel gear pairs of approximately equal hardness  $C_H = Z_W = 1$ .

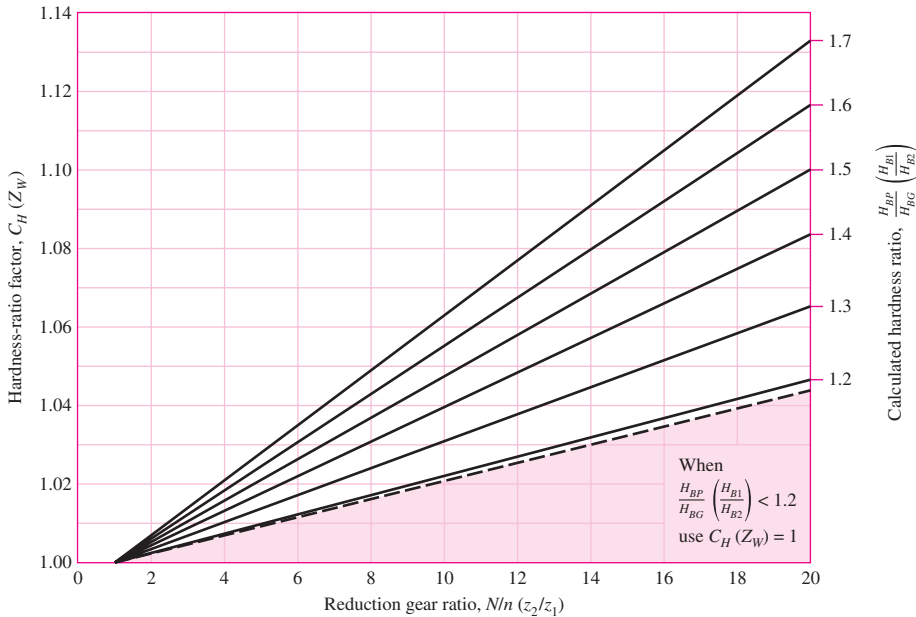
### Temperature Factor $K_T$ ( $K_\theta$ )

$$\begin{aligned} K_T &= \begin{cases} 1 & 32^\circ\text{F} \leq t \leq 250^\circ\text{F} \\ (460 + t)/710 & t > 250^\circ\text{F} \end{cases} \\ K_\theta &= \begin{cases} 1 & 0^\circ\text{C} \leq \theta \leq 120^\circ\text{C} \\ (273 + \theta)/393 & \theta > 120^\circ\text{C} \end{cases} \end{aligned} \quad (15-18)$$

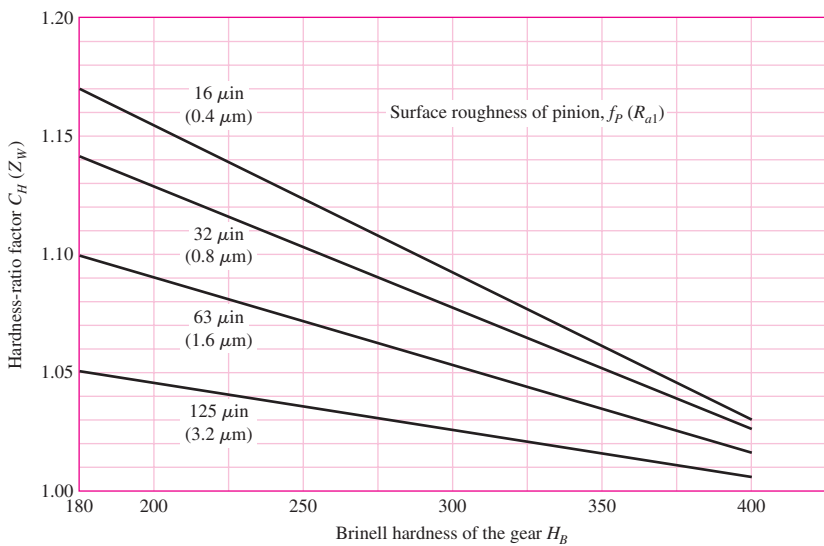
**Figure 15-10**

Hardness-ratio factor  $C_H (Z_W)$  for through-hardened pinion and gear.

(Source: ANSI/AGMA 2003-B97.)

**Figure 15-11**

Hardness-ratio factor  $C_H (Z_W)$  for surface-hardened pinions.  
(Source: ANSI/AGMA 2003-B97.)



### Reliability Factors $C_R (Z_Z)$ and $K_R (Y_Z)$

Table 15-3 displays the reliability factors. Note that  $C_R = \sqrt{K_R}$  and  $Z_Z = \sqrt{Y_Z}$ . Logarithmic interpolation equations are

$$Y_Z = K_R = \begin{cases} 0.50 - 0.25 \log(1 - R) & 0.99 \leq R \leq 0.999 \\ 0.70 - 0.15 \log(1 - R) & 0.90 \leq R < 0.99 \end{cases} \quad (15-19)$$

$$(15-20)$$

The reliability of the stress (fatigue) numbers allowable in Tables 15-4, 15-5, 15-6, and 15-7 is 0.99.

**Table 15-3**

## Reliability Factors

Source: ANSI/AGMA  
2003-B97.

Requirements of Application	Reliability Factors for Steel*	
	$C_R (Z_Z)$	$K_R (Y_Z)^\dagger$
Fewer than one failure in 10 000	1.22	1.50
Fewer than one failure in 1000	1.12	1.25
Fewer than one failure in 100	1.00	1.00
Fewer than one failure in 10	0.92	0.85‡
Fewer than one failure in 2	0.84	0.70§

\*At the present time there are insufficient data concerning the reliability of bevel gears made from other materials.

†Tooth breakage is sometimes considered a greater hazard than pitting. In such cases a greater value of  $K_R (Y_Z)$  is selected for bending.

‡At this value plastic flow might occur rather than pitting.

§From test data extrapolation.

**Table 15-4**

Allowable Contact Stress Number for Steel Gears,  $s_{ac} (\sigma_H \text{ lim})$  Source: ANSI/AGMA 2003-B97.

Material Designation	Heat Treatment	Minimum Surface Hardness	Allowable Contact Stress Number, $s_{ac} (\sigma_H \text{ lim}) \text{ lbf/in}^2 (\text{N/mm}^2)$		
			Grade 1†	Grade 2†	Grade 3†
Steel	Through-hardened‡	Fig. 15-12	Fig. 15-12	Fig. 15-12	
	Flame or induction hardened§	50 HRC	175 000 (1210)	190 000 (1310)	
	Carburized and case hardened§	2003-B97 Table 8	200 000 (1380)	225 000 (1550)	250 000 (1720)
AISI 4140	Nitrided§	84.5 HR15N		145 000 (1000)	
Nitr alloy 135M	Nitrided§	90.0 HR15N		160 000 (1100)	

\*Hardness to be equivalent to that at the tooth middepth in the center of the face width.

†See ANSI/AGMA 2003-B97, Tables 8 through 11, for metallurgical factors for each stress grade of steel gears.

‡These materials must be annealed or normalized as a minimum.

§The allowable stress numbers indicated may be used with the case depths prescribed in 21.1, ANSI/AGMA 2003-B97.

**Elastic Coefficient for Pitting Resistance  $C_p (Z_E)$** 

$$C_p = \sqrt{\frac{1}{\pi[(1 - v_P^2)/E_P + (1 - v_G^2)/E_G]}} \quad (15-21)$$

$$Z_E = \sqrt{\frac{1}{\pi[(1 - v_1^2)/E_1 + (1 - v_2^2)/E_2]}}$$

**Table 15-5**Allowable Contact Stress Number for Iron Gears,  $s_{ac}$  ( $\sigma_H$  lim)   Source: ANSI/AGMA 2003-B97.

Material	Material Designation		Heat Treatment	Typical Minimum Surface Hardness	Allowable Contact Stress Number, $s_{ac}$ ( $\sigma_H$ lim) lbf/in <sup>2</sup> (N/mm <sup>2</sup> )
	ASTM	ISO			
Cast iron	ASTM A48	ISO/DR 185	As cast	175 HB	50 000 (345)
	Class 30	Grade 200			65 000 (450)
	Class 40	Grade 300		200 HB	
Ductile (nodular) iron	ASTM A536	ISO/DIS 1083	Quenched and tempered	180 HB	94 000 (650)
	Grade 80-55-06	Grade 600-370-03			
	Grade 120-90-02	Grade 800-480-02		300 HB	135 000 (930)

**Table 15-6**Allowable Bending Stress Numbers for Steel Gears,  $s_{at}$  ( $\sigma_F$  lim)   Source: ANSI/AGMA 2003-B97.

Material Designation	Heat Treatment	Minimum Surface Hardness	Bending Stress Number (Allowable), $s_{at}$ ( $\sigma_F$ lim) lbf/in <sup>2</sup> (N/mm <sup>2</sup> )		
			Grade 1*	Grade 2*	Grade 3*
Steel	Through-hardened	Fig. 15-13	Fig. 15-13	Fig. 15-13	
	Flame or induction hardened				
	Unhardened roots	50 HRC	15 000 (85)	13 500 (95)	
	Hardened roots		22 500 (154)		
	Carburized and case hardened <sup>†</sup>	2003-B97			
		Table 8	30 000 (205)	35 000 (240)	40 000 (275)
AISI 4140	Nitrided <sup>‡,§</sup>	84.5 HR15N		22 000 (150)	
Nitralloy 135M	Nitrided <sup>‡,§</sup>	90.0 HR15N		24 000 (165)	

<sup>\*</sup>See ANSI/AGMA 2003-B97, Tables 8–11, for metallurgical factors for each stress grade of steel gears.<sup>†</sup>The allowable stress numbers indicated may be used with the case depths prescribed in 21.1, ANSI/AGMA 2003-B97.<sup>‡</sup>The overload capacity of nitrided gears is low. Since the shape of the effective S-N curve is flat, the sensitivity to shock should be investigated before proceeding with the design.

where

 $C_p$  = elastic coefficient,  $2290 \sqrt{\text{psi}}$  for steel $Z_E$  = elastic coefficient,  $190 \sqrt{\text{N/mm}^2}$  for steel $E_P$  and  $E_G$  = Young's moduli for pinion and gear respectively, psi $E_1$  and  $E_2$  = Young's moduli for pinion and gear respectively, N/mm<sup>2</sup>

### Allowable Contact Stress

Tables 15-4 and 15-5 provide values of  $s_{ac}$  ( $\sigma_H$ ) for steel gears and for iron gears, respectively. Figure 15-12 graphically displays allowable stress for grade 1 and 2 materials.

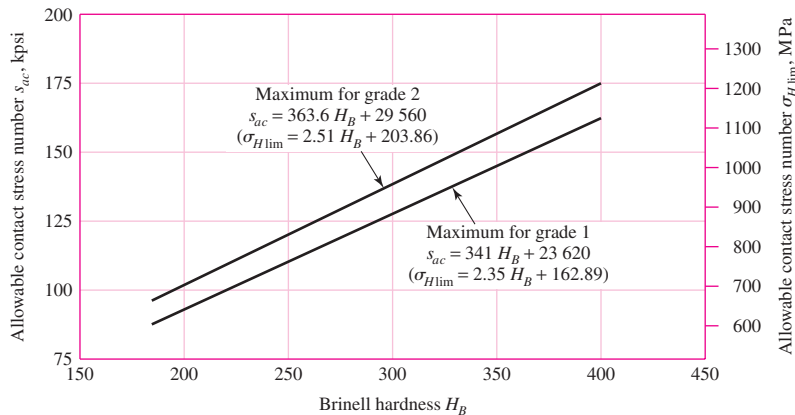
**Table 15–7**

Allowable Bending Stress Number for Iron Gears,  $s_{at}$  ( $\sigma_F$  lim)    Source: ANSI/AGMA 2003-B97.

Material	Material Designation		Heat Treatment	Surface Hardness	Typical Minimum Bending Stress Number (Allowable), $s_{at}$ ( $\sigma_F$ lim) lbf/in <sup>2</sup> (N/mm <sup>2</sup> )	
	ASTM	ISO			( $\sigma_F$ lim)	lbf/in <sup>2</sup> (N/mm <sup>2</sup> )
Cast iron	ASTM A48	ISO/DR 185	As cast	175 HB	4500 (30)	6500 (45)
	Class 30	Grade 200				
	Class 40	Grade 300				
Ductile (nodular) iron	ASTM A536	ISO/DIS 1083	Quenched and tempered	180 HB	10 000 (70)	13 500 (95)
	Grade 80-55-06	Grade 600-370-03				
	Grade 120-90-02	Grade 800-480-02				

**Figure 15–12**

Allowable contact stress number for through-hardened steel gears,  $s_{ac}$  ( $\sigma_H$  lim).  
(Source: ANSI/AGMA 2003-B97.)



The equations are

$$\begin{aligned} s_{ac} &= 341H_B + 23\,620 \text{ psi} && \text{grade 1} \\ \sigma_H \text{ lim} &= 2.35H_B + 162.89 \text{ MPa} && \text{grade 1} \\ s_{ac} &= 363.6H_B + 29\,560 \text{ psi} && \text{grade 2} \\ \sigma_H \text{ lim} &= 2.51H_B + 203.86 \text{ MPa} && \text{grade 2} \end{aligned} \quad (15-22)$$

### Allowable Bending Stress Numbers

Tables 15–6 and 15–7 provide  $s_{at}$  ( $\sigma_F$  lim) for steel gears and for iron gears, respectively. Figure 15–13 shows graphically allowable bending stress  $s_{at}$  ( $\sigma_H$  lim) for through-hardened steels. The equations are

$$\begin{aligned} s_{at} &= 44H_B + 2100 \text{ psi} && \text{grade 1} \\ \sigma_F \text{ lim} &= 0.30H_B + 14.48 \text{ MPa} && \text{grade 1} \\ s_{at} &= 48H_B + 5980 \text{ psi} && \text{grade 2} \\ \sigma_H \text{ lim} &= 0.33H_B + 41.24 \text{ MPa} && \text{grade 2} \end{aligned} \quad (15-23)$$

### Reversed Loading

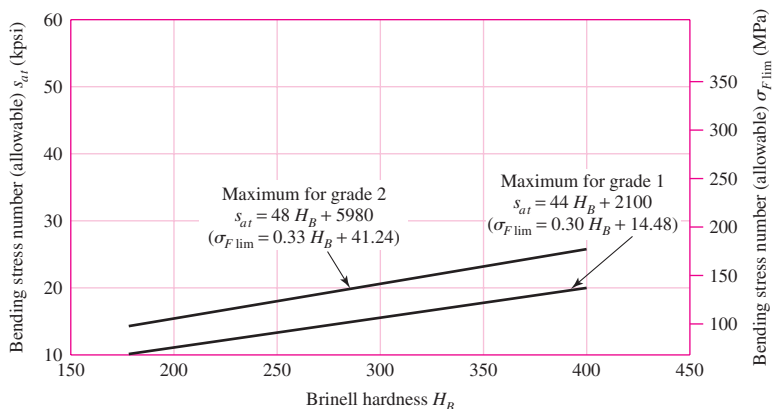
AGMA recommends use of 70 percent of allowable strength in cases where tooth load is completely reversed, as in idler gears and reversing mechanisms.

### Summary

Figure 15–14 is a “roadmap” for straight-bevel gear wear relations using 2003-B97. Figure 15–15 is a similar guide for straight-bevel gear bending using 2003-B97.

**Figure 15-13**

Allowable bending stress number for through-hardened steel gears,  $s_{at}(\sigma_F)_{lim}$ .  
(Source: ANSI/AGMA 2003-B97.)

**Figure 15-14**

“Roadmap” summary of principal straight-bevel gear wear equations and their parameters.

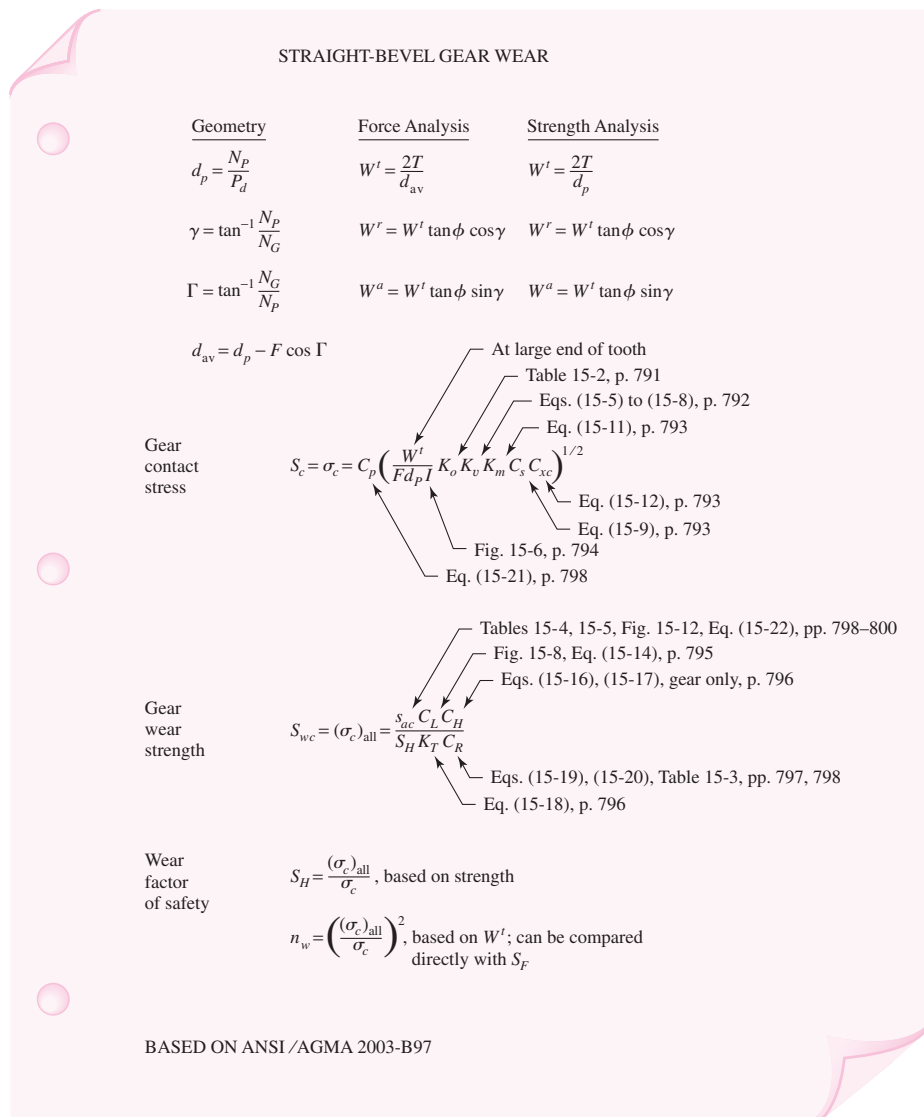


**Figure 15-15**

“Roadmap” summary of principal straight-bevel gear bending equations and their parameters.

## STRAIGHT-BEVEL GEAR BENDING

## Geometry

$$d_p = \frac{N_p}{P}$$

$$\gamma = \tan^{-1} \frac{N_p}{N_G}$$

$$\Gamma = \tan^{-1} \frac{N_G}{N_p}$$

$$d_{av} = d_p - F \cos \Gamma$$

Gear  
bending  
stress

Gear  
bending  
strength

Bending  
factor  
of safety

## Force Analysis

$$W^t = \frac{2T}{d_{av}}$$

$$W^r = W^t \tan \phi \cos \gamma$$

$$W^a = W^t \tan \phi \sin \gamma$$

Table 15-2, p. 791

Eqs. (15-5) to (15-8), p. 792

Eq. (15-10), p. 793

Eq. (15-11), p. 793

Fig. 15-7, p. 794

Eq. (15-13), p. 793

$$S_t = \sigma = \frac{W^t}{F} P_d K_o K_v \frac{K_s K_m}{K_x J}$$

Table 15-6 or 15-7, pp. 799, 800

Fig. 15-9, Eq. (15-15), pp. 795, 796

Eqs. (15-19), (15-20), Table 15-3, pp. 797, 798

Eq. (15-18), p. 796

$S_{wt} = \sigma_{all} = \frac{S_{ult} K_L}{S_F K_T K_R}$

$n_B = \frac{\sigma_{all}}{\sigma}$ , based on  $W^t$ , same as  $S_F$

BASED ON ANSI /AGMA 2003-B97

The standard does not mention specific steel but mentions the hardness attainable by heat treatments such as through-hardening, carburizing and case-hardening, flame-hardening, and nitriding. Through-hardening results depend on size (diametral pitch). Through-hardened materials and the corresponding Rockwell C-scale hardness at the 90 percent martensite shown in parentheses following include 1045 (50), 1060 (54), 1335 (46), 2340 (49), 3140 (49), 4047 (52), 4130 (44), 4140 (49), 4340 (49), 5145 (51), E52100 (60), 6150 (53), 8640 (50), and 9840 (49). For carburized case-hard materials the approximate core hardnesses are 1015 (22), 1025 (37), 1118 (33), 1320 (35), 2317 (30), 4320 (35), 4620 (35), 4820 (35), 6120 (35), 8620 (35), and E9310 (30). The conversion from HRC to  $H_B$  (300-kg load, 10-mm ball) is

HRC	42	40	38	36	34	32	30	28	26	24	22	20	18	16	14	12	10
$H_B$	388	375	352	331	321	301	285	269	259	248	235	223	217	207	199	192	187

Most bevel-gear sets are made from carburized case-hardened steel, and the factors incorporated in 2003-B97 largely address these high-performance gears. For through-hardened gears, 2003-B97 is silent on  $K_L$  and  $C_L$ , and Figs. 15–8 and 15–9 should prudently be considered as approximate.

## 15–4 Straight-Bevel Gear Analysis

### EXAMPLE 15–1

A pair of identical straight-tooth miter gears listed in a catalog has a diametral pitch of 5 at the large end, 25 teeth, a 1.10-in face width, and a  $20^\circ$  normal pressure angle; the gears are grade 1 steel through-hardened with a core and case hardness of 180 Brinell. The gears are uncrowned and intended for general industrial use. They have a quality number of  $Q_v = 7$ . It is likely that the application intended will require outboard mounting of the gears. Use a safety factor of 1, a  $10^7$  cycle life, and a 0.99 reliability. (a) For a speed of 600 rev/min find the power rating of this gearset based on AGMA bending strength.

(b) For the same conditions as in part (a) find the power rating of this gearset based on AGMA wear strength.

(c) For a reliability of 0.995, a gear life of  $10^9$  revolutions, and a safety factor of  $S_F = S_H = 1.5$ , find the power rating for this gearset using AGMA strengths.

**Solution** From Figs. 15–14 and 15–15,

$$d_P = N_P/P = 25/5 = 5.000 \text{ in}$$

$$v_t = \pi d_P n_P / 12 = \pi(5)(600)/12 = 785.4 \text{ ft/min}$$

Overload factor: uniform-uniform loading, Table 15–2,  $K_o = 1.00$ .

Safety factor:  $S_F = 1$ ,  $S_H = 1$ .

Dynamic factor  $K_v$ : from Eq. (15–6),

$$B = 0.25(12 - 7)^{2/3} = 0.731$$

$$A = 50 + 56(1 - 0.731) = 65.06$$

$$K_v = \left( \frac{65.06 + \sqrt{785.4}}{65.06} \right)^{0.731} = 1.299$$

From Eq. (15–8),

$$v_{t \max} = [65.06 + (7 - 3)]^2 = 4769 \text{ ft/min}$$

$v_t < v_{t \max}$ , that is,  $785.4 < 4769$  ft/min, therefore  $K_v$  is valid. From Eq. (15–10),

$$K_s = 0.4867 + 0.2132/5 = 0.529$$

From Eq. (15–11),

$$K_{mb} = 1.25 \quad \text{and} \quad K_m = 1.25 + 0.0036(1.10)^2 = 1.254$$

From Eq. (15–13),  $K_x = 1$ . From Fig. 15–6,  $I = 0.065$ ; from Fig. 15–7,  $J_P = 0.216$ ,  $J_G = 0.216$ . From Eq. (15–15),

$$K_L = 1.683(10^7)^{-0.0323} = 0.999\ 96 \doteq 1$$

From Eq. (15–14),

$$C_L = 3.4822(10^7)^{-0.0602} = 1.32$$

Since  $H_{BP}/H_{BG} = 1$ , then from Fig. 15–10,  $C_H = 1$ . From Eqs. (15–13) and (15–18),  $K_x = 1$  and  $K_T = 1$ , respectively. From Eq. (15–20),

$$K_R = 0.70 - 0.15 \log(1 - 0.99) = 1, \quad C_R = \sqrt{K_R} = \sqrt{1} = 1$$

(a) *Bending*: From Eq. (15–23),

$$s_{at} = 44(180) + 2100 = 10\,020 \text{ psi}$$

From Eq. (15–3),

$$\begin{aligned} s_t = \sigma &= \frac{W^t}{F} P_d K_o K_v \frac{K_s K_m}{K_x J} = \frac{W^t}{1.10}(5)(1)1.299 \frac{0.529(1.254)}{(1)0.216} \\ &= 18.13 W^t \end{aligned}$$

From Eq. (15–4),

$$s_{wt} = \frac{s_{at} K_L}{S_F K_T K_R} = \frac{10\,020(1)}{(1)(1)(1)} = 10\,020 \text{ psi}$$

Equating  $s_t$  and  $s_{wt}$ ,

$$18.13 W^t = 10\,020 \quad W^t = 552.6 \text{ lbf}$$

**Answer**

$$H = \frac{W^t v_t}{33\,000} = \frac{552.6(785.4)}{33\,000} = 13.2 \text{ hp}$$

(b) *Wear*: From Fig. 15–12,

$$s_{ac} = 341(180) + 23\,620 = 85\,000 \text{ psi}$$

From Eq. (15–2),

$$\sigma_{c,\text{all}} = \frac{s_{ac} C_L C_H}{S_H K_T C_R} = \frac{85\,000(1.32)(1)}{(1)(1)(1)} = 112\,200 \text{ psi}$$

Now  $C_p = 2290\sqrt{\text{psi}}$  from definitions following Eq. (15–21). From Eq. (15–9),

$$C_s = 0.125(1.1) + 0.4375 = 0.575$$

From Eq. (15–12),  $C_{xc} = 2$ . Substituting in Eq. (15–1) gives

$$\begin{aligned} \sigma_c &= C_p \left( \frac{W^t}{F d_P I} K_o K_v K_m C_s C_{xc} \right)^{1/2} \\ &= 2290 \left[ \frac{W^t}{1.10(5)0.065} (1)1.299(1.254)0.575(2) \right]^{1/2} = 5242\sqrt{W^t} \end{aligned}$$

Equating  $\sigma_c$  and  $\sigma_{c,\text{all}}$  gives

$$5242\sqrt{W^t} = 112\,200, \quad W^t = 458.1 \text{ lbf}$$

$$H = \frac{458.1(785.4)}{33\,000} = 10.9 \text{ hp}$$

Rated power for the gearset is

**Answer**

$$H = \min(12.9, 10.9) = 10.9 \text{ hp}$$

(c) Life goal  $10^9$  cycles,  $R = 0.995$ ,  $S_F = S_H = 1.5$ , and from Eq. (15–15),

$$K_L = 1.683(10^9)^{-0.0323} = 0.8618$$

From Eq. (15–19),

$$K_R = 0.50 - 0.25 \log(1 - 0.995) = 1.075, \quad C_R = \sqrt{K_R} = \sqrt{1.075} = 1.037$$

From Eq. (15–14),

$$C_L = 3.4822(10^9)^{-0.0602} = 1$$

*Bending:* From Eq. (15–23) and part (a),  $s_{at} = 10\ 020$  psi. From Eq. (15–3),

$$s_t = \sigma = \frac{W^t}{1.10} 5(1) 1.299 \frac{0.529(1.254)}{(1) 0.216} = 18.13 W^t$$

From Eq. (15–4),

$$s_{wt} = \frac{s_{at} K_L}{S_F K_T K_R} = \frac{10\ 020(0.8618)}{1.5(1)1.075} = 5355 \text{ psi}$$

Equating  $s_t$  to  $s_{wt}$  gives

$$18.13 W^t = 5355 \quad W^t = 295.4 \text{ lbf}$$

$$H = \frac{295.4(785.4)}{33\ 000} = 7.0 \text{ hp}$$

*Wear:* From Eq. (15–22), and part (b),  $s_{ac} = 85\ 000$  psi.

Substituting into Eq. (15–2) gives

$$\sigma_{c,\text{all}} = \frac{s_{ac} C_L C_H}{S_H K_T C_R} = \frac{85\ 000(1)(1)}{1.5(1)1.037} = 54\ 640 \text{ psi}$$

Substituting into Eq. (15–1) gives, from part (b),  $\sigma_c = 5242\sqrt{W^t}$ .

Equating  $\sigma_c$  to  $\sigma_{c,\text{all}}$  gives

$$\sigma_c = \sigma_{c,\text{all}} = 54\ 640 = 5242\sqrt{W^t} \quad W^t = 108.6 \text{ lbf}$$

The wear power is

$$H = \frac{108.6(785.4)}{33\ 000} = 2.58 \text{ hp}$$

**Answer**

The mesh rated power is  $H = \min(7.0, 2.58) = 2.6$  hp.

## 15-5 Design of a Straight-Bevel Gear Mesh

A useful decision set for straight-bevel gear design is

- Function
- Design factor
- Tooth system
- Tooth count
- Pitch and face width
- Quality number
- Gear material, core and case hardness
- Pinion material, core and case hardness

A priori decisions

Design variables

In bevel gears the quality number is linked to the wear strength. The  $J$  factor for the gear can be smaller than for the pinion. Bending strength is not linear with face width, because added material is placed at the small end of the teeth. Consequently, face width is roughly prescribed as

$$F = \min(0.3A_0, 10/P_d) \quad (15-24)$$

where  $A_0$  is the cone distance (see Fig. 13-20), given by

$$A_0 = \frac{d_P}{2 \sin \gamma} = \frac{d_G}{2 \sin \Gamma} \quad (15-25)$$

### EXAMPLE 15-2

Design a straight-bevel gear mesh for shaft centerlines that intersect perpendicularly, to deliver 6.85 hp at 900 rev/min with a gear ratio of 3:1, temperature of 300°F, normal pressure angle of 20°, using a design factor of 2. The load is uniform-uniform. Although the minimum number of teeth on the pinion is 13, which will mesh with 31 or more teeth without interference, use a pinion of 20 teeth. The material is to be AGMA grade 1 and the teeth are to be crowned. The reliability goal is 0.995 with a pinion life of  $10^9$  revolutions.

#### Solution

First we list the a priori decisions and their immediate consequences.

*Function:* 6.85 hp at 900 rev/min, gear ratio  $m_G = 3$ , 300°F environment, neither gear straddle-mounted,  $K_{mb} = 1.25$  [Eq. (15-11)],  $R = 0.995$  at  $10^9$  revolutions of the pinion,

$$\text{Eq. (15-14): } (C_L)_G = 3.4822(10^9/3)^{-0.0602} = 1.068$$

$$(C_L)_P = 3.4822(10^9)^{-0.0602} = 1$$

$$\text{Eq. (15-15): } (K_L)_G = 1.683(10^9/3)^{-0.0323} = 0.8929$$

$$(K_L)_P = 1.683(10^9)^{-0.0323} = 0.8618$$

$$\text{Eq. (15-19): } K_R = 0.50 - 0.25 \log(1 - 0.995) = 1.075$$

$$C_R = \sqrt{K_R} = \sqrt{1.075} = 1.037$$

$$\text{Eq. (15-18): } K_T = C_T = (460 + 300)/710 = 1.070$$

*Design factor:*  $n_d = 2$ ,  $S_F = 2$ ,  $S_H = \sqrt{2} = 1.414$ .

*Tooth system:* crowned, straight-bevel gears, normal pressure angle  $20^\circ$ ,

$$\text{Eq. (15-13):} \quad K_x = 1$$

$$\text{Eq. (15-12):} \quad C_{xc} = 1.5.$$

With  $N_P = 20$  teeth,  $N_G = (3)20 = 60$  teeth and from Fig. 15-14,

$$\gamma = \tan^{-1}(N_P/N_G) = \tan^{-1}(20/60) = 18.43^\circ \quad \Gamma = \tan^{-1}(60/20) = 71.57^\circ$$

From Figs. 15-6 and 15-7,  $I = 0.0825$ ,  $J_P = 0.248$ , and  $J_G = 0.202$ . Note that  $J_P > J_G$ .

*Decision 1:* Trial diametral pitch,  $P_d = 8$  teeth/in.

$$\text{Eq. (15-10):} \quad K_s = 0.4867 + 0.2132/8 = 0.5134$$

$$d_P = N_P/P_d = 20/8 = 2.5 \text{ in}$$

$$d_G = 2.5(3) = 7.5 \text{ in}$$

$$v_t = \pi d_P n_P / 12 = \pi(2.5)900/12 = 589.0 \text{ ft/min}$$

$$W^t = 33\,000 \text{ hp}/v_t = 33\,000(6.85)/589.0 = 383.8 \text{ lbf}$$

$$\text{Eq. (15-25):} \quad A_0 = d_P/(2 \sin \gamma) = 2.5/(2 \sin 18.43^\circ) = 3.954 \text{ in}$$

*Eq. (15-24):*

$$F = \min(0.3A_0, 10/P_d) = \min[0.3(3.954), 10/8] = \min(1.186, 1.25) = 1.186 \text{ in}$$

*Decision 2:* Let  $F = 1.25$  in. Then,

$$\text{Eq. (15-9):} \quad C_s = 0.125(1.25) + 0.4375 = 0.5937$$

$$\text{Eq. (15-11):} \quad K_m = 1.25 + 0.0036(1.25)^2 = 1.256$$

*Decision 3:* Let the transmission accuracy number be 6. Then, from Eq. (15-6),

$$B = 0.25(12 - 6)^{2/3} = 0.8255$$

$$A = 50 + 56(1 - 0.8255) = 59.77$$

$$\text{Eq. (15-5):} \quad K_v = \left( \frac{59.77 + \sqrt{589.0}}{59.77} \right)^{0.8255} = 1.325$$

*Decision 4:* Pinion and gear material and treatment. Carburize and case-harden grade ASTM 1320 to

Core 21 HRC ( $H_B$  is 229 Brinell)

Case 55-64 HRC ( $H_B$  is 515 Brinell)

From Table 15-4,  $s_{ac} = 200\,000$  psi and from Table 15-6,  $s_{at} = 30\,000$  psi.

**Gear bending:** From Eq. (15-3), the bending stress is

$$(s_t)_G = \frac{W^t}{F} P_d K_o K_v \frac{K_s K_m}{K_x J_G} = \frac{383.8}{1.25} 8(1)1.325 \frac{0.5134(1.256)}{(1)0.202}$$

$$= 10\,390 \text{ psi}$$

The bending strength, from Eq. (15–4), is given by

$$(s_{wt})_G = \left( \frac{s_{at} K_L}{S_F K_T K_R} \right)_G = \frac{30\,000(0.8929)}{2(1.070)1.075} = 11\,640 \text{ psi}$$

The strength exceeds the stress by a factor of  $11\,640/10\,390 = 1.12$ , giving an actual factor of safety of  $(S_F)_G = 2(1.12) = 2.24$ .

**Pinion bending:** The bending stress can be found from

$$(s_t)_P = (s_t)_G \frac{J_G}{J_P} = 10\,390 \frac{0.202}{0.248} = 8463 \text{ psi}$$

The bending strength, again from Eq. (15–4), is given by

$$(s_{wt})_P = \left( \frac{s_{at} K_L}{S_F K_T K_R} \right)_P = \frac{30\,000(0.8618)}{2(1.070)1.075} = 11\,240 \text{ psi}$$

The strength exceeds the stress by a factor of  $11\,240/8463 = 1.33$ , giving an actual factor of safety of  $(S_F)_P = 2(1.33) = 2.66$ .

**Gear wear:** The load-induced contact stress for the pinion and gear, from Eq. (15–1), is

$$\begin{aligned} s_c &= C_p \left( \frac{W^t}{F d_p I} K_o K_v K_m C_s C_{xc} \right)^{1/2} \\ &= 2290 \left[ \frac{383.8}{1.25(2.5)0.0825} (1)1.325(1.256)0.5937(1.5) \right]^{1/2} \\ &= 107\,560 \text{ psi} \end{aligned}$$

From Eq. (15–2) the contact strength of the gear is

$$(s_{wc})_G = \left( \frac{s_{ac} C_L C_H}{S_H K_T C_R} \right)_G = \frac{200\,000(1.068)(1)}{\sqrt{2}(1.070)1.037} = 136\,120 \text{ psi}$$

The strength exceeds the stress by a factor of  $136\,120/107\,560 = 1.266$ , giving an actual factor of safety of  $(S_H)_G^2 = 1.266^2(2) = 3.21$ .

**Pinion wear:** From Eq. (15–2) the contact strength of the pinion is

$$(s_{wc})_P = \left( \frac{s_{ac} C_L C_H}{S_H K_T C_R} \right)_P = \frac{200\,000(1)(1)}{\sqrt{2}(1.070)1.037} = 127\,450 \text{ psi}$$

The strength exceeds the stress by a factor of  $136\,120/127\,450 = 1.068$ , giving an actual factor of safety of  $(S_H)_P^2 = 1.068^2(2) = 2.28$ .

The actual factors of safety are 2.24, 2.66, 3.21, and 2.28. Making a direct comparison of the factors, we note that the threat from gear bending and pinion wear are practically equal. We also note that three of the ratios are comparable. Our goal would be to make changes in the design decisions that drive the factors closer to 2. The next step would be to adjust the design variables. It is obvious that an iterative process is involved. We need a figure of merit to order the designs. A computer program clearly is desirable.

## 15-6

**Worm Gearing—AGMA Equation**

Since they are essentially nonenveloping worm gears, the *crossed helical gears*, shown in Fig. 15–16, can be considered with other worm gearing. Because the teeth of worm gears have *point contact* changing to *line contact* as the gears are used, worm gears are said to “wear in,” whereas other types “wear out.”

Crossed helical gears, and worm gears too, usually have a  $90^\circ$  shaft angle, though this need not be so. The relation between the shaft and helix angles is

$$\sum = \psi_P \pm \psi_G \quad (15-26)$$

where  $\sum$  is the shaft angle. The plus sign is used when both helix angles are of the same hand, and the minus sign when they are of opposite hand. The subscript  $P$  in Eq. (15–26) refers to the pinion (worm); the subscript  $W$  is used for this same purpose. The subscript  $G$  refers to the gear, also called *gear wheel*, *worm wheel*, or simply the *wheel*. Table 15–8 gives cylindrical worm dimensions common to worm and gear.

Section 13–11 introduced worm gears, and Sec. 13–17 developed the force analysis and efficiency of worm gearing to which we will refer. Here our interest is in strength and durability. Good proportions indicate the pitch worm diameter  $d$  falls in the range

$$\frac{C^{0.875}}{3} \leq d \leq \frac{C^{0.875}}{1.6} \quad (15-27)$$

**Figure 15–16**

View of the pitch cylinders of a pair of crossed helical gears.

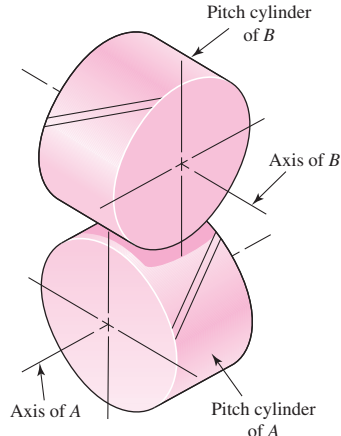


**Table 15–8**

Cylindrical Worm Dimensions Common to Both Worm and Gear\*

Quantity	Symbol	$\phi_n$		
		14.5°	20°	25°
Addendum	$a$	$0.3183p_x$	$0.3183p_x$	$0.286p_x$
Dedendum	$b$	$0.3683p_x$	$0.3683p_x$	$0.349p_x$
Whole depth	$h_t$	$0.6866p_x$	$0.6866p_x$	$0.635p_x$

\*The table entries are for a tangential diametral pitch of the gear of  $P_t = 1$ .

where  $C$  is the center-to-center distance.<sup>2</sup> AGMA relates the allowable tangential force on the worm-gear tooth ( $W^t$ )<sub>all</sub> to other parameters by

$$(W^t)_{\text{all}} = C_s D_m^{0.8} F_e C_m C_v \quad (15-28)$$

where  $C_s$  = materials factor

$D_m$  = mean gear diameter, in (mm)

$F_e$  = effective face width of the gear (actual face width, but not to exceed  $0.67d_m$ , the mean worm diameter), in (mm)

$C_m$  = ratio correction factor

$C_v$  = velocity factor

The friction force  $W_f$  is given by

$$W_f = \frac{f W^t}{\cos \lambda \cos \phi_n} \quad (15-29)$$

where  $f$  = coefficient of friction

$\lambda$  = lead angle at mean worm diameter

$\phi_n$  = normal pressure angle

The sliding velocity  $V_s$  is

$$V_s = \frac{\pi n_W d_m}{12 \cos \lambda} \quad (15-30)$$

where  $n_W$  = rotative speed of the worm and  $d_m$  = mean worm diameter. The torque at the worm gear is

$$T_G = \frac{W^t D_m}{2} \quad (15-31)$$

where  $D_m$  is the mean gear diameter.

The parameters in Eq. (15-28) are, quantitatively,

$$C_s = 270 + 10.37C^3 \quad C \leq 3 \text{ in} \quad (15-32)$$

For sand-cast gears,

$$C_s = \begin{cases} 1000 & C > 3 \quad d_G \leq 2.5 \text{ in} \\ 1190 - 477 \log d_G & C > 3 \quad d_G > 2.5 \text{ in} \end{cases} \quad (15-33)$$

For chilled-cast gears,

$$C_s = \begin{cases} 1000 & C > 3 \quad d_G \leq 8 \text{ in} \\ 1412 - 456 \log d_G & C > 3 \quad d_G > 8 \text{ in} \end{cases} \quad (15-34)$$

---

<sup>2</sup>ANSI/AGMA 6034-B92, February 1992, *Practice for Enclosed Cylindrical Wormgear Speed-Reducers and Gear Motors*; and ANSI/AGMA 6022-C93, Dec. 1993, *Design Manual for Cylindrical Wormgearing*.

Note: Equations (15-32) to (15-38) are contained in Annex C of 6034-B92 for informational purposes only. To comply with ANSI/AGMA 6034-B92, use the tabulations of these rating factors provided in the standard.

For centrifugally cast gears,

$$C_s = \begin{cases} 1000 & C > 3 \\ 1251 - 180 \log d_G & C > 3 \end{cases} \quad \begin{array}{ll} d_G \leq 25 \text{ in} & \\ d_G > 25 \text{ in} & \end{array} \quad (15-35)$$

The ratio correction factor  $C_m$  is given by

$$C_m = \begin{cases} 0.02\sqrt{-m_G^2 + 40m_G - 76} + 0.46 & 3 < m_G \leq 20 \\ 0.0107\sqrt{-m_G^2 + 56m_G + 5145} & 20 < m_G \leq 76 \\ 1.1483 - 0.00658m_G & m_G > 76 \end{cases} \quad (15-36)$$

The velocity factor  $C_v$  is given by

$$C_v = \begin{cases} 0.659 \exp(-0.0011V_s) & V_s < 700 \text{ ft/min} \\ 13.31V_s^{-0.571} & 700 \leq V_s < 3000 \text{ ft/min} \\ 65.52V_s^{-0.774} & V_s > 3000 \text{ ft/min} \end{cases} \quad (15-37)$$

AGMA reports the coefficient of friction  $f$  as

$$f = \begin{cases} 0.15 & V_s = 0 \\ 0.124 \exp(-0.074V_s^{0.645}) & 0 < V_s \leq 10 \text{ ft/min} \\ 0.103 \exp(-0.110V_s^{0.450}) + 0.012 & V_s > 10 \text{ ft/min} \end{cases} \quad (15-38)$$

Now we examine some worm-gear mesh geometry. The addendum  $a$  and dedendum  $b$  are

$$a = \frac{p_x}{\pi} = 0.3183p_x \quad (15-39)$$

$$b = \frac{1.157p_x}{\pi} = 0.3683p_x \quad (15-40)$$

The full depth  $h_t$  is

$$h_t = \begin{cases} \frac{2.157p_x}{\pi} = 0.6866p_x & p_x \geq 0.16 \text{ in} \\ \frac{2.200p_x}{\pi} + 0.002 = 0.7003p_x + 0.002 & p_x < 0.16 \text{ in} \end{cases} \quad (15-41)$$

The worm outside diameter  $d_0$  is

$$d_0 = d + 2a \quad (15-42)$$

The worm root diameter  $d_r$  is

$$d_r = d - 2b \quad (15-43)$$

The worm-gear throat diameter  $D_t$  is

$$D_t = D + 2a \quad (15-44)$$

where  $D$  is the worm-gear pitch diameter. The worm-gear root diameter  $D_r$  is

$$D_r = D - 2b \quad (15-45)$$

The clearance  $c$  is

$$c = b - a \quad (15-46)$$

The worm face width (maximum)  $(F_W)_{\max}$  is

$$(F_W)_{\max} = 2\sqrt{\left(\frac{D_t}{2}\right)^2 - \left(\frac{D}{2} - a\right)^2} = 2\sqrt{2Da} \quad (15-47)$$

which was simplified using Eq. (15-44). The worm-gear face width  $F_G$  is

$$F_G = \begin{cases} 2d_m/3 & p_x > 0.16 \text{ in} \\ 1.125\sqrt{(d_0 + 2c)^2 - (d_0 - 4a)^2} & p_x \leq 0.16 \text{ in} \end{cases} \quad (15-48)$$

The heat loss rate  $H_{\text{loss}}$  from the worm-gear case in  $\text{ft} \cdot \text{lbf}/\text{min}$  is

$$H_{\text{loss}} = 33\,000(1 - e)H_{\text{in}} \quad (15-49)$$

where  $e$  is efficiency, given by Eq. (13-46), and  $H_{\text{in}}$  is the input horsepower from the worm. The overall coefficient  $h_{\text{CR}}$  for combined convective and radiative heat transfer from the worm-gear case in  $\text{ft} \cdot \text{lbf}/(\text{min} \cdot \text{in}^2 \cdot {}^\circ\text{F})$  is

$$h_{\text{CR}} = \begin{cases} \frac{n_w}{6494} + 0.13 & \text{no fan on worm shaft} \\ \frac{n_w}{3939} + 0.13 & \text{fan on worm shaft} \end{cases} \quad (15-50)$$

When the case lateral area  $A$  is expressed in  $\text{in}^2$ , the temperature of the oil sump  $t_s$  is given by

$$t_s = t_a + \frac{H_{\text{loss}}}{h_{\text{CR}}A} = \frac{33\,000(1 - e)(H_{\text{in}})}{h_{\text{CR}}A} + t_a \quad (15-51)$$

Bypassing Eqs. (15-49), (15-50), and (15-51) one can apply the AGMA recommendation for minimum lateral area  $A_{\min}$  in  $\text{in}^2$  using

$$A_{\min} = 43.20C^{1.7} \quad (15-52)$$

Because worm teeth are inherently much stronger than worm-gear teeth, they are not considered. The teeth in worm gears are short and thick on the edges of the face; midplane they are thinner as well as curved. Buckingham<sup>3</sup> adapted the Lewis equation for this case:

$$\sigma_a = \frac{W_G^t}{p_n F_e y} \quad (15-53)$$

where  $p_n = p_x \cos \lambda$  and  $y$  is the Lewis form factor related to circular pitch. For  $\phi_n = 14.5^\circ$ ,  $y = 0.100$ ;  $\phi_n = 20^\circ$ ,  $y = 0.125$ ;  $\phi_n = 25^\circ$ ,  $y = 0.150$ ;  $\phi_n = 30^\circ$ ,  $y = 0.175$ .

<sup>3</sup>Earle Buckingham, *Analytical Mechanics of Gears*, McGraw-Hill, New York, 1949, p. 495.

## 15-7 Worm-Gear Analysis

Compared to other gearing systems worm-gear meshes have a much lower mechanical efficiency. Cooling, for the benefit of the lubricant, becomes a design constraint sometimes resulting in what appears to be an oversize gear case in light of its contents. If the heat can be dissipated by natural cooling, or simply with a fan on the wormshaft, simplicity persists. Water coils within the gear case or lubricant outpumping to an external cooler is the next level of complexity. For this reason, gear-case area is a design decision.

To reduce cooling load, use multiple-thread worms. Also keep the worm pitch diameter as small as possible.

Multiple-thread worms can remove the self-locking feature of many worm-gear drives. When the worm drives the gearset, the mechanical efficiency  $e_W$  is given by

$$e_W = \frac{\cos \phi_n - f \tan \lambda}{\cos \phi_n + f \cot \lambda} \quad (15-54)$$

With the gear driving the gearset, the mechanical efficiency  $e_G$  is given by

$$e_G = \frac{\cos \phi_n - f \cot \lambda}{\cos \phi_n + f \tan \lambda} \quad (15-55)$$

To ensure that the worm gear will drive the worm,

$$f_{\text{stat}} < \cos \phi_n \tan \lambda \quad (15-56)$$

where values of  $f_{\text{stat}}$  can be found in ANSI/AGMA 6034-B92. To prevent the worm gear from driving the worm, refer to clause 9 of 6034-B92 for a discussion of self-locking in the static condition.

It is important to have a way to relate the tangential component of the gear force  $W_G^t$  to the tangential component of the worm force  $W_W^t$ , which includes the role of friction and the angularities of  $\phi_n$  and  $\lambda$ . Refer to Eq. (13-45) solved for  $W_W^t$ :

$$W_W^t = W_G^t \frac{\cos \phi_n \sin \lambda + f \cos \lambda}{\cos \phi_n \cos \lambda - f \sin \lambda} \quad (15-57)$$

In the absence of friction

$$W_W^t = W_G^t \tan \lambda$$

The mechanical efficiency of most gearing is very high, which allows power in and power out to be used almost interchangeably. Worm gearsets have such poor efficiencies that we work with, and speak of, output power. The magnitude of the gear transmitted force  $W_G^t$  can be related to the output horsepower  $H_0$ , the application factor  $K_a$ , the efficiency  $e$ , and design factor  $n_d$  by

$$W_G^t = \frac{33\,000 n_d H_0 K_a}{V_G e} \quad (15-58)$$

We use Eq. (15-57) to obtain the corresponding worm force  $W_W^t$ . It follows that

$$H_W = \frac{W_W^t V_W}{33\,000} = \frac{\pi d_W n_W W_W^t}{12(33\,000)} \text{ hp} \quad (15-59)$$

$$H_G = \frac{W_G^t V_G}{33\,000} = \frac{\pi d_G n_G W_G^t}{12(33\,000)} \text{ hp} \quad (15-60)$$

**Table 15–9**

	<b><math>\phi_n</math></b>	<b>Maximum Lead Angle <math>\lambda_{\max}</math></b>
Largest Lead Angle		
Associated with a	14.5°	16°
Normal Pressure Angle	20°	25°
$\phi_n$ for Worm Gearing	25°	35°
	30°	45°

From Eq. (13–44),

$$W_f = \frac{f W_G^t}{f \sin \lambda - \cos \phi_n \cos \lambda} \quad (15-61)$$

The sliding velocity of the worm at the pitch cylinder  $V_s$  is

$$V_s = \frac{\pi d n_W}{12 \cos \lambda} \quad (15-62)$$

and the friction power  $H_f$  is given by

$$H_f = \frac{|W_f| V_s}{33,000} \text{ hp} \quad (15-63)$$

Table 15–9 gives the largest lead angle  $\lambda_{\max}$  associated with normal pressure angle  $\phi_n$ .

### EXAMPLE 15–3

A single-thread steel worm rotates at 1800 rev/min, meshing with a 24-tooth worm gear transmitting 3 hp to the output shaft. The worm pitch diameter is 3 in and the tangential diametral pitch of the gear is 4 teeth/in. The normal pressure angle is 14.5°. The ambient temperature is 70°F. The application factor is 1.25 and the design factor is 1; gear face width is 2 in, lateral case area 600 in<sup>2</sup>, and the gear is chill-cast bronze.

- (a) Find the gear geometry.
- (b) Find the transmitted gear forces and the mesh efficiency.
- (c) Is the mesh sufficient to handle the loading?
- (d) Estimate the lubricant sump temperature.

#### Solution

(a)  $m_G = N_G/N_W = 24/1 = 24$ , gear:  $D = N_G/P_t = 24/4 = 6.000$  in, worm:  $d = 3.000$  in. The axial circular pitch  $p_x$  is  $p_x = \pi/P_t = \pi/4 = 0.7854$  in.  $C = (3 + 6)/2 = 4.5$  in.

$$\text{Eq. (15–39): } a = p_x/\pi = 0.7854/\pi = 0.250 \text{ in}$$

$$\text{Eq. (15–40): } b = 0.3683 p_x = 0.3683(0.7854) = 0.289 \text{ in}$$

$$\text{Eq. (15–41): } h_t = 0.6866 p_x = 0.6866(0.7854) = 0.539 \text{ in}$$

$$\text{Eq. (15–42): } d_0 = 3 + 2(0.250) = 3.500 \text{ in}$$

$$\text{Eq. (15–43): } d_r = 3 - 2(0.289) = 2.422 \text{ in}$$

$$\text{Eq. (15–44): } D_t = 6 + 2(0.250) = 6.500 \text{ in}$$

$$\text{Eq. (15–45): } D_r = 6 - 2(0.289) = 5.422 \text{ in}$$

$$\text{Eq. (15–46): } c = 0.289 - 0.250 = 0.039 \text{ in}$$

$$\text{Eq. (15–47): } (F_w)_{\max} = 2\sqrt{2(6)0.250} = 3.464 \text{ in}$$

The tangential speeds of the worm,  $V_W$ , and gear,  $V_G$ , are, respectively,

$$V_W = \pi(3)1800/12 = 1414 \text{ ft/min} \quad V_G = \frac{\pi(6)1800/24}{12} = 117.8 \text{ ft/min}$$

The lead of the worm, from Eq. (13–27), is  $L = p_x N_W = 0.7854(1) = 0.7854$  in. The lead angle  $\lambda$ , from Eq. (13–28), is

$$\lambda = \tan^{-1} \frac{L}{\pi d} = \tan^{-1} \frac{0.7854}{\pi(3)} = 4.764^\circ$$

The normal diametral pitch for a worm gear is the same as for a helical gear, which from Eq. (13–18) with  $\psi = \lambda$  is

$$P_n = \frac{P_t}{\cos \lambda} = \frac{4}{\cos 4.764^\circ} = 4.014$$

$$p_n = \frac{\pi}{P_n} = \frac{\pi}{4.014} = 0.7827 \text{ in}$$

The sliding velocity, from Eq. (15–62), is

$$V_s = \frac{\pi d n_W}{12 \cos \lambda} = \frac{\pi(3)1800}{12 \cos 4.764^\circ} = 1419 \text{ ft/min}$$

(b) The coefficient of friction, from Eq. (15–38), is

$$f = 0.103 \exp[-0.110(1419)^{0.450}] + 0.012 = 0.0178$$

The efficiency  $e$ , from Eq. (13–46), is

**Answer**

$$e = \frac{\cos \phi_n - f \tan \lambda}{\cos \phi_n + f \cot \lambda} = \frac{\cos 14.5^\circ - 0.0178 \tan 4.764^\circ}{\cos 14.5^\circ + 0.0178 \cot 4.764^\circ} = 0.818$$

The designer used  $n_d = 1$ ,  $K_a = 1.25$  and an output horsepower of  $H_0 = 3$  hp. The gear tangential force component  $W_G^t$ , from Eq. (15–58), is

**Answer**

$$W_G^t = \frac{33\,000 n_d H_0 K_a}{V_G e} = \frac{33\,000(1)3(1.25)}{117.8(0.818)} = 1284 \text{ lbf}$$

**Answer** The tangential force on the worm is given by Eq. (15–57):

$$W_W^t = W_G^t \frac{\cos \phi_n \sin \lambda + f \cos \lambda}{\cos \phi_n \cos \lambda - f \sin \lambda}$$

$$= 1284 \frac{\cos 14.5^\circ \sin 4.764^\circ + 0.0178 \cos 4.764^\circ}{\cos 14.5^\circ \cos 4.764^\circ - 0.0178 \sin 4.764^\circ} = 131 \text{ lbf}$$

(c)

Eq. (15–34):  $C_s = 1000$

Eq. (15–36):  $C_m = 0.0107 \sqrt{-24^2 + 56(24) + 5145} = 0.823$

Eq. (15–37):  $C_v = 13.31(1419)^{-0.571} = 0.211^4$

---

<sup>4</sup>Note: From ANSI/AGMA 6034-B92, the rating factors are  $C_s = 1000$ ,  $C_m = 0.825$ ,  $C_v = 0.214$ , and  $f = 0.0185$ .

$$\text{Eq. (15-28): } (W^t)_{\text{all}} = C_s D^{0.8} (F_e)_G C_m C_v \\ = 1000(6)^{0.8}(2)0.823(0.211) = 1456 \text{ lbf}$$

Since  $W_G^t < (W^t)_{\text{all}}$ , the mesh will survive at least 25 000 h. The friction force  $W_f$  is given by Eq. (15-61):

$$W_f = \frac{f W_G^t}{f \sin \lambda - \cos \phi_n \cos \lambda} = \frac{0.0178(1284)}{0.0178 \sin 4.764^\circ - \cos 14.5^\circ \cos 4.764^\circ} \\ = -23.7 \text{ lbf}$$

The power dissipated in frictional work  $H_f$  is given by Eq. (15-63):

$$H_f = \frac{|W_f| V_s}{33 \text{ 000}} = \frac{|-23.7| 1419}{33 \text{ 000}} = 1.02 \text{ hp}$$

The worm and gear powers,  $H_W$  and  $H_G$ , are given by

$$H_W = \frac{W_W^t V_W}{33 \text{ 000}} = \frac{131(1414)}{33 \text{ 000}} = 5.61 \text{ hp} \quad H_G = \frac{W_G^t V_G}{33 \text{ 000}} = \frac{1284(117.8)}{33 \text{ 000}} = 4.58 \text{ hp}$$

**Answer** Gear power is satisfactory. Now,

$$P_n = P_t / \cos \lambda = 4 / \cos 4.764^\circ = 4.014$$

$$p_n = \pi / P_n = \pi / 4.014 = 0.7827 \text{ in}$$

The bending stress in a gear tooth is given by Buckingham's adaptation of the Lewis equation, Eq. (15-53), as

$$(\sigma)_G = \frac{W_G^t}{p_n F_G y} = \frac{1284}{0.7827(2)(0.1)} = 8200 \text{ psi}$$

**Answer** Stress in gear satisfactory.

(d)

$$\text{Eq. (15-52): } A_{\min} = 43.2 C^{1.7} = 43.2(4.5)^{1.7} = 557 \text{ in}^2$$

The gear case has a lateral area of 600 in<sup>2</sup>.

$$\text{Eq. (15-49): } H_{\text{loss}} = 33 \text{ 000}(1 - e) H_{\text{in}} = 33 \text{ 000}(1 - 0.818)5.61 \\ = 33 \text{ 690 ft} \cdot \text{lbf/min}$$

$$\text{Eq. (15-50): } \bar{h}_{\text{CR}} = \frac{n_w}{3939} + 0.13 = \frac{1800}{3939} + 0.13 = 0.587 \text{ ft} \cdot \text{lbf}/(\text{min} \cdot \text{in}^2 \cdot {}^\circ\text{F})$$

**Answer** Eq. (15-51):  $t_s = t_a + \frac{H_{\text{loss}}}{\bar{h}_{\text{CR}} A} = 70 + \frac{33 \text{ 690}}{0.587(600)} = 166 {}^\circ\text{F}$

## 15-8 Designing a Worm-Gear Mesh

A usable decision set for a worm-gear mesh includes

- Function: power, speed,  $m_G$ ,  $K_a$
- Design factor:  $n_d$
- Tooth system
- Materials and processes
- Number of threads on the worm:  $N_W$
- Axial pitch of worm:  $p_x$
- Pitch diameter of the worm:  $d_W$
- Face width of gear:  $F_G$
- Lateral area of case:  $A$

A priori decisions  
Design variables

Reliability information for worm gearing is not well developed at this time. The use of Eq. (15–28) together with the factors  $C_s$ ,  $C_m$ , and  $C_v$ , with an alloy steel case-hardened worm together with customary nonferrous worm-wheel materials, will result in lives in excess of 25 000 h. The worm-gear materials in the experience base are principally bronzes:

- Tin- and nickel-bronzes (chilled-casting produces hardest surfaces)
- Lead-bronze (high-speed applications)
- Aluminum- and silicon-bronze (heavy load, slow-speed application)

The factor  $C_s$  for bronze in the spectrum sand-cast, chilled-cast, and centrifugally cast increases in the same order.

Standardization of tooth systems is not as far along as it is in other types of gearing. For the designer this represents freedom of action, but acquisition of tooling for tooth-forming is more of a problem for in-house manufacturing. When using a subcontractor the designer must be aware of what the supplier is capable of providing with on-hand tooling.

Axial pitches for the worm are usually integers, and quotients of integers are common. Typical pitches are  $\frac{1}{4}$ ,  $\frac{5}{16}$ ,  $\frac{3}{8}$ ,  $\frac{1}{2}$ ,  $\frac{3}{4}$ , 1,  $\frac{5}{4}$ ,  $\frac{6}{4}$ ,  $\frac{7}{4}$ , and 2, but others are possible. Table 15–8 shows dimensions common to both worm gear and cylindrical worm for proportions often used. Teeth frequently are stubbed when lead angles are  $30^\circ$  or larger.

Worm-gear design is constrained by available tooling, space restrictions, shaft center-to-center distances, gear ratios needed, and the designer's experience. ANSI/AGMA 6022-C93, *Design Manual for Cylindrical Wormgearing* offers the following guidance. Normal pressure angles are chosen from  $14.5^\circ$ ,  $17.5^\circ$ ,  $20^\circ$ ,  $22.5^\circ$ ,  $25^\circ$ ,  $27.5^\circ$ , and  $30^\circ$ . The recommended minimum number of gear teeth is given in Table 15–10. The normal range of the number of threads on the worm is 1 through 10. Mean worm pitch diameter is usually chosen in the range given by Eq. (15–27).

A design decision is the axial pitch of the worm. Since acceptable proportions are couched in terms of the center-to-center distance, which is not yet known, one chooses a trial axial pitch  $p_x$ . Having  $N_W$  and a trial worm diameter  $d$ ,

$$N_G = m_G N_W \quad P_t = \frac{\pi}{p_x} \quad D = \frac{N_G}{P_t}$$

**Table 15-10**

	$\phi_n$	$(N_G)_{\min}$
Minimum Number of Gear Teeth for Normal Pressure Angle $\phi_n$	14.5	40
	17.5	27
	20	21
	22.5	17
	25	14
	27.5	12
	30	10

Then

$$(d)_{lo} = C^{0.875}/3 \quad (d)_{hi} = C^{0.875}/1.6$$

Examine  $(d)_{lo} \leq d \leq (d)_{hi}$ , and refine the selection of mean worm-pitch diameter to  $d_1$  if necessary. Recompute the center-to-center distance as  $C = (d_1 + D)/2$ . There is even an opportunity to make  $C$  a round number. Choose  $C$  and set

$$d_2 = 2C - D$$

Equations (15-39) through (15-48) apply to one usual set of proportions.

### EXAMPLE 15-4

Design a 10-hp 11:1 worm-gear speed-reducer mesh for a lumber mill planer feed drive for 3- to 10-h daily use. A 1720-rev/min squirrel-cage induction motor drives the planer feed ( $K_a = 1.25$ ), and the ambient temperature is 70°F.

#### Solution

*Function:*  $H_0 = 10$  hp,  $m_G = 11$ ,  $n_W = 1720$  rev/min.

*Design factor:*  $n_d = 1.2$ .

*Materials and processes:* case-hardened alloy steel worm, sand-cast bronze gear.

*Worm threads:* double,  $N_W = 2$ ,  $N_G = m_G N_W = 11(2) = 22$  gear teeth acceptable for  $\phi_n = 20^\circ$ , according to Table 15-10.

*Decision 1:* Choose an axial pitch of worm  $p_x = 1.5$  in. Then,

$$P_t = \pi/p_x = \pi/1.5 = 2.0944$$

$$D = N_G/P_t = 22/2.0944 = 10.504 \text{ in}$$

$$\text{Eq. (15-39): } a = 0.3183p_x = 0.3183(1.5) = 0.4775 \text{ in (addendum)}$$

$$\text{Eq. (15-40): } b = 0.3683(1.5) = 0.5525 \text{ in (dedendum)}$$

$$\text{Eq. (15-41): } h_t = 0.6866(1.5) = 1.030 \text{ in}$$

*Decision 2:* Choose a mean worm diameter  $d = 2.000$  in. Then

$$C = (d + D)/2 = (2.000 + 10.504)/2 = 6.252 \text{ in}$$

$$(d)_{lo} = 6.252^{0.875}/3 = 1.657 \text{ in}$$

$$(d)_{hi} = 6.252^{0.875}/1.6 = 3.107 \text{ in}$$

The range, given by Eq. (15-27), is  $1.657 \leq d \leq 3.107$  in, which is satisfactory. Try  $d = 2.500$  in. Recompute  $C$ :

$$C = (2.5 + 10.504)/2 = 6.502 \text{ in}$$

The range is now  $1.715 \leq d \leq 3.216$  in, which is still satisfactory. Decision:  $d = 2.500$  in. Then

$$\text{Eq. (13-27):} \quad L = p_x N_W = 1.5(2) = 3.000 \text{ in}$$

$$\text{Eq. (13-28):}$$

$$\lambda = \tan^{-1}[L/(\pi d)] = \tan^{-1}[3/(\pi 2.5)] = 20.905^\circ \quad (\text{from Table 15-9 lead angle OK})$$

$$\text{Eq. (15-62):} \quad V_s = \frac{\pi d n_W}{12 \cos \lambda} = \frac{\pi (2.5) 1720}{12 \cos 20.905^\circ} = 1205.1 \text{ ft/min}$$

$$V_W = \frac{\pi d n_W}{12} = \frac{\pi (2.5) 1720}{12} = 1125.7 \text{ ft/min}$$

$$V_G = \frac{\pi D n_G}{12} = \frac{\pi (10.504) 1720 / 11}{12} = 430.0 \text{ ft/min}$$

$$\text{Eq. (15-33):} \quad C_s = 1190 - 477 \log 10.504 = 702.8$$

$$\text{Eq. (15-36):} \quad C_m = 0.02\sqrt{-11^2 + 40(11) - 76} + 0.46 = 0.772$$

$$\text{Eq. (15-37):} \quad C_v = 13.31(1205.1)^{-0.571} = 0.232$$

$$\text{Eq. (15-38):} \quad f = 0.103 \exp[-0.11(1205.1)^{0.45}] + 0.012 = 0.0191^5$$

$$\text{Eq. (15-54):} \quad e_W = \frac{\cos 20^\circ - 0.0191 \tan 20.905^\circ}{\cos 20^\circ + 0.0191 \cot 20.905^\circ} = 0.942$$

(If the worm gear drives,  $e_G = 0.939$ .) To ensure nominal 10-hp output, with adjustments for  $K_a$ ,  $n_d$ , and  $e$ ,

$$\text{Eq. (15-57):} \quad W_W^t = 1222 \frac{\cos 20^\circ \sin 20.905^\circ + 0.0191 \cos 20.905^\circ}{\cos 20^\circ \cos 20.905^\circ - 0.0191 \sin 20.905^\circ} = 495.4 \text{ lbf}$$

$$\text{Eq. (15-58):} \quad W_G^t = \frac{33\ 000(1.2)10(1.25)}{430(0.942)} = 1222 \text{ lbf}$$

$$\text{Eq. (15-59):} \quad H_W = \frac{\pi(2.5)1720(495.4)}{12(33\ 000)} = 16.9 \text{ hp}$$

$$\text{Eq. (15-60):} \quad H_G = \frac{\pi(10.504)1720/11(1222)}{12(33\ 000)} = 15.92 \text{ hp}$$

$$\text{Eq. (15-61):} \quad W_f = \frac{0.0191(1222)}{0.0191 \sin 20.905^\circ - \cos 20^\circ \cos 20.905^\circ} = -26.8 \text{ lbf}$$

$$\text{Eq. (15-63):} \quad H_f = \frac{|-26.8|1205.1}{33\ 000} = 0.979 \text{ hp}$$

With  $C_s = 702.8$ ,  $C_m = 0.772$ , and  $C_v = 0.232$ ,

$$(F_e)_{\text{req}} = \frac{W_G^t}{C_s D^{0.8} C_m C_v} = \frac{1222}{702.8(10.504)^{0.8} 0.772(0.232)} = 1.479 \text{ in}$$

---

<sup>5</sup>Note: From ANSI/AGMA 6034-B92, the rating factors are  $C_s = 703$ ,  $C_m = 0.773$ ,  $C_v = 0.2345$ , and  $f = 0.01995$ .

*Decision 3:* The available range of  $(F_e)_G$  is  $1.479 \leq (F_e)_G \leq 2d/3$  or  $1.479 \leq (F_e)_G \leq 1.667$  in. Set  $(F_e)_G = 1.5$  in.

$$\text{Eq. (15-28): } W_{\text{all}}^t = 702.8(10.504)^{0.8}1.5(0.772)0.232 = 1239 \text{ lbf}$$

This is greater than 1222 lbf. There is a little excess capacity. The force analysis stands.

*Decision 4:*

$$\text{Eq. (15-50): } \dot{h}_{\text{CR}} = \frac{n_W}{6494} + 0.13 = \frac{1720}{6494} + 0.13 = 0.395 \text{ ft} \cdot \text{lbf}/(\text{min} \cdot \text{in}^2 \cdot {}^\circ\text{F})$$

$$\text{Eq. (15-49): } H_{\text{loss}} = 33\ 000(1 - e)H_W = 33\ 000(1 - 0.942)16.9 = 32\ 347 \text{ ft} \cdot \text{lbf}/\text{min}$$

The AGMA area, from Eq. (15-52), is  $A_{\text{min}} = 43.2C^{1.7} = 43.2(6.502)^{1.7} = 1041.5 \text{ in}^2$ . A rough estimate of the lateral area for 6-in clearances:

$$\text{Vertical: } d + D + 6 = 2.5 + 10.5 + 6 = 19 \text{ in}$$

$$\text{Width: } D + 6 = 10.5 + 6 = 16.5 \text{ in}$$

$$\text{Thickness: } d + 6 = 2.5 + 6 = 8.5 \text{ in}$$

$$\text{Area: } 2(19)16.5 + 2(8.5)19 + 16.5(8.5) \doteq 1090 \text{ in}^2$$

Expect an area of 1100 in<sup>2</sup>. Choose: Air-cooled, no fan on worm, with an ambient temperature of 70°F.

$$t_s = t_a + \frac{H_{\text{loss}}}{\dot{h}_{\text{CR}}A} = 70 + \frac{32\ 350}{0.395(1100)} = 70 + 74.5 = 144.5 {}^\circ\text{F}$$

Lubricant is safe with some margin for smaller area.

$$\text{Eq. (13-18): } P_n = \frac{P_t}{\cos \lambda} = \frac{2.094}{\cos 20.905^\circ} = 2.242$$

$$p_n = \frac{\pi}{P_n} = \frac{\pi}{2.242} = 1.401 \text{ in}$$

Gear bending stress, for reference, is

$$\text{Eq. (15-53): } \sigma = \frac{W_G^t}{p_n F_{ey}} = \frac{1222}{1.401(1.5)0.125} = 4652 \text{ psi}$$

The risk is from wear, which is addressed by the AGMA method that provides  $(W_G^t)_{\text{all}}$ .

## 15-9 Buckingham Wear Load

A precursor to the AGMA method was the method of Buckingham, which identified an allowable wear load in worm gearing. Buckingham showed that the allowable gear-tooth loading for wear can be estimated from

$$(W_G^t)_{\text{all}} = K_w d_G F_e \quad (15-64)$$

where  $K_w$  = worm-gear load factor

$d_G$  = gear-pitch diameter

$F_e$  = worm-gear effective face width

**Table 15-11**

Wear Factor  $K_w$  for Worm Gearing

*Source:* Earle Buckingham, *Design of Worm and Spiral Gears*, Industrial Press, New York, 1981.

<b>Worm</b>	<b>Gear</b>	<b>Material</b>	<b>Thread Angle <math>\phi_n</math></b>			
			<b>14<math>\frac{1}{2}</math></b>	<b>20°</b>	<b>25°</b>	<b>30°</b>
Hardened steel*	Chilled bronze	90	125	150	180	
Hardened steel*	Bronze	60	80	100	120	
Steel, 250 BHN (min.)	Bronze	36	50	60	72	
High-test cast iron	Bronze	80	115	140	165	
Gray iron†	Aluminum	10	12	15	18	
High-test cast iron	Gray iron	90	125	150	180	
High-test cast iron	Cast steel	22	31	37	45	
High-test cast iron	High-test cast iron	135	185	225	270	
Steel 250 BHN (min.)	Laminated phenolic	47	64	80	95	
Gray iron	Laminated phenolic	70	96	120	140	

\*Over 500 BHN surface.

†For steel worms, multiply given values by 0.6.

Table 15–11 gives values for  $K_w$  for worm gearsets as a function of the material pairing and the normal pressure angle.

### EXAMPLE 15-5

Estimate the allowable gear wear load ( $W_G^t$ )<sub>all</sub> for the gearset of Ex. 15–4 using Buckingham's wear equation.

#### Solution

From Table 15–11 for a hardened steel worm and a bronze gear,  $K_w$  is given as 80 for  $\phi_n = 20^\circ$ . Equation (15–64) gives

$$(W_G^t)_{\text{all}} = 80(10.504)1.5 = 1260 \text{ lbf}$$

which is larger than the 1239 lbf of the AGMA method. The method of Buckingham does not have refinements of the AGMA method. [Is  $(W_G^t)_{\text{all}}$  linear with gear diameter?]

For material combinations not addressed by AGMA, Buckingham's method allows quantitative treatment.

## PROBLEMS

### 15-1

An uncrowned straight-bevel pinion has 20 teeth, a diametral pitch of 6 teeth/in, and a transmission accuracy number of 6. Both the pinion and gear are made of through-hardened steel with a Brinell hardness of 300. The driven gear has 60 teeth. The gearset has a life goal of  $10^9$  revolutions of the pinion with a reliability of 0.999. The shaft angle is  $90^\circ$ ; the pinion speed is 900 rev/min. The face width is 1.25 in, and the normal pressure angle is  $20^\circ$ . The pinion is mounted outboard of its bearings, and the gear is straddle-mounted. Based on the AGMA bending strength, what is the power rating of the gearset? Use  $K_0 = 1$ ,  $S_F = 1$ , and  $S_H = 1$ .

**15-2** For the gearset and conditions of Prob. 15–1, find the power rating based on the AGMA surface durability.

**15-3** An uncrowned straight-bevel pinion has 30 teeth, a diametral pitch of 6, and a transmission accuracy number of 6. The driven gear has 60 teeth. Both are made of No. 30 cast iron. The shaft angle is  $90^\circ$ . The face width is 1.25 in, the pinion speed is 900 rev/min, and the normal pressure angle is  $20^\circ$ . The pinion is mounted outboard of its bearings; the bearings of the gear straddle it. What is the power rating based on AGMA bending strength? (For cast iron gearsets reliability information has not yet been developed. We say the life is greater than  $10^7$  revolutions; set  $K_L = 1$ ,  $C_L = 1$ ,  $C_R = 1$ ,  $K_R = 1$ ; and apply a factor of safety. Use  $S_F = 2$  and  $S_H = \sqrt{2}$ .)

**15-4** For the gearset and conditions of Prob. 15–3, find the power rating based on AGMA surface durability. For the solutions to Probs. 15–3 and 15–4, what is the power rating of the gearset?

**15-5** An uncrowned straight-bevel pinion has 22 teeth, a module of 4 mm, and a transmission accuracy number of 5. The pinion and the gear are made of through-hardened steel, both having core and case hardnesses of 180 Brinell. The pinion drives the 24-tooth bevel gear. The shaft angle is  $90^\circ$ , the pinion speed is 1800 rev/min, the face width is 25 mm, and the normal pressure angle is  $20^\circ$ . Both gears have an outboard mounting. Find the power rating based on AGMA pitting resistance if the life goal is  $10^9$  revolutions of the pinion at 0.999 reliability.

**15-6** For the gearset and conditions of Prob. 15–5, find the power rating for AGMA bending strength.

**15-7** In straight-bevel gearing, there are some analogs to Eqs. (14–44) and (14–45). If we have a pinion core with a hardness of  $(H_B)_{11}$  and we try equal power ratings, the transmitted load  $W^t$  can be made equal in all four cases. It is possible to find these relations:

	<b>Core</b>	<b>Case</b>
Pinion	$(H_B)_{11}$	$(H_B)_{12}$
Gear	$(H_B)_{21}$	$(H_B)_{22}$

(a) For carburized case-hardened gear steel with core AGMA bending strength  $(s_{at})_G$  and pinion core strength  $(s_{at})_P$ , show that the relationship is

$$(s_{at})_G = (s_{at})_P \frac{J_P}{J_G} m_G^{-0.0323}$$

This allows  $(H_B)_{21}$  to be related to  $(H_B)_{11}$ .

(b) Show that the AGMA contact strength of the gear case  $(s_{ac})_G$  can be related to the AGMA core bending strength of the pinion core  $(s_{at})_P$  by

$$(s_{ac})_G = \frac{C_p}{(C_L)_G C_H} \sqrt{\frac{S_H^2}{S_F} \frac{(s_{at})_P (K_L)_P K_x J_P K_T C_s C_{xc}}{N_P I K_s}}$$

If factors of safety are applied to the transmitted load  $W_t$ , then  $S_H = \sqrt{S_F}$  and  $S_H^2/S_F$  is unity. The result allows  $(H_B)_{22}$  to be related to  $(H_B)_{11}$ .

(c) Show that the AGMA contact strength of the gear  $(s_{ac})_G$  is related to the contact strength of the pinion  $(s_{ac})_P$  by

$$(s_{ac})_P = (s_{ac})_G m_G^{0.0602} C_H$$

- 15-8** Refer to your solution to Probs. 15-1 and 15-2, which is to have a pinion core hardness of 300 Brinell. Use the relations from Prob. 15-7 to establish the hardness of the gear core and the case hardesses of both gears.

- 15-9** Repeat Probs. 15-1 and 15-2 with the hardness protocol

	<b>Core</b>	<b>Case</b>
Pinion	300	372
Gear	352	344

which can be established by relations in Prob. 15-7, and see if the result matches transmitted loads  $W^t$  in all four cases.

- 15-10** A catalog of stock bevel gears lists a power rating of 5.2 hp at 1200 rev/min pinion speed for a straight-bevel gearset consisting of a 20-tooth pinion driving a 40-tooth gear. This gear pair has a  $20^\circ$  normal pressure angle, a face width of 0.71 in, and a diametral pitch of 10 teeth/in and is through-hardened to 300 BHN. Assume the gears are for general industrial use, are generated to a transmission accuracy number of 5, and are uncrowned. Given these data, what do you think about the stated catalog power rating?
- 15-11** Apply the relations of Prob. 15-7 to Ex. 15-1 and find the Brinell case hardness of the gears for equal allowable load  $W^t$  in bending and wear. Check your work by reworking Ex. 15-1 to see if you are correct. How would you go about the heat treatment of the gears?
- 15-12** Your experience with Ex. 15-1 and problems based on it will enable you to write an interactive computer program for power rating of through-hardened steel gears. Test your understanding of bevel-gear analysis by noting the ease with which the coding develops. The hardness protocol developed in Prob. 15-7 can be incorporated at the end of your code, first to display it, then as an option to loop back and see the consequences of it.
- 15-13** Use your experience with Prob. 15-11 and Ex. 15-2 to design an interactive computer-aided design program for straight-steel bevel gears, implementing the ANSI/AGMA 2003-B97 standard. It will be helpful to follow the decision set in Sec. 15-5, allowing the return to earlier decisions for revision as the consequences of earlier decisions develop.
- 15-14** A single-threaded steel worm rotates at 1725 rev/min, meshing with a 56-tooth worm gear transmitting 1 hp to the output shaft. The pitch diameter of the worm is 1.50. The tangential diametral pitch of the gear is 8 teeth per inch and the normal pressure angle is  $20^\circ$ . The ambient temperature is  $70^\circ\text{F}$ , the application factor is 1.25, the design factor is 1, the gear face is 0.5 in, the lateral case area is  $850 \text{ in}^2$ , and the gear is sand-cast bronze.  
 (a) Determine and evaluate the geometric properties of the gears.  
 (b) Determine the transmitted gear forces and the mesh efficiency.  
 (c) Is the mesh sufficient to handle the loading?  
 (d) Estimate the lubricant sump temperature.
- 15-15 to  
15-22** As in Ex. 15-4, design a cylindrical worm-gear mesh to connect a squirrel-cage induction motor to a liquid agitator. The motor speed is 1125 rev/min, and the velocity ratio is to be 10:1. The output power requirement is 25 hp. The shaft axes are  $90^\circ$  to each other. An overload factor  $K_o$  (see Table 15-2) makes allowance for external dynamic excursions of load from the nominal or average load  $W^t$ . For this service  $K_o = 1.25$  is appropriate. Additionally, a design factor  $n_d$  of 1.1 is to be included to address other unquantifiable risks. For Probs. 15-15 to 15-17 use the AGMA method for  $(W_G^t)_{\text{all}}$  whereas for Probs. 15-18 to 15-22, use the Buckingham method. See Table 15-12.

**Table 15-12**

Table Supporting

Problems 15-15 to 15-22

<b>Problem No.</b>	<b>Method</b>	<b>Materials</b>	
		<b>Worm</b>	<b>Gear</b>
<b>15-15</b>	AGMA	Steel, HRC 58	Sand-cast bronze
<b>15-16</b>	AGMA	Steel, HRC 58	Chilled-cast bronze
<b>15-17</b>	AGMA	Steel, HRC 58	Centrifugal-cast bronze
<b>15-18</b>	Buckingham	Steel, 500 Bhn	Chilled-cast bronze
<b>15-19</b>	Buckingham	Steel, 500 Bhn	Cast bronze
<b>15-20</b>	Buckingham	Steel, 250 Bhn	Cast bronze
<b>15-21</b>	Buckingham	High-test cast iron	Cast bronze
<b>15-22</b>	Buckingham	High-test cast iron	High-test cast iron

# 16

## Clutches, Brakes, Couplings, and Flywheels

### Chapter Outline

- 16-1** Static Analysis of Clutches and Brakes **827**
- 16-2** Internal Expanding Rim Clutches and Brakes **832**
- 16-3** External Contracting Rim Clutches and Brakes **840**
- 16-4** Band-Type Clutches and Brakes **844**
- 16-5** Frictional-Contact Axial Clutches **845**
- 16-6** Disk Brakes **849**
- 16-7** Cone Clutches and Brakes **853**
- 16-8** Energy Considerations **856**
- 16-9** Temperature Rise **857**
- 16-10** Friction Materials **861**
- 16-11** Miscellaneous Clutches and Couplings **864**
- 16-12** Flywheels **866**

This chapter is concerned with a group of elements usually associated with rotation that have in common the function of storing and/or transferring rotating energy. Because of this similarity of function, clutches, brakes, couplings, and flywheels are treated together in this book.

A simplified dynamic representation of a friction clutch or brake is shown in Fig. 16-1a. Two inertias,  $I_1$  and  $I_2$ , traveling at the respective angular velocities  $\omega_1$  and  $\omega_2$ , one of which may be zero in the case of brakes, are to be brought to the same speed by engaging the clutch or brake. Slippage occurs because the two elements are running at different speeds and energy is dissipated during actuation, resulting in a temperature rise. In analyzing the performance of these devices we shall be interested in:

- 1 The actuating force
- 2 The torque transmitted
- 3 The energy loss
- 4 The temperature rise

The torque transmitted is related to the actuating force, the coefficient of friction, and the geometry of the clutch or brake. This is a problem in statics, which will have to be studied separately for each geometric configuration. However, temperature rise is related to energy loss and can be studied without regard to the type of brake or clutch, because the geometry of interest is that of the heat-dissipating surfaces.

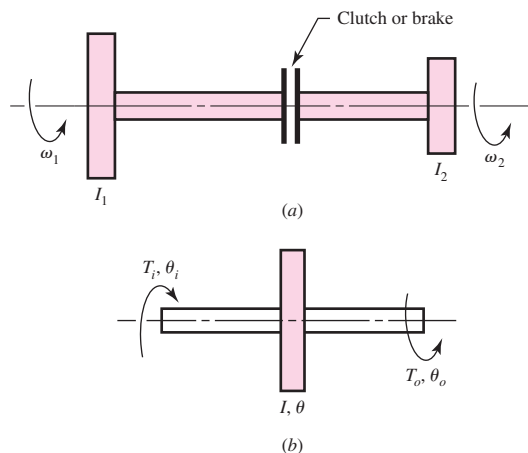
The various types of devices to be studied may be classified as follows:

- 1 Rim types with internal expanding shoes
- 2 Rim types with external contracting shoes
- 3 Band types
- 4 Disk or axial types
- 5 Cone types
- 6 Miscellaneous types

A flywheel is an inertial energy-storage device. It absorbs mechanical energy by increasing its angular velocity and delivers energy by decreasing its velocity. Figure 16-1b is a mathematical representation of a flywheel. An input torque  $T_i$ , corresponding to a coordinate  $\theta_i$ , will cause the flywheel speed to increase. And a load or output torque  $T_o$ , with coordinate  $\theta_o$ , will absorb energy from the flywheel and cause it to slow down. We shall be interested in designing flywheels so as to obtain a specified amount of speed regulation.

**Figure 16-1**

- (a) Dynamic representation of a clutch or brake;  
 (b) mathematical representation of a flywheel.



## 16-1 Static Analysis of Clutches and Brakes

Many types of clutches and brakes can be analyzed by following a general procedure. The procedure entails the following tasks:

- Estimate, model, or measure the pressure distribution on the friction surfaces.
- Find a relationship between the largest pressure and the pressure at any point.
- Use the conditions of static equilibrium to find the braking force or torque and the support reactions.

Let us apply these tasks to the doorstop depicted in Fig. 16–2a. The stop is hinged at pin A. A normal pressure distribution  $p(u)$  is shown under the friction pad as a function of position  $u$ , taken from the right edge of the pad. A similar distribution of shearing frictional traction is on the surface, of intensity  $fp(u)$ , in the direction of the motion of the floor relative to the pad, where  $f$  is the coefficient of friction. The width of the pad into the page is  $w_2$ . The net force in the  $y$  direction and moment about C from the pressure are respectively,

$$N = w_2 \int_0^{w_1} p(u) du = p_{av} w_1 w_2 \quad (a)$$

$$w_2 \int_0^{w_1} p(u)u du = \bar{u} w_2 \int_0^{w_1} p(u) du = p_{av} w_1 w_2 \bar{u} \quad (b)$$

We sum the forces in the  $x$ -direction to obtain

$$\sum F_x = R_x \mp w_2 \int_0^{w_1} fp(u) du = 0$$

where  $-$  or  $+$  is for rightward or leftward relative motion of the floor, respectively. Assuming  $f$  constant, solving for  $R_x$  gives

$$R_x = \pm w_2 \int_0^{w_1} fp(u) du = \pm f w_1 w_2 p_{av} \quad (c)$$

Summing the forces in the  $y$  direction gives

$$\sum F_y = -F + w_2 \int_0^{w_1} p(u) du + R_y = 0$$

from which

$$R_y = F - w_2 \int_0^{w_1} p(u) du = F - p_{av} w_1 w_2 \quad (d)$$

for either direction. Summing moments about the pin located at A we have

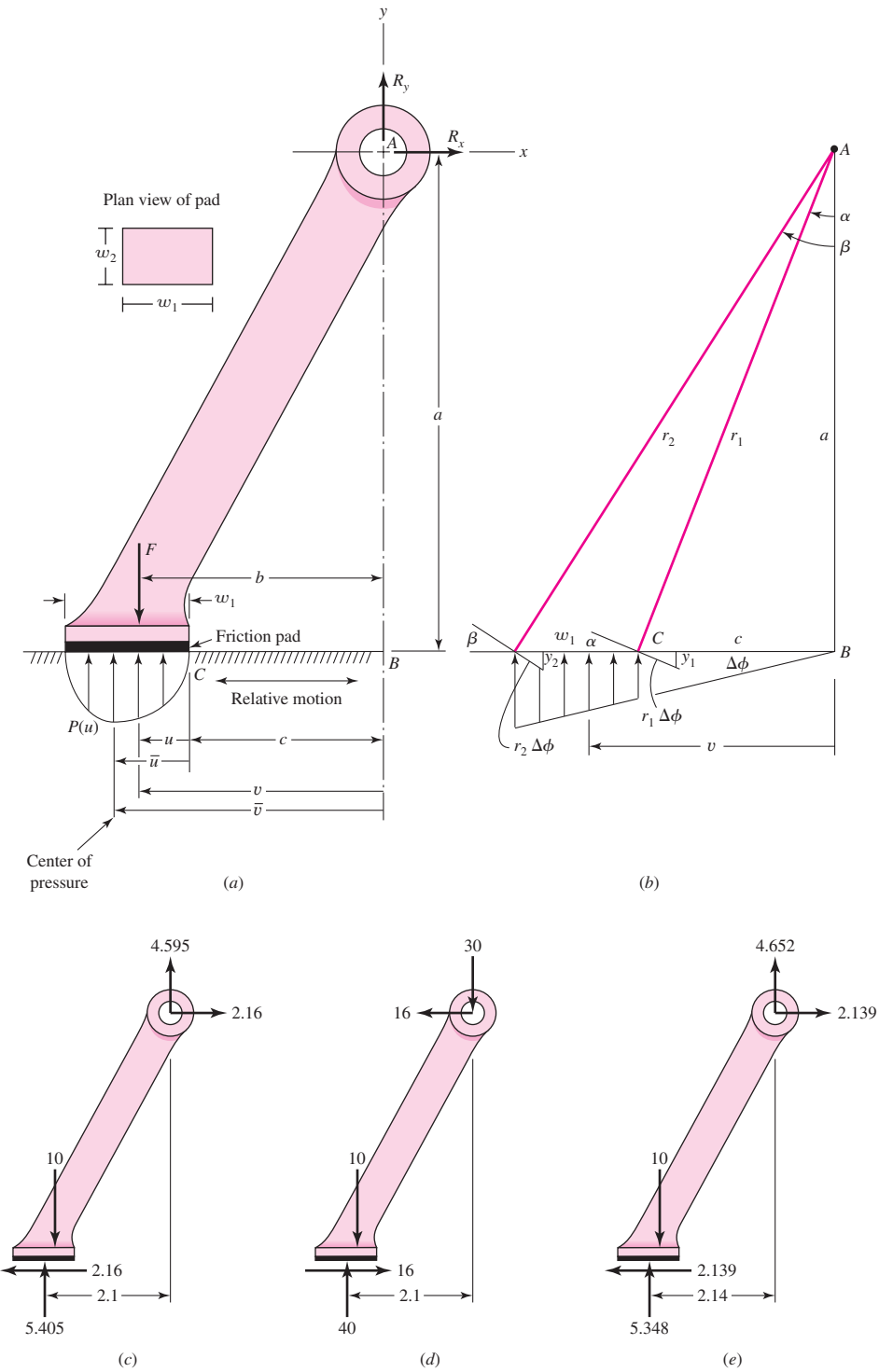
$$\sum M_A = Fb - w_2 \int_0^{w_1} p(u)(c+u) du \mp af w_2 \int_0^{w_1} p(u) du = 0$$

A brake shoe is *self-energizing* if its moment sense helps set the brake, *self-deenergizing* if the moment resists setting the brake. Continuing,

$$F = \frac{w_2}{b} \left[ \int_0^{w_1} p(u)(c+u) du \pm af \int_0^{w_1} p(u) du \right] \quad (e)$$

**Figure 16–2**

A common doorstop.  
 (a) Free body of the doorstop.  
 (b) Trapezoidal pressure distribution on the foot pad based on linear deformation of pad. (c) Free-body diagram for leftward movement of the floor, uniform pressure, Ex. 16–1.  
 (d) Free-body diagram for rightward movement of the floor, uniform pressure, Ex. 16–1. (e) Free-body diagram for leftward movement of the floor, trapezoidal pressure, Ex. 16–1.



Can  $F$  be equal to or less than zero? Only during rightward motion of the floor when the expression in brackets in Eq. (e) is equal to or less than zero. We set the brackets to zero or less:

$$\int_0^{w_1} p(u)(c+u) du - af \int_0^{w_1} p(u) du \leq 0$$

from which

$$f_{cr} \geq \frac{1}{a} \frac{\int_0^{w_1} p(u)(c+u) du}{\int_0^{w_1} p(u) du} = \frac{1}{a} \frac{c \int_0^{w_1} p(u) du + \int_0^{w_1} p(u)u du}{\int_0^{w_1} p(u) du}$$

$$f_{cr} \geq \frac{c + \bar{u}}{a} \quad (f)$$

where  $\bar{u}$  is the distance of the center of pressure from the right edge of the pad. The conclusion that a *self-acting* or *self-locking* phenomenon is present is independent of our knowledge of the normal pressure distribution  $p(u)$ . Our ability to find the critical value of the coefficient of friction  $f_{cr}$  is dependent on our knowledge of  $p(u)$ , from which we derive  $\bar{u}$ .

### EXAMPLE 16-1

The doorstop depicted in Fig. 16-2a has the following dimensions:  $a = 4$  in,  $b = 2$  in,  $c = 1.6$  in,  $w_1 = 1$  in,  $w_2 = 0.75$  in, where  $w_2$  is the depth of the pad into the plane of the paper.

(a) For a leftward relative movement of the floor, an actuating force  $F$  of 10 lbf, a coefficient of friction of 0.4, use a uniform pressure distribution  $p_{av}$ , find  $R_x$ ,  $R_y$ ,  $p_{av}$ , and the largest pressure  $p_a$ .

(b) Repeat part a for rightward relative movement of the floor.

(c) Model the normal pressure to be the “crush” of the pad, much as if it were composed of many small helical coil springs. Find  $R_x$ ,  $R_y$ ,  $p_{av}$ , and  $p_a$  for leftward relative movement of the floor and other conditions as in part a.

(d) For rightward relative movement of the floor, is the doorstop a self-acting brake?

#### Solution

(a)

$$\text{Eq. (c): } R_x = fp_{av}w_1w_2 = 0.4(1)(0.75)p_{av} = 0.3p_{av}$$

$$\text{Eq. (d): } R_y = F - p_{av}w_1w_2 = 10 - p_{av}(1)(0.75) = 10 - 0.75p_{av}$$

$$\text{Eq. (e): } F = \frac{w_2}{b} \left[ \int_0^1 p_{av}(c+u) du + af \int_0^1 p_{av} du \right]$$

$$= \frac{w_2}{b} \left( p_{av}c \int_0^1 du + p_{av} \int_0^1 u du + afp_{av} \int_0^1 du \right)$$

$$= \frac{w_2 p_{av}}{b} (c + 0.5 + af) = \frac{0.75}{2} [1.6 + 0.5 + 4(0.4)] p_{av}$$

$$= 1.3875 p_{av}$$

Solving for  $p_{av}$  gives

$$p_{av} = \frac{F}{1.3875} = \frac{10}{1.3875} = 7.207 \text{ psi}$$

We evaluate  $R_x$  and  $R_y$  as

**Answer**  $R_x = 0.3(7.207) = 2.162 \text{ lbf}$

**Answer**  $R_y = 10 - 0.75(7.207) = 4.595 \text{ lbf}$

The normal force  $N$  on the pad is  $F - R_y = 10 - 4.595 = 5.405 \text{ lbf}$ , upward. The line of action is through the center of pressure, which is at the center of the pad. The friction force is  $fN = 0.4(5.405) = 2.162 \text{ lbf}$  directed to the left. A check of the moments about  $A$  gives

$$\begin{aligned} \sum M_A &= Fb - fNa - N(w_1/2 + c) \\ &= 10(2) - 0.4(5.405)4 - 5.405(1/2 + 1.6) \doteq 0 \end{aligned}$$

**Answer** The maximum pressure  $p_a = p_{av} = 7.207 \text{ psi}$ .

(b)

Eq. (c):  $R_x = -fp_{av}w_1w_2 = -0.4(1)(0.75)p_{av} = -0.3p_{av}$

Eq. (d):  $R_y = F - p_{av}w_1w_2 = 10 - p_{av}(1)(0.75) = 10 - 0.75p_{av}$

$$\begin{aligned} \text{Eq. (e): } F &= \frac{w_2}{b} \left[ \int_0^1 p_{av}(c+u) du + af \int_0^1 p_{av} du \right] \\ &= \frac{w_2}{b} \left( p_{av}c \int_0^1 du + p_{av} \int_0^1 u du + afp_{av} \int_0^1 du \right) \\ &= \frac{0.75}{2} p_{av}[1.6 + 0.5 - 4(0.4)] = 0.1875p_{av} \end{aligned}$$

from which

$$p_{av} = \frac{F}{0.1875} = \frac{10}{0.1875} = 53.33 \text{ psi}$$

which makes

**Answer**  $R_x = -0.3(53.33) = -16 \text{ lbf}$

**Answer**  $R_y = 10 - 0.75(53.33) = -30 \text{ lbf}$

The normal force  $N$  on the pad is  $10 + 30 = 40 \text{ lbf}$  upward. The friction shearing force is  $fN = 0.4(40) = 16 \text{ lbf}$  to the right. We now check the moments about  $A$ :

$$M_A = fNa + Fb - N(c + 0.5) = 16(4) + 10(2) - 40(1.6 + 0.5) = 0$$

Note the change in average pressure from 7.207 psi in part *a* to 53.3 psi. Also note how directions of forces have changed. The maximum pressure  $p_a$  is the same as  $p_{av}$ , which has changed from 7.207 psi to 53.3 psi.

(c) We will model the deformation of the pad as follows. If the doorstop rotates  $\Delta\phi$  counterclockwise, the right and left edges of the pad will deform down  $y_1$  and  $y_2$ , respectively (Fig. 16-2b). From similar triangles,  $y_1/(r_1 \Delta\phi) = c/r_1$  and  $y_2/(r_2 \Delta\phi) = (c + w_1)/r_2$ . Thus,  $y_1 = c \Delta\phi$  and  $y_2 = (c + w_1) \Delta\phi$ . This means that  $y$  is directly

proportional to the horizontal distance from the pivot point  $A$ ; that is,  $y = C_1v$ , where  $C_1$  is a constant (see Fig. 16–2b). Assuming the pressure is directly proportional to deformation, then  $p(v) = C_2v$ , where  $C_2$  is a constant. In terms of  $u$ , the pressure is  $p(u) = C_2(c + u) = C_2(1.6 + u)$ .

Eq. (e):

$$\begin{aligned} F &= \frac{w_2}{b} \left[ \int_0^{w_1} p(u)c \, du + \int_0^{w_1} p(u)u \, du + af \int_0^{w_1} p(u) \, du \right] \\ &= \frac{0.75}{2} \left[ \int_0^1 C_2(1.6 + u)1.6 \, du + \int_0^1 C_2(1.6 + u)u \, du + af \int_0^1 C_2(1.6 + u) \, du \right] \\ &= 0.375C_2[(1.6 + 0.5)1.6 + (0.8 + 0.3333) + 4(0.4)(1.6 + 0.5)] = 2.945C_2 \end{aligned}$$

Since  $F = 10 \text{ lbf}$ , then  $C_2 = 10/2.945 = 3.396 \text{ psi/in}$ , and  $p(u) = 3.396(1.6 + u)$ . The average pressure is given by

**Answer**  $p_{av} = \frac{1}{w_1} \int_0^{w_1} p(u) \, du = \frac{1}{1} \int_0^1 3.396(1.6 + u) \, du = 3.396(1.6 + 0.5) = 7.132 \text{ psi}$

The maximum pressure occurs at  $u = 1 \text{ in}$ , and is

**Answer**  $p_a = 3.396(1.6 + 1) = 8.83 \text{ psi}$

Equations (c) and (d) of Sec. 16–1 are still valid. Thus,

**Answer**  $R_x = 0.3p_{av} = 0.3(7.131) = 2.139 \text{ lbf}$

$$R_y = 10 - 0.75p_{av} = 10 - 0.75(7.131) = 4.652 \text{ lbf}$$

The average pressure is  $p_{av} = 7.13 \text{ psi}$  and the maximum pressure is  $p_a = 8.83 \text{ psi}$ , which is approximately 24 percent higher than the average pressure. The presumption that the pressure was uniform in part *a* (because the pad was small, or because the arithmetic would be easier?) underestimated the peak pressure. Modeling the pad as a one-dimensional springset is better, but the pad is really a three-dimensional continuum. A theory of elasticity approach or a finite element modeling may be overkill, given uncertainties inherent in this problem, but it still represents better modeling.

(d) To evaluate  $\bar{u}$  we need to evaluate two integrations

$$\begin{aligned} \int_0^c p(u)u \, du &= \int_0^1 3.396(1.6 + u)u \, du = 3.396(0.8 + 0.3333) = 3.849 \text{ lbf} \\ \int_0^c p(u) \, du &= \int_0^1 3.396(1.6 + u) \, du = 3.396(1.6 + 0.5) = 7.132 \text{ lbf/in} \end{aligned}$$

Thus  $\bar{u} = 3.849/7.132 = 0.5397 \text{ in}$ . Then, from Eq. (f) of Sec. 16–1, the critical coefficient of friction is

**Answer**  $f_{cr} \geq \frac{c + \bar{u}}{a} = \frac{1.6 + 0.5397}{4} = 0.535$

The doorstop friction pad does not have a high enough coefficient of friction to make the doorstop a self-acting brake. The configuration must change and/or the pad material specification must be changed to sustain the function of a doorstop.

## 16-2 Internal Expanding Rim Clutches and Brakes

The internal-shoe rim clutch shown in Fig. 16-3 consists essentially of three elements: the mating frictional surface, the means of transmitting the torque to and from the surfaces, and the actuating mechanism. Depending upon the operating mechanism, such clutches are further classified as *expanding-ring*, *centrifugal*, *magnetic*, *hydraulic*, and *pneumatic*.

The expanding-ring clutch is often used in textile machinery, excavators, and machine tools where the clutch may be located within the driving pulley. Expanding-ring clutches benefit from centrifugal effects; transmit high torque, even at low speeds; and require both positive engagement and ample release force.

The centrifugal clutch is used mostly for automatic operation. If no spring is used, the torque transmitted is proportional to the square of the speed. This is particularly useful for electric-motor drives where, during starting, the driven machine comes up to speed without shock. Springs can also be used to prevent engagement until a certain motor speed is reached, but some shock may occur.

Magnetic clutches are particularly useful for automatic and remote-control systems. Such clutches are also useful in drives subject to complex load cycles (see Sec. 11-7).

Hydraulic and pneumatic clutches are also useful in drives having complex loading cycles and in automatic machinery, or in robots. Here the fluid flow can be controlled remotely using solenoid valves. These clutches are also available as disk, cone, and multiple-plate clutches.

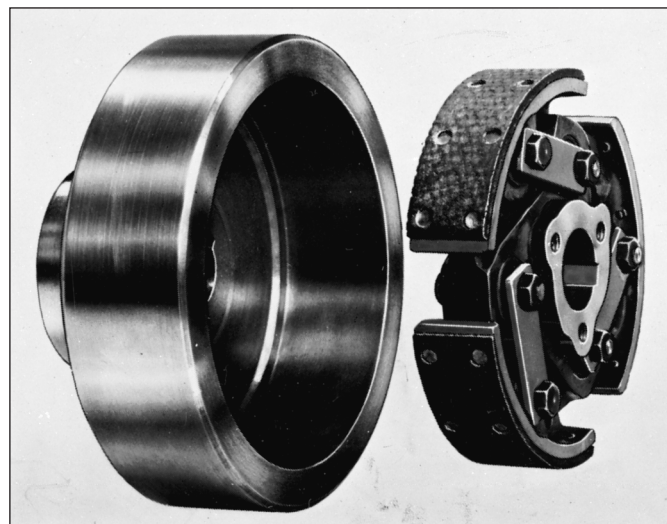
In braking systems, the *internal-shoe* or *drum* brake is used mostly for automotive applications.

To analyze an internal-shoe device, refer to Fig. 16-4, which shows a shoe pivoted at point A, with the actuating force acting at the other end of the shoe. Since the shoe is long, we cannot make the assumption that the distribution of normal forces is uniform. The mechanical arrangement permits no pressure to be applied at the heel, and we will therefore assume the pressure at this point to be zero.

It is the usual practice to omit the friction material for a short distance away from the heel (point A). This eliminates interference, and the material would contribute little to the performance anyway, as will be shown. In some designs the hinge pin is made movable to provide additional heel pressure. This gives the effect of a floating shoe.

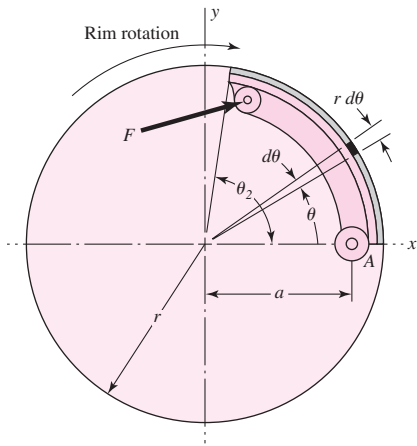
**Figure 16-3**

An internal expanding centrifugal-acting rim clutch.  
(Courtesy of the Hilliard Corporation.)

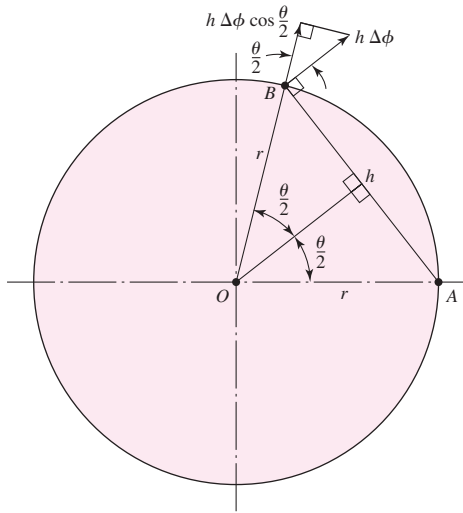


**Figure 16–4**

Internal friction shoe geometry.

**Figure 16–5**

The geometry associated with an arbitrary point on the shoe.



(Floating shoes will not be treated in this book, although their design follows the same general principles.)

Let us consider the pressure  $p$  acting upon an element of area of the frictional material located at an angle  $\theta$  from the hinge pin (Fig. 16–4). We designate the maximum pressure  $p_a$  located at an angle  $\theta_a$  from the hinge pin. To find the pressure distribution on the periphery of the internal shoe, consider point  $B$  on the shoe (Fig. 16–5). As in Ex. 16–1, if the shoe deforms by an infinitesimal rotation  $\Delta\phi$  about the pivot point  $A$ , deformation perpendicular to  $AB$  is  $h \Delta\phi$ . From the isosceles triangle  $AOB$ ,  $h = 2r \sin(\theta/2)$ , so

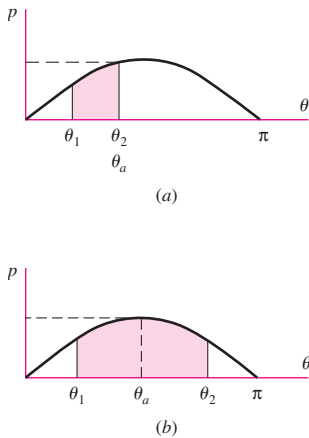
$$h \Delta\phi = 2r \Delta\phi \sin(\theta/2)$$

The deformation perpendicular to the rim is  $h \Delta\phi \cos(\theta/2)$ , which is

$$h \Delta\phi \cos(\theta/2) = 2r \Delta\phi \sin(\theta/2) \cos(\theta/2) = r \Delta\phi \sin \theta$$

Thus, the deformation, and consequently the pressure, is proportional to  $\sin \theta$ . In terms of the pressure at  $B$  and where the pressure is a maximum, this means

$$\frac{P}{\sin \theta} = \frac{p_a}{\sin \theta_a} \quad (a)$$



Rearranging gives

$$p = \frac{p_a}{\sin \theta_a} \sin \theta \quad (16-1)$$

This pressure distribution has interesting and useful characteristics:

- The pressure distribution is sinusoidal with respect to the angle  $\theta$ .
- If the shoe is short, as shown in Fig. 16-6a, the largest pressure *on the shoe* is  $p_a$  occurring at the end of the shoe,  $\theta_2$ .
- If the shoe is long, as shown in Fig. 16-6b, the largest pressure on the shoe is  $p_a$  occurring at  $\theta_a = 90^\circ$ .

Since limitations on friction materials are expressed in terms of the largest allowable pressure on the lining, the designer wants to think in terms of  $p_a$  and not about the amplitude of the sinusoidal distribution that addresses locations off the shoe.

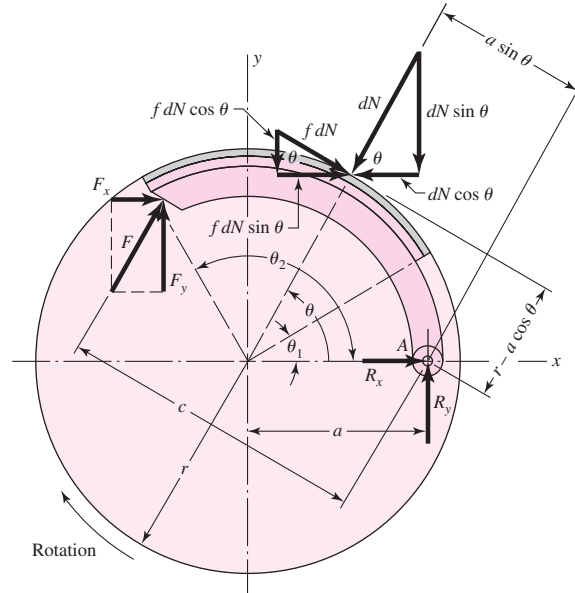
When  $\theta = 0$ , Eq. (16-1) shows that the pressure is zero. The frictional material located at the heel therefore contributes very little to the braking action and might as well be omitted. A good design would concentrate as much frictional material as possible in the neighborhood of the point of maximum pressure. Such a design is shown in Fig. 16-7. In this figure the frictional material begins at an angle  $\theta_1$ , measured from the hinge pin  $A$ , and ends at an angle  $\theta_2$ . Any arrangement such as this will give a good distribution of the frictional material.

Proceeding now (Fig. 16-7), the hinge-pin reactions are  $R_x$  and  $R_y$ . The actuating force  $F$  has components  $F_x$  and  $F_y$  and operates at distance  $c$  from the hinge pin. At any angle  $\theta$  from the hinge pin there acts a differential normal force  $dN$  whose magnitude is

$$dN = pbr d\theta \quad (b)$$

**Figure 16-7**

Forces on the shoe.



where  $b$  is the face width (perpendicular to the paper) of the friction material. Substituting the value of the pressure from Eq. (16-1), the normal force is

$$dN = \frac{p_a br \sin \theta d\theta}{\sin \theta_a} \quad (c)$$

The normal force  $dN$  has horizontal and vertical components  $dN \cos \theta$  and  $dN \sin \theta$ , as shown in the figure. The frictional force  $f dN$  has horizontal and vertical components whose magnitudes are  $f dN \sin \theta$  and  $f dN \cos \theta$ , respectively. By applying the conditions of static equilibrium, we may find the actuating force  $F$ , the torque  $T$ , and the pin reactions  $R_x$  and  $R_y$ .

We shall find the actuating force  $F$ , using the condition that the summation of the moments about the hinge pin is zero. The frictional forces have a moment arm about the pin of  $r - a \cos \theta$ . The moment  $M_f$  of these frictional forces is

$$M_f = \int f dN (r - a \cos \theta) = \frac{fp_a br}{\sin \theta_a} \int_{\theta_1}^{\theta_2} \sin \theta (r - a \cos \theta) d\theta \quad (16-2)$$

which is obtained by substituting the value of  $dN$  from Eq. (c). It is convenient to integrate Eq. (16-2) for each problem, and we shall therefore retain it in this form. The moment arm of the normal force  $dN$  about the pin is  $a \sin \theta$ . Designating the moment of the normal forces by  $M_N$  and summing these about the hinge pin give

$$M_N = \int dN (a \sin \theta) = \frac{p_a bra}{\sin \theta_a} \int_{\theta_1}^{\theta_2} \sin^2 \theta d\theta \quad (16-3)$$

The actuating force  $F$  must balance these moments. Thus

$$F = \frac{M_N - M_f}{c} \quad (16-4)$$

We see here that a condition for zero actuating force exists. In other words, if we make  $M_N = M_f$ , self-locking is obtained, and no actuating force is required. This furnishes us with a method for obtaining the dimensions for some self-energizing action. Thus the dimension  $a$  in Fig. 16-7 must be such that

$$M_N > M_f \quad (16-5)$$

The torque  $T$  applied to the drum by the brake shoe is the sum of the frictional forces  $f dN$  times the radius of the drum:

$$\begin{aligned} T &= \int fr dN = \frac{fp_a br^2}{\sin \theta_a} \int_{\theta_1}^{\theta_2} \sin \theta d\theta \\ &= \frac{fp_a br^2 (\cos \theta_1 - \cos \theta_2)}{\sin \theta_a} \end{aligned} \quad (16-6)$$

The hinge-pin reactions are found by taking a summation of the horizontal and vertical forces. Thus, for  $R_x$ , we have

$$\begin{aligned} R_x &= \int dN \cos \theta - \int f dN \sin \theta - F_x \\ &= \frac{p_a br}{\sin \theta_a} \left( \int_{\theta_1}^{\theta_2} \sin \theta \cos \theta d\theta - f \int_{\theta_1}^{\theta_2} \sin^2 \theta d\theta \right) - F_x \end{aligned} \quad (d)$$

The vertical reaction is found in the same way:

$$\begin{aligned} R_y &= \int dN \sin \theta + \int f dN \cos \theta - F_y \\ &= \frac{p_a br}{\sin \theta_a} \left( \int_{\theta_1}^{\theta_2} \sin^2 \theta d\theta + f \int_{\theta_1}^{\theta_2} \sin \theta \cos \theta d\theta \right) - F_y \end{aligned} \quad (e)$$

The direction of the frictional forces is reversed if the rotation is reversed. Thus, for counterclockwise rotation the actuating force is

$$F = \frac{M_N + M_f}{c} \quad (16-7)$$

and since both moments have the same sense, the self-energizing effect is lost. Also, for counterclockwise rotation the signs of the frictional terms in the equations for the pin reactions change, and Eqs. (d) and (e) become

$$R_x = \frac{p_a br}{\sin \theta_a} \left( \int_{\theta_1}^{\theta_2} \sin \theta \cos \theta d\theta + f \int_{\theta_1}^{\theta_2} \sin^2 \theta d\theta \right) - F_x \quad (f)$$

$$R_y = \frac{p_a br}{\sin \theta_a} \left( \int_{\theta_1}^{\theta_2} \sin^2 \theta d\theta - f \int_{\theta_1}^{\theta_2} \sin \theta \cos \theta d\theta \right) - F_y \quad (g)$$

Equations (d), (e), (f), and (g) can be simplified to ease computations. Thus, let

$$\begin{aligned} A &= \int_{\theta_1}^{\theta_2} \sin \theta \cos \theta d\theta = \left( \frac{1}{2} \sin^2 \theta \right)_{\theta_1}^{\theta_2} \\ B &= \int_{\theta_1}^{\theta_2} \sin^2 \theta d\theta = \left( \frac{\theta}{2} - \frac{1}{4} \sin 2\theta \right)_{\theta_1}^{\theta_2} \end{aligned} \quad (16-8)$$

Then, for clockwise rotation as shown in Fig. 16-7, the hinge-pin reactions are

$$\begin{aligned} R_x &= \frac{p_a br}{\sin \theta_a} (A - fB) - F_x \\ R_y &= \frac{p_a br}{\sin \theta_a} (B + fA) - F_y \end{aligned} \quad (16-9)$$

For counterclockwise rotation, Eqs. (f) and (g) become

$$\begin{aligned} R_x &= \frac{p_a br}{\sin \theta_a} (A + fB) - F_x \\ R_y &= \frac{p_a br}{\sin \theta_a} (B - fA) - F_y \end{aligned} \quad (16-10)$$

In using these equations, the reference system always has its origin at the center of the drum. The positive  $x$  axis is taken through the hinge pin. The positive  $y$  axis is always in the direction of the shoe, even if this should result in a left-handed system.

The following assumptions are implied by the preceding analysis:

- 1 The pressure at any point on the shoe is assumed to be proportional to the distance from the hinge pin, being zero at the heel. This should be considered from the standpoint that pressures specified by manufacturers are averages rather than maxima.

- 2 The effect of centrifugal force has been neglected. In the case of brakes, the shoes are not rotating, and no centrifugal force exists. In clutch design, the effect of this force must be considered in writing the equations of static equilibrium.
- 3 The shoe is assumed to be rigid. Since this cannot be true, some deflection will occur, depending upon the load, pressure, and stiffness of the shoe. The resulting pressure distribution may be different from that which has been assumed.
- 4 The entire analysis has been based upon a coefficient of friction that does not vary with pressure. Actually, the coefficient may vary with a number of conditions, including temperature, wear, and environment.

### EXAMPLE 16-2

The brake shown in Fig. 16-8 is 300 mm in diameter and is actuated by a mechanism that exerts the same force  $F$  on each shoe. The shoes are identical and have a face width of 32 mm. The lining is a molded asbestos having a coefficient of friction of 0.32 and a pressure limitation of 1000 kPa. Estimate the maximum

- (a) Actuating force  $F$ .
- (b) Braking capacity.
- (c) Hinge-pin reactions.

#### Solution

(a) The right-hand shoe is self-energizing, and so the force  $F$  is found on the basis that the maximum pressure will occur on this shoe. Here  $\theta_1 = 0^\circ$ ,  $\theta_2 = 126^\circ$ ,  $\theta_a = 90^\circ$ , and  $\sin \theta_a = 1$ . Also,

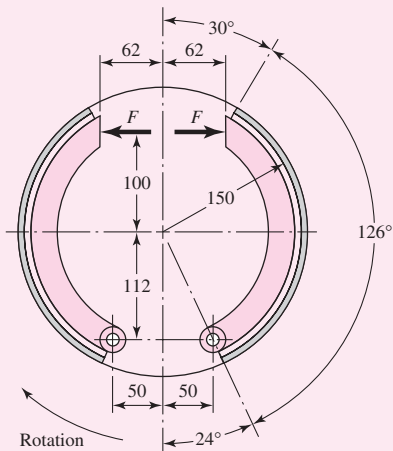
$$a = \sqrt{(112)^2 + (50)^2} = 122.7 \text{ mm}$$

Integrating Eq. (16-2) from 0 to  $\theta_2$  yields

$$\begin{aligned} M_f &= \frac{fp_a br}{\sin \theta_a} \left[ \left( -r \cos \theta \right)_0^{\theta_2} - a \left( \frac{1}{2} \sin^2 \theta \right)_0^{\theta_2} \right] \\ &= \frac{fp_a br}{\sin \theta_a} \left( r - r \cos \theta_2 - \frac{a}{2} \sin^2 \theta_2 \right) \end{aligned}$$

**Figure 16-8**

Brake with internal expanding shoes; dimensions in millimeters.



Changing all lengths to meters, we have

$$\begin{aligned} M_f &= (0.32)[1000(10)^3](0.032)(0.150) \\ &\quad \times \left[ 0.150 - 0.150 \cos 126^\circ - \left( \frac{0.1227}{2} \right) \sin^2 126^\circ \right] \\ &= 304 \text{ N} \cdot \text{m} \end{aligned}$$

The moment of the normal forces is obtained from Eq. (16–3). Integrating from 0 to  $\theta_2$  gives

$$\begin{aligned} M_N &= \frac{p_a b r a}{\sin \theta_a} \left( \frac{\theta}{2} - \frac{1}{4} \sin 2\theta \right)_0^{\theta_2} \\ &= \frac{p_a b r a}{\sin \theta_a} \left( \frac{\theta_2}{2} - \frac{1}{4} \sin 2\theta_2 \right) \\ &= [1000(10)^3](0.032)(0.150)(0.1227) \left\{ \frac{\pi}{2} \frac{126}{180} - \frac{1}{4} \sin[(2)(126^\circ)] \right\} \\ &= 788 \text{ N} \cdot \text{m} \end{aligned}$$

From Eq. (16–4), the actuating force is

**Answer**

$$F = \frac{M_N - M_f}{c} = \frac{788 - 304}{100 + 112} = 2.28 \text{ kN}$$

(b) From Eq. (16–6), the torque applied by the right-hand shoe is

$$\begin{aligned} T_R &= \frac{f p_a b r^2 (\cos \theta_1 - \cos \theta_2)}{\sin \theta_a} \\ &= \frac{0.32[1000(10)^3](0.032)(0.150)^2(\cos 0^\circ - \cos 126^\circ)}{\sin 90^\circ} = 366 \text{ N} \cdot \text{m} \end{aligned}$$

The torque contributed by the left-hand shoe cannot be obtained until we learn its maximum operating pressure. Equations (16–2) and (16–3) indicate that the frictional and normal moments are proportional to this pressure. Thus, for the left-hand shoe,

$$M_N = \frac{788 p_a}{1000} \quad M_f = \frac{304 p_a}{1000}$$

Then, from Eq. (16–7),

$$F = \frac{M_N + M_f}{c}$$

or

$$2.28 = \frac{(788/1000)p_a + (304/1000)p_a}{100 + 112}$$

Solving gives  $p_a = 443$  kPa. Then, from Eq. (16–6), the torque on the left-hand shoe is

$$T_L = \frac{f p_a b r^2 (\cos \theta_1 - \cos \theta_2)}{\sin \theta_a}$$

Since  $\sin \theta_a = \sin 90^\circ = 1$ , we have

$$T_L = 0.32[443(10)^3](0.032)(0.150)^2(\cos 0^\circ - \cos 126^\circ) = 162 \text{ N} \cdot \text{m}$$

The braking capacity is the total torque:

### Answer

$$T = T_R + T_L = 366 + 162 = 528 \text{ N} \cdot \text{m}$$

(c) In order to find the hinge-pin reactions, we note that  $\sin \theta_a = 1$  and  $\theta_1 = 0$ . Then Eq. (16–8) gives

$$A = \frac{1}{2} \sin^2 \theta_2 = \frac{1}{2} \sin^2 126^\circ = 0.3273$$

$$B = \frac{\theta_2}{2} - \frac{1}{4} \sin 2\theta_2 = \frac{\pi(126)}{2(180)} - \frac{1}{4} \sin[(2)(126^\circ)] = 1.3373$$

Also, let

$$D = \frac{p_a br}{\sin \theta_a} = \frac{1000(0.032)(0.150)}{1} = 4.8 \text{ kN}$$

where  $p_a = 1000 \text{ kPa}$  for the right-hand shoe. Then, using Eq. (16–9), we have

$$\begin{aligned} R_x &= D(A - fB) - F_x = 4.8[0.3273 - 0.32(1.3373)] - 2.28 \sin 24^\circ \\ &= -1.410 \text{ kN} \end{aligned}$$

$$\begin{aligned} R_y &= D(B + fA) - F_y = 4.8[1.3373 + 0.32(0.3273)] - 2.28 \cos 24^\circ \\ &= 4.839 \text{ kN} \end{aligned}$$

The resultant on this hinge pin is

### Answer

$$R = \sqrt{(-1.410)^2 + (4.839)^2} = 5.04 \text{ kN}$$

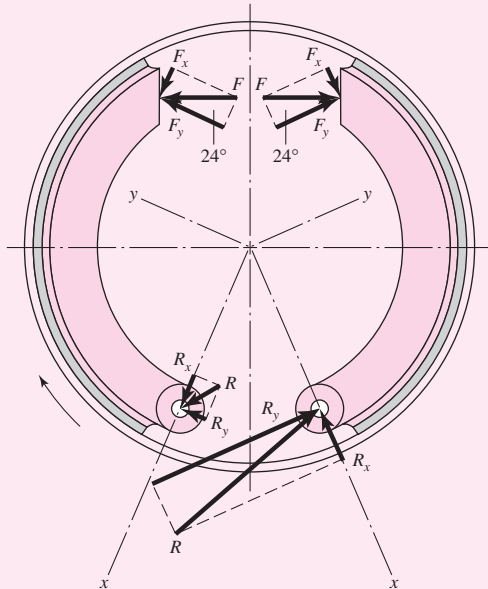
The reactions at the hinge pin of the left-hand shoe are found using Eqs. (16–10) for a pressure of 443 kPa. They are found to be  $R_x = 0.678 \text{ kN}$  and  $R_y = 0.538 \text{ kN}$ . The resultant is

### Answer

$$R = \sqrt{(0.678)^2 + (0.538)^2} = 0.866 \text{ kN}$$

The reactions for both hinge pins, together with their directions, are shown in Fig. 16–9.

| Figure 16–9



This example dramatically shows the benefit to be gained by arranging the shoes to be self-energizing. If the left-hand shoe were turned over so as to place the hinge pin at the top, it could apply the same torque as the right-hand shoe. This would make the capacity of the brake  $(2)(366) = 732 \text{ N} \cdot \text{m}$  instead of the present  $528 \text{ N} \cdot \text{m}$ , a 30 percent improvement. In addition, some of the friction material at the heel could be eliminated without seriously affecting the capacity, because of the low pressure in this area. This change might actually improve the overall design because the additional rim exposure would improve the heat-dissipation capacity.

### 16-3

## External Contracting Rim Clutches and Brakes

The patented clutch-brake of Fig. 16-10 has external contracting friction elements, but the actuating mechanism is pneumatic. Here we shall study only pivoted external shoe brakes and clutches, though the methods presented can easily be adapted to the clutch-brake of Fig. 16-10.

Operating mechanisms can be classified as:

- 1 Solenoids
- 2 Levers, linkages, or toggle devices
- 3 Linkages with spring loading
- 4 Hydraulic and pneumatic devices

The static analysis required for these devices has already been covered in Sec. 3-1. The methods there apply to any mechanism system, including all those used in brakes and clutches. It is not necessary to repeat the material in Chap. 3 that applies directly to such mechanisms. Omitting the operating mechanisms from consideration allows us to concentrate on brake and clutch performance without the extraneous influences introduced by the need to analyze the statics of the control mechanisms.

The notation for external contracting shoes is shown in Fig. 16-11. The moments of the frictional and normal forces about the hinge pin are the same as for the internal

**Figure 16-10**

An external contracting clutch-brake that is engaged by expanding the flexible tube with compressed air. (Courtesy of Twin Disc Clutch Company.)

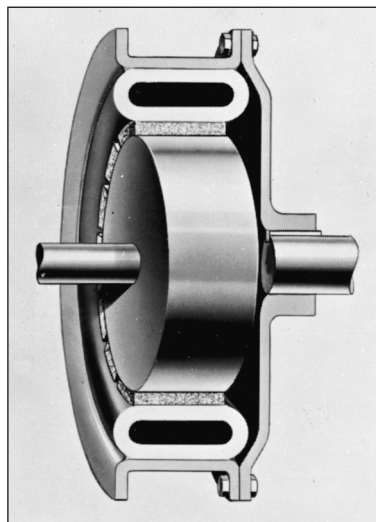
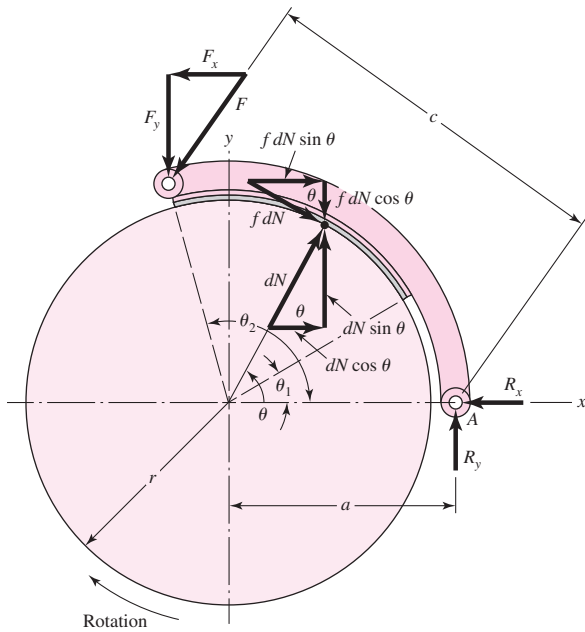


**Figure 16-11**

Notation of external contracting shoes.



expanding shoes. Equations (16-2) and (16-3) apply and are repeated here for convenience:

$$M_f = \frac{fp_a br}{\sin \theta_a} \int_{\theta_1}^{\theta_2} \sin \theta (r - a \cos \theta) d\theta \quad (16-2)$$

$$M_N = \frac{p_a bra}{\sin \theta_a} \int_{\theta_1}^{\theta_2} \sin^2 \theta d\theta \quad (16-3)$$

Both these equations give positive values for clockwise moments (Fig. 16-11) when used for external contracting shoes. The actuating force must be large enough to balance both moments:

$$F = \frac{M_N + M_f}{c} \quad (16-11)$$

The horizontal and vertical reactions at the hinge pin are found in the same manner as for internal expanding shoes. They are

$$R_x = \int dN \cos \theta + \int f dN \sin \theta - F_x \quad (a)$$

$$R_y = \int f dN \cos \theta - \int dN \sin \theta + F_y \quad (b)$$

By using Eq. (16-8) and Eq. (c) from Sec. 16-2, we have

$$R_x = \frac{p_a br}{\sin \theta_a} (A + fB) - F_x \quad (16-12)$$

$$R_y = \frac{p_a br}{\sin \theta_a} (fA - B) + F_y$$

If the rotation is counterclockwise, the sign of the frictional term in each equation is reversed. Thus Eq. (16–11) for the actuating force becomes

$$F = \frac{M_N - M_f}{c} \quad (16-13)$$

and self-energization exists for counterclockwise rotation. The horizontal and vertical reactions are found, in the same manner as before, to be

$$R_x = \frac{p_a br}{\sin \theta_a} (A - fB) - F_x \quad (16-14)$$

$$R_y = \frac{p_a br}{\sin \theta_a} (-fA - B) + F_y$$

It should be noted that, when external contracting designs are used as clutches, the effect of centrifugal force is to decrease the normal force. Thus, as the speed increases, a larger value of the actuating force  $F$  is required.

A special case arises when the pivot is symmetrically located and also placed so that the moment of the friction forces about the pivot is zero. The geometry of such a brake will be similar to that of Fig. 16–12a. To get a pressure-distribution relation, we note that lining wear is such as to retain the cylindrical shape, much as a milling machine cutter feeding in the  $x$  direction would do to the shoe held in a vise. See Fig. 16–12b. This means the abscissa component of wear is  $w_0$  for all positions  $\theta$ . If wear in the radial direction is expressed as  $w(\theta)$ , then

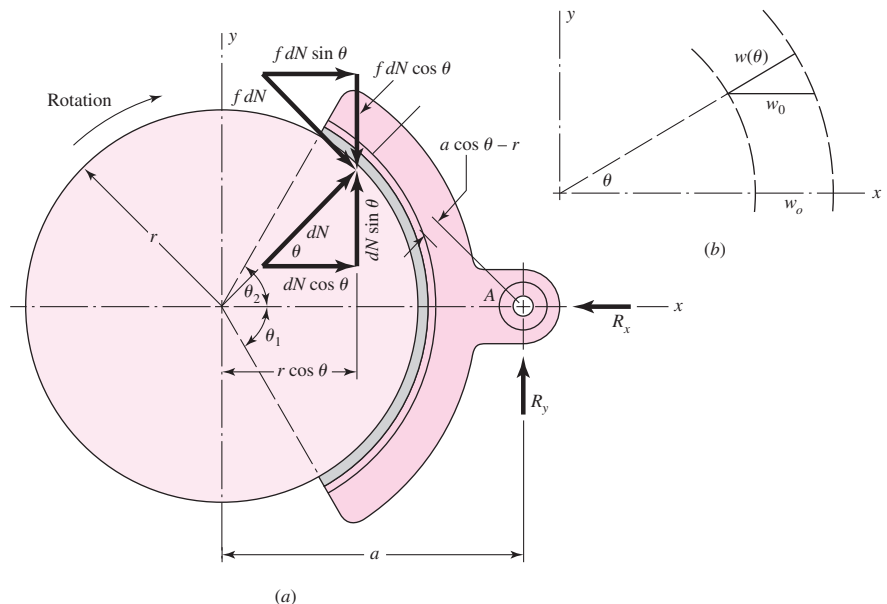
$$w(\theta) = w_0 \cos \theta$$

Using Eq. (12–26), p. 662, to express radial wear  $w(\theta)$  as

$$w(\theta) = K P V t$$

**Figure 16–12**

(a) Brake with symmetrical pivoted shoe; (b) wear of brake lining.



where  $K$  is a material constant,  $P$  is pressure,  $V$  is rim velocity, and  $t$  is time. Then, denoting  $P$  as  $p(\theta)$  above and solving for  $p(\theta)$  gives

$$p(\theta) = \frac{w(\theta)}{KVt} = \frac{w_0 \cos \theta}{KVt}$$

Since all elemental surface areas of the friction material see the same rubbing speed for the same duration,  $w_0/(KVt)$  is a constant and

$$p(\theta) = (\text{constant}) \cos \theta = p_a \cos \theta \quad (c)$$

where  $p_a$  is the maximum value of  $p(\theta)$ .

Proceeding to the force analysis, we observe from Fig. 16–12a that

$$dN = pbr d\theta \quad (d)$$

or

$$dN = p_a br \cos \theta d\theta \quad (e)$$

The distance  $a$  to the pivot is chosen by finding where the moment of the frictional forces  $M_f$  is zero. First, this ensures that reaction  $R_y$  is at the correct location to establish symmetrical wear. Second, a cosinusoidal pressure distribution is sustained, preserving our predictive ability. Symmetry means  $\theta_1 = \theta_2$ , so

$$M_f = 2 \int_0^{\theta_2} (f dN)(a \cos \theta - r) = 0$$

Substituting Eq. (e) gives

$$2fp_a br \int_0^{\theta_2} (a \cos^2 \theta - r \cos \theta) d\theta = 0$$

from which

$$a = \frac{4r \sin \theta_2}{2\theta_2 + \sin 2\theta_2} \quad (16-15)$$

The distance  $a$  depends on the pressure distribution. Mislocating the pivot makes  $M_f$  zero about a different location, so the brake lining adjusts its local contact pressure, through wear, to compensate. The result is unsymmetrical wear, retiring the shoe lining, hence the shoe, sooner.

With the pivot located according to Eq. (16–15), the moment about the pin is zero, and the horizontal and vertical reactions are

$$R_x = 2 \int_0^{\theta_2} dN \cos \theta = \frac{p_a br}{2} (2\theta_2 + \sin 2\theta_2) \quad (16-16)$$

where, because of symmetry,

$$\int f dN \sin \theta = 0$$

Also,

$$R_y = 2 \int_0^{\theta_2} f dN \cos \theta = \frac{p_a br f}{2} (2\theta_2 + \sin 2\theta_2) \quad (16-17)$$

where

$$\int dN \sin \theta = 0$$

also because of symmetry. Note, too, that  $R_x = -N$  and  $R_y = -fN$ , as might be expected for the particular choice of the dimension  $a$ . Therefore the torque is

$$T = afN \quad (16-18)$$

## 16-4 Band-Type Clutches and Brakes

Flexible clutch and brake bands are used in power excavators and in hoisting and other machinery. The analysis follows the notation of Fig. 16-13.

Because of friction and the rotation of the drum, the actuating force  $P_2$  is less than the pin reaction  $P_1$ . Any element of the band, of angular length  $d\theta$ , will be in equilibrium under the action of the forces shown in the figure. Summing these forces in the vertical direction, we have

$$(P + dP) \sin \frac{d\theta}{2} + P \sin \frac{d\theta}{2} - dN = 0 \quad (a)$$

$$dN = Pd\theta \quad (b)$$

since for small angles  $\sin d\theta/2 = d\theta/2$ . Summing the forces in the horizontal direction gives

$$(P + dP) \cos \frac{d\theta}{2} - P \cos \frac{d\theta}{2} - f dN = 0 \quad (c)$$

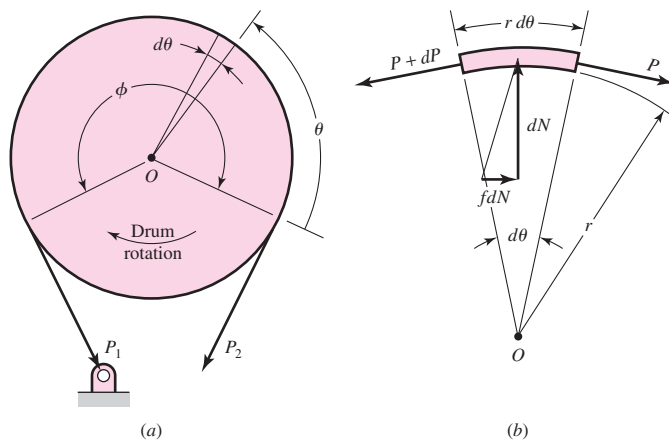
$$dP - f dN = 0 \quad (d)$$

since for small angles,  $\cos(d\theta/2) \doteq 1$ . Substituting the value of  $dN$  from Eq. (b) in (d) and integrating give

$$\int_{P_2}^{P_1} \frac{dP}{P} = f \int_0^\phi d\theta \quad \text{or} \quad \ln \frac{P_1}{P_2} = f\phi$$

**Figure 16-13**

Forces on a brake band.



and

$$\frac{P_1}{P_2} = e^{f\phi} \quad (16-19)$$

The torque may be obtained from the equation

$$T = (P_1 - P_2) \frac{D}{2} \quad (16-20)$$

The normal force  $dN$  acting on an element of area of width  $b$  and length  $rd\theta$  is

$$dN = pbr d\theta \quad (e)$$

where  $p$  is the pressure. Substitution of the value of  $dN$  from Eq. (b) gives

$$P d\theta = pbr d\theta$$

Therefore

$$p = \frac{P}{br} = \frac{2P}{bD} \quad (16-21)$$

The pressure is therefore proportional to the tension in the band. The maximum pressure  $p_a$  will occur at the toe and has the value

$$p_a = \frac{2P_1}{bD} \quad (16-22)$$

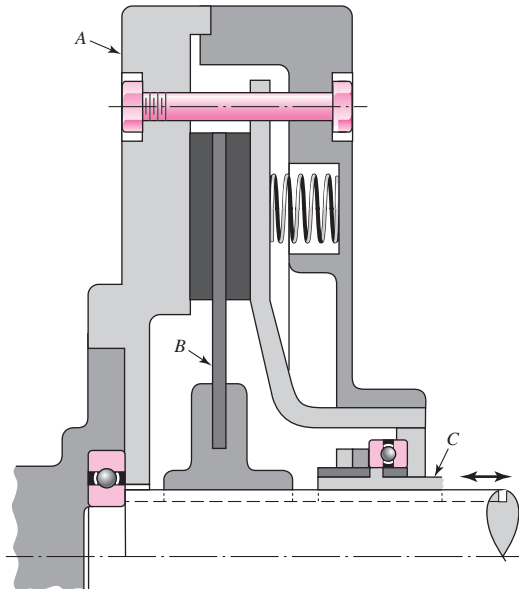
## 16-5

### Frictional-Contact Axial Clutches

An axial clutch is one in which the mating frictional members are moved in a direction parallel to the shaft. One of the earliest of these is the cone clutch, which is simple in construction and quite powerful. However, except for relatively simple installations, it has been largely displaced by the disk clutch employing one or more disks as the operating members. Advantages of the disk clutch include the freedom from centrifugal effects, the large frictional area that can be installed in a small space, the more effective heat-dissipation surfaces, and the favorable pressure distribution. Figure 16-14 shows a

**Figure 16-14**

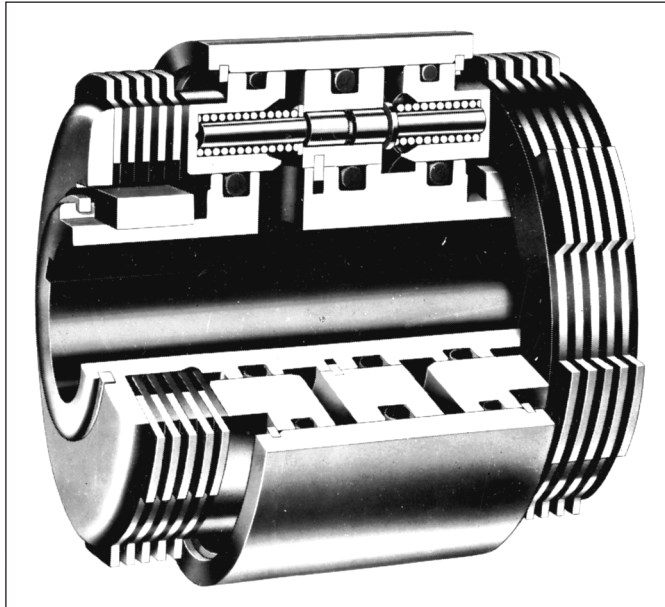
Cross-sectional view of a single-plate clutch; A, driver; B, driven plate (keyed to driven shaft); C, actuator.



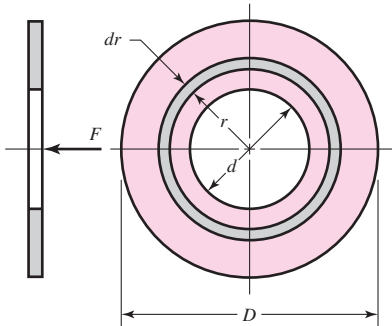
**Figure 16-15**

An oil-actuated multiple-disk clutch-brake for operation in an oil bath or spray. It is especially useful for rapid cycling.

(Courtesy of Twin Disc Clutch Company.)

**Figure 16-16**

Disk friction member.



single-plate disk clutch; a multiple-disk clutch-brake is shown in Fig. 16-15. Let us now determine the capacity of such a clutch or brake in terms of the material and geometry.

Figure 16-16 shows a friction disk having an outside diameter  $D$  and an inside diameter  $d$ . We are interested in obtaining the axial force  $F$  necessary to produce a certain torque  $T$  and pressure  $p$ . Two methods of solving the problem, depending upon the construction of the clutch, are in general use. If the disks are rigid, then the greatest amount of wear will at first occur in the outer areas, since the work of friction is greater in those areas. After a certain amount of wear has taken place, the pressure distribution will change so as to permit the wear to be uniform. This is the basis of the first method of solution.

Another method of construction employs springs to obtain a uniform pressure over the area. It is this assumption of uniform pressure that is used in the second method of solution.

### **Uniform Wear**

After initial wear has taken place and the disks have worn down to a point where uniform wear is established, the axial wear can be expressed by Eq. (12-27), p. 663, as

$$w = f_1 f_2 K P V t$$

in which only  $P$  and  $V$  vary from place to place in the rubbing surfaces. By definition uniform wear is constant from place to place; therefore,

$$\begin{aligned} PV &= (\text{constant}) = C_1 \\ pr\omega &= C_2 \\ pr &= C_3 = p_{\max}r_i = p_a r_i = p_a \frac{d}{2} \end{aligned} \quad (a)$$

We can take an expression from Eq. (a), which is the condition for having the same amount of work done at radius  $r$  as is done at radius  $d/2$ . Referring to Fig. 16-16, we have an element of area of radius  $r$  and thickness  $dr$ . The area of this element is  $2\pi r dr$ , so that the normal force acting upon this element is  $dF = 2\pi pr dr$ . We can find the total normal force by letting  $r$  vary from  $d/2$  to  $D/2$  and integrating. Thus, with  $pr$  constant,

$$F = \int_{d/2}^{D/2} 2\pi pr dr = \pi p_a d \int_{d/2}^{D/2} dr = \frac{\pi p_a d}{2} (D - d) \quad (16-23)$$

The torque is found by integrating the product of the frictional force and the radius:

$$T = \int_{d/2}^{D/2} 2\pi fpr^2 dr = \pi f p_a d \int_{d/2}^{D/2} r dr = \frac{\pi f p_a d}{8} (D^2 - d^2) \quad (16-24)$$

By substituting the value of  $F$  from Eq. (16-23) we may obtain a more convenient expression for the torque. Thus

$$T = \frac{Ff}{4} (D + d) \quad (16-25)$$

In use, Eq. (16-23) gives the actuating force for the selected maximum pressure  $p_a$ . This equation holds for any number of friction pairs or surfaces. Equation (16-25), however, gives the torque capacity for only a single friction surface.

### Uniform Pressure

When uniform pressure can be assumed over the area of the disk, the actuating force  $F$  is simply the product of the pressure and the area. This gives

$$F = \frac{\pi p_a}{4} (D^2 - d^2) \quad (16-26)$$

As before, the torque is found by integrating the product of the frictional force and the radius:

$$T = 2\pi fp \int_{d/2}^{D/2} r^2 dr = \frac{\pi fp}{12} (D^3 - d^3) \quad (16-27)$$

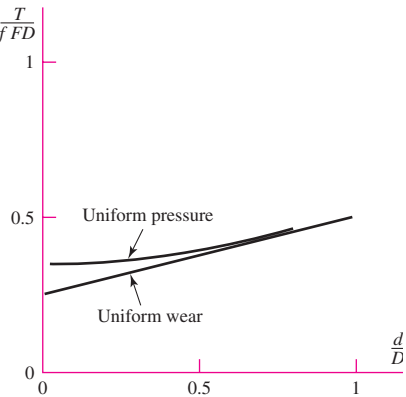
Since  $p = p_a$ , from Eq. (16-26) we can rewrite Eq. (16-27) as

$$T = \frac{Ff}{3} \frac{D^3 - d^3}{D^2 - d^2} \quad (16-28)$$

It should be noted for both equations that the torque is for a single pair of mating surfaces. This value must therefore be multiplied by the number of pairs of surfaces in contact.

**Figure 16-17**

Dimensionless plot of Eqs. (b) and (c).



Let us express Eq. (16–25) for torque during uniform wear as

$$\frac{T}{fFD} = \frac{1 + d/D}{4} \quad (b)$$

and Eq. (16–28) for torque during uniform pressure (new clutch) as

$$\frac{T}{fFD} = \frac{1}{3} \frac{1 - (d/D)^3}{1 - (d/D)^2} \quad (c)$$

and plot these in Fig. 16–17. What we see is a dimensionless presentation of Eqs. (b) and (c) which reduces the number of variables from five ( $T$ ,  $f$ ,  $F$ ,  $D$ , and  $d$ ) to three ( $T/FD$ ,  $f$ , and  $d/D$ ) which are dimensionless. This is the method of Buckingham. The dimensionless groups (called pi terms) are

$$\pi_1 = \frac{T}{FD} \quad \pi_2 = f \quad \pi_3 = \frac{d}{D}$$

This allows a five-dimensional space to be reduced to a three-dimensional space. Further, because of the “multiplicative” relation between  $f$  and  $T$  in Eqs. (b) and (c), it is possible to plot  $\pi_1/\pi_2$  versus  $\pi_3$  in a two-dimensional space (the plane of a sheet of paper) to view all cases over the domain of existence of Eqs. (b) and (c) and to compare, without risk of oversight! By examining Fig. 16–17 we can conclude that a new clutch, Eq. (b), always transmits more torque than an old clutch, Eq. (c). Furthermore, since clutches of this type are proportioned to make the diameter ratio  $d/D$  fall in the range  $0.6 \leq d/D \leq 1$ , the largest discrepancy between Eq. (b) and Eq. (c) will be

$$\frac{T}{fFD} = \frac{1 + 0.6}{4} = 0.400 \quad (\text{old clutch, uniform wear})$$

$$\frac{T}{fFD} = \frac{1}{3} \frac{1 - 0.6^3}{1 - 0.6^2} = 0.4083 \quad (\text{new clutch, uniform pressure})$$

so the proportional error is  $(0.4083 - 0.400)/0.400 = 0.021$ , or about 2 percent. Given the uncertainties in the actual coefficient of friction and the certainty that new clutches get old, there is little reason to use anything but Eqs. (16–23), (16–24), and (16–25).

## 16-6 Disk Brakes

As indicated in Fig. 16-16, there is no fundamental difference between a disk clutch and a disk brake. The analysis of the preceding section applies to disk brakes too.

We have seen that rim or drum brakes can be designed for self-energization. While this feature is important in reducing the braking effort required, it also has a disadvantage. When drum brakes are used as vehicle brakes, only a slight change in the coefficient of friction will cause a large change in the pedal force required for braking. A not unusual 30 percent reduction in the coefficient of friction due to a temperature change or moisture, for example, can result in a 50 percent change in the pedal force required to obtain the same braking torque obtainable prior to the change. The disk brake has no self-energization, and hence is not so susceptible to changes in the coefficient of friction.

Another type of disk brake is the *floating caliper brake*, shown in Fig. 16-18. The caliper supports a single floating piston actuated by hydraulic pressure. The action is much like that of a screw clamp, with the piston replacing the function of the screw. The floating action also compensates for wear and ensures a fairly constant pressure over the area of the friction pads. The seal and boot of Fig. 16-18 are designed to obtain clearance by backing off from the piston when the piston is released.

Caliper brakes (named for the nature of the actuating linkage) and disk brakes (named for the shape of the unlined surface) press friction material against the face(s)

**Figure 16-18**

An automotive disk brake.  
(Courtesy DaimlerChrysler Corporation.)

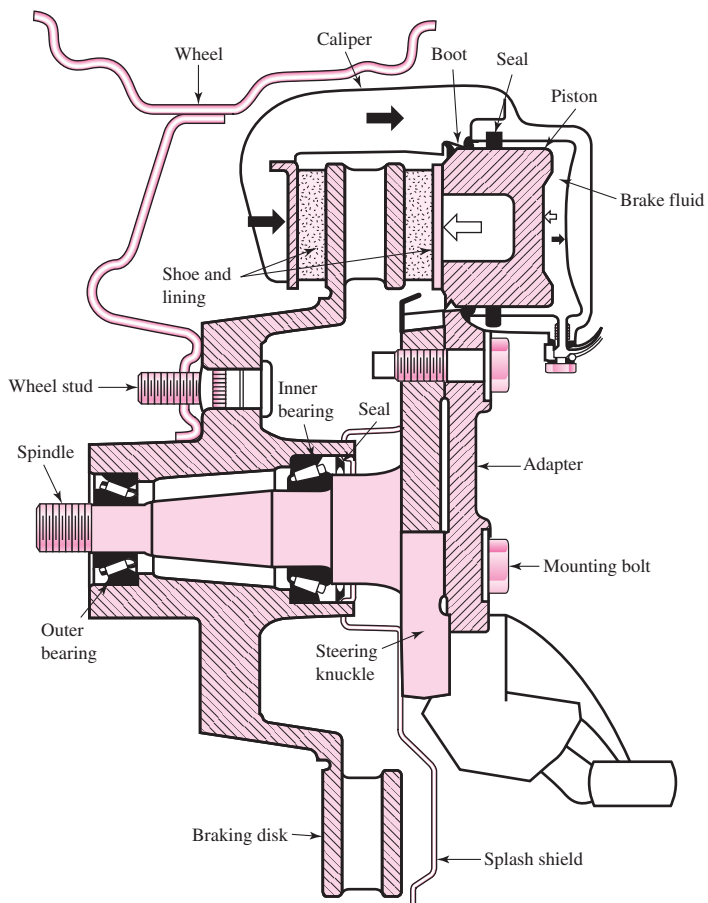
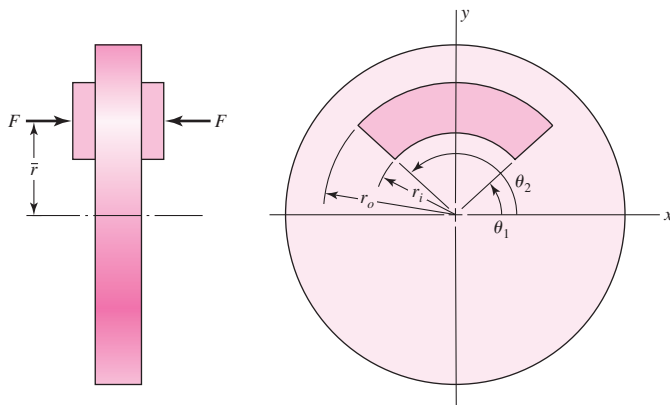


**Figure 16-19**

Geometry of contact area of an annular-pad segment of a caliper brake.



of a rotating disk. Depicted in Fig. 16-19 is the geometry of an annular-pad brake contact area. The governing axial wear equation is Eq. (12-27), p. 663,

$$w = f_1 f_2 K P V t$$

The coordinate  $\bar{r}$  locates the line of action of force  $F$  that intersects the  $y$  axis. Of interest also is the effective radius  $r_e$ , which is the radius of an equivalent shoe of infinitesimal radial thickness. If  $p$  is the local contact pressure, the actuating force  $F$  and the friction torque  $T$  are given by

$$F = \int_{\theta_1}^{\theta_2} \int_{r_i}^{r_o} pr dr d\theta = (\theta_2 - \theta_1) \int_{r_i}^{r_o} pr dr \quad (16-29)$$

$$T = \int_{\theta_1}^{\theta_2} \int_{r_i}^{r_o} fpr^2 dr d\theta = (\theta_2 - \theta_1) f \int_{r_i}^{r_o} pr^2 dr \quad (16-30)$$

The equivalent radius  $r_e$  can be found from  $fFr_e = T$ , or

$$r_e = \frac{T}{fF} = \frac{\int_{r_i}^{r_o} pr^2 dr}{\int_{r_i}^{r_o} pr dr} \quad (16-31)$$

The locating coordinate  $\bar{r}$  of the activating force is found by taking moments about the  $x$  axis:

$$M_x = F\bar{r} = \int_{\theta_1}^{\theta_2} \int_{r_i}^{r_o} pr(r \sin \theta) dr d\theta = (\cos \theta_1 - \cos \theta_2) \int_{r_i}^{r_o} pr^2 dr$$

$$\bar{r} = \frac{M_x}{F} = \frac{(\cos \theta_1 - \cos \theta_2)}{\theta_2 - \theta_1} r_e \quad (16-32)$$

### Uniform Wear

It is clear from Eq. (12-27) that for the axial wear to be the same everywhere, the product  $PV$  must be a constant. From Eq. (a), Sec. 16-5, the pressure  $p$  can be expressed in terms of the largest allowable pressure  $p_a$  (which occurs at the inner radius  $r_i$ ) as

$p = p_a r_i / r$ . Equation (16–29) becomes

$$F = (\theta_2 - \theta_1) p_a r_i (r_o - r_i) \quad (16-33)$$

Equation (16–30) becomes

$$T = (\theta_2 - \theta_1) f p_a r_i \int_{r_i}^{r_o} r dr = \frac{1}{2} (\theta_2 - \theta_1) f p_a r_i (r_o^2 - r_i^2) \quad (16-34)$$

Equation (16–31) becomes

$$r_e = \frac{p_a r_i \int_{r_i}^{r_o} r dr}{p_a r_i \int_{r_i}^{r_o} dr} = \frac{r_o^2 - r_i^2}{2} \frac{1}{r_o - r_i} = \frac{r_o + r_i}{2} \quad (16-35)$$

Equation (16–32) becomes

$$\bar{r} = \frac{\cos \theta_1 - \cos \theta_2}{\theta_2 - \theta_1} \frac{r_o + r_i}{2} \quad (16-36)$$

### Uniform Pressure

In this situation, approximated by a new brake,  $p = p_a$ . Equation (16–29) becomes

$$F = (\theta_2 - \theta_1) p_a \int_{r_i}^{r_o} r dr = \frac{1}{2} (\theta_2 - \theta_1) p_a (r_o^2 - r_i^2) \quad (16-37)$$

Equation (16–30) becomes

$$T = (\theta_2 - \theta_1) f p_a \int_{r_i}^{r_o} r^2 dr = \frac{1}{3} (\theta_2 - \theta_1) f p_a (r_o^3 - r_i^3) \quad (16-38)$$

Equation (16–31) becomes

$$r_e = \frac{p_a \int_{r_i}^{r_o} r^2 dr}{p_a \int_{r_i}^{r_o} r dr} = \frac{r_o^3 - r_i^3}{3} \frac{2}{r_o^2 - r_i^2} = \frac{2}{3} \frac{r_o^3 - r_i^3}{r_o^2 - r_i^2} \quad (16-39)$$

Equation (16–32) becomes

$$\bar{r} = \frac{\cos \theta_1 - \cos \theta_2}{\theta_2 - \theta_1} \frac{2}{3} \frac{r_o^3 - r_i^3}{r_o^2 - r_i^2} = \frac{2}{3} \frac{r_o^3 - r_i^3}{r_o^2 - r_i^2} \frac{\cos \theta_1 - \cos \theta_2}{\theta_2 - \theta_1} \quad (16-40)$$

### EXAMPLE 16–3

Two annular pads,  $r_i = 3.875$  in,  $r_o = 5.50$  in, subtend an angle of  $108^\circ$ , have a coefficient of friction of 0.37, and are actuated by a pair of hydraulic cylinders 1.5 in in diameter. The torque requirement is 13 000 lbf · in. For uniform wear

- (a) Find the largest normal pressure  $p_a$ .
- (b) Estimate the actuating force  $F$ .
- (c) Find the equivalent radius  $r_e$  and force location  $\bar{r}$ .
- (d) Estimate the required hydraulic pressure.

**Solution**

(a) From Eq. (16–34), with  $T = 13\,000/2 = 6500 \text{ lbf} \cdot \text{in}$  for each pad,

**Answer**

$$p_a = \frac{2T}{(\theta_2 - \theta_1)fr_i(r_o^2 - r_i^2)}$$

$$= \frac{2(6500)}{(144^\circ - 36^\circ)(\pi/180)0.37(3.875)(5.5^2 - 3.875^2)} = 315.8 \text{ psi}$$

(b) From Eq. (16–33),

**Answer**

$$F = (\theta_2 - \theta_1)p_a r_i(r_o - r_i) = (144^\circ - 36^\circ)(\pi/180)315.8(3.875)(5.5 - 3.875)$$

$$= 3748 \text{ lbf}$$

(c) From Eq. (16–35),

**Answer**

$$r_e = \frac{r_o + r_i}{2} = \frac{5.50 + 3.875}{2} = 4.688 \text{ in}$$

From Eq. (16–36),

**Answer**

$$\bar{r} = \frac{\cos \theta_1 - \cos \theta_2}{\theta_2 - \theta_1} \frac{r_o + r_i}{2} = \frac{\cos 36^\circ - \cos 144^\circ}{(144^\circ - 36^\circ)(\pi/180)} \frac{5.50 + 3.875}{2}$$

$$= 4.024 \text{ in}$$

(d) Each cylinder supplies the actuating force, 3748 lbf.

**Answer**

$$p_{\text{hydraulic}} = \frac{F}{A_P} = \frac{3748}{\pi(1.5^2/4)} = 2121 \text{ psi}$$

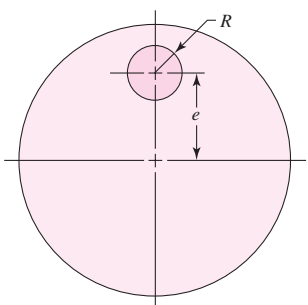


**Figure 16–20**

Geometry of circular pad of a caliper brake.

**Circular (Button or Puck) Pad Caliper Brake**

Figure 16–20 displays the pad geometry. Numerical integration is necessary to analyze this brake since the boundaries are difficult to handle in closed form. Table 16–1 gives the parameters for this brake as determined by Fazekas. The effective radius is given by

$$r_e = \delta e \quad (16-41)$$

The actuating force is given by

$$F = \pi R^2 p_{\text{av}} \quad (16-42)$$

and the torque is given by

$$T = f Fr_e \quad (16-43)$$

**Table 16-1**

Parameters for a

Circular-Pad Caliper

Brake

Source: G. A. Fazekas, "On Circular Spot Brakes," *Trans. ASME, J. Engineering for Industry*, vol. 94, Series B, No. 3, August 1972, pp. 859–863.

$\frac{R}{e}$	$\delta = \frac{r_e}{e}$	$\frac{p_{\max}}{p_{av}}$
0.0	1.000	1.000
0.1	0.983	1.093
0.2	0.969	1.212
0.3	0.957	1.367
0.4	0.947	1.578
0.5	0.938	1.875

**EXAMPLE 16-4**

A button-pad disk brake uses dry sintered metal pads. The pad radius is  $\frac{1}{2}$  in, and its center is 2 in from the axis of rotation of the  $3\frac{1}{2}$ -in-diameter disk. Using half of the largest allowable pressure,  $p_{\max} = 350$  psi, find the actuating force and the brake torque. The coefficient of friction is 0.31.

**Solution**

Since the pad radius  $R = 0.5$  in and eccentricity  $e = 2$  in,

$$\frac{R}{e} = \frac{0.5}{2} = 0.25$$

From Table 16-1, by interpolation,  $\delta = 0.963$  and  $p_{\max}/p_{av} = 1.290$ . It follows that the effective radius  $e$  is found from Eq. (16-41):

$$r_e = \delta e = 0.963(2) = 1.926 \text{ in}$$

and the average pressure is

$$p_{av} = \frac{p_{\max}/2}{1.290} = \frac{350/2}{1.290} = 135.7 \text{ psi}$$

The actuating force  $F$  is found from Eq. (16-42) to be

**Answer**  $F = \pi R^2 p_{av} = \pi(0.5)^2 135.7 = 106.6 \text{ lbf}$  (one side)

The brake torque  $T$  is

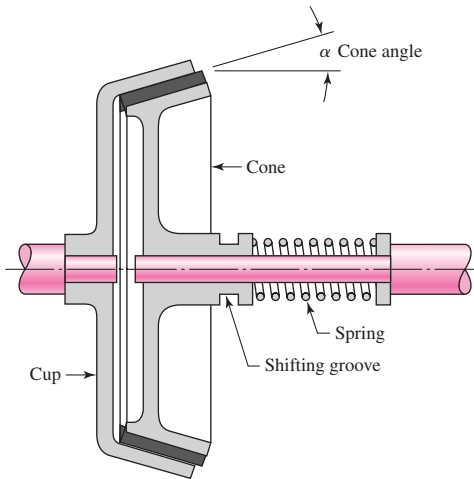
**Answer**  $T = f Fr_e = 0.31(106.6)1.926 = 63.65 \text{ lbf} \cdot \text{in}$  (one side)

**16-7****Cone Clutches and Brakes**

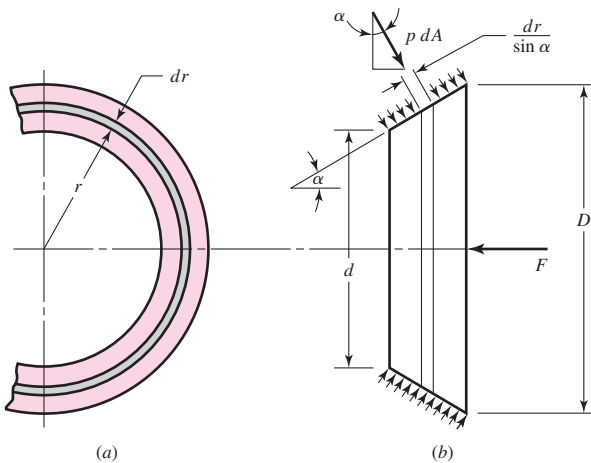
The drawing of a *cone clutch* in Fig. 16-21 shows that it consists of a *cup* keyed or splined to one of the shafts, a *cone* that must slide axially on splines or keys on the mating shaft, and a helical *spring* to hold the clutch in engagement. The clutch is disengaged by means of a fork that fits into the shifting groove on the friction cone. The *cone angle*  $\alpha$  and the diameter and face width of the cone are the important geometric design parameters. If the

**Figure 16–21**

Cross section of a cone clutch.

**Figure 16–22**

Contact area of a cone clutch.



cone angle is too small, say, less than about  $8^\circ$ , then the force required to disengage the clutch may be quite large. And the wedging effect lessens rapidly when larger cone angles are used. Depending upon the characteristics of the friction materials, a good compromise can usually be found using cone angles between  $10$  and  $15^\circ$ .

To find a relation between the operating force  $F$  and the torque transmitted, designate the dimensions of the friction cone as shown in Figure 16–22. As in the case of the axial clutch, we can obtain one set of relations for a uniform-wear and another set for a uniform-pressure assumption.

### Uniform Wear

The pressure relation is the same as for the axial clutch:

$$p = p_a \frac{d}{2r} \quad (a)$$

Next, referring to Fig. 16–22, we see that we have an element of area  $dA$  of radius  $r$  and width  $dr/\sin \alpha$ . Thus  $dA = (2\pi r dr)/\sin \alpha$ . As shown in Fig. 16–22, the operating

force will be the integral of the axial component of the differential force  $p dA$ . Thus

$$\begin{aligned} F &= \int p dA \sin \alpha = \int_{d/2}^{D/2} \left( p_a \frac{d}{2r} \right) \left( \frac{2\pi r dr}{\sin \alpha} \right) (\sin \alpha) \\ &= \pi p_a d \int_{d/2}^{D/2} dr = \frac{\pi p_a d}{2} (D - d) \end{aligned} \quad (16-44)$$

which is the same result as in Eq. (16-23).

The differential friction force is  $fp dA$ , and the torque is the integral of the product of this force with the radius. Thus

$$\begin{aligned} T &= \int r fp dA = \int_{d/2}^{D/2} (rf) \left( p_a \frac{d}{2r} \right) \left( \frac{2\pi r dr}{\sin \alpha} \right) \\ &= \frac{\pi f p_a d}{\sin \alpha} \int_{d/2}^{D/2} r dr = \frac{\pi f p_a d}{8 \sin \alpha} (D^2 - d^2) \end{aligned} \quad (16-45)$$

Note that Eq. (16-24) is a special case of Eq. (16-45), with  $\alpha = 90^\circ$ . Using Eq. (16-44), we find that the torque can also be written

$$T = \frac{Ff}{4 \sin \alpha} (D + d) \quad (16-46)$$

### Uniform Pressure

Using  $p = p_a$ , the actuating force is found to be

$$F = \int p_a dA \sin \alpha = \int_{d/2}^{D/2} (p_a) \left( \frac{2\pi r dr}{\sin \alpha} \right) (\sin \alpha) = \frac{\pi p_a}{4} (D^2 - d^2) \quad (16-47)$$

The torque is

$$T = \int r fp_a dA = \int_{d/2}^{D/2} (rf p_a) \left( \frac{2\pi r dr}{\sin \alpha} \right) = \frac{\pi f p_a}{12 \sin \alpha} (D^3 - d^3) \quad (16-48)$$

Using Eq. (16-47) in Eq. (16-48) gives

$$T = \frac{Ff}{3 \sin \alpha} \frac{D^3 - d^3}{D^2 - d^2} \quad (16-49)$$

As in the case of the axial clutch, we can write Eq. (16-46) dimensionlessly as

$$\frac{T \sin \alpha}{f F d} = \frac{1 + d/D}{4} \quad (b)$$

and write Eq. (16-49) as

$$\frac{T \sin \alpha}{f F d} = \frac{1}{3} \frac{1 - (d/D)^3}{1 - (d/D)^2} \quad (c)$$

This time there are six ( $T, \alpha, f, F, D$ , and  $d$ ) parameters and four pi terms:

$$\pi_1 = \frac{T}{FD} \quad \pi_2 = f \quad \pi_3 = \sin \alpha \quad \pi_4 = \frac{d}{D}$$

As in Fig. 16-17, we plot  $T \sin \alpha / (f F D)$  as ordinate and  $d/D$  as abscissa. The plots and conclusions are the same. There is little reason for using equations other than Eqs. (16-44), (16-45), and (16-46).

## 16-8 Energy Considerations

When the rotating members of a machine are caused to stop by means of a brake, the kinetic energy of rotation must be absorbed by the brake. This energy appears in the brake in the form of heat. In the same way, when the members of a machine that are initially at rest are brought up to speed, slipping must occur in the clutch until the driven members have the same speed as the driver. Kinetic energy is absorbed during slippage of either a clutch or a brake, and this energy appears as heat.

We have seen how the torque capacity of a clutch or brake depends upon the coefficient of friction of the material and upon a safe normal pressure. However, the character of the load may be such that, if this torque value is permitted, the clutch or brake may be destroyed by its own generated heat. The capacity of a clutch is therefore limited by two factors, the characteristics of the material and the ability of the clutch to dissipate heat. In this section we shall consider the amount of heat generated by a clutching or braking operation. If the heat is generated faster than it is dissipated, we have a temperature-rise problem; that is the subject of the next section.

To get a clear picture of what happens during a simple clutching or braking operation, refer to Fig. 16-1a, which is a mathematical model of a two-inertia system connected by a clutch. As shown, inertias  $I_1$  and  $I_2$  have initial angular velocities of  $\omega_1$  and  $\omega_2$ , respectively. During the clutch operation both angular velocities change and eventually become equal. We assume that the two shafts are rigid and that the clutch torque is constant.

Writing the equation of motion for inertia 1 gives

$$I_1 \ddot{\theta}_1 = -T \quad (a)$$

where  $\ddot{\theta}_1$  is the angular acceleration of  $I_1$  and  $T$  is the clutch torque. A similar equation for  $I_2$  is

$$I_2 \ddot{\theta}_2 = T \quad (b)$$

We can determine the instantaneous angular velocities  $\dot{\theta}_1$  and  $\dot{\theta}_2$  of  $I_1$  and  $I_2$  after any period of time  $t$  has elapsed by integrating Eqs. (a) and (b). The results are

$$\dot{\theta}_1 = -\frac{T}{I_1}t + \omega_1 \quad (c)$$

$$\dot{\theta}_2 = \frac{T}{I_2}t + \omega_2 \quad (d)$$

where  $\dot{\theta}_1 = \omega_1$  and  $\dot{\theta}_2 = \omega_2$  at  $t = 0$ . The difference in the velocities, sometimes called the relative velocity, is

$$\begin{aligned} \dot{\theta} &= \dot{\theta}_1 - \dot{\theta}_2 = -\frac{T}{I_1}t + \omega_1 - \left( \frac{T}{I_2}t + \omega_2 \right) \\ &= \omega_1 - \omega_2 - T \left( \frac{I_1 + I_2}{I_1 I_2} \right) t \end{aligned} \quad (16-50)$$

The clutching operation is completed at the instant in which the two angular velocities  $\dot{\theta}_1$  and  $\dot{\theta}_2$  become equal. Let the time required for the entire operation be  $t_1$ . Then  $\dot{\theta} = 0$  when  $\dot{\theta}_1 = \dot{\theta}_2$ , and so Eq. (16-50) gives the time as

$$t_1 = \frac{I_1 I_2 (\omega_1 - \omega_2)}{T(I_1 + I_2)} \quad (16-51)$$

This equation shows that the time required for the engagement operation is directly proportional to the velocity difference and inversely proportional to the torque.

We have assumed the clutch torque to be constant. Therefore, using Eq. (16–50), we find the rate of energy-dissipation during the clutching operation to be

$$u = T\dot{\theta} = T \left[ \omega_1 - \omega_2 - T \left( \frac{I_1 + I_2}{I_1 I_2} \right) t \right] \quad (e)$$

This equation shows that the energy-dissipation rate is greatest at the start, when  $t = 0$ .

The total energy dissipated during the clutching operation or braking cycle is obtained by integrating Eq. (e) from  $t = 0$  to  $t = t_1$ . The result is found to be

$$\begin{aligned} E &= \int_0^{t_1} u dt = T \int_0^{t_1} \left[ \omega_1 - \omega_2 - T \left( \frac{I_1 + I_2}{I_1 I_2} \right) t \right] dt \\ &= \frac{I_1 I_2 (\omega_1 - \omega_2)^2}{2(I_1 + I_2)} \end{aligned} \quad (16-52)$$

where Eq. (16–51) was employed. Note that the energy dissipated is proportional to the velocity difference squared and is independent of the clutch torque.

Note that  $E$  in Eq. (16–52) is the energy lost or dissipated; this is the energy that is absorbed by the clutch or brake. If the inertias are expressed in U.S. customary units ( $\text{lbf} \cdot \text{in} \cdot \text{s}^2$ ), then the energy absorbed by the clutch assembly is in  $\text{in} \cdot \text{lbf}$ . Using these units, the heat generated in Btu is

$$H = \frac{E}{9336} \quad (16-53)$$

In SI, the inertias are expressed in kilogram-meter<sup>2</sup> units, and the energy dissipated is expressed in joules.

## 16-9 Temperature Rise

The temperature rise of the clutch or brake assembly can be approximated by the classic expression

$$\Delta T = \frac{H}{C_p W} \quad (16-54)$$

where  $\Delta T$  = temperature rise, °F

$C_p$  = specific heat capacity,  $\text{Btu}/(\text{lb}_m \cdot {}^\circ\text{F})$ ; use 0.12 for steel or cast iron

$W$  = mass of clutch or brake parts,  $\text{lbm}$

A similar equation can be written for SI units. It is

$$\Delta T = \frac{E}{C_p m} \quad (16-55)$$

where  $\Delta T$  = temperature rise, °C

$C_p$  = specific heat capacity; use  $500 \text{ J/kg} \cdot {}^\circ\text{C}$  for steel or cast iron

$m$  = mass of clutch or brake parts,  $\text{kg}$

The temperature-rise equations above can be used to explain what happens when a clutch or brake is operated. However, there are so many variables involved that it would

be most unlikely that such an analysis would even approximate experimental results. For this reason such analyses are most useful, for repetitive cycling, in pinpointing those design parameters that have the greatest effect on performance.

If an object is at initial temperature  $T_1$  in an environment of temperature  $T_\infty$ , then Newton's cooling model is expressed as

$$\frac{T - T_\infty}{T_1 - T_\infty} = \exp\left(-\frac{\hbar_{\text{CR}} A}{W C_p} t\right) \quad (16-56)$$

where  $T$  = temperature at time  $t$ , °F

$T_1$  = initial temperature, °F

$T_\infty$  = environmental temperature, °F

$\hbar_{\text{CR}}$  = overall coefficient of heat transfer, Btu/(in<sup>2</sup> · s · °F)

$A$  = lateral surface area, in<sup>2</sup>

$W$  = mass of the object, lbm

$C_p$  = specific heat capacity of the object, Btu/(lbm · °F)

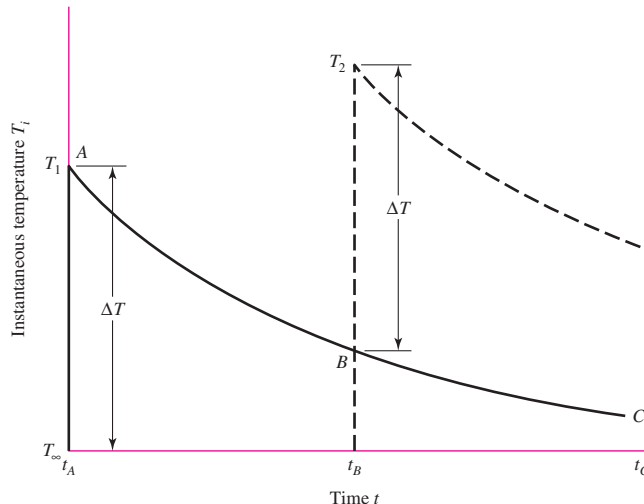
Figure 16–23 shows an application of Eq. (16–56). The curve ABC is the exponential decline of temperature given by Eq. (16–56). At time  $t_B$  a second application of the brake occurs. The temperature quickly rises to temperature  $T_2$ , and a new cooling curve is started. For repetitive brake applications, subsequent temperature peaks  $T_3, T_4, \dots$ , occur until the brake is able to dissipate by cooling between operations an amount of heat equal to the energy absorbed in the application. If this is a production situation with brake applications every  $t_1$  seconds, then a steady state develops in which all the peaks  $T_{\max}$  and all the valleys  $T_{\min}$  are repetitive.

The heat-dissipation capacity of disk brakes has to be planned to avoid reaching the temperatures of disk and pad that are detrimental to the parts. When a disk brake has a rhythm such as discussed above, then the rate of heat transfer is described by another Newtonian equation:

$$H_{\text{loss}} = \hbar_{\text{CR}} A(T - T_\infty) = (h_r + f_v h_c)A(T - T_\infty) \quad (16-57)$$

**Figure 16–23**

The effect of clutching or braking operations on temperature.  $T_\infty$  is the ambient temperature. Note that the temperature rise  $\Delta T$  may be different for each operation.



where  $H_{\text{loss}}$  = rate of energy loss, Btu/s

$\bar{h}_{\text{CR}}$  = overall coefficient of heat transfer, Btu/(in<sup>2</sup> · s · °F)

$h_r$  = radiation component of  $\bar{h}_{\text{CR}}$ , Btu/(in<sup>2</sup> · s · °F), Fig. 16–24a

$h_c$  = convective component of  $\bar{h}_{\text{CR}}$ , Btu/(in<sup>2</sup> · s · °F), Fig. 16–24a

$f_v$  = ventilation factor, Fig. 16–24b

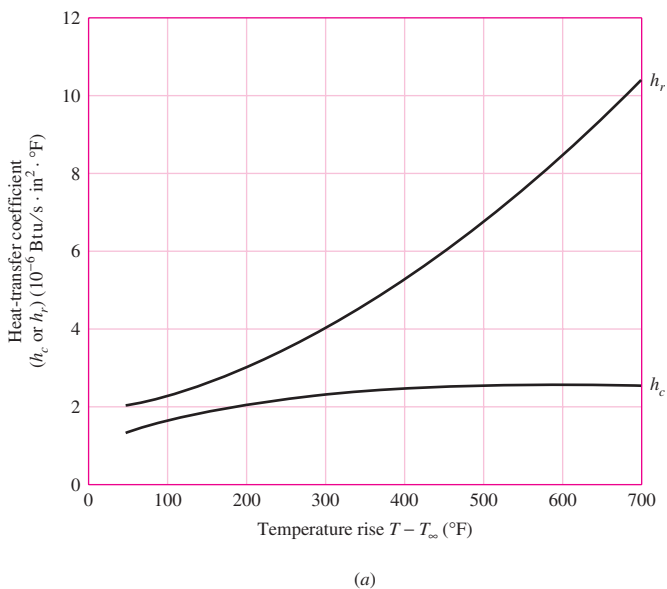
$T$  = disk temperature, °F

$T_\infty$  = ambient temperature, °F

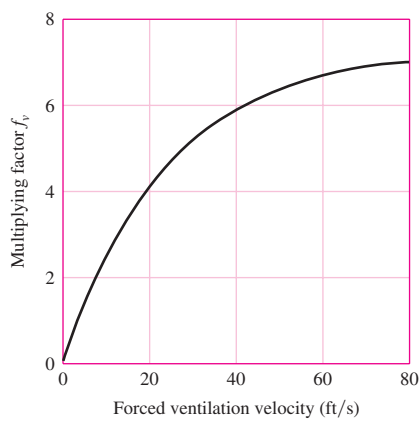
The energy  $E$  absorbed by the brake stopping an equivalent rotary inertia  $I$  in terms of original and final angular velocities  $\omega_o$  and  $\omega_f$  is given by Eq. (16–53) with  $I_1 = I$

**Figure 16–24**

(a) Heat-transfer coefficient in still air. (b) Ventilation factors.  
(Courtesy of Tolo-o-matic.)



(a)



(b)

and  $I_2 = 0$ ,

$$E = \frac{1}{2} \frac{I}{9336} (\omega_o^2 - \omega_f^2) \quad (16-58)$$

in Btu. The temperature rise  $\Delta T$  due to a single stop is

$$\Delta T = \frac{E}{WC} \quad (16-59)$$

$T_{\max}$  has to be high enough to transfer  $E$  Btu in  $t_1$  seconds. For steady state, rearrange Eq. (16-56) as

$$\frac{T_{\min} - T_{\infty}}{T_{\max} - T_{\infty}} = \exp(-\beta t_1)$$

where  $\beta = \hbar_{\text{CR}} A / (W C_p)$ . Cross-multiply, add  $T_{\max}$  to both sides, set  $T_{\max} - T_{\min} = \Delta T$ , and rearrange, obtaining

$$T_{\max} = T_{\infty} + \frac{\Delta T}{1 - \exp(-\beta t_1)} \quad (16-60)$$

### EXAMPLE 16-5

A caliper brake is used 24 times per hour to arrest a machine shaft from a speed of 250 rev/min to rest. The ventilation of the brake provides a mean air speed of 25 ft/s. The equivalent rotary inertia of the machine as seen from the brake shaft is 289 lbm · in · s. The disk is steel with a density  $\gamma = 0.282 \text{ lbm/in}^3$ , a specific heat capacity of 0.108 Btu/(lbm · °F), a diameter of 6 in, a thickness of  $\frac{1}{4}$  in. The pads are dry sintered metal. The lateral area of the brake surface is 50 in<sup>2</sup>. Find  $T_{\max}$  and  $T_{\min}$  for the steady-state operation.

#### Solution

$$t_1 = 60^2 / 24 = 150 \text{ s}$$

Assuming a temperature rise of  $T_{\max} - T_{\infty} = 200^\circ\text{F}$ , from Fig. 16-24a,

$$h_r = 3.0(10^{-6}) \text{ Btu}/(\text{in}^2 \cdot \text{s} \cdot {}^\circ\text{F})$$

$$h_c = 2.0(10^{-6}) \text{ Btu}/(\text{in}^2 \cdot \text{s} \cdot {}^\circ\text{F})$$

Fig. 16-24b

$$f_v = 4.8$$

$$\hbar_{\text{CR}} = h_r + f_v h_c = 3.0(10^{-6}) + 4.8(2.0)10^{-6} = 12.6(10^{-6}) \text{ Btu}/(\text{in}^2 \cdot \text{s} \cdot {}^\circ\text{F})$$

The mass of the disk is

$$W = \frac{\pi \gamma D^2 h}{4} = \frac{\pi(0.282)6^2(0.25)}{4} = 1.99 \text{ lbm}$$

$$\text{Eq. (16-58): } E = \frac{1}{2} \frac{I}{9336} (\omega_o^2 - \omega_f^2) = \frac{289}{2(9336)} \left( \frac{2\pi}{60} 250 \right)^2 = 10.6 \text{ Btu}$$

$$\beta = \frac{\hbar_{\text{CR}} A}{W C_p} = \frac{12.6(10^{-6})50}{1.99(0.108)} = 2.93(10^{-3}) \text{ s}^{-1}$$

$$\text{Eq. (16-59): } \Delta T = \frac{E}{WC_p} = \frac{10.6}{1.99(0.108)} = 49.3^\circ\text{F}$$

**Answer** Eq. (16-60):  $T_{\max} = 70 + \frac{49.3}{1 - \exp[-2.93(10^{-3})150]} = 209^\circ\text{F}$

**Answer**  $T_{\min} = 209 - 49.3 = 160^\circ\text{F}$

The predicted temperature rise here is  $T_{\max} - T_\infty = 139^\circ\text{F}$ . Iterating with revised values of  $h_r$  and  $h_c$  from Fig. 16-24a, we can make the solution converge to  $T_{\max} = 220^\circ\text{F}$  and  $T_{\min} = 171^\circ\text{F}$ .

Table 16-3 for dry sintered metal pads gives a continuous operating maximum temperature of 570–660°F. There is no danger of overheating.

## 16-10 Friction Materials

A brake or friction clutch should have the following lining material characteristics to a degree that is dependent on the severity of service:

- High and reproducible coefficient of friction
- Imperviousness to environmental conditions, such as moisture
- The ability to withstand high temperatures, together with good thermal conductivity and diffusivity, as well as high specific heat capacity
- Good resiliency
- High resistance to wear, scoring, and galling
- Compatible with the environment
- Flexibility

Table 16-2 gives area of friction surface required for several braking powers. Table 16-3 gives important characteristics of some friction materials for brakes and clutches.

**Table 16-2**

Area of Friction Material Required for a Given Average Braking Power   Sources: M. J. Neale, *The Tribology Handbook*, Butterworth, London, 1973; *Friction Materials for Engineers*, Ferodo Ltd., Chapel-en-le-Frith, England, 1968.

<b>Duty Cycle</b>	<b>Typical Applications</b>	<b>Ratio of Area to Average Braking Power, in<sup>2</sup>/(Btu/s)</b>		
		<b>Band and Drum Brakes</b>	<b>Plate Disk Brakes</b>	<b>Caliper Disk Brakes</b>
Infrequent	Emergency brakes	0.85	2.8	0.28
Intermittent	Elevators, cranes, and winches	2.8	7.1	0.70
Heavy-duty	Excavators, presses	5.6–6.9	13.6	1.41

**Table 16-3**

Characteristics of Friction Materials for Brakes and Clutches   Sources: Ferodo Ltd., Chapel-en-le-frith, England; Scan-pac, Mequon, Wisc.; Raybestos, New York, N.Y. and Stratford, Conn.; Gatke Corp., Chicago, Ill.; General Metals Powder Co., Akron, Ohio; D. A. B. Industries, Troy, Mich.; Friction Products Co., Medina, Ohio.

Material	Friction Coefficient <i>f</i>	Maximum Pressure <i>p</i> <sub>max</sub> , psi	Maximum Temperature Instantaneous, °F	Continuous, °F	Maximum Velocity <i>V</i> <sub>max</sub> , ft/min	Applications
Cermet	0.32	150	1500	750		Brakes and clutches
Sintered metal (dry)	0.29–0.33	300–400	930–1020	570–660	3600	Clutches and caliper disk brakes
Sintered metal (wet)	0.06–0.08	500	930	570	3600	Clutches
Rigid molded asbestos (dry)	0.35–0.41	100	660–750	350	3600	Drum brakes and clutches
Rigid molded asbestos (wet)	0.06	300	660	350	3600	Industrial clutches
Rigid molded asbestos pads	0.31–0.49	750	930–1380	440–660	4800	Disk brakes
Rigid molded nonasbestos	0.33–0.63	100–150		500–750	4800–7500	Clutches and brakes
Semirigid molded asbestos	0.37–0.41	100	660	300	3600	Clutches and brakes
Flexible molded asbestos	0.39–0.45	100	660–750	300–350	3600	Clutches and brakes
Wound asbestos yarn and wire	0.38	100	660	300	3600	Vehicle clutches
Woven asbestos yarn and wire	0.38	100	500	260	3600	Industrial clutches and brakes
Woven cotton	0.47	100	230	170	3600	Industrial clutches and brakes
Resilient paper (wet)	0.09–0.15	400	300		<i>PV</i> < 500 000 psi · ft/min	Clutches and transmission bands

The manufacture of friction materials is a highly specialized process, and it is advisable to consult manufacturers' catalogs and handbooks, as well as manufacturers directly, in selecting friction materials for specific applications. Selection involves a consideration of the many characteristics as well as the standard sizes available.

The *woven-cotton lining* is produced as a fabric belt that is impregnated with resins and polymerized. It is used mostly in heavy machinery and is usually supplied in rolls up to 50 ft in length. Thicknesses available range from  $\frac{1}{8}$  to 1 in, in widths up to about 12 in.

A *woven-asbestos lining* is made in a similar manner to the cotton lining and may also contain metal particles. It is not quite as flexible as the cotton lining and comes in a smaller range of sizes. Along with the cotton lining, the asbestos lining was widely used as a brake material in heavy machinery.

*Molded-asbestos linings* contain asbestos fiber and friction modifiers; a thermoset polymer is used, with heat, to form a rigid or semirigid molding. The principal use was in drum brakes.

*Molded-asbestos pads* are similar to molded linings but have no flexibility; they were used for both clutches and brakes.

*Sintered-metal pads* are made of a mixture of copper and/or iron particles with friction modifiers, molded under high pressure and then heated to a high temperature to fuse the material. These pads are used in both brakes and clutches for heavy-duty applications.

*Cermet pads* are similar to the sintered-metal pads and have a substantial ceramic content.

Table 16–4 lists properties of typical brake linings. The linings may consist of a mixture of fibers to provide strength and ability to withstand high temperatures, various friction particles to obtain a degree of wear resistance as well as a higher coefficient of friction, and bonding materials.

Table 16–5 includes a wider variety of clutch friction materials, together with some of their properties. Some of these materials may be run wet by allowing them to dip in oil or to be sprayed by oil. This reduces the coefficient of friction somewhat but carries away more heat and permits higher pressures to be used.

**Table 16–4**

Some Properties  
of Brake Linings

	<b>Woven Lining</b>	<b>Molded Lining</b>	<b>Rigid Block</b>
Compressive strength, kpsi	10–15	10–18	10–15
Compressive strength, MPa	70–100	70–125	70–100
Tensile strength, kpsi	2.5–3	4–5	3–4
Tensile strength, MPa	17–21	27–35	21–27
Max. temperature, °F	400–500	500	750
Max. temperature, °C	200–260	260	400
Max. speed, ft/min	7500	5000	7500
Max. speed, m/s	38	25	38
Max. pressure, psi	50–100	100	150
Max. pressure, kPa	340–690	690	1000
Frictional coefficient, mean	0.45	0.47	0.40–45

**Table 16–5**

Friction Materials for Clutches

<b>Material</b>	<b>Friction Coefficient</b>		<b>Max. Temperature</b>		<b>Max. Pressure</b>	
	<b>Wet</b>	<b>Dry</b>	<b>°F</b>	<b>°C</b>	<b>psi</b>	<b>kPa</b>
Cast iron on cast iron	0.05	0.15–0.20	600	320	150–250	1000–1750
Powdered metal* on cast iron	0.05–0.1	0.1–0.4	1000	540	150	1000
Powdered metal* on hard steel	0.05–0.1	0.1–0.3	1000	540	300	2100
Wood on steel or cast iron	0.16	0.2–0.35	300	150	60–90	400–620
Leather on steel or cast iron	0.12	0.3–0.5	200	100	10–40	70–280
Cork on steel or cast iron	0.15–0.25	0.3–0.5	200	100	8–14	50–100
Felt on steel or cast iron	0.18	0.22	280	140	5–10	35–70
Woven asbestos* on steel or cast iron	0.1–0.2	0.3–0.6	350–500	175–260	50–100	350–700
Molded asbestos* on steel or cast iron	0.08–0.12	0.2–0.5	500	260	50–150	350–1000
Impregnated asbestos* on steel or cast iron	0.12	0.32	500–750	260–400	150	1000
Carbon graphite on steel	0.05–0.1	0.25	700–1000	370–540	300	2100

\*The friction coefficient can be maintained with  $\pm 5$  percent for specific materials in this group.

## 16–11 Miscellaneous Clutches and Couplings

The square-jaw clutch shown in Fig. 16–25a is one form of positive-contact clutch. These clutches have the following characteristics:

- 1 They do not slip.
- 2 No heat is generated.
- 3 They cannot be engaged at high speeds.
- 4 Sometimes they cannot be engaged when both shafts are at rest.
- 5 Engagement at any speed is accompanied by shock.

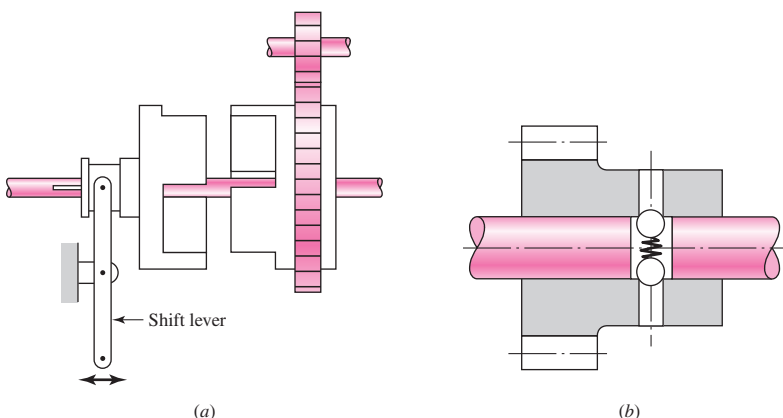
The greatest differences among the various types of positive clutches are concerned with the design of the jaws. To provide a longer period of time for shift action during engagement, the jaws may be ratchet-shaped, spiral-shaped, or gear-tooth-shaped. Sometimes a great many teeth or jaws are used, and they may be cut either circumferentially, so that they engage by cylindrical mating, or on the faces of the mating elements.

Although positive clutches are not used to the extent of the frictional-contact types, they do have important applications where synchronous operation is required, as, for example, in power presses or rolling-mill screw-downs.

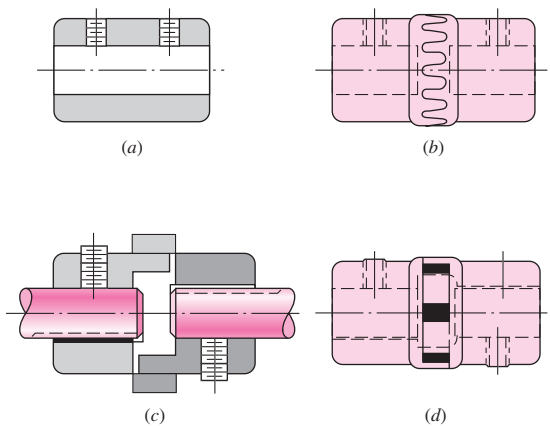
Devices such as linear drives or motor-operated screwdrivers must run to a definite limit and then come to a stop. An overload-release type of clutch is required for these applications. Figure 16–25b is a schematic drawing illustrating the principle of operation of such a clutch. These clutches are usually spring-loaded so as to release at a

**Figure 16–25**

- (a) Square-jaw clutch;  
(b) overload release clutch  
using a detent.

**Figure 16–26**

- Shaft couplings. (a) Plain.  
(b) Light-duty toothed coupling.  
(c) BOST-FLEX® through-bore design having elastomer insert to transmit torque by compression; insert permits 1° misalignment.  
(d) Three-jaw coupling available with bronze, rubber, or polyurethane insert to minimize vibration. (Reproduced by permission, Boston Gear Division, Colfax Corp.)



predetermined torque. The clicking sound which is heard when the overload point is reached is considered to be a desirable signal.

Both fatigue and shock loads must be considered in obtaining the stresses and deflections of the various portions of positive clutches. In addition, wear must generally be considered. The application of the fundamentals discussed in Parts 1 and 2 is usually sufficient for the complete design of these devices.

An overrunning clutch or coupling permits the driven member of a machine to "freewheel" or "overrun" because the driver is stopped or because another source of power increases the speed of the driven mechanism. The construction uses rollers or balls mounted between an outer sleeve and an inner member having cam flats machined around the periphery. Driving action is obtained by wedging the rollers between the sleeve and the cam flats. This clutch is therefore equivalent to a pawl and ratchet with an infinite number of teeth.

There are many varieties of overrunning clutches available, and they are built in capacities up to hundreds of horsepower. Since no slippage is involved, the only power loss is that due to bearing friction and windage.

The shaft couplings shown in Fig. 16–26 are representative of the selection available in catalogs.

## 16-12 Flywheels

The equation of motion for the flywheel represented in Fig. 16-1b is

$$\sum M = T_i(\theta_i, \dot{\theta}_i) - T_o(\theta_o, \dot{\theta}_o) - I\ddot{\theta} = 0$$

or

$$I\ddot{\theta} = T_i(\theta_i, \omega_i) - T_o(\theta_o, \omega_o) \quad (a)$$

where  $T_i$  is considered positive and  $T_o$  negative, and where  $\dot{\theta}$  and  $\ddot{\theta}$  are the first and second time derivatives of  $\theta$ , respectively. Note that both  $T_i$  and  $T_o$  may depend for their values on the angular displacements  $\theta_i$  and  $\theta_o$  as well as their angular velocities  $\omega_i$  and  $\omega_o$ . In many cases the torque characteristic depends upon only one of these. Thus, the torque delivered by an induction motor depends upon the speed of the motor. In fact, motor manufacturers publish charts detailing the torque-speed characteristics of their various motors.

When the input and output torque functions are given, Eq. (a) can be solved for the motion of the flywheel using well-known techniques for solving linear and nonlinear differential equations. We can dispense with this here by assuming a rigid shaft, giving  $\theta_i = \theta = \theta_o$  and  $\omega_i = \omega = \omega_o$ . Thus, Eq. (a) becomes

$$I\ddot{\theta} = T_i(\theta, \omega) - T_o(\theta, \omega) \quad (b)$$

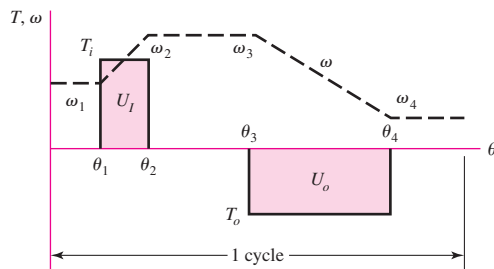
When the two torque functions are known and the starting values of the displacement  $\theta$  and velocity  $\omega$  are given, Eq. (b) can be solved for  $\theta$ ,  $\omega$ , and  $\ddot{\theta}$  as functions of time. However, we are not really interested in the instantaneous values of these terms at all. Primarily we want to know the overall performance of the flywheel. What should its moment of inertia be? How do we match the power source to the load? And what are the resulting performance characteristics of the system that we have selected?

To gain insight into the problem, a hypothetical situation is diagrammed in Fig. 16-27. An input power source subjects a flywheel to a constant torque  $T_i$  while the shaft rotates from  $\theta_1$  to  $\theta_2$ . This is a positive torque and is plotted upward. Equation (b) indicates that a positive acceleration  $\ddot{\theta}$  will be the result, and so the shaft velocity increases from  $\omega_1$  to  $\omega_2$ . As shown, the shaft now rotates from  $\theta_2$  to  $\theta_3$  with zero torque and hence, from Eq. (b), with zero acceleration. Therefore  $\omega_3 = \omega_2$ . From  $\theta_3$  to  $\theta_4$  a load, or output torque, of constant magnitude is applied, causing the shaft to slow down from  $\omega_3$  to  $\omega_4$ . Note that the output torque is plotted in the negative direction in accordance with Eq. (b).

The work input to the flywheel is the area of the rectangle between  $\theta_1$  and  $\theta_2$ , or

$$U_i = T_i(\theta_2 - \theta_1) \quad (c)$$

| Figure 16-27



The work output of the flywheel is the area of the rectangle from  $\theta_3$  to  $\theta_4$ , or

$$U_o = T_o(\theta_4 - \theta_3) \quad (d)$$

If  $U_o$  is greater than  $U_i$ , the load uses more energy than has been delivered to the flywheel and so  $\omega_4$  will be less than  $\omega_1$ . If  $U_o = U_i$ ,  $\omega_4$  will be equal to  $\omega_1$  because the gains and losses are equal; we are assuming no friction losses. And finally,  $\omega_4$  will be greater than  $\omega_1$  if  $U_i > U_o$ .

We can also write these relations in terms of kinetic energy. At  $\theta = \theta_1$  the flywheel has a velocity of  $\omega_1$  rad/s, and so its kinetic energy is

$$E_1 = \frac{1}{2} I \omega_1^2 \quad (e)$$

At  $\theta = \theta_2$  the velocity is  $\omega_2$ , and so

$$E_2 = \frac{1}{2} I \omega_2^2 \quad (f)$$

Thus the change in kinetic energy is

$$E_2 - E_1 = \frac{1}{2} I (\omega_2^2 - \omega_1^2) \quad (16-61)$$

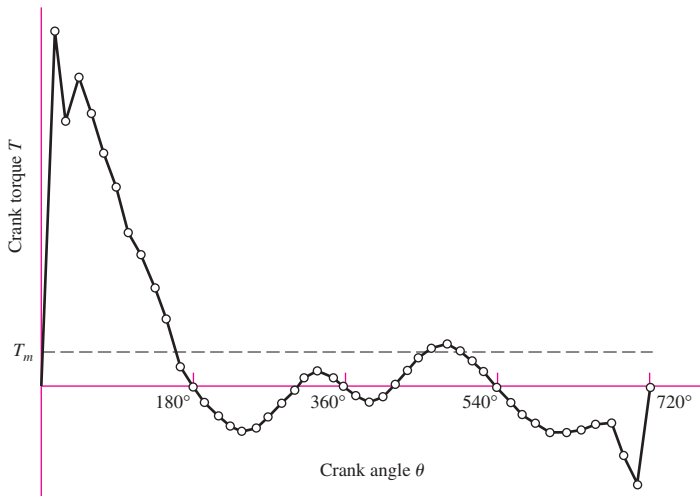
Many of the torque displacement functions encountered in practical engineering situations are so complicated that they must be integrated by numerical methods. Figure 16–28, for example, is a typical plot of the engine torque for one cycle of motion of a single-cylinder internal combustion engine. Since a part of the torque curve is negative, the flywheel must return part of the energy back to the engine. Integrating this curve from  $\theta = 0$  to  $4\pi$  and dividing the result by  $4\pi$  yields the mean torque  $T_m$  available to drive a load during the cycle.

It is convenient to define a *coefficient of speed fluctuation* as

$$C_s = \frac{\omega_2 - \omega_1}{\omega} \quad (16-62)$$

**Figure 16–28**

Relation between torque and crank angle for a one-cylinder, four-stroke-cycle internal combustion engine.



where  $\omega$  is the nominal angular velocity, given by

$$\omega = \frac{\omega_2 + \omega_1}{2} \quad (16-63)$$

Equation (16–61) can be factored to give

$$E_2 - E_1 = \frac{I}{2}(\omega_2 - \omega_1)(\omega_2 + \omega_1)$$

Since  $\omega_2 - \omega_1 = C_s \omega$  and  $\omega_2 + \omega_1 = 2\omega$ , we have

$$E_2 - E_1 = C_s I \omega^2 \quad (16-64)$$

Equation (16–64) can be used to obtain an appropriate flywheel inertia corresponding to the energy change  $E_2 - E_1$ .

### EXAMPLE 16–6

Table 16–6 lists values of the torque used to plot Fig. 16–28. The nominal speed of the engine is to be 250 rad/s.

- (a) Integrate the torque-displacement function for one cycle and find the energy that can be delivered to a load during the cycle.
- (b) Determine the mean torque  $T_m$  (see Fig. 16–28).
- (c) The greatest energy fluctuation is approximately between  $\theta = 15^\circ$  and  $\theta = 150^\circ$  on the torque diagram; see Fig. 16–28 and note that  $T_o = -T_m$ . Using a coefficient of speed fluctuation  $C_s = 0.1$ , find a suitable value for the flywheel inertia.
- (d) Find  $\omega_2$  and  $\omega_1$ .

#### Solution

- (a) Using  $n = 48$  intervals of  $\Delta\theta = 4\pi/48$ , numerical integration of the data of Table 16–6 yields  $E = 3368 \text{ in} \cdot \text{lbf}$ . This is the energy that can be delivered to the load.

**Table 16–6**

Plotting Data for  
Fig. 16–29

$\theta, \text{ deg}$	$T, \text{ lbf} \cdot \text{in}$	$\theta, \text{ deg}$	$T, \text{ lbf} \cdot \text{in}$	$\theta, \text{ deg}$	$T, \text{ lbf} \cdot \text{in}$	$\theta, \text{ deg}$	$T, \text{ lbf} \cdot \text{in}$
0	0	195	-107	375	-85	555	-107
15	2800	210	-206	390	-125	570	-206
30	2090	225	-260	405	-89	585	-292
45	2430	240	-323	420	8	600	-355
60	2160	255	-310	435	126	615	-371
75	1840	270	-242	450	242	630	-362
90	1590	285	-126	465	310	645	-312
105	1210	300	-8	480	323	660	-272
120	1066	315	89	495	280	675	-274
135	803	330	125	510	206	690	-548
150	532	345	85	525	107	705	-760
165	184	360	0	540	0	720	0
180	0						

**Answer**

(b)

$$T_m = \frac{3368}{4\pi} = 268 \text{ lbf} \cdot \text{in}$$

(c) The largest positive loop on the torque-displacement diagram occurs between  $\theta = 0^\circ$  and  $\theta = 180^\circ$ . We select this loop as yielding the largest speed change. Subtracting 268 lbf · in from the values in Table 16–6 for this loop gives, respectively, -268, 2532, 1822, 2162, 1892, 1572, 1322, 942, 798, 535, 264, -84, and -268 lbf · in. Numerically integrating  $T - T_m$  with respect to  $\theta$  yields  $E_2 - E_1 = 3531 \text{ lbf} \cdot \text{in}$ . We now solve Eq. (16–64) for  $I$ . This gives

**Answer**

$$I = \frac{E_2 - E_1}{C_s \omega^2} = \frac{3531}{0.1(250)^2} = 0.565 \text{ lbf} \cdot \text{s}^2 \text{ in}$$

(d) Equations (16–62) and (16–63) can be solved simultaneously for  $\omega_2$  and  $\omega_1$ . Substituting appropriate values in these two equations yields

**Answer**

$$\omega_2 = \frac{\omega}{2}(2 + C_s) = \frac{250}{2}(2 + 0.1) = 262.5 \text{ rad/s}$$

**Answer**

$$\omega_1 = 2\omega - \omega_2 = 2(250) - 262.5 = 237.5 \text{ rad/s}$$

These two speeds occur at  $\theta = 180^\circ$  and  $\theta = 0^\circ$ , respectively.

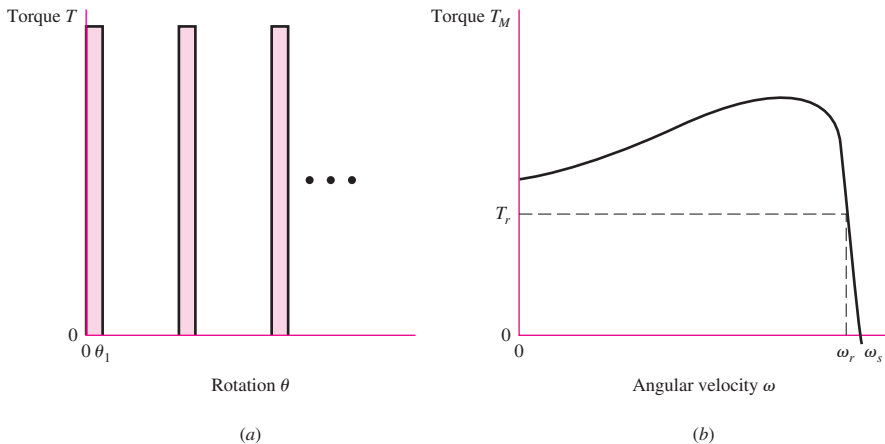
Punch-press torque demand often takes the form of a severe impulse and the running friction of the drive train. The motor overcomes the minor task of overcoming friction while attending to the major task of restoring the flywheel's angular speed. The situation can be idealized as shown in Fig. 16–29. Neglecting the running friction, Euler's equation can be written as

$$T(\theta_1 - 0) = \frac{1}{2}I(\omega_1^2 - \omega_2^2) = E_2 - E_1$$

where the only significant inertia is that of the flywheel. Punch presses can have the motor and flywheel on one shaft, then, through a gear reduction, drive a slider-crank mechanism that carries the punching tool. The motor can be connected to the punch

**Figure 16–29**

(a) Punch-press torque demand during punching. (b) Squirrel-cage electric motor torque-speed characteristic.



continuously, creating a punching rhythm, or it can be connected on command through a clutch that allows one punch and a disconnect. The motor and flywheel must be sized for the most demanding service, which is steady punching. The work done is given by

$$W = \int_{\theta_1}^{\theta_2} [T(\theta) - T] d\theta = \frac{1}{2} I (\omega_{\max}^2 - \omega_{\min}^2)$$

This equation can be arranged to include the coefficient of speed fluctuation  $C_s$  as follows:

$$\begin{aligned} W &= \frac{1}{2} I (\omega_{\max}^2 - \omega_{\min}^2) = \frac{I}{2} (\omega_{\max} - \omega_{\min}) (\omega_{\max} + \omega_{\min}) \\ &= \frac{I}{2} (C_s \bar{\omega}) (2\omega_0) = IC_s \bar{\omega} \omega_0 \end{aligned}$$

When the speed fluctuation is low,  $\omega_0 \doteq \bar{\omega}$ , and

$$I = \frac{W}{C_s \bar{\omega}^2}$$

An induction motor has a linear torque characteristic  $T = a\omega + b$  in the range of operation. The constants  $a$  and  $b$  can be found from the nameplate speed  $\omega_r$  and the synchronous speed  $\omega_s$ :

$$\begin{aligned} a &= \frac{T_r - T_s}{\omega_r - \omega_s} = \frac{T_r}{\omega_r - \omega_s} = -\frac{T_r}{\omega_s - \omega_r} \\ b &= \frac{T_r \omega_s - T_s \omega_r}{\omega_s - \omega_r} = \frac{T_r \omega_s}{\omega_s - \omega_r} \end{aligned} \quad (16-65)$$

For example, a 3-hp three-phase squirrel-cage ac motor rated at 1125 rev/min has a torque of  $63025(3)/1125 = 168.1 \text{ lbf}\cdot\text{in}$ . The rated angular velocity is  $\omega_r = 2\pi n_r/60 = 2\pi(1125)/60 = 117.81 \text{ rad/s}$ , and the synchronous angular velocity  $\omega_s = 2\pi(1200)/60 = 125.66 \text{ rad/s}$ . Thus  $a = -21.41 \text{ lbf}\cdot\text{in}\cdot\text{s/rad}$ , and  $b = 2690.9 \text{ lbf}\cdot\text{in}$ , and we can express  $T(\omega)$  as  $a\omega + b$ . During the interval from  $t_1$  to  $t_2$  the motor accelerates the flywheel according to  $I\ddot{\theta} = T_M$  (i.e.,  $Td\omega/dt = T_M$ ). Separating the equation  $T_M = I d\omega/dt$  we have

$$\int_{t_1}^{t_2} dt = \int_{\omega_r}^{\omega_2} \frac{I d\omega}{T_M} = I \int_{\omega_r}^{\omega_2} \frac{d\omega}{a\omega + b} = \frac{I}{a} \ln \frac{a\omega_2 + b}{a\omega_r + b} = \frac{I}{a} \ln \frac{T_2}{T_r}$$

or

$$t_2 - t_1 = \frac{I}{a} \ln \frac{T_2}{T_r} \quad (16-66)$$

For the deceleration interval when the motor and flywheel feel the punch torque on the shaft as  $T_L$ ,  $(T_M - T_L) = I d\omega/dt$ , or

$$\int_0^{t_1} dt = I \int_{\omega_2}^{\omega_r} \frac{d\omega}{T_M - T_L} = I \int_{\omega_2}^{\omega_r} \frac{d\omega}{a\omega + b - T_L} = \frac{I}{a} \ln \frac{a\omega_r + b - T_L}{a\omega_2 + b - T_L}$$

or

$$t_1 = \frac{I}{a} \ln \frac{T_r - T_L}{T_2 - T_L} \quad (16-67)$$

We can divide Eq. (16–66) by Eq. (16–67) to obtain

$$\frac{T_2}{T_r} = \left( \frac{T_L - T_r}{T_L - T_2} \right)^{(t_2 - t_1)/t_1} \quad (16-68)$$

Equation (16–68) can be solved for  $T_2$  numerically. Having  $T_2$  the flywheel inertia is, from Eq. (16–66),

$$I = \frac{a(t_2 - t_1)}{\ln(T_2/T_r)} \quad (16-69)$$

It is important that  $a$  be in units of  $\text{lbf} \cdot \text{in} \cdot \text{s}/\text{rad}$  so that  $I$  has proper units. The constant  $a$  should not be in  $\text{lbf} \cdot \text{in}$  per rev/min or  $\text{lbf} \cdot \text{in}$  per rev/s.

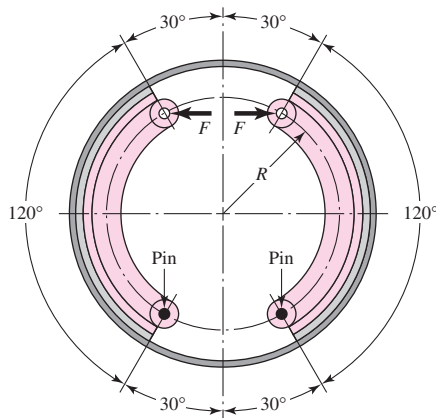
## PROBLEMS

### 16-1

The figure shows an internal rim-type brake having an inside rim diameter of 300 mm and a dimension  $R = 125$  mm. The shoes have a face width of 40 mm and are both actuated by a force of 2.2 kN. The mean coefficient of friction is 0.28.

- (a) Find the maximum pressure and indicate the shoe on which it occurs.
- (b) Estimate the braking torque effected by each shoe, and find the total braking torque.
- (c) Estimate the resulting hinge-pin reactions.

Problem 16-1



### 16-2

For the brake in Prob. 16–1, consider the pin and actuator locations to be the same. However, instead of 120°, let the friction surface of the brake shoes be 90° and centrally located. Find the maximum pressure and the total braking torque.

### 16-3

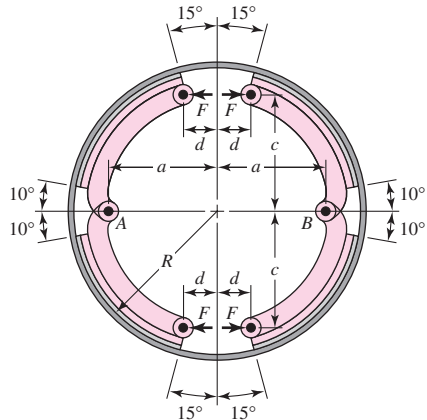
In the figure for Prob. 16–1, the inside rim diameter is 11 in and the dimension  $R$  is 3.5 in. The shoes have a face width of 1.25 in. Find the braking torque and the maximum pressure for each shoe if the actuating force is 225 lbf, the drum rotation is counterclockwise, and  $f = 0.30$ .

### 16-4

The figure shows a 400-mm-diameter brake drum with four internally expanding shoes. Each of the hinge pins A and B supports a pair of shoes. The actuating mechanism is to be arranged to produce the same force  $F$  on each shoe. The face width of the shoes is 75 mm. The material used permits a coefficient of friction of 0.24 and a maximum pressure of 1000 kPa.

**Problem 16-4**

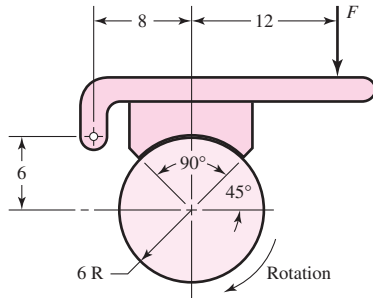
The dimensions in millimeters are  
 $a = 150$ ,  $c = 165$ ,  $R = 200$ ,  
and  $d = 50$ .



- (a) Determine the actuating force.
- (b) Estimate the brake capacity.
- (c) Noting that rotation may be in either direction, estimate the hinge-pin reactions.

**16-5**

The block-type hand brake shown in the figure has a face width of 1.25 in and a mean coefficient of friction of 0.25. For an estimated actuating force of 90 lbf, find the maximum pressure on the shoe and find the braking torque.

**Problem 16-5**  
Dimensions in inches.**16-6**

Suppose the standard deviation of the coefficient of friction in Prob. 16-5 is  $\hat{\sigma}_f = 0.025$ , where the deviation from the mean is due entirely to environmental conditions. Find the brake torques corresponding to  $\pm 3\hat{\sigma}_f$ .

**16-7**

The brake shown in the figure has a coefficient of friction of 0.30, a face width of 2 in, and a limiting shoe lining pressure of 150 psi. Find the limiting actuating force  $F$  and the torque capacity.

**16-8**

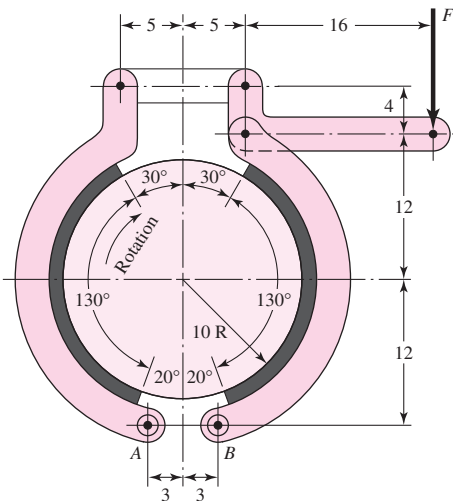
Refer to the symmetrical pivoted external brake shoe of Fig. 16-12 and Eq. (16-15). Suppose the pressure distribution was uniform, that is, the pressure  $p$  is independent of  $\theta$ . What would the pivot distance  $a'$  be? If  $\theta_1 = \theta_2 = 60^\circ$ , compare  $a$  with  $a'$ .

**16-9**

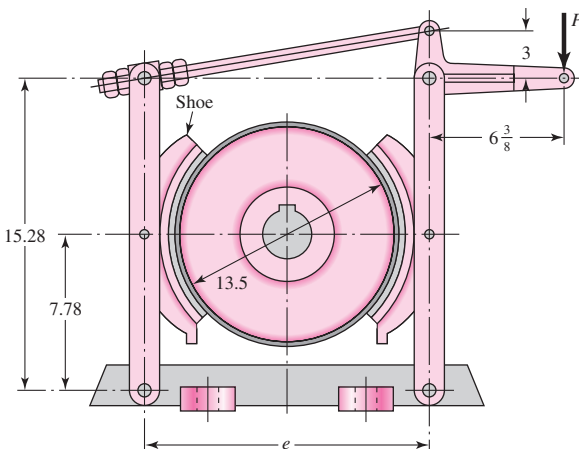
The shoes on the brake depicted in the figure subtend a  $90^\circ$  arc on the drum of this external pivoted-shoe brake. The actuation force  $P$  is applied to the lever. The rotation direction of the drum is counterclockwise, and the coefficient of friction is 0.30.

- (a) What should the dimension  $e$  be?
- (b) Draw the free-body diagrams of the handle lever and both shoe levers, with forces expressed in terms of the actuation force  $P$ .
- (c) Does the direction of rotation of the drum affect the braking torque?

*Problem 16-7*  
Dimensions in inches.



*Problem 16-9*  
Dimensions in inches.



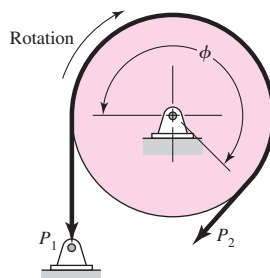
### 16-10

Problem 16-9 is preliminary to analyzing the brake. A rigid molded non-asbestos lining is used dry in the brake of Prob. 16-9 on a cast iron drum. The shoes are 6 in wide and subtend a  $90^\circ$  arc. Find the maximum allowable actuation force and the braking torque.

### 16-11

The maximum band interface pressure on the brake shown in the figure is 620 kPa. Use a 350 mm-diameter drum, a band width of 25 mm, a coefficient of friction of 0.30, and an angle-of-wrap of  $270^\circ$ . Find the band tensions and the torque capacity.

*Problem 16-11*



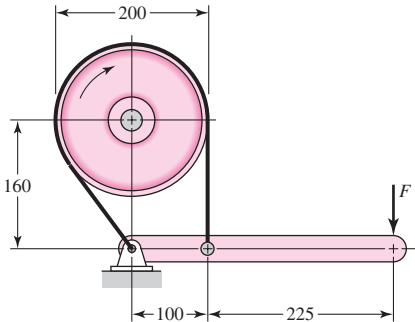
**16-12**

The drum for the band brake in Prob. 16-11 is 12 in in diameter. The band selected has a mean coefficient of friction of 0.28 and a width of 3.25 in. It can safely support a tension of 1.8 kip. If the angle of wrap is  $270^\circ$ , find the lining pressure and the torque capacity.

**16-13**

The brake shown in the figure has a coefficient of friction of 0.30 and is to operate using a maximum force  $F$  of 400 N. If the band width is 50 mm, find the band tensions and the braking torque.

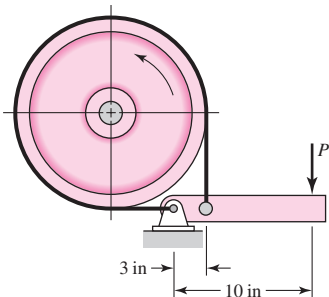
*Problem 16-13*  
Dimensions in millimeters.

**16-14**

The figure depicts a band brake whose drum rotates counterclockwise at 200 rev/min. The drum diameter is 16 in and the band lining 3 in wide. The coefficient of friction is 0.20. The maximum lining interface pressure is 70 psi.

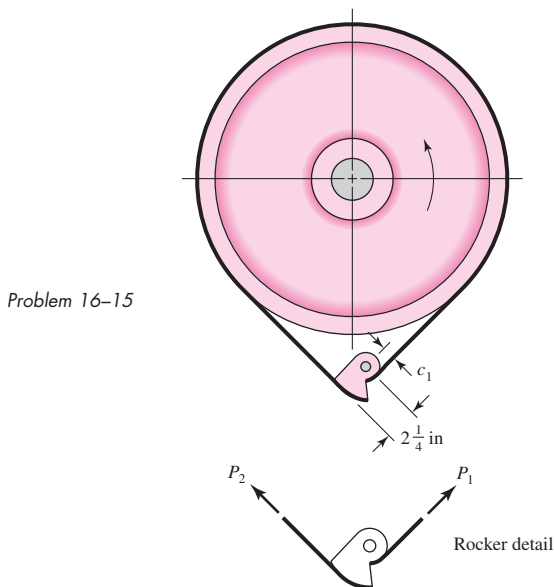
- Find the brake torque, necessary force  $P$ , and steady-state power.
- Complete the free-body diagram of the drum. Find the bearing radial load that a pair of straddle-mounted bearings would have to carry.
- What is the lining pressure  $p$  at both ends of the contact arc?

*Problem 16-14*

**16-15**

The figure shows a band brake designed to prevent “backward” rotation of the shaft. The angle of wrap is  $270^\circ$ , the band width is  $2\frac{1}{8}$  in, and the coefficient of friction is 0.20. The torque to be resisted by the brake is 150 lbf · ft. The diameter of the pulley is  $8\frac{1}{4}$  in.

- What dimension  $c_1$  will just prevent backward motion?
- If the rocker was designed with  $c_1 = 1$  in, what is the maximum pressure between the band and drum at 150 lbf · ft back torque?
- If the back-torque demand is 100 lbf · in, what is the largest pressure between the band and drum?

**16-16**

A plate clutch has a single pair of mating friction surfaces 250-mm OD by 175-mm ID. The mean value of the coefficient of friction is 0.30, and the actuating force is 4 kN.

- (a) Find the maximum pressure and the torque capacity using the uniform-wear model.
- (b) Find the maximum pressure and the torque capacity using the uniform-pressure model.

**16-17**

A hydraulically operated multidisk plate clutch has an effective disk outer diameter of 6.5 in and an inner diameter of 4 in. The coefficient of friction is 0.24, and the limiting pressure is 120 psi. There are six planes of sliding present.

- (a) Using the uniform wear model, estimate the axial force  $F$  and the torque  $T$ .
- (b) Let the inner diameter of the friction pairs  $d$  be a variable. Complete the following table:

$d$ , in	2	3	4	5	6
$T$ , lbf · in					

(c) What does the table show?

**16-18**

Look again at Prob. 16-17.

- (a) Show how the optimal diameter  $d^*$  is related to the outside diameter  $D$ .
- (b) What is the optimal inner diameter?
- (c) What does the tabulation show about maxima?
- (d) Common proportions for such plate clutches lie in the range  $0.45 \leq d/D \leq 0.80$ . Is the result in part a useful?

**16-19**

A cone clutch has  $D = 12$  in,  $d = 11$  in, a cone length of 2.25 in, and a coefficient of friction of 0.28. A torque of 1.8 kip · in is to be transmitted. For this requirement, estimate the actuating force and pressure by both models.

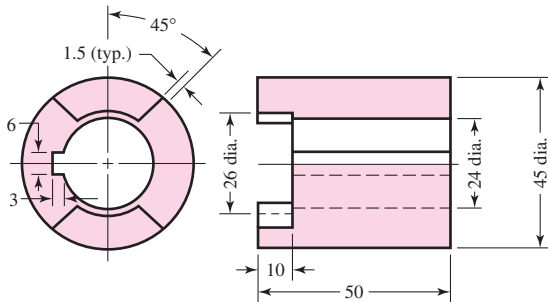
**16-20**

Show that for the caliper brake the  $T/(fFD)$  versus  $d/D$  plots are the same as Eqs. (b) and (c) of Sec. 16-5.

**16-21**

A two-jaw clutch has the dimensions shown in the figure and is made of ductile steel. The clutch has been designed to transmit 2 kW at 500 rev/min. Find the bearing and shear stresses in the key and the jaws.

*Problem 16-21*  
Dimensions in millimeters.

**16-22**

A brake has a normal braking torque of 2.8 kip · in and heat-dissipating surfaces whose mass is 40 lbm. Suppose a load is brought to rest in 8.0 s from an initial angular speed of 1600 rev/min using the normal braking torque; estimate the temperature rise of the heat-dissipating surfaces.

**16-23**

A cast-iron flywheel has a rim whose OD is 1.5 m and whose ID is 1.4 m. The flywheel weight is to be such that an energy fluctuation of 6.75 J will cause the angular speed to vary no more than 240 to 260 rev/min. Estimate the coefficient of speed fluctuation. If the weight of the spokes is neglected, what should be the width of the rim?

**16-24**

A single-geared blanking press has a stroke of 200 mm and a rated capacity of 320 kN. A cam-driven ram is assumed to be capable of delivering the full press load at constant force during the last 15 percent of a constant-velocity stroke. The camshaft has an average speed of 90 rev/min and is geared to the flywheel shaft at a 6:1 ratio. The total work done is to include an allowance of 16 percent for friction.

(a) Estimate the maximum energy fluctuation.

(b) Find the rim weight for an effective diameter of 1.2 m and a coefficient of speed fluctuation of 0.10.

**16-25**

Using the data of Table 16-6, find the mean output torque and flywheel inertia required for a three-cylinder in-line engine corresponding to a nominal speed of 2400 rev/min. Use  $C_s = 0.30$ .

**16-26**

When a motor armature inertia, a pinion inertia, and a motor torque reside on a motor shaft, and a gear inertia, a load inertia, and a load torque exist on a second shaft, it is useful to reflect all the torques and inertias to one shaft, say, the armature shaft. We need some rules to make such reflection easy. Consider the pinion and gear as disks of pitch radius.

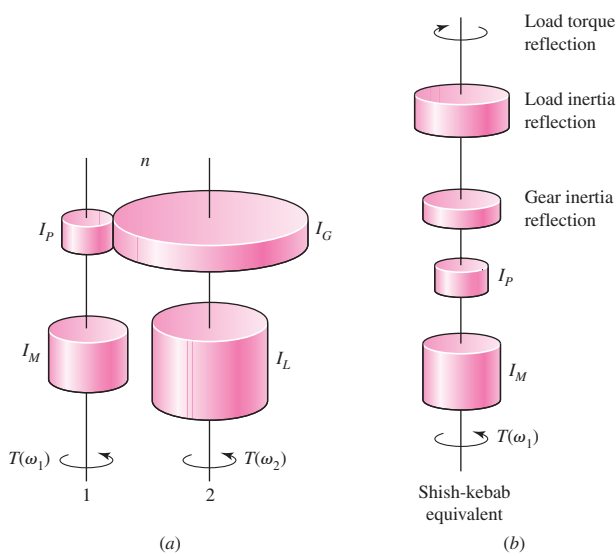
- A torque on a second shaft is reflected to the motor shaft as the load torque divided by the negative of the stepdown ratio.
- An inertia on a second shaft is reflected to the motor shaft as its inertia divided by the stepdown ratio squared.
- The inertia of a disk gear on a second shaft in mesh with a disk pinion on the motor shaft is reflected to the pinion shaft as the *pinion* inertia multiplied by the stepdown ratio squared.

(a) Verify the three rules.

(b) Using the rules, reduce the two-shaft system in the figure to a motor-shaft shish-kebab equivalent. Correctly done, the dynamic response of the shish kebab and the real system are identical.

(c) For a stepdown ratio of  $n = 10$  compare the shish-kebab inertias.

**Problem 16-26**  
Dimensions in millimeters.

**16-27**

Apply the rules of Prob. 16-26 to the three-shaft system shown in the figure to create a motor shaft shish kebab.

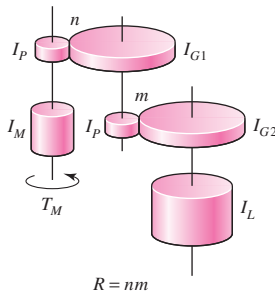
(a) Show that the equivalent inertia  $I_e$  is given by

$$I_e = I_M + I_P + n^2 I_P + \frac{I_P}{n^2} + \frac{m^2 I_P}{n^2} + \frac{I_L}{m^2 n^2}$$

(b) If the overall gear reduction  $R$  is a constant  $nm$ , show that the equivalent inertia becomes

$$I_e = I_M + I_P + n^2 I_P + \frac{I_P}{n^2} + \frac{R^2 I_P}{n^4} + \frac{I_L}{R^2}$$

(c) If the problem is to minimize the gear-train inertia, find the ratios  $n$  and  $m$  for the values of  $I_P = 1$ ,  $I_M = 10$ ,  $I_L = 100$ , and  $R = 10$ .

**Problem 16-27****16-28**

For the conditions of Prob. 16-27, make a plot of the equivalent inertia  $I_e$  as ordinate and the stepdown ratio  $n$  as abscissa in the range  $1 \leq n \leq 10$ . How does the minimum inertia compare to the single-step inertia?

**16-29**

A punch-press geared 10:1 is to make six punches per minute under circumstances where the torque on the crankshaft is  $1300 \text{ lbf} \cdot \text{ft}$  for  $\frac{1}{2} \text{ s}$ . The motor's nameplate reads 3 bhp at 1125 rev/min for continuous duty. Design a satisfactory flywheel for use on the motor shaft to the extent of specifying material and rim inside and outside diameters as well as its width. As you prepare your

specifications, note  $\omega_{\max}$ ,  $\omega_{\min}$ , the coefficient of speed fluctuation  $C_s$ , energy transfer, and peak power that the flywheel transmits to the punch-press. Note power and shock conditions imposed on the gear train because the flywheel is on the motor shaft.

**16-30**

The punch-press of Prob. 16-29 needs a flywheel for service on the crankshaft of the punch-press. Design a satisfactory flywheel to the extent of specifying material, rim inside and outside diameters, and width. Note  $\omega_{\max}$ ,  $\omega_{\min}$ ,  $C_s$ , energy transfer, and peak power the flywheel transmits to the punch. What is the peak power seen in the gear train? What power and shock conditions must the gear-train transmit?

**16-31**

Compare the designs resulting from the tasks assigned in Probs. 16-29 and 16-30. What have you learned? What recommendations do you have?

# 17

## Flexible Mechanical Elements

### Chapter Outline

<b>17-1</b>	Belts	<b>880</b>
<b>17-2</b>	Flat- and Round-Belt Drives	<b>883</b>
<b>17-3</b>	V Belts	<b>898</b>
<b>17-4</b>	Timing Belts	<b>906</b>
<b>17-5</b>	Roller Chain	<b>907</b>
<b>17-6</b>	Wire Rope	<b>916</b>
<b>17-7</b>	Flexible Shafts	<b>924</b>

Belts, ropes, chains, and other similar elastic or flexible machine elements are used in conveying systems and in the transmission of power over comparatively long distances. It often happens that these elements can be used as a replacement for gears, shafts, bearings, and other relatively rigid power-transmission devices. In many cases their use simplifies the design of a machine and substantially reduces the cost.

In addition, since these elements are elastic and usually quite long, they play an important part in absorbing shock loads and in damping out and isolating the effects of vibration. This is an important advantage as far as machine life is concerned.

Most flexible elements do not have an infinite life. When they are used, it is important to establish an inspection schedule to guard against wear, aging, and loss of elasticity. The elements should be replaced at the first sign of deterioration.

## 17-1 Belts

The four principal types of belts are shown, with some of their characteristics, in Table 17-1. *Crowned pulleys* are used for flat belts, and *grooved pulleys*, or *sheaves*, for round and V belts. Timing belts require *toothed wheels*, or *sprockets*. In all cases, the pulley axes must be separated by a certain minimum distance, depending upon the belt type and size, to operate properly. Other characteristics of belts are:

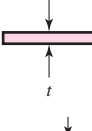
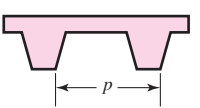
- They may be used for long center distances.
- Except for timing belts, there is some slip and creep, and so the angular-velocity ratio between the driving and driven shafts is neither constant nor exactly equal to the ratio of the pulley diameters.
- In some cases an idler or tension pulley can be used to avoid adjustments in center distance that are ordinarily necessitated by age or the installation of new belts.

Figure 17-1 illustrates the geometry of open and closed flat-belt drives. For a flat belt with this drive the belt tension is such that the sag or droop is visible in Fig. 17-2a, when the belt is running. Although the top is preferred for the loose side of the belt, for other belt types either the top or the bottom may be used, because their installed tension is usually greater.

Two types of reversing drives are shown in Fig. 17-2. Notice that both sides of the belt contact the pulleys in Figs. 17-2b and 17-2c, and so these drives cannot be used with V belts or timing belts.

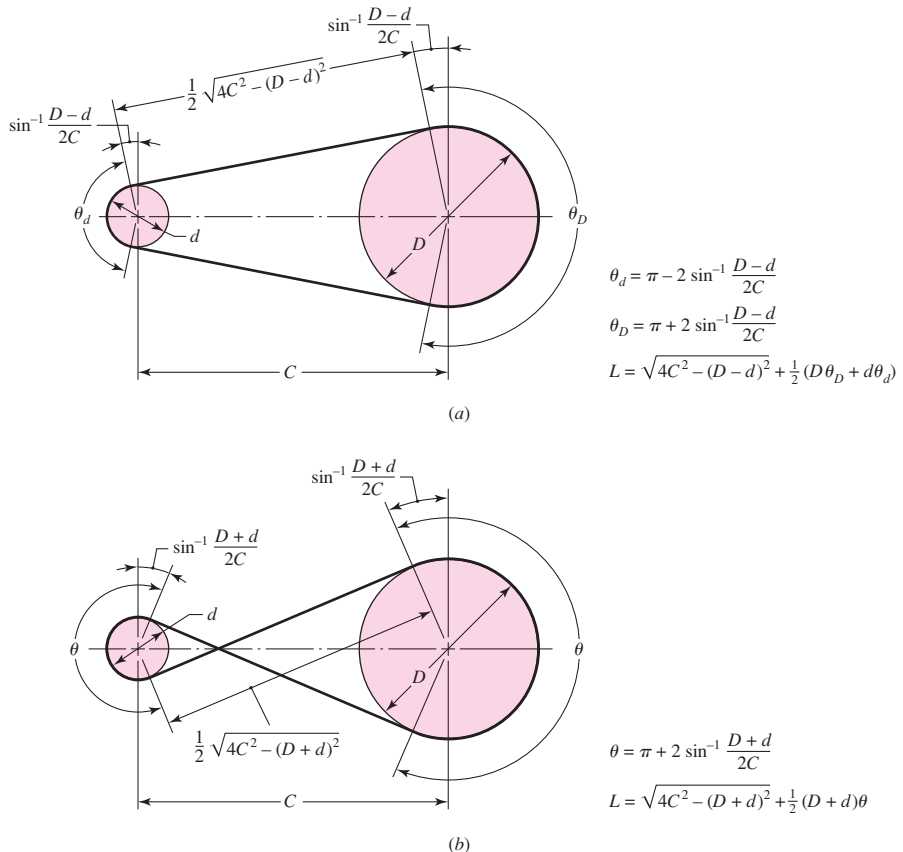
**Table 17-1**

Characteristics of Some Common Belt Types  
(Figures are cross sections except for the timing belt, which is a side view).

Belt Type	Figure	Joint	Size Range	Center Distance
Flat		Yes	$t = \begin{cases} 0.03 \text{ to } 0.20 \text{ in} \\ 0.75 \text{ to } 5 \text{ mm} \end{cases}$	No upper limit
Round		Yes	$d = \frac{1}{8} \text{ to } \frac{3}{4} \text{ in}$	No upper limit
V		None	$b = \begin{cases} 0.31 \text{ to } 0.91 \text{ in} \\ 8 \text{ to } 19 \text{ mm} \end{cases}$	Limited
Timing		None	$p = 2 \text{ mm and up}$	Limited

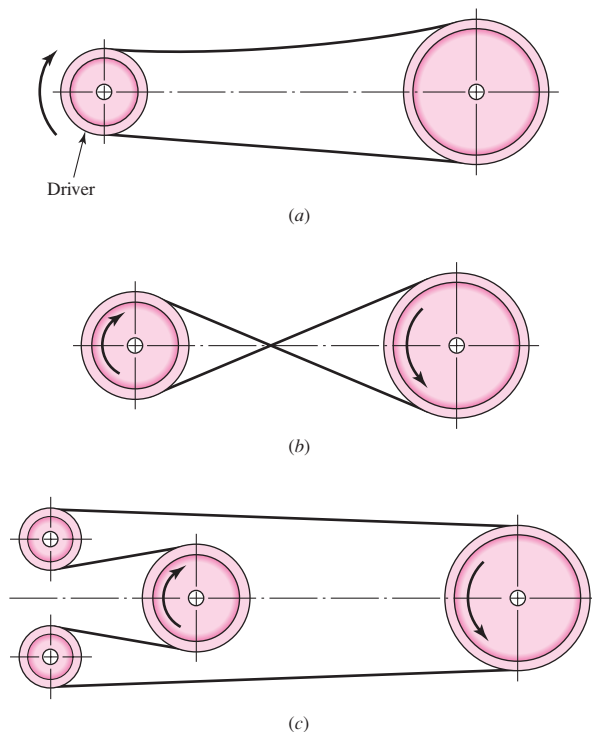
**Figure 17-1**

Flat-belt geometry. (a) Open belt. (b) Crossed belt.

**Figure 17-2**

Nonreversing and reversing belt drives. (a) Nonreversing open belt. (b) Reversing crossed belt. Crossed belts must be separated to prevent rubbing if high-friction materials are used.

(c) Reversing open-belt drive.



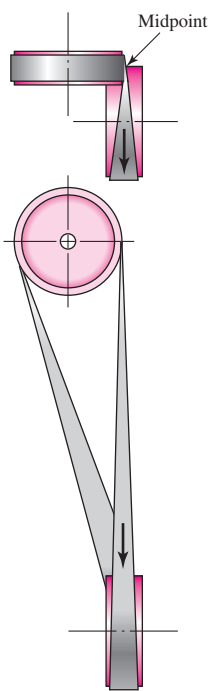


**Figure 17-3**

Quarter-twist belt drive;  
an idler guide pulley must be  
used if motion is to be in both  
directions.

Figure 17-3 shows a flat-belt drive with out-of-plane pulleys. The shafts need not be at right angles as in this case. Note the top view of the drive in Fig. 17-3. The pulleys must be positioned so that the belt leaves each pulley in the midplane of the other pulley face. Other arrangements may require guide pulleys to achieve this condition.

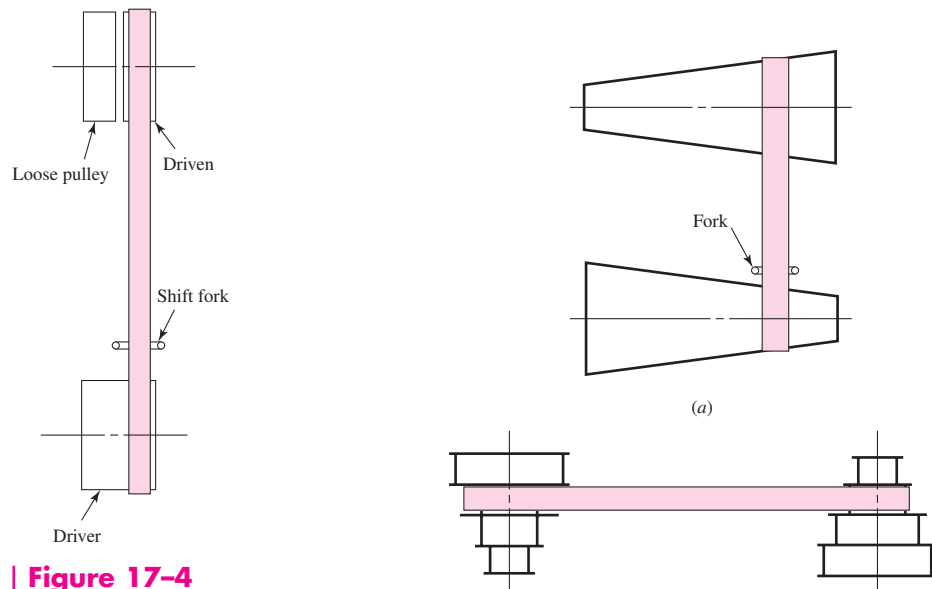
Another advantage of flat belts is shown in Fig. 17-4, where clutching action is obtained by shifting the belt from a loose to a tight or driven pulley.

Figure 17-5 shows two variable-speed drives. The drive in Fig. 17-5a is commonly used only for flat belts. The drive of Fig. 17-5b can also be used for V belts and round belts by using grooved sheaves.

Flat belts are made of urethane and also of rubber-impregnated fabric reinforced with steel wire or nylon cords to take the tension load. One or both surfaces may have a friction surface coating. Flat belts are quiet, they are efficient at high speeds, and they can transmit large amounts of power over long center distances. Usually, flat belting is purchased by the roll and cut and the ends are joined by using special kits furnished by the manufacturer. Two or more flat belts running side by side, instead of a single wide belt, are often used to form a conveying system.

A V belt is made of fabric and cord, usually cotton, rayon, or nylon, and impregnated with rubber. In contrast with flat belts, V belts are used with similar sheaves and at shorter center distances. V belts are slightly less efficient than flat belts, but a number of them can be used on a single sheave, thus making a multiple drive. V belts are made only in certain lengths and have no joints.

Timing belts are made of rubberized fabric and steel wire and have teeth that fit into grooves cut on the periphery of the sprockets. The timing belt does not stretch or slip and consequently transmits power at a constant angular-velocity ratio. The fact that the belt is toothed provides several advantages over ordinary belting. One of these is that no initial tension is necessary, so that fixed-center drives may be used. Another is



**Figure 17-4**

This drive eliminates the need  
for a clutch. Flat belt can be  
shifted left or right by use of  
a fork.

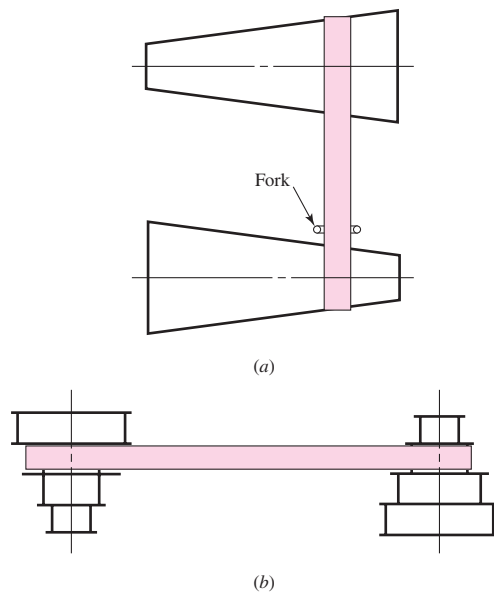


**Figure 17-5**

Variable-speed belt drives.

the elimination of the restriction on speeds; the teeth make it possible to run at nearly any speed, slow or fast. Disadvantages are the first cost of the belt, the necessity of grooving the sprockets, and the attendant dynamic fluctuations caused at the belt-tooth meshing frequency.

## 17-2

### Flat- and Round-Belt Drives

Modern flat-belt drives consist of a strong elastic core surrounded by an elastomer; these drives have distinct advantages over gear drives or V-belt drives. A flat-belt drive has an efficiency of about 98 percent, which is about the same as for a gear drive. On the other hand, the efficiency of a V-belt drive ranges from about 70 to 96 percent.<sup>1</sup> Flat-belt drives produce very little noise and absorb more torsional vibration from the system than either V-belt or gear drives.

When an open-belt drive (Fig. 17-1a) is used, the contact angles are found to be

$$\begin{aligned}\theta_d &= \pi - 2 \sin^{-1} \frac{D-d}{2C} \\ \theta_D &= \pi + 2 \sin^{-1} \frac{D-d}{2C}\end{aligned}\quad (17-1)$$

where  $D$  = diameter of large pulley

$d$  = diameter of small pulley

$C$  = center distance

$\theta$  = angle of contact

The length of the belt is found by summing the two arc lengths with twice the distance between the beginning and end of contact. The result is

$$L = [4C^2 - (D-d)^2]^{1/2} + \frac{1}{2}(D\theta_D + d\theta_d) \quad (17-2)$$

A similar set of equations can be derived for the crossed belt of Fig. 17-2b. For this belt, the angle of wrap is the same for both pulleys and is

$$\theta = \pi + 2 \sin^{-1} \frac{D+d}{2C} \quad (17-3)$$

The belt length for crossed belts is found to be

$$L = [4C^2 - (D+d)^2]^{1/2} + \frac{1}{2}(D+d)\theta \quad (17-4)$$

Firbank<sup>2</sup> explains flat-belt-drive theory in the following way. A change in belt tension due to friction forces between the belt and pulley will cause the belt to elongate or contract and move relative to the surface of the pulley. This motion is caused by *elastic creep* and is associated with sliding friction as opposed to static friction. The action at the driving pulley, through that portion of the angle of contact that is actually transmitting power, is such that the belt moves more slowly than the surface speed of the pulley because of the elastic creep. The angle of contact is made up of the *effective arc*,

<sup>1</sup>A. W. Wallin, "Efficiency of Synchronous Belts and V-Belts," *Proc. Nat. Conf. Power Transmission*, vol. 5, Illinois Institute of Technology, Chicago, Nov. 7-9, 1978, pp. 265-271.

<sup>2</sup>T. C. Firbank, *Mechanics of the Flat Belt Drive*, ASME paper no. 72-PTG-21.

through which power is transmitted, and the *idle arc*. For the driving pulley the belt first contacts the pulley with a *tight-side tension*  $F_1$  and a velocity  $V_1$ , which is the same as the surface velocity of the pulley. The belt then passes through the idle arc with no change in  $F_1$  or  $V_1$ . Then creep or sliding contact begins, and the belt tension changes in accordance with the friction forces. At the end of the effective arc the belt leaves the pulley with a *loose-side tension*  $F_2$  and a reduced speed  $V_2$ .

Firbank has used this theory to express the mechanics of flat-belt drives in mathematical form and has verified the results by experiment. His observations include the finding that substantially more power is transmitted by static friction than sliding friction. He also found that the coefficient of friction for a belt having a nylon core and leather surface was typically 0.7, but that it could be raised to 0.9 by employing special surface finishes.

Our model will assume that the friction force on the belt is proportional to the normal pressure along the arc of contact. We seek first a relationship between the tight side tension and slack side tension, similar to that of band brakes but incorporating the consequences of movement, that is, centrifugal tension in the belt. In Fig. 17–6 we see a free body of a small segment of the belt. The differential force  $dS$  is due to centrifugal force,  $dN$  is the normal force between the belt and pulley, and  $f dN$  is the shearing traction due to friction at the point of slip. The belt width is  $b$  and the thickness is  $t$ . The belt mass per unit length is  $m$ . The centrifugal force  $dS$  can be expressed as

$$dS = (mr d\theta)r\omega^2 = mr^2\omega^2 d\theta = mV^2 d\theta = F_c d\theta \quad (a)$$

where  $V$  is the belt speed. Summing forces radially gives

$$\sum F_r = -(F + dF) \frac{d\theta}{2} - F \frac{d\theta}{2} + dN + dS = 0$$

Ignoring the higher-order term, we have

$$dN = F d\theta - dS \quad (b)$$

Summing forces tangentially gives

$$\sum F_t = -f dN - F + (F + dF) = 0$$

from which, incorporating Eqs. (a) and (b), we obtain

$$dF = f dN = f F d\theta - f dS = f F d\theta - f m r^2 \omega^2 d\theta$$

or

$$\frac{dF}{d\theta} - f F = -f m r^2 \omega^2 \quad (c)$$

The solution to this nonhomogeneous first-order linear differential equation is

$$F = A \exp(f\theta) + m r^2 \omega^2 \quad (d)$$

where  $A$  is an arbitrary constant. Assuming  $\theta$  starts at the loose side, the boundary condition that  $F$  at  $\theta = 0$  equals  $F_2$  gives  $A = F_2 - m r^2 \omega^2$ . The solution is

$$F = (F_2 - m r^2 \omega^2) \exp(f\theta) + m r^2 \omega^2 \quad (17-5)$$

At the end of the angle of wrap  $\phi$ , the tight side,

$$F|_{\theta=\phi} = F_1 = (F_2 - m r^2 \omega^2) \exp(f\phi) + m r^2 \omega^2 \quad (17-6)$$

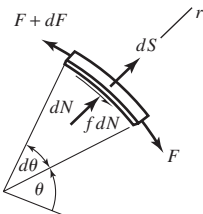


**Figure 17–6**

Free body of an infinitesimal element of a flat belt in contact with a pulley.

Now we can write

$$\frac{F_1 - mr^2\omega^2}{F_2 - mr^2\omega^2} = \frac{F_1 - F_c}{F_2 - F_c} = \exp(f\phi) \quad (17-7)$$

where, from Eq. (a),  $F_c = mr^2\omega^2$ . It is also useful that Eq. (17-7) can be written as

$$F_1 - F_2 = (F_1 - F_c) \frac{\exp(f\phi) - 1}{\exp(f\phi)} \quad (17-8)$$

Now  $F_c$  is found as follows: with  $n$  being the rotational speed, in rev/min, of the pulley of diameter  $d$ , the belt speed is

$$V = \pi dn/12 \quad \text{ft/min}$$

The weight  $w$  of a foot of belt is given in terms of the weight density  $\gamma$  in lbf/in<sup>3</sup> as  $w = 12\gamma bt$  lbf/ft where  $b$  and  $t$  are in inches.  $F_c$  is written as

$$F_c = \frac{w}{g} \left( \frac{V}{60} \right)^2 = \frac{w}{32.17} \left( \frac{V}{60} \right)^2 \quad (e)$$

Figure 17-7 shows a free body of a pulley and part of the belt. The tight side tension  $F_1$  and the loose side tension  $F_2$  have the following additive components:

$$F_1 = F_i + F_c + \Delta F/2 = F_i + F_c + T/d \quad (f)$$

$$F_2 = F_i + F_c - \Delta F/2 = F_i + F_c - T/d \quad (g)$$

where  $F_i$  = initial tension

$F_c$  = hoop tension due to centrifugal force

$\Delta F/2$  = tension due to the transmitted torque  $T$

$d$  = diameter of the pulley

The difference between  $F_1$  and  $F_2$  is related to the pulley torque. Subtracting Eq. (g) from Eq. (f) gives

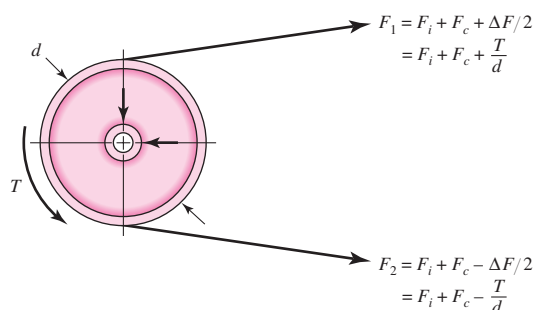
$$F_1 - F_2 = \frac{2T}{d} \quad (h)$$

Adding Eqs. (f) and (g) gives

$$F_1 + F_2 = 2F_i + 2F_c$$

**Figure 17-7**

Forces and torques on a pulley.



from which

$$F_i = \frac{F_1 + F_2}{2} - F_c \quad (i)$$

Dividing Eq. (i) by Eq. (h), manipulating, and using Eq. (17-7) gives

$$\begin{aligned} \frac{F_i}{T/d} &= \frac{(F_1 + F_2)/2 - F_c}{(F_1 - F_2)/2} = \frac{F_1 + F_2 - 2F_c}{F_1 - F_2} = \frac{(F_1 - F_c) + (F_2 - F_c)}{(F_1 - F_c) - (F_2 - F_c)} \\ &= \frac{(F_1 - F_c)/(F_2 - F_c) + 1}{(F_1 - F_c)/(F_2 - F_c) - 1} = \frac{\exp(f\phi) + 1}{\exp(f\phi) - 1} \end{aligned}$$

from which

$$F_i = \frac{T}{d} \frac{\exp(f\phi) + 1}{\exp(f\phi) - 1} \quad (17-9)$$

Equation (17-9) give us a fundamental insight into flat belting. If  $F_i$  equals zero, then  $T$  equals zero: no initial tension, no torque transmitted. The torque is in proportion to the initial tension. This means that if there is to be a satisfactory flat-belt drive, the initial tension must be (1) provided, (2) sustained, (3) in the proper amount, and (4) maintained by routine inspection.

From Eq. (f), incorporating Eq. (17-9) gives

$$\begin{aligned} F_1 &= F_i + F_c + \frac{T}{d} = F_c + F_i + F_i \frac{\exp(f\phi) - 1}{\exp(f\phi) + 1} \\ &= F_c + \frac{F_i[\exp(f\phi) + 1] + F_i[\exp(f\phi) - 1]}{\exp(f\phi) + 1} \end{aligned}$$

$$F_1 = F_c + F_i \frac{2\exp(f\phi)}{\exp(f\phi) + 1} \quad (17-10)$$

From Eq. (g), incorporating Eq. (17-9) gives

$$\begin{aligned} F_2 &= F_i + F_c - \frac{T}{d} = F_c + F_i - F_i \frac{\exp(f\phi) - 1}{\exp(f\phi) + 1} \\ &= F_c + \frac{F_i[\exp(f\phi) + 1] - F_i[\exp(f\phi) - 1]}{\exp(f\phi) + 1} \end{aligned}$$

$$F_2 = F_c + F_i \frac{2}{\exp(f\phi) + 1} \quad (17-11)$$

Equation (17–7) is called the *belting equation*, but Eqs. (17–9), (17–10), and (17–11) reveal how belting works. We plot Eqs. (17–10) and (17–11) as shown in Fig. 17–8 against  $F_i$  as abscissa. The initial tension needs to be sufficient so that the difference between the  $F_1$  and  $F_2$  curve is  $2T/d$ . With no torque transmitted, the least possible belt tension is  $F_1 = F_2 = F_c$ .

The transmitted horsepower is given by

$$H = \frac{(F_1 - F_2)V}{33\,000} \quad (\text{J})$$

Manufacturers provide specifications for their belts that include allowable tension  $F_a$  (or stress  $\sigma_{\text{all}}$ ), the tension being expressed in units of force per unit width. Belt life is usually several years. The severity of flexing at the pulley and its effect on life is reflected in a pulley correction factor  $C_p$ . Speed in excess of 600 ft/min and its effect on life is reflected in a velocity correction factor  $C_v$ . For polyamide and urethane belts use  $C_v = 1$ . For leather belts see Fig. 17–9. A service factor  $K_s$  is used for excursions of

**Figure 17–8**

Plot of initial tension  $F_i$  against belt tension  $F_1$  or  $F_2$ , showing the intercept  $F_c$ , the equations of the curves, and where  $2T/d$  is to be found.

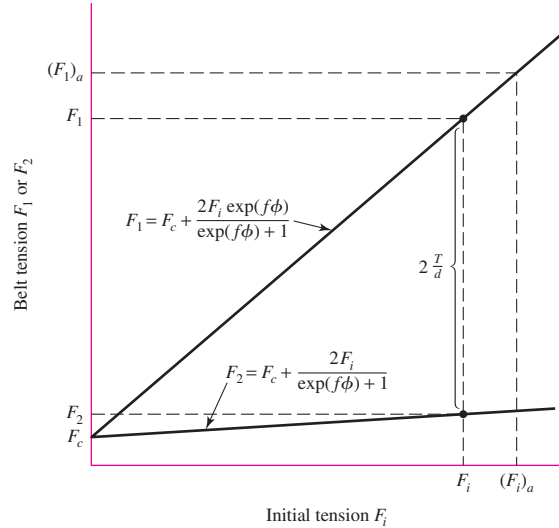
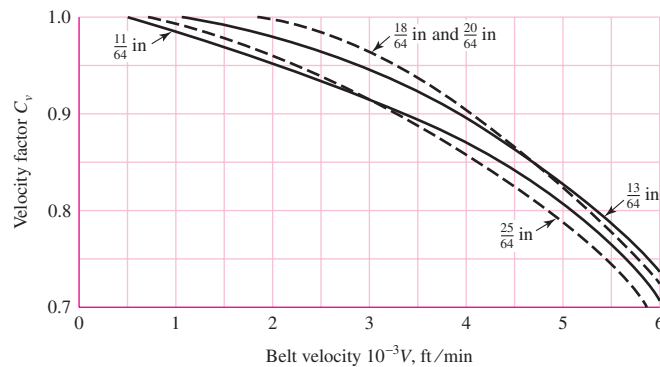


**Figure 17–9**

Velocity correction factor  $C_v$  for leather belts for various thicknesses. (Data source: Machinery's Handbook, 20th ed., Industrial Press, New York, 1976, p. 1047.)



load from nominal, applied to the nominal power as  $H_d = H_{\text{nom}}K_s n_d$ , where  $n_d$  is the design factor for exigencies. These effects are incorporated as follows:

$$(F_1)_a = b F_a C_p C_v \quad (17-12)$$

where  $(F_1)_a$  = allowable largest tension, lbf

$b$  = belt width, in

$F_a$  = manufacturer's allowed tension, lbf/in

$C_p$  = pulley correction factor (Table 17-4)

$C_v$  = velocity correction factor

The steps in analyzing a flat-belt drive can include (see Ex. 17-1)

- 1 Find  $\exp(f\phi)$  from belt-drive geometry and friction
- 2 From belt geometry and speed find  $F_c$
- 3 From  $T = 63.025 H_{\text{nom}} K_s n_d / n$  find necessary torque
- 4 From torque  $T$  find the necessary  $(F_1)_a - F_2 = 2T/d$
- 5 From Tables 17-2 and 17-4, and Eq. (17-12) determine  $(F_1)_a$ .
- 6 Find  $F_2$  from  $(F_1)_a - [(F_1)_a - F_2]$
- 7 From Eq. (i) find the necessary initial tension  $F_i$
- 8 Check the friction development,  $f' < f$ . Use Eq. (17-7) solved for  $f'$ :

$$f' = \frac{1}{\phi} \ln \frac{(F_1)_a - F_c}{F_2 - F_c}$$

- 9 Find the factor of safety from  $n_{fs} = H_a / (H_{\text{nom}} K_s)$

It is unfortunate that many of the available data on belting are from sources in which they are presented in a very simplistic manner. These sources use a variety of charts, nomographs, and tables to enable someone who knows nothing about belting to apply them. Little, if any, computation is needed for such a person to obtain valid results. Since a basic understanding of the process, in many cases, is lacking, there is no way this person can vary the steps in the process to obtain a better design.

Incorporating the available belt-drive data into a form that provides a good understanding of belt mechanics involves certain adjustments in the data. Because of this, the results from the analysis presented here will not correspond exactly with those of the sources from which they were obtained.

A moderate variety of belt materials, with some of their properties, are listed in Table 17-2. These are sufficient for solving a large variety of design and analysis problems. The design equation to be used is Eq. (j).

The values given in Table 17-2 for the allowable belt tension are based on a belt speed of 600 ft/min. For higher speeds, use Fig. 17-9 to obtain  $C_v$  values for leather belts. For polyamide and urethane belts, use  $C_v = 1.0$ .

The service factors  $K_s$  for V-belt drives, given in Table 17-15 in Sec. 17-3, are also recommended here for flat- and round-belt drives.

Minimum pulley sizes for the various belts are listed in Tables 17-2 and 17-3. The pulley correction factor accounts for the amount of bending or flexing of the belt and how this affects the life of the belt. For this reason it is dependent on the size and material of the belt used. See Table 17-4. Use  $C_p = 1.0$  for urethane belts.

Flat-belt pulleys should be crowned to keep belts from running off the pulleys. If only one pulley is crowned, it should be the larger one. Both pulleys must be crowned whenever the pulley axes are not in a horizontal position. Use Table 17-5 for the crown height.

**Table 17-2**Properties of Some Flat- and Round-Belt Materials. (Diameter =  $d$ , thickness =  $t$ , width =  $w$ )

Material	Specification	Size, in	Minimum Pulley Diameter, in	Allowable Tension per Unit Width at 600 ft/min, lbf/in	Specific Weight, lbf/in <sup>3</sup>	Coefficient of Friction
Leather	1 ply	$t = \frac{11}{64}$	3	30	0.035–0.045	0.4
		$t = \frac{13}{64}$	$3\frac{1}{2}$	33	0.035–0.045	0.4
	2 ply	$t = \frac{18}{64}$	$4\frac{1}{2}$	41	0.035–0.045	0.4
		$t = \frac{20}{64}$	$6^a$	50	0.035–0.045	0.4
		$t = \frac{23}{64}$	$9^a$	60	0.035–0.045	0.4
	Polyamide <sup>b</sup>	$t = 0.03$	0.60	10	0.035	0.5
	F-1 <sup>c</sup>	$t = 0.05$	1.0	35	0.035	0.5
Polyamide <sup>b</sup>	F-2 <sup>c</sup>	$t = 0.07$	2.4	60	0.051	0.5
	A-2 <sup>c</sup>	$t = 0.11$	2.4	60	0.037	0.8
	A-3 <sup>c</sup>	$t = 0.13$	4.3	100	0.042	0.8
	A-4 <sup>c</sup>	$t = 0.20$	9.5	175	0.039	0.8
	A-5 <sup>c</sup>	$t = 0.25$	13.5	275	0.039	0.8
	Urethane <sup>d</sup>	$w = 0.50$	$t = 0.062$	See	5.2 <sup>e</sup>	0.038–0.045
		$w = 0.75$	$t = 0.078$	Table	9.8 <sup>e</sup>	0.038–0.045
Urethane <sup>d</sup>		$w = 1.25$	$t = 0.090$	17-3	18.9 <sup>e</sup>	0.038–0.045
	Round	$d = \frac{1}{4}$	See	8.3 <sup>e</sup>	0.038–0.045	0.7
		$d = \frac{3}{8}$	Table	18.6 <sup>e</sup>	0.038–0.045	0.7
		$d = \frac{1}{2}$	17-3	33.0 <sup>e</sup>	0.038–0.045	0.7
		$d = \frac{3}{4}$		74.3 <sup>e</sup>	0.038–0.045	0.7

<sup>a</sup>Add 2 in to pulley size for belts 8 in wide or more.<sup>b</sup>Source: Habasit Engineering Manual, Habasit Belting, Inc., Chamblee (Atlanta), Ga.<sup>c</sup>Friction cover of acrylonitrile-butadiene rubber on both sides.<sup>d</sup>Source: Eagle Belting Co., Des Plaines, Ill.<sup>e</sup>At 6% elongation; 12% is maximum allowable value.**Table 17-3**

Minimum Pulley Sizes for Flat and Round

Urethane Belts (Listed are the pulley diameters in inches).

Source: Eagle Belting Co., Des Plaines, Ill.

Belt Style	Belt Size, in	Ratio of Pulley Speed to Belt Length, rev/(ft · min)		
		Up to 250	250 to 499	500 to 1000
Flat	$0.50 \times 0.062$	0.38	0.44	0.50
	$0.75 \times 0.078$	0.50	0.63	0.75
	$1.25 \times 0.090$	0.50	0.63	0.75
Round	$\frac{1}{4}$	1.50	1.75	2.00
	$\frac{3}{8}$	2.25	2.62	3.00
	$\frac{1}{2}$	3.00	3.50	4.00
	$\frac{3}{4}$	5.00	6.00	7.00

**Table 17-4**Pulley Correction Factor  $C_P$  for Flat Belts\*

Material	Small-Pulley Diameter, in					
	1.6 to 4	4.5 to 8	9 to 12.5	14, 16	18 to 31.5	Over 31.5
Leather	0.5	0.6	0.7	0.8	0.9	1.0
Polyamide, F-0	0.95	1.0	1.0	1.0	1.0	1.0
F-1	0.70	0.92	0.95	1.0	1.0	1.0
F-2	0.73	0.86	0.96	1.0	1.0	1.0
A-2	0.73	0.86	0.96	1.0	1.0	1.0
A-3	—	0.70	0.87	0.94	0.96	1.0
A-4	—	—	0.71	0.80	0.85	0.92
A-5	—	—	—	0.72	0.77	0.91

\*Average values of  $C_P$  for the given ranges were approximated from curves in the *Habasit Engineering Manual*, Habasit Belting, Inc., Chamblee (Atlanta), Ga.

**Table 17-5**

Crown Height and ISO Pulley Diameters for Flat Belts\*

ISO Pulley Diameter, in	Crown Height, in	ISO Pulley Diameter, in	Crown Height, in	
			w ≤ 10 in	w > 10 in
1.6, 2, 2.5	0.012	12.5, 14	0.03	0.03
2.8, 3.15	0.012	12.5, 14	0.04	0.04
3.55, 4, 4.5	0.012	22.4, 25, 28	0.05	0.05
5, 5.6	0.016	31.5, 35.5	0.05	0.06
6.3, 7.1	0.020	40	0.05	0.06
8, 9	0.024	45, 50, 56	0.06	0.08
10, 11.2	0.030	63, 71, 80	0.07	0.10

\*Crown should be rounded, not angled; maximum roughness is  $R_a = AA\ 63\ \mu\text{in}$ .

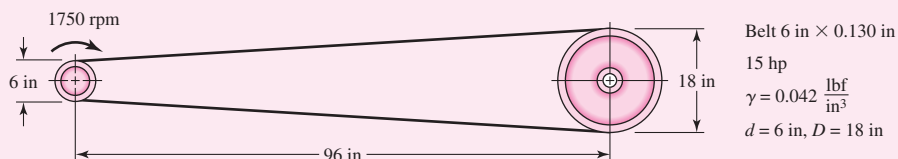
**EXAMPLE 17-1**

A polyamide A-3 flat belt 6 in wide is used to transmit 15 hp under light shock conditions where  $K_s = 1.25$ , and a factor of safety equal to or greater than 1.1 is appropriate. The pulley rotational axes are parallel and in the horizontal plane. The shafts are 8 ft apart. The 6-in driving pulley rotates at 1750 rev/min in such a way that the loose side is on top. The driven pulley is 18 in in diameter. See Fig. 17-10. The factor of safety is for unquantifiable exigencies.

- (a) Estimate the centrifugal tension  $F_c$  and the torque  $T$ .
- (b) Estimate the allowable  $F_1$ ,  $F_2$ ,  $F_i$  and allowable power  $H_a$ .
- (c) Estimate the factor of safety. Is it satisfactory?

**Figure 17-10**

The flat-belt drive of Ex. 17-1.



**Solution** (a) Eq. (17-1):  $\phi = \theta_d = \pi - 2 \sin^{-1} \left[ \frac{18 - 6}{2(8)12} \right] = 3.0165 \text{ rad}$

$$\exp(f\phi) = \exp[0.8(3.0165)] = 11.17$$

$$V = \pi(6)1750/12 = 2749 \text{ ft/min}$$

Table 17-2:  $w = 12\gamma bt = 12(0.042)6(0.130) = 0.393 \text{ lbf/ft}$

**Answer** Eq. (e):  $F_c = \frac{w}{g} \left( \frac{V}{60} \right)^2 = \frac{0.393}{32.17} \left( \frac{2749}{60} \right)^2 = 25.6 \text{ lbf}$

$$T = \frac{63,025 H_{\text{nom}} K_s n_d}{n} = \frac{63,025(15)1.25(1.1)}{1750}$$

**Answer**  $= 742.8 \text{ lbf} \cdot \text{in}$

(b) The necessary  $(F_1)_a - F_2$  to transmit the torque  $T$ , from Eq. (h), is

$$(F_1)_a - F_2 = \frac{2T}{d} = \frac{2(742.8)}{6} = 247.6 \text{ lbf}$$

From Table 17-2  $F_a = 100 \text{ lbf}$ . For polyamide belts  $C_v = 1$ , and from Table 17-4  $C_p = 0.70$ . From Eq. (17-12) the allowable largest belt tension  $(F_1)_a$  is

**Answer**  $(F_1)_a = b F_a C_p C_v = 6(100)0.70(1) = 420 \text{ lbf}$

then

**Answer**  $F_2 = (F_1)_a - [(F_1)_a - F_2] = 420 - 247.6 = 172.4 \text{ lbf}$

and from Eq. (i)

$$F_i = \frac{(F_1)_a + F_2}{2} - F_c = \frac{420 + 172.4}{2} - 25.6 = 270.6 \text{ lbf}$$

**Answer** The combination  $(F_1)_a$ ,  $F_2$ , and  $F_i$  will transmit the design power of  $15(1.25)(1.1) = 20.6 \text{ hp}$  and protect the belt. We check the friction development by solving Eq. (17-7) for  $f'$ :

$$f' = \frac{1}{\phi} \ln \frac{(F_1)_a - F_c}{F_2 - F_c} = \frac{1}{3.0165} \ln \frac{420 - 25.6}{172.4 - 25.6} = 0.328$$

From Table 17-2,  $f = 0.8$ . Since  $f' < f$ , that is,  $0.328 < 0.80$ , there is no danger of slipping.

(c)

**Answer**  $n_{fs} = \frac{H}{H_{\text{nom}} K_s} = \frac{20.6}{15(1.25)} = 1.1 \quad (\text{as expected})$

**Answer** The belt is satisfactory and the maximum allowable belt tension exists. If the initial tension is maintained, the capacity is the design power of  $20.6 \text{ hp}$ .

Initial tension is the key to the functioning of the flat belt as intended. There are ways of controlling initial tension. One way is to place the motor and drive pulley on a pivoted mounting plate so that the weight of the motor, pulley, and mounting plate and a share of the belt weight induces the correct initial tension and maintains it. A second way is use of a spring-loaded idler pulley, adjusted to the same task. Both of these methods accommodate to temporary or permanent belt stretch. See Fig. 17-11.

Because flat belts were used for long center-to-center distances, the weight of the belt itself can provide the initial tension. The static belt deflects to an approximate catenary curve, and the dip from a straight belt can be measured against a stretched music wire. This provides a way of measuring and adjusting the dip. From catenary theory the dip is related to the initial tension by

$$dip = \frac{12(C/12)^2 w}{8F_i} = \frac{C^2 w}{96F_i} \quad (17-13)$$

where  $dip$  = dip, in

$C$  = center-to-center distance, in

$w$  = weight per foot of the belt, lbf/ft

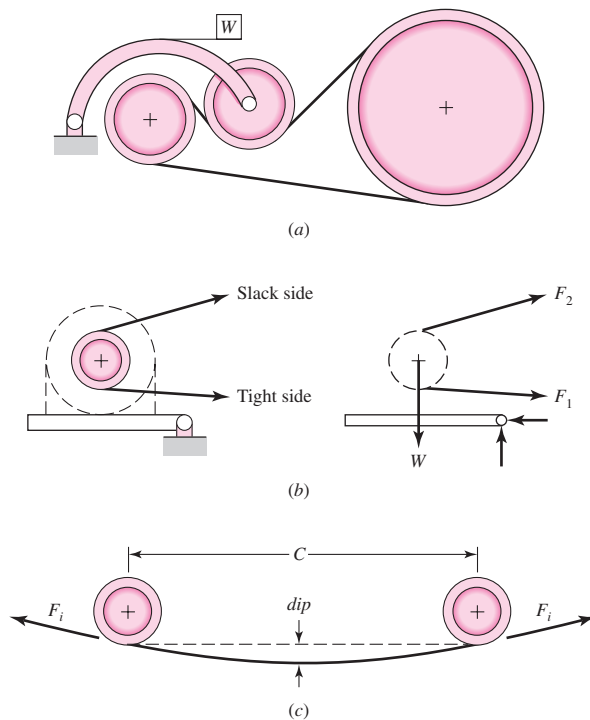
$F_i$  = initial tension, lbf

In Ex. 17-1 the dip corresponding to a 270.6-lbf initial tension is

$$dip = \frac{(96^2)0.393}{96(270.6)} = 0.14 \text{ in}$$

**Figure 17-11**

- Belt-tensioning schemes.  
 (a) Weighted idler pulley.  
 (b) Pivoted motor mount.  
 (c) Catenary-induced tension.



A decision set for a flat belt can be

- Function: power, speed, durability, reduction, service factor,  $C$
- Design factor:  $n_d$
- Initial tension maintenance
- Belt material
- Drive geometry,  $d, D$
- Belt thickness:  $t$
- Belt width:  $b$

Depending on the problem, some or all of the last four could be design variables. Belt cross-sectional area is really the design decision, but available belt thicknesses and widths are discrete choices. Available dimensions are found in suppliers' catalogs.

### EXAMPLE 17-2

Design a flat-belt drive to connect horizontal shafts on 16-ft centers. The velocity ratio is to be 2.25:1. The angular speed of the small driving pulley is 860 rev/min, and the nominal power transmission is to be 60 hp under very light shock.

#### Solution

- Function:  $H_{\text{nom}} = 60 \text{ hp}$ , 860 rev/min, 2.25:1 ratio,  $K_s = 1.15$ ,  $C = 16 \text{ ft}$
- Design factor:  $n_d = 1.05$
- Initial tension maintenance: catenary
- Belt material: polyamide
- Drive geometry,  $d, D$
- Belt thickness:  $t$
- Belt width:  $b$

The last four could be design variables. Let's make a few more a priori decisions.

#### Decision

$$d = 16 \text{ in}, D = 2.25d = 2.25(16) = 36 \text{ in}.$$

#### Decision

Use polyamide A-3 belt; therefore  $t = 0.13 \text{ in}$  and  $C_v = 1$ .

Now there is one design decision remaining to be made, the belt width  $b$ .

Table 17-2:  $\gamma = 0.042 \text{ lbf/in}^3$        $f = 0.8$        $F_a = 100 \text{ lbf/in}$  at 600 rev/min

Table 17-4:  $C_p = 0.94$

Eq. (17-12):  $F_{1a} = b(100)0.94(1) = 94.0b \text{ lbf}$

(1)

$$H_d = H_{\text{nom}}K_s n_d = 60(1.15)1.05 = 72.5 \text{ hp}$$

$$T = \frac{63\ 025 H_d}{n} = \frac{63\ 025(72.5)}{860} = 5310 \text{ lbf} \cdot \text{in}$$

Estimate  $\exp(f\phi)$  for full friction development:

$$\text{Eq. (17-1): } \phi = \theta_d = \pi - 2 \sin^{-1} \frac{36 - 16}{2(16)12} = 3.037 \text{ rad}$$

$$\exp(f\phi) = \exp[0.80(3.037)] = 11.35$$

Estimate centrifugal tension  $F_c$  in terms of belt width  $b$ :

$$w = 12\gamma bt = 12(0.042)b(0.13) = 0.0655b \text{ lbf/ft}$$

$$V = \pi dn/12 = \pi(16)860/12 = 3602 \text{ ft/min}$$

$$\text{Eq. (e):} \quad F_c = \frac{w}{g} \left( \frac{V}{60} \right)^2 = \frac{0.0655b}{32.17} \left( \frac{3602}{60} \right)^2 = 7.34b \text{ lbf} \quad (2)$$

For design conditions, that is, at  $H_d$  power level, using Eq. (h) gives

$$(F_1)_a - F_2 = 2T/d = 2(5310)/16 = 664 \text{ lbf} \quad (3)$$

$$F_2 = (F_1)_a - [(F_1)_a - F_2] = 94.0b - 664 \text{ lbf} \quad (4)$$

Using Eq. (i) gives

$$F_i = \frac{(F_1)_a + F_2}{2} - F_c = \frac{94.0b + 94.0b - 664}{2} - 7.34b = 86.7b - 332 \text{ lbf} \quad (5)$$

Place friction development at its highest level, using Eq. (17-7):

$$f\phi = \ln \frac{(F_1)_a - F_c}{F_2 - F_c} = \ln \frac{94.0b - 7.34b}{94.0b - 664 - 7.34b} = \ln \frac{86.7b}{86.7b - 664}$$

Solving the preceding equation for belt width  $b$  at which friction is fully developed gives

$$b = \frac{664}{86.7} \frac{\exp(f\phi)}{\exp(f\phi) - 1} = \frac{664}{86.7} \frac{11.38}{11.38 - 1} = 8.40 \text{ in}$$

A belt width greater than 8.40 in will develop friction less than  $f = 0.80$ . The manufacturer's data indicate that the next available larger width is 10 in.

### Decision

Use 10-in-wide belt.

It follows that for a 10-in-wide belt

$$\text{Eq. (2):} \quad F_c = 7.34(10) = 73.4 \text{ lbf}$$

$$\text{Eq. (1):} \quad (F_1)_a = 94(10) = 940 \text{ lbf}$$

$$\text{Eq. (4):} \quad F_2 = 94(10) - 664 = 276 \text{ lbf}$$

$$\text{Eq. (5):} \quad F_i = 86.7(10) - 332 = 535 \text{ lbf}$$

The transmitted power, from Eq. (3), is

$$H_t = \frac{[(F_1)_a - F_2]V}{33\ 000} = \frac{664(3602)}{33\ 000} = 72.5 \text{ hp}$$

and the level of friction development  $f'$ , from Eq. (17-7) is

$$f' = \frac{1}{\phi} \ln \frac{(F_1)_a - F_c}{F_2 - F_c} = \frac{1}{3.037} \ln \frac{940 - 73.4}{276 - 73.4} = 0.479$$

which is less than  $f = 0.8$ , and thus is satisfactory. Had a 9-in belt width been available, the analysis would show  $(F_1)_a = 846$  lbf,  $F_2 = 182$  lbf,  $F_i = 448$  lbf, and  $f' = 0.63$ . With a figure of merit available reflecting cost, thicker belts (A-4 or A-5) could be examined to ascertain which of the satisfactory alternatives is best. From Eq. (17-13) the catenary dip is

$$\text{dip} = \frac{C^2 w}{96 F_i} = \frac{[16(12)]^2 0.0655(10)}{96(535)} = 0.470 \text{ in}$$

**Figure 17-12**

Flat-belt tensions.

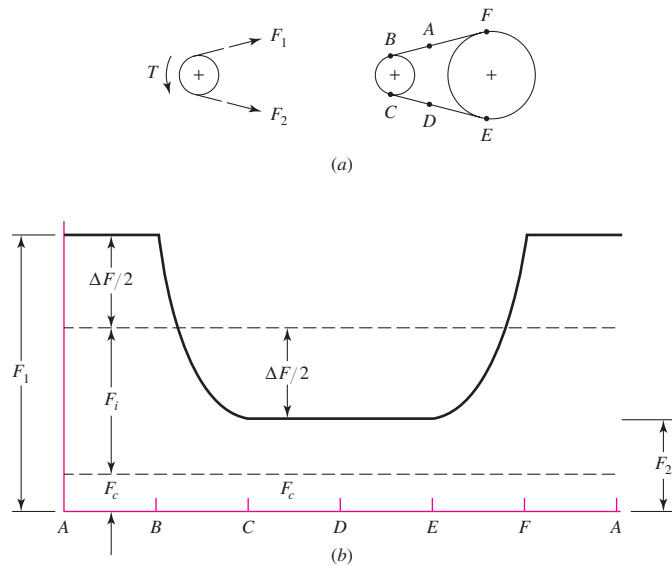


Figure 17–12 illustrates the variation of flexible flat-belt tensions at some cardinal points during a belt pass.

### Flat Metal Belts

Thin flat metal belts with their attendant strength and geometric stability could not be fabricated until laser welding and thin rolling technology made possible belts as thin as 0.002 in and as narrow as 0.026 in. The introduction of perforations allows no-slip applications. Thin metal belts exhibit

- High strength-to-weight ratio
- Dimensional stability
- Accurate timing
- Usefulness to temperatures up to 700°F
- Good electrical and thermal conduction properties

In addition, stainless steel alloys offer “inert,” nonabsorbent belts suitable to hostile (corrosive) environments, and can be made sterile for food and pharmaceutical applications.

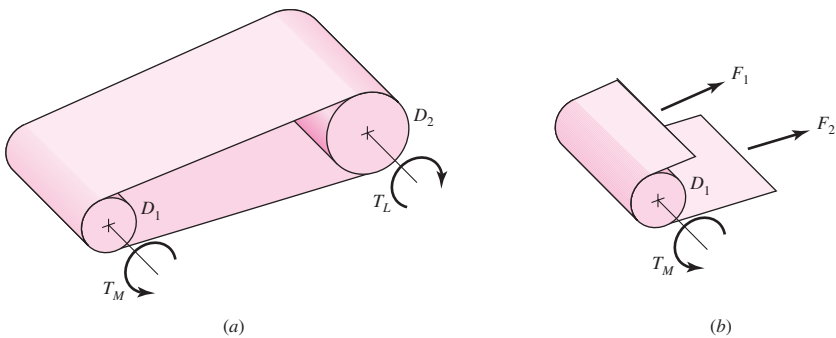
Thin metal belts can be classified as friction drives, timing or positioning drives, or tape drives. Among friction drives are plain, metal-coated, and perforated belts. Crowned pulleys are used to compensate for tracking errors.

Figure 17–13 shows a thin flat metal belt with the tight tension  $F_1$  and the slack side tension  $F_2$  revealed. The relationship between  $F_1$  and  $F_2$  and the driving torque  $T$  is the same as in Eq. (h). Equations (17–9), (17–10), and (17–11) also apply. The largest allowable tension, as in Eq. (17–12), is posed in terms of stress in metal belts. A bending stress is created by making the belt conform to the pulley, and its tensile magnitude  $\sigma_b$  is given by

$$\sigma_b = \frac{Et}{(1 - \nu^2)D} = \frac{E}{(1 - \nu^2)(D/t)} \quad (17-14)$$

**Figure 17-13**

Metal-belt tensions and torques.



where  $E$  = Young's modulus

$t$  = belt thickness

$\nu$  = Poisson's ratio

$D$  = pulley diameter

The tensile stresses  $(\sigma)_1$  and  $(\sigma)_2$  imposed by the belt tensions  $F_1$  and  $F_2$  are

$$(\sigma)_1 = F_1/(bt) \quad \text{and} \quad (\sigma)_2 = F_2/(bt)$$

The largest tensile stress is  $(\sigma_b)_1 + F_1/(bt)$  and the smallest is  $(\sigma_b)_2 + F_2/(bt)$ . During a belt pass both levels of stress appear.

Although the belts are of simple geometry, the method of Marin is not used because the condition of the butt weldment (to form the loop) is not accurately known, and the testing of coupons is difficult. The belts are run to failure on two equal-sized pulleys. Information concerning fatigue life, as shown in Table 17-6, is obtainable. Tables 17-7 and 17-8 give additional information.

Table 17-6 shows metal belt life expectancies for a stainless steel belt. From Eq. (17-14) with  $E = 28$  Mpsi and  $\nu = 0.29$ , the bending stresses corresponding to the four entries of the table are 48 914, 76 428, 91 805, and 152 855 psi. Using a natural log transformation on stress and passes shows that the regression line ( $r = -0.96$ ) is

$$\sigma = 14\ 169\ 982 N^{-0.407} = 14.17(10^6) N_p^{-0.407} \quad (17-15)$$

where  $N_p$  is the number of belt passes.

**Table 17-6**

Belt Life for Stainless Steel Friction Drives\*

$\frac{D}{t}$	Belt Passes
625	$\geq 10^6$
400	$0.500 \cdot 10^6$
333	$0.165 \cdot 10^6$
200	$0.085 \cdot 10^6$

\*Data courtesy of Belt Technologies, Agawam, Mass.

**Table 17-7**

Minimum Pulley  
Diameter\*

	Belt Thickness, in	Minimum Pulley Diameter, in
	0.002	1.2
	0.003	1.8
	0.005	3.0
	0.008	5.0
	0.010	6.0
	0.015	10
	0.020	12.5
	0.040	25.0

\*Data courtesy of Belt Technologies, Agawam, Mass.

**Table 17-8**

Typical Material  
Properties, Metal Belts\*

Alloy	Yield Strength, ksi	Young's Modulus, GPa	Poisson's Ratio
301 or 302 stainless steel	175	28	0.285
BeCu	170	17	0.220
1075 or 1095 carbon steel	230	30	0.287
Titanium	150	15	—
Inconel	160	30	0.284

\*Data courtesy of Belt Technologies, Agawam, Mass.

The selection of a metal flat belt can consist of the following steps:

- 1 Find  $\exp(f\phi)$  from geometry and friction
- 2 Find endurance strength

$$S_f = 14.17(10^6)N_p^{-0.407} \quad \text{301, 302 stainless}$$

$$S_f = S_y/3 \quad \text{others}$$

- 3 Allowable tension

$$F_{1a} = \left[ S_f - \frac{Et}{(1-\nu^2)D} \right] tb = ab$$

$$4 \quad \Delta F = 2T/D$$

$$5 \quad F_2 = F_{1a} - \Delta F = ab - \Delta F$$

$$6 \quad F_i = \frac{F_{1a} + F_2}{2} = \frac{ab + ab - \Delta F}{2} = ab - \frac{\Delta F}{2}$$

$$7 \quad b_{\min} = \frac{\Delta F}{a} \frac{\exp(f\phi)}{\exp(f\phi) - 1}$$

$$8 \quad \text{Choose } b > b_{\min}, F_1 = ab, F_2 = ab - \Delta F, F_i = ab - \Delta F/2, T = \Delta FD/2$$

**9** Check frictional development  $f'$ :

$$f' = \frac{1}{\phi} \ln \frac{F_1}{F_2} \quad f' < f$$

### EXAMPLE 17-3

A friction-drive stainless steel metal belt runs over two 4-in metal pulleys ( $f = 0.35$ ). The belt thickness is to be 0.003 in. For a life exceeding  $10^6$  belt passes with smooth torque ( $K_s = 1$ ), (a) select the belt if the torque is to be 30 lbf · in, and (b) find the initial tension  $F_i$ .

#### Solution

(a) From step 1,  $\phi = \theta_d = \pi$ , therefore  $\exp(0.35\pi) = 3.00$ . From step 2,

$$(S_f)_{10^6} = 14.17(10^6)(10^6)^{-0.407} = 51\,210 \text{ psi}$$

From steps 3, 4, 5, and 6,

$$F_{1a} = \left[ 51\,210 - \frac{28(10^6)0.003}{(1 - 0.285^2)4} \right] 0.003b = 85.1b \text{ lbf} \quad (1)$$

$$\Delta F = 2T/D = 2(30)/4 = 15 \text{ lbf}$$

$$F_2 = F_{1a} - \Delta F = 85.1b - 15 \text{ lbf} \quad (2)$$

$$F_i = \frac{F_{1a} + F_2}{2} = \frac{85.1b + 15}{2} \text{ lbf} \quad (3)$$

From step 7,

$$b_{\min} = \frac{\Delta F}{a} \frac{\exp(f\phi)}{\exp(f\phi) - 1} = \frac{15}{85.1} \frac{3.00}{3.00 - 1} = 0.264 \text{ in}$$

#### Decision

Select an available 0.75-in-wide belt 0.003 in thick.

$$\text{Eq. (1):} \quad F_1 = 85.1(0.75) = 63.8 \text{ lbf}$$

$$\text{Eq. (2):} \quad F_2 = 85.1(0.75) - 15 = 48.8 \text{ lbf}$$

$$\text{Eq. (3):} \quad F_i = (63.8 + 48.8)/2 = 56.3 \text{ lbf}$$

$$f' = \frac{1}{\phi} \ln \frac{F_1}{F_2} = \frac{1}{\pi} \ln \frac{63.8}{48.8} = 0.0853$$

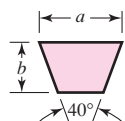
Note  $f' < f$ , that is,  $0.0853 < 0.35$ .

## 17-3 V Belts

The cross-sectional dimensions of V belts have been standardized by manufacturers, with each section designated by a letter of the alphabet for sizes in inch dimensions. Metric sizes are designated in numbers. Though these have not been included here, the procedure for analyzing and designing them is the same as presented here. Dimensions, minimum sheave diameters, and the horsepower range for each of the lettered sections are listed in Table 17-9.

**Table 17-9**

Standard V-Belt Sections



Belt Section	Width <i>a</i> , in	Thickness <i>b</i> , in	Minimum Sheave Diameter, in	hp Range, One or More Belts
A	$\frac{1}{2}$	$\frac{11}{32}$	3.0	$\frac{1}{4}$ –10
B	$\frac{21}{32}$	$\frac{7}{16}$	5.4	1–25
C	$\frac{7}{8}$	$\frac{17}{32}$	9.0	15–100
D	$1\frac{1}{4}$	$\frac{3}{4}$	13.0	50–250
E	$1\frac{1}{2}$	1	21.6	100 and up

**Table 17-10**

Inside Circumferences of Standard V Belts

Section	Circumference, in
A	26, 31, 33, 35, 38, 42, 46, 48, 51, 53, 55, 57, 60, 62, 64, 66, 68, 71, 75, 78, 80, 85, 90, 96, 105, 112, 120, 128
B	35, 38, 42, 46, 48, 51, 53, 55, 57, 60, 62, 64, 65, 66, 68, 71, 75, 78, 79, 81, 83, 85, 90, 93, 97, 100, 103, 105, 112, 120, 128, 131, 136, 144, 158, 173, 180, 195, 210, 240, 270, 300
C	51, 60, 68, 75, 81, 85, 90, 96, 105, 112, 120, 128, 136, 144, 158, 162, 173, 180, 195, 210, 240, 270, 300, 330, 360, 390, 420
D	120, 128, 144, 158, 162, 173, 180, 195, 210, 240, 270, 300, 330, 360, 390, 420, 480, 540, 600, 660
E	180, 195, 210, 240, 270, 300, 330, 360, 390, 420, 480, 540, 600, 660

**Table 17-11**

Length Conversion Dimensions (Add the listed quantity to the inside circumference to obtain the pitch length in inches).

Belt section	A	B	C	D	E
Quantity to be added	1.3	1.8	2.9	3.3	4.5

To specify a V belt, give the belt-section letter, followed by the inside circumference in inches (standard circumferences are listed in Table 17-10). For example, B75 is a B-section belt having an inside circumference of 75 in.

Calculations involving the belt length are usually based on the pitch length. For any given belt section, the pitch length is obtained by adding a quantity to the inside circumference (Tables 17-10 and 17-11). For example, a B75 belt has a pitch length of 76.8 in. Similarly, calculations of the velocity ratios are made using the pitch diameters of the sheaves, and for this reason the stated diameters are usually understood to be the pitch diameters even though they are not always so specified.

The groove angle of a sheave is made somewhat smaller than the belt-section angle. This causes the belt to wedge itself into the groove, thus increasing friction. The exact value of this angle depends on the belt section, the sheave diameter, and the angle of contact. If it is made too much smaller than the belt, the force required to pull the belt out of the groove as the belt leaves the pulley will be excessive. Optimum values are given in the commercial literature.

The minimum sheave diameters have been listed in Table 17–9. For best results, a V belt should be run quite fast: 4000 ft/min is a good speed. Trouble may be encountered if the belt runs much faster than 5000 ft/min or much slower than 1000 ft/min.

The *pitch length*  $L_p$  and the center-to-center distance  $C$  are

$$L_p = 2C + \pi(D + d)/2 + (D - d)^2/(4C) \quad (17-16a)$$

$$C = 0.25 \left\{ \left[ L_p - \frac{\pi}{2}(D + d) \right] + \sqrt{\left[ L_p - \frac{\pi}{2}(D + d) \right]^2 - 2(D - d)^2} \right\} \quad (17-16b)$$

where  $D$  = pitch diameter of the large sheave and  $d$  = pitch diameter of the small sheave.

In the case of flat belts, there is virtually no limit to the center-to-center distance. Long center-to-center distances are not recommended for V belts because the excessive vibration of the slack side will shorten the belt life materially. In general, the center-to-center distance should be no greater than 3 times the sum of the sheave diameters and no less than the diameter of the larger sheave. Link-type V belts have less vibration, because of better balance, and hence may be used with longer center-to-center distances.

The basis for power ratings of V belts depends somewhat on the manufacturer; it is not often mentioned quantitatively in vendors' literature but is available from vendors. The basis may be a number of hours, 24 000, for example, or a life of  $10^8$  or  $10^9$  belt passes. Since the number of belts must be an integer, an undersized belt set that is augmented by one belt can be substantially oversized. Table 17–12 gives power ratings of standard V belts.

The rating, whether in terms of hours or belt passes, is for a belt running on equal-diameter sheaves ( $180^\circ$  of wrap), of moderate length, and transmitting a steady load. Deviations from these laboratory test conditions are acknowledged by multiplicative adjustments. If the tabulated power of a belt for a C-section belt is 9.46 hp for a 12-in.-diameter sheave at a peripheral speed of 3000 ft/min (Table 17–12), then, when the belt is used under other conditions, the tabulated value  $H_{\text{tab}}$  is adjusted as follows:

$$H_a = K_1 K_2 H_{\text{tab}} \quad (17-17)$$

where  $H_a$  = allowable power, per belt

$K_1$  = angle-of-wrap correction factor, Table 17–13

$K_2$  = belt length correction factor, Table 17–14

The allowable power can be near to  $H_{\text{tab}}$ , depending upon circumstances.

In a V belt the effective coefficient of friction  $f'$  is  $f/\sin(\phi/2)$ , which amounts to an augmentation by a factor of about 3 due to the grooves. The effective coefficient of friction  $f'$  is sometimes tabulated against *sheave* groove angles of  $30^\circ$ ,  $34^\circ$ , and  $38^\circ$ , the tabulated values being 0.50, 0.45, and 0.40, respectively, revealing a belt material-on-metal coefficient of friction of 0.13 for each case. The Gates Rubber Company declares its effective coefficient of friction to be 0.5123 for grooves. Thus

$$\frac{F_1 - F_c}{F_2 - F_c} = \exp(0.5123\phi) \quad (17-18)$$

The design power is given by

$$H_d = H_{\text{nom}} K_s n_d \quad (17-19)$$

where  $H_{\text{nom}}$  is the nominal power,  $K_s$  is the service factor given in Table 17–15, and  $n_d$  is the design factor. The number of belts,  $N_b$ , is usually the next higher integer to  $H_d/H_a$ .

**Table 17-12**

Horsepower Ratings of Standard V Belts

Belt Section	Sheave Pitch Diameter, in	Belt Speed, ft/min				
		1000	2000	3000	4000	5000
A	2.6	0.47	0.62	0.53	0.15	
	3.0	0.66	1.01	1.12	0.93	0.38
	3.4	0.81	1.31	1.57	1.53	1.12
	3.8	0.93	1.55	1.92	2.00	1.71
	4.2	1.03	1.74	2.20	2.38	2.19
	4.6	1.11	1.89	2.44	2.69	2.58
	5.0 and up	1.17	2.03	2.64	2.96	2.89
B	4.2	1.07	1.58	1.68	1.26	0.22
	4.6	1.27	1.99	2.29	2.08	1.24
	5.0	1.44	2.33	2.80	2.76	2.10
	5.4	1.59	2.62	3.24	3.34	2.82
	5.8	1.72	2.87	3.61	3.85	3.45
	6.2	1.82	3.09	3.94	4.28	4.00
	6.6	1.92	3.29	4.23	4.67	4.48
C	7.0 and up	2.01	3.46	4.49	5.01	4.90
	6.0	1.84	2.66	2.72	1.87	
	7.0	2.48	3.94	4.64	4.44	3.12
	8.0	2.96	4.90	6.09	6.36	5.52
	9.0	3.34	5.65	7.21	7.86	7.39
	10.0	3.64	6.25	8.11	9.06	8.89
	11.0	3.88	6.74	8.84	10.0	10.1
D	12.0 and up	4.09	7.15	9.46	10.9	11.1
	10.0	4.14	6.13	6.55	5.09	1.35
	11.0	5.00	7.83	9.11	8.50	5.62
	12.0	5.71	9.26	11.2	11.4	9.18
	13.0	6.31	10.5	13.0	13.8	12.2
	14.0	6.82	11.5	14.6	15.8	14.8
	15.0	7.27	12.4	15.9	17.6	17.0
E	16.0	7.66	13.2	17.1	19.2	19.0
	17.0 and up	8.01	13.9	18.1	20.6	20.7
	16.0	8.68	14.0	17.5	18.1	15.3
	18.0	9.92	16.7	21.2	23.0	21.5
	20.0	10.9	18.7	24.2	26.9	26.4
	22.0	11.7	20.3	26.6	30.2	30.5
	24.0	12.4	21.6	28.6	32.9	33.8
F	26.0	13.0	22.8	30.3	35.1	36.7
	28.0 and up	13.4	23.7	31.8	37.1	39.1

That is,

$$N_b \geq \frac{H_d}{H_a} \quad N_b = 1, 2, 3, \dots \quad (17-20)$$

Designers work on a per-belt basis.

The flat-belt tensions shown in Fig. 17-12 ignored the tension induced by bending the belt about the pulleys. This is more pronounced with V belts, as shown in Fig. 17-14.

The centrifugal tension  $F_c$  is given by

$$F_c = K_c \left( \frac{V}{1000} \right)^2 \quad (17-21)$$

where  $K_c$  is from Table 17-16.

**Table 17-13**

	$\frac{D-d}{C}$	$\theta$ , deg	$K_1$	V Flat
			VV	
Angle of Contact				
Correction Factor $K_1$ for VV* and V-Flat Drives	0.00	180	1.00	0.75
	0.10	174.3	0.99	0.76
	0.20	166.5	0.97	0.78
	0.30	162.7	0.96	0.79
	0.40	156.9	0.94	0.80
	0.50	151.0	0.93	0.81
	0.60	145.1	0.91	0.83
	0.70	139.0	0.89	0.84
	0.80	132.8	0.87	0.85
	0.90	126.5	0.85	0.85
	1.00	120.0	0.82	0.82
	1.10	113.3	0.80	0.80
	1.20	106.3	0.77	0.77
	1.30	98.9	0.73	0.73
	1.40	91.1	0.70	0.70
	1.50	82.8	0.65	0.65

\*A curve fit for the VV column in terms of  $\theta$  is

$$K_1 = 0.143\ 543 + 0.007\ 46\ 8 \theta - 0.000\ 015\ 052 \theta^2$$

in the range  $90^\circ \leq \theta \leq 180^\circ$ .

**Table 17-14**

Belt-Length Correction Factor  $K_2^*$

Length Factor	Nominal Belt Length, in				
	A Belts	B Belts	C Belts	D Belts	E Belts
0.85	Up to 35	Up to 46	Up to 75	Up to 128	
0.90	38–46	48–60	81–96	144–162	Up to 195
0.95	48–55	62–75	105–120	173–210	210–240
1.00	60–75	78–97	128–158	240	270–300
1.05	78–90	105–120	162–195	270–330	330–390
1.10	96–112	128–144	210–240	360–420	420–480
1.15	120 and up	158–180	270–300	480	540–600
1.20		195 and up	330 and up	540 and up	660

\*Multiply the rated horsepower per belt by this factor to obtain the corrected horsepower.

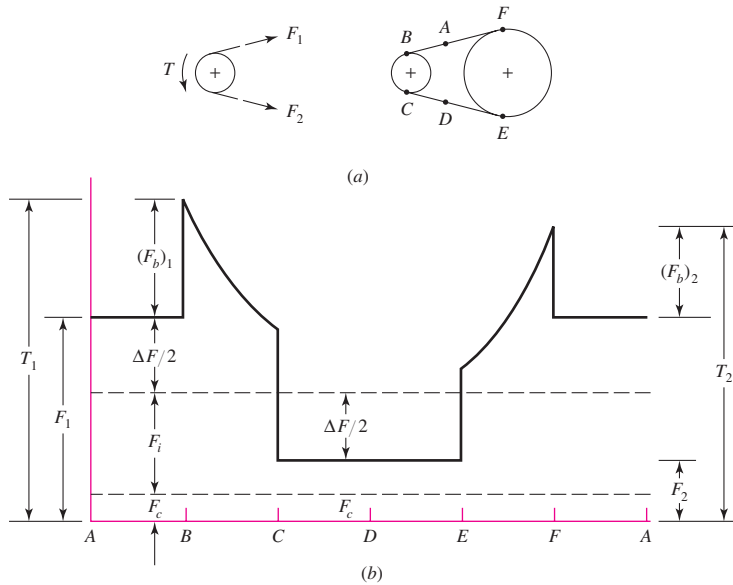
**Table 17-15**

Suggested Service Factors  $K_S$  for V-Belt Drives

Driven Machinery	Source of Power	
	Normal Torque Characteristic	High or Nonuniform Torque
Uniform	1.0 to 1.2	1.1 to 1.3
Light shock	1.1 to 1.3	1.2 to 1.4
Medium shock	1.2 to 1.4	1.4 to 1.6
Heavy shock	1.3 to 1.5	1.5 to 1.8

**Figure 17-14**

V-belt tensions.

**Table 17-16**

Some V-Belt Parameters\*

Belt Section	$K_b$	$K_c$
A	220	0.561
B	576	0.965
C	1 600	1.716
D	5 680	3.498
E	10 850	5.041
3V	230	0.425
5V	1098	1.217
8V	4830	3.288

\*Data courtesy of Gates Rubber Co., Denver, Colo.

The power that is transmitted per belt is based on  $\Delta F = F_1 - F_2$ , where

$$\Delta F = \frac{63\,025 H_d / N_b}{n(d/2)} \quad (17-22)$$

then from Eq. (17-8) the largest tension  $F_1$  is given by

$$F_1 = F_c + \frac{\Delta F \exp(f\phi)}{\exp(f\phi) - 1} \quad (17-23)$$

From the definition of  $\Delta F$ , the least tension  $F_2$  is

$$F_2 = F_1 - \Delta F \quad (17-24)$$

From Eq. (j) in Sec. 17-2

$$F_i = \frac{F_1 + F_2}{2} - F_c \quad (17-25)$$

The factor of safety is

$$n_{fs} = \frac{H_a N_b}{H_{\text{nom}} K_s} \quad (17-26)$$

Durability (life) correlations are complicated by the fact that the bending induces flexural stresses in the belt; the corresponding belt tension that induces the same maximum tensile stress is  $F_{b1}$  at the driving sheave and  $F_{b2}$  at the driven pulley. These equivalent tensions are added to  $F_1$  as

$$T_1 = F_1 + (F_b)_1 = F_1 + \frac{K_b}{d}$$

$$T_2 = F_1 + (F_b)_2 = F_1 + \frac{K_b}{D}$$

where  $K_b$  is given in Table 17-16. The equation for the tension versus pass trade-off used by the Gates Rubber Company is of the form

$$T^b N_P = K^b$$

where  $N_P$  is the number of passes and  $b$  is approximately 11. See Table 17-17. The Miner rule is used to sum damage incurred by the two tension peaks:

$$\frac{1}{N_P} = \left( \frac{K}{T_1} \right)^{-b} + \left( \frac{K}{T_2} \right)^{-b}$$

or

$$N_P = \left[ \left( \frac{K}{T_1} \right)^{-b} + \left( \frac{K}{T_2} \right)^{-b} \right]^{-1} \quad (17-27)$$

The lifetime  $t$  in hours is given by

$$t = \frac{N_P L_p}{720V} \quad (17-28)$$

**Table 17-17**

Durability Parameters for Some V-Belt Sections

Source: M. E. Spotts, *Design of Machine Elements*, 6th ed. Prentice Hall, Englewood Cliffs, N.J., 1985.

Belt Section	10 <sup>8</sup> to 10 <sup>9</sup> Force Peaks		10 <sup>9</sup> to 10 <sup>10</sup> Force Peaks		Minimum Sheave Diameter, in
	K	b	K	b	
A	674	11.089			3.0
B	1193	10.926			5.0
C	2038	11.173			8.5
D	4208	11.105			13.0
E	6061	11.100			21.6
3V	728	12.464	1062	10.153	2.65
5V	1654	12.593	2394	10.283	7.1
8V	3638	12.629	5253	10.319	12.5

The constants  $K$  and  $b$  have their ranges of validity. If  $N_P > 10^9$ , report that  $N_P = 10^9$  and  $t > N_P L_p / (720V)$  without placing confidence in numerical values beyond the validity interval. See the statement about  $N_P$  and  $t$  near the conclusion of Ex. 17–4.

The analysis of a V-belt drive can consist of the following steps:

- Find  $V$ ,  $L_p$ ,  $C$ ,  $\phi$ , and  $\exp(0.5123\phi)$
- Find  $H_d$ ,  $H_a$ , and  $N_b$  from  $H_d/H_a$  and round up
- Find  $F_c$ ,  $\Delta F$ ,  $F_1$ ,  $F_2$ , and  $F_i$ , and  $n_{fs}$
- Find belt life in number of passes, or hours, if possible

### EXAMPLE 17–4

A 10-hp split-phase motor running at 1750 rev/min is used to drive a rotary pump, which operates 24 hours per day. An engineer has specified a 7.4-in small sheave, an 11-in large sheave, and three B112 belts. The service factor of 1.2 was augmented by 0.1 because of the continuous-duty requirement. Analyze the drive and estimate the belt life in passes and hours.

#### Solution

The peripheral speed  $V$  of the belt is

$$V = \pi dn/12 = \pi(7.4)1750/12 = 3390 \text{ ft/min}$$

Table 17–11:  $L_p = L + L_c = 112 + 1.8 = 113.8$  in

$$\begin{aligned} \text{Eq. (17–16b): } C &= 0.25 \left\{ \left[ 113.8 - \frac{\pi}{2}(11 + 7.4) \right] \right. \\ &\quad \left. + \sqrt{\left[ 113.8 - \frac{\pi}{2}(11 + 7.4) \right]^2 - 2(11 - 7.4)^2} \right\} \\ &= 42.4 \text{ in} \end{aligned}$$

$$\text{Eq. (17–1): } \phi = \theta_d = \pi - 2 \sin^{-1}(11 - 7.4)/[2(42.4)] = 3.057 \text{ rad}$$

$$\exp[0.5123(3.057)] = 4.788$$

Interpolating in Table 17–12 for  $V = 3390$  ft/min gives  $H_{\text{tab}} = 4.693$  hp. The wrap angle in degrees is  $3.057(180)/\pi = 175^\circ$ . From Table 17–13,  $K_1 = 0.99$ . From Table 17–14,  $K_2 = 1.05$ . Thus, from Eq. (17–17),

$$H_a = K_1 K_2 H_{\text{tab}} = 0.99(1.05)4.693 = 4.878 \text{ hp}$$

$$\text{Eq. (17–19): } H_d = H_{\text{nom}} K_s n_d = 10(1.2 + 0.1)(1) = 13 \text{ hp}$$

$$\text{Eq. (17–20): } N_b \geq H_d/H_a = 13/4.878 = 2.67 \rightarrow 3$$

From Table 17–16,  $K_c = 0.965$ . Thus, from Eq. (17–21),

$$F_c = 0.965(3390/1000)^2 = 11.1 \text{ lbf}$$

$$\text{Eq. (17–22): } \Delta F = \frac{63.025(13)/3}{1750(7.4/2)} = 42.2 \text{ lbf}$$

$$\text{Eq. (17–23): } F_1 = 11.1 + \frac{42.2(4.788)}{4.788 - 1} = 64.4 \text{ lbf}$$

$$\text{Eq. (17-24): } F_2 = F_1 - \Delta F = 64.4 - 42.2 = 22.2 \text{ lbf}$$

$$\text{Eq. (17-25): } F_i = \frac{64.4 + 22.2}{2} - 11.1 = 32.2 \text{ lbf}$$

$$\text{Eq. (17-26): } n_{fs} = \frac{H_a N_b}{H_{\text{nom}} K_s} = \frac{4.878(3)}{10(1.3)} = 1.13$$

*Life:* From Table 17-16,  $K_b = 576$ .

$$F_{b1} = \frac{K_b}{d} = \frac{576}{7.4} = 77.8 \text{ lbf}$$

$$F_{b2} = \frac{576}{11} = 52.4 \text{ lbf}$$

$$T_1 = F_1 + F_{b1} = 64.4 + 77.8 = 142.2 \text{ lbf}$$

$$T_2 = F_1 + F_{b2} = 64.4 + 52.4 = 116.8 \text{ lbf}$$

From Table 17-17,  $K = 1193$  and  $b = 10.926$ .

$$\text{Eq. (17-27): } N_P = \left[ \left( \frac{1193}{142.2} \right)^{-10.926} + \left( \frac{1193}{116.8} \right)^{-10.926} \right]^{-1} = 11(10^9) \text{ passes}$$

**Answer** Since  $N_P$  is out of the validity range of Eq. (17-27), life is reported as greater than  $10^9$  passes. Then

**Answer** Eq. (17-28):  $t > \frac{10^9(113.8)}{720(3390)} = 46,600 \text{ h}$

## 17-4

### Timing Belts

A timing belt is made of a rubberized fabric coated with a nylon fabric, and has steel wire within to take the tension load. It has teeth that fit into grooves cut on the periphery of the pulleys (Fig. 17-15). A timing belt does not stretch appreciably or slip and consequently transmits power at a constant angular-velocity ratio. No initial tension is needed.

**Figure 17-15**

Timing-belt drive showing portions of the pulley and belt. Note that the pitch diameter of the pulley is greater than the diametral distance across the top lands of the teeth.

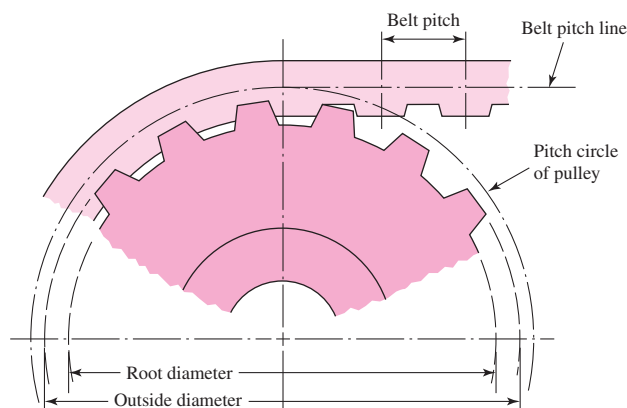


**Table 17-18**

Standard Pitches  
of Timing Belts

Service	Designation	Pitch $p$ , in
Extra light	XL	$\frac{1}{5}$
Light	L	$\frac{3}{8}$
Heavy	H	$\frac{1}{2}$
Extra heavy	XH	$\frac{7}{8}$
Double extra heavy	XXH	$1\frac{1}{4}$

Such belts can operate over a very wide range of speeds, have efficiencies in the range of 97 to 99 percent, require no lubrication, and are quieter than chain drives. There is no chordal-speed variation, as in chain drives (see Sec. 17-5), and so they are an attractive solution for precision-drive requirements.

The steel wire, the tension member of a timing belt, is located at the belt pitch line (Fig. 17-15). Thus the pitch length is the same regardless of the thickness of the backing.

The five standard inch-series pitches available are listed in Table 17-18 with their letter designations. Standard pitch lengths are available in sizes from 6 to 180 in. Pulleys come in sizes from 0.60 in pitch diameter up to 35.8 in and with groove numbers from 10 to 120.

The design and selection process for timing belts is so similar to that for V belts that the process will not be presented here. As in the case of other belt drives, the manufacturers will provide an ample supply of information and details on sizes and strengths.

## 17-5

### Roller Chain

Basic features of chain drives include a constant ratio, since no slippage or creep is involved; long life; and the ability to drive a number of shafts from a single source of power.

Roller chains have been standardized as to sizes by the ANSI. Figure 17-16 shows the nomenclature. The pitch is the linear distance between the centers of the rollers. The width is the space between the inner link plates. These chains are manufactured in single, double, triple, and quadruple strands. The dimensions of standard sizes are listed in Table 17-19.

**Figure 17-16**

Portion of a double-strand roller chain.

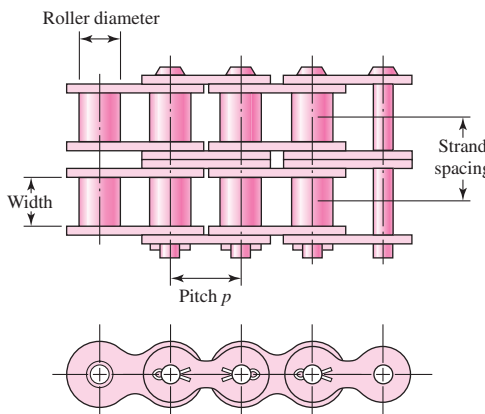


**Table 17-19**

Dimensions of American Standard Roller Chains—Single Strand

*Source:* Compiled from ANSI B29.1-1975.

ANSI Chain Number	Pitch, in (mm)	Width, in (mm)	Minimum Tensile Strength, lbf (N)	Average Weight, lbf/ft (N/m)	Roller Diameter, in (mm)	Multiple- Strand Spacing, in (mm)
25	0.250 (6.35)	0.125 (3.18)	780 (3 470)	0.09 (1.31)	0.130 (3.30)	0.252 (6.40)
35	0.375 (9.52)	0.188 (4.76)	1 760 (7 830)	0.21 (3.06)	0.200 (5.08)	0.399 (10.13)
41	0.500 (12.70)	0.25 (6.35)	1 500 (6 670)	0.25 (3.65)	0.306 (7.77)	— —
40	0.500 (12.70)	0.312 (7.94)	3 130 (13 920)	0.42 (6.13)	0.312 (7.92)	0.566 (14.38)
50	0.625 (15.88)	0.375 (9.52)	4 880 (21 700)	0.69 (10.1)	0.400 (10.16)	0.713 (18.11)
60	0.750 (19.05)	0.500 (12.7)	7 030 (31 300)	1.00 (14.6)	0.469 (11.91)	0.897 (22.78)
80	1.000 (25.40)	0.625 (15.88)	12 500 (55 600)	1.71 (25.0)	0.625 (15.87)	1.153 (29.29)
100	1.250 (31.75)	0.750 (19.05)	19 500 (86 700)	2.58 (37.7)	0.750 (19.05)	1.409 (35.76)
120	1.500 (38.10)	1.000 (25.40)	28 000 (124 500)	3.87 (56.5)	0.875 (22.22)	1.789 (45.44)
140	1.750 (44.45)	1.000 (25.40)	38 000 (169 000)	4.95 (72.2)	1.000 (25.40)	1.924 (48.87)
160	2.000 (50.80)	1.250 (31.75)	50 000 (222 000)	6.61 (96.5)	1.125 (28.57)	2.305 (58.55)
180	2.250 (57.15)	1.406 (35.71)	63 000 (280 000)	9.06 (132.2)	1.406 (35.71)	2.592 (65.84)
200	2.500 (63.50)	1.500 (38.10)	78 000 (347 000)	10.96 (159.9)	1.562 (39.67)	2.817 (71.55)
240	3.00 (76.70)	1.875 (47.63)	112 000 (498 000)	16.4 (239)	1.875 (47.62)	3.458 (87.83)

Figure 17–17 shows a sprocket driving a chain and rotating in a counterclockwise direction. Denoting the chain pitch by  $p$ , the pitch angle by  $\gamma$ , and the pitch diameter of the sprocket by  $D$ , from the trigonometry of the figure we see

$$\sin \frac{\gamma}{2} = \frac{p/2}{D/2} \quad \text{or} \quad D = \frac{p}{\sin(\gamma/2)} \quad (a)$$

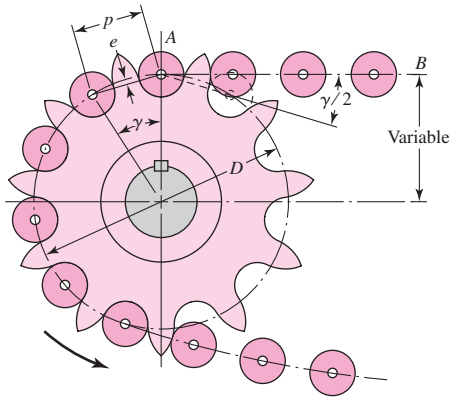
Since  $\gamma = 360^\circ/N$ , where  $N$  is the number of sprocket teeth, Eq. (a) can be written

$$D = \frac{p}{\sin(180^\circ/N)} \quad (17-29)$$

The angle  $\gamma/2$ , through which the link swings as it enters contact, is called the *angle of articulation*. It can be seen that the magnitude of this angle is a function of the number of teeth. Rotation of the link through this angle causes impact between the

**Figure 17-17**

Engagement of a chain and sprocket.



rollers and the sprocket teeth and also wear in the chain joint. Since the life of a properly selected drive is a function of the wear and the surface fatigue strength of the rollers, it is important to reduce the angle of articulation as much as possible.

The number of sprocket teeth also affects the velocity ratio during the rotation through the pitch angle  $\gamma$ . At the position shown in Fig. 17-17, the chain  $AB$  is tangent to the pitch circle of the sprocket. However, when the sprocket has turned an angle of  $\gamma/2$ , the chain line  $AB$  moves closer to the center of rotation of the sprocket. This means that the chain line  $AB$  is moving up and down, and that the lever arm varies with rotation through the pitch angle, all resulting in an uneven chain exit velocity. You can think of the sprocket as a polygon in which the exit velocity of the chain depends upon whether the exit is from a corner, or from a flat of the polygon. Of course, the same effect occurs when the chain first enters into engagement with the sprocket.

The chain velocity  $V$  is defined as the number of feet coming off the sprocket per unit time. Thus the chain velocity in feet per minute is

$$V = \frac{Npn}{12} \quad (17-30)$$

where  $N$  = number of sprocket teeth

$p$  = chain pitch, in

$n$  = sprocket speed, rev/min

The maximum exit velocity of the chain is

$$v_{\max} = \frac{\pi Dn}{12} = \frac{\pi np}{12 \sin(\gamma/2)} \quad (b)$$

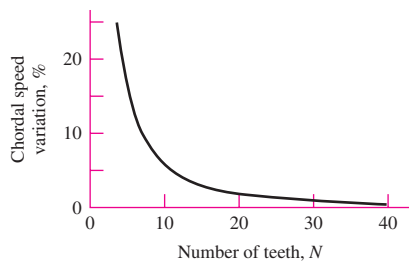
where Eq. (a) has been substituted for the pitch diameter  $D$ . The minimum exit velocity occurs at a diameter  $d$ , smaller than  $D$ . Using the geometry of Fig. 17-17, we find

$$d = D \cos \frac{\gamma}{2} \quad (c)$$

Thus the minimum exit velocity is

$$v_{\min} = \frac{\pi dn}{12} = \frac{\pi np}{12} \frac{\cos(\gamma/2)}{\sin(\gamma/2)} \quad (d)$$

| Figure 17-18



Now substituting  $\gamma/2 = 180^\circ/N$  and employing Eqs. (17-30), (b), and (d), we find the speed variation to be

$$\frac{\Delta V}{V} = \frac{v_{\max} - v_{\min}}{V} = \frac{\pi}{N} \left[ \frac{1}{\sin(180^\circ/N)} - \frac{1}{\tan(180^\circ/N)} \right] \quad (17-31)$$

This is called the *chordal speed variation* and is plotted in Fig. 17-18. When chain drives are used to synchronize precision components or processes, due consideration must be given to these variations. For example, if a chain drive synchronized the cutting of photographic film with the forward drive of the film, the lengths of the cut sheets of film might vary too much because of this chordal speed variation. Such variations can also cause vibrations within the system.

Although a large number of teeth is considered desirable for the driving sprocket, in the usual case it is advantageous to obtain as small a sprocket as possible, and this requires one with a small number of teeth. For smooth operation at moderate and high speeds it is considered good practice to use a driving sprocket with at least 17 teeth; 19 or 21 will, of course, give a better life expectancy with less chain noise. Where space limitations are severe or for very slow speeds, smaller tooth numbers may be used by sacrificing the life expectancy of the chain.

Driven sprockets are not made in standard sizes over 120 teeth, because the pitch elongation will eventually cause the chain to “ride” high long before the chain is worn out. The most successful drives have velocity ratios up to 6:1, but higher ratios may be used at the sacrifice of chain life.

Roller chains seldom fail because they lack tensile strength; they more often fail because they have been subjected to a great many hours of service. Actual failure may be due either to wear of the rollers on the pins or to fatigue of the surfaces of the rollers. Roller-chain manufacturers have compiled tables that give the horsepower capacity corresponding to a life expectancy of 15 kh for various sprocket speeds. These capacities are tabulated in Table 17-20 for 17-tooth sprockets. Table 17-21 displays available tooth counts on sprockets of one supplier. Table 17-22 lists the tooth correction factors for other than 17 teeth. Table 17-23 shows the multiple-strand factors  $K_2$ .

The capacities of chains are based on the following:

- 15 000 h at full load
- Single strand
- ANSI proportions
- Service factor of unity
- 100 pitches in length
- Recommended lubrication

- Elongation maximum of 3 percent
- Horizontal shafts
- Two 17-tooth sprockets

The fatigue strength of link plates governs capacity at lower speeds. The American Chain Association (ACA) publication *Chains for Power Transmission and Materials Handling* (1982) gives, for single-strand chain, the nominal power  $H_1$ , link-plate limited, as

$$H_1 = 0.004N_1^{1.08}n_1^{0.9}p^{(3-0.07p)} \quad \text{hp} \quad (17-32)$$

and the nominal power  $H_2$ , roller-limited, as

$$H_2 = \frac{1000K_r N_1^{1.5} p^{0.8}}{n_1^{1.5}} \quad \text{hp} \quad (17-33)$$

where  $N_1$  = number of teeth in the smaller sprocket

$n_1$  = sprocket speed, rev/min

$p$  = pitch of the chain, in

$K_r = 29$  for chain numbers 25, 35; 3.4 for chain 41; and 17 for chains 40–240

**Table 17-20**

Rated Horsepower Capacity of Single-Strand Single-Pitch Roller Chain for a 17-Tooth Sprocket

Source: Compiled from ANSI B29.1-1975 information only section, and from B29.9-1958.

Sprocket Speed, rev/min	ANSI Chain Number					
	25	35	40	41	50	60
50	0.05	0.16	0.37	0.20	0.72	1.24
100	0.09	0.29	0.69	0.38	1.34	2.31
150	0.13*	0.41*	0.99*	0.55*	1.92*	3.32
200	0.16*	0.54*	1.29	0.71	2.50	4.30
300	0.23	0.78	1.85	1.02	3.61	6.20
400	0.30*	1.01*	2.40	1.32	4.67	8.03
500	0.37	1.24	2.93	1.61	5.71	9.81
600	0.44*	1.46*	3.45*	1.90*	6.72*	11.6
700	0.50	1.68	3.97	2.18	7.73	13.3
800	0.56*	1.89*	4.48*	2.46*	8.71*	15.0
900	0.62	2.10	4.98	2.74	9.69	16.7
1000	0.68*	2.31*	5.48	3.01	10.7	18.3
1200	0.81	2.73	6.45	3.29	12.6	21.6
1400	0.93*	3.13*	7.41	2.61	14.4	18.1
1600	1.05*	3.53*	8.36	2.14	12.8	14.8
1800	1.16	3.93	8.96	1.79	10.7	12.4
2000	1.27*	4.32*	7.72*	1.52*	9.23*	10.6
2500	1.56	5.28	5.51*	1.10*	6.58*	7.57
3000	1.84	5.64	4.17	0.83	4.98	5.76
	Type A	Type B	Type C			

\*Estimated from ANSI tables by linear interpolation.

Note: Type A—manual or drip lubrication; type B—bath or disk lubrication; type C—oil-stream lubrication.

(Continued)

**Table 17-20**

Rated Horsepower Capacity of Single- Strand Single-Pitch Roller Chain for a 17-Tooth Sprocket (Continued)	Sprocket Speed, rev/min	ANSI Chain Number							
		80	100	120	140	160	180	200	240
50	Type A	2.88	5.52	9.33	14.4	20.9	28.9	38.4	61.8
100		5.38	10.3	17.4	26.9	39.1	54.0	71.6	115
150		7.75	14.8	25.1	38.8	56.3	77.7	103	166
200		10.0	19.2	32.5	50.3	72.9	101	134	215
300		14.5	27.7	46.8	72.4	105	145	193	310
400		18.7	35.9	60.6	93.8	136	188	249	359
500	Type B	22.9	43.9	74.1	115	166	204	222	0
600		27.0	51.7	87.3	127	141	155	169	
700		31.0	59.4	89.0	101	112	123	0	
800		35.0	63.0	72.8	82.4	91.7	101		
900		39.9	52.8	61.0	69.1	76.8	84.4		
1000		37.7	45.0	52.1	59.0	65.6	72.1		
1200		28.7	34.3	39.6	44.9	49.9	0		
1400		22.7	27.2	31.5	35.6	0			
1600		18.6	22.3	25.8	0				
1800		15.6	18.7	21.6					
2000		13.3	15.9	0					
2500		9.56	0.40						
3000			7.25	0					

**Type C****Type C'**

Note: Type A—manual or drip lubrication; type B—bath or disk lubrication; type C—oil-stream lubrication; type C'—type C, but this is a galling region; submit design to manufacturer for evaluation.

**Table 17-21**

Single-Strand Sprocket Tooth Counts Available from One Supplier\*

No.	Available Sprocket Tooth Counts
25	8-30, 32, 34, 35, 36, 40, 42, 45, 48, 54, 60, 64, 65, 70, 72, 76, 80, 84, 90, 95, 96, 102, 112, 120
35	4-45, 48, 52, 54, 60, 64, 65, 68, 70, 72, 76, 80, 84, 90, 95, 96, 102, 112, 120
41	6-60, 64, 65, 68, 70, 72, 76, 80, 84, 90, 95, 96, 102, 112, 120
40	8-60, 64, 65, 68, 70, 72, 76, 80, 84, 90, 95, 96, 102, 112, 120
50	8-60, 64, 65, 68, 70, 72, 76, 80, 84, 90, 95, 96, 102, 112, 120
60	8-60, 62, 63, 64, 65, 66, 67, 68, 70, 72, 76, 80, 84, 90, 95, 96, 102, 112, 120
80	8-60, 64, 65, 68, 70, 72, 76, 78, 80, 84, 90, 95, 96, 102, 112, 120
100	8-60, 64, 65, 67, 68, 70, 72, 74, 76, 80, 84, 90, 95, 96, 102, 112, 120
120	9-45, 46, 48, 50, 52, 54, 55, 57, 60, 64, 65, 67, 68, 70, 72, 76, 80, 84, 90, 95, 96, 102, 112, 120
140	9-28, 30, 31, 32, 33, 34, 35, 36, 37, 39, 40, 42, 43, 45, 48, 54, 60, 64, 65, 68, 70, 72, 76, 80, 84, 96
160	8-30, 32-36, 38, 40, 45, 46, 50, 52, 53, 54, 56, 57, 60, 62, 63, 64, 65, 66, 68, 70, 72, 73, 80, 84, 96
180	13-25, 28, 35, 39, 40, 45, 54, 60
200	9-30, 32, 33, 35, 36, 39, 40, 42, 44, 45, 48, 50, 51, 54, 56, 58, 59, 60, 63, 64, 65, 68, 70, 72
240	9-30, 32, 35, 36, 40, 44, 45, 48, 52, 54, 60

\*Morse Chain Company, Ithaca, NY, Type B hub sprockets.

**Table 17-22**

Tooth Correction Factors,  $K_1$

Number of Teeth on Driving Sprocket	$K_1$ Pre-extreme Horsepower	$K_1$ Post-extreme Horsepower
11	0.62	0.52
12	0.69	0.59
13	0.75	0.67
14	0.81	0.75
15	0.87	0.83
16	0.94	0.91
17	1.00	1.00
18	1.06	1.09
19	1.13	1.18
20	1.19	1.28
$N$	$(N_1/17)^{1.08}$	$(N_1/17)^{1.5}$

**Table 17-23**

Multiple-Strand Factors,  $K_2$

Number of Strands	$K_2$
1	1.0
2	1.7
3	2.5
4	3.3
5	3.9
6	4.6
8	6.0

The constant 0.004 becomes 0.0022 for no. 41 lightweight chain. The nominal horsepower in Table 17-20 is  $H_{\text{nom}} = \min(H_1, H_2)$ . For example, for  $N_1 = 17$ ,  $n_1 = 1000$  rev/min, no. 40 chain with  $p = 0.5$  in, from Eq. (17-32),

$$H_1 = 0.004(17)^{1.08} 1000^{0.9} 0.5^{[3-0.07(0.5)]} = 5.48 \text{ hp}$$

From Eq. (17-33),

$$H_2 = \frac{1000(17)17^{1.5}(0.5^{0.8})}{1000^{1.5}} = 21.64 \text{ hp}$$

The tabulated value in Table 17-20 is  $H_{\text{tab}} = \min(5.48, 21.64) = 5.48$  hp.

It is preferable to have an odd number of teeth on the driving sprocket (17, 19, . . .) and an even number of pitches in the chain to avoid a special link. The approximate length of the chain  $L$  in pitches is

$$\frac{L}{p} \doteq \frac{2C}{p} + \frac{N_1 + N_2}{2} + \frac{(N_2 - N_1)^2}{4\pi^2 C/p} \quad (17-34)$$

The center-to-center distance  $C$  is given by

$$C = \frac{p}{4} \left[ -A + \sqrt{A^2 - 8 \left( \frac{N_2 - N_1}{2\pi} \right)^2} \right] \quad (17-35)$$

where

$$A = \frac{N_1 + N_2}{2} - \frac{L}{p} \quad (17-36)$$

The allowable power  $H_a$  is given by

$$H_a = K_1 K_2 H_{\text{tab}} \quad (17-37)$$

where  $K_1$  = correction factor for tooth number other than 17 (Table 17-22)

$K_2$  = strand correction (Table 17-23)

The horsepower that must be transmitted  $H_d$  is given by

$$H_d = H_{\text{nom}} K_s n_d \quad (17-38)$$

Equation (17-32) is the basis of the pre-extreme power entries (vertical entries) of Table 17-20, and the chain power is limited by link-plate fatigue. Equation (17-33) is the basis for the post-extreme power entries of these tables, and the chain power performance is limited by impact fatigue. The entries are for chains of 100 pitch length and 17-tooth sprocket. For a deviation from this

$$H_2 = 1000 \left[ K_r \left( \frac{N_1}{n_1} \right)^{1.5} p^{0.8} \left( \frac{L_p}{100} \right)^{0.4} \left( \frac{15000}{h} \right)^{0.4} \right] \quad (17-39)$$

where  $L_p$  is the chain length in pitches and  $h$  is the chain life in hours. Viewed from a deviation viewpoint, Eq. (17-39) can be written as a trade-off equation in the following form:

$$\frac{H_2^{2.5} h}{N_1^{3.75} L_p} = \text{constant} \quad (17-40)$$

If tooth-correction factor  $K_1$  is used, then omit the term  $N_1^{3.75}$ . Note that  $(N_1^{1.5})^{2.5} = N_1^{3.75}$ .

In Eq. (17-40) one would expect the  $h/L_p$  term because doubling the hours can require doubling the chain length, other conditions constant, for the same number of cycles. Our experience with contact stresses leads us to expect a load (tension) life relation of the form  $F^a L = \text{constant}$ . In the more complex circumstance of roller-bushing impact, the Diamond Chain Company has identified  $a = 2.5$ .

The maximum speed (rev/min) for a chain drive is limited by galling between the pin and the bushing. Tests suggest

$$n_1 \leq 1000 \left[ \frac{82.5}{7.95^p (1.0278)^{N_1} (1.323)^{F/1000}} \right]^{1/(1.59 \log p + 1.873)} \text{ rev/min}$$

where  $F$  is the chain tension in pounds.

### EXAMPLE 17-5

Select drive components for a 2:1 reduction, 90-hp input at 300 rev/min, moderate shock, an abnormally long 18-hour day, poor lubrication, cold temperatures, dirty surroundings, short drive  $C/p = 25$ .

**Solution**

Function:  $H_{\text{nom}} = 90 \text{ hp}$ ,  $n_1 = 300 \text{ rev/min}$ ,  $C/p = 25$ ,  $K_s = 1.3$

Design factor:  $n_d = 1.5$

Sprocket teeth:  $N_1 = 17$  teeth,  $N_2 = 34$  teeth,  $K_1 = 1$ ,  $K_2 = 1, 1.7, 2.5, 3.3$

Chain number of strands:

$$H_{\text{tab}} = \frac{n_d K_s H_{\text{nom}}}{K_1 K_2} = \frac{1.5(1.3)90}{(1)K_2} = \frac{176}{K_2}$$

Form a table:

Number of Strands	176/K2 (Table 17-23)	Chain Number (Table 17-19)	Lubrication Type
1	$176/1 = 176$	200	C'
2	$176/1.7 = 104$	160	C
3	$176/2.5 = 70.4$	140	B
4	$176/3.3 = 53.3$	140	B

### Decision

3 strands of number 140 chain ( $H_{\text{tab}}$  is 72.4 hp).

Number of pitches in the chain:

$$\begin{aligned} \frac{L}{p} &= \frac{2C}{p} + \frac{N_1 + N_2}{2} + \frac{(N_2 - N_1)^2}{4\pi^2 C/p} \\ &= 2(25) + \frac{17 + 34}{2} + \frac{(34 - 17)^2}{4\pi^2(25)} = 75.79 \text{ pitches} \end{aligned}$$

### Decision

Use 76 pitches. Then  $L/p = 76$ .

Identify the center-to-center distance: From Eqs. (17-35) and (17-36),

$$\begin{aligned} A &= \frac{N_1 + N_2}{2} - \frac{L}{p} = \frac{17 + 34}{2} - 76 = -50.5 \\ C &= \frac{p}{4} \left[ -A + \sqrt{A^2 - 8 \left( \frac{N_2 - N_1}{2\pi} \right)^2} \right] \\ &= \frac{p}{4} \left[ 50.5 + \sqrt{50.5^2 - 8 \left( \frac{34 - 17}{2\pi} \right)^2} \right] = 25.104p \end{aligned}$$

For a 140 chain,  $p = 1.75$  in. Thus,

$$C = 25.104p = 25.104(1.75) = 43.93 \text{ in}$$

Lubrication: Type B

Comment: This is operating on the pre-extreme portion of the power, so durability estimates other than 15 000 h are not available. Given the poor operating conditions, life will be much shorter.

Lubrication of roller chains is essential in order to obtain a long and trouble-free life. Either a drip feed or a shallow bath in the lubricant is satisfactory. A medium or light mineral oil, without additives, should be used. Except for unusual conditions, heavy oils and greases are not recommended, because they are too viscous to enter the small clearances in the chain parts.

## 17-6 Wire Rope

Wire rope is made with two types of winding, as shown in Fig. 17-19. The *regular lay*, which is the accepted standard, has the wire twisted in one direction to form the strands, and the strands twisted in the opposite direction to form the rope. In the completed rope the visible wires are approximately parallel to the axis of the rope. Regular-lay ropes do not kink or untwist and are easy to handle.

*Lang-lay* ropes have the wires in the strand and the strands in the rope twisted in the same direction, and hence the outer wires run diagonally across the axis of the rope. Lang-lay ropes are more resistant to abrasive wear and failure due to fatigue than are regular-lay ropes, but they are more likely to kink and untwist.

Standard ropes are made with a hemp core, which supports and lubricates the strands. When the rope is subjected to heat, either a steel center or a wire-strand center must be used.

Wire rope is designated as, for example, a  $1\frac{1}{8}$ -in  $6 \times 7$  haulage rope. The first figure is the diameter of the rope (Fig. 17-19c). The second and third figures are the number of strands and the number of wires in each strand, respectively. Table 17-24 lists some of the various ropes that are available, together with their characteristics and properties. The area of the metal in standard hoisting and haulage rope is  $A_m = 0.38d^2$ .

When a wire rope passes around a sheave, there is a certain amount of readjustment of the elements. Each of the wires and strands must slide on several others, and presumably some individual bending takes place. It is probable that in this complex action there exists some stress concentration. The stress in one of the wires of a rope passing around a sheave may be calculated as follows. From solid mechanics, we have

$$M = \frac{EI}{\rho} \quad \text{and} \quad M = \frac{\sigma I}{c} \quad (a)$$

where the quantities have their usual meaning. Eliminating  $M$  and solving for the stress gives

$$\sigma = \frac{Ec}{\rho} \quad (b)$$

For the radius of curvature  $\rho$ , we can substitute the sheave radius  $D/2$ . Also,  $c = d_w/2$ , where  $d_w$  is the wire diameter. These substitutions give

$$\sigma = E_r \frac{d_w}{D} \quad (c)$$

where  $E_r$  is the *modulus of elasticity of the rope*, not the wire. To understand this equation, observe that the individual wire makes a corkscrew figure in space and if you pull on it to determine  $E$  it will stretch or give more than its native  $E$  would suggest. Therefore

**Figure 17-19**

Types of wire rope; both lays are available in either right or left hand.

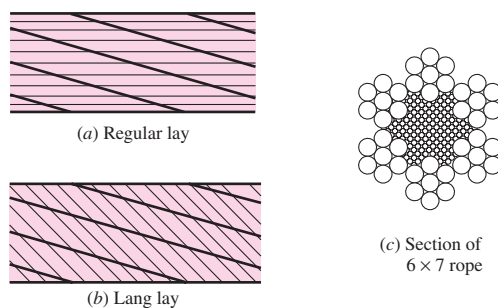


**Table 17-24**Wire-Rope Data *Source:* Compiled from American Steel and Wire Company Handbook.

Rope	Weight per Foot, lbf	Minimum Sheave Diameter, in	Standard Sizes $d$ , in	Material	Size of Outer Wires	Modulus of Elasticity,* Mpsi	Strength, <sup>†</sup> kpsi
6 × 7 haulage	1.50d <sup>2</sup>	42d	$\frac{1}{4}$ – $1\frac{1}{2}$	Monitor steel	$d/9$	14	100
				Plow steel	$d/9$	14	88
				Mild plow steel	$d/9$	14	76
6 × 19 standard hoisting	1.60d <sup>2</sup>	26d–34d	$\frac{1}{4}$ – $2\frac{3}{4}$	Monitor steel	$d/13$ – $d/16$	12	106
				Plow steel	$d/13$ – $d/16$	12	93
				Mild plow steel	$d/13$ – $d/16$	12	80
6 × 37 special flexible	1.55d <sup>2</sup>	18d	$\frac{1}{4}$ – $3\frac{1}{2}$	Monitor steel	$d/22$	11	100
				Plow steel	$d/22$	11	88
8 × 19 extra flexible	1.45d <sup>2</sup>	21d–26d	$\frac{1}{4}$ – $1\frac{1}{2}$	Monitor steel	$d/15$ – $d/19$	10	92
				Plow steel	$d/15$ – $d/19$	10	80
7 × 7 aircraft	1.70d <sup>2</sup>	—	$\frac{1}{16}$ – $1\frac{3}{8}$	Corrosion-resistant steel	—	—	124
				Carbon steel	—	—	124
				Corrosion-resistant steel	—	—	135
7 × 9 aircraft	1.75d <sup>2</sup>	—	$\frac{1}{8}$ – $1\frac{3}{8}$	Carbon steel	—	—	143
				Corrosion-resistant steel	—	—	165
				Carbon steel	—	—	165

\*The modulus of elasticity is only approximate; it is affected by the loads on the rope and, in general, increases with the life of the rope.

<sup>†</sup>The strength is based on the nominal area of the rope. The figures given are only approximate and are based on 1-in rope sizes and  $\frac{1}{4}$ -in aircraft-cable sizes.

$E$  is still the modulus of elasticity of the wire, but in its peculiar configuration as part of the rope, its modulus is smaller. For this reason we say that  $E_r$  in Eq. (c) is the modulus of elasticity of the rope, not the wire, recognizing that one can quibble over the name used.

Equation (c) gives the tensile stress  $\sigma$  in the outer wires. The sheave diameter is represented by  $D$ . This equation reveals the importance of using a large-diameter sheave. The suggested minimum sheave diameters in Table 17-24 are based on a  $D/d_w$  ratio of 400. If possible, the sheaves should be designed for a larger ratio. For elevators and mine hoists,  $D/d_w$  is usually taken from 800 to 1000. If the ratio is less than 200, heavy loads will often cause a permanent set in the rope.

A wire rope tension giving the same tensile stress as the sheave bending is called the *equivalent bending load*  $F_b$ , given by

$$F_b = \sigma A_m = \frac{E_r d_w A_m}{D} \quad (17-41)$$

A wire rope may fail because the static load exceeds the ultimate strength of the rope. Failure of this nature is generally not the fault of the designer, but rather that of the operator in permitting the rope to be subjected to loads for which it was not designed.

The first consideration in selecting a wire rope is to determine the static load. This load is composed of the following items:

- The known or dead weight
- Additional loads caused by sudden stops or starts
- Shock loads
- Sheave-bearing friction

When these loads are summed, the total can be compared with the ultimate strength of the rope to find a factor of safety. However, the ultimate strength used in this determination must be reduced by the strength loss that occurs when the rope passes over a curved surface such as a stationary sheave or a pin; see Fig. 17–20.

For an average operation, use a factor of safety of 5. Factors of safety up to 8 or 9 are used if there is danger to human life and for very critical situations. Table 17–25

**Figure 17–20**

Percent strength loss due to different  $D/d$  ratios; derived from standard test data for  $6 \times 19$  and  $6 \times 17$  class ropes. (Materials provided by the Wire Rope Technical Board (WRTB), Wire Rope Users Manual Third Edition, Second printing. Reprinted by permission.)

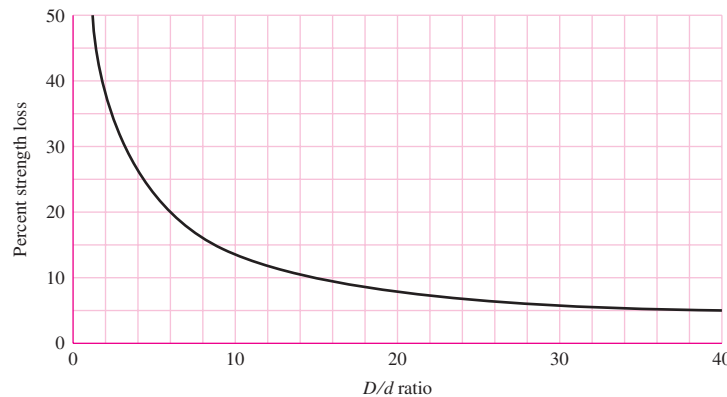


**Table 17–25**

**Minimum Factors of Safety for Wire Rope\***

*Source:* Compiled from a variety of sources, including ANSI A17.1-1978.

Track cables	3.2	Passenger elevators, ft/min:	
Guys	3.5	50	7.60
Mine shafts, ft:		300	9.20
Up to 500	8.0	800	11.25
1000–2000	7.0	1200	11.80
2000–3000	6.0	1500	11.90
Over 3000	5.0	Freight elevators, ft/min:	
Hoisting	5.0	50	6.65
Haulage	6.0	300	8.20
Cranes and derricks	6.0	800	10.00
Electric hoists	7.0	1200	10.50
Hand elevators	5.0	1500	10.55
Powered dumbwaiters, ft/min:			
Hand elevators	5.0	50	4.8
Private elevators	7.5	300	6.6
Hand dumbwaiter	4.5	500	8.0
Grain elevators	7.5		

\*Use of these factors does not preclude a fatigue failure.

lists minimum factors of safety for a variety of design situations. Here, the factor of safety is defined as

$$n = \frac{F_u}{F_t}$$

where  $F_u$  is the ultimate wire load and  $F_t$  is the largest working tension.

Once you have made a tentative selection of a rope based upon static strength, the next consideration is to ensure that the wear life of the rope and the sheave or sheaves meets certain requirements. When a loaded rope is bent over a sheave, the rope stretches like a spring, rubs against the sheave, and causes wear of both the rope and the sheave. The amount of wear that occurs depends upon the pressure of the rope in the sheave groove. This pressure is called the *bearing pressure*; a good estimate of its magnitude is given by

$$p = \frac{2F}{dD} \quad (17-42)$$

where  $F$  = tensile force on rope

$d$  = rope diameter

$D$  = sheave diameter

The allowable pressures given in Table 17–26 are to be used only as a rough guide; they may not prevent a fatigue failure or severe wear. They are presented here because they represent past practice and furnish a starting point in design.

A fatigue diagram not unlike an *S-N* diagram can be obtained for wire rope. Such a diagram is shown in Fig. 17–21. Here the ordinate is the pressure-strength ratio  $p/S_u$ , and  $S_u$  is the ultimate tensile strength of the *wire*. The abscissa is the number of bends that occur in the total life of the rope. The curve implies that a wire rope has a fatigue limit; but this is not true at all. A wire rope that is used over sheaves will eventually fail

**Table 17-26**

Maximum Allowable Bearing Pressures of Ropes on Sheaves (in psi)

Source: Wire Rope Users Manual, AISI, 1979.

<b>Rope</b>	<b>Sheave Material</b>				
	<b>Wood<sup>a</sup></b>	<b>Cast Iron<sup>b</sup></b>	<b>Cast Steel<sup>c</sup></b>	<b>Chilled Cast Irons<sup>d</sup></b>	<b>Manganese Steel<sup>e</sup></b>
Regular lay:					
6 × 7	150	300	550	650	1470
6 × 19	250	480	900	1100	2400
6 × 37	300	585	1075	1325	3000
8 × 19	350	680	1260	1550	3500
Lang lay:					
6 × 7	165	350	600	715	1650
6 × 19	275	550	1000	1210	2750
6 × 37	330	660	1180	1450	3300

<sup>a</sup>On end grain of beech, hickory, or gum.

<sup>b</sup>For  $H_B$  (min.) = 125.

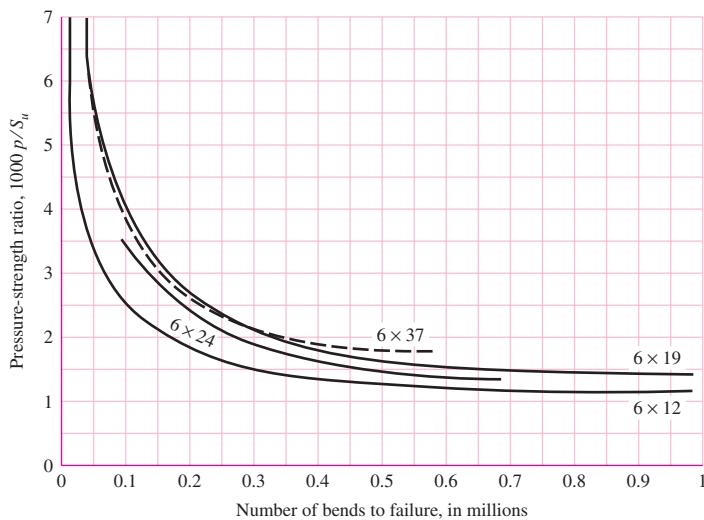
<sup>c</sup>30–40 carbon;  $H_B$  (min.) = 160.

<sup>d</sup>Use only with uniform surface hardness.

<sup>e</sup>For high speeds with balanced sheaves having ground surfaces.

**Figure 17-21**

Experimentally determined relation between the fatigue life of wire rope and the sheave pressure.



in fatigue or in wear. However, the graph does show that the rope will have a long life if the ratio  $p/S_u$  is less than 0.001. Substitution of this ratio in Eq. (17-42) gives

$$S_u = \frac{2000F}{dD} \quad (17-43)$$

where  $S_u$  is the ultimate strength of the wire, not the rope, and the units of  $S_u$  are related to the units of  $F$ . This interesting equation contains the wire strength, the load, the rope diameter, and the sheave diameter—all four variables in a single equation! Dividing both sides of Eq. (17-42) by the ultimate strength of the wires  $S_u$  and solving for  $F$  gives

$$F_f = \frac{(p/S_u)S_u d D}{2} \quad (17-44)$$

where  $F_f$  is interpreted as the allowable fatigue tension as the wire is flexed a number of times corresponding to  $p/S_u$  selected from Fig. 17-21 for a particular rope and life expectancy. The factor of safety can be defined in fatigue as

$$n_f = \frac{F_f - F_b}{F_t} \quad (17-45)$$

where  $F_f$  is the rope tension strength under flexing and  $F_t$  is the tension at the place where the rope is flexing. Unfortunately, the designer often has vendor information that tabulates ultimate rope tension and gives no ultimate-strength  $S_u$  information concerning the wires from which the rope is made. Some guidance in strength of individual wires is

Improved plow steel (monitor)	$240 < S_u < 280$ kpsi
Plow steel	$210 < S_u < 240$ kpsi
Mild plow steel	$180 < S_u < 210$ kpsi

In wire-rope usage, the factor of safety has been defined in static loading as  $n = F_u/F_t$  or  $n = (F_u - F_b)/F_t$ , where  $F_b$  is the rope tension that would induce the same outer-wire stress as that given by Eq. (c). The factor of safety in fatigue loading can be defined as in Eq. (17-45), or by using a static analysis and compensating with a large factor of safety applicable to static loading, as in Table 17-25. When using factors of safety expressed in codes, standards, corporate design manuals, or wire-rope manufacturers'

recommendations or from the literature, be sure to ascertain upon which basis the factor of safety is to be evaluated, and proceed accordingly.

If the rope is made of plow steel, the wires are probably hard-drawn AISI 1070 or 1080 carbon steel. Referring to Table 10–3, we see that this lies somewhere between hard-drawn spring wire and music wire. But the constants  $m$  and  $A$  needed to solve Eq. (10–14), p. 523, for  $S_u$  are lacking.

Practicing engineers who desire to solve Eq. (17–43) should determine the wire strength  $S_u$  for the rope under consideration by unraveling enough wire to test for the Brinell hardness. Then  $S_u$  can be found using Eq. (2–17), p. 40. Fatigue failure in wire rope is not sudden, as in solid bodies, but progressive, and shows as the breaking of an outside wire. This means that the beginning of fatigue can be detected by periodic routine inspection.

Figure 17–22 is another graph showing the gain in life to be obtained by using large  $D/d$  ratios. In view of the fact that the life of wire rope used over sheaves is only finite, it is extremely important that the designer specify and insist that periodic inspection, lubrication, and maintenance procedures be carried out during the life of the rope. Table 17–27 gives useful properties of some wire ropes.

For a mine-hoist problem we can develop working equations from the preceding presentation. The wire rope tension  $F_t$  due to load and acceleration/deceleration is

$$F_t = \left( \frac{W}{m} + wl \right) \left( 1 + \frac{a}{g} \right) \quad (17-46)$$

**Figure 17–22**

Service-life curve based on bending and tensile stresses only. This curve shows that the life corresponding to  $D/d = 48$  is twice that of  $D/d = 33$ . (Materials provided by the Wire Rope Technical Board (WRTB), Wire Rope Users Manual Third Edition, Second printing. Reprinted by permission.)

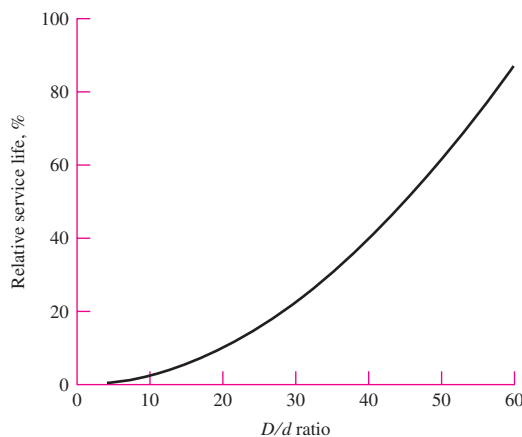


**Table 17–27**

Some Useful Properties of  $6 \times 7$ ,  $6 \times 19$ , and  $6 \times 37$  Wire Ropes

Wire Rope	Weight per Foot $w$ , lbf/ft	Weight per Foot Including Core $w$ , lbf/ft	Minimum Sheave Diameter $D$ , in	Better Sheave Diameter $D$ , in	Diameter of Wires $d_w$ , in	Area of Metal $A_m$ , in <sup>2</sup>	Rope Young's Modulus $E_r$ , psi
$6 \times 7$	$1.50d^2$		$42d$	$72d$	$0.111d$	$0.38d^2$	$13 \times 10^6$
$6 \times 19$	$1.60d^2$	$1.76d^2$	$30d$	$45d$	$0.067d$	$0.40d^2$	$12 \times 10^6$
$6 \times 37$	$1.55d^2$	$1.71d^2$	$18d$	$27d$	$0.048d$	$0.40d^2$	$12 \times 10^6$

- where  $W$  = weight at the end of the rope (cage and load), lbf  
 $m$  = number of wire ropes supporting the load  
 $w$  = weight/foot of the wire rope, lbf/ft  
 $l$  = suspended length of rope, ft  
 $a$  = maximum acceleration/deceleration experienced, ft/s<sup>2</sup>  
 $g$  = acceleration of gravity, ft/s<sup>2</sup>

The fatigue tensile strength in pounds for a specified life  $F_f$  is

$$F_f = \frac{(p/S_u)S_u D d}{2} \quad (17-47)$$

where  $(p/S_u)$  = specified life, from Fig. 17-21

- $S_u$  = ultimate tensile strength of the wires, psi  
 $D$  = sheave or winch drum diameter, in  
 $d$  = nominal wire rope size, in

The equivalent bending load  $F_b$  is

$$F_b = \frac{E_r d_w A_m}{D} \quad (17-48)$$

where  $E_r$  = Young's modulus for the wire rope, Table 17-24 or 17-27, psi

$d_w$  = diameter of the wires, in

$A_m$  = metal cross-sectional area, Table 17-24 or 17-28, in<sup>2</sup>

$D$  = sheave or winch drum diameter, in

The static factor of safety  $n_s$  is

$$n_s = \frac{F_u - F_b}{F_t} \quad (17-49)$$

Be careful when comparing recommended static factors of safety to Eq. (17-49), as  $n_s$  is sometimes defined as  $F_u/F_t$ . The fatigue factor of safety  $n_f$  is

$$n_f = \frac{F_f - F_b}{F_t} \quad (17-50)$$

### EXAMPLE 17-6

Given a 6 × 19 monitor steel ( $S_u = 240$  ksi) wire rope.

(a) Develop the expressions for rope tension  $F_t$ , fatigue tension  $F_f$ , equivalent bending tensions  $F_b$ , and fatigue factor of safety  $n_f$  for a 531.5-ft, 1-ton cage-and-load mine hoist with a starting acceleration of 2 ft/s<sup>2</sup> as depicted in Fig. 17-23. The sheave diameter is 72 in.

(b) Using the expressions developed in part (a), examine the variation in factor of safety  $n_f$  for various wire rope diameters  $d$  and number of supporting ropes  $m$ .

#### Solution

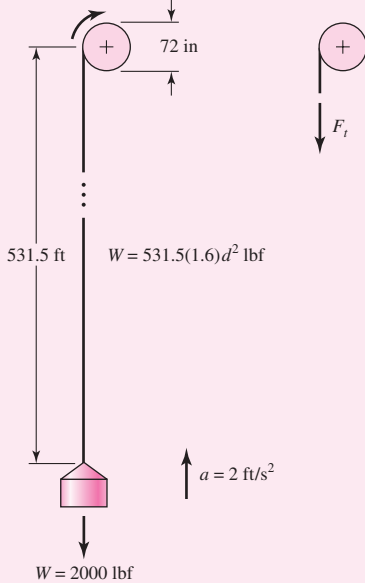
(a) Rope tension  $F_t$  from Eq. (17-46) is given by

**Answer**

$$\begin{aligned} F_t &= \left( \frac{W}{m} + wl \right) \left( 1 + \frac{a}{g} \right) = \left[ \frac{2000}{m} + 1.60d^2(531.5) \right] \left( 1 + \frac{2}{32.2} \right) \\ &= \frac{2124}{m} + 903d^2 \text{ lbf} \end{aligned}$$

**Figure 17-23**

Geometry of the mine hoist of Ex. 17-6.



From Fig. 17-21, use  $p/S_u = 0.0014$ . Fatigue tension  $F_f$  from Eq. (17-47) is given by

**Answer** 
$$F_f = \frac{(p/S_u)S_u D d}{2} = \frac{0.0014(240\,000)72d}{2} = 12\,096d \text{ lbf}$$

Equivalent bending tension  $F_b$  from Eq. (17-48) and Table 17-27 is given by

**Answer** 
$$F_b = \frac{E_r d_w A_m}{D} = \frac{12(10^6)0.067d(0.40d^2)}{72} = 4467d^3 \text{ lbf}$$

Factor of safety  $n_f$  in fatigue from Eq. (17-50) is given by

**Answer** 
$$n_f = \frac{F_f - F_b}{F_t} = \frac{12\,096d - 4467d^3}{2124/m + 903d^2}$$

(b) Form a table as follows:

<b>d</b>	<b><math>n_f</math></b>			
	<b><math>m = 1</math></b>	<b><math>m = 2</math></b>	<b><math>m = 3</math></b>	<b><math>m = 4</math></b>
0.25	1.355	2.641	3.865	5.029
0.375	1.910	3.617	5.150	6.536
0.500	2.336	4.263	5.879	7.254
0.625	2.612	4.573	6.099	7.331
0.750	2.731	4.578	5.911	6.918
0.875	2.696	4.330	5.425	6.210
1.000	2.520	3.882	4.736	5.320

Wire rope sizes are discrete, as is the number of supporting ropes. Note that for each  $m$  the factor of safety exhibits a maximum. Predictably the largest factor of safety increases with  $m$ . If the required factor of safety were to be 6, only three or four ropes could meet the requirement. The sizes are different:  $\frac{5}{8}$ -in ropes with three ropes or  $\frac{3}{8}$ -in ropes with four ropes. The costs include not only the wires, but the grooved winch drums.

## 17-7 Flexible Shafts

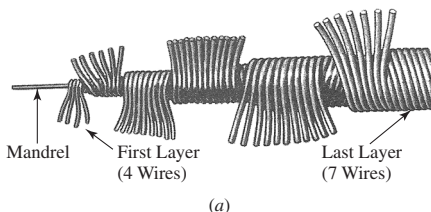
One of the greatest limitations of the solid shaft is that it cannot transmit motion or power around corners. It is therefore necessary to resort to belts, chains, or gears, together with bearings and the supporting framework associated with them. The flexible shaft may often be an economical solution to the problem of transmitting motion around corners. In addition to the elimination of costly parts, its use may reduce noise considerably.

There are two main types of flexible shafts: the power-drive shaft for the transmission of power in a single direction, and the remote-control or manual-control shaft for the transmission of motion in either direction.

The construction of a flexible shaft is shown in Fig. 17-24. The cable is made by winding several layers of wire around a central core. For the power-drive shaft, rotation should be in a direction such that the outer layer is wound up. Remote-control cables

**Figure 17-24**

Flexible shaft: (a) construction details; (b) a variety of configurations. (Courtesy of S. S. White Technologies, Inc.)



have a different lay of the wires forming the cable, with more wires in each layer, so that the torsional deflection is approximately the same for either direction of rotation.

Flexible shafts are rated by specifying the torque corresponding to various radii of curvature of the casing. A 15-in radius of curvature, for example, will give from 2 to 5 times more torque capacity than a 7-in radius. When flexible shafts are used in a drive in which gears are also used, the gears should be placed so that the flexible shaft runs at as high a speed as possible. This permits the transmission of the maximum amount of horsepower.

## PROBLEMS

- 17-1** A 6-in-wide polyamide F-1 flat belt is used to connect a 2-in-diameter pulley to drive a larger pulley with an angular velocity ratio of 0.5. The center-to-center distance is 9 ft. The angular speed of the small pulley is 1750 rev/min as it delivers 2 hp. The service is such that a service factor  $K_s$  of 1.25 is appropriate.  
 (a) Find  $F_c$ ,  $F_i$ ,  $F_{1a}$ , and  $F_2$ .  
 (b) Find  $H_a$ ,  $n_{fs}$ , and belt length.  
 (c) Find the dip.

- 17-2** Perspective and insight can be gained by doubling all geometric dimensions and observing the effect on problem parameters. Take the drive of Prob. 17-1, double the dimensions, and compare.

- 17-3** A flat-belt drive is to consist of two 4-ft-diameter cast-iron pulleys spaced 16 ft apart. Select a belt type to transmit 60 hp at a pulley speed of 380 rev/min. Use a service factor of 1.1 and a design factor of 1.0.

- 17-4** In solving problems and examining examples, you probably have noticed some recurring forms:

$$w = 12\gamma bt = (12\gamma t)b = a_1 b,$$

$$(F_1)_a = F_a b C_p C_v = (F_a C_p C_v)b = a_0 b$$

$$F_c = \frac{wV^2}{g} = \frac{a_1 b}{32.174} \left( \frac{V}{60} \right)^2 = a_2 b$$

$$(F_1)_a - F_2 = 2T/d = 33\,000H_d/V = 33\,000H_{\text{nom}}K_s n_d/V$$

$$F_2 = (F_1)_a - [(F_1)_a - F_2] = a_0 b - 2T/d$$

$$f\phi = \ln \frac{(F_1)_a - F_c}{F_2 - F_c} = \ln \frac{(a_0 - a_2)b}{(a_0 - a_2)b - 2T/d}$$

Show that

$$b = \frac{1}{a_0 - a_2} \frac{33\,000H_d}{V} \frac{\exp(f\phi)}{\exp(f\phi) - 1}$$

- 17-5** Return to Ex. 17-1 and complete the following.  
 (a) Find the torque capacity that would put the drive as built at the point of slip, as well as the initial tension  $F_i$ .  
 (b) Find the belt width  $b$  that exhibits  $n_{fs} = n_d = 1.1$ .  
 (c) For part b find the corresponding  $F_{1a}$ ,  $F_c$ ,  $F_i$ ,  $F_2$ , power, and  $n_{fs}$ .  
 (d) What have you learned?

- 17-6** Take the drive of Prob. 17-5 and double the belt width. Compare  $F_c$ ,  $F_i$ ,  $F_{1a}$ ,  $F_2$ ,  $H_a$ ,  $n_{fs}$ , and dip.

**17-7** Belted pulleys place loads on shafts, inducing bending and loading bearings. Examine Fig. 17-7 and develop an expression for the load the belt places on the pulley, and then apply it to Ex. 17-2.

**17-8** Example 17-2 resulted in selection of a 10-in-wide A-3 polyamide flat belt. Show that the value of  $F_1$  restoring  $f$  to 0.80 is

$$F_1 = \frac{(\Delta F + F_c) \exp f\phi - F_c}{\exp f\phi - 1}$$

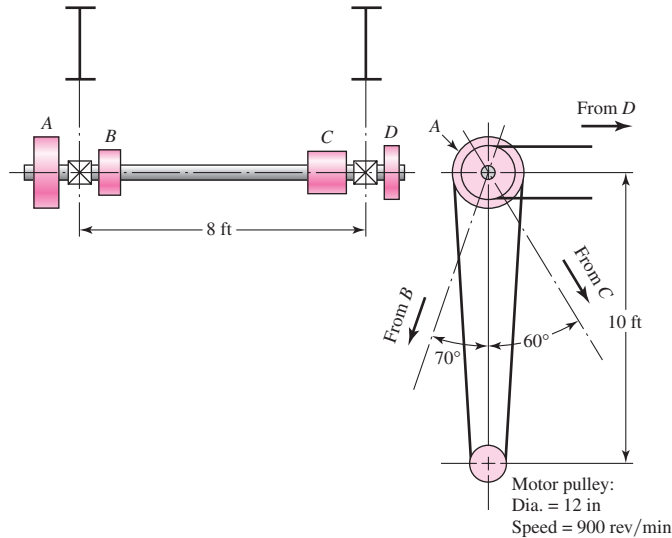
and compare the initial tensions.

**17-9** The line shaft illustrated in the figure is used to transmit power from an electric motor by means of flat-belt drives to various machines. Pulley A is driven by a vertical belt from the motor pulley. A belt from pulley B drives a machine tool at an angle of  $70^\circ$  from the vertical and at a center-to-center distance of 9 ft. Another belt from pulley C drives a grinder at a center-to-center distance of 11 ft. Pulley C has a double width to permit belt shifting as shown in Fig. 17-4. The belt from pulley D drives a dust-extractor fan whose axis is located horizontally 8 ft from the axis of the lineshaft. Additional data are

Machine	Speed, rev/min	Power, hp	Lineshaft Pulley	Diameter, in
Machine tool	400	12.5	B	16
Grinder	300	4.5	C	14
Dust extractor	500	8.0	D	18

Problem 17-9

(Courtesy of Dr. Ahmed F. Abdel Azim, Zagazig University, Cairo.)



The power requirements, listed above, account for the overall efficiencies of the equipment. The two line-shaft bearings are mounted on hangers suspended from two overhead wide-flange beams. Select the belt types and sizes for each of the four drives. Make provision for replacing belts from time to time because of wear or permanent stretch.

**17-10** Two shafts 20 ft apart, with axes in the same horizontal plane, are to be connected with a flat belt in which the driving pulley, powered by a six-pole squirrel-cage induction motor with a 100 brake hp rating at 1140 rev/min, drives the second shaft at half its angular speed. The driven shaft drives light-shock machinery loads. Select a flat belt.

**17-11** The mechanical efficiency of a flat-belt drive is approximately 98 percent. Because of its high value, the efficiency is often neglected. If a designer should choose to include it, where would he or she insert it in the flat-belt protocol?

**17-12** In metal belts, the centrifugal tension  $F_c$  is ignored as negligible. Convince yourself that this is a reasonable problem simplification.

**17-13** A designer has to select a metal-belt drive to transmit a power of  $H_{\text{nom}}$  under circumstances where a service factor of  $K_s$  and a design factor of  $n_d$  are appropriate. The design goal becomes  $H_d = H_{\text{nom}} K_s n_d$ . Use Eq. (17-8) to show that the minimum belt width is given by

$$b_{\min} = \frac{1}{a} \left( \frac{33\,000 H_d}{V} \right) \frac{\exp f\theta}{\exp f\theta - 1}$$

where  $a$  is the constant from  $F_{1a} = ab$ .

**17-14** Design a friction metal flat-belt drive to connect a 1-hp, four-pole squirrel-cage motor turning at 1750 rev/min to a shaft 15 in away, running at half speed. The circumstances are such that a service factor of 1.2 and a design factor of 1.05 are appropriate. The life goal is  $10^6$  belt passes,  $f = 0.35$ , and the environmental considerations require a stainless steel belt.

**17-15** A beryllium-copper metal flat belt with  $S_f = 56.67$  kpsi is to transmit 5 hp at 1125 rev/min with a life goal of  $10^6$  belt passes between two shafts 20 in apart whose centerlines are in a horizontal plane. The coefficient of friction between belt and pulley is 0.32. The conditions are such that a service factor of 1.25 and a design factor of 1.1 are appropriate. The driven shaft rotates at one-third the motor-pulley speed. Specify your belt, pulley sizes, and initial tension at installation.

**17-16** For the conditions of Prob. 17-15 use a 1095 plain carbon-steel heat-treated belt. Conditions at the driving pulley hub require a pulley outside diameter of 3 in or more. Specify your belt, pulley sizes, and initial tension at installation.

**17-17** A single V belt is to be selected to deliver engine power to the wheel-drive transmission of a riding tractor. A 5-hp single-cylinder engine is used. At most, 60 percent of this power is transmitted to the belt. The driving sheave has a diameter of 6.2 in, the driven, 12.0 in. The belt selected should be as close to a 92-in pitch length as possible. The engine speed is governor-controlled to a maximum of 3100 rev/min. Select a satisfactory belt and assess the factor of safety and the belt life in passes.

**17-18** Two B85 V belts are used in a drive composed of a 5.4-in driving sheave, rotating at 1200 rev/min, and a 16-in driven sheave. Find the power capacity of the drive based on a service factor of 1.25, and find the center-to-center distance.

**17-19** A 60-hp four-cylinder internal combustion engine is used to drive a brick-making machine under a schedule of two shifts per day. The drive consists of two 26-in sheaves spaced about 12 ft apart, with a sheave speed of 400 rev/min. Select a V-belt arrangement. Find the factor of safety, and estimate the life in passes and hours.

**17-20** A reciprocating air compressor has a 5-ft-diameter flywheel 14 in wide, and it operates at 170 rev/min. An eight-pole squirrel-cage induction motor has nameplate data 50 bhp at 875 rev/min.

(a) Design a V-belt drive.

(b) Can cutting the V-belt grooves in the flywheel be avoided by using a V-flat drive?

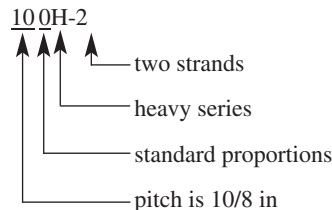
**17-21** The geometric implications of a V-flat drive are interesting.

(a) If the earth's equator was an inextensible string, snug to the spherical earth, and you spliced 6 ft of string into the equatorial cord and arranged it to be concentric to the equator, how far off the ground is the string?

- (b) Using the solution to part *a*, formulate the modifications to the expressions for  $m_G$ ,  $\theta_d$  and  $\theta_D$ ,  $L_p$ , and  $C$ .
- (c) As a result of this exercise, how would you revise your solution to part *b* of Prob. 17–20?

**17–22** A 2-hp electric motor running at 1720 rev/min is to drive a blower at a speed of 240 rev/min. Select a V-belt drive for this application and specify standard V belts, sheave sizes, and the resulting center-to-center distance. The motor size limits the center distance to at least 22 in.

**17–23** The standard roller-chain number indicates the chain pitch in inches, construction proportions, series, and number of strands as follows:



This convention makes the pitch directly readable from the chain number. In Ex. 17–5 ascertain the pitch from the selected chain number and confirm from Table 17–19.

**17–24** Equate Eqs. (17–32) and (17–33) to find the rotating speed  $n_1$  at which the power equates and marks the division between the premaximum and the postmaximum power domains.

(*a*) Show that

$$n_1 = \left[ \frac{0.25(10^6)K_r N_1^{0.42}}{p^{(2.2-0.07p)}} \right]^{1/2.4}$$

(*b*) Find the speed  $n_1$  for a no. 60 chain,  $p = 0.75$  in,  $N_1 = 17$ ,  $K_r = 17$ , and confirm from Table 17–20.

(*c*) At which speeds is Eq. (17–40) applicable?

**17–25** A double-strand no. 60 roller chain is used to transmit power between a 13-tooth driving sprocket rotating at 300 rev/min and a 52-tooth driven sprocket.

(*a*) What is the allowable horsepower of this drive?

(*b*) Estimate the center-to-center distance if the chain length is 82 pitches.

(*c*) Estimate the torque and bending force on the driving shaft by the chain if the actual horsepower transmitted is 30 percent less than the corrected (allowable) power.

**17–26** A four-strand no. 40 roller chain transmits power from a 21-tooth driving sprocket to an 84-tooth driven sprocket. The angular speed of the driving sprocket is 2000 rev/min.

(*a*) Estimate the chain length if the center-to-center distance has to be about 20 in.

(*b*) Estimate the tabulated horsepower entry  $H_{tab}^*$  for a 20 000-h life goal.

(*c*) Estimate the allowable horsepower for a 20 000-h life.

(*d*) Estimate the tension in the chain at the allowable power.

**17–27** A 700 rev/min 25-hp squirrel-cage induction motor is to drive a two-cylinder reciprocating pump, out-of-doors under a shed. A service factor  $K_s$  of 1.5 and a design factor of 1.1 are appropriate. The pump speed is 140 rev/min. Select a suitable chain and sprocket sizes.

**17–28** A centrifugal pump is driven by a 50-hp synchronous motor at a speed of 1800 rev/min. The pump is to operate at 900 rev/min. Despite the speed, the load is smooth ( $K_s = 1.2$ ). For a design factor of 1.1 specify a chain and sprockets that will realize a 50 000-h life goal. Let the sprockets be 19T and 38T.

**17-29**

A mine hoist uses a 2-in  $6 \times 19$  monitor-steel wire rope. The rope is used to haul loads of 4 tons from the shaft 480 ft deep. The drum has a diameter of 6 ft, the sheaves are of good-quality cast steel, and the smallest is 3 ft in diameter.

(a) Using a maximum hoisting speed of 1200 ft/min and a maximum acceleration of  $2 \text{ ft/s}^2$ , estimate the stresses in the rope.

(b) Estimate the various factors of safety.

**17-30**

A temporary construction elevator is to be designed to carry workers and materials to a height of 90 ft. The maximum estimated load to be hoisted is 5000 lbf at a velocity not to exceed 2 ft/s. For minimum sheave diameters and acceleration of  $4 \text{ ft/s}^2$ , specify the number of ropes required if the 1-in plow-steel  $6 \times 19$  hoisting strand is used.

**17-31**

A 2000-ft mine hoist operates with a 72-in drum using  $6 \times 19$  monitor-steel wire rope. The cage and load weigh 8000 lbf, and the cage is subjected to an acceleration of  $2 \text{ ft/s}^2$  when starting.

(a) For a single-strand hoist how does the factor of safety  $n = F_f/F_t$  vary with the choice of rope diameter?

(b) For four supporting strands of wire rope attached to the cage, how does the factor of safety vary with the choice of rope diameter?

**17-32**

Generalize the results of Prob. 17-31 by representing the factor of safety  $n$  as

$$n = \frac{ad}{(b/m) + cd^2}$$

where  $m$  is the number of ropes supporting the cage, and  $a$ ,  $b$ , and  $c$  are constants. Show that the optimal diameter is  $d^* = [b/(mc)]^{1/2}$  and the corresponding maximum attainable factor of safety is  $n^* = a[m/(bc)]^{1/2}/2$ .

**17-33**

From your results in Prob. 17-32, show that to meet a fatigue factor of safety  $n_1$  the optimal solution is

$$m = \frac{4bcn_1}{a^2} \text{ ropes}$$

having a diameter of

$$d = \frac{a}{2cn_1}$$

Solve Prob. 17-31 if a factor of safety of 2 is required. Show what to do in order to accommodate to the necessary discreteness in the rope diameter  $d$  and the number of ropes  $m$ .

**17-34**

For Prob. 17-29 estimate the elongation of the rope if a 9000-lbf loaded mine cart is placed on the cage. The results of Prob. 4-6 may be useful.

### Computer Programs

In approaching the ensuing computer problems, the following suggestions may be helpful:

- Decide whether an analysis program or a design program would be more useful. In problems as simple as these, you will find the programs similar. For maximum instructional benefit, try the design problem.
- Creating a design program without a figure of merit precludes ranking alternative designs but does not hinder the attainment of satisfactory designs. Your instructor can provide the class design library with commercial catalogs, which not only have price information but define available sizes.

- Quantitative understanding and logic of interrelations are required for programming. Difficulty in programming is a signal to you and your instructor to increase your understanding. The following programs can be accomplished in 100 to 500 lines of code.
- Make programs interactive and user-friendly.
- Let the computer do what it can do best; the user should do what a human can do best.
- Assume the user has a copy of the text and can respond to prompts for information.
- If interpolating in a table is in order, solicit table entries in the neighborhood, and let the computer crunch the numbers.
- In decision steps, allow the user to make the necessary decision, even if it is undesirable. This allows learning of consequences and the use of the program for analysis.
- Display a lot of information in the summary. Show the decision set used up-front for user perspective.
- When a summary is complete, adequacy assessment can be accomplished with ease, so consider adding this feature.

**17-35**

Your experience with Probs. 17-1 through 17-11 has placed you in a position to write an interactive computer program to design/select flat-belt drive components. A possible decision set is

*A Priori Decisions*

- Function:  $H_{\text{nom}}$ , rev/min, velocity ratio, approximate  $C$
- Design factor:  $n_d$
- Initial tension maintenance: catenary
- Belt material:  $t$ ,  $d_{\min}$ , allowable tension, density,  $f$
- Drive geometry:  $d$ ,  $D$
- Belt thickness:  $t$  (in material decision)

*Design Decisions*

- Belt width:  $b$

**17-36**

Problems 17-12 through 17-16 have given you some experience with flat metal friction belts, indicating that a computer program could be helpful in the design/selection process. A possible decision set is

*A Priori Decisions*

- Function:  $H_{\text{nom}}$ , rev/min, velocity ratio approximate  $C$
- Design factor:  $n_d$
- Belt material:  $S_y$ ,  $E$ ,  $v$ ,  $d_{\min}$
- Drive geometry:  $d$ ,  $D$
- Belt thickness:  $t$

*Design Decisions*

- Belt width:  $b$
- Length of belt (often standard loop periphery)

**17-37** Problems 17–17 through 17–22 have given you enough experience with V belts to convince you that a computer program would be helpful in the design/selection of V-belt drive components. Write such a program.

**17-38** Experience with Probs. 17–23 through 17–28 can suggest an interactive computer program to help in the design/selection process of roller-chain elements. A possible decision set is

*A Priori Decisions*

- Function: power, speed, space,  $K_s$ , life goal
- Design factor:  $n_d$
- Sprocket tooth counts:  $N_1, N_2, K_1, K_2$

*Design Decisions*

- Chain number
- Strand count
- Lubrication system
- Chain length in pitches

(center-to-center distance for reference)

*This page intentionally left blank*

# 18

## Power Transmission Case Study

### Chapter Outline

<b>18-1</b>	Design Sequence for Power Transmission	<b>935</b>
<b>18-2</b>	Power and Torque Requirements	<b>936</b>
<b>18-3</b>	Gear Specification	<b>936</b>
<b>18-4</b>	Shaft Layout	<b>943</b>
<b>18-5</b>	Force Analysis	<b>945</b>
<b>18-6</b>	Shaft Material Selection	<b>945</b>
<b>18-7</b>	Shaft Design for Stress	<b>946</b>
<b>18-8</b>	Shaft Design for Deflection	<b>946</b>
<b>18-9</b>	Bearing Selection	<b>947</b>
<b>18-10</b>	Key and Retaining Ring Selection	<b>948</b>
<b>18-11</b>	Final Analysis	<b>951</b>

Transmission of power from a source, such as an engine or motor, through a machine to an output actuation is one of the most common machine tasks. An efficient means of transmitting power is through rotary motion of a shaft that is supported by bearings. Gears, belt pulleys, or chain sprockets may be incorporated to provide for torque and speed changes between shafts. Most shafts are cylindrical (solid or hollow), and include stepped diameters with shoulders to accommodate the positioning and support of bearings, gears, etc.

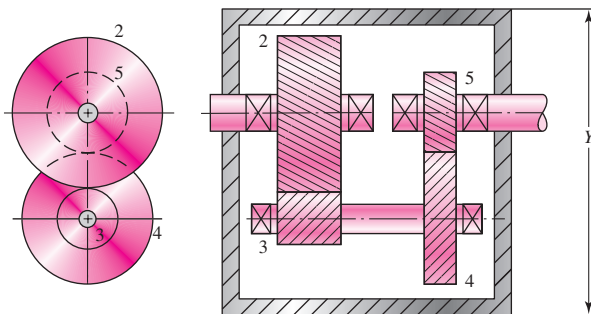
The design of a system to transmit power requires attention to the design and selection of individual components (gears, bearings, shaft, etc.). However, as is often the case in design, these components are not independent. For example, in order to design the shaft for stress and deflection, it is necessary to know the applied forces. If the forces are transmitted through gears, it is necessary to know the gear specifications in order to determine the forces that will be transmitted to the shaft. But stock gears come with certain bore sizes, requiring knowledge of the necessary shaft diameter. It is no surprise that the design process is interdependent and iterative, but where should a designer start?

The nature of machine design textbooks is to focus on each component separately. This chapter will focus on an overview of a power transmission system design, demonstrating how to incorporate the details of each component into an overall design process. A typical two-stage gear reduction such as shown in Fig. 18-1 will be assumed for this discussion. The design sequence is similar for variations of this particular transmission system.

The following outline will help clarify a logical design sequence. Discussion of how each part of the outline affects the overall design process will be given in sequence in this chapter. Details on the specifics for designing and selecting major components are covered in separate chapters, particularly Chap. 7 on shaft design, Chap. 11 on bearing selection, and Chaps. 13 and 14 on gear specification. A complete case study is presented as a specific vehicle to demonstrate the process.

**Figure 18-1**

A compound reverted gear train.



## CASE STUDY PART 1 PROBLEM SPECIFICATION

Section 1-17, p. 24, presents the background for this case study involving a speed reducer. A two-stage, compound reverted gear train such as shown in Fig. 18-1 will be designed. In this chapter, the design of the intermediate shaft and its components is presented, taking into account the other shafts as necessary.

A subset of the pertinent design specifications that will be needed for this part of the design are given here.

*Power to be delivered:* 20 hp

*Input speed:* 1750 rpm

*Output speed:* 82-88 rev/min

Usually low shock levels, occasional moderate shock

Input and output shafts extend 4 in outside gearbox

*Maximum gearbox size:* 14-in  $\times$  14-in base, 22-in height

Output shaft and input shaft in-line

Gear and bearing life  $> 12\,000$  hours; infinite shaft life

## 18-1

### Design Sequence for Power Transmission

There is not a precise sequence of steps for any design process. By nature, design is an iterative process in which it is necessary to make some tentative choices, and to build a skeleton of a design, and to determine which parts of the design are critical. However, much time can be saved by understanding the dependencies between the parts of the problem, allowing the designer to know what parts will be affected by any given change. In this section, only an outline is presented, with a short explanation of each step. Further details will be discussed in the following sections.

- *Power and torque requirements.* Power considerations should be addressed first, as this will determine the overall sizing needs for the entire system. Any necessary speed or torque ratio from input to output must be determined before addressing gear/pulley sizing.
- *Gear specification.* Necessary gear ratios and torque transmission issues can now be addressed with selection of appropriate gears. Note that a full force analysis of the shafts is not yet needed, as only the transmitted loads are required to specify the gears.
- *Shaft layout.* The general layout of the shaft, including axial location of gears and bearings must now be specified. Decisions on how to transmit the torque from the gears to the shaft need to be made (keys, splines, etc.), as well as how to hold gears and bearings in place (retaining rings, press fits, nuts, etc.). However, it is not necessary at this point to size these elements, since their standard sizes allow estimation of stress-concentration factors.
- *Force analysis.* Once the gear/pulley diameters are known, and the axial locations of the gears and bearings are known, the free-body, shear force, and bending moment diagrams for the shafts can be produced. Forces at the bearings can be determined.
- *Shaft material selection.* Since fatigue design depends so heavily on the material choice, it is usually easier to make a reasonable material selection first, then check for satisfactory results.
- *Shaft design for stress (fatigue and static).* At this point, a stress design of the shaft should look very similar to a typical design problem from the shaft chapter (Chap. 7). Shear force and bending moment diagrams are known, critical locations can be predicted, approximate stress concentrations can be used, and estimates for shaft diameters can be determined.

- *Shaft design for deflection.* Since deflection analysis is dependent on the entire shaft geometry, it is saved until this point. With all shaft geometry now estimated, the critical deflections at the bearing and gear locations can be checked by analysis.
- *Bearing selection.* Specific bearings from a catalog may now be chosen to match the estimated shaft diameters. The diameters can be adjusted slightly as necessary to match the catalog specifications.
- *Key and retaining ring selection.* With shaft diameters settling in to stable values, appropriate keys and retaining rings can be specified in standard sizes. This should make little change in the overall design if reasonable stress-concentration factors were assumed in previous steps.
- *Final analysis.* Once everything has been specified, iterated, and adjusted as necessary for any specific part of the task, a complete analysis from start to finish will provide a final check and specific safety factors for the actual system.

## 18-2

### Power and Torque Requirements

Power transmission systems will typically be specified by a power capacity, for example, a 40-horsepower gearbox. This rating specifies the combination of torque and speed that the unit can endure. Remember that, in the ideal case, *power in* equals *power out*, so that we can refer to the power being the same throughout the system. In reality, there are small losses due to factors like friction in the bearings and gears. In many transmission systems, the losses in the rolling bearings will be negligible. Gears have a reasonably high efficiency, with about 1 to 2 percent power loss in a pair of meshed gears. Thus, in the double-reduction gearbox in Fig. 18-1, with two pairs of meshed gears the output power is likely to be about 2 to 4 percent less than the input power. Since this is a small loss, it is common to speak of simply the power of the system, rather than input power and output power. Flat belts and timing belts have efficiencies typically in the mid to upper 90 percent range. V belts and worm gears have efficiencies that may dip much lower, requiring a distinction between the necessary input power to obtain a desired output power.

Torque, on the other hand, is typically not constant throughout a transmission system. Remember that power equals the product of torque and speed. Since *power in* = *power out*, we know that for a gear train

$$H = T_i \omega_i = T_o \omega_o \quad (18-1)$$

With a constant power, a gear ratio to decrease the angular velocity will simultaneously increase torque. The gear ratio, or train value, for the gear train is

$$e = \omega_o / \omega_i = T_i / T_o \quad (18-2)$$

A typical power transmission design problem will specify the desired power capacity, along with either the input and output angular velocities, or the input and output torques. There will usually be a tolerance specified for the output values. After the specific gears are specified, the actual output values can be determined.

## 18-3

### Gear Specification

With the gear train value known, the next step is to determine appropriate gears. As a rough guideline, a train value of up to 10 to 1 can be obtained with one pair of gears. Greater ratios can be obtained by compounding additional pairs of gears (See Sec. 13-13, p. 698). The compound reverted gear train in Fig. 18-1 can obtain a train value of up to 100 to 1.

Since numbers of teeth on gears must be integers, it is best to design with teeth numbers rather than diameters. See Ex. 13–3, 13–4, and 13–5, pp. 700–702, for details on designing appropriate numbers of teeth to satisfy the gear train value and any necessary geometry condition, such as in-line condition of input and output shaft. Care should be taken at this point to find the best combination of teeth numbers to minimize the overall package size. If the train value only needs to be approximate, use this flexibility to try different options of teeth numbers to minimize the package size. A difference of one tooth on the smallest gear can result in a significant increase in size of the overall package.

If designing for large production quantities, gears can be purchased in large enough quantities that it is not necessary to worry about preferred sizes. For small lot production, consideration should be given to the tradeoffs between smaller gearbox size and extra cost for odd gear sizes that are difficult to purchase off the shelf. If stock gears are to be used, their availability in prescribed numbers of teeth with anticipated diametral pitch should be checked at this time. If necessary, iterate the design for numbers of teeth that are available.

## CASE STUDY PART 2 SPEED, TORQUE, AND GEAR RATIOS

Continue the case study by determining appropriate tooth counts to reduce the input speed of  $\omega_i = 1750 \text{ rev/min}$  to an output speed within the range

$$82 \text{ rev/min} < \omega_o < 88 \text{ rev/min}$$

Once final tooth counts are specified, determine values of

- (a) Speeds for the intermediate and output shafts
- (b) Torques for the input, intermediate and output shafts, to transmit 20 hp.

### Solution

Use the notation for gear numbers from Fig. 18-1. Choose mean value for initial design,  $\omega_5 = 85 \text{ rev/min}$ .

$$e = \frac{\omega_5}{\omega_2} = \frac{85}{1750} = \frac{1}{20.59} \quad \text{Eq. (18-2)}$$

For a compound reverted geartrain,

$$e = \frac{1}{20.59} = \frac{N_2}{N_3} \frac{N_4}{N_5} \quad \text{Eq. (13-30), p. 699}$$

For smallest package size, let both stages be the same reduction. Also, by making the two stages identical, the in-line condition on the input and output shaft will automatically be satisfied.

$$\frac{N_2}{N_3} = \frac{N_4}{N_5} = \sqrt{\frac{1}{20.59}} = \frac{1}{4.54}$$

For this ratio, the minimum number of teeth from Eq. (13-11), p. 686, is 16.

$$N_2 = N_4 = 16 \text{ teeth}$$

$$N_3 = 4.54(N_2) = 72.64$$

Try rounding down and check if  $\omega_5$  is within limits.

$$\omega_5 = \left(\frac{16}{72}\right) \left(\frac{16}{72}\right) (1750) = 86.42 \text{ rev/min} \quad \text{Acceptable}$$

Proceed with

$$N_2 = N_4 = 16 \text{ teeth}$$

$$N_3 = N_5 = 72 \text{ teeth}$$

$$e = \left(\frac{16}{72}\right) \left(\frac{16}{72}\right) = \frac{1}{20.25}$$

$$\omega_5 = 86.42 \text{ rev/min}$$

$$\omega_3 = \omega_4 = \left(\frac{16}{72}\right) (1750) = 388.9 \text{ rev/min}$$

To determine the torques, return to the power relationship,

$$H = T_2 \omega_2 = T_5 \omega_5 \quad \text{Eq. (18-1)}$$

$$T_2 = H/\omega_2 = \left(\frac{20 \text{ hp}}{1750 \text{ rev/min}}\right) \left(550 \frac{\text{ft-lbf/s}}{\text{hp}}\right) \left(\frac{1 \text{ rev}}{2\pi \text{ rad}}\right) \left(\frac{60 \text{ s}}{\text{min}}\right)$$

$$T_2 = 60.0 \text{ lbf} \cdot \text{ft}$$

$$T_3 = T_2 \frac{\omega_2}{\omega_3} = 60.0 \frac{1750}{388.9} = 270 \text{ lbf} \cdot \text{ft}$$

$$T_5 = T_2 \frac{\omega_2}{\omega_5} = 60.0 \frac{1750}{86.42} = 1215 \text{ lbf} \cdot \text{ft}$$

If a maximum size for the gearbox has been specified in the problem specification, a minimum diametral pitch (maximum tooth size) can be estimated at this point by writing an expression for gearbox size in terms of gear diameters, and converting to numbers of teeth through the diametral pitch. For example, from Fig. 18-1, the overall height of the gearbox is

$$Y = d_3 + d_2/2 + d_5/2 + 2/P + \text{clearances} + \text{wall thicknesses}$$

where the  $2/P$  term accounts for the addendum height of the teeth on gears 2 and 5 that extend beyond the pitch diameters. Substituting  $d_i = N_i/P$  gives

$$Y = N_3/P + N_2/(2P) + N_5/(2P) + 2/P + \text{clearances} + \text{wall thicknesses}$$

Solving this for  $P$ , we find

$$P = (N_3 + N_2/2 + N_5/2 + 2)/(Y - \text{clearances} - \text{wall thicknesses}) \quad \text{(18-3)}$$

This is the minimum value that can be used for diametral pitch, and therefore the maximum tooth size, to stay within the overall gearbox constraint. It should be rounded *up* to the next standard diametral pitch, which reduces the maximum tooth size.

The AGMA approach, as described in Chap. 14, for both bending and contact stress should be applied next to determine suitable gear parameters. The primary design parameters to be specified by the designer include material, diametral pitch, and face width. A recommended procedure is to start with an estimated diametral pitch. This allows determination of gear diameters ( $d = N/P$ ), pitch-line velocities [Eq. (13–34), p. 707], and transmitted loads [Eq. (13–35) or (13–36), p. 707]. Typical spur gears are available with face widths from 3 to 5 times the circular pitch  $p$ . Using an average of 4, a first estimate can be made for face width  $F = 4p = 4\pi/P$ . Alternatively, the designer can simply perform a quick search of on-line gear catalogs to find available face widths for the diametral pitch and number of teeth.

Next, the AGMA equations in Chap. 14 can be used to determine appropriate material choices to provide desired safety factors. It is generally most efficient to attempt to analyze the most critical gear first, as it will determine the limiting values of diametral pitch and material strength. Usually, the critical gear will be the smaller gear, on the high-torque (low-speed) end of the gearbox.

If the required material strengths are too high, such that they are either too expensive or not available, iteration with a smaller diametral pitch (larger tooth) will help. Of course, this will increase the overall gearbox size. Often the excessive stress will be in one of the small gears. Rather than increase the tooth size for all gears, it is sometimes better to reconsider the design of tooth counts, shifting more of the gear ratio to the pair of gears with less stress, and less ratio to the pair of gears with the excessive stress. This will allow the offending gear to have more teeth and therefore larger diameter, decreasing its stress.

If contact stress turns out to be more limiting than bending stress, consider gear materials that have been heat treated or case hardened to increase the surface strength. Adjustments can be made to the diametral pitch if necessary to achieve a good balance of size, material, and cost. If the stresses are all much lower than the material strengths, a larger diametral pitch is in order, which will reduce the size of the gears and the gearbox.

Everything up to this point should be iterated until acceptable results are obtained, as this portion of the design process can usually be accomplished independently from the next stages of the process. The designer should be satisfied with the gear selection before proceeding to the shaft. Selection of specific gears from catalogs at this point will be helpful in later stages, particularly in knowing overall width, bore size, recommended shoulder support, and maximum fillet radius.

## CASE STUDY PART 3 GEAR SPECIFICATION

Continue the case study by specifying appropriate gears, including pitch diameter, diametral pitch, face width, and material. Achieve safety factors of at least 1.2 for wear and bending.

### Solution

Estimate the minimum diametral pitch for overall gearbox height = 22 in.

From Eq. (18-3) and Fig. 18-1,

$$P_{\min} = \frac{\left( N_3 + \frac{N_2}{2} + \frac{N_5}{2} + 2 \right)}{(Y - \text{clearances} - \text{wall thickness})}$$

Allow 1.5 in for clearances and wall thicknesses:

$$P_{\min} = \frac{\left( 72 + \frac{16}{2} + \frac{72}{2} + 2 \right)}{(22 - 1.5)} = 5.76 \text{ teeth/in}$$

Start with  $P = 6 \text{ teeth/in}$

$d_2 = d_4 = N_2/P = 16/6 = 2.67 \text{ in}$
$d_3 = d_5 = 72/6 = 12.0 \text{ in}$

Shaft speeds were previously determined to be

$$\omega_2 = 1750 \text{ rev/min} \quad \omega_3 = \omega_4 = 388.9 \text{ rev/min} \quad \omega_5 = 86.4 \text{ rev/min}$$

Get pitch-line velocities and transmitted loads for later use.

$$V_{23} = \frac{\pi d_2 \omega_2}{12} = \frac{\pi (2.67)(1750)}{12} = 1223 \text{ ft/min} \quad \text{Eq. (13-34), p. 707}$$

$$V_{45} = \frac{\pi d_5 \omega_5}{12} = 271.5 \text{ ft/min}$$

$$W_{23}^t = 33000 \frac{H}{V_{23}} = 33000 \left( \frac{20}{1223} \right) = 540.0 \text{ lbf} \quad \text{Eq. (13-35), p. 707}$$

$$W_{45}^t = 33000 \frac{H}{V_{45}} = 2431 \text{ lbf}$$

Start with gear 4, since it is the smallest gear, transmitting the largest load. It will likely be critical. Start with wear by contact stress, since it is often the limiting factor.

### Gear 4 Wear

$$I = \frac{\cos 20^\circ \sin 20^\circ}{2(1)} \left( \frac{4.5}{4.5 + 1} \right) = 0.1315 \quad \text{Eq. (14-23), p. 755}$$

For  $K_v$ , assume  $Q_v = 7$ .  $B = 0.731$ ,  $A = 65.1$   $\text{Eq. (14-29), p. 756}$

$$K_v = \left( \frac{65.1 + \sqrt{271.5}}{65.1} \right)^{0.731} = 1.18 \quad \text{Eq. (14-27), p. 756}$$

Face width  $F$  is typically from 3 to 5 times circular pitch. Try

$$F = 4 \left( \frac{\pi}{P} \right) = 4 \left( \frac{\pi}{6} \right) = 2.09 \text{ in.}$$

Since gear specifications are readily available on the Internet, we might as well check for commonly available face widths. On [www.globalspec.com](http://www.globalspec.com), entering  $P = 6$  teeth/in and  $d = 2.67$  in, stock spur gears from several sources have face widths of 1.5 in or 2.0 in. These are also available for the meshing gear 5 with  $d = 12$  in.

Choose  $F = 2.0 \text{ in.}$

For  $K_m$ ,  $C_{pf} = 0.0624$

$\text{Eq. (14-32), p. 760}$

$$C_{mc} = 1 \text{ uncrowned teeth} \quad \text{Eq. (14-31), p. 760}$$

$$C_{pm} = 1 \text{ straddle-mounted} \quad \text{Eq. (14-33), p. 760}$$

$$C_{ma} = 0.15 \text{ commercial enclosed unit} \quad \text{Eq. (14-34), p. 760}$$

$$C_e = 1 \quad \text{Eq. (14-35), p. 760}$$

$$K_m = 1.21 \quad \text{Eq. (14-30), p. 759}$$

$$C_p = 2300 \quad \text{Table 14-8, p. 757}$$

$$K_o = K_s = C_f = 1$$

$$\sigma_c = 2300 \sqrt{\frac{2431(1.18)(1.21)}{2.67(2)(0.1315)}} = \underline{161\ 700 \text{ psi}} \quad \text{Eq. (14-16), p. 746}$$

Get factors for  $\sigma_{c,\text{all}}$ . For life factor  $Z_N$ , get number of cycles for specified life of 12 000 h.

$$L_4 = (12\ 000 \text{ h}) \left( 60 \frac{\text{min}}{\text{h}} \right) \left( 389 \frac{\text{rev}}{\text{min}} \right) = 2.8 \times 10^8 \text{ rev}$$

$$Z_N = 0.9$$

Fig. 14-15, p. 763

$$K_R = K_T = C_H = 1$$

For a design factor of 1.2,

$$\sigma_{c,\text{all}} = S_c Z_N / S_H = \sigma_c \quad \text{Eq. (14-18), p. 750}$$

$$S_c = \frac{S_H \sigma_c}{Z_N} = \frac{1.2(161\ 700)}{0.9} = \underline{215\ 600 \text{ psi}}$$

From Table 14-6, p. 751, this strength is achievable with Grade 2 carburized and hardened with  $S_c = 225\ 000 \text{ psi}$ . To find the achieved factor of safety,  $n_c = \sigma_{c,\text{all}} / \sigma_c$  with  $S_H = 1$ . The factor of safety for wear of gear 4 is

$$n_c = \frac{\sigma_{c,\text{all}}}{\sigma_c} = \frac{S_c Z_N}{\sigma_c} = \frac{225\ 000(0.9)}{161\ 700} = \underline{1.25}$$

### Gear 4 Bending

$$J = 0.27$$

Fig. 14-6, p. 753

$$K_B = 1$$

Everything else is the same as before.

$$\sigma = W_t K_v \frac{P_d}{F} \frac{K_m}{J} = (2431)(1.18) \left( \frac{6}{2} \right) \left( \frac{1.21}{0.27} \right) \quad \text{Eq. (14-15), p. 746}$$

$$\underline{\sigma = 38\ 570 \text{ psi}}$$

$$Y_N = 0.9$$

Fig. 14-14, p. 763

Using Grade 2 carburized and hardened, same as chosen for wear, find  $S_t = 65\,000$  psi (Table 14-3, p. 748).

$$\sigma_{\text{all}} = S_t Y_N = 58\,500 \text{ psi}$$

The factor of safety for bending of gear 4 is

$$n = \frac{\sigma_{\text{all}}}{\sigma} = \frac{58\,500}{38\,570} = 1.52$$

### Gear 5 Bending and Wear

Everything is the same as for gear 4, except  $J$ ,  $Y_N$ , and  $Z_N$ .

$$J = 0.41$$

Fig. 14-6, p. 753

$$L_5 = (12\,000\text{h})(60 \text{ min/h})(86.4 \text{ rev/min}) = 6.2 \times 10^7 \text{ rev}$$

$$Y_N = 0.97$$

Fig. 14-14, p. 763

$$Z_N = 1.0$$

Fig. 14-15, p. 763

$$\sigma_c = 2300 \sqrt{\frac{2431(1.18)(1.21)}{2.67(2)(0.1315)}} = 161\,700 \text{ psi}$$

$$\sigma = (2431)(1.18) \left(\frac{6}{2}\right) \left(\frac{1.21}{0.41}\right) = 25\,400 \text{ psi}$$

Choose Grade 2 carburized and hardened, the same as gear 4

$$n_c = \frac{\sigma_{c,\text{all}}}{\sigma_c} = \frac{225\,000}{161\,700} = 1.39$$

$$n = \frac{\sigma_{\text{all}}}{\sigma} = \frac{65\,000(0.97)}{25\,400} = 2.48$$

### Gear 2 Wear

Gears 2 and 3 are evaluated similarly. Only selected results are shown.

$$K_v = 1.37$$

Try  $F = 1.5$  in, since the loading is less on gears 2 and 3.

$$K_m = 1.19$$

All other factors are the same as those for gear 4.

$$\sigma_c = 2300 \sqrt{\frac{(539.7)(1.37)(1.19)}{2.67(1.5)(0.1315)}} = 94\,000 \text{ psi}$$

$$L_2 = (12\,000 \text{ h})(60 \text{ min/h})(1750 \text{ rev/min}) = 1.26 \times 10^9 \text{ rev} \quad Z_N = 0.8$$

Try grade 1 flame-hardened,  $S_c = 170\,000$  psi

$$n_c = \frac{\sigma_{c,\text{all}}}{\sigma_c} = \frac{170\,000(0.8)}{94\,000} = 1.40$$

### Gear 2 Bending

$$J = 0.27 \quad Y_N = 0.88$$

$$\sigma = 539.7(1.37) \frac{(6)(1.19)}{(1.5)(0.27)} = 13\,040 \text{ psi}$$

$$n = \frac{\sigma_{\text{all}}}{\sigma} = \frac{45\,000(0.88)}{13\,040} = 3.04$$

### Gear 3 Wear and Bending

$$J = 0.41 \quad Y_N = 0.9 \quad Z_N = 0.9$$

$$\sigma_c = 2300 \sqrt{\frac{(539.7)(1.37)(1.19)}{2.67(1.5)(0.1315)}} = 94\,000 \text{ psi}$$

$$\sigma = 539.7(1.37) \frac{(6)(1.19)}{1.5(0.41)} = 8584 \text{ psi}$$

Try Grade 1 steel, through-hardened to 300  $H_B$ . From Fig. 14-2, p. 747,  $S_t = 36\,000 \text{ psi}$  and from Fig. 14-5, p. 750,  $S_c = 126\,000 \text{ psi}$ .

$$n_c = \frac{126\,000(0.9)}{94\,000} = 1.21$$

$$n = \frac{\sigma_{\text{all}}}{\sigma} = \frac{36\,000(0.9)}{8584} = 3.77$$

In summary, the resulting gear specifications are:

All gears,  $P = 6$  teeth/in

Gear 2, Grade 1 flame-hardened,  $S_c = 170\,000 \text{ psi}$  and  $S_t = 45\,000 \text{ psi}$   
 $d_2 = 2.67 \text{ in}$ , face width = 1.5 in

Gear 3, Grade 1 through-hardened to 300  $H_B$ ,  $S_c = 126\,000 \text{ psi}$  and  $S_t = 36\,000 \text{ psi}$   
 $d_3 = 12.0 \text{ in}$ , face width = 1.5 in

Gear 4, Grade 2 carburized and hardened,  $S_c = 225\,000 \text{ psi}$  and  $S_t = 65\,000 \text{ psi}$   
 $d_4 = 2.67 \text{ in}$ , face width = 2.0 in

Gear 5, Grade 2 carburized and hardened,  $S_c = 225\,000 \text{ psi}$  and  $S_t = 65\,000 \text{ psi}$   
 $d_5 = 12.0 \text{ in}$ , face width = 2.0 in

## 18-4 Shaft Layout

The general layout of the shafts, including axial location of gears and bearings, must now be specified in order to perform a free-body force analysis and to obtain shear force and bending moment diagrams. If there is no existing design to use as a starter, then the determination of the shaft layout may have many solutions. Section 7-3, p. 361, discusses the issues involved in shaft layout. In this section the focus will be on how the decisions relate to the overall process.

A free-body force analysis can be performed without knowing shaft diameters, but can not be performed without knowing axial distances between gears and bearings. It is extremely important to keep axial distances small. Even small forces can create large bending moments if the moment arms are large. Also, recall that beam deflection equations typically include length terms raised to the third power.

It is worth examining the entirety of the gearbox at this time, to determine what factors drive the length of the shaft and the placement of the components. A rough sketch, such as shown in Fig. 18-2, is sufficient for this purpose.

## CASE STUDY PART 4 SHAFT LAYOUT

Continue the case study by preparing a sketch of the gearbox sufficient to determine the axial dimensions. In particular, estimate the overall length, and the distance between the gears of the intermediate shaft, in order to fit with the mounting requirements of the other shafts.

### Solution

Fig. 18-2 shows the rough sketch. It includes all three shafts, with consideration of how the bearings are to mount in the case. The gear widths are known at this point. Bearing widths are guessed, allowing a little more space for larger bearings on the intermediate shaft where bending moments will be greater. Small changes in bearing widths will have minimal effect on the force analysis, since the location of the ground reaction force will change very little. The 4-in distance between the two gears on the countershaft is dictated by the requirements of the input and output shafts, including the space for the case to mount the bearings. Small allotments are given for the retaining rings, and for space behind the bearings. Adding it all up gives the intermediate shaft length as 11.5 in.

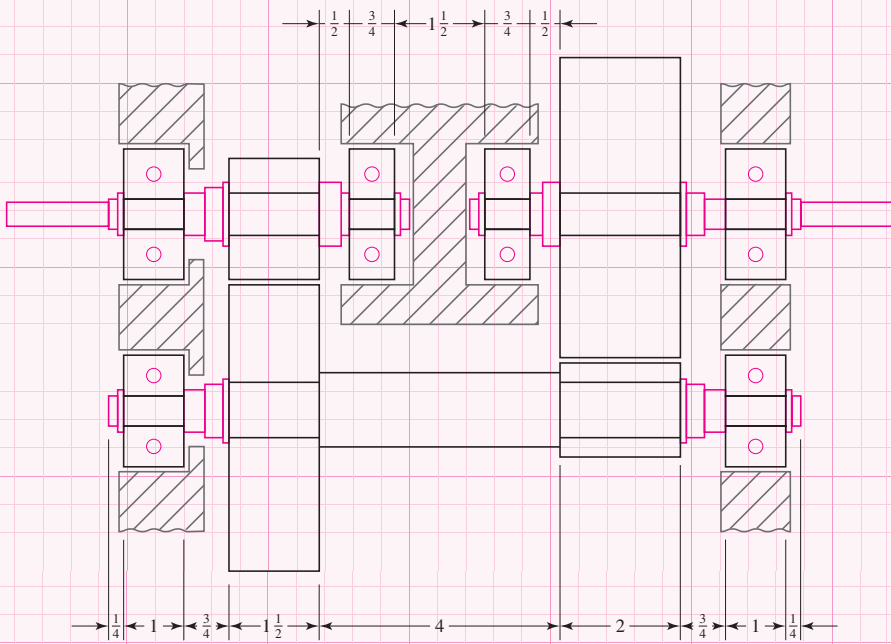


**Figure 18-2**

Sketch for shaft layout. Dimensions are in inches.

Wider face widths on gears require more shaft length. Originally, gears with hubs were considered for this design to allow the use of set screws instead of high-stress-concentration retaining rings. However, the extra hub lengths added several inches to the shaft lengths and the gearbox housing.

Several points are worth noting in the layout in Fig. 18–2. The gears and bearings are positioned against shoulders, with retaining rings to hold them in position. While it is desirable to place gears near the bearings, a little extra space is provided between them to accommodate any housing that extends behind the bearing, and to allow for a bearing puller to have space to access the back of the bearing. The extra change in diameter between the bearings and the gears allows the shoulder height for the bearing and the bore size for the gear to be different. This diameter can have loose tolerances and large fillet radius.

Each bearing is restrained axially on its shaft, but only one bearing on each shaft is axially fixed in the housing, allowing for slight axial thermal expansion of the shafts.

## 18–5 Force Analysis

Once the gear diameters are known, and the axial locations of the components are set, the free-body diagrams and shear force and bending moment diagrams for the shafts can be produced. With the known transmitted loads, determine the radial and axial loads transmitted through the gears (see Secs. 13–14 through 13–17, pp. 705–714). From summation of forces and moments on each shaft, ground reaction forces at the bearings can be determined. For shafts with gears and pulleys, the forces and moments will usually have components in two planes along the shaft. For rotating shafts, usually only the resultant magnitude is needed, so force components at bearings are summed as vectors. Shear force and bending moment diagrams are usually obtained in two planes, then summed as vectors at any point of interest. A torque diagram should also be generated to clearly visualize the transfer of torque from an input component, through the shaft, and to an output component.

See the beginning of Ex. 7–2, p. 374, for the force analysis portion of the case study for the intermediate shaft. The bending moment is largest at gear 4. This is predictable, since gear 4 is smaller, and must transmit the same torque that entered the shaft through the much larger gear 3.

While the force analysis is not difficult to perform manually, if beam software is to be used for the deflection analysis, it will necessarily calculate reaction forces, along with shear force and bending moment diagrams in the process of calculating deflections. The designer can enter guessed values for diameters into the software at this point, just to get the force information, and later enter actual diameters to the same model to determine deflections.

## 18–6 Shaft Material Selection

A trial material for the shaft can be selected at any point before the stress design of the shaft, and can be modified as necessary during the stress design process. Section 7–2, p. 360, provides details for decisions regarding material selection. For the case study, an inexpensive steel, 1020 CD, is initially selected. After the stress analysis, a slightly higher strength 1050 CD is chosen to reduce the critical stresses without further increasing the shaft diameters.

## 18-7 Shaft Design for Stress

The critical shaft diameters are to be determined by stress analysis at critical locations. Section 7-4, p. 366, provides a detailed examination of the issues involved in shaft design for stress.

### CASE STUDY PART 5 DESIGN FOR STRESS

Proceed with the next phase of the case study design, in which appropriate diameters for each section of the shaft are estimated, based on providing sufficient fatigue and static stress capacity for infinite life of the shaft, with minimum safety factor of 1.5.

#### Solution

The solution to this phase of the design is presented in Ex. 7-2, p. 374.

Since the bending moment is highest at gear 4, potentially critical stress points are at its shoulder, keyway, and retaining ring groove. It turns out that the keyway is the critical location. It seems that shoulders often get the most attention. This example demonstrates the danger of neglecting other stress concentration sources, such as keyways.

The material choice was changed in the course of this phase, choosing to pay for a higher strength to limit the shaft diameter to 2 in. If the shaft were to get much bigger, the small gear would not be able to provide an adequate bore size. If it becomes necessary to increase the shaft diameter any more, the gearing specification will need to be redesigned.

## 18-8 Shaft Design for Deflection

Section 7-5, p. 379, provides a detailed discussion of deflection considerations for shafts. Typically, a deflection problem in a shaft will not cause catastrophic failure of the shaft, but will lead to excess noise and vibration, and premature failure of the gears or bearings.

### CASE STUDY PART 6 DEFLECTION CHECK

Proceed with the next phase of the case study by checking that deflections and slopes at the gears and bearings on the intermediate shaft are within acceptable ranges.

#### Solution

The solution to this phase of the design is presented in Ex. 7-3, p. 380.

It turns out that in this problem all the deflections are within recommended limits for bearings and gears. This is not always the case, and it would be a poor choice to neglect the deflection analysis. In a first iteration of this case study, with longer shafts due to using gears with hubs, the deflections were more critical than the stresses.

18-9

## Bearing Selection

Bearing selection is straightforward now that the bearing reaction forces and the approximate bore diameters are known. See Chap. 11 for general details on bearing selection. Rolling-contact bearings are available with a wide range of load capacities and dimensions, so it is usually not a problem to find a suitable bearing that is close to the estimated bore diameter and width.

### CASE STUDY PART 7 BEARING SELECTION

Continue the case study by selecting appropriate bearings for the intermediate shaft, with a reliability of 99 percent. The problem specifies a design life of 12 000 h. The intermediate shaft speed is 389 rev/min. The estimated bore size is 1 in, and the estimated bearing width is 1 in.

#### Solution

From the free-body diagram (see Ex. 7-2, p. 374),

$$\begin{aligned} R_{Az} &= 115.0 \text{ lbf} & R_{Ay} &= 356.7 \text{ lbf} & R_A &= 375 \text{ lbf} \\ R_{Bz} &= 1776.0 \text{ lbf} & R_{By} &= 725.3 \text{ lbf} & R_B &= 1918 \text{ lbf} \end{aligned}$$

At the shaft speed of 389 rev/min, the design life of 12 000 h correlates to a bearing life of  $L_D = (12\,000 \text{ h})(60 \text{ min/h})(389 \text{ rev/min}) = 2.8 \times 10^8 \text{ rev}$ .

Start with bearing B since it has the higher loads and will likely raise any lurking problems. From Eq. (11-7), p. 578, assuming a ball bearing with  $a = 3$  and  $L = 2.8 \times 10^6 \text{ rev}$ ,

$$F_{RB} = 1918 \left[ \frac{2.8 \times 10^8 / 10^6}{0.02 + 4.439(1 - 0.99)^{1/1.483}} \right]^{1/3} = 20\,820 \text{ lbf}$$

A check on the Internet for available bearings ([www.globalspec.com](http://www.globalspec.com) is one good starting place) shows that this load is relatively high for a ball bearing with bore size in the neighborhood of 1 in. Try a cylindrical roller bearing. Recalculating  $F_{RB}$  with the exponent  $a = 3/10$  for roller bearings, we obtain

$$F_{RB} = 16\,400 \text{ lbf}$$

Cylindrical roller bearings are available from several sources in this range. A specific one is chosen from SKF, a common supplier of bearings, with the following specifications:

Cylindrical roller bearing at right end of shaft

$C = 18\,658 \text{ lbf}$ , ID = 1.1811 in, OD = 2.8346 in,  $W = 1.063 \text{ in}$

Shoulder diameter = 1.45 in to 1.53 in, and maximum fillet radius = 0.043 in

For bearing A, again assuming a ball bearing,

$$F_{RA} = 375 \left[ \frac{2.8 \times 10^8 / 10^6}{0.02 + 4.439(1 - 0.99)^{1/1.483}} \right]^{1/3} = 407 \text{ lbf}$$

A specific ball bearing is chosen from the SKF Internet catalog.

Deep-groove ball bearing at left end of shaft

$C = 5058 \text{ lbf}$ , ID = 1.000 in, OD = 2.500 in,  $W = 0.75 \text{ in}$

Shoulder diameter = 1.3 in to 1.4 in, and maximum fillet radius = 0.08 in

At this point, the actual bearing dimensions can be checked against the initial assumptions. For bearing B the bore diameter of 1.1811 in is slightly larger than the original 1.0 in. There is no reason for this to be a problem as long as there is room for the shoulder diameter. The original estimate for shoulder support diameters was 1.4 in. As long as this diameter is less than 1.625 in, the next step of the shaft, there should not be any problem. In the case study, the recommended shoulder support diameters are within the acceptable range. The original estimates for stress concentration at the bearing shoulder assumed a fillet radius such that  $r/d = 0.02$ . The actual bearings selected have ratios of 0.036 and 0.080. This allows the fillet radii to be increased from the original design, decreasing the stress-concentration factors.

The bearing widths are close to the original estimates. Slight adjustments should be made to the shaft dimensions to match the bearings. No redesign should be necessary.

## 18-10

### Key and Retaining Ring Selection

The sizing and selection of keys is discussed in Sec. 7–7, p. 388, with an example in Ex. 7–6, p. 394. The cross-sectional size of the key will be dictated to correlate with the shaft size (see Tables 7–6 and 7–8, pp. 391, 393), and must certainly match an integral keyway in the gear bore. The design decision includes the length of the key, and if necessary an upgrade in material choice.

The key could fail by shearing across the key, or by crushing due to bearing stress. For a square key, it turns out that checking only the crushing failure is adequate, since the shearing failure will be less critical according to the distortion energy failure theory, and equal according to the maximum shear stress failure theory. Check Ex. 7–6 to investigate why.

## CASE STUDY PART 8 KEY DESIGN

Continue the case study by specifying appropriate keys for the two gears on the intermediate shaft to provide a factor of safety of 2. The gears are to be custom bored and keyed to the required specifications. Previously obtained information includes the following:

Transmitted torque:  $T = 3240 \text{ lbf-in}$

Bore diameters:  $d_3 = d_4 = 1.625 \text{ in}$

Gear hub lengths:  $l_3 = 1.5 \text{ in}$ ,  $l_4 = 2.0 \text{ in}$

### Solution

From Table 7-6, p. 391, for a shaft diameter of 1.625 in, choose a square key with side dimension  $t = \frac{3}{8}$  in. Choose 1020 CD material, with  $S_y = 57$  ksi. The force on the key at the surface of the shaft is

$$F = \frac{T}{r} = \frac{3240}{1.625/2} = 3988 \text{ lbf}$$

Checking for failure by crushing, we find the area of one-half the face of the key is used.

$$n = \frac{S_y}{\sigma} = \frac{S_y}{F/(tl/2)}$$

Solving for  $l$  gives

$$l = \frac{2Fn}{tS_y} = \frac{2(3988)(2)}{(0.375)(57000)} = 0.75 \text{ in}$$

Since both gears have the same bore diameter and transmit the same torque, the same key specification can be used for both.

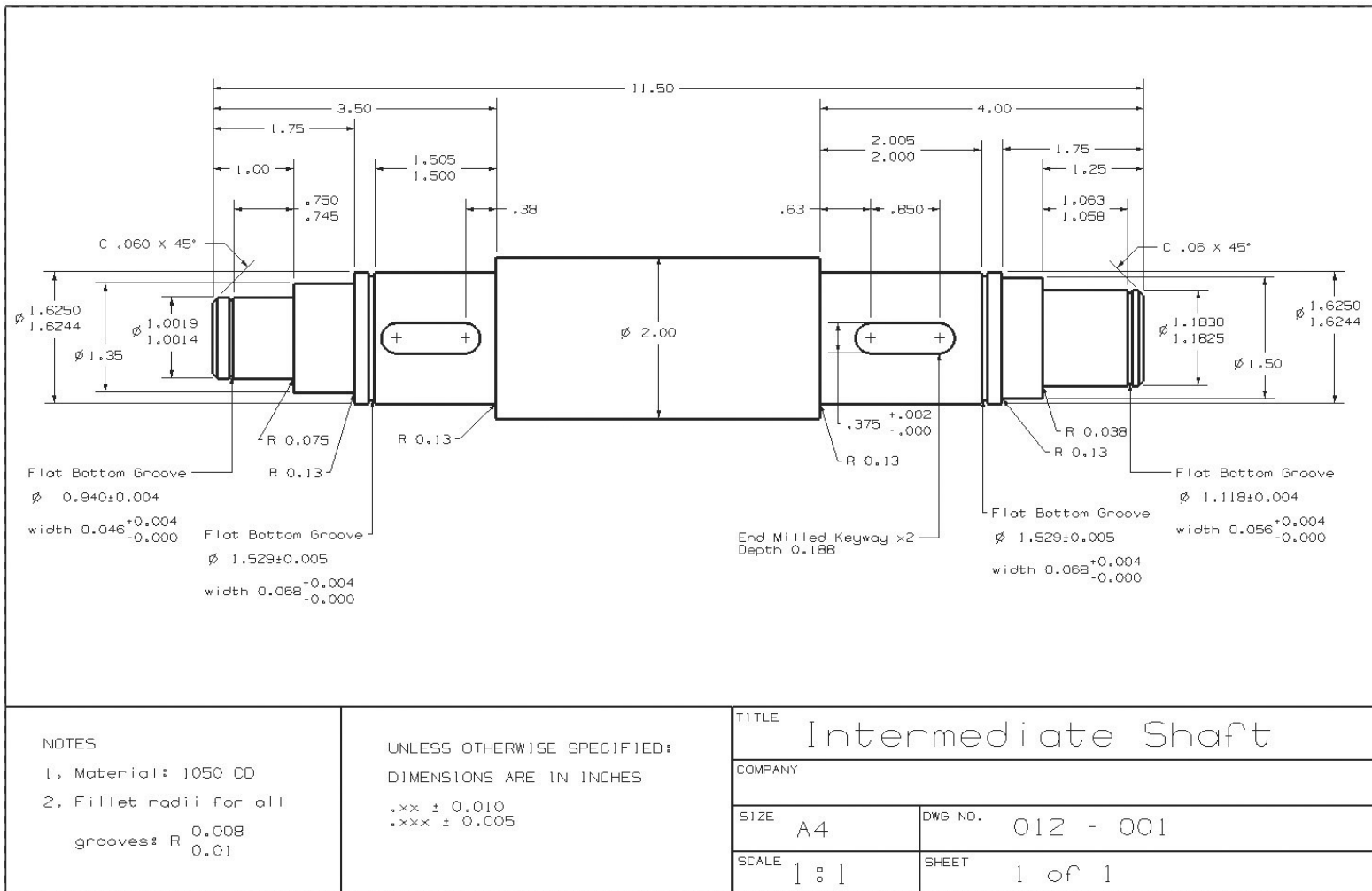
Retaining ring selection is simply a matter of checking catalog specifications. The retaining rings are listed for nominal shaft diameter, and are available with different axial load capacities. Once selected, the designer should make note of the depth of the groove, the width of the groove, and the fillet radius in the bottom of the groove. The catalog specification for the retaining ring also includes an edge margin, which is the minimum distance to the next smaller diameter change. This is to ensure support for the axial load carried by the ring. It is important to check stress-concentration factors with actual dimensions, as these factors can be rather large. In the case study, a specific retaining ring was already chosen during the stress analysis (see Ex. 7-2, p. 374) at the potentially critical location of gear 4. The other locations for retaining rings were not at points of high stress, so it is not necessary to worry about the stress concentration due to the retaining rings in these locations. Specific retaining rings should be selected at this time to complete the dimensional specifications of the shaft.

For the case study, retaining rings specifications are entered into globalspec, and specific rings are selected from Truarc Co., with the following specifications:

	<b>Both Gears</b>	<b>Left Bearing</b>	<b>Right Bearing</b>
Nominal Shaft diameter	1.625 in	1.000 in	1.181 in
Groove diameter	$1.529 \pm 0.005$ in	$0.940 \pm 0.004$ in	$1.118 \pm 0.004$ in
Groove width	$0.068^{+0.004}_{-0.000}$ in	$0.046^{+0.004}_{-0.000}$ in	$0.046^{+0.004}_{-0.000}$ in
Nominal groove depth	0.048 in	0.030 in	0.035 in
Max groove fillet radius	0.010 in	0.010 in	0.010 in
Minimum edge margin	0.144 in	0.105 in	0.105 in
Allowable axial thrust	11 850 lbf	6000 lbf	7000 lbf

These are within the estimates used for the initial shaft layout, and should not require any redesign. The final shaft should be updated with these dimensions.

| Figure 18-3



## 18-11 Final Analysis

At this point in the design, everything seems to check out. Final details include determining dimensions and tolerances for appropriate fits with the gears and bearings. See Section 7–8, p. 395, for details on obtaining specific fits. Any small changes from the nominal diameters already specified will have negligible effect on the stress and deflection analysis. However, for manufacturing and assembly purposes, the designer should not overlook the tolerance specification. Improper fits can lead to failure of the design. The final drawing for the intermediate shaft is shown in Fig. 18–3.

For documentation purposes, and for a check on the design work, the design process should conclude with a complete analysis of the final design. Remember that analysis is much more straightforward than design, so the investment of time for the final analysis will be relatively small.

## PROBLEMS

- 18–1** For the case study problem, design the input shaft, including complete specification of the gear, bearings, key, retaining rings, and shaft.
- 18–2** For the case study problem, design the output shaft, including complete specification of the gear, bearings, key, retaining rings, and shaft.
- 18–3** For the case study problem, use helical gears and design the intermediate shaft. Compare your results with the spur gear design presented in this chapter.
- 18–4** Perform a final analysis for the resulting design of the intermediate shaft of the case study problem presented in this chapter. Produce a final drawing with dimensions and tolerances for the shaft. Does the final design satisfy all the requirements? Identify the critical aspects of the design with the lowest factor of safety.
- 18–5** For the case study problem, change the power requirement to 40 horsepower. Design the intermediate shaft, including complete specification of the gears, bearings, keys, retaining rings, and shaft.

**PART**

# 4

## **Analysis Tools**

---

# 19

## Finite-Element Analysis

### Chapter Outline

<b>19-1</b>	The Finite-Element Method	<b>955</b>
<b>19-2</b>	Element Geometries	<b>957</b>
<b>19-3</b>	The Finite-Element Solution Process	<b>959</b>
<b>19-4</b>	Mesh Generation	<b>962</b>
<b>19-5</b>	Load Application	<b>964</b>
<b>19-6</b>	Boundary Conditions	<b>965</b>
<b>19-7</b>	Modeling Techniques	<b>966</b>
<b>19-8</b>	Thermal Stresses	<b>969</b>
<b>19-9</b>	Critical Buckling Load	<b>969</b>
<b>19-10</b>	Vibration Analysis	<b>971</b>
<b>19-11</b>	Summary	<b>972</b>

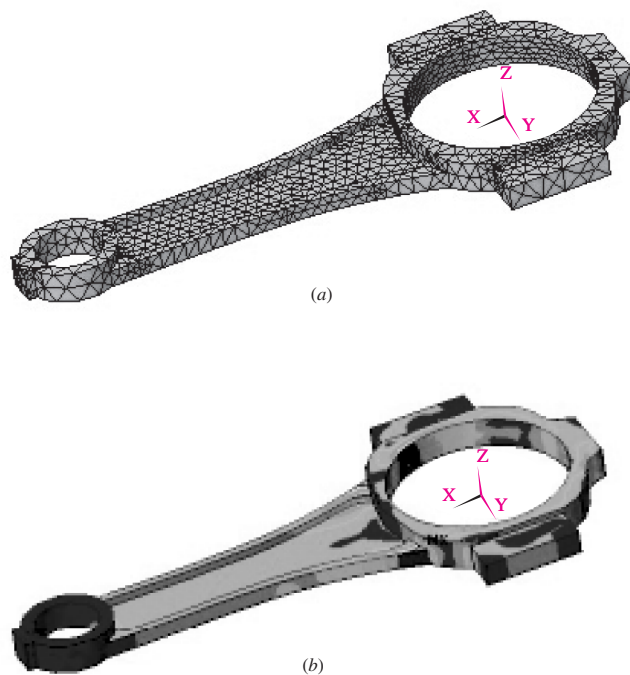
Mechanical components in the form of simple bars, beams, etc., can be analyzed quite easily by basic methods of mechanics that provide closed-form solutions. Actual components, however, are rarely so simple, and the designer is forced to less effective approximations of closed-form solutions, experimentation, or numerical methods. There are a great many numerical techniques used in engineering applications for which the digital computer is very useful. In mechanical design, where computer-aided design (CAD) software is heavily employed, the analysis method that integrates well with CAD is *finite-element analysis* (FEA). The mathematical theory and applications of the method are vast. There is also a number of commercial FEA software packages that are available, such as ANSYS, NASTRAN, Algor, etc.

The purpose of this chapter is only to expose the reader to some of the fundamental aspects of FEA, and therefore the coverage is extremely introductory in nature. For further detail, the reader is urged to consult the many references cited at the end of this chapter. Figure 19–1 shows a finite-element model of a connecting rod that was developed to study the effects of dynamic elastohydrodynamic lubrication on bearing and structural performance.<sup>1</sup>

There are a multitude of FEA applications such as static and dynamic, linear and nonlinear, stress and deflection analysis; free and forced vibrations; heat transfer (which can be combined with stress and deflection analysis to provide thermally induced stresses and deflections); elastic instability (buckling); acoustics; electrostatics and

**Figure 19–1**

Model of a connecting rod using ANSYS finite-element software. (a) Meshed model; (b) stress contours. *Courtesy of S. Boedo (see footnote 1).*



<sup>1</sup>S. Boedo, "Elastohydrodynamic Lubrication of Conformal Bearing Systems," *Proceedings of 2002 ANSYS Users Conference*, Pittsburgh, PA, April 22–24, 2002.

magnetics (which can be combined with heat transfer); fluid dynamics; piping analysis; and multiphysics. For purposes of this chapter, we will limit ourselves to basic mechanics analyses.

An actual mechanical component is a continuous elastic structure (continuum). FEA divides (discretizes) the structure into small but finite, well-defined, elastic substructures (elements). By using polynomial functions, together with matrix operations, the continuous elastic behavior of each element is developed in terms of the element's material and geometric properties. Loads can be applied within the element (gravity, dynamic, thermal, etc.), on the surface of the element, or at the *nodes* of the element. The element's nodes are the fundamental governing entities of the element, as it is the node where the element connects to other elements, where elastic properties of the element are eventually established, where boundary conditions are assigned, and where forces (contact or body) are ultimately applied. A node possesses *degrees of freedom* (dof's). Degrees of freedom are the independent translational and rotational motions that can exist at a node. At most, a node can possess three translational and three rotational degrees of freedom. Once each element within a structure is defined *locally* in matrix form, the elements are then *globally* assembled (attached) through their common nodes (dof's) into an overall system matrix. Applied loads and boundary conditions are then specified and through matrix operations the values of all unknown displacement degrees of freedom are determined. Once this is done, it is a simple matter to use these displacements to determine strains and stresses through the constitutive equations of elasticity.

## 19-1

### The Finite-Element Method

The modern development of the finite-element method began in the 1940s in the field of structural mechanics with the work of Hrennikoff,<sup>2</sup> McHenry,<sup>3</sup> and Newmark,<sup>4</sup> who used a lattice of line elements (rods and beams) for the solution of stresses in continuous solids. In 1943, from a 1941 lecture, Courant<sup>5</sup> suggested piecewise polynomial interpolation over triangular subregions as a method to model torsional problems. With the advent of digital computers in the 1950s it became practical for engineers to write and solve the stiffness equations in matrix form.<sup>6,7,8</sup> A classic paper by Turner, Clough, Martin, and Topp published in 1956 presented the matrix stiffness equations for the

<sup>2</sup>A. Hrennikoff, "Solution of Problems in Elasticity by the Frame Work Method," *Journal of Applied Mechanics*, Vol. 8, No. 4, pp. 169–175, December 1941.

<sup>3</sup>D. McHenry, "A Lattice Analogy for the Solution of Plane Stress Problems," *Journal of Institution of Civil Engineers*, Vol. 21, pp. 59–82, December 1943.

<sup>4</sup>N. M. Newmark, "Numerical Methods of Analysis in Bars, Plates, and Elastic Bodies," *Numerical Methods in Analysis in Engineering* (ed. L. E. Grinter), Macmillan, 1949.

<sup>5</sup>R. Courant, "Variational Methods for the Solution of Problems of Equilibrium and Vibrations," *Bulletin of the American Mathematical Society*, Vol. 49, pp. 1–23, 1943.

<sup>6</sup>S. Levy, "Structural Analysis and Influence Coefficients for Delta Wings," *Journal of Aeronautical Sciences*, Vol. 20, No. 7, pp. 449–454, July 1953.

<sup>7</sup>J. H. Argyris, "Energy Theorems and Structural Analysis," *Aircraft Engineering*, October, November, December 1954 and February, March, April, May 1955.

<sup>8</sup>J. H. Argyris and S. Kelsey, *Energy Theorems and Structural Analysis*, Butterworths, London, 1960 (reprinted from *Aircraft Engineering*, 1954–55).

truss, beam, and other elements.<sup>9</sup> The expression *finite element* is first attributed to Clough.<sup>10</sup> Since these early beginnings, a great deal of effort has been expended in the development of the finite element method in the areas of element formulations and computer implementation of the entire solution process. The major advances in computer technology include the rapidly expanding computer hardware capabilities, efficient and accurate matrix solver routines, and computer graphics for ease in the visual preprocessing stages of model building, including automatic adaptive mesh generation, and in the postprocessing stages of reviewing the solution results. A great abundance of literature has been presented on the subject, including many textbooks. A partial list of some textbooks, introductory and more comprehensive, is given at the end of this chapter.

Since the finite-element method is a numerical technique that discretizes the domain of a continuous structure, errors are inevitable. These errors are:

- 1 Computational errors.** These are due to round-off errors from the computer floating-point calculations and the formulations of the numerical integration schemes that are employed. Most commercial finite-element codes concentrate on reducing these errors, and consequently the analyst generally is concerned with discretization factors.
- 2 Discretization errors.** The geometry and the displacement distribution of a true structure continuously vary. Using a finite number of elements to model the structure introduces errors in matching geometry and the displacement distribution due to the inherent mathematical limitations of the elements.

For an example of discretization errors, consider the constant thickness, thin plate structure shown in Fig. 19–2a. Figure 19–2b shows a finite-element model

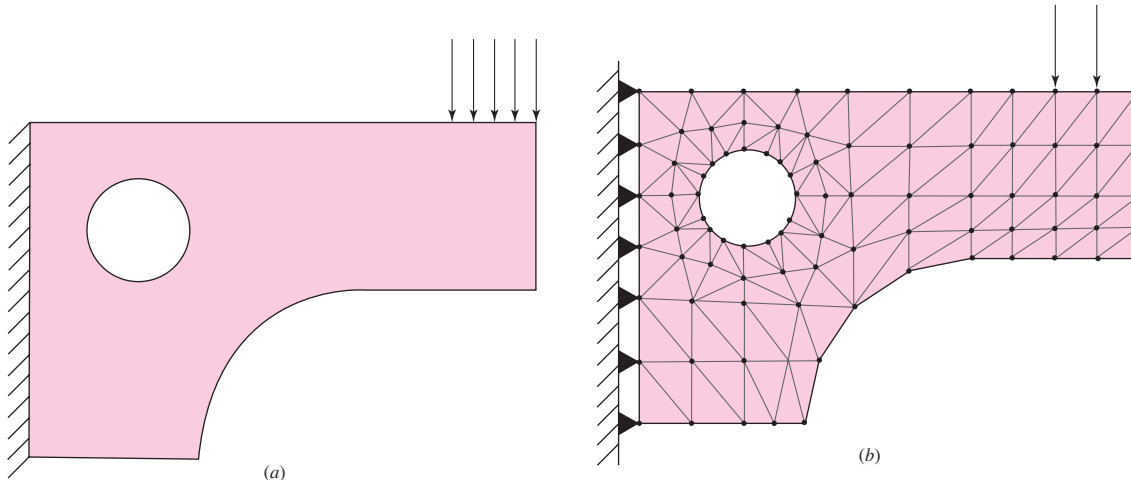


**Figure 19-2**

Structural problem. (a) Idealized model; (b) finite-element model.

<sup>9</sup>M. J. Turner, R. W. Clough, H. C. Martin, and L. J. Topp, "Stiffness and Deflection Analysis of Complex Structures," *Journal of Aeronautical Sciences*, Vol. 23, No. 9, pp. 805–824, September 1956.

<sup>10</sup>R. W. Clough, "The Finite Element Method in Plane Stress Analysis," *Proceedings of the Second Conference on Electronic Computation*, American Society of Civil Engineers, Pittsburgh, PA, pp. 345–378, September 1960.

of the structure where three-node, plane stress, simplex triangular elements are employed. This element type has a flaw that creates two basic problems. The element has straight sides that remain straight after deformation. The strains throughout the plane stress triangular element are constant. The first problem, a geometric one, is the modeling of curved edges. Note that the surface of the model with a large curvature appears poorly modeled, whereas the surface of the hole seems to be reasonably modeled. The second problem, which is much more severe, is that the strains in various regions of the actual structure are changing rapidly, and the constant strain element will provide only an approximation of the average strain at the center of the element. So, in a nutshell, the results predicted by this model will be extremely poor. The results can be improved by significantly increasing the number of elements (increased mesh density). Alternatively, using a better element, such as an eight-node quadrilateral, which is more suited to the application, will provide the improved results. Because of higher-order interpolation functions, the eight-node quadrilateral element can model curved edges and provide for a higher-order function for the strain distribution.

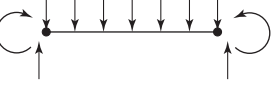
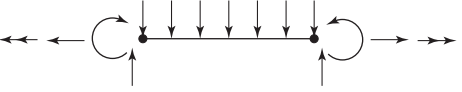
In Fig. 19–2b, the triangular elements are shaded and the nodes of the elements are represented by the black dots. Forces and constraints can be placed only at the nodes. The nodes of a simplex triangular plane stress elements have only two degrees of freedom, translation in the plane. Thus, the solid black, simple support triangles on the left edge represent the fixed support of the model. Also, the distributed load can be applied only to three nodes as shown. The modeled load has to be statically consistent with the actual load.

## 19–2 Element Geometries

Many geometric shapes of elements are used in finite-element analysis for specific applications. The various elements used in a general-purpose commercial FEM software code constitute what is referred to as the *element library* of the code. Elements can be placed in the following categories: *line elements*, *surface elements*, *solid elements*, and *special-purpose elements*. Table 19–1 provides some, but not all, of the

**Table 19–1**

Sample Finite-Element Library

Element Type	None	Shape	Number of Nodes	Applications
Line	Truss		2	Pin-ended bar in tension or compression
	Beam		2	Bending
	Frame		2	Axial, torsional, and bending. With or without load stiffening.

(continued)

| Table 19-1 (Continued)

Element Type	None	Shape	Number of Nodes	Applications
Surface	4-node quadrilateral		4	Plane stress or strain, axisymmetry, shear panel, thin flat plate in bending
	8-node quadrilateral		8	Plane stress or strain, thin plate or shell in bending
	3-node triangular		3	Plane stress or strain, axisymmetry, shear panel, thin flat plate in bending. Prefer quad where possible. Used for transitions of quads.
	6-node triangular		6	Plane stress or strain, axisymmetry, thin plate or shell in bending. Prefer quad where possible. Used for transitions of quads.
Solid <sup>†</sup>	8-node hexagonal (brick)		8	Solid, thick plate
	6-node pentagonal (wedge)		6	Solid, thick plate. Used for transitions.
	4-node tetrahedron (tet)		4	Solid, thick plate. Used for transitions.
Special purpose	Gap		2	Free displacement for prescribed compressive gap
	Hook		2	Free displacement for prescribed extension gap
	Rigid		Variable	Rigid constraints between nodes

<sup>†</sup>These elements are also available with midside nodes.

types of elements available for finite-element analysis for structural problems. Not all elements support all degrees of freedom. For example, the 3-D truss element supports only three translational degrees of freedom at each node. Connecting elements with differing dof's generally requires some manual modification. For example, consider connecting a truss element to a frame element. The frame element supports all six dof's at each node. A truss member, when connected to it, can rotate freely at the connection.

### 19-3 The Finite-Element Solution Process

We will describe the finite-element solution process on a very simple one-dimensional problem, using the linear truss element. A truss element is a bar loaded in tension or compression and is of constant cross-sectional area  $A$ , length  $l$ , and elastic modulus  $E$ . The basic truss element has two nodes, and for a one-dimensional problem, each node will have only one degree of freedom. A truss element can be modeled as a simple linear spring with a spring rate, given by Eq. (4-4) as

$$k = \frac{AE}{l} \quad (19-1)$$

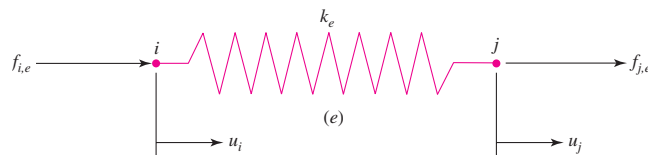
Consider a spring element ( $e$ ) of spring rate  $k_e$ , with nodes  $i$  and  $j$ , as shown in Fig. 19-3. Nodes and elements will be numbered. So, to avoid confusion as to what a number corresponds to, elements will be numbered within parentheses. Assuming all forces  $f$  and displacements  $u$  directed toward the right as positive, the forces at each node can be written as

$$\begin{aligned} f_{i,e} &= k_e(u_i - u_j) = k_e u_i - k_e u_j \\ f_{j,e} &= k_e(u_j - u_i) = -k_e u_i + k_e u_j \end{aligned} \quad (19-2)$$

The two equations can be written in matrix form as

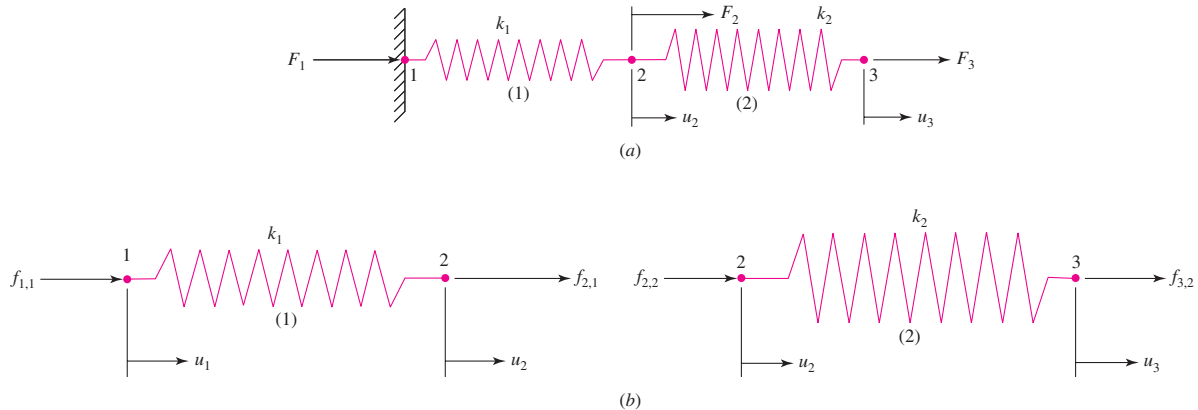
$$\begin{Bmatrix} f_{i,e} \\ f_{j,e} \end{Bmatrix} = \begin{bmatrix} k_e & -k_e \\ -k_e & k_e \end{bmatrix} \begin{Bmatrix} u_i \\ u_j \end{Bmatrix} \quad (19-3)$$

Next, consider a two-spring system as shown in Fig. 19-4a. Here we have numbered the nodes and elements. We have also labeled the forces at each node. However, these forces are the total external forces at each node,  $F_1$ ,  $F_2$ , and  $F_3$ . If we draw separate free-body diagrams we will expose the internal forces as shown in Fig. 19-4b.



**Figure 19-3**

A simple spring element.

**Figure 19-4**

A two-element spring system. (a) System model, (b) separate free-body diagrams.

Using Eq. (19-3) for each spring gives

$$\text{Element 1} \quad \begin{Bmatrix} f_{1,1} \\ f_{2,1} \end{Bmatrix} = \begin{bmatrix} k_1 & -k_1 \\ -k_1 & k_1 \end{bmatrix} \begin{Bmatrix} u_1 \\ u_2 \end{Bmatrix} \quad (19-4a)$$

$$\text{Element 2} \quad \begin{Bmatrix} f_{2,2} \\ f_{3,2} \end{Bmatrix} = \begin{bmatrix} k_2 & -k_2 \\ -k_2 & k_2 \end{bmatrix} \begin{Bmatrix} u_2 \\ u_3 \end{Bmatrix} \quad (19-4b)$$

The total force at each node is the external force,  $F_1 = f_{1,1}$ ,  $F_2 = f_{2,1} + f_{2,2}$ , and  $F_3 = f_{3,2}$ . Combining the two matrices in terms of the external forces gives

$$\begin{Bmatrix} f_{1,1} \\ f_{2,1} + f_{2,2} \\ f_3 \end{Bmatrix} = \begin{Bmatrix} F_1 \\ F_2 \\ F_3 \end{Bmatrix} = \begin{bmatrix} k_1 & -k_1 & 0 \\ -k_1 & (k_1 + k_2) & -k_2 \\ 0 & -k_2 & k_2 \end{bmatrix} \begin{Bmatrix} u_1 \\ u_2 \\ u_3 \end{Bmatrix} \quad (19-5)$$

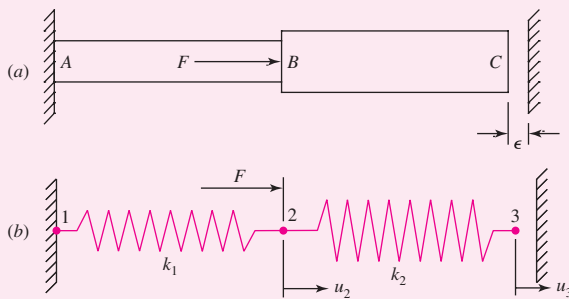
If we know the displacement of a node, then the force at the node will be unknown. For example, in Fig. 19-4a, the displacement of node 1 at the wall is zero, so  $F_1$  is the unknown reaction force (note, up to this point, we have not applied a static solution of the system). If we do not know the displacement of a node, then we know the force. For example, in Fig. 19-4a, the displacements at nodes 2 and 3 are unknown, and the forces  $F_2$  and  $F_3$  are to be specified. To see how the remainder of the solution process can be implemented, let us consider the following example.

**EXAMPLE 19-1**

Consider the aluminum step-shaft shown in Fig. 19-5a. The areas of sections *AB* and *BC* are  $0.100 \text{ in}^2$  and  $0.150 \text{ in}^2$ , respectively. The lengths of sections *AB* and *BC* are 10 in and 12 in, respectively. A force  $F = 1000 \text{ lbf}$  is applied to *B*. Initially, a gap of  $\epsilon = 0.002 \text{ in}$  exists between end *C* and the right rigid wall. Determine the wall

**Figure 19–5**

(a) Step shaft; (b) spring model.



reactions, the internal forces in the members, and the deflection of point *B*. Let  $E = 10$  Mpsi and assume that end *C* hits the wall. Check the validity of the assumption.

**Solution** The step-shaft is modeled by the two-spring system of Fig. 19–5b where

$$k_1 = \left( \frac{AE}{l} \right)_{AB} = \frac{0.1(10)10^6}{10} = 1(10^5) \text{ lbf/in}$$

$$k_2 = \left( \frac{AE}{l} \right)_{BC} = \frac{0.15(10)10^6}{12} = 1.25(10^5) \text{ lbf/in}$$

With  $u_1 = 0$ ,  $F_2 = 1000$  lbf and the assumption that  $u_3 = \epsilon = 0.002$  in, Eq. (19–5) becomes

$$\begin{Bmatrix} F_1 \\ 1000 \\ F_3 \end{Bmatrix} = 10^5 \begin{bmatrix} 1 & -1 & 0 \\ -1 & 2.25 & -1.25 \\ 0 & -1.25 & 1.25 \end{bmatrix} \begin{Bmatrix} 0 \\ u_2 \\ 0.002 \end{Bmatrix} \quad (1)$$

For large problems, there is a systematic method of solving equations like Eq. (1), called *partitioning* or *the elimination approach*.<sup>11</sup> However, for this simple problem, the solution is quite simple. From the second equation of the matrix equation

$$1000 = 10^5[-1(0) + 2.25u_2 - 1.25(0.002)]$$

or,

**Answer**  $u_B = u_2 = \frac{1000/10^5 + 1.25(0.002)}{2.25} = 5.556(10^{-3}) \text{ in}$

Since  $u_B > \epsilon$ , it is verified that point *C* hits the wall.

The reactions at the walls are  $F_1$  and  $F_3$ . From the first and third equations of matrix Eq. (1),

**Answer**  $F_1 = 10^5[-1(u_2)] = 10^5[-1(5.556)10^{-3}] = -555.6 \text{ lbf}$

<sup>11</sup>See T. R. Chandrupatla and A. D. Belegundu, *Introduction to Finite Elements in Engineering*, 3rd ed., Prentice Hall, Upper Saddle River, NJ, 2002, pp. 63–68.

and

**Answer**

$$\begin{aligned} F_3 &= 10^5[-1.25u_2 + 1.25(0.002)] \\ &= 10^5[-1.25(5.556)10^{-3} + 1.25(0.002)] = -444.4 \text{ lbf} \end{aligned}$$

Since  $F_3$  is negative, this also verifies that C hits the wall. Note that  $F_1 + F_3 = -555.6 - 444.4 = -1000$  lbf, balancing the applied force (with no statics equations necessary).

For internal forces, it is necessary to return to the individual (local) equations. From Eq. (19-4a),

$$\begin{Bmatrix} f_{1,1} \\ f_{2,1} \end{Bmatrix} = \begin{bmatrix} k_1 & -k_1 \\ -k_1 & k_1 \end{bmatrix} \begin{Bmatrix} u_1 \\ u_2 \end{Bmatrix} = 10^5 \begin{bmatrix} 1 & -1 \\ -1 & 1 \end{bmatrix} \begin{Bmatrix} 0 \\ 5.556(10^{-3}) \end{Bmatrix} = \begin{Bmatrix} -555.6 \\ 555.6 \end{Bmatrix} \text{ lbf}$$

**Answer**

Since  $f_{1,1}$  is directed to the left and  $f_{2,1}$  is directed to the right, the element is in tension, with a force of 555.6 lbf. If the stress is desired, it is simply  $\sigma_{AB} = f_{2,1}/A_{AB} = 555.6/0.1 = 5556$  psi.

For element BC, from Eq. (19.4b),

$$\begin{Bmatrix} f_{2,2} \\ f_{3,2} \end{Bmatrix} = \begin{bmatrix} k_2 & -k_2 \\ -k_2 & k_2 \end{bmatrix} \begin{Bmatrix} u_2 \\ u_3 \end{Bmatrix} = 10^5 \begin{bmatrix} 1.25 & -1.25 \\ -1.25 & 1.25 \end{bmatrix} \begin{Bmatrix} 5.556(10^{-3}) \\ 0.002 \end{Bmatrix} = \begin{Bmatrix} 444.5 \\ -444.5 \end{Bmatrix} \text{ lbf}$$

**Answer**

Since  $f_{2,2}$  is directed to the right and  $f_{3,2}$  is directed to the left, the element is in compression, with a force of 444.5 lbf. If the stress is desired, it is simply  $\sigma_{BC} = -f_{2,2}/A_{BC} = -444.5/0.15 = -2963$  psi.

## 19-4

## Mesh Generation

The network of elements and nodes that discretize a region is referred to as a *mesh*. The *mesh density* increases as more elements are placed within a given region. *Mesh refinement* is when the mesh is modified from one analysis of a model to the next analysis to yield improved results. Results generally improve when the mesh density is increased in areas of high stress gradients and/or when geometric transition zones are meshed smoothly. Generally, but not always, the FEA results converge toward the exact results as the mesh is continuously refined. To assess improvement, in regions where high stress gradients appear, the structure can be remeshed with a higher mesh density at this location. If there is a minimal change in the maximum stress value, it is reasonable to presume that the solution has converged. There are three basic ways to generate an element mesh, manually, semiautomatically, or fully automated.

- 1 Manual mesh generation.** This is how the element mesh was created in the early days of the finite-element method. This is a very labor intensive method of creating the mesh, and except for some quick modifications of a model is it rarely done. *Note:* Care must be exercised in editing an input text file. With

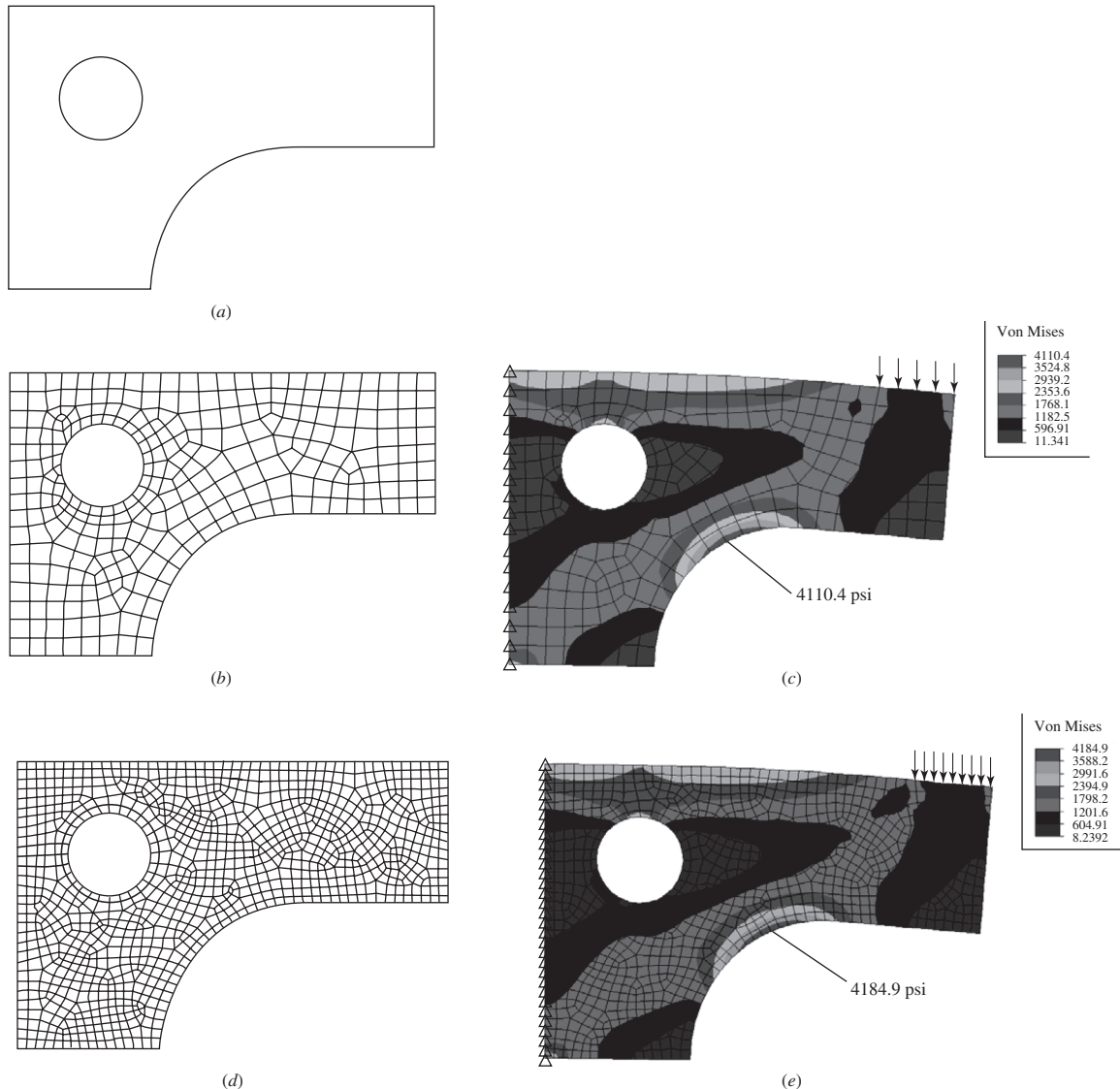
some FEA software, other files such as the preprocessor binary graphics file may not change. Consequently, the files may no longer be compatible with each other.

- 2 **Semiautomatic mesh generation.** Over the years, computer algorithms have been developed that enable the modeler to automatically mesh regions of the structure that he or she has divided up, using well-defined boundaries. Since the modeler has to define these regions, the technique is deemed *semiautomatic*. The development of the many computer algorithms for mesh generation emanates from the field of computer graphics. If the reader desires more information on this subject, a review the literature available from this field is recommended.
- 3 **Fully automated mesh generation.** Many software vendors have concentrated their efforts on developing fully automatic mesh generation, and in some instances, automatic *self-adaptive* mesh refinement. The obvious goal is to significantly reduce the modeler's preprocessing time and effort to arrive at a final well-constructed FEA mesh. Once the complete boundary of the structure is defined, without subdivisions as in semiautomatic mesh generation and with a minimum of user intervention, various schemes are available to discretize the region with *one element type*. For plane elastic problems the boundary is defined by a series of internal and external geometric lines and the element type to be automeshed would be the plane elastic element. For thin-walled structures, the geometry would be defined by three-dimensional surface representations and the automeshed element type would be the three-dimensional plate element. For solid structures, the boundary could be constructed by using *constructive solid geometry (CSG)* or *boundary representation (B-rep)* techniques. The finite-element types for automeshing would be the brick and/or tetrahedron.

Automatic self-adaptive mesh refinement programs estimate the error of the FEA solution. On the basis of the error, the mesh is automatically revised and reanalyzed. The process is repeated until some convergence or termination criterion is satisfied.

Returning to the thin-plate model of Fig. 19–2, the boundaries of the structure are constructed as shown in Fig. 19–6a. The boundaries were then automeshed as shown in Fig. 19–6b, where 294 elements and 344 nodes were generated. Note the uniformity of the element generation at the boundaries. The finite-element solver then generated the deflections and von Mises stresses shown in Fig. 19–6c. The maximum von Mises stress at the location shown is 4110.4 psi. The model was then automeshed with an increased mesh density as shown in Fig. 19–6d, where the model has 1008 elements and 1096 nodes. The results are shown in Fig. 19–6e where the maximum von Mises stress is found to be 4184.9 psi, which is only 1.8 percent higher. In all likelihood, the solution has nearly converged. *Note:* The stress contours of Figs. 19–6c and e are better visualized in color.

When stress concentrations are present, it is necessary to have a very fine mesh at the stress-concentration region in order to get realistic results. What is important is that the mesh density needs to be increased only in the region around the stress concentration and that the transition mesh from the rest of the structure to the stress-concentration region be gradual. An abrupt mesh transition, in itself, will have the same effect as a stress concentration. Stress concentration will be discussed further in Sec. 19–7, Modeling Techniques.

**Figure 19-6**

Automatic meshing the thin-plate model of Fig. 19-2. (a) Model boundaries; (b) automesh with 294 elements and 344 nodes; (c) deflected (exaggerated scale) with stress contours; (d) automesh with 1008 elements and 1096 nodes, (e) deflected (exaggerated scale) with stress contours.

## 19-5 Load Application

There are two basic forms of specifying loads on a structure, nodal and element loading. However, element loads are eventually applied to the nodes by using equivalent nodal loads. One aspect of load application is related to Saint-Venant's principle. If one is not concerned about the stresses near points of load application, it is

not necessary to attempt to distribute the loading very precisely. The net force and/or moment can be applied to a single node, provided the element supports the dof associated with the force and/or moment at the node. However, the analyst should not be surprised, or concerned, when reviewing the results and the stresses in the vicinity of the load application point are found to be very large. Concentrated moments can be applied to the nodes of beam and most plate elements. However, concentrated moments cannot be applied to truss, two-dimensional plane elastic, axisymmetric, or brick elements. They do not support rotational degrees of freedom. A pure moment can be applied to these elements only by using forces in the form of a couple. From the mechanics of statics, a couple can be generated by using two or more forces acting in a plane where the net force from the forces is zero. The net moment from the forces is a vector perpendicular to the plane and is the summation of the moments from the forces taken about any common point.

Element loads include static loads due to gravity (weight), thermal effects, surface loads such as uniform and hydrostatic pressure, and dynamic loads due to constant acceleration and steady-state rotation (centrifugal acceleration). As stated earlier, element loads are converted by the software to equivalent nodal loads and in the end are treated as concentrated loads applied to nodes.

For gravity loading, the gravity constant in appropriate units and the direction of gravity must be supplied by the modeler. If the model length and force units are inches and lbf,  $g = 386.1 \text{ ips}^2$ . If the model length and force units are meters and Newtons,  $g = 9.81 \text{ m/s}^2$ . The gravity direction is normally toward the center of the earth.

For thermal loading, the thermal expansion coefficient  $\alpha$  must be given for each material, as well as the initial temperature of the structure, and the final nodal temperatures. Most software packages have the capability of first performing a finite-element heat transfer analysis on the structure to determine the final nodal temperatures. The temperature results are written to a file, which can be transferred to the static stress analysis. Here the heat transfer model should have the same nodes and element type the static stress analysis model has.

Surface loading can generally be applied to most elements. For example, uniform or linear transverse line loads (force/length) can be specified on beams. Uniform and linear pressure can normally be applied on the edges of two-dimensional plane and axisymmetric elements. Lateral pressure can be applied on plate elements, and pressure can be applied on the surface of solid brick elements. Each software package has its unique manner in which to specify these surface loads, usually in a combination of text and graphic modes.

## 19-6 Boundary Conditions

The simulation of boundary conditions and other forms of constraint is probably the single most difficult part of the accurate modeling of a structure for a finite-element analysis. In specifying constraints, it is relatively easy to make mistakes of omission or misrepresentation. It may be necessary for the analyst to test different approaches to model esoteric constraints such as bolted joints, welds, etc., which are not as simple as the idealized pinned or fixed joints. Testing should be confined to simple problems and not to a large, complex structure. Sometimes, when the exact nature of a boundary condition is uncertain, only limits of behavior may be possible. For example, we have modeled shafts with bearings as being simply supported. It is more likely that the support is something between simply supported and

fixed, and we could analyze both constraints to establish the limits. However, by assuming simply supported, the results of the solution are conservative for stress and deflections. That is, the solution would predict stresses and deflections larger than the actual.

For another example, consider beam 16 in Table A-9. The horizontal beam is uniformly loaded and is fixed at both ends. Although not explicitly stated, tables such as these assume that the beams are not restrained in the horizontal direction. That is, it is assumed that the beam can slide horizontally in the supports. If the ends were completely or partially restrained, a beam-column solution would be necessary.<sup>12</sup> With a finite-element analysis, a special element, a beam with stiffening, could be used.

*Multipoint constraint equations* are quite often used to model boundary conditions or rigid connections between elastic members. When used in the latter form, the equations are acting as elements and are thus referred to as *rigid elements*. Rigid elements can rotate or translate only rigidly.

*Boundary elements* are used to force specific nonzero displacements on a structure. Boundary elements can also be useful in modeling boundary conditions that are askew from the global coordinate system.

## 19-7 Modeling Techniques

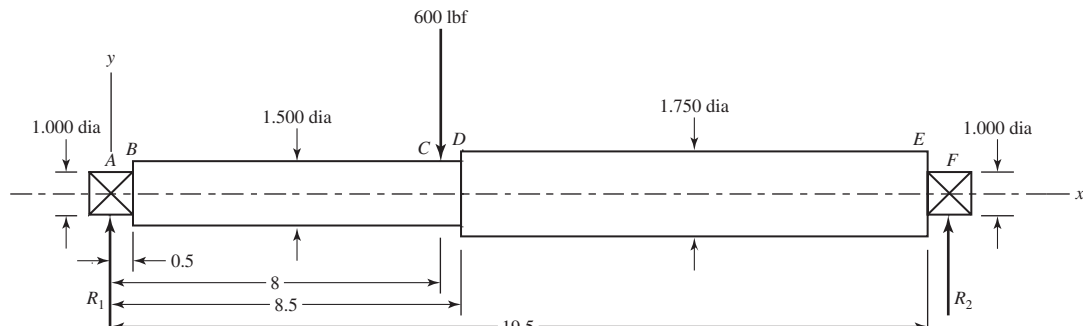
With today's CAD packages and automatic mesh generators, it is an easy task to create a solid model and mesh the volume with finite elements. With today's computing speeds and with gobs of computer memory, it is very easy to create a model with extremely large numbers of elements and nodes. The finite-element modeling techniques of the past now seem passé and unnecessary. However, much unnecessary time can be spent on a very complex model when a much simpler model will do. The complex model may not even provide an accurate solution, whereas a simpler one will. What is important is what solution the analyst is looking for: deflections, stresses, or both?

For example, consider the steel step-shaft of Ex. 4-7, repeated here as Fig. 19-7a. Let the fillets at the steps have a radius of 0.02 in. If only deflections and slopes were sought at the steps, a highly meshed solid model would not yield much more than the simple five-element beam model, shown in Fig. 19-7b, would. The fillets at the steps, which could not be modeled easily with beam elements, would not contribute much to a difference in results between the two models. Nodes are necessary wherever boundary conditions, applied forces, and changes in cross section and/or material occur. The displacement results for the FEA model are shown in Fig. 19-7c.

The FE model of Fig. 19-7b is not capable of providing the stress at the fillet of the step at D. Here, a full-blown solid model would have to be developed and meshed, using solid elements with a high mesh density at the fillet as shown in Fig. 19-8a. Here, the steps at the bearing supports are not modeled, as we are concerned only with the stress concentration at  $x = 8.5$  in. The brick and tetrahedron elements do not support rotational

---

<sup>12</sup>See R. B. Budynas, *Advanced Strength and Applied Stress Analysis*, 2nd ed., McGraw-Hill, New York, 1999, pp. 471–482.



(a) Dimensions in inches



(b)

Displacements/rotations (degrees) of nodes

Node No.	x Translation	y Translation	z Translation	$\theta_x$ Rotation (deg)	$\theta_y$ Rotation (deg)	$\theta_z$ Rotation (deg)
1	0.0000 E + 00	0.0000 E + 00	0.0000 E + 00	0.0000 E + 00	0.0000 E + 00	-9.7930 E - 02
2	0.0000 E + 00	-8.4951 E - 04	0.0000 E + 00	0.0000 E + 00	0.0000 E + 00	-9.6179 E - 02
3	0.0000 E + 00	-9.3649 E - 03	0.0000 E + 00	0.0000 E + 00	0.0000 E + 00	-7.9874 E - 03
4	0.0000 E + 00	-9.3870 E - 03	0.0000 E + 00	0.0000 E + 00	0.0000 E + 00	2.8492 E - 03
5	0.0000 E + 00	-6.0507 E - 04	0.0000 E + 00	0.0000 E + 00	0.0000 E + 00	6.8558 E - 02
6	0.0000 E + 00	0.0000 E + 00	0.0000 E + 00	0.0000 E + 00	0.0000 E + 00	6.9725 E - 02

(c)

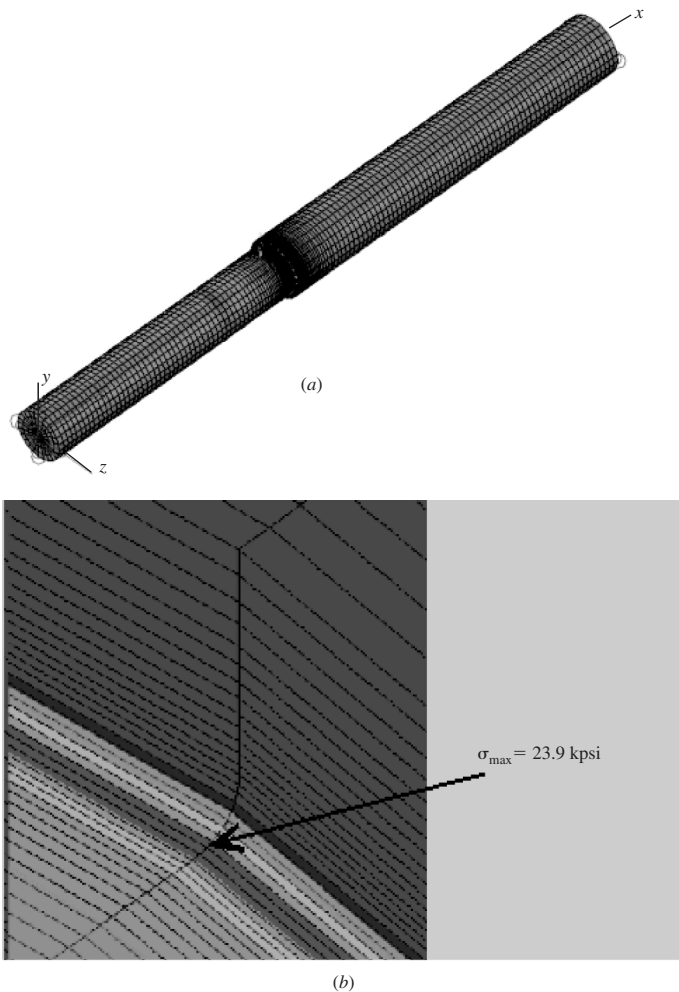
**Figure 19-7**

(a) Steel step shaft of Ex. 4-7; (b) finite-element model using five beam elements; (c) displacement results for FEA model.

degrees of freedom. To model the simply supported boundary condition at the left end, nodes along the  $z$  axis were constrained from translating in the  $x$  and  $y$  directions. Nodes along the  $y$  axis were constrained from translating in the  $z$  direction. Nodes on the right end on an axis parallel with the  $z$  axis through the center of the shaft were constrained from translating in the  $y$  direction, and nodes on an axis parallel with the  $y$  axis through the center of the shaft were constrained from translating in the  $z$  direction. This ensures no rigid-body translation or rotation and no overconstraint at the ends. The maximum tensile stress at the fillet at the beam bottom is found to be  $\sigma_{\max} = 23.9$  kpsi. Performing an analytical check at the step yields  $D/d = 1.75/1.5 = 1.167$ , and  $r/d = 0.02/1.5 = 0.0133$ . Figure A-15-9 is not very accurate for these values.

**Figure 19–8**

(a) Solid model of the step-shaft of Ex. 4–7 using 56 384 brick and tetrahedron elements; (b) view of stress contours at step, rotated 180° about  $x$  axis, showing maximum tension.



Resorting to another source,<sup>13</sup> the stress-concentration factor is found to be  $K_t = 3.00$ . The reaction at the right support is  $R_F = (8/20)600 = 240$  lbf. The bending moment at the start of the fillet is  $M = 240(11.52) = 2765$  lbf · in = 2.765 kip · in. The analytical prediction of the maximum stress is thus

$$\sigma_{\max} = K_t \left( \frac{32M}{\pi d^3} \right) = 3.00 \left[ \frac{32(2.765)}{\pi(1.5^3)} \right] = 25.03 \text{ kpsi}$$

The finite-element model is 4.5 percent lower. If more elements were used in the fillet region, the results would undoubtedly be closer. However, the results are within engineering acceptability.

If we want to check deflections, we should compare the results with the three-element beam model, not the five-element model. This is because we did not model the bearing steps in the solid model. The vertical deflection, at  $x = 8.5$  in, for the solid

<sup>13</sup>See, W. D. Pilkey and D. F. Pilkey, *Peterson's Stress-Concentration Factors*, 3rd ed. John Wiley & Sons, New York, 2008, Chart 3.11.

model was found to be  $-0.00981$  in. This is 4.6 percent higher in magnitude than the  $-0.00938$  in deflection for the three-element beam model,. For slopes, the brick element does not support rotational degrees of freedom, so the rotation at the ends has to be computed from the displacements of adjacent nodes at the ends. This results in the slopes at the ends of  $\theta_A = -0.103^\circ$  and  $\theta_F = 0.0732^\circ$ ; these are 6.7 and 6.6 percent higher in magnitude than the three-element beam model, respectively. However, the point of this exercise is, if deflections were the only result desired, which model would you use?

There are countless modeling situations which could be examined. The reader is urged to read the literature, and peruse the tutorials available from the software vendors.<sup>14</sup>

## 19–8

### Thermal Stresses

A heat transfer analysis can be performed on a structural component including the effects of heat conduction, convection, and/or radiation. After the heat transfer analysis is completed, the same model can be used to determine the resulting thermal stresses. For sake of a simple illustration, we will model a 10 in  $\times$  4 in, 0.25-in-thick steel plate with a centered 1.0-in-diameter hole. The plate is supported as shown in Fig. 19–9a, and the temperatures of the ends are maintained at temperatures of 100°F and 0°F. Other than at the walls, all surfaces are thermally insulated. Before placing the plate between the walls, the initial temperature of the plate was 0°F. The thermal coefficient of expansion for steel is  $\alpha_s = 6.5 \times 10^{-6} \text{ } ^\circ\text{F}^{-1}$ . The plate was meshed with 1312 two-dimensional elements, with the mesh refined along the border of the hole. Figure 19–9b shows the temperature contours of the steady-state temperature distribution obtained by the FEA. Using the same elements for a linear stress analysis, where the temperatures were transferred from the heat transfer analysis, Fig. 19–9c shows the resulting stress contours. As expected, the maximum compressive stresses occurred at the top and bottom of the hole; with a magnitude of 31.9 kpsi.

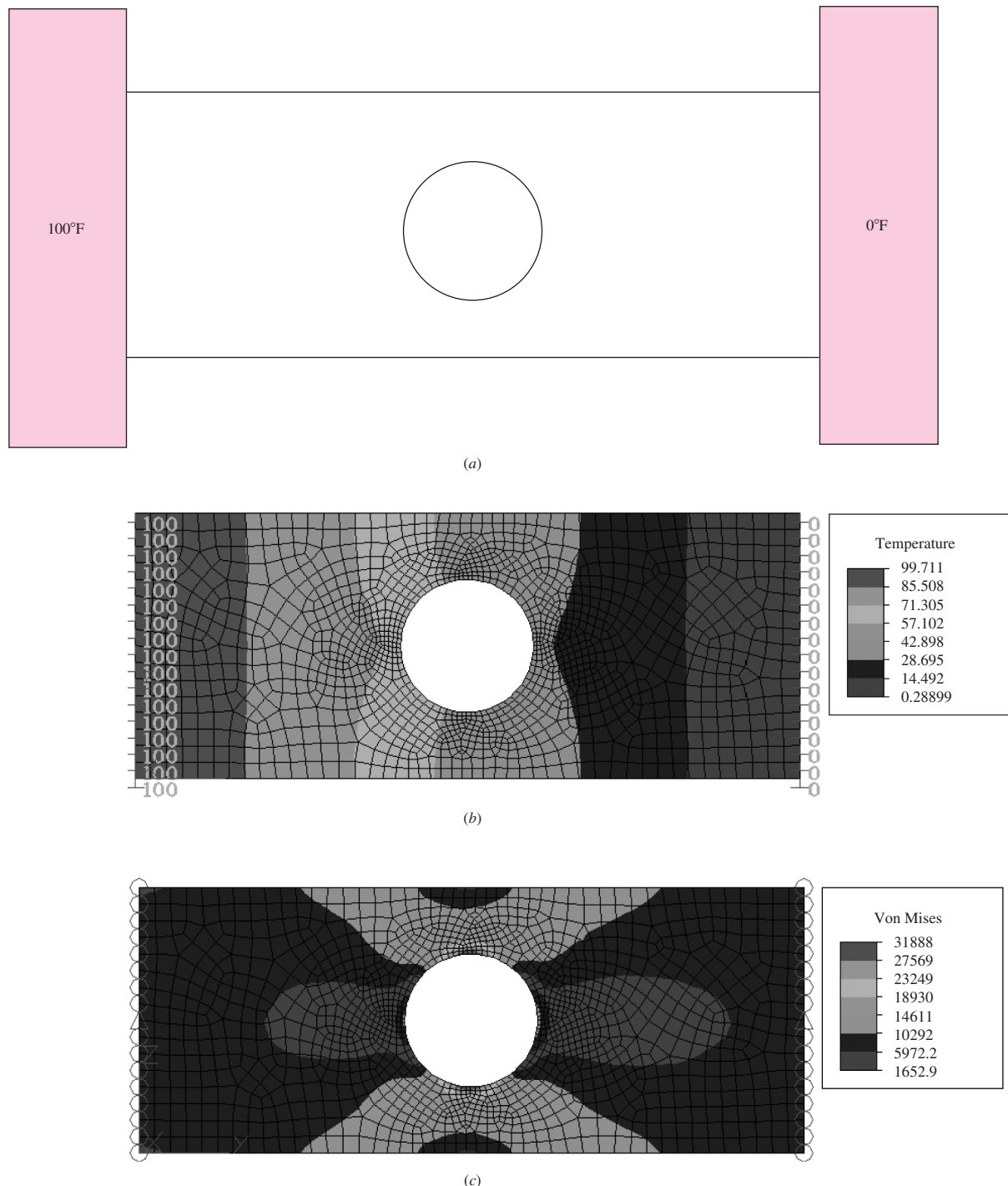
## 19–9

### Critical Buckling Load

Finite elements can be used to predict the *critical buckling load* for a thin-walled structure. An example was shown in Fig. 4–25 (p. 190). Another example can be seen in Fig. 19–10a, which is a thin-walled aluminum beverage can. A specific pressure was applied to the top surface. The bottom of the can was constrained in translation vertically, the center node of the bottom of the can was constrained in translation in all three directions, and one outer node on the can bottom was constrained in translation tangentially. This prevents rigid-body motion, and provides vertical support for the bottom of the can with unconstrained motion of the bottom of the can horizontally. The finite element software returns a value of the load multiplier, which, when multiplied with the total applied force, indicates the critical buckling load. Buckling analysis is an eigenvalue problem, and a reader who reviews a basic mechanics of materials

---

<sup>14</sup>See, for example, R. D. Cook, *Finite Element Modeling for Stress Analysis*, Wiley & Sons, New York, 1995; and R. G. Budynas, *Advanced Strength and Applied Stress Analysis*, 2nd ed., McGraw-Hill, New York, 1999, Chap. 10.

**Figure 19-9**

(a) Plate supported at ends and maintained at the temperatures shown; (b) steady-state temperature contours; (c) thermal stress contours where the initial temperature of the plate was  $0^{\circ}\text{F}$ .

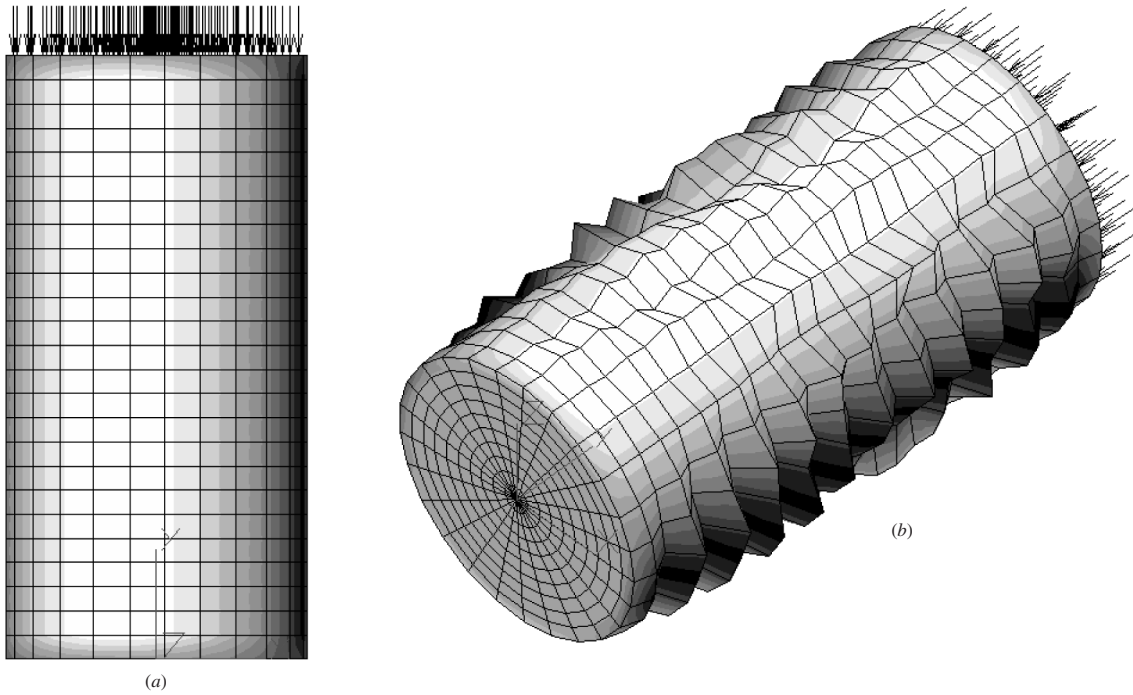


**Figure 19-10**

(a) Thin-walled aluminum beverage container loaded vertically downward on the top surface; (b) isometric view of the buckled can (deflections greatly exaggerated).

textbook would find there is a deflection mode shape associated with the critical load. The buckling mode shape for the buckled beverage can is shown in Fig. 19–10b.

## 19–10

### Vibration Analysis

The design engineer may be concerned as to how a component behaves relative to dynamic input, which results in vibration. For vibration, most finite element packages start with a *modal analysis* of the component. This provides the natural frequencies and mode shapes that the component naturally vibrates at. These are called the eigenvalues and eigenvectors of the component. Next, this solution can be transferred (much the same as for thermal stresses) to solvers for forced vibration analyses, such as frequency response, transient impact, or random vibration, to see how the component's modes behave to dynamic input. The mode shape analysis is primarily based on stiffness and the resulting deflections. Thus, similar to static stress analysis, simpler models will suffice. However, if, when solving forced response problems, stresses are desired, a more detailed model is necessary (similar to the shaft illustration given in Sec. 19–7).

A modal analysis of the beam model without the bearing steps was performed for a 20-element beam model,<sup>15</sup> and the 56 384-element brick and tetrahedron model.

<sup>15</sup>For static deflection analysis, only three beam elements were necessary. However, because of mass distribution for the dynamics problem, more beam elements are necessary.

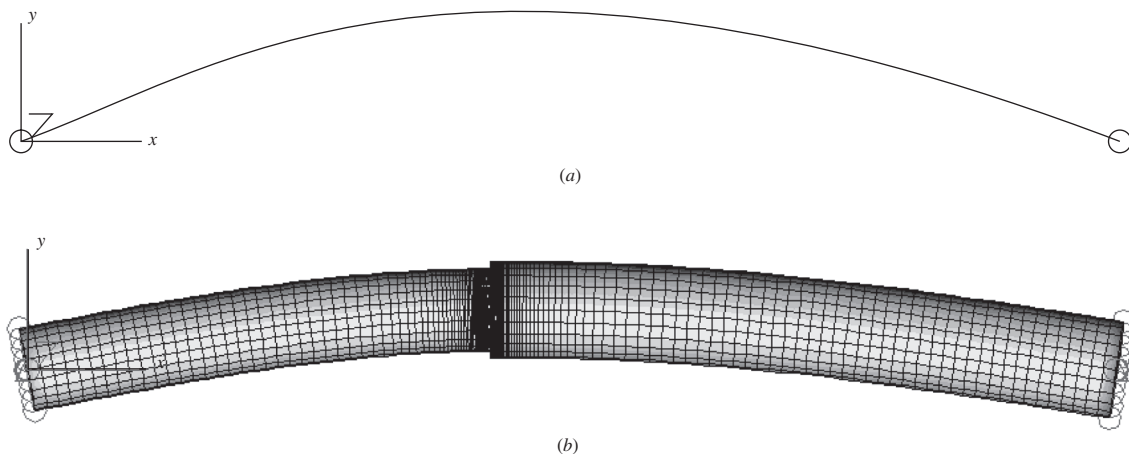


**Figure 19-11**

First free vibration mode of step beam. (a) Twenty-element beam model,  $f_1 = 322$  Hz; (b) 56 384-element brick and tetrahedron model,  $f_1 = 316$  Hz.

Needless to say, the beam model took less than 9 seconds to solve, whereas the solid model took *considerably* longer. The first (fundamental) vibration mode was bending and is shown in Fig. 19-11 for both models, together with the respective frequencies. The difference between the frequencies is about 1.9 percent. Further note that the mode shape is just that, a shape. The actual magnitudes of the deflections are unknown, only their relative values are known. Thus, any scale factor can be used to exaggerate the view of the deflection shape.

The convergence of the 20-element model was checked by doubling the number of elements. This resulted in no change.

Figure 19-12 provides the frequencies and shapes for the second mode.<sup>16</sup> Here, the difference between the models is 3.6 percent.

As stated earlier, once the mode shapes are obtained, the response of the structure to various dynamic loadings, such as harmonic, transient, or random input, can be obtained. This is accomplished by using the mode shapes together with modal superposition. The method is called *modal analysis*.<sup>17</sup>

## 19-11 Summary

As stated in Sec. 1-4, the mechanical design engineer has many powerful computational tools available today. Finite-element analysis is one of the most important and is easily integrated into the computer-aided engineering environment. Solid-modeling

---

<sup>16</sup>Note: Both models exhibited repeated frequencies and mode shapes for each bending mode. Since the beam and the bearing supports (boundary conditions) are axisymmetric, the bending modes are the same in all transverse planes. So, the second mode shown in Fig. 19-12 is the next unrepeated mode.

<sup>17</sup>See S. S. Rao, *Mechanical Vibrations*, 4th ed., Pearson Prentice Hall, Upper Saddle River, NJ, 2004, Sec. 6.14.

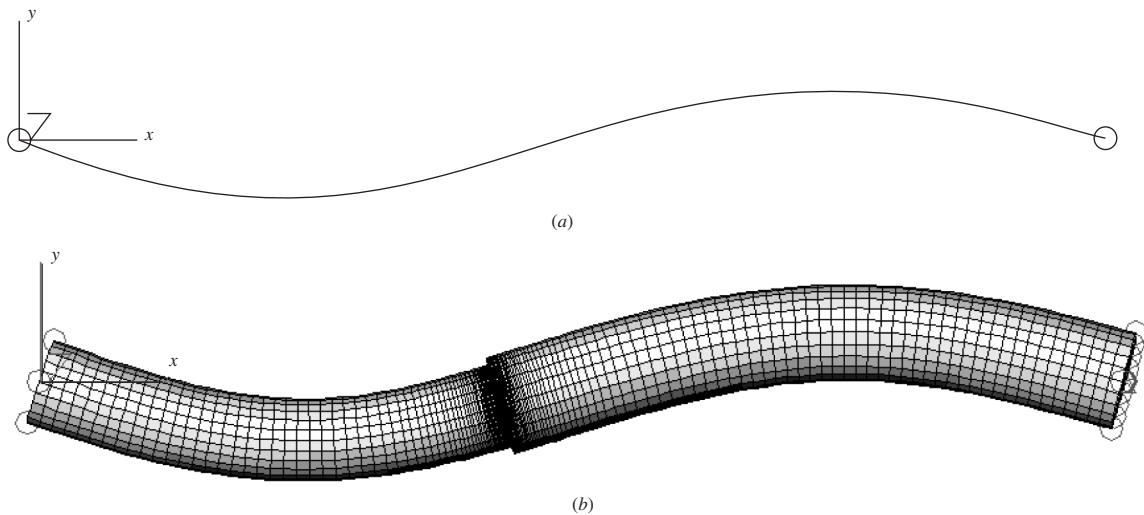


**Figure 19-12**

Second free-vibration mode of step beam. (a) Twenty-element beam model,  $f_2 = 1296$  Hz; (b) 56 384-element brick and tetrahedron model,  $f_2 = 1249$  Hz.

CAD software provides an excellent platform for the easy creation of FEA models. Several types of analysis have been described in this chapter, using some fairly simple illustrative problems. The purpose of this chapter, however, was to discuss some basic considerations of FEA element configurations, parameters, modeling considerations, and solvers, and not to necessarily describe complex geometric situations. Finite-element theory and applications is a vast subject, and will take years of experience before one becomes knowledgeable and skilled with the technique. There are many sources of information on the topic in various textbooks; FEA software suppliers (such as ANSYS, MSC/NASTRAN, and Algor) provide case studies, user's guides, user's group newsletters, tutorials, etc.; and the Internet provides many sources. Footnotes 11, 12, and 14 referenced some textbooks on FEA. Additional references are cited below.

### Additional FEA References

- K. J. Bathe, *Finite Element Procedures*, Prentice Hall, Englewood Cliffs, NJ, 1996.
- R. D. Cook, D. S. Malkus, M. E. Plesha, and R. J. Witt, *Concepts and Applications of Finite Element Analysis*, 4th ed., Wiley, New York, 2001.
- D. L. Logan, *A First Course in the Finite Element Method*, 4th ed., Nelson, a division of Thomson Canada Limited, Toronto, 2007.
- J. N. Reddy, *An Introduction to the Finite Element Method*, 3rd ed., McGraw-Hill, New York, 2002.
- O. C. Zienkiewicz and R. L. Taylor, *The Finite Element Method*, 4th ed., Vols. 1 and 2, McGraw-Hill, New York, 1989 and 1991.

## PROBLEMS

The following problems are to be solved by FEA. It is recommended that you also solve the problems analytically, compare the two results, and explain any differences.

**19-1**

Solve Ex. 3-6.

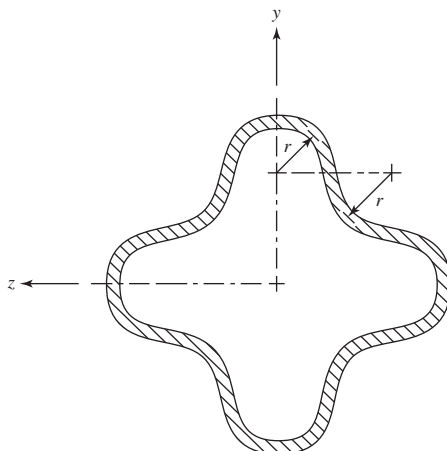
**19-2**

For Ex. 3-10, apply a torque of 23 730 lbf · in, and determine the maximum shear stress and angle of twist. Use  $\frac{1}{8}$ -in-thick plate elements.

**19-3**

The steel tube with the cross section shown is transmitting a torsional moment of 100 N · m. The tube wall thickness is 2.5 mm, all radii are  $r = 6.25$  mm, and the tube is 500 mm long. For steel, let  $E = 207$  GPa and  $\nu = 0.29$ . Determine the average shear stress in the wall and the angle of twist over the given length. Use 2.5-mm-thick plate elements.

Problem 19-3


**19-4**

For Fig. A-15-1, let  $w = 2$  in,  $d = 0.3$  in, and estimate  $K_t$ . Use 1/4 symmetry and 1/8-in-thick 2-D elements.

**19-5**

For Fig. A-15-3, let  $w = 1.5$  in,  $d = 1.0$  in,  $r = 0.10$  in, and estimate  $K_t$ . Use 1/4 symmetry and 1/8-in-thick 2-D elements.

**19-6**

For Fig. A-15-5, let  $D = 3$  in,  $d = 2$  in,  $r = 0.25$  in, and estimate  $K_t$ . Use 1/2 symmetry and 1/8-in-thick 2-D elements.

**19-7**

Solve Prob. 3-122, using solid elements. *Note:* You may omit the top part of the eyebolt above the applied force.

**19-8**

Solve Prob. 3-132, using solid elements. *Note:* Since there is a plane of symmetry, a one-half model can be constructed. However, be very careful to constrain the plane of symmetry properly to assure symmetry without overconstraint.

**19-9**

Solve Ex. 4-11, with  $F = 10$  lbf,  $d = 1/8$  in,  $a = 0.5$  in,  $b = 1$  in,  $c = 2$  in,  $E = 30$  Mpsi, and  $\nu = 0.29$ , using beam elements.

**19-10**

Solve Ex. 4-13, modeling Fig. 4-14b with 2-D elements of 2-in thickness. Since this example uses symmetry, be careful to constrain the boundary conditions of the bottom horizontal surface appropriately.

- 19-11** Solve Prob. 4-12, using beam elements.
- 19-12** Solve Prob. 4-47, using beam elements. Pick a diameter, and solve for the slopes. Then, use Eq. 7-18, p. 381, to readjust the diameter. Use the new diameter to verify.
- 19-13** Solve Prob. 4-63, using beam elements.
- 19-14** Solve Prob. 4-78, using solid elements. Use a one-half model with symmetry. Be very careful to constrain the plane of symmetry properly to assure symmetry without overconstraint.
- 19-15** Solve Prob. 4-79, using beam elements. Use a one-half model with symmetry. At the plane of symmetry, constrain translation and rotation.
- 19-16** Solve Prob. 4-80, using beam elements. Model the problem two ways: (a) Model the entire wire form, using, 200 elements. (b) Model half the entire wire form, using 100 elements and symmetry. That is, model the form from point *A* to point *C*. Apply half the force at the top, and constrain the top horizontally and in rotation in the plane.
- 19-17** Solve Prob. 4-88, using beam elements.
- 19-18** Solve Prob. 10-42, using beam elements.
- 19-19** An aluminum cylinder ( $E_a = 70 \text{ MPa}$ ,  $\nu_a = 0.33$ ) with an outer diameter of 150 mm and inner diameter of 100 mm is to be press-fitted over a stainless-steel cylinder ( $E_s = 190 \text{ MPa}$ ,  $\nu_s = 0.30$ ) with an outer diameter of 100.20 mm and inner diameter of 50 mm. Determine (a) the interface pressure  $p$  and (b) the maximum tangential stresses in the cylinders.

Solve the press-fit problem, using the following procedure. Using the plane-stress two-dimensional element, utilizing symmetry, create a quarter model meshing elements in the radial and tangential directions. The elements for each cylinder should be assigned their unique material properties. The interface between the two cylinders should have common nodes. To simulate the press fit, the inner cylinder will be forced to expand thermally. Assign a coefficient of expansion and temperature increase,  $\alpha$  and  $\Delta T$ , respectively, for the inner cylinder. Do this according to the relation  $\delta = \alpha \Delta T b$ , where  $\delta$  and  $b$  are the radial interference and the outer radius of the inner member, respectively. Nodes along the straight edges of the quarter model should be fixed in the tangential directions, and free to deflect in the radial direction.

*This page intentionally left blank*

# 20

## Statistical Considerations

### Chapter Outline

#### **20-1**

Random Variables **978**

#### **20-2**

Arithmetic Mean, Variance, and Standard Deviation **980**

#### **20-3**

Probability Distributions **985**

#### **20-4**

Propagation of Error **992**

#### **20-5**

Linear Regression **994**

Statistics in mechanical design provides a method of dealing with characteristics whose values are variable. Products manufactured in large quantities—automobiles, watches, lawnmowers, washing machines, for example—have a life that is variable. One automobile may have so many defects that it must be repaired repeatedly during the first few months of operation while another may operate satisfactorily for years, requiring only minor maintenance.

Methods of quality control are deeply rooted in the use of statistics, and engineering designers need a knowledge of statistics to conform to quality-control standards. The variability inherent in limits and fits, in stress and strength, in bearing clearances, and in a multitude of other characteristics must be described numerically for proper control. It is not satisfactory to say that a product is expected to have a long and troublefree life. We must express such things as product life and product reliability in numerical form in order to achieve a specific quality goal. As noted in Sec. 1–10, uncertainties abound and require quantitative treatment. The algebra of real numbers, by itself, is not well-suited to describing the presence of variation.

It is clear that consistencies in nature are stable, not in magnitude, but in the *pattern of variation*. Evidence gathered from nature by measurement is a mixture of systematic and random effects. It is the role of statistics to separate these, and, through the sensitive use of data, illuminate the obscure.

Some students will start this book after completing a formal course in statistics while others may have had brief encounters with statistics in their engineering courses. This contrast in background, together with space and time constraints, makes it very difficult to present an extensive integration of statistics with mechanical engineering design at this stage. Beyond first courses in mechanical design and engineering statistics, the student can begin to meaningfully integrate the two in a second course in design.

The intent of this chapter is to introduce some statistical concepts associated with basic reliability goals.

## 20–1

### Random Variables

Consider an experiment to measure strength in a collection of 20 tensile-test specimens that have been machined from a like number of samples selected at random from a car-load shipment of, say, UNS G10200 cold-drawn steel. It is reasonable to expect that there will be differences in the ultimate tensile strengths  $S_{ut}$  of each of the individual test specimens. Such differences may occur because of differences in the sizes of the specimens, in the strength of the material itself, or both. Such an experiment is called a *random experiment*, because the specimens are selected at random. The strength  $S_{ut}$  determined by this experiment is called a *random*, or a *stochastic, variable*. So a random variable is a variable quantity, such as strength, size, or weight, whose value depends on the outcome of a random experiment.

Let us define a random variable  $x$  as the sum of the numbers obtained when two dice are tossed. Either die can display any number from 1 to 6. Figure 20–1 displays all possible outcomes in what is called the *sample space*. Note that  $x$  has a specific value

**Figure 20–1**

Sample space showing all possible outcomes of the toss of two dice.

1,1	1,2	1,3	1,4	1,5	1,6
2,1	2,2	2,3	2,4	2,5	2,6
3,1	3,2	3,3	3,4	3,5	3,6
4,1	4,2	4,3	4,4	4,5	4,6
5,1	5,2	5,3	5,4	5,5	5,6
6,1	6,2	6,3	6,4	6,5	6,6

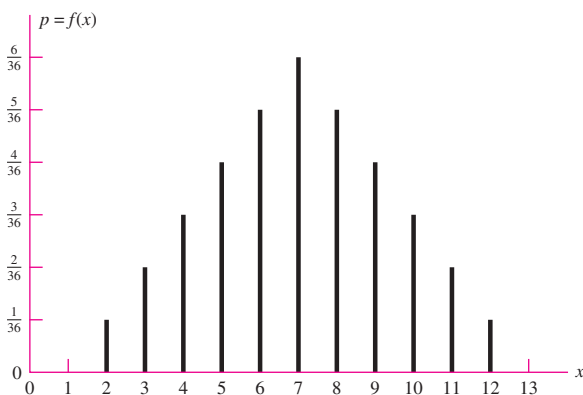
**Table 20-1**

A Probability Distribution

<b>x</b>	<b>2</b>	<b>3</b>	<b>4</b>	<b>5</b>	<b>6</b>	<b>7</b>	<b>8</b>	<b>9</b>	<b>10</b>	<b>11</b>	<b>12</b>
$f(x)$	$\frac{1}{36}$	$\frac{2}{36}$	$\frac{3}{36}$	$\frac{4}{36}$	$\frac{5}{36}$	$\frac{6}{36}$	$\frac{5}{36}$	$\frac{4}{36}$	$\frac{3}{36}$	$\frac{2}{36}$	$\frac{1}{36}$

**Figure 20-2**

Frequency distribution.

**Table 20-2**

A Cumulative Probability Distribution

<b>x</b>	<b>2</b>	<b>3</b>	<b>4</b>	<b>5</b>	<b>6</b>	<b>7</b>	<b>8</b>	<b>9</b>	<b>10</b>	<b>11</b>	<b>12</b>
$F(x)$	$\frac{1}{36}$	$\frac{3}{36}$	$\frac{6}{36}$	$\frac{10}{36}$	$\frac{15}{36}$	$\frac{21}{36}$	$\frac{26}{36}$	$\frac{30}{36}$	$\frac{33}{36}$	$\frac{35}{36}$	$\frac{36}{36}$

for each possible outcome—for example, the event 5, 4;  $x = 5 + 4 = 9$ . It is useful to form a table showing the values of  $x$  and the corresponding values of the probability of  $x$ , called  $p = f(x)$ . This is easily done from Fig. 20-1 merely by adding each outcome, determining how many times a specific value of  $x$  arises, and dividing by the total number of possible outcomes. The results are shown in Table 20-1. Any table like this, listing all possible values of a random variable and with the corresponding probabilities, is called a *probability distribution*.

The values of Table 20-1 are plotted in graphical form in Fig. 20-2. Here it is clear that the probability is a function of  $x$ . This *probability function*  $p = f(x)$  is often called the *frequency function* or, sometimes, the *probability density function* (PDF). The probability that  $x$  is less than or equal to a certain value  $x_i$  can be obtained from the probability function by summing the probability of all  $x$ 's up to and including  $x_i$ . If we do this with Table 20-1, letting  $x_i$  equal 2, then 3, and so on, up to 12, we get Table 20-2, which is called a *cumulative probability distribution*. The function  $F(x)$  in Table 20-2 is called a *cumulative density function* (CDF) of  $x$ . In terms of  $f(x)$  it may be expressed mathematically in the general form

$$F(x_i) = \sum_{x_j \leq x_i} f(x_j) \quad (20-1)$$

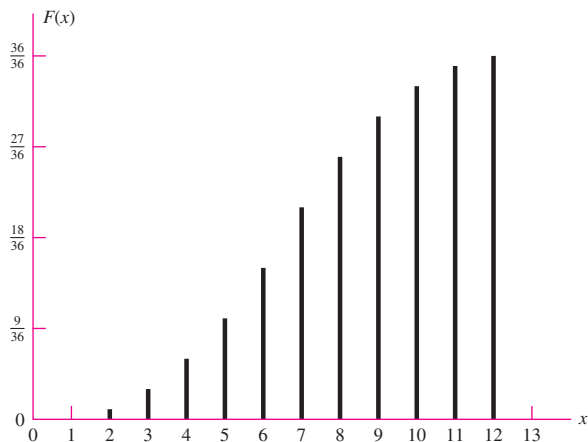
The cumulative distribution may also be plotted as a graph (Fig. 20-3).

The variable  $x$  of this example is called a *discrete random variable*, because  $x$  has only discrete values. A *continuous random variable* is one that can take on any value in a specified interval; for such variables, graphs like Figs. 20-2 and 20-3 would be plotted as continuous curves. For a continuous probability density function  $F(x)$ , the probability of obtaining an observation equal to or less than  $x$  is given by

$$F(x) = \int_{-\infty}^x f(x) dx \quad (20-2)$$

**Figure 20–3**

Cumulative frequency distribution.



where  $f(x)$  is the probability per unit  $x$ . When  $x \rightarrow \infty$ , then

$$\int_{-\infty}^{\infty} f(x) dx = 1 \quad (20-3)$$

Differentiation of Eq. (20-2) gives

$$\frac{dF(x)}{dx} = f(x) \quad (20-4)$$

## 20-2

### Arithmetic Mean, Variance, and Standard Deviation

In studying the variations in the mechanical properties and characteristics of mechanical elements, we shall generally be dealing with a finite number of elements. The total number of elements, called the *population*, may in some cases be quite large. In such cases it is usually impractical to measure the characteristics of each member of the population, because this involves destructive testing in some cases, and so we select a small part of the group, called a *sample*, for these determinations. Thus the *population* is the entire group, and the *sample* is a part of the population.

The arithmetic mean of a sample, called the *sample mean*, consisting of  $N$  elements, is defined by the equation

$$\bar{x} = \frac{x_1 + x_2 + x_3 + \cdots + x_N}{N} = \frac{1}{N} \sum_{i=1}^N x_i \quad (20-5)$$

Besides the arithmetic mean, it is useful to have another kind of measure that will tell us something about the spread, or dispersion, of the distribution. For any random variable  $x$ , the deviation of the  $i$ th observation from the mean is  $x_i - \bar{x}$ . But since the sum of the deviations so defined is always zero, we square them, and define *sample variance* as

$$s_x^2 = \frac{(x_1 - \bar{x})^2 + (x_2 - \bar{x})^2 + \cdots + (x_N - \bar{x})^2}{N-1} = \frac{1}{N-1} \sum_{i=1}^N (x_i - \bar{x})^2 \quad (20-6)$$

The *sample standard deviation*, defined as the square root of the sample variance, is

$$s_x = \sqrt{\frac{1}{N-1} \sum_{i=1}^N (x_i - \bar{x})^2} \quad (20-7)$$

Equation (20-7) is not well-suited for use in a calculator. For such purposes, use the alternative form

$$s_x = \sqrt{\frac{\sum_{i=1}^N x_i^2 - \left(\sum_{i=1}^N x_i\right)^2 / N}{N-1}} = \sqrt{\frac{\sum_{i=1}^N x_i^2 - N\bar{x}^2}{N-1}} \quad (20-8)$$

for the standard deviation.

It should be observed that some authors define the variance and the standard deviation by using  $N$  instead of  $N - 1$  in the denominator. For large values of  $N$ , there is very little difference. For small values, the denominator  $N - 1$  actually gives a better estimate of the variance of the population from which the sample is taken.

Equations (20-5) to (20-8) apply specifically to the *sample* of a population. When an entire population is considered, the same equations apply, but  $\bar{x}$  and  $s_x$  are replaced with the symbols  $\mu_x$  and,  $\hat{\sigma}_x$  respectively. The circumflex accent mark  $\hat{\cdot}$ , or “hat,” is used to avoid confusion with normal stress. For the population variance and standard deviation,  $N$  weighting is used in the denominators instead of  $N - 1$ .

Sometimes we are going to be dealing with the standard deviation of the strength of an element. So you must be careful not to be confused by the notation. Note that we are using the *capital letter S* for *strength* and the *lowercase letter s* for *standard deviation* as shown in the caption of the histogram in Fig. 20-4.

Figure 20-4 is called a *discrete frequency histogram*, which gives the number of occurrences, or class frequency  $f_i$ , within a given range. If the data are grouped in this fashion, then the mean and standard deviation are given by

$$\bar{x} = \frac{1}{N} \sum_{i=1}^k f_i x_i \quad (20-9)$$

and

$$s_x = \sqrt{\frac{\sum_{i=1}^k f_i x_i^2 - \left[\left(\sum_{i=1}^k f_i x_i\right)^2 / N\right]}{N-1}} = \sqrt{\frac{\sum_{i=1}^k f_i x_i^2 - N\bar{x}^2}{N-1}} \quad (20-10)$$

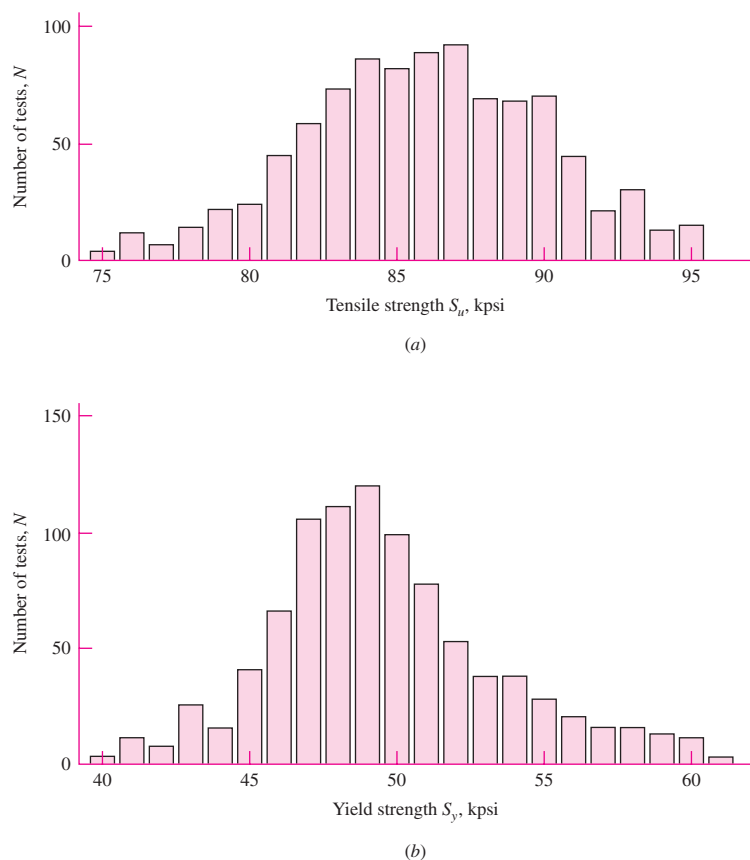
Here  $x_i$ ,  $f_i$ , and  $k$  are class midpoint, frequency of occurrences within the range of the class, and the total number of classes, respectively. Also, the cumulative density function that gives the probability of an occurrence at class mark of  $x_i$  or less is

$$F_i = \frac{f_i w_i}{2} + \sum_{j=1}^{i-1} f_j w_j \quad (20-11)$$

where  $w_i$  represents the class width at  $x_i$ . For Fig. 20-4a,  $k = 21$  and the class width is constant at  $w = 1$  kpsi.

**Figure 20-4**

Distribution of tensile properties of hot-rolled UNS G10350 steel, as rolled. These tests were made from round bars varying in diameter from 1 to 9 in. (a) Tensile-strength distributions from 930 heats;  $\bar{S}_u = 86.0$  kpsi,  $s_{S_u} = 4.94$  kpsi. (b) Yield-strength distribution from 899 heats;  $\bar{S}_y = 49.5$  kpsi,  $s_{S_y} = 5.36$  kpsi. (From Metals Handbook, vol. 1, 8th ed., American Society for Metals, Materials Park, OH 44073-0002, fig. 22, p. 64. Reprinted by permission of ASM International®, www.asminternational.org.)



### Notation

In this book, we follow the convention of designating vectors by boldface characters, indicative of the fact that two or three quantities, such as direction and magnitude, are necessary to describe them. The same convention is widely used for random variables that can be characterized by specifying a mean and a standard deviation. We shall therefore use boldface characters to designate random variables as well as vectors. No confusion between the two is likely to arise.

The terms *stochastic variable* and *variate* are also used to mean a random variable. A *deterministic quantity* is something that has a single specific value. The mean value of a population is a deterministic quantity, and so is its standard deviation. A stochastic variable can be partially described by the mean and the standard deviation, or by the mean and the *coefficient of variation* defined by

$$C_x = \frac{s_x}{\bar{x}} \quad (20-12)$$

Thus the variate  $\mathbf{x}$  for the sample can be expressed in the following two ways:

$$\mathbf{x} = \mathbf{X}(\bar{x}, s_x) = \bar{x} \mathbf{X}(1, C_x) \quad (20-13)$$

where  $\mathbf{X}$  represents a variate probability distribution function. Note that the deterministic quantities  $\bar{x}$ ,  $s_x$ , and  $C_x$  are all in normal italic font.

**EXAMPLE 20-1**

Five tons of 2-in round rod of 1030 hot-rolled steel has been received for workpiece stock. Nine standard-geometry tensile test specimens have been machined from random locations in various rods. In the test report, the ultimate tensile strength was given in kpsi. In ascending order (not necessary), these are displayed in Table 20-3. Find the mean  $\bar{x}$ , the standard deviation  $s_x$ , and the coefficient of variation  $C_x$  from the sample, such that these are best estimates of the parent population (the stock your plant will convert to product).

**Table 20-3**

Data Worksheet from  
Nine Tensile Test  
Specimens Taken from  
a Shipment of 1030  
Hot-Rolled Steel  
Barstock

$S_{ut}$ , kpsi	
x	$x^2$
62.8	3 943.84
64.4	4 147.36
65.8	4 329.64
66.3	4 395.69
68.1	4 637.61
69.1	4 774.81
69.8	4 872.04
71.5	5 112.25
74.0	5 476.00
$\sum 611.8$	41 689.24

**Solution** From Eqs. (20-5) and (20-8),

$$\bar{x} = \frac{1}{N} \sum_{i=1}^9 x_i$$

and

$$s_x = \sqrt{\frac{\sum x_i^2 - (\sum x_i)^2/N}{N-1}}$$

It is computationally efficient to generate  $\sum x$  and  $\sum x^2$  before evaluating  $\bar{x}$  and  $s_x$ . This has been done in Table 20-3.

**Answer**

$$\bar{x} = \frac{1}{9}(611.8) = 67.98 \text{ kpsi}$$

**Answer**

$$s_x = \sqrt{\frac{41 689.24 - 611.8^2/9}{9-1}} = 3.543 \text{ kpsi}$$

From Eq. (20-12),

**Answer**

$$C_x = \frac{s_x}{\bar{x}} = \frac{3.543}{67.98} = 0.0521$$

All three statistics are estimates of the parent population statistical parameters. Note that these results are independent of the distribution.

Multiple data entries may be identical or may be grouped in histogramic form to suggest a distributional shape. If the original data are lost to the designer, the grouped data can still be reduced, although with some loss in computational precision.

### EXAMPLE 20-2

The data in Ex. 20-1 have come to the designer in the histogramic form of the first two columns of Table 20-4. Using the data in this form, find the mean  $\bar{x}$ , standard deviation  $s_x$ , and the coefficient of variation  $C_x$ .

**Table 20-4**

Grouped Data of  
Ultimate Tensile  
Strength from Nine  
Tensile Test Specimens  
from a Shipment of  
1030 Hot-Rolled Steel  
Barstock

Class Midpoint $x$ , kpsi	Class Frequency $f$	Extension $fx$	Extension $fx^2$
63.5	2	127	8 064.50
66.5	2	133	8 844.50
69.5	3	208.5	14 480.75
72.5	2	145	10 513.50
	$\sum f = 9$	613.5	41 912.25

The data in Table 20-4 have been extended to provide  $\sum f_i x_i$  and  $\sum f_i x_i^2$ .

**Solution** From Eq. (20-9),

$$\text{Answer} \quad \bar{x} = \frac{1}{N} \sum_{i=1}^4 f_i x_i = \frac{1}{9}(613.5) = 68.17 \text{ kpsi}$$

From Eq. (20-10),

$$\text{Answer} \quad s_x = \sqrt{\frac{41 912.25 - 613.5^2/9}{9 - 1}} = 3.391 \text{ kpsi}$$

From Eq. (20-12),

$$\text{Answer} \quad C_x = \frac{s_x}{\bar{x}} = \frac{3.391}{68.17} = 0.0497$$

Note the small changes in  $\bar{x}$ ,  $s_x$ , and  $C_x$  due to small changes in the summation terms.

The descriptive statistics developed, whether from ungrouped or grouped data, describe the ultimate tensile strength  $S_{ut}$  of the material from which we will form parts. Such description is not possible with a single number. In fact, sometimes two or three numbers plus identification or, at least, a robust approximation of the distribution are needed. As you look at the data in Ex. 20-1, consider the answers to these questions:

- Can we characterize the ultimate tensile strength by the mean,  $\bar{S}_{ut}$ ?
- Can we take the lowest ultimate tensile strength of 62.8 kpsi as a minimum? If we do, we will encounter some lesser ultimate strengths, because some of 100 specimens will be lower.
- Can we find the distribution of the ultimate tensile strength of the 1030 stock in Ex. 20-1? Yes, but it will take more specimens and require plotting on coordinates that rectify the data string.

## 20–3 Probability Distributions

There are a number of standard discrete and continuous probability distributions that are commonly applicable to engineering problems. In this section, we will discuss four important continuous probability distributions; the *Gaussian, or normal, distribution*; the *lognormal distribution*; the *uniform distribution*; and the *Weibull distribution*.

### The Gaussian (Normal) Distribution

When Gauss asked the question, What distribution is the most likely parent to a set of data?, the answer was the distribution that bears his name. The *Gaussian, or normal, distribution* is an important one whose probability density function is expressed in terms of its mean  $\mu_x$  and its standard deviation  $\hat{\sigma}_x$  as

$$f(x) = \frac{1}{\hat{\sigma}_x \sqrt{2\pi}} \exp \left[ -\frac{1}{2} \left( \frac{x - \mu_x}{\hat{\sigma}_x} \right)^2 \right] \quad (20-14)$$

With the notation described in Sec. 20–2, the normally distributed variate  $x$  can be expressed as

$$\mathbf{x} = \mathbf{N}(\mu_x, \hat{\sigma}_x) = \mu_x \mathbf{N}(1, C_x) \quad (20-15)$$

where  $\mathbf{N}$  represents the normal distribution function given by Eq. (20–14).

Since Eq. (20–14) is a probability density function, the area under it, as required, is unity. Plots of Eq. (20–14) are shown in Fig. 20–5 for small and large standard deviations. The bell-shaped curve is taller and narrower for small values of  $\hat{\sigma}$  and shorter and broader for large values of  $\hat{\sigma}$ . Integration of Eq. (20–14) to find the cumulative density function  $F(x)$  is not possible in closed form, but must be accomplished numerically. To avoid the need for many tables for different values of  $\mu$  and  $\hat{\sigma}$ , the deviation from the mean is expressed in units of standard deviation by the transform

$$z = \frac{x - \mu_x}{\hat{\sigma}_x} \quad (20-16)$$

The integral of the transform is tabulated in Table A–10 and sketched in Fig. 20–6. The value of the normal cumulative density function is used so often, and manipulated in so

**Figure 20–5**

The shape of the normal distribution curve: (a) small  $\hat{\sigma}$ ; (b) large  $\hat{\sigma}$ .

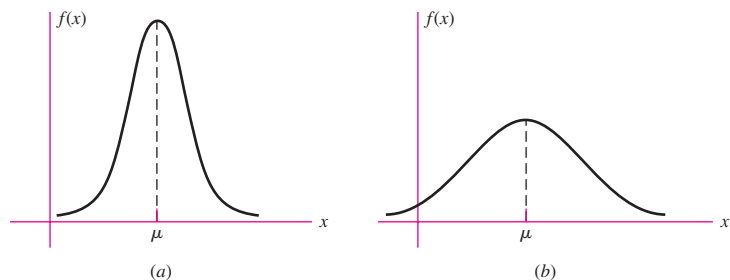
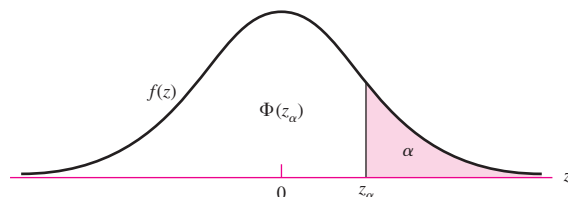


**Figure 20–6**

The standard normal distribution.



many equations, that it has its own particular symbol,  $\Phi(z)$ . The transformation variate  $z$  is normally distributed, with a mean of zero and a standard deviation and variance of unity. That is,  $z = N(0, 1)$ . The probability of an observation less than  $z$  is  $\Phi(z)$  for negative values of  $z$  and  $1 - \Phi(z)$  for positive values of  $z$  in Table A-10.

### EXAMPLE 20-3

In a shipment of 250 connecting rods, the mean tensile strength is found to be 45 kpsi and the standard deviation 5 kpsi.

- Assuming a normal distribution, how many rods can be expected to have a strength less than 39.5 kpsi?
- How many are expected to have a strength between 39.5 and 59.5 kpsi?

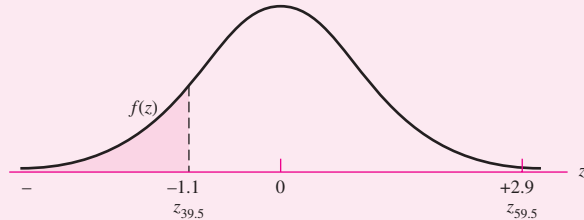
**Solution**

(a) Substituting in Eq. (20-16) gives the standardized  $z$  variable as

$$z_{39.5} = \frac{x - \mu_x}{\hat{\sigma}_x} = \frac{S - \bar{S}}{\hat{\sigma}_S} = \frac{39.5 - 45}{5} = -1.10$$

The probability that the strength is less than 39.5 kpsi can be designated as  $F(z) = \Phi(-1.10)$ . Using Table A-10, and referring to Fig. 20-7, we find  $\Phi(z_{39.5}) = 0.1357$ . So the number of rods having a strength less than 39.5 kpsi is,

| **Figure 20-7**



**Answer**

$$N\Phi(z_{39.5}) = 250(0.1357) = 33.9 \approx 34$$

because  $\Phi(z_{39.5})$  represents the proportion of the population  $N$  having a strength less than 39.5 kpsi.

- Corresponding to  $S = 59.5$  kpsi, we have

$$z_{59.5} = \frac{59.5 - 45}{5} = 2.90$$

Referring again to Fig. 20-7, we see that the probability that the strength is less than 59.5 kpsi is  $F(z) = \Phi(z_{59.5})$ . Since the  $z$  variable is positive, we need to find the value complementary to unity. Thus, from Table A-10,

$$\Phi(2.90) = 1 - \Phi(-2.90) = 1 - 0.00187 = 0.99813$$

The probability that the strength lies between 39.5 and 59.5 kpsi is the area between the ordinates at  $z_{39.5}$  and  $z_{59.5}$  in Fig. 20-7. This probability is found to be

$$\begin{aligned} p &= \Phi(z_{59.5}) - \Phi(z_{39.5}) = \Phi(2.90) - \Phi(-1.10) \\ &= 0.99813 - 0.1357 = 0.86243 \end{aligned}$$

Therefore the number of rods expected to have strengths between 39.5 and 59.5 kpsi is

**Answer**

$$Np = 250(0.862) = 215.5 \approx 216$$

### The Lognormal Distribution

Sometimes random variables have the following two characteristics:

- The distribution is asymmetrical about the mean.
- The variables have only positive values.

Such characteristics rule out the use of the normal distribution. There are several other distributions that are potentially useful in such situations, one of them being the log-normal (written as a single word) distribution. Especially when life is involved, such as fatigue life under stress or the wear life of rolling bearings, the lognormal distribution may be a very appropriate one to use.

The *lognormal distribution* is one in which the logarithms of the variate have a normal distribution. Thus the variate itself is said to be lognormally distributed. Let this variate be expressed as

$$x = LN(\mu_x, \hat{\sigma}_x) \quad (a)$$

Equation (a) states that the random variable  $x$  is distributed lognormally (*not a logarithm*) and that its mean value is  $\mu_x$  and its standard deviation is  $\hat{\sigma}_x$ .

Now use the transformation

$$y = \ln x \quad (b)$$

Since, by definition,  $y$  has a normal distribution, we can write

$$y = N(\mu_y, \hat{\sigma}_y) \quad (c)$$

This equation states that the random variable  $y$  is normally distributed, its mean value is  $\mu_y$ , and its standard deviation is  $\hat{\sigma}_y$ .

It is convenient to think of Eq. (a) as designating the *parent, or principal, distribution* while Eq. (b) represents the *companion, or subsidiary, distribution*.

The probability density function (PDF) for  $x$  can be derived from that for  $y$ ; see Eq. (20–14), and substitute  $y$  for  $x$  in that equation. Thus the PDF for the companion distribution is found to be

$$f(x) = \begin{cases} \frac{1}{x\hat{\sigma}_y\sqrt{2\pi}} \exp\left[-\frac{1}{2}\left(\frac{\ln x - \mu_y}{\hat{\sigma}_y}\right)^2\right] & \text{for } x > 0 \\ 0 & \text{for } x \leq 0 \end{cases} \quad (20-17)$$

The companion mean  $\mu_y$  and standard deviation  $\hat{\sigma}_y$  in Eq. (20–17) are obtained from

$$\mu_y = \ln \mu_x - \ln \sqrt{1 + C_x^2} \approx \ln \mu_x - \frac{1}{2} C_x^2 \quad (20-18)$$

$$\hat{\sigma}_y = \sqrt{\ln(1 + C_x^2)} \approx C_x \quad (20-19)$$

These equations make it possible to use Table A–10 for statistical computations and eliminate the need for a special table for the lognormal distribution.

#### EXAMPLE 20–4

One thousand specimens of 1020 steel were tested to rupture and the ultimate tensile strengths were reported as grouped data in Table 20–5. From Eq. (20–9),

$$\bar{x} = \frac{63,625}{1000} = 63.625 \text{ kpsi}$$

**Table 20–5**

Worksheet for Ex. 20–4

Class Midpoint, kpsi	Frequency $f_i$	Extension $x_i f_i$	$x_i^2 f_i$	Observed PDF $f_i/(Nw)^*$	Normal Density $f(x)$	Lognormal Density $g(x)$
56.5	2	113.0	6 384.5	0.002	0.0035	0.0026
57.5	18	1 035.0	59 512.5	0.018	0.0095	0.0082
58.5	23	1 345.5	78 711.75	0.023	0.0218	0.0209
59.5	31	1 844.5	109 747.75	0.031	0.0434	0.0440
60.5	83	5 021.5	303 800.75	0.083	0.0744	0.0773
61.5	109	6 703.5	412 265.25	0.109	0.110	0.1143
62.5	138	8 625.0	539 062.5	0.138	0.140	0.1434
63.5	151	9 588.5	608 869.75	0.151	0.1536	0.1539
64.5	139	8 965.5	578 274.75	0.139	0.1453	0.1424
65.5	130	8 515.0	577 732.5	0.130	0.1184	0.1142
66.5	82	5 453.0	362 624.5	0.082	0.0832	0.0800
67.5	49	3 307.5	223 256.25	0.049	0.0504	0.0493
68.5	28	1 918.0	131 382.0	0.028	0.0263	0.0268
69.5	11	764.5	53 132.75	0.011	0.0118	0.0129
70.5	4	282.0	19 881.0	0.004	0.0046	0.0056
71.5	2	143.0	10 224.5	0.002	0.0015	0.0022
$\sum$	1 000	63 625	4 054 864	1.000		

\*To compare discrete frequency data with continuous probability density functions  $f_i$  must be divided by  $Nw$ . Here,  $N$  = sample size = 1000;  $w$  = width of class interval = 1 kpsi.

From Eq. (20–10),

$$s_x = \sqrt{\frac{4 054 864 - 63 625^2/1000}{1000 - 1}} = 2.594 245 = 2.594 \text{ kpsi}$$

$$C_x = \frac{s_x}{\bar{x}} = \frac{2.594 245}{63.625} = 0.040 773 = 0.0408$$

From Eq. (20–14) the probability density function for a normal distribution with a mean of 63.625 and a standard deviation of 2.594 245 is

$$f(x) = \frac{1}{2.594 245 \sqrt{2\pi}} \exp \left[ -\frac{1}{2} \left( \frac{x - 63.625}{2.594 245} \right)^2 \right]$$

For example,  $f(63.625) = 0.1538$ . The probability density  $f(x)$  is evaluated at class midpoints to form the column of normal density in Table 20–5.

**EXAMPLE 20–5**

Continue Ex. 20–4, but fit a lognormal density function.

**Solution**

From Eqs. (20–18) and (20–19),

$$\mu_y = \ln \mu_x - \ln \sqrt{1 + C_x^2} = \ln 63.625 - \frac{1}{2} \ln(1 + 0.040773^2) = 4.1522$$

$$\hat{\sigma}_y = \sqrt{\ln(1 + C_x^2)} = \sqrt{\ln(1 + 0.040773^2)} = 0.0408$$

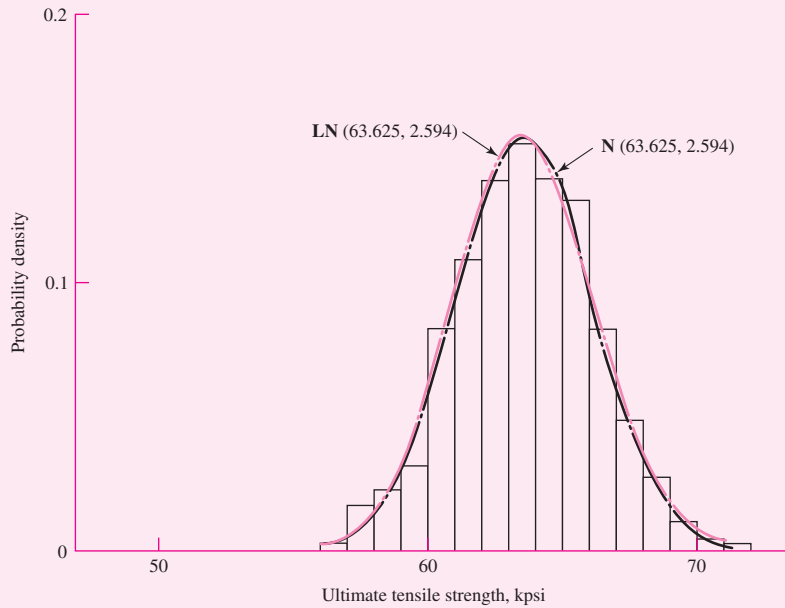
The probability density of a lognormal distribution is given in Eq. (20–17) as

$$g(x) = \frac{1}{x (0.0408) \sqrt{2\pi}} \exp \left[ -\frac{1}{2} \left( \frac{\ln x - 4.1522}{0.0408} \right)^2 \right] \quad \text{for } x > 0$$

For example,  $g(63.625) = 0.1537$ . This lognormal density has been added to Table 20–5. Plot the lognormal PDF superposed on the histogram of Ex. 20–4 along with the normal density. As seen in Fig. 20–8, both normal and lognormal densities fit well.

**Figure 20–8**

Histogram for Ex. 20–4 and Ex. 20–5 with normal and lognormal probability density functions superposed.

**The Uniform Distribution**

The uniform distribution is a closed-interval distribution that arises when the chance of an observation is the same as the chance for any other observation. If  $a$  is the lower bound and  $b$  is the upper bound, then the probability density function (PDF) for the uniform distribution is

$$f(x) = \begin{cases} 1/(b-a) & a \leq x \leq b \\ 0 & a > x > b \end{cases} \quad (20-20)$$

The cumulative density function (CDF), the integral of  $f(x)$ , is thus linear in the range  $a \leq x \leq b$  given by

$$F(x) = \begin{cases} 0 & x < a \\ (x - a)/(b - a) & a \leq x \leq b \\ 1 & x > b \end{cases} \quad (20-21)$$

The mean and standard deviation are given by

$$\mu_x = \frac{a + b}{2} \quad (20-22)$$

$$\hat{\sigma}_x = \frac{b - a}{2\sqrt{3}} \quad (20-23)$$

The uniform distribution arises, among other places in manufacturing, where a part is mass-produced in an automatic operation and the dimension gradually changes through tool wear and increased tool forces between setups. If  $n$  is the part sequence or processing number, and  $n_f$  is the sequence number of the final-produced part before another setup, then the dimension  $x$  graphs linearly when plotted against the sequence number  $n$ . If the last part made during the setup has a dimension  $x_i$ , and the final part produced has the dimension  $x_f$ , the magnitude of the dimension at sequence number  $n$  is given by

$$x = x_i + (x_f - x_i) \frac{n}{n_f} = x_i + (x_f - x_i) F(x) \quad (a)$$

since  $n/n_f$  is a good approximation to the CDF. Solving Eq. (a) for  $F(x)$  gives

$$F(x) = \frac{x - x_i}{x_f - x_i} \quad (b)$$

Compare this equation with the middle form of Eq. (20-21).

### The Weibull Distribution

The Weibull distribution does not arise from classical statistics and is usually not included in elementary statistics textbooks. It is far more likely to be discussed and used in works dealing with experimental results, particularly reliability. It is a chameleon distribution, asymmetrical, with different values for the mean and the median. It contains within it a good approximation of the normal distribution as well as an exact representation of the exponential distribution. Most reliability information comes from laboratory and field service data, and because of its flexibility, the Weibull distribution is widely used.

The expression for reliability is the value of the cumulative density function complementary to unity. For the Weibull this value is both explicit and simple. The reliability given by the *three-parameter Weibull distribution* is

$$R(x) = \exp \left[ - \left( \frac{x - x_0}{\theta - x_0} \right)^b \right] \quad x \geq x_0 \geq 0 \quad (20-24)$$

where the three parameters are

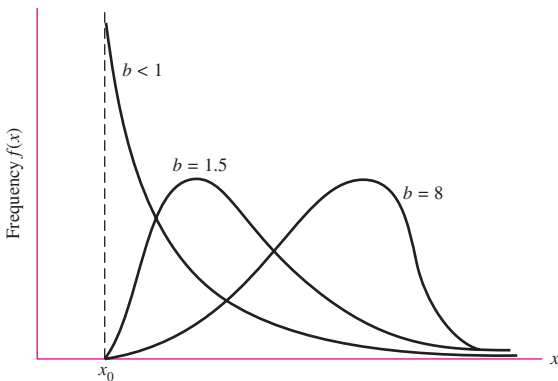
$x_0$  = minimum, guaranteed, value of  $x$

$\theta$  = a characteristic or scale value ( $\theta \geq x_0$ )

$b$  = a shape parameter ( $b > 0$ )

**Figure 20–9**

The density function of the Weibull distribution showing the effect of skewness of the shape parameter  $b$ .



For the special case when  $x_0 = 0$ , Eq. (20–24) becomes the two-parameter Weibull

$$R(x) = \exp\left[-\left(\frac{x}{\theta}\right)^b\right] \quad x \geq 0 \quad (20-25)$$

The characteristic variate  $\theta$  serves a role similar to the mean and represents a value of  $x$  below which lie 63.2 percent of the observations.

The shape parameter  $b$  controls the skewness of the distribution. Figure 20–9 shows that large  $b$ 's skew the distribution to the right and small  $b$ 's skew it to the left. In the range  $3.3 < b < 3.5$ , approximate symmetry is obtained along with a good approximation to the normal distribution. When  $b = 1$ , the distribution is exponential.

Given a specific required reliability, solving Eq. (20–24) for  $x$  yields

$$x = x_0 + (\theta - x_0) \left( \ln \frac{1}{R} \right)^{1/b} \quad (20-26)$$

To find the probability function, we note that

$$F(x) = 1 - R(x) \quad (a)$$

$$f(x) = \frac{dF(x)}{dx} = -\frac{dR(x)}{dx} \quad (b)$$

Thus, for the Weibull,

$$f(x) = \begin{cases} \frac{b}{\theta - x_0} \left( \frac{x - x_0}{\theta - x_0} \right)^{b-1} \exp\left[-\left(\frac{x - x_0}{\theta - x_0}\right)^b\right] & x \geq x_0 \geq 0 \\ 0 & x \leq x_0 \end{cases} \quad (20-27)$$

The mean and standard deviation are given by

$$\mu_x = x_0 + (\theta - x_0) \Gamma(1 + 1/b) \quad (20-28)$$

$$\hat{\sigma}_x = (\theta - x_0) \sqrt{\Gamma(1 + 2/b) - \Gamma^2(1 + 1/b)} \quad (20-29)$$

where  $\Gamma$  is the gamma function and may be found tabulated in Table A–34. The notation for a Weibull distribution is<sup>1</sup>

$$\mathbf{x} = \mathbf{W}(x_0, \theta, b) \quad (20-30)$$

<sup>1</sup>To estimate the Weibull parameters from data, see J. E. Shigley and C. R. Mischke, *Mechanical Engineering Design*, 5th ed., 1989, McGraw-Hill, New York, Sec. 4–12. The Weibull parameters are determined for the data given in Ex. 2–4.

**EXAMPLE 20–6**

The Weibull is used extensively for expressing the reliability of rolling-contact bearings (see Sec. 11–4). Here, the variate  $x$  is put in dimensionless form as  $x = L/L_{10}$  where  $L$  is bearing life, in say, number of cycles; and  $L_{10}$  is the manufacturer's rated life of the bearing where 10 percent of the bearings have failed (90 percent reliability).

Construct the distributional properties of a 02–30 mm deep-groove ball bearing if the Weibull parameters are  $x_0 = 0.0200$ ,  $\theta = 4.459$ , and  $b = 1.483$ . Find the mean, median,  $L_{90}$ , and standard deviation.

**Solution** From Eq. (20–28) the mean dimensionless life is

$$\begin{aligned}\text{Answer} \quad \mu_x &= x_0 + (\theta - x_0)\Gamma(1 + 1/b) \\ &= 0.0200 + (4.459 - 0.0200)\Gamma(1 + 1/1.483) = 4.033\end{aligned}$$

This says that the average bearing life is  $4.033 L_{10}$ . The median dimensionless life corresponds to  $R = 0.5$ , or  $L_{50}$ , and from Eq. (20–26) is

$$\begin{aligned}\text{Answer} \quad x_{0.5} &= x_0 + (\theta - x_0) \left( \ln \frac{1}{0.5} \right)^{1/b} = 0.0200 + (4.459 - 0.0200) \left( \ln \frac{1}{0.5} \right)^{1/1.483} \\ &= 3.487\end{aligned}$$

For  $L_{90}$ ,  $R = 0.1$ , the dimensionless life  $x$  is

$$\text{Answer} \quad x_{0.90} = 0.0200 + (4.459 - 0.0200) \left( \ln \frac{1}{0.1} \right)^{1/1.483} = 7.810$$

The standard deviation of the dimensionless life is given by Eq. (20–29):

$$\begin{aligned}\text{Answer} \quad \hat{\sigma}_x &= (\theta - x_0) \sqrt{\Gamma(1 + 2/b) - \Gamma^2(1 + 1/b)} \\ &= (4.459 - 0.0200) \sqrt{\Gamma(1 + 2/1.483) - \Gamma^2(1 + 1/1.483)} = 2.753\end{aligned}$$

## 20–4 Propagation of Error

In the equation for axial stress

$$\sigma = \frac{F}{A} \quad (a)$$

suppose both the force  $F$  and the area  $A$  are random variables. Then Eq. (a) is written as

$$\sigma = \frac{\mathbf{F}}{\mathbf{A}} \quad (b)$$

and we see that the stress  $\sigma$  is also a random variable. When Eq. (b) is solved, the errors inherent in  $\mathbf{F}$  and in  $\mathbf{A}$  are said to be *propagated* to the stress variate  $\sigma$ . It is not hard to think of many other relations where this will occur.

Suppose we wish to add the two variates  $\mathbf{x}$  and  $\mathbf{y}$  to form a third variate  $\mathbf{z}$ . This is written as

$$\mathbf{z} = \mathbf{x} + \mathbf{y} \quad (c)$$

The mean is given as

$$\mu_z = \mu_x + \mu_y \quad (d)$$

**Table 20–6**

Means and Standard Deviations for Simple Algebraic Operations on Independent (Uncorrelated) Random Variables

Function	Mean ( $\mu$ )	Standard Deviation ( $\hat{\sigma}$ )
$a$	$a$	0
$x$	$\mu_x$	$\hat{\sigma}_x$
$x + a$	$\mu_x + a$	$\hat{\sigma}_x$
$ax$	$a\mu_x$	$a\hat{\sigma}_x$
$x + y$	$\mu_x + \mu_y$	$(\hat{\sigma}_x^2 + \hat{\sigma}_y^2)^{1/2}$
$x - y$	$\mu_x - \mu_y$	$(\hat{\sigma}_x^2 + \hat{\sigma}_y^2)^{1/2}$
$xy$	$\mu_x \mu_y$	$\mu_x \mu_y (C_x^2 + C_y^2 + C_x^2 C_y^2)^{1/2}$
$x/y$	$\mu_x / \mu_y$	$\mu_x / \mu_y \left[ (C_x^2 + C_y^2) / (1 + C_y^2) \right]^{1/2}$
$x^n$	$\mu_x^n \left[ 1 + \frac{n(n-1)}{2} C_x^2 \right]$	$ n  \mu_x^n C_x \left[ 1 + \frac{(n-1)^2}{4} C_x^2 \right]$
$1/x$	$\frac{1}{\mu_x} (1 + C_x^2)$	$\frac{C_x}{\mu_x} (1 + C_x^2)$
$1/x^2$	$\frac{1}{\mu_x^2} (1 + 3 C_x^2)$	$\frac{2 C_x}{\mu_x^2} \left( 1 + \frac{9}{4} C_x^2 \right)$
$1/x^3$	$\frac{1}{\mu_x^3} (1 + 6 C_x^2)$	$\frac{3 C_x}{\mu_x^3} (1 + 4 C_x^2)$
$1/x^4$	$\frac{1}{\mu_x^4} (1 + 10 C_x^2)$	$\frac{4 C_x}{\mu_x^4} \left( 1 + \frac{25}{4} C_x^2 \right)$
$\sqrt{x}$	$\sqrt{\mu_x} \left( 1 - \frac{1}{8} C_x^2 \right)$	$\frac{\sqrt{\mu_x}}{2} C_x \left( 1 + \frac{1}{16} C_x^2 \right)$
$x^2$	$\mu_x^2 (1 + C_x^2)$	$2 \mu_x^2 C_x \left( 1 + \frac{1}{4} C_x^2 \right)$
$x^3$	$\mu_x^3 (1 + 3 C_x^2)$	$3 \mu_x^3 C_x (1 + C_x^2)$
$x^4$	$\mu_x^4 (1 + 6 C_x^2)$	$4 \mu_x^4 C_x \left( 1 + \frac{9}{4} C_x^2 \right)$

Note: The coefficient of variation of variate  $x$  is  $C_x = \hat{\sigma}_x / \mu_x$ . For small COVs their square is small compared to unity, so the first term in the powers of  $x$  expressions are excellent approximations. For correlated products and quotients see Charles R. Mischke, *Mathematical Model Building*, 2nd rev. ed., Iowa State University Press, Ames, 1980, App. C.

The standard deviation follows the Pythagorean theorem. Thus the standard deviation for both addition and subtraction of independent variables is

$$\hat{\sigma}_z = \sqrt{\hat{\sigma}_x^2 + \hat{\sigma}_y^2} \quad (\text{e})$$

Similar relations have been worked out for a variety of functions and are displayed in Table 20–6. The results shown can easily be combined to form other functions.

An unanswered question here is what is the distribution that results from the various operations? For answers to this question, statisticians use closure theorems and the central limit theorem.<sup>2</sup>

<sup>2</sup>See E. B. Haugen, *Probabilistic Mechanical Design*, Wiley, New York, 1980, pp. 49–54.

**EXAMPLE 20-7**

A round bar subject to a bending load has a diameter  $\mathbf{d} = \text{LN}(2.000, 0.002)$  in. This equivalency states that the mean diameter is  $\mu_d = 2.000$  in and the standard deviation is  $\hat{\sigma}_d = 0.002$  in. Find the mean and the standard deviation of the second moment of area.

**Solution**

The second moment of area is given by the equation

$$\mathbf{I} = \frac{\pi \mathbf{d}^4}{64}$$

The coefficient of variation of the diameter is

$$C_d = \frac{\hat{\sigma}_d}{\mu_d} = \frac{0.002}{2} = 0.001$$

Using Table 20–6, we find

**Answer**  $\mu_I = (\pi/64)\mu_d^4(1 + 6C_d^2) = (\pi/64)(2.000)^4[1 + 6(0.001)^2] = 0.785 \text{ in}^4$

**Answer**  $\hat{\sigma}_I = 4\mu_d^4 C_d [1 + (9/4)C_d^2] = 4(2.000)^4(0.001)[1 + (9/4)(0.001)^2] = 0.064 \text{ in}^4$

These results can be expressed in the form

$$\mathbf{I} = \text{LN}(0.785, 0.064) = 0.785\text{LN}(1, 0.0815) \text{ in}^4$$

**20–5****Linear Regression**

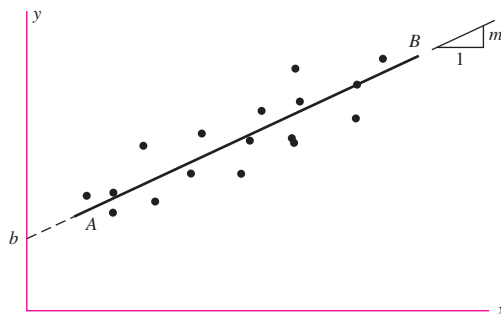
Statisticians use a process of analysis called *regression* to obtain a curve that best fits a set of data points. The process is called *linear regression* when the best-fitting straight line is to be found. The meaning of the word *best* is open to argument, because there can be many meanings. The usual method, and the one employed here, regards a line as “best” if it minimizes the squares of the deviations of the data points from the line.

Figure 20–10 shows a set of data points approximated by the line  $AB$ . The standard equation of a straight line is

$$y = mx + b \quad (20-31)$$

**Figure 20–10**

Set of data points approximated by regression line  $AB$ .



where  $m$  is the slope and  $b$  is the  $y$  intercept. Consider a set of  $N$  data points  $(x_i, y_i)$ . In general, the best-fit line will not intersect a data point. Thus, we can write

$$y_i = mx_i + b + \epsilon_i \quad (b)$$

where  $\epsilon_i = y_i - y$  is the deviation between the data point and the line. The sum of the squares of the deviations is given by<sup>3</sup>

$$\mathcal{E} = \sum \epsilon_i^2 = \sum (y_i - mx_i - b)^2 \quad (c)$$

Minimizing  $\mathcal{E}$ , the sum of the squared errors, expecting a stationary point minimum, requires  $\partial\mathcal{E}/\partial m = 0$  and  $\partial\mathcal{E}/\partial b = 0$ . This results in two simultaneous equations for the slope and  $y$  intercept denoted as  $\hat{m}$  and  $\hat{b}$ , respectively. Solving these equations results in

$$\hat{m} = \frac{N \sum x_i y_i - \sum x_i \sum y_i}{N \sum x_i^2 - (\sum x_i)^2} = \frac{\sum x_i y_i - N \bar{x} \bar{y}}{\sum x_i^2 - N \bar{x}^2} \quad (20-32)$$

$$\hat{b} = \frac{\sum y_i - \hat{m} \sum x_i}{N} = \bar{y} - \hat{m} \bar{x} \quad (20-33)$$

Once you have established a slope and an intercept, the next point of interest is to discover how well  $x$  and  $y$  correlate with each other. If the data points are scattered all over the  $xy$  plane, there is obviously no correlation. But if all the data points coincide with the regression line, then there is perfect correlation. Most statistical data will be in between these extremes. A *correlation coefficient*  $r$ , having the range  $-1 \leq r \leq +1$ , has been devised to answer this question. The formula is

$$r = \hat{m} \frac{s_x}{s_y} \quad (20-34)$$

where  $s_x$  and  $s_y$  are the standard deviations of the  $x$  coordinates and  $y$  coordinates of the data, respectively. If  $r = 0$ , there is no correlation; if  $r = \pm 1$ , there is perfect correlation. A positive or negative  $r$  indicates that the regression line has a positive or negative slope, respectively.

The standard deviations for  $\hat{m}$  and  $\hat{b}$  are given by

$$s_{\hat{m}} = \frac{s_{y \cdot x}}{\sqrt{\sum (x_i - \bar{x})^2}} \quad (20-35)$$

$$s_{\hat{b}} = s_{y \cdot x} \sqrt{\frac{1}{N} + \frac{\bar{x}^2}{\sum (x_i - \bar{x})^2}} \quad (20-36)$$

where

$$s_{y \cdot x} = \sqrt{\frac{\sum y_i^2 - \hat{b} \sum y_i - \hat{m} \sum x_i y_i}{N - 2}} \quad (20-37)$$

is the standard deviation of the scatter of the data from the regression line.

---

<sup>3</sup>From this point on, for economy of notation, the limits of the summation of  $i(1, N)$  will not be displayed.

**EXAMPLE 20-8**

A specimen of a medium carbon steel was tested in tension. With an extensometer in place, the specimen was loaded then unloaded, to see if the extensometer reading returned to the no-load reading, then the next higher load was applied. The loads and extensometer elongations were reduced to stress  $\sigma$  and strain  $\epsilon$ , producing the following data:

$\sigma$ , psi	5033	10 068	15 104	20 143	35 267
$\epsilon$	0.000 20	0.000 30	0.000 50	0.000 65	0.001 15

Find the mean Young's modulus  $\bar{E}$  and its standard deviation. Since the extensometer seems to have an initial reading at no load, use a  $y = mx + b$  regression.

**Solution**

From Table 20-7,  $\bar{x} = 0.00280/5 = 0.00056$ ,  $\bar{y} = 85615/5 = 17123$ . Note that a regression line always contains the data centroid. From Eq. (20-32)

**Answer**

$$\hat{m} = \frac{5(65.229) - 0.0028(85615)}{5(0.000002125) - 0.0028^2} = 31.03(10^6) \text{ psi} = \bar{E}$$

From Eq. (20-33)

$$\hat{b} = \frac{0.000002125(85615) - 0.0028(65.229)}{5(0.000002125) - 0.0028^2} = -254.69 \text{ psi}$$

From Eq. (20-34), obtaining  $s_x$  and  $s_y$  from a statistics calculator routine,

$$\hat{r} = \frac{\hat{m}s_x}{s_y} = \frac{31031597.85(316216310^{-4})}{11601.11} = 0.998$$

From Eq. (20-37), the scatter about the regression line is measured by the standard deviation  $s_{y,x}$  and is equal to

$$\begin{aligned} s_{y,x} &= \sqrt{\frac{\sum y^2 - \hat{b} \sum y - \hat{m} \sum xy}{N - 2}} \\ &= \sqrt{\frac{2004328267 - (-254.69)85615 - 31.03(10^6)(65.229)}{5 - 2}} \\ &= 811.1 \text{ psi} \end{aligned}$$

**Table 20-7**

Worksheet for Ex. 20-6

<b>y</b> $\sigma$ , psi	<b>x</b> $\epsilon$	<b><math>x^2</math></b>	<b><math>xy</math></b>	<b><math>y^2</math></b>	<b><math>(x - \bar{x})^2</math></b>
5 033	0.000 20	0.000 000 040	1.006 600	25 330 089	0.000 000 130
10 068	0.000 30	0.000 000 090	3.020 400	101 364 624	0.000 000 069
15 104	0.000 50	0.000 000 250	7.552 000	228 130 816	0.000 000 004
20 143	0.000 65	0.000 000 423	13.092 950	405 740 449	0.000 000 008
35 261	0.001 15	0.000 001 323	40.557 050	1 243 761 289	0.000 000 348
$\Sigma$ 85 615	0.002 80	0.000 002 125	65.229 000	2 004 328 267	0.000 000 556

Note:  $\bar{y} = 85615/5 = 17123$  psi,  $\bar{x} = 0.00280/5 = 0.00056$ .

From Eq. (20–35), the standard deviation of  $\hat{m}$  is

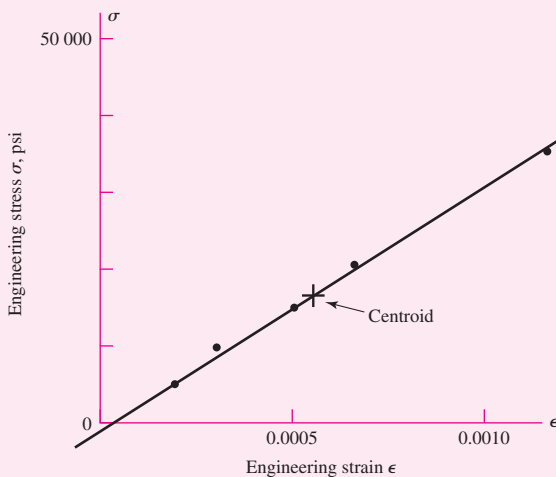
**Answer**

$$s_{\hat{m}} = \frac{s_{y,x}}{\sqrt{\sum(x - \bar{x})^2}} = \frac{811.1}{\sqrt{0.000\ 000\ 558}} = 1.086(10^6) \text{ psi} = s_E$$

See Fig. 20–11 for the regression plot.

**Figure 20–11**

The data from Ex. 20–8 are plotted. The regression line passes through the data centroid and among the data points, minimizing the squared deviations.



## PROBLEMS

### 20–1

At a constant amplitude, completely reversed bending stress level, the cycles-to-failure experience with 69 specimens of 5160H steel from 1.25-in hexagonal bar stock was as follows:

$L$	60	70	80	90	100	110	120	130	140	150	160	170	180	190	200	210
$f$	2	1	3	5	8	12	6	10	8	5	2	3	2	1	0	1

where  $L$  is the life in thousands of cycles, and  $f$  is the class frequency of failures.

(a) Construct a histogram with class frequency  $f$  as ordinate.

(b) Estimate the mean and standard deviation of the life for the population from which the sample was drawn.

### 20–2

Determinations of the ultimate tensile strength  $S_{ut}$  of stainless steel sheet (17-7PH, condition TH 1050), in sizes from 0.016 to 0.062 in, in 197 tests combined into seven classes were

$S_{ut}$ , ksi	174	182	190	198	206	214	222
Frequency, $f$	6	9	44	67	53	12	6

where  $f$  is the class frequency. Find the mean and standard deviation.

**20-3**

A total of 58 AISI 1018 cold-drawn steel bars were tested to determine the 0.2 percent offset yield strength  $S_y$ . The results were

$S_y$ , kpsi	64	68	72	76	80	84	88	92
$f$	2	6	6	9	19	10	4	2

where  $S_y$  is the class midpoint and  $f$  is the class frequency. Estimate the mean and standard deviation of  $S_y$  and its PDF assuming a normal distribution.

**20-4**

The base 10 logarithm of 55 cycles-to-failure observations on specimens subjected to a constant stress level in fatigue have been classified as follows:

$y$	5.625	5.875	6.125	6.375	6.625	6.875	7.125	7.375	7.625	7.875	8.125
$f$	1	0	0	3	3	6	14	15	10	2	1

Here  $y$  is the class midpoint and  $f$  is the class frequency.

- (a) Estimate the mean and standard deviation of the population from which the sample was taken and establish the normal PDF.
- (b) Plot the histogram and superpose the predicted class frequency from the normal fit.

**20-5**

A  $\frac{1}{2}$ -in nominal diameter round is formed in an automatic screw machine operation that is initially set to produce a 0.5000-in diameter and is reset when tool wear produces diameters in excess of 0.5008 in. The stream of parts is thoroughly mixed and produces a uniform distribution of diameters.

- (a) Estimate the mean and standard deviation of the large batch of parts from setup to reset.
- (b) Find the expressions for the PDF and CDF of the population.
- (c) If, by inspection, the diameters less than 0.5002 in are removed, what are the new PDF and CDF as well as the mean and standard deviation of the diameters of the survivors of the inspection?

**20-6**

The only detail drawing of a machine part has a dimension smudged beyond legibility. The round in question was created in an automatic screw machine and 1000 parts are in stock. A random sample of 50 parts gave a mean dimension of  $\bar{d} = 0.6241$  in and a standard deviation of  $s = 0.000581$  in. Toleranced dimensions elsewhere are given in integral thousandths of an inch. Estimate the missing information on the drawing.

**20-7**

- (a) The CDF of the variate  $x$  is  $F(x) = 0.555x - 33$ , where  $x$  is in millimeters. Find the PDF, the mean, the standard deviation, and the range numbers of the distribution.
- (b) In the expression  $\sigma = F/A$ , the force  $F = LN(3600, 300)$  lbf and the area is  $A = LN(0.112, 0.001)$  in<sup>2</sup>. Estimate the mean, standard deviation, coefficient of variation, and distribution of  $\sigma$ .

**20-8**

A regression model of the form  $y = a_1x + a_2x^2$  is desired. From the normal equations

$$\sum y = a_1 \sum x + a_2 \sum x^2$$

$$\sum xy = a_1 \sum x^2 + a_2 \sum x^3$$

show that

$$a_1 = \frac{\sum y \sum x^3 - \sum xy \sum x^2}{\sum x \sum x^3 - (\sum x^2)^2} \quad \text{and} \quad a_2 = \frac{\sum x \sum xy - \sum y \sum x^2}{\sum x \sum x^3 - (\sum x^2)^2}$$

For the data set

$x$	0.0	0.2	0.4	0.6	0.8	1.0
$y$	0.01	0.15	0.25	0.25	0.17	-0.01

find the regression equation and plot the data with the regression model.

### 20-9

R. W. Landgraf reported the following axial (push-pull) endurance strengths for steels of differing ultimate strengths:

$S_u$	$S'_e$	$S_u$	$S'_e$	$S_u$	$S'_e$
65	29.5	325	114	280	96
60	30	238	109	295	99
82	45	130	67	120	48
64	48	207	87	180	84
101	51	205	96	213	75
119	50	225	99	242	106
195	78	325	117	134	60
210	87	355	122	145	64
230	105	225	87	227	116
265	105				

(a) Plot the data with  $S'_e$  as ordinate and  $S_u$  as abscissa.

(b) Using the  $y = mx + b$  linear regression model, find the regression line and plot.

### 20-10

In fatigue studies a parabola of the Gerber type

$$\frac{\sigma_a}{S_e} + \left( \frac{\sigma_m}{S_{ut}} \right)^2 = 1$$

is useful (see Sec. 6-12). Solved for  $\sigma_a$  the preceding equation becomes

$$\sigma_a = S_e - \frac{S_e}{S_{ut}^2} \sigma_m^2$$

This implies a regression model of the form  $y = a_0 + a_2 x^2$ . Show that the normal equations are

$$\begin{aligned}\sum y &= n a_0 + a_2 \sum x^2 \\ \sum xy &= a_0 \sum x + a_2 \sum x^3\end{aligned}$$

and that

$$a_0 = \frac{\sum x^3 \sum y - \sum x^2 \sum xy}{n \sum x^3 - \sum x \sum x^2} \quad \text{and} \quad a_2 = \frac{n \sum xy - \sum x \sum y}{n \sum x^3 - \sum x \sum x^2}$$

Plot the data

$x$	20	40	60	80
$y$	19	17	13	7

superposed on a plot of the regression line.

**20-11**

Consider the following data collected on a single helical coil extension spring with an initial extension  $F_i$  and a spring rate  $k$  suspected of being related by the equation  $F = F_i + kx$  where  $x$  is the deflection beyond initial. The data are

$x$ , in	0.2	0.4	0.6	0.8	1.0	2.0
$F$ , lbf	7.1	10.3	12.1	13.8	16.2	25.2

- (a) Estimate the mean and standard deviation of the initial tension  $F_i$ .
- (b) Estimate the mean and standard deviation of the spring rate  $k$ .

**20-12**

In the expression for uniaxial strain  $\epsilon = \delta/l$ , the elongation is specified as  $\delta \sim (0.0015, 0.000\,092)$  in and the length as  $l \sim (2.0000, 0.0081)$  in. What are the mean, the standard deviation, and the coefficient of variation of the corresponding strain  $\epsilon$ .

**20-13**

In Hooke's law for uniaxial stress,  $\sigma = \epsilon E$ , the strain is given as  $\epsilon \sim (0.0005, 0.000\,034)$  and Young's modulus as  $E \sim (29.5, 0.885)$  Mpsi. Find the mean, the standard deviation, and the coefficient of variation of the corresponding stress  $\sigma$  in psi.

**20-14**

The stretch of a uniform rod in tension is given by the formula  $\delta = Fl/AE$ . Suppose the terms in this equation are random variables and have parameters as follows:

$$\begin{aligned} F &\sim (14.7, 1.3) \text{ kip} & A &\sim (0.226, 0.003) \text{ in}^2 \\ l &\sim (1.5, 0.004) \text{ in} & E &\sim (29.5, 0.885) \text{ Mpsi} \end{aligned}$$

Estimate the mean, the standard deviation, and the coefficient of variation of the corresponding elongation  $\delta$  in inches.

**20-15**

The maximum bending stress in a round bar in flexure occurs in the outer surface and is given by the equation  $\sigma = 32M/\pi d^3$ . If the moment is specified as  $M \sim (15\,000, 1350)$  lbf · in and the diameter is  $d \sim (2.00, 0.005)$  in, find the mean, the standard deviation, and the coefficient of variation of the corresponding stress  $\sigma$  in psi.

**20-16**

When a production process is wider than the tolerance interval, inspection rejects a low-end scrap fraction  $\alpha$  with  $x < x_1$  and an upper-end scrap fraction  $\beta$  with dimensions  $x > x_2$ . The surviving population has a new density function  $g(x)$  related to the original  $f(x)$  by a multiplier  $a$ . This is because any two observations  $x_i$  and  $x_j$  will have the same relative probability of occurrence as before. Show that

$$a = \frac{1}{F(x_2) - F(x_1)} = \frac{1}{1 - (\alpha + \beta)}$$

and

$$g(x) = \begin{cases} \frac{f(x)}{F(x_2) - F(x_1)} = \frac{f(x)}{1 - (\alpha + \beta)} & x_1 \leq x \leq x_2 \\ 0 & \text{otherwise} \end{cases}$$

**20-17**

An automatic screw machine produces a run of parts with a uniform distribution  $d = U[0.748, 0.751]$  in because it was not reset when the diameters reached 0.750 in. The square brackets contain range numbers.

- (a) Estimate the mean, standard deviation, and PDF of the original production run if the parts are thoroughly mixed.
- (b) Using the results of Prob. 20-16, find the new mean, standard deviation, and PDF. Superpose the PDF plots and compare.

- 20-18** A springmaker is supplying helical coil springs meeting the requirement for a spring rate  $k$  of  $10 \pm 1$  lbf/in. The test program of the springmaker shows that the distribution of spring rate is well approximated by a normal distribution. The experience with inspection has shown that 8.1 percent are scrapped with  $k < 9$  and 5.5 percent are scrapped with  $k > 11$ . Estimate the probability density function.
- 20-19** The lives of parts are often expressed as the number of cycles of operation that a specified percentage of a population will exceed before experiencing failure. The symbol  $L$  is used to designate this definition of life. Thus we can speak of  $L_{10}$  life as the number of cycles to failure exceeded by 90 percent of a population of parts. Using the mean and standard deviation for the data of Prob. 20-1, a normal distribution model, estimate the corresponding  $L_{10}$  life.
- 20-20** Fit a normal distribution to the histogram of Prob. 20-1. Superpose the probability density function on the  $f/(Nw)$  histographic plot.
- 20-21** For Prob. 20-2, plot the histogram with  $f/(Nw)$  as ordinate and superpose a normal distribution density function on the histographic plot.
- 20-22** For Prob. 20-3, plot the histogram with  $f/(Nw)$  as ordinate and superpose a normal distribution probability density function on the histographic plot.
- 20-23** A 1018 cold-drawn steel has a 0.2 percent tensile yield strength  $S_y = N(78.4, 5.90)$  kpsi. A round rod in tension is subjected to a load  $\mathbf{P} = N(40, 8.5)$  kip. If rod diameter  $d$  is 1.000 in, what is the probability that a random static tensile load  $P$  from  $\mathbf{P}$  imposed on the shank with a 0.2 percent tensile load  $S_y$  from  $S_y$  will not yield?
- 20-24** A hot-rolled 1035 steel has a 0.2 percent tensile yield strength  $S_y = LN(49.6, 3.81)$  kpsi. A round rod in tension is subjected to a load  $\mathbf{P} = LN(30, 5.1)$  kip. If the rod diameter  $d$  is 1.000 in, what is the probability that a random static tensile load  $P$  from  $\mathbf{P}$  on a shank with a 0.2 percent yield strength  $S_y$  from  $S_y$  will not yield?
- 20-25** The tensile 0.2 percent offset yield strength of AISI 1137 cold-drawn steel rounds up to 1 inch in diameter from 2 mills and 25 heats is reported histographically as follows:
- | $S_y$ | 93 | 95 | 97 | 99 | 101 | 103 | 105 | 107 | 109 | 111 |
|-------|----|----|----|----|-----|-----|-----|-----|-----|-----|
| $f$   | 19 | 25 | 38 | 17 | 12  | 10  | 5   | 4   | 4   | 2   |
- where  $S_y$  is the class midpoint in kpsi and  $f$  is the number in each class. Presuming the distribution is normal, what is the yield strength exceeded by 99 percent of the population?
- 20-26** Repeat Prob. 20-25, presuming the distribution is lognormal. What is the yield strength exceeded by 99 percent of the population? Compare the normal fit of Prob. 20-25 with the lognormal fit by superposing the PDFs and the histographic PDF.
- 20-27** A 1046 steel, water-quenched and tempered for 2 h at  $1210^{\circ}\text{F}$ , has a mean tensile strength of 105 kpsi and a yield mean strength of 82 kpsi. Test data from endurance strength testing at  $10^4$ -cycle life give  $(S'_{fe})_{10^4} = W[79, 86.2, 2.60]$  kpsi. What are the mean, standard deviation, and coefficient of variation of  $(S'_{fe})_{10^4}$ ?
- 20-28** An ASTM grade 40 cast iron has the following result from testing for ultimate tensile strength:  $S_{ut} = W[27.7, 46.2, 4.38]$  kpsi. Find the mean and standard deviation of  $S_{ut}$ , and estimate the chance that the ultimate strength is less than 40 kpsi.
- 20-29** A cold-drawn 301SS stainless steel has an ultimate tensile strength given by  $S_{ut} = W[151.9, 193.6, 8.00]$  kpsi. Find the mean and standard deviation.

- 20-30** A 100-70-04 nodular iron has tensile and yield strengths described by

$$\mathbf{S}_{ut} = \mathbf{W}[47.6, 125.6, 11.84] \text{ kpsi}$$

$$\mathbf{S}_y = \mathbf{W}[64.1, 81.0, 3.77] \text{ kpsi}$$

What is the chance that  $S_{ut}$  is less than 100 kpsi? What is the chance that  $S_y$  is less than 70 kpsi?

- 20-31** A 1038 heat-treated steel bolt in finished form provided the material from which a tensile test specimen was made. The testing of many such bolts led to the description  $\mathbf{S}_{ut} = \mathbf{W}[122.3, 134.6, 3.64]$  kpsi. What is the probability that the bolts meet the SAE grade 5 requirement of a minimum tensile strength of 120 kpsi? What is the probability that the bolts meet the SAE grade 7 requirement of a minimum tensile strength of 133 kpsi?

- 20-32** A 5160H steel was tested in fatigue and the distribution of cycles to failure at constant stress level was found to be  $\mathbf{n} = \mathbf{W}[36.9, 133.6, 2.66]$  in  $10^3$  cycles. Plot the PDF of  $n$  and the PDF of the lognormal distribution having the same mean and standard deviation. What is the L10 life (see Prob. 20-19) predicted by both distributions?

- 20-33** A material was tested at steady fully reversed loading to determine the number of cycles to failure using 100 specimens. The results were

$(10^{-5})L$	3.05	3.55	4.05	4.55	5.05	5.55	6.05	6.55	7.05	7.55	8.05	8.55	9.05	9.55	10.05
$f$	3	7	11	16	21	13	13	6	2	0	4	3	0	0	1

where  $L$  is the life in cycles and  $f$  is the number in each class. Assuming a lognormal distribution, plot the theoretical PDF and the histographic PDF for comparison.

- 20-34** The ultimate tensile strength of an AISI 1117 cold-drawn steel is Weibullian, with  $\mathbf{S}_u = \mathbf{W}[70.3, 84.4, 2.01]$ . What are the mean, the standard deviation, and the coefficient of variation?

- 20-35** A 60-45-15 nodular iron has a 0.2 percent yield strength  $S_y$  with a mean of 49.0 kpsi, a standard deviation of 4.2 kpsi, and a guaranteed yield strength of 33.8 kpsi. What are the Weibull parameters  $\theta$  and  $b$ ?

- 20-36** A 35018 malleable iron has a 0.2 percent offset yield strength given by the Weibull distribution  $\mathbf{S}_y = \mathbf{W}[34.7, 39.0, 2.93]$  kpsi. What are the mean, the standard deviation, and the coefficient of variation?

- 20-37** The histographic results of steady load tests on 237 rolling-contact bearings are:

$L$	1	2	3	4	5	6	7	8	9	10	11	12
$f$	11	22	38	57	31	19	15	12	11	9	7	5

where  $L$  is the life in millions of revolutions and  $f$  is the number of failures. Fit a lognormal distribution to these data and plot the PDF with the histographic PDF superposed. From the lognormal distribution, estimate the life at which 10 percent of the bearings under this steady loading will have failed.

# A

## Useful Tables

## Appendix

### Appendix Outline

- A-1** Standard SI Prefixes **1005**  
**A-2** Conversion Factors **1006**  
**A-3** Optional SI Units for Bending, Torsion, Axial, and Direct Shear Stresses **1007**  
**A-4** Optional SI Units for Bending and Torsional Deflections **1007**  
**A-5** Physical Constants of Materials **1007**  
**A-6** Properties of Structural-Steel Angles **1008-1009**  
**A-7** Properties of Structural-Steel Channels **1010-1011**  
**A-8** Properties of Round Tubing **1012**  
**A-9** Shear, Moment, and Deflection of Beams **1013-1020**  
**A-10** Cumulative Distribution Function of Normal (Gaussian) Distribution **1021-1022**  
**A-11** A Selection of International Tolerance Grades—Metric Series **1022**  
**A-12** Fundamental Deviations for Shafts—Metric Series **1023**  
**A-13** A Selection of International Tolerance Grades—Inch Series **1024**  
**A-14** Fundamental Deviations for Shafts—Inch Series **1025**  
**A-15** Charts of Theoretical Stress-Concentration Factors  $K_t$  **1026-1032**  
**A-16** Approximate Stress-Concentration Factors  $K_t$  and  $K_{ts}$  for Bending a Round Bar or Tube with a Transverse Round Hole **1033-1034**  
**A-17** Preferred Sizes and Renard (R-Series) Numbers **1035**  
**A-18** Geometric Properties **1036-1038**  
**A-19** American Standard Pipe **1039**  
**A-20** Deterministic ASTM Minimum Tensile and Yield Strengths for HR and CD Steels **1040**  
**A-21** Mean Mechanical Properties of Some Heat-Treated Steels **1041-1042**  
**A-22** Results of Tensile Tests of Some Metals **1043**  
**A-23** Mean Monotonic and Cyclic Stress-Strain Properties of Selected Steels **1044-1045**  
**A-24** Mechanical Properties of Three Non-Steel Metals **1046-1047**  
**A-25** Stochastic Yield and Ultimate Strengths for Selected Materials **1048**  
**A-26** Stochastic Parameters from Finite Life Fatigue Tests in Selected Metals **1049**

- A-27** Finite Life Fatigue Strengths of Selected Plain Carbon Steels **1050**
- A-28** Decimal Equivalents of Wire and Sheet-Metal Gauges **1051-1052**
- A-29** Dimensions of Square and Hexagonal Bolts **1053**
- A-30** Dimensions of Hexagonal Cap Screws and Heavy Hexagonal Screws **1054**
- A-31** Dimensions of Hexagonal Nuts **1055**
- A-32** Basic Dimensions of American Standard Plain Washers **1056**
- A-33** Dimensions of Metric Plain Washers **1057**
- A-34** Gamma Function **1058**

**Table A-1**

Standard SI Prefixes\*†

Name	Symbol	Factor
exa	E	$1\ 000\ 000\ 000\ 000\ 000\ 000 = 10^{18}$
peta	P	$1\ 000\ 000\ 000\ 000\ 000\ 000 = 10^{15}$
tera	T	$1\ 000\ 000\ 000\ 000 = 10^{12}$
giga	G	$1\ 000\ 000\ 000 = 10^9$
mega	M	$1\ 000\ 000 = 10^6$
kilo	k	$1\ 000 = 10^3$
hecto‡	h	$100 = 10^2$
deka‡	da	$10 = 10^1$
deci‡	d	$0.1 = 10^{-1}$
centi‡	c	$0.01 = 10^{-2}$
milli	m	$0.001 = 10^{-3}$
micro	$\mu$	$0.000\ 001 = 10^{-6}$
nano	n	$0.000\ 000\ 001 = 10^{-9}$
pico	p	$0.000\ 000\ 000\ 001 = 10^{-12}$
femto	f	$0.000\ 000\ 000\ 000\ 001 = 10^{-15}$
atto	a	$0.000\ 000\ 000\ 000\ 000\ 001 = 10^{-18}$

\*If possible use multiple and submultiple prefixes in steps of 1000.

†Spaces are used in SI instead of commas to group numbers to avoid confusion with the practice in some European countries of using commas for decimal points.

‡Not recommended but sometimes encountered.

**Table A-2**Conversion Factors A to Convert Input X to Output Y Using the Formula  $Y = AX^*$ 

Multiply Input X	By Factor A	To Get Output Y	Multiply Input X	By Factor A	To Get Output Y
British thermal unit, Btu	1055	joule, J	mile, mi	1.610	kilometer, km
Btu/second, Btu/s	1.05	kilowatt, kW	mile/hour, mi/h	1.61	kilometer/hour, km/h
calorie	4.19	joule, J	mile/hour, mi/h	0.447	meter/second, m/s
centimeter of mercury ( $0^\circ\text{C}$ )	1.333	kilopascal, kPa	moment of inertia, $\text{lbf} \cdot \text{ft}^2$	0.0421	kilogram-meter <sup>2</sup> , $\text{kg} \cdot \text{m}^2$
centipoise, cP	0.001	pascal-second, $\text{Pa} \cdot \text{s}$	moment of inertia, $\text{lbf} \cdot \text{in}^2$	293	kilogram-millimeter <sup>2</sup> , $\text{kg} \cdot \text{mm}^2$
degree (angle)	0.0174	radian, rad	moment of section (second moment of area), $\text{in}^4$	41.6	centimeter <sup>4</sup> , $\text{cm}^4$
foot, ft	0.305	meter, m	ounce-force, oz	0.278	newton, N
foot <sup>2</sup> , ft <sup>2</sup>	0.0929	meter <sup>2</sup> , m <sup>2</sup>	ounce-mass	0.0311	kilogram, kg
foot/minute, ft/min	0.0051	meter/second, m/s	pound, lbf <sup>†</sup>	4.45	newton, N
foot-pound, ft · lbf	1.35	joule, J	pound-foot, lbf · ft	1.36	newton-meter, N · m
foot-pound/second, ft · lbf/s	1.35	watt, W	pound/foot <sup>2</sup> , lbf/ft <sup>2</sup>	47.9	pascal, Pa
foot/second, ft/s	0.305	meter/second, m/s	pound-inch, lbf · in	0.113	joule, J
gallon (U.S.), gal	3.785	liter, L	pound-inch, lbf · in	0.113	newton-meter, N · m
horsepower, hp	0.746	kilowatt, kW	pound/inch, lbf/in	175	newton/meter, N/m
inch, in	0.0254	meter, m	pound/inch <sup>2</sup> , psi (lbf/in <sup>2</sup> )	6.89	kilopascal, kPa
inch, in	25.4	millimeter, mm	pound-mass, lbf	0.454	kilogram, kg
inch <sup>2</sup> , in <sup>2</sup>	645	millimeter <sup>2</sup> , mm <sup>2</sup>	pound-mass/second, lbf/s	0.454	kilogram/second, kg/s
inch of mercury ( $32^\circ\text{F}$ )	3.386	kilopascal, kPa	quart (U.S. liquid), qt	946	milliliter, mL
kilopound, kip	4.45	kilonewton, kN	section modulus, in <sup>3</sup>	16.4	centimeter <sup>3</sup> , cm <sup>3</sup>
kilopound/inch <sup>2</sup> , ksi	6.89	megapascal, MPa (N/mm <sup>2</sup> )	slug	14.6	kilogram, kg
mass, lbf · s <sup>2</sup> /in	175	kilogram, kg	ton (short 2000 lbf)	907	kilogram, kg
			yard, yd	0.914	meter, m

\*Approximate.

<sup>†</sup>The U.S. Customary system unit of the pound-force is often abbreviated as lbf to distinguish it from the pound-mass, which is abbreviated as lbf.

**Table A-3**

Optional SI Units for Bending Stress

$\sigma = Mc/l$ , Torsion Stress

$\tau = Tr/J$ , Axial Stress

$\sigma = F/A$ , and Direct Shear Stress  $\tau = F/A$

Bending and Torsion				Axial and Direct Shear		
<b>M, T</b>	<b>I, J</b>	<b>c, r</b>	<b><math>\sigma, \tau</math></b>	<b>F</b>	<b>A</b>	<b><math>\sigma, \tau</math></b>
N · m*	m <sup>4</sup>	m	Pa	N*	m <sup>2</sup>	Pa
N · m	cm <sup>4</sup>	cm	MPa (N/mm <sup>2</sup> )	N†	mm <sup>2</sup>	MPa (N/mm <sup>2</sup> )
N · m†	mm <sup>4</sup>	mm	GPa	kN	m <sup>2</sup>	kPa
kN · m	cm <sup>4</sup>	cm	GPa	kN†	mm <sup>2</sup>	GPa
N · mm†	mm <sup>4</sup>	mm	MPa (N/mm <sup>2</sup> )			

\*Basic relation.

†Often preferred.

**Table A-4**

Optional SI Units for Bending Deflection

$y = f(Fl^3/EI)$  or

$y = f(wl^4/EI)$  and

Torsional Deflection

$\theta = Tl/GJ$

Bending Deflection					Torsional Deflection				
<b>F, wl</b>	<b>I</b>	<b>E</b>	<b>y</b>	<b>T</b>	<b>I</b>	<b>J</b>	<b>G</b>	<b><math>\theta</math></b>	
N*	m	m <sup>4</sup>	Pa	m	N · m*	m	m <sup>4</sup>	Pa	rad
kN†	mm	mm <sup>4</sup>	GPa	mm	N · m†	mm	mm <sup>4</sup>	GPa	rad
kN	m	m <sup>4</sup>	GPa	$\mu\text{m}$	N · mm	mm	mm <sup>4</sup>	MPa (N/mm <sup>2</sup> )	rad
N	mm	mm <sup>4</sup>	kPa	m	N · m	cm	cm <sup>4</sup>	MPa (N/mm <sup>2</sup> )	rad

\*Basic relation.

†Often preferred.

**Table A-5**

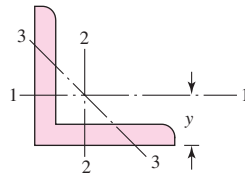
Physical Constants of Materials

<b>Material</b>	<b>Modulus of Elasticity E</b>		<b>Modulus of Rigidity G</b>		<b>Poisson's Ratio <math>\nu</math></b>	<b>Unit Weight w</b>		
	<b>Mpsi</b>	<b>GPa</b>	<b>Mpsi</b>	<b>GPa</b>		<b>Ibf/in<sup>3</sup></b>	<b>Ibf/ft<sup>3</sup></b>	<b>kN/m<sup>3</sup></b>
Aluminum (all alloys)	10.4	71.7	3.9	26.9	0.333	0.098	169	26.6
Beryllium copper	18.0	124.0	7.0	48.3	0.285	0.297	513	80.6
Brass	15.4	106.0	5.82	40.1	0.324	0.309	534	83.8
Carbon steel	30.0	207.0	11.5	79.3	0.292	0.282	487	76.5
Cast iron (gray)	14.5	100.0	6.0	41.4	0.211	0.260	450	70.6
Copper	17.2	119.0	6.49	44.7	0.326	0.322	556	87.3
Douglas fir	1.6	11.0	0.6	4.1	0.33	0.016	28	4.3
Glass	6.7	46.2	2.7	18.6	0.245	0.094	162	25.4
Inconel	31.0	214.0	11.0	75.8	0.290	0.307	530	83.3
Lead	5.3	36.5	1.9	13.1	0.425	0.411	710	111.5
Magnesium	6.5	44.8	2.4	16.5	0.350	0.065	112	17.6
Molybdenum	48.0	331.0	17.0	117.0	0.307	0.368	636	100.0
Monel metal	26.0	179.0	9.5	65.5	0.320	0.319	551	86.6
Nickel silver	18.5	127.0	7.0	48.3	0.322	0.316	546	85.8
Nickel steel	30.0	207.0	11.5	79.3	0.291	0.280	484	76.0
Phosphor bronze	16.1	111.0	6.0	41.4	0.349	0.295	510	80.1
Stainless steel (18-8)	27.6	190.0	10.6	73.1	0.305	0.280	484	76.0
Titanium alloys	16.5	114.0	6.2	42.4	0.340	0.160	276	43.4

**Table A-6**

Properties of Structural-  
Steel Equal Legs  
Angles\*†

$w$  = weight per foot, lbf/ft  
 $m$  = mass per meter, kg/m  
 $A$  = area, in<sup>2</sup> (cm<sup>2</sup>)  
 $I$  = second moment of area, in<sup>4</sup> (cm<sup>4</sup>)  
 $k$  = radius of gyration, in (cm)  
 $y$  = centroidal distance, in (cm)  
 $Z$  = section modulus, in<sup>3</sup>, (cm<sup>3</sup>)



Size, in	w	A	$I_{1-1}$	$k_{1-1}$	$Z_{1-1}$	y	$k_{3-3}$	
$1 \times 1 \times \frac{1}{8}$	0.80	0.234	0.021	0.298	0.029	0.290	0.191	
	$\times \frac{1}{4}$	1.49	0.437	0.036	0.287	0.054	0.336	0.193
$1\frac{1}{2} \times 1\frac{1}{2} \times \frac{1}{8}$	1.23	0.36	0.074	0.45	0.068	0.41	0.29	
	$\times \frac{1}{4}$	2.34	0.69	0.135	0.44	0.130	0.46	0.29
$2 \times 2 \times \frac{1}{8}$	1.65	0.484	0.190	0.626	0.131	0.546	0.398	
	$\times \frac{1}{4}$	3.19	0.938	0.348	0.609	0.247	0.592	0.391
	$\times \frac{3}{8}$	4.7	1.36	0.479	0.594	0.351	0.636	0.389
$2\frac{1}{2} \times 2\frac{1}{2} \times \frac{1}{4}$	4.1	1.19	0.703	0.769	0.394	0.717	0.491	
	$\times \frac{3}{8}$	5.9	1.73	0.984	0.753	0.566	0.762	0.487
$3 \times 3 \times \frac{1}{4}$	4.9	1.44	1.24	0.930	0.577	0.842	0.592	
	$\times \frac{3}{8}$	7.2	2.11	1.76	0.913	0.833	0.888	0.587
	$\times \frac{1}{2}$	9.4	2.75	2.22	0.898	1.07	0.932	0.584
$3\frac{1}{2} \times 3\frac{1}{2} \times \frac{1}{4}$	5.8	1.69	2.01	1.09	0.794	0.968	0.694	
	$\times \frac{3}{8}$	8.5	2.48	2.87	1.07	1.15	1.01	0.687
$4 \times 4 \times \frac{1}{4}$	11.1	3.25	3.64	1.06	1.49	1.06	0.683	
	$\times \frac{3}{8}$	6.6	1.94	3.04	1.25	1.05	1.09	0.795
$4 \times 4 \times \frac{1}{2}$	9.8	2.86	4.36	1.23	1.52	1.14	0.788	
	$\times \frac{1}{2}$	12.8	3.75	5.56	1.22	1.97	1.18	0.782
$4 \times 4 \times \frac{5}{8}$	15.7	4.61	6.66	1.20	2.40	1.23	0.779	
	$\times \frac{3}{4}$	14.9	4.36	15.4	1.88	3.53	1.64	1.19
$6 \times 6 \times \frac{3}{8}$	19.6	5.75	19.9	1.86	4.61	1.68	1.18	
	$\times \frac{5}{8}$	24.2	7.11	24.2	1.84	5.66	1.73	1.18
$6 \times 6 \times \frac{3}{4}$	28.7	8.44	28.2	1.83	6.66	1.78	1.17	

**Table A-6**

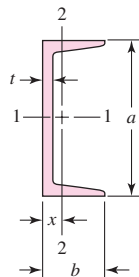
	<b>Size, mm</b>	<b>m</b>	<b>A</b>	<b><math>I_{1-1}</math></b>	<b><math>k_{1-1}</math></b>	<b><math>Z_{1-1}</math></b>	<b>y</b>	<b><math>k_{3-3}</math></b>
Properties of Structural-Steel Equal Legs Angles*†	25 × 25 × 3	1.11	1.42	0.80	0.75	0.45	0.72	0.48
(Continued)	× 4	1.45	1.85	1.01	0.74	0.58	0.76	0.48
	× 5	1.77	2.26	1.20	0.73	0.71	0.80	0.48
	40 × 40 × 4	2.42	3.08	4.47	1.21	1.55	1.12	0.78
	× 5	2.97	3.79	5.43	1.20	1.91	1.16	0.77
	× 6	3.52	4.48	6.31	1.19	2.26	1.20	0.77
	50 × 50 × 5	3.77	4.80	11.0	1.51	3.05	1.40	0.97
	× 6	4.47	5.59	12.8	1.50	3.61	1.45	0.97
	× 8	5.82	7.41	16.3	1.48	4.68	1.52	0.96
	60 × 60 × 5	4.57	5.82	19.4	1.82	4.45	1.64	1.17
	× 6	5.42	6.91	22.8	1.82	5.29	1.69	1.17
	× 8	7.09	9.03	29.2	1.80	6.89	1.77	1.16
	× 10	8.69	11.1	34.9	1.78	8.41	1.85	1.16
	80 × 80 × 6	7.34	9.35	55.8	2.44	9.57	2.17	1.57
	× 8	9.63	12.3	72.2	2.43	12.6	2.26	1.56
	× 10	11.9	15.1	87.5	2.41	15.4	2.34	1.55
	100 × 100 × 8	12.2	15.5	145	3.06	19.9	2.74	1.96
	× 12	17.8	22.7	207	3.02	29.1	2.90	1.94
	× 15	21.9	27.9	249	2.98	35.6	3.02	1.93
	150 × 150 × 10	23.0	29.3	624	4.62	56.9	4.03	2.97
	× 12	27.3	34.8	737	4.60	67.7	4.12	2.95
	× 15	33.8	43.0	898	4.57	83.5	4.25	2.93
	× 18	40.1	51.0	1050	4.54	98.7	4.37	2.92

\*Metric sizes also available in sizes of 45, 70, 90, 120, and 200 mm.

†These sizes are also available in aluminum alloy.

**Table A-7**

Properties of Structural-Steel Channels\*

 $a, b$  = size, in (mm) $w$  = weight per foot, lbf/ft $m$  = mass per meter, kg/m $t$  = web thickness, in (mm) $A$  = area, in<sup>2</sup> (cm<sup>2</sup>) $I$  = second moment of area, in<sup>4</sup> (cm<sup>4</sup>) $k$  = radius of gyration, in (cm) $x$  = centroidal distance, in (cm) $Z$  = section modulus, in<sup>3</sup> (cm<sup>3</sup>)

<b><i>a, in</i></b>	<b><i>b, in</i></b>	<b><i>t</i></b>	<b><i>A</i></b>	<b><i>w</i></b>	<b><i>I<sub>1-1</sub></i></b>	<b><i>k<sub>1-1</sub></i></b>	<b><i>Z<sub>1-1</sub></i></b>	<b><i>I<sub>2-2</sub></i></b>	<b><i>k<sub>2-2</sub></i></b>	<b><i>Z<sub>2-2</sub></i></b>	<b><i>x</i></b>
3	1.410	0.170	1.21	4.1	1.66	1.17	1.10	0.197	0.404	0.202	0.436
3	1.498	0.258	1.47	5.0	1.85	1.12	1.24	0.247	0.410	0.233	0.438
3	1.596	0.356	1.76	6.0	2.07	1.08	1.38	0.305	0.416	0.268	0.455
4	1.580	0.180	1.57	5.4	3.85	1.56	1.93	0.319	0.449	0.283	0.457
4	1.720	0.321	2.13	7.25	4.59	1.47	2.29	0.433	0.450	0.343	0.459
5	1.750	0.190	1.97	6.7	7.49	1.95	3.00	0.479	0.493	0.378	0.484
5	1.885	0.325	2.64	9.0	8.90	1.83	3.56	0.632	0.489	0.450	0.478
6	1.920	0.200	2.40	8.2	13.1	2.34	4.38	0.693	0.537	0.492	0.511
6	2.034	0.314	3.09	10.5	15.2	2.22	5.06	0.866	0.529	0.564	0.499
6	2.157	0.437	3.83	13.0	17.4	2.13	5.80	1.05	0.525	0.642	0.514
7	2.090	0.210	2.87	9.8	21.3	2.72	6.08	0.968	0.581	0.625	0.540
7	2.194	0.314	3.60	12.25	24.2	2.60	6.93	1.17	0.571	0.703	0.525
7	2.299	0.419	4.33	14.75	27.2	2.51	7.78	1.38	0.564	0.779	0.532
8	2.260	0.220	3.36	11.5	32.3	3.10	8.10	1.30	0.625	0.781	0.571
8	2.343	0.303	4.04	13.75	36.2	2.99	9.03	1.53	0.615	0.854	0.553
8	2.527	0.487	5.51	18.75	44.0	2.82	11.0	1.98	0.599	1.01	0.565
9	2.430	0.230	3.91	13.4	47.7	3.49	10.6	1.75	0.669	0.962	0.601
9	2.485	0.285	4.41	15.0	51.0	3.40	11.3	1.93	0.661	1.01	0.586
9	2.648	0.448	5.88	20.0	60.9	3.22	13.5	2.42	0.647	1.17	0.583
10	2.600	0.240	4.49	15.3	67.4	3.87	13.5	2.28	0.713	1.16	0.634
10	2.739	0.379	5.88	20.0	78.9	3.66	15.8	2.81	0.693	1.32	0.606
10	2.886	0.526	7.35	25.0	91.2	3.52	18.2	3.36	0.676	1.48	0.617
10	3.033	0.673	8.82	30.0	103	3.43	20.7	3.95	0.669	1.66	0.649
12	3.047	0.387	7.35	25.0	144	4.43	24.1	4.47	0.780	1.89	0.674
12	3.170	0.510	8.82	30.0	162	4.29	27.0	5.14	0.763	2.06	0.674

**Table A-7**Properties of Structural-Steel Channels (*Continued*)

<b>a × b, mm</b>	<b>m</b>	<b>t</b>	<b>A</b>	<b>I<sub>1-1</sub></b>	<b>k<sub>1-1</sub></b>	<b>Z<sub>1-1</sub></b>	<b>I<sub>2-2</sub></b>	<b>k<sub>2-2</sub></b>	<b>Z<sub>2-2</sub></b>	<b>x</b>
76 × 38	6.70	5.1	8.53	74.14	2.95	19.46	10.66	1.12	4.07	1.19
102 × 51	10.42	6.1	13.28	207.7	3.95	40.89	29.10	1.48	8.16	1.51
127 × 64	14.90	6.4	18.98	482.5	5.04	75.99	67.23	1.88	15.25	1.94
152 × 76	17.88	6.4	22.77	851.5	6.12	111.8	113.8	2.24	21.05	2.21
152 × 89	23.84	7.1	30.36	1166	6.20	153.0	215.1	2.66	35.70	2.86
178 × 76	20.84	6.6	26.54	1337	7.10	150.4	134.0	2.25	24.72	2.20
178 × 89	26.81	7.6	34.15	1753	7.16	197.2	241.0	2.66	39.29	2.76
203 × 76	23.82	7.1	30.34	1950	8.02	192.0	151.3	2.23	27.59	2.13
203 × 89	29.78	8.1	37.94	2491	8.10	245.2	264.4	2.64	42.34	2.65
229 × 76	26.06	7.6	33.20	2610	8.87	228.3	158.7	2.19	28.22	2.00
229 × 89	32.76	8.6	41.73	3387	9.01	296.4	285.0	2.61	44.82	2.53
254 × 76	28.29	8.1	36.03	3367	9.67	265.1	162.6	2.12	28.21	1.86
254 × 89	35.74	9.1	45.42	4448	9.88	350.2	302.4	2.58	46.70	2.42
305 × 89	41.69	10.2	53.11	7061	11.5	463.3	325.4	2.48	48.49	2.18
305 × 102	46.18	10.2	58.83	8214	11.8	539.0	499.5	2.91	66.59	2.66

\*These sizes are also available in aluminum alloy.

**Table A-8**

Properties of Round  
Tubing

$w_a$  = unit weight of aluminum tubing, lbf/ft  
 $w_s$  = unit weight of steel tubing, lbf/ft  
 $m$  = unit mass, kg/m  
 $A$  = area, in<sup>2</sup> (cm<sup>2</sup>)  
 $I$  = second moment of area, in<sup>4</sup> (cm<sup>4</sup>)  
 $J$  = second polar moment of area, in<sup>4</sup> (cm<sup>4</sup>)  
 $k$  = radius of gyration, in (cm)  
 $Z$  = section modulus, in<sup>3</sup> (cm<sup>3</sup>)  
 $d, t$  = size (OD) and thickness, in (mm)

Size, in	$w_a$	$w_s$	$A$	$I$	$k$	$Z$	$J$
$1 \times \frac{1}{8}$	0.416	1.128	0.344	0.034	0.313	0.067	0.067
$1 \times \frac{1}{4}$	0.713	2.003	0.589	0.046	0.280	0.092	0.092
$1\frac{1}{2} \times \frac{1}{8}$	0.653	1.769	0.540	0.129	0.488	0.172	0.257
$1\frac{1}{2} \times \frac{1}{4}$	1.188	3.338	0.982	0.199	0.451	0.266	0.399
$2 \times \frac{1}{8}$	0.891	2.670	0.736	0.325	0.664	0.325	0.650
$2 \times \frac{1}{4}$	1.663	4.673	1.374	0.537	0.625	0.537	1.074
$2\frac{1}{2} \times \frac{1}{8}$	1.129	3.050	0.933	0.660	0.841	0.528	1.319
$2\frac{1}{2} \times \frac{1}{4}$	2.138	6.008	1.767	1.132	0.800	0.906	2.276
$3 \times \frac{1}{4}$	2.614	7.343	2.160	2.059	0.976	1.373	4.117
$3 \times \frac{3}{8}$	3.742	10.51	3.093	2.718	0.938	1.812	5.436
$4 \times \frac{3}{16}$	2.717	7.654	2.246	4.090	1.350	2.045	8.180
$4 \times \frac{3}{8}$	5.167	14.52	4.271	7.090	1.289	3.544	14.180

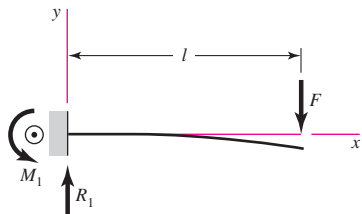
  

Size, mm	$m$	$A$	$I$	$k$	$Z$	$J$
$12 \times 2$	0.490	0.628	0.082	0.361	0.136	0.163
$16 \times 2$	0.687	0.879	0.220	0.500	0.275	0.440
$16 \times 3$	0.956	1.225	0.273	0.472	0.341	0.545
$20 \times 4$	1.569	2.010	0.684	0.583	0.684	1.367
$25 \times 4$	2.060	2.638	1.508	0.756	1.206	3.015
$25 \times 5$	2.452	3.140	1.669	0.729	1.336	3.338
$30 \times 4$	2.550	3.266	2.827	0.930	1.885	5.652
$30 \times 5$	3.065	3.925	3.192	0.901	2.128	6.381
$42 \times 4$	3.727	4.773	8.717	1.351	4.151	17.430
$42 \times 5$	4.536	5.809	10.130	1.320	4.825	20.255
$50 \times 4$	4.512	5.778	15.409	1.632	6.164	30.810
$50 \times 5$	5.517	7.065	18.118	1.601	7.247	36.226

**Table A-9**

Shear, Moment, and Deflection of Beams  
(Note: Force and moment reactions are positive in the directions shown; equations for shear force  $V$  and bending moment  $M$  follow the sign conventions given in Sec. 3-2.)

## 1 Cantilever—end load

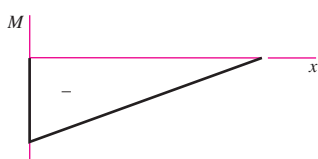


$$R_1 = V = F \quad M_1 = Fl$$

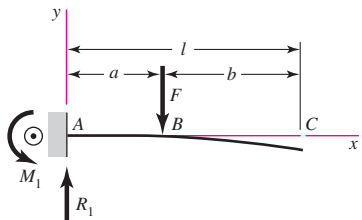
$$M = F(x - l)$$

$$y = \frac{Fx^2}{6EI}(x - 3l)$$

$$y_{\max} = -\frac{Fl^3}{3EI}$$



## 2 Cantilever—intermediate load



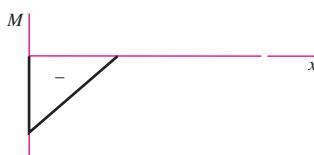
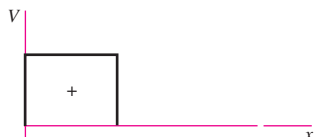
$$R_1 = V = F \quad M_1 = Fa$$

$$M_{AB} = F(x - a) \quad M_{BC} = 0$$

$$y_{AB} = \frac{Fx^2}{6EI}(x - 3a)$$

$$y_{BC} = \frac{Fa^2}{6EI}(a - 3x)$$

$$y_{\max} = \frac{Fa^2}{6EI}(a - 3l)$$

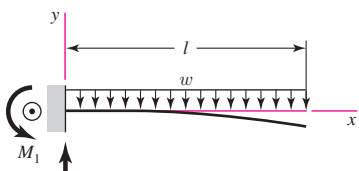


(continued)

**Table A-9**

**Shear, Moment, and Deflection of Beams  
(Continued)**

(Note: Force and moment reactions are positive in the directions shown; equations for shear force  $V$  and bending moment  $M$  follow the sign conventions given in Sec. 3-2.)

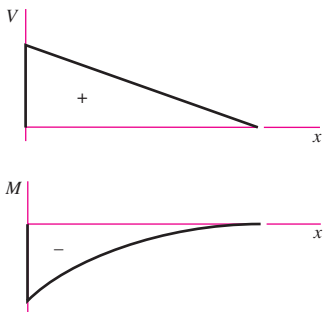
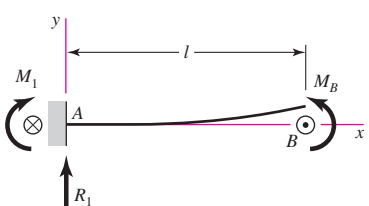
**3 Cantilever—uniform load**

$$R_1 = wl \quad M_1 = \frac{wl^2}{2}$$

$$V = w(l - x) \quad M = -\frac{w}{2}(l - x)^2$$

$$y = \frac{wx^2}{24EI}(4lx - x^2 - 6l^2)$$

$$y_{\max} = -\frac{wl^4}{8EI}$$

**4 Cantilever—moment load**

$$R_1 = V = 0 \quad M_1 = M = M_B$$

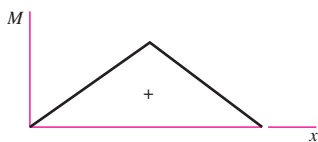
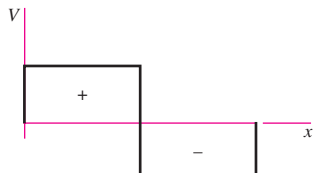
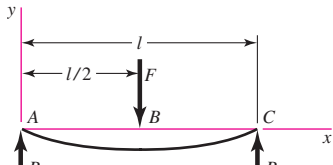
$$y = \frac{M_B x^2}{2EI} \quad y_{\max} = \frac{M_B l^2}{2EI}$$



**Table A-9**

**Shear, Moment, and Deflection of Beams  
(Continued)**

(Note: Force and moment reactions are positive in the directions shown; equations for shear force  $V$  and bending moment  $M$  follow the sign conventions given in Sec. 3-2.)

**5 Simple supports—center load**

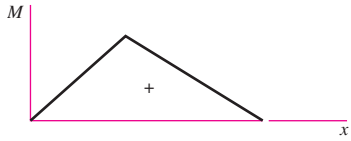
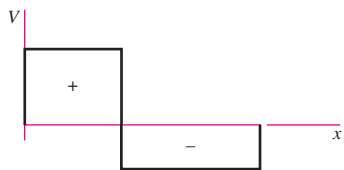
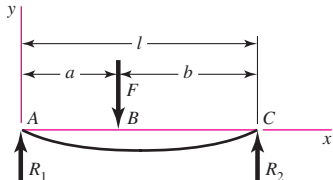
$$R_1 = R_2 = \frac{F}{2}$$

$$V_{AB} = R_1 \quad V_{BC} = -R_2$$

$$M_{AB} = \frac{Fx}{2} \quad M_{BC} = \frac{F}{2}(l-x)$$

$$y_{AB} = \frac{Fx}{48EI}(4x^2 - 3l^2)$$

$$y_{\max} = -\frac{Fl^3}{48EI}$$

**6 Simple supports—intermediate load**

$$R_1 = \frac{Fb}{l} \quad R_2 = \frac{Fa}{l}$$

$$V_{AB} = R_1 \quad V_{BC} = -R_2$$

$$M_{AB} = \frac{Fbx}{l} \quad M_{BC} = \frac{Fa}{l}(l-x)$$

$$y_{AB} = \frac{Fbx}{6EI}(x^2 + b^2 - l^2)$$

$$y_{BC} = \frac{Fa(l-x)}{6EI}(x^2 + a^2 - 2lx)$$

(continued)

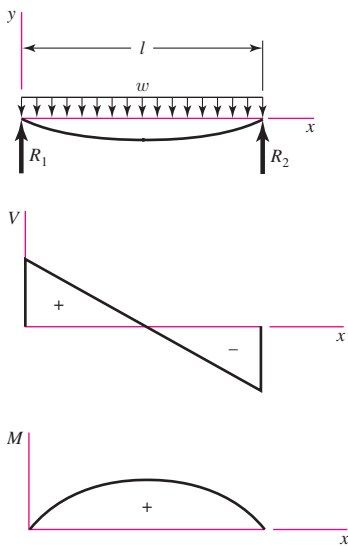
**Table A-9**

## Shear, Moment, and

## Deflection of Beams

(Continued)

(Note: Force and moment reactions are positive in the directions shown; equations for shear force  $V$  and bending moment  $M$  follow the sign conventions given in Sec. 3-2.)

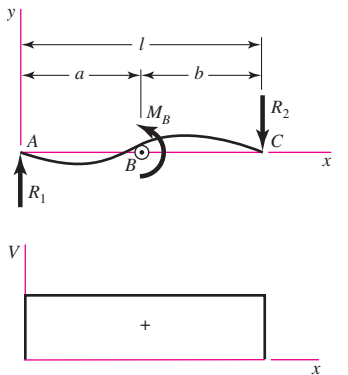
**7 Simple supports—uniform load**

$$R_1 = R_2 = \frac{wl}{2} \quad V = \frac{wl}{2} - wx$$

$$M = \frac{wx}{2}(l-x)$$

$$y = \frac{wx}{24EI}(2lx^2 - x^3 - l^3)$$

$$y_{\max} = -\frac{5wl^4}{384EI}$$

**8 Simple supports—moment load**

$$R_1 = R_2 = \frac{M_B}{l} \quad V = \frac{M_B}{l}$$

$$M_{AB} = \frac{M_B x}{l} \quad M_{BC} = \frac{M_B}{l}(x-l)$$

$$y_{AB} = \frac{M_B x}{6EI l} (x^2 + 3a^2 - 6al + 2l^2)$$

$$y_{BC} = \frac{M_B}{6EI l} [x^3 - 3lx^2 + x(2l^2 + 3a^2) - 3a^2 l]$$

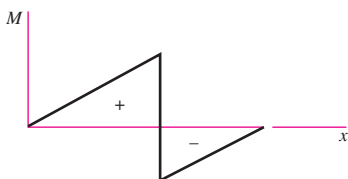
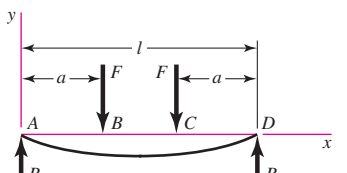


**Table A-9**

**Shear, Moment, and Deflection of Beams  
(Continued)**

(Note: Force and moment reactions are positive in the directions shown; equations for shear force  $V$  and bending moment  $M$  follow the sign conventions given in Sec. 3-2.)

9 Simple supports—twin loads



$$R_1 = R_2 = F \quad V_{AB} = F \quad V_{BC} = 0$$

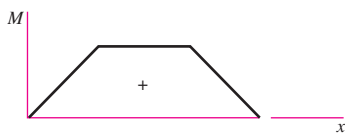
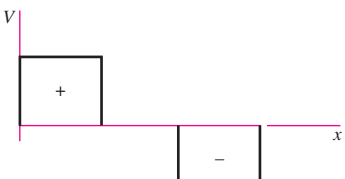
$$V_{CD} = -F$$

$$M_{AB} = Fx \quad M_{BC} = Fa \quad M_{CD} = F(l - x)$$

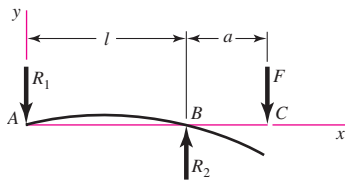
$$y_{AB} = \frac{Fx}{6EI}(x^2 + 3a^2 - 3la)$$

$$y_{BC} = \frac{Fa}{6EI}(3x^2 + a^2 - 3lx)$$

$$y_{\max} = \frac{Fa}{24EI}(4a^2 - 3l^2)$$



10 Simple supports—overhanging load



$$R_1 = \frac{Fa}{l} \quad R_2 = \frac{F}{l}(l + a)$$

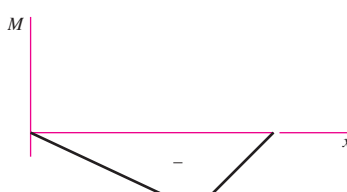
$$V_{AB} = -\frac{Fa}{l} \quad V_{BC} = F$$

$$M_{AB} = -\frac{Fax}{l} \quad M_{BC} = F(x - l - a)$$

$$y_{AB} = \frac{Fax}{6EIl}(l^2 - x^2)$$

$$y_{BC} = \frac{F(x - l)}{6EI}[(x - l)^2 - a(3x - l)]$$

$$y_C = -\frac{Fa^2}{3EI}(l + a)$$



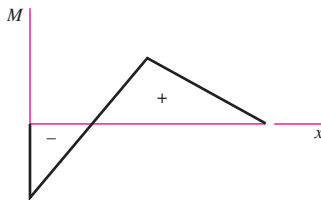
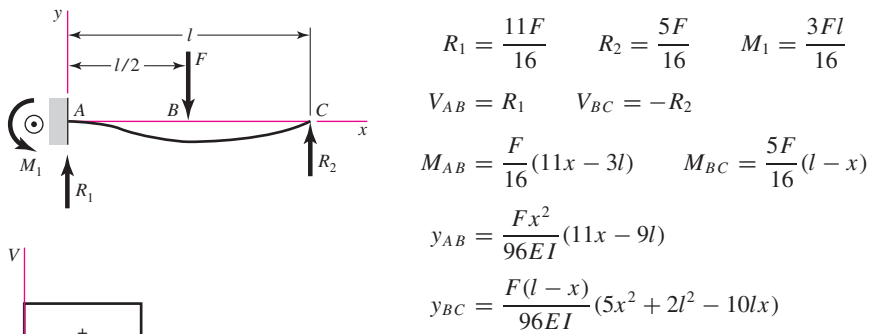
(continued)

**Table A-9**

**Shear, Moment, and Deflection of Beams  
(Continued)**

(Note: Force and moment reactions are positive in the directions shown; equations for shear force  $V$  and bending moment  $M$  follow the sign conventions given in Sec. 3-2.)

11 One fixed and one simple support—center load



12 One fixed and one simple support—intermediate load

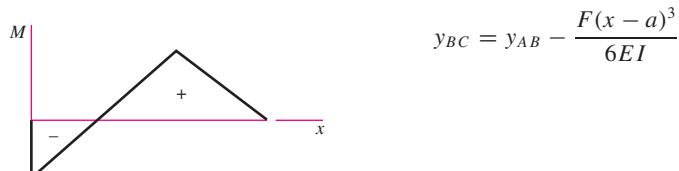
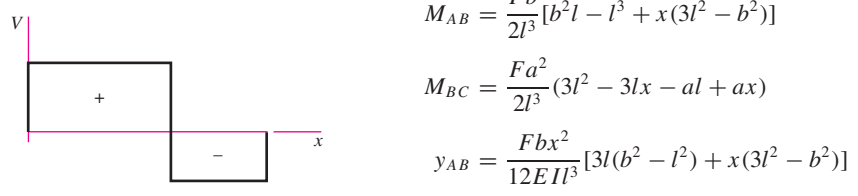
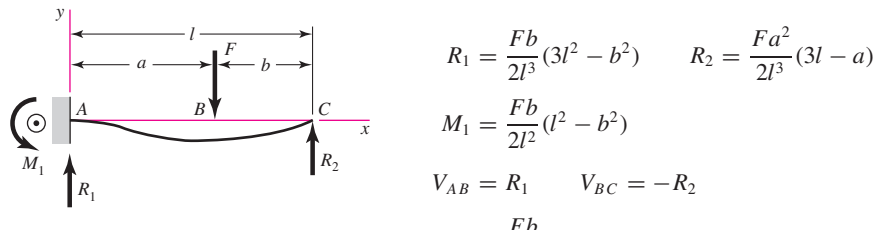
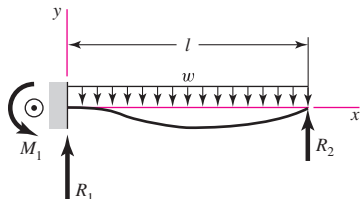


**Table A-9**

**Shear, Moment, and Deflection of Beams  
(Continued)**  
(Note: Force and moment reactions are positive in the directions shown; equations for shear force  $V$  and bending moment  $M$  follow the sign conventions given in Sec. 3-2.)

13 One fixed and one simple support—uniform load

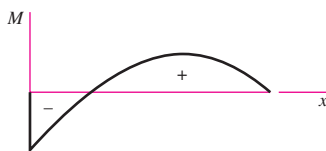
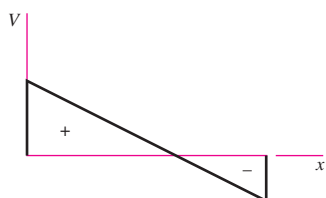


$$R_1 = \frac{5wl}{8} \quad R_2 = \frac{3wl}{8} \quad M_1 = \frac{wl^2}{8}$$

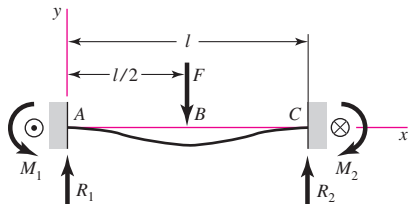
$$V = \frac{5wl}{8} - wx$$

$$M = -\frac{w}{8}(4x^2 - 5lx + l^2)$$

$$y = \frac{wx^2}{48EI}(l-x)(2x-3l)$$



14 Fixed supports—center load



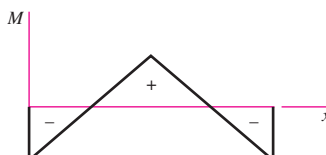
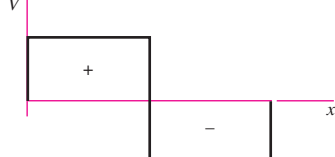
$$R_1 = R_2 = \frac{F}{2} \quad M_1 = M_2 = \frac{Fl}{8}$$

$$V_{AB} = -V_{BC} = \frac{F}{2}$$

$$M_{AB} = \frac{F}{8}(4x-l) \quad M_{BC} = \frac{F}{8}(3l-4x)$$

$$y_{AB} = \frac{Fx^2}{48EI}(4x-3l)$$

$$y_{\max} = -\frac{Fl^3}{192EI}$$

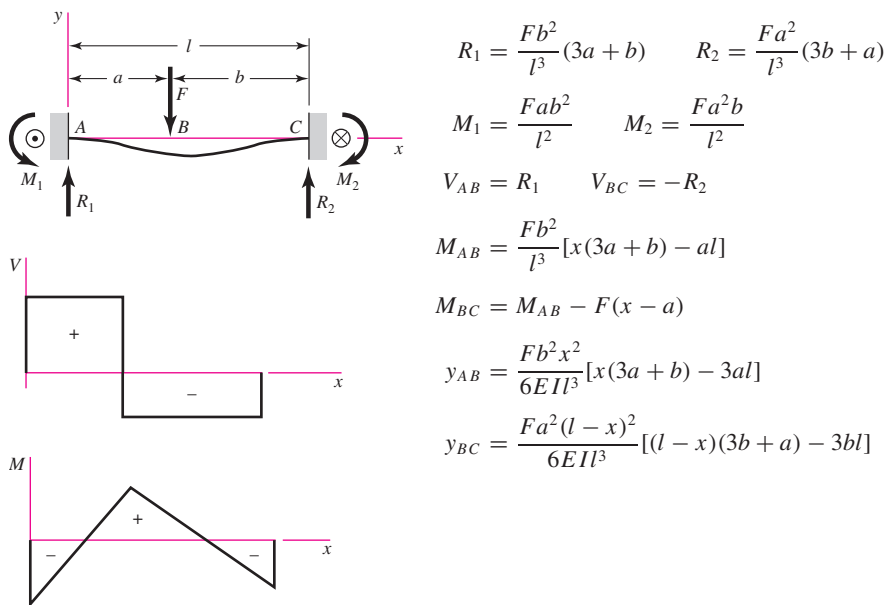


(continued)

**Table A-9**

**Shear, Moment, and Deflection of Beams (Continued)**  
**(Note:** Force and moment reactions are positive in the directions shown; equations for shear force  $V$  and bending moment  $M$  follow the sign conventions given in Sec. 3-2.)

15 Fixed supports—intermediate load



16 Fixed supports—uniform load

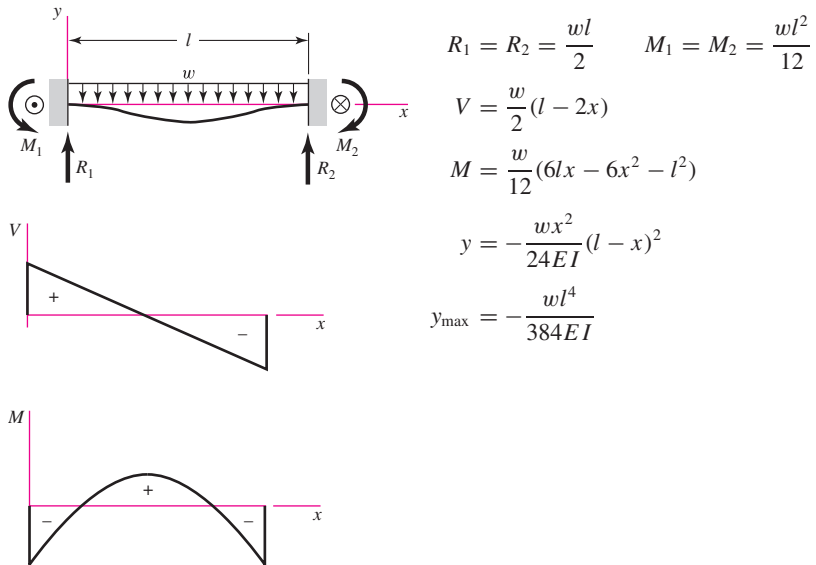
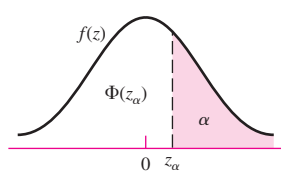


**Table A-10**

Cumulative Distribution Function of Normal (Gaussian) Distribution

$$\Phi(z_\alpha) = \int_{-\infty}^{z_\alpha} \frac{1}{\sqrt{2\pi}} \exp\left(-\frac{u^2}{2}\right) du$$

$$= \begin{cases} \alpha & z_\alpha \leq 0 \\ 1 - \alpha & z_\alpha > 0 \end{cases}$$



<b>Z<sub>α</sub></b>	<b>0.00</b>	<b>0.01</b>	<b>0.02</b>	<b>0.03</b>	<b>0.04</b>	<b>0.05</b>	<b>0.06</b>	<b>0.07</b>	<b>0.08</b>	<b>0.09</b>
0.0	0.5000	0.4960	0.4920	0.4880	0.4840	0.4801	0.4761	0.4721	0.4681	0.4641
0.1	0.4602	0.4562	0.4522	0.4483	0.4443	0.4404	0.4364	0.4325	0.4286	0.4247
0.2	0.4207	0.4168	0.4129	0.4090	0.4052	0.4013	0.3974	0.3936	0.3897	0.3859
0.3	0.3821	0.3783	0.3745	0.3707	0.3669	0.3632	0.3594	0.3557	0.3520	0.3483
0.4	0.3446	0.3409	0.3372	0.3336	0.3300	0.3264	0.3238	0.3192	0.3156	0.3121
0.5	0.3085	0.3050	0.3015	0.2981	0.2946	0.2912	0.2877	0.2843	0.2810	0.2776
0.6	0.2743	0.2709	0.2676	0.2643	0.2611	0.2578	0.2546	0.2514	0.2483	0.2451
0.7	0.2420	0.2389	0.2358	0.2327	0.2296	0.2266	0.2236	0.2206	0.2177	0.2148
0.8	0.2119	0.2090	0.2061	0.2033	0.2005	0.1977	0.1949	0.1922	0.1894	0.1867
0.9	0.1841	0.1814	0.1788	0.1762	0.1736	0.1711	0.1685	0.1660	0.1635	0.1611
1.0	0.1587	0.1562	0.1539	0.1515	0.1492	0.1469	0.1446	0.1423	0.1401	0.1379
1.1	0.1357	0.1335	0.1314	0.1292	0.1271	0.1251	0.1230	0.1210	0.1190	0.1170
1.2	0.1151	0.1131	0.1112	0.1093	0.1075	0.1056	0.1038	0.1020	0.1003	0.0985
1.3	0.0968	0.0951	0.0934	0.0918	0.0901	0.0885	0.0869	0.0853	0.0838	0.0823
1.4	0.0808	0.0793	0.0778	0.0764	0.0749	0.0735	0.0721	0.0708	0.0694	0.0681
1.5	0.0668	0.0655	0.0643	0.0630	0.0618	0.0606	0.0594	0.0582	0.0571	0.0559
1.6	0.0548	0.0537	0.0526	0.0516	0.0505	0.0495	0.0485	0.0475	0.0465	0.0455
1.7	0.0446	0.0436	0.0427	0.0418	0.0409	0.0401	0.0392	0.0384	0.0375	0.0367
1.8	0.0359	0.0351	0.0344	0.0336	0.0329	0.0322	0.0314	0.0307	0.0301	0.0294
1.9	0.0287	0.0281	0.0274	0.0268	0.0262	0.0256	0.0250	0.0244	0.0239	0.0233
2.0	0.0228	0.0222	0.0217	0.0212	0.0207	0.0202	0.0197	0.0192	0.0188	0.0183
2.1	0.0179	0.0174	0.0170	0.0166	0.0162	0.0158	0.0154	0.0150	0.0146	0.0143
2.2	0.0139	0.0136	0.0132	0.0129	0.0125	0.0122	0.0119	0.0116	0.0113	0.0110
2.3	0.0107	0.0104	0.0102	0.00990	0.00964	0.00939	0.00914	0.00889	0.00866	0.00842
2.4	0.00820	0.00798	0.00776	0.00755	0.00734	0.00714	0.00695	0.00676	0.00657	0.00639
2.5	0.00621	0.00604	0.00587	0.00570	0.00554	0.00539	0.00523	0.00508	0.00494	0.00480
2.6	0.00466	0.00453	0.00440	0.00427	0.00415	0.00402	0.00391	0.00379	0.00368	0.00357
2.7	0.00347	0.00336	0.00326	0.00317	0.00307	0.00298	0.00289	0.00280	0.00272	0.00264
2.8	0.00256	0.00248	0.00240	0.00233	0.00226	0.00219	0.00212	0.00205	0.00199	0.00193
2.9	0.00187	0.00181	0.00175	0.00169	0.00164	0.00159	0.00154	0.00149	0.00144	0.00139

(continued)

**Table A-10**Cumulative Distribution Function of Normal (Gaussian) Distribution (*Continued*)

<b><math>Z_\alpha</math></b>	<b>0.0</b>	<b>0.1</b>	<b>0.2</b>	<b>0.3</b>	<b>0.4</b>	<b>0.5</b>	<b>0.6</b>	<b>0.7</b>	<b>0.8</b>	<b>0.9</b>
3	0.00135	0.0 <sup>3</sup> 968	0.0 <sup>3</sup> 687	0.0 <sup>3</sup> 483	0.0 <sup>3</sup> 337	0.0 <sup>3</sup> 233	0.0 <sup>3</sup> 159	0.0 <sup>3</sup> 108	0.0 <sup>4</sup> 723	0.0 <sup>4</sup> 481
4	0.0 <sup>4</sup> 317	0.0 <sup>4</sup> 207	0.0 <sup>4</sup> 133	0.0 <sup>5</sup> 854	0.0 <sup>5</sup> 541	0.0 <sup>5</sup> 340	0.0 <sup>5</sup> 211	0.0 <sup>5</sup> 130	0.0 <sup>6</sup> 793	0.0 <sup>6</sup> 479
5	0.0 <sup>6</sup> 287	0.0 <sup>6</sup> 170	0.0 <sup>7</sup> 996	0.0 <sup>7</sup> 579	0.0 <sup>7</sup> 333	0.0 <sup>7</sup> 190	0.0 <sup>7</sup> 107	0.0 <sup>8</sup> 599	0.0 <sup>8</sup> 332	0.0 <sup>8</sup> 182
6	0.0 <sup>9</sup> 987	0.0 <sup>9</sup> 530	0.0 <sup>9</sup> 282	0.0 <sup>9</sup> 149	0.0 <sup>10</sup> 777	0.0 <sup>10</sup> 402	0.0 <sup>10</sup> 206	0.0 <sup>10</sup> 104	0.0 <sup>11</sup> 523	0.0 <sup>11</sup> 260
$z_\alpha$	-1.282	-1.643	-1.960	-2.326	-2.576	-3.090	-3.291	-3.891	-4.417	
F( $z_\alpha$ )	0.10	0.05	0.025	0.010	0.005	0.001	0.0005	0.0001	0.000005	
R( $z_\alpha$ )	0.90	0.95	0.975	0.990	0.995	0.999	0.9995	0.9999	0.999995	

**Table A-11**

A Selection of International Tolerance Grades—Metric Series (Size Ranges Are for Over the Lower Limit and Including the Upper Limit. All Values Are in Millimeters)	<b>Basic Sizes</b>	<b>Tolerance Grades</b>				
		<b>IT6</b>	<b>IT7</b>	<b>IT8</b>	<b>IT9</b>	<b>IT10</b>
0–3	0.006	0.010	0.014	0.025	0.040	0.060
3–6	0.008	0.012	0.018	0.030	0.048	0.075
6–10	0.009	0.015	0.022	0.036	0.058	0.090
10–18	0.011	0.018	0.027	0.043	0.070	0.110
18–30	0.013	0.021	0.033	0.052	0.084	0.130
30–50	0.016	0.025	0.039	0.062	0.100	0.160
50–80	0.019	0.030	0.046	0.074	0.120	0.190
80–120	0.022	0.035	0.054	0.087	0.140	0.220
120–180	0.025	0.040	0.063	0.100	0.160	0.250
180–250	0.029	0.046	0.072	0.115	0.185	0.290
250–315	0.032	0.052	0.081	0.130	0.210	0.320
315–400	0.036	0.057	0.089	0.140	0.230	0.360

*Source: Preferred Metric Limits and Fits, ANSI B4.2-1978.*

See also BSI 4500.

**Table A-12**

Fundamental Deviations for Shafts—Metric Series

(Size Ranges Are for *Over* the Lower Limit and *Including* the Upper Limit. All Values Are in Millimeters)Source: *Preferred Metric Limits and Fits*, ANSI B4.2-1978. See also BSI 4500.

<b>Basic Sizes</b>	<b>Upper-Deviation Letter</b>						<b>Lower-Deviation Letter</b>				
	<b>c</b>	<b>d</b>	<b>f</b>	<b>g</b>	<b>h</b>	<b>k</b>	<b>n</b>	<b>p</b>	<b>s</b>	<b>u</b>	
0–3	−0.060	−0.020	−0.006	−0.002	0	0	+0.004	+0.006	+0.014	+0.018	
3–6	−0.070	−0.030	−0.010	−0.004	0	+0.001	+0.008	+0.012	+0.019	+0.023	
6–10	−0.080	−0.040	−0.013	−0.005	0	+0.001	+0.010	+0.015	+0.023	+0.028	
10–14	−0.095	−0.050	−0.016	−0.006	0	+0.001	+0.012	+0.018	+0.028	+0.033	
14–18	−0.095	−0.050	−0.016	−0.006	0	+0.001	+0.012	+0.018	+0.028	+0.033	
18–24	−0.110	−0.065	−0.020	−0.007	0	+0.002	+0.015	+0.022	+0.035	+0.041	
24–30	−0.110	−0.065	−0.020	−0.007	0	+0.002	+0.015	+0.022	+0.035	+0.048	
30–40	−0.120	−0.080	−0.025	−0.009	0	+0.002	+0.017	+0.026	+0.043	+0.060	
40–50	−0.130	−0.080	−0.025	−0.009	0	+0.002	+0.017	+0.026	+0.043	+0.070	
50–65	−0.140	−0.100	−0.030	−0.010	0	+0.002	+0.020	+0.032	+0.053	+0.087	
65–80	−0.150	−0.100	−0.030	−0.010	0	+0.002	+0.020	+0.032	+0.059	+0.102	
80–100	−0.170	−0.120	−0.036	−0.012	0	+0.003	+0.023	+0.037	+0.071	+0.124	
100–120	−0.180	−0.120	−0.036	−0.012	0	+0.003	+0.023	+0.037	+0.079	+0.144	
120–140	−0.200	−0.145	−0.043	−0.014	0	+0.003	+0.027	+0.043	+0.092	+0.170	
140–160	−0.210	−0.145	−0.043	−0.014	0	+0.003	+0.027	+0.043	+0.100	+0.190	
160–180	−0.230	−0.145	−0.043	−0.014	0	+0.003	+0.027	+0.043	+0.108	+0.210	
180–200	−0.240	−0.170	−0.050	−0.015	0	+0.004	+0.031	+0.050	+0.122	+0.236	
200–225	−0.260	−0.170	−0.050	−0.015	0	+0.004	+0.031	+0.050	+0.130	+0.258	
225–250	−0.280	−0.170	−0.050	−0.015	0	+0.004	+0.031	+0.050	+0.140	+0.284	
250–280	−0.300	−0.190	−0.056	−0.017	0	+0.004	+0.034	+0.056	+0.158	+0.315	
280–315	−0.330	−0.190	−0.056	−0.017	0	+0.004	+0.034	+0.056	+0.170	+0.350	
315–355	−0.360	−0.210	−0.062	−0.018	0	+0.004	+0.037	+0.062	+0.190	+0.390	
355–400	−0.400	−0.210	−0.062	−0.018	0	+0.004	+0.037	+0.062	+0.208	+0.435	

**Table A-13**

A Selection of International Tolerance Grades—Inch Series (Size Ranges Are for Over the Lower Limit and Including the Upper Limit. All Values Are in Inches, Converted from Table A-11)	<b>Basic Sizes</b>	<b>Tolerance Grades</b>				
		<b>IT6</b>	<b>IT7</b>	<b>IT8</b>	<b>IT9</b>	<b>IT10</b>
0–0.12	0.0002	0.0004	0.0006	0.0010	0.0016	0.0024
0.12–0.24	0.0003	0.0005	0.0007	0.0012	0.0019	0.0030
0.24–0.40	0.0004	0.0006	0.0009	0.0014	0.0023	0.0035
0.40–0.72	0.0004	0.0007	0.0011	0.0017	0.0028	0.0043
0.72–1.20	0.0005	0.0008	0.0013	0.0020	0.0033	0.0051
1.20–2.00	0.0006	0.0010	0.0015	0.0024	0.0039	0.0063
2.00–3.20	0.0007	0.0012	0.0018	0.0029	0.0047	0.0075
3.20–4.80	0.0009	0.0014	0.0021	0.0034	0.0055	0.0087
4.80–7.20	0.0010	0.0016	0.0025	0.0039	0.0063	0.0098
7.20–10.00	0.0011	0.0018	0.0028	0.0045	0.0073	0.0114
10.00–12.60	0.0013	0.0020	0.0032	0.0051	0.0083	0.0126
12.60–16.00	0.0014	0.0022	0.0035	0.0055	0.0091	0.0142

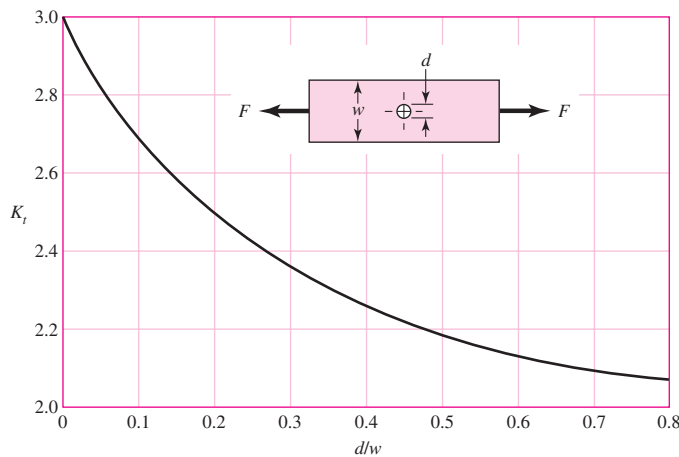
**Table A-14**

Fundamental Deviations for Shafts—Inch Series (Size Ranges Are for *Over* the Lower Limit and *Including* the Upper Limit. All Values Are in Inches, Converted from Table A-12)

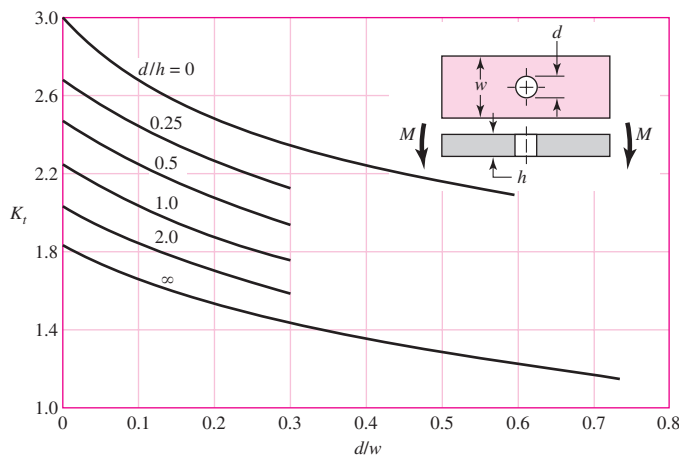
Basic Sizes	Upper-Deviation Letter					Lower-Deviation Letter				
	c	d	f	g	h	k	n	p	s	u
0–0.12	-0.0024	-0.0008	-0.0002	-0.0001	0	0	+0.0002	+0.0002	+0.0006	+0.0007
0.12–0.24	-0.0028	-0.0012	-0.0004	-0.0002	0	0	+0.0003	+0.0005	+0.0007	+0.0009
0.24–0.40	-0.0031	-0.0016	-0.0005	-0.0002	0	0	+0.0004	+0.0006	+0.0009	+0.0011
0.40–0.72	-0.0037	-0.0020	-0.0006	-0.0002	0	0	+0.0005	+0.0007	+0.0011	+0.0013
0.72–0.96	-0.0043	-0.0026	-0.0008	-0.0003	0	+0.0001	+0.0006	+0.0009	+0.0014	+0.0016
0.96–1.20	-0.0043	-0.0026	-0.0008	-0.0003	0	+0.0001	+0.0006	+0.0009	+0.0014	+0.0019
1.20–1.60	-0.0047	-0.0031	-0.0010	-0.0004	0	+0.0001	+0.0007	+0.0010	+0.0017	+0.0024
1.60–2.00	-0.0051	-0.0031	-0.0010	-0.0004	0	+0.0001	+0.0007	+0.0010	+0.0017	+0.0028
2.00–2.60	-0.0055	-0.0039	-0.0012	-0.0004	0	+0.0001	+0.0008	+0.0013	+0.0021	+0.0034
2.60–3.20	-0.0059	-0.0039	-0.0012	-0.0004	0	+0.0001	+0.0008	+0.0013	+0.0023	+0.0040
3.20–4.00	-0.0067	-0.0047	-0.0014	-0.0005	0	+0.0001	+0.0009	+0.0015	+0.0028	+0.0049
4.00–4.80	-0.0071	-0.0047	-0.0014	-0.0005	0	+0.0001	+0.0009	+0.0015	+0.0031	+0.0057
4.80–5.60	-0.0079	-0.0057	-0.0017	-0.0006	0	+0.0001	+0.0011	+0.0017	+0.0036	+0.0067
5.60–6.40	-0.0083	-0.0057	-0.0017	-0.0006	0	+0.0001	+0.0011	+0.0017	+0.0039	+0.0075
6.40–7.20	-0.0091	-0.0057	-0.0017	-0.0006	0	+0.0001	+0.0011	+0.0017	+0.0043	+0.0083
7.20–8.00	-0.0094	-0.0067	-0.0020	-0.0006	0	+0.0002	+0.0012	+0.0020	+0.0048	+0.0093
8.00–9.00	-0.0102	-0.0067	-0.0020	-0.0006	0	+0.0002	+0.0012	+0.0020	+0.0051	+0.0102
9.00–10.00	-0.0110	-0.0067	-0.0020	-0.0006	0	+0.0002	+0.0012	+0.0020	+0.0055	+0.0112
10.00–11.20	-0.0118	-0.0075	-0.0022	-0.0007	0	+0.0002	+0.0013	+0.0022	+0.0062	+0.0124
11.20–12.60	-0.0130	-0.0075	-0.0022	-0.0007	0	+0.0002	+0.0013	+0.0022	+0.0067	+0.0130
12.60–14.20	-0.0142	-0.0083	-0.0024	-0.0007	0	+0.0002	+0.0015	+0.0024	+0.0075	+0.0154
14.20–16.00	-0.0157	-0.0083	-0.0024	-0.0007	0	+0.0002	+0.0015	+0.0024	+0.0082	+0.0171

**Table A-15**Charts of Theoretical Stress-Concentration Factors  $K_t^*$ **Figure A-15-1**

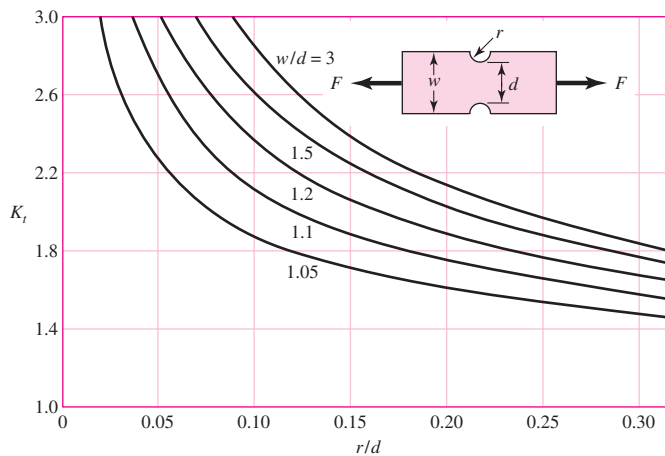
Bar in tension or simple compression with a transverse hole.  $\sigma_0 = F/A$ , where  $A = (w - d)t$  and  $t$  is the thickness.

**Figure A-15-2**

Rectangular bar with a transverse hole in bending.  $\sigma_0 = Mc/I$ , where  $I = (w - d)h^3/12$ .

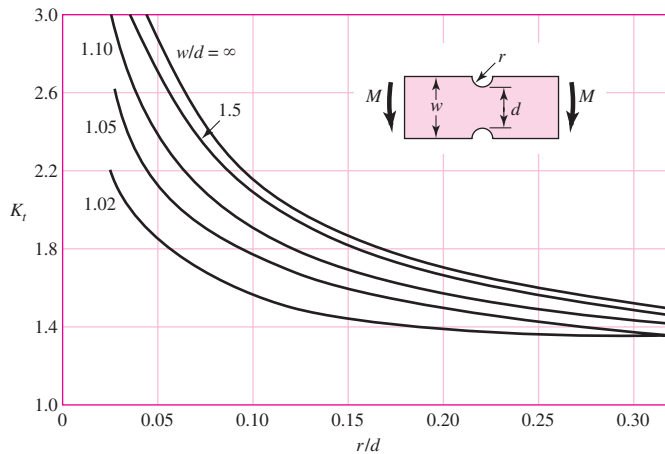
**Figure A-15-3**

Notched rectangular bar in tension or simple compression.  $\sigma_0 = F/A$ , where  $A = dt$  and  $t$  is the thickness.

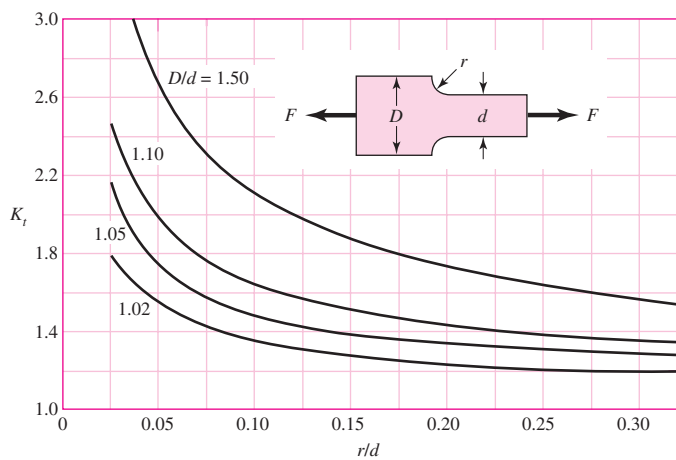


**Table A-15**Charts of Theoretical Stress-Concentration Factors  $K_t^*$  (Continued)**Figure A-15-4**

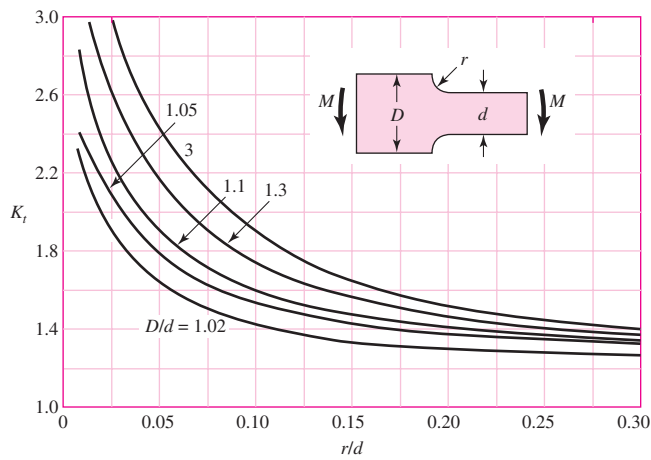
Notched rectangular bar in bending.  $\sigma_0 = Mc/I$ , where  $c = d/2$ ,  $I = td^3/12$ , and  $t$  is the thickness.

**Figure A-15-5**

Rectangular filleted bar in tension or simple compression.  $\sigma_0 = F/A$ , where  $A = dt$  and  $t$  is the thickness.

**Figure A-15-6**

Rectangular filleted bar in bending.  $\sigma_0 = Mc/I$ , where  $c = d/2$ ,  $I = td^3/12$ ,  $t$  is the thickness.

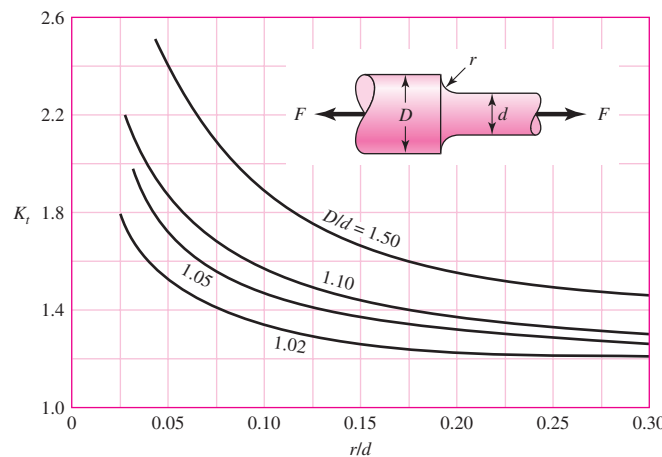


(continued)

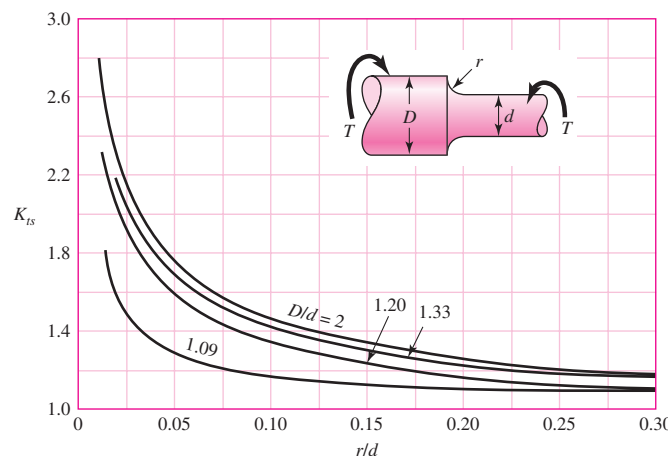
\*Factors from R. E. Peterson, "Design Factors for Stress Concentration," Machine Design, vol. 23, no. 2, February 1951, p. 169; no. 3, March 1951, p. 161; no. 5, May 1951, p. 159; no. 6, June 1951, p. 173; no. 7, July 1951, p. 155. Reprinted with permission from Machine Design, a Penton Media Inc. publication.

**Table A-15**Charts of Theoretical Stress-Concentration Factors  $K_t^*$  (Continued)**Figure A-15-7**

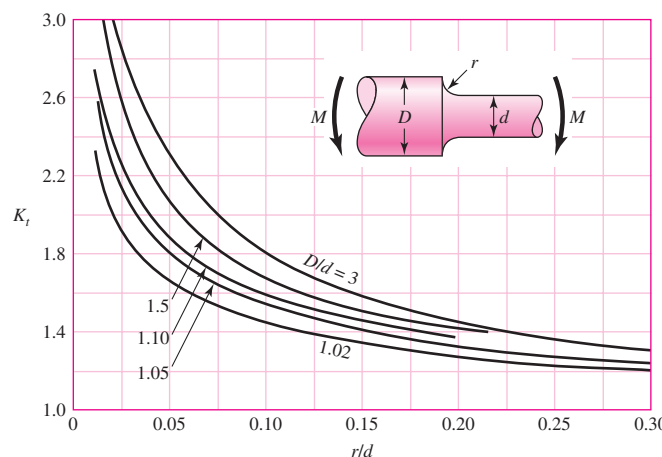
Round shaft with shoulder fillet in tension.  $\sigma_0 = F/A$ , where  $A = \pi d^2/4$ .

**Figure A-15-8**

Round shaft with shoulder fillet in torsion.  $\tau_0 = Tc/J$ , where  $c = d/2$  and  $J = \pi d^4/32$ .

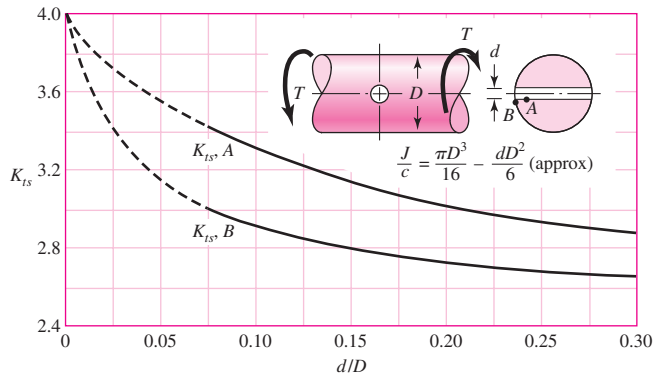
**Figure A-15-9**

Round shaft with shoulder fillet in bending.  $\sigma_0 = Mc/I$ , where  $c = d/2$  and  $I = \pi d^4/64$ .



**Table A-15**Charts of Theoretical Stress-Concentration Factors  $K_t^*$  (Continued)**Figure A-15-10**

Round shaft in torsion with transverse hole.

**Figure A-15-11**

Round shaft in bending with a transverse hole.  $\sigma_0 = M/[(\pi D^3/32) - (dD^2/6)]$ , approximately.

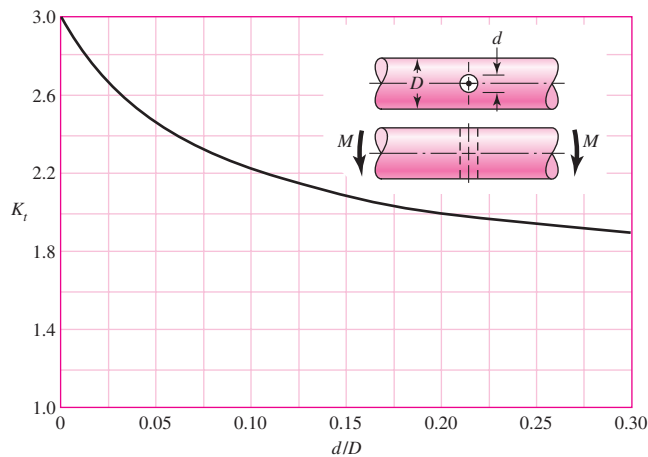
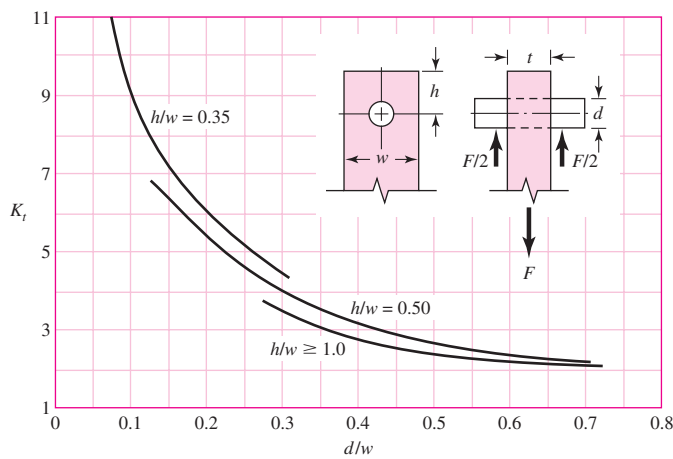
**Figure A-15-12**

Plate loaded in tension by a pin through a hole.  $\sigma_0 = F/A$ , where  $A = (w - d)t$ . When clearance exists, increase  $K_t$  35 to 50 percent. (M. M. Frocht and H. N. Hill, "Stress-Concentration Factors around a Central Circular Hole in a Plate Loaded through a Pin in Hole," *J. Appl. Mechanics*, vol. 7, no. 1, March 1940, p. A-5.)

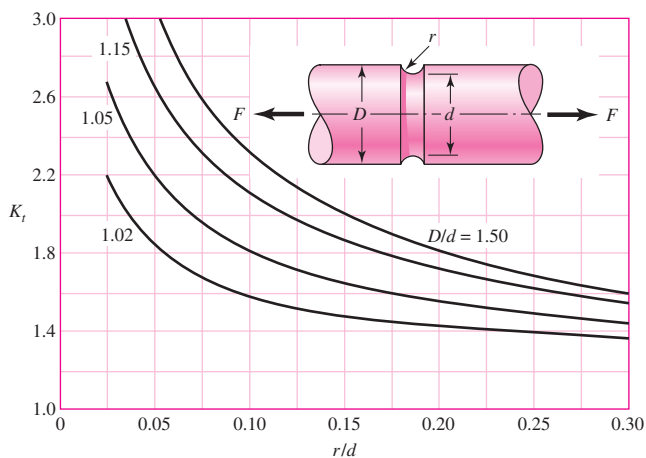


(continued)

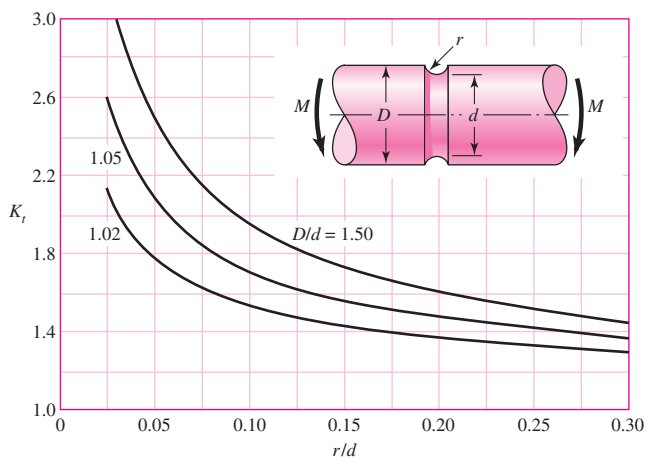
\*Factors from R. E. Peterson, "Design Factors for Stress Concentration," *Machine Design*, vol. 23, no. 2, February 1951, p. 169; no. 3, March 1951, p. 161; no. 5, May 1951, p. 159; no. 6, June 1951, p. 173; no. 7, July 1951, p. 155. Reprinted with permission from *Machine Design*, a Penton Media Inc. publication.

**Table A-15**Charts of Theoretical Stress-Concentration Factors  $K_t^*$  (Continued)**Figure A-15-13**

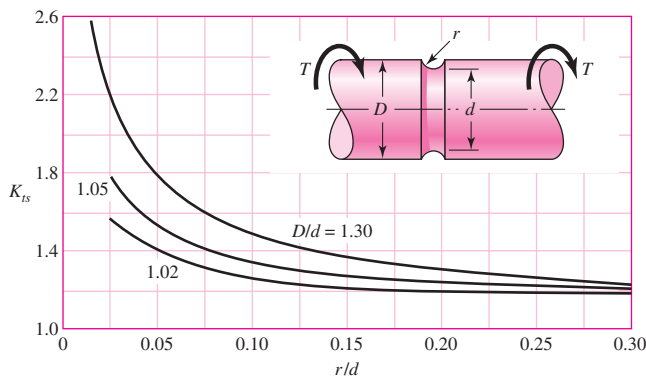
Grooved round bar in tension.  
 $\sigma_0 = F/A$ , where  $A = \pi d^2/4$ .

**Figure A-15-14**

Grooved round bar in bending.  
 $\sigma_0 = Mc/l$ , where  $c = d/2$   
and  $I = \pi d^4/64$ .

**Figure A-15-15**

Grooved round bar in torsion.  
 $\tau_0 = Tc/J$ , where  $c = d/2$  and  
 $J = \pi d^4/32$ .



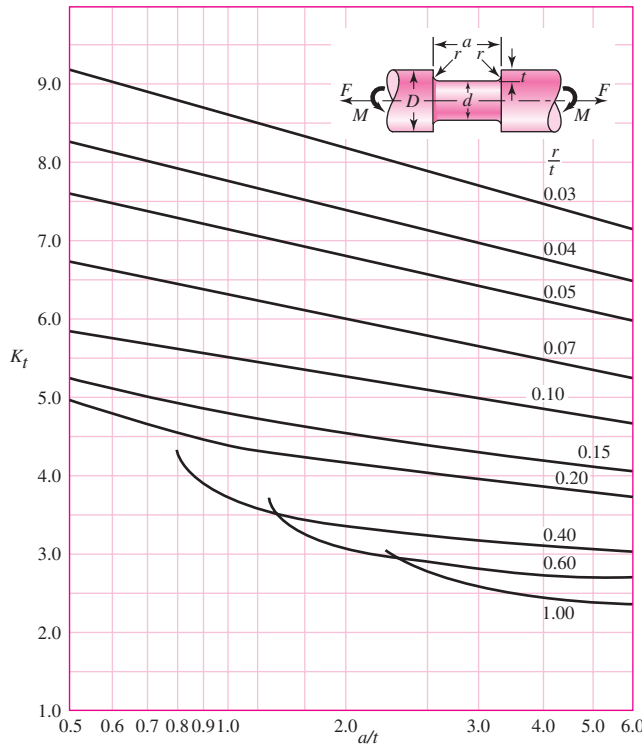
\*Factors from R. E. Peterson, "Design Factors for Stress Concentration," Machine Design, vol. 23, no. 2, February 1951, p. 169; no. 3, March 1951, p. 161, no. 5, May 1951, p. 159; no. 6, June 1951, p. 173; no. 7, July 1951, p. 155. Reprinted with permission from Machine Design, a Penton Media Inc. publication.

**Table A-15**Charts of Theoretical Stress-Concentration Factors  $K_t^*$  (*Continued*)**Figure A-15-16**

Round shaft with flat-bottom groove in bending and/or tension.

$$\sigma_0 = \frac{4F}{\pi d^2} + \frac{32M}{\pi d^3}$$

Source: W. D. Pilkey, *Peterson's Stress-Concentration Factors*, 2nd ed. John Wiley & Sons, New York, 1997, p. 115.



(continued)

**Table A-15**Charts of Theoretical Stress-Concentration Factors  $K_t^*$  (*Continued*)**Figure A-15-17**

Round shaft with flat-bottom groove in torsion.

$$\tau_0 = \frac{16T}{\pi d^3}$$

Source: W. D. Pilkey, *Peterson's Stress-Concentration Factors*, 2nd ed. John Wiley & Sons, New York, 1997, p. 133

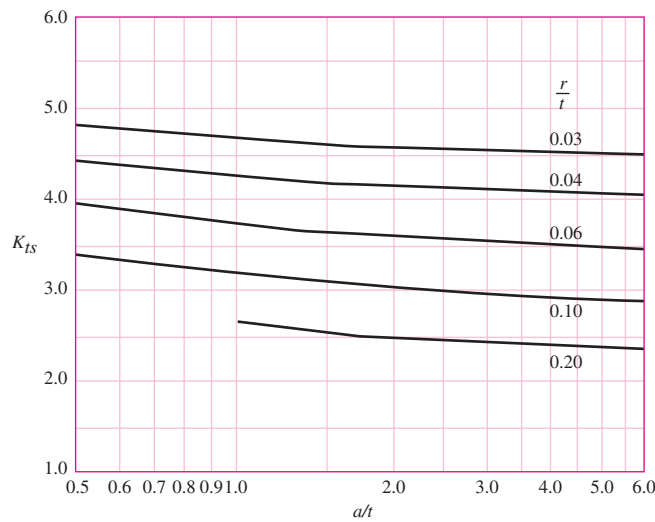
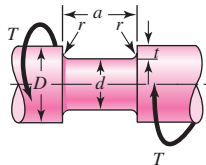
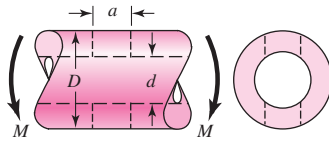


**Table A-16**

Approximate Stress-Concentration Factor  $K_t$  for Bending of a Round Bar or Tube with a Transverse Round Hole

Source: R. E. Peterson, *Stress-Concentration Factors*, Wiley, New York, 1974, pp. 146, 235.



The nominal bending stress is  $\sigma_0 = M/Z_{\text{net}}$  where  $Z_{\text{net}}$  is a reduced value of the section modulus and is defined by

$$Z_{\text{net}} = \frac{\pi A}{32D}(D^4 - d^4)$$

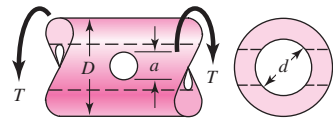
Values of  $A$  are listed in the table. Use  $d = 0$  for a solid bar

$a/D$	0.9		0.6		0	
	$A$	$K_t$	$A$	$K_t$	$A$	$K_t$
0.050	0.92	2.63	0.91	2.55	0.88	2.42
0.075	0.89	2.55	0.88	2.43	0.86	2.35
0.10	0.86	2.49	0.85	2.36	0.83	2.27
0.125	0.82	2.41	0.82	2.32	0.80	2.20
0.15	0.79	2.39	0.79	2.29	0.76	2.15
0.175	0.76	2.38	0.75	2.26	0.72	2.10
0.20	0.73	2.39	0.72	2.23	0.68	2.07
0.225	0.69	2.40	0.68	2.21	0.65	2.04
0.25	0.67	2.42	0.64	2.18	0.61	2.00
0.275	0.66	2.48	0.61	2.16	0.58	1.97
0.30	0.64	2.52	0.58	2.14	0.54	1.94

(continued)

**Table A-16** (Continued)

Approximate Stress-Concentration Factors  $K_{ts}$  for a Round Bar or Tube Having a Transverse Round Hole and Loaded in Torsion    Source: R. E. Peterson, *Stress-Concentration Factors*, Wiley, New York, 1974, pp. 148, 244.



The maximum stress occurs on the inside of the hole, slightly below the shaft surface. The nominal shear stress is  $\tau_0 = TD/2J_{\text{net}}$ , where  $J_{\text{net}}$  is a reduced value of the second polar moment of area and is defined by

$$J_{\text{net}} = \frac{\pi A(D^4 - d^4)}{32}$$

Values of  $A$  are listed in the table. Use  $d = 0$  for a solid bar.

$a/D$	$d/D$									
	0.9		0.8		0.6		0.4		0	
$a/D$	$A$	$K_{ts}$	$A$	$K_{ts}$	$A$	$K_{ts}$	$A$	$K_{ts}$	$A$	$K_{ts}$
0.05	0.96	1.78							0.95	1.77
0.075	0.95	1.82							0.93	1.71
0.10	0.94	1.76	0.93	1.74	0.92	1.72	0.92	1.70	0.92	1.68
0.125	0.91	1.76	0.91	1.74	0.90	1.70	0.90	1.67	0.89	1.64
0.15	0.90	1.77	0.89	1.75	0.87	1.69	0.87	1.65	0.87	1.62
0.175	0.89	1.81	0.88	1.76	0.87	1.69	0.86	1.64	0.85	1.60
0.20	0.88	1.96	0.86	1.79	0.85	1.70	0.84	1.63	0.83	1.58
0.25	0.87	2.00	0.82	1.86	0.81	1.72	0.80	1.63	0.79	1.54
0.30	0.80	2.18	0.78	1.97	0.77	1.76	0.75	1.63	0.74	1.51
0.35	0.77	2.41	0.75	2.09	0.72	1.81	0.69	1.63	0.68	1.47
0.40	0.72	2.67	0.71	2.25	0.68	1.89	0.64	1.63	0.63	1.44

**Table A-17**

Preferred Sizes and Renard (R-Series) Numbers  
 (When a choice can be made, use one of these sizes; however, not all parts or items are available in all the sizes shown in the table.)

Fraction of Inches
$\frac{1}{64}, \frac{1}{32}, \frac{1}{16}, \frac{3}{32}, \frac{1}{8}, \frac{5}{32}, \frac{3}{16}, \frac{1}{4}, \frac{5}{16}, \frac{3}{8}, \frac{7}{16}, \frac{1}{2}, \frac{9}{16}, \frac{5}{8}, \frac{11}{16}, \frac{3}{4}, \frac{7}{8}, 1, 1\frac{1}{4}, 1\frac{1}{2}, 1\frac{3}{4}, 2, 2\frac{1}{4}, 2\frac{1}{2}, 2\frac{3}{4}, 3, 3\frac{1}{4}, 3\frac{1}{2}, 3\frac{3}{4}, 4, 4\frac{1}{4}, 4\frac{1}{2}, 4\frac{3}{4}, 5, 5\frac{1}{4}, 5\frac{1}{2}, 5\frac{3}{4}, 6, 6\frac{1}{2}, 7, 7\frac{1}{2}, 8, 8\frac{1}{2}, 9, 9\frac{1}{2}, 10, 10\frac{1}{2}, 11, 11\frac{1}{2}, 12, 12\frac{1}{2}, 13, 13\frac{1}{2}, 14, 14\frac{1}{2}, 15, 15\frac{1}{2}, 16, 16\frac{1}{2}, 17, 17\frac{1}{2}, 18, 18\frac{1}{2}, 19, 19\frac{1}{2}, 20$
Decimal Inches
0.010, 0.012, 0.016, 0.020, 0.025, 0.032, 0.040, 0.05, 0.06, 0.08, 0.10, 0.12, 0.16, 0.20, 0.24, 0.30, 0.40, 0.50, 0.60, 0.80, 1.00, 1.20, 1.40, 1.60, 1.80, 2.0, 2.4, 2.6, 2.8, 3.0, 3.2, 3.4, 3.6, 3.8, 4.0, 4.2, 4.4, 4.6, 4.8, 5.0, 5.2, 5.4, 5.6, 5.8, 6.0, 7.0, 7.5, 8.5, 9.0, 9.5, 10.0, 10.5, 11.0, 11.5, 12.0, 12.5, 13.0, 13.5, 14.0, 14.5, 15.0, 15.5, 16.0, 16.5, 17.0, 17.5, 18.0, 18.5, 19.0, 19.5, 20
Millimeters
0.05, 0.06, 0.08, 0.10, 0.12, 0.16, 0.20, 0.25, 0.30, 0.40, 0.50, 0.60, 0.70, 0.80, 0.90, 1.0, 1.1, 1.2, 1.4, 1.5, 1.6, 1.8, 2.0, 2.2, 2.5, 2.8, 3.0, 3.5, 4.0, 4.5, 5.0, 5.5, 6.0, 6.5, 7.0, 8.0, 9.0, 10, 11, 12, 14, 16, 18, 20, 22, 25, 28, 30, 32, 35, 40, 45, 50, 60, 80, 100, 120, 140, 160, 180, 200, 250, 300
Renard Numbers*
1st choice, R5: 1, 1.6, 2.5, 4, 6.3, 10 2d choice, R10: 1.25, 2, 3.15, 5, 8 3d choice, R20: 1.12, 1.4, 1.8, 2.24, 2.8, 3.55, 4.5, 5.6, 7.1, 9 4th choice, R40: 1.06, 1.18, 1.32, 1.5, 1.7, 1.9, 2.12, 2.36, 2.65, 3, 3.35, 3.75, 4.25, 4.75, 5.3, 6, 6.7, 7.5, 8.5, 9.5

\*May be multiplied or divided by powers of 10.

**Table A-18****Part 1 Properties of Sections**

## Geometric Properties

 $A$  = area $G$  = location of centroid

$$I_x = \int y^2 dA = \text{second moment of area about } x \text{ axis}$$

$$I_y = \int x^2 dA = \text{second moment of area about } y \text{ axis}$$

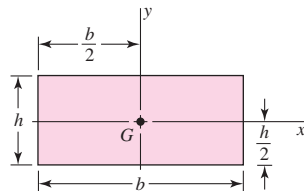
$$I_{xy} = \int xy dA = \text{mixed moment of area about } x \text{ and } y \text{ axes}$$

$$J_G = \int r^2 dA = \int (x^2 + y^2) dA = I_x + I_y$$

= second polar moment of area about axis through  $G$ 

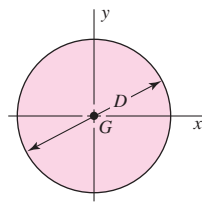
$$k_x^2 = I_x/A = \text{squared radius of gyration about } x \text{ axis}$$

## Rectangle



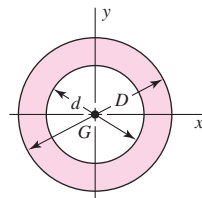
$$A = bh \quad I_x = \frac{bh^3}{12} \quad I_y = \frac{b^3h}{12} \quad I_{xy} = 0$$

## Circle



$$A = \frac{\pi D^2}{4} \quad I_x = I_y = \frac{\pi D^4}{64} \quad I_{xy} = 0 \quad J_G = \frac{\pi D^4}{32}$$

## Hollow circle

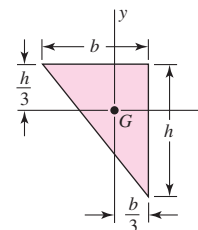
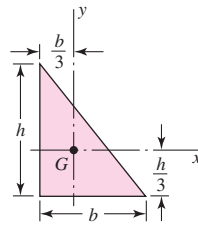


$$A = \frac{\pi}{4}(D^2 - d^2) \quad I_x = I_y = \frac{\pi}{64}(D^4 - d^4) \quad I_{xy} = 0 \quad J_G = \frac{\pi}{32}(D^4 - d^4)$$

**Table A-18**

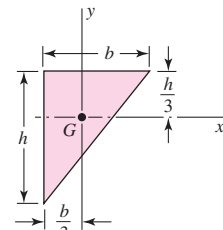
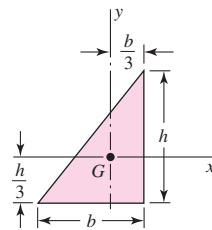
Geometric Properties  
(Continued)

## Right triangles



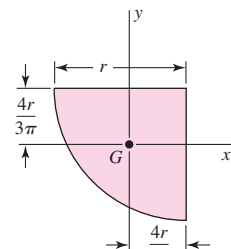
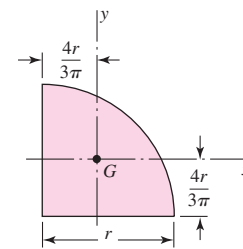
$$A = \frac{bh}{2} \quad I_x = \frac{bh^3}{36} \quad I_y = \frac{b^3h}{36} \quad I_{xy} = \frac{-b^2h^2}{72}$$

## Right triangles



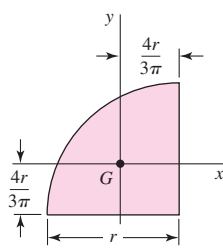
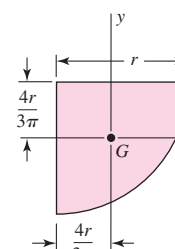
$$A = \frac{bh}{2} \quad I_x = \frac{bh^3}{36} \quad I_y = \frac{b^3h}{36} \quad I_{xy} = \frac{b^2h^2}{72}$$

## Quarter-circles



$$A = \frac{\pi r^2}{4} \quad I_x = I_y = r^4 \left( \frac{\pi}{16} - \frac{4}{9\pi} \right) \quad I_{xy} = r^4 \left( \frac{1}{8} - \frac{4}{9\pi} \right)$$

## Quarter-circles



$$A = \frac{\pi r^2}{4} \quad I_x = I_y = r^4 \left( \frac{\pi}{16} - \frac{4}{9\pi} \right) \quad I_{xy} = r^4 \left( \frac{4}{9\pi} - \frac{1}{8} \right)$$

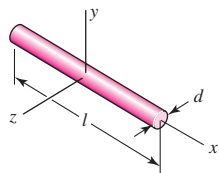
(continued)

**Table A-18**

Geometric Properties  
(Continued)

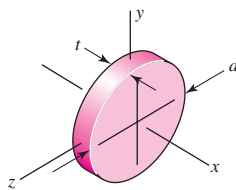
**Part 2 Properties of Solids ( $\rho$  = Density, Weight per Unit Volume)**

Rods



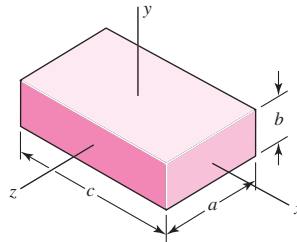
$$m = \frac{\pi d^2 l \rho}{4g} \quad I_y = I_z = \frac{ml^2}{12}$$

Round disks



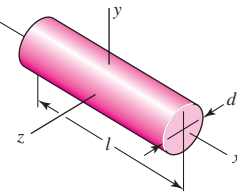
$$m = \frac{\pi d^2 t \rho}{4g} \quad I_x = \frac{md^2}{8} \quad I_y = I_z = \frac{md^2}{16}$$

Rectangular prisms



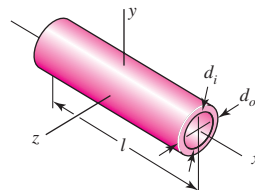
$$m = \frac{abc\rho}{g} \quad I_x = \frac{m}{12}(a^2 + b^2) \quad I_y = \frac{m}{12}(a^2 + c^2) \quad I_z = \frac{m}{12}(b^2 + c^2)$$

Cylinders



$$m = \frac{\pi d^2 l \rho}{4g} \quad I_x = \frac{md^2}{8} \quad I_y = I_z = \frac{m}{48}(3d^2 + 4l^2)$$

Hollow cylinders



$$m = \frac{\pi (d_o^2 - d_i^2) l \rho}{4g} \quad I_x = \frac{m}{8} (d_o^2 + d_i^2) \quad I_y = I_z = \frac{m}{48} (3d_o^2 + 3d_i^2 + 4l^2)$$

**Table A-19**

American Standard Pipe

<b>Nominal Size, in</b>	<b>Outside Diameter, in</b>	<b>Threads per inch</b>	<b>Standard No. 40</b>	<b>Wall Thickness, in</b>	
				<b>Extra Strong No. 80</b>	<b>Double Extra Strong</b>
$\frac{1}{8}$	0.405	27	0.070	0.098	
$\frac{1}{4}$	0.540	18	0.090	0.122	
$\frac{3}{8}$	0.675	18	0.093	0.129	
$\frac{1}{2}$	0.840	14	0.111	0.151	0.307
$\frac{3}{4}$	1.050	14	0.115	0.157	0.318
1	1.315	$11\frac{1}{2}$	0.136	0.183	0.369
$\frac{1}{4}$	1.660	$11\frac{1}{2}$	0.143	0.195	0.393
$\frac{1}{2}$	1.900	$11\frac{1}{2}$	0.148	0.204	0.411
2	2.375	$11\frac{1}{2}$	0.158	0.223	0.447
$2\frac{1}{2}$	2.875	8	0.208	0.282	0.565
3	3.500	8	0.221	0.306	0.615
$3\frac{1}{2}$	4.000	8	0.231	0.325	
4	4.500	8	0.242	0.344	0.690
5	5.563	8	0.263	0.383	0.768
6	6.625	8	0.286	0.441	0.884
8	8.625	8	0.329	0.510	0.895

**Table A-20**

Deterministic ASTM Minimum Tensile and Yield Strengths for Some Hot-Rolled (HR) and Cold-Drawn (CD) Steels [The strengths listed are estimated ASTM minimum values in the size range 18 to 32 mm ( $\frac{3}{4}$  to  $1\frac{1}{4}$  in). These strengths are suitable for use with the design factor defined in Sec. 1–10, provided the materials conform to ASTM A6 or A568 requirements or are required in the purchase specifications. Remember that a numbering system is not a specification.] *Source:* 1986 SAE Handbook, p. 2.15.

1 UNS No.	2 SAE and/or AISI No.	3 Process- ing	4 Tensile Strength, MPa (kpsi)	5 Yield Strength, MPa (kpsi)	6 Elongation in 2 in, %	7 Reduction in Area, %	8 Brinell Hardness
			HR	CD	HR	CD	HR
G10060	1006	HR	300 (43)	170 (24)	30	55	86
		CD	330 (48)	280 (41)	20	45	95
G10100	1010	HR	320 (47)	180 (26)	28	50	95
		CD	370 (53)	300 (44)	20	40	105
G10150	1015	HR	340 (50)	190 (27.5)	28	50	101
		CD	390 (56)	320 (47)	18	40	111
G10180	1018	HR	400 (58)	220 (32)	25	50	116
		CD	440 (64)	370 (54)	15	40	126
G10200	1020	HR	380 (55)	210 (30)	25	50	111
		CD	470 (68)	390 (57)	15	40	131
G10300	1030	HR	470 (68)	260 (37.5)	20	42	137
		CD	520 (76)	440 (64)	12	35	149
G10350	1035	HR	500 (72)	270 (39.5)	18	40	143
		CD	550 (80)	460 (67)	12	35	163
G10400	1040	HR	520 (76)	290 (42)	18	40	149
		CD	590 (85)	490 (71)	12	35	170
G10450	1045	HR	570 (82)	310 (45)	16	40	163
		CD	630 (91)	530 (77)	12	35	179
G10500	1050	HR	620 (90)	340 (49.5)	15	35	179
		CD	690 (100)	580 (84)	10	30	197
G10600	1060	HR	680 (98)	370 (54)	12	30	201
G10800	1080	HR	770 (112)	420 (61.5)	10	25	229
G10950	1095	HR	830 (120)	460 (66)	10	25	248

**Table A-21**

## Mean Mechanical Properties of Some Heat-Treated Steels

[These are typical properties for materials normalized and annealed. The properties for quenched and tempered (Q&T) steels are from a single heat. Because of the many variables, the properties listed are global averages. In all cases, data were obtained from specimens of diameter 0.505 in, machined from 1-in rounds, and of gauge length 2 in. unless noted, all specimens were oil-quenched.] *Source: ASM Metals Reference Book, 2d ed., American Society for Metals, Metals Park, Ohio, 1983.*

1 AISI No.	2 Treatment	3 Temperature °C (°F)	4 Tensile Strength MPa (kpsi)	5 Yield Strength, MPa (kpsi)	6 Elongation, %	7 Reduction in Area, %	8 Brinell Hardness
1030	Q&T*	205 (400)	848 (123)	648 (94)	17	47	495
	Q&T*	315 (600)	800 (116)	621 (90)	19	53	401
	Q&T*	425 (800)	731 (106)	579 (84)	23	60	302
	Q&T*	540 (1000)	669 (97)	517 (75)	28	65	255
	Q&T*	650 (1200)	586 (85)	441 (64)	32	70	207
	Normalized	925 (1700)	521 (75)	345 (50)	32	61	149
	Annealed	870 (1600)	430 (62)	317 (46)	35	64	137
1040	Q&T	205 (400)	779 (113)	593 (86)	19	48	262
	Q&T	425 (800)	758 (110)	552 (80)	21	54	241
	Q&T	650 (1200)	634 (92)	434 (63)	29	65	192
	Normalized	900 (1650)	590 (86)	374 (54)	28	55	170
	Annealed	790 (1450)	519 (75)	353 (51)	30	57	149
1050	Q&T*	205 (400)	1120 (163)	807 (117)	9	27	514
	Q&T*	425 (800)	1090 (158)	793 (115)	13	36	444
	Q&T*	650 (1200)	717 (104)	538 (78)	28	65	235
	Normalized	900 (1650)	748 (108)	427 (62)	20	39	217
	Annealed	790 (1450)	636 (92)	365 (53)	24	40	187
1060	Q&T	425 (800)	1080 (156)	765 (111)	14	41	311
	Q&T	540 (1000)	965 (140)	669 (97)	17	45	277
	Q&T	650 (1200)	800 (116)	524 (76)	23	54	229
	Normalized	900 (1650)	776 (112)	421 (61)	18	37	229
	Annealed	790 (1450)	626 (91)	372 (54)	22	38	179
1095	Q&T	315 (600)	1260 (183)	813 (118)	10	30	375
	Q&T	425 (800)	1210 (176)	772 (112)	12	32	363
	Q&T	540 (1000)	1090 (158)	676 (98)	15	37	321
	Q&T	650 (1200)	896 (130)	552 (80)	21	47	269
	Normalized	900 (1650)	1010 (147)	500 (72)	9	13	293
	Annealed	790 (1450)	658 (95)	380 (55)	13	21	192
1141	Q&T	315 (600)	1460 (212)	1280 (186)	9	32	415
	Q&T	540 (1000)	896 (130)	765 (111)	18	57	262

(continued)

**Table A-21** (Continued)

## Mean Mechanical Properties of Some Heat-Treated Steels

[These are typical properties for materials normalized and annealed. The properties for quenched and tempered (Q&T) steels are from a single heat. Because of the many variables, the properties listed are global averages. In all cases, data were obtained from specimens of diameter 0.505 in., machined from 1-in rounds, and of gauge length 2 in. Unless noted, all specimens were oil-quenched.] *Source: ASM Metals Reference Book, 2d ed., American Society for Metals, Metals Park, Ohio, 1983.*

AISI No.	Treatment	1	2	3	4	5	6	7	8
				Temperature °C (°F)	Tensile Strength MPa (kpsi)	Yield Strength, MPa (kpsi)	Elongation, %	Reduction in Area, %	Brinell Hardness
4130	Q&T*	205 (400)		1630 (236)	1460 (212)	10	41	467	
	Q&T*	315 (600)		1500 (217)	1380 (200)	11	43	435	
	Q&T*	425 (800)		1280 (186)	1190 (173)	13	49	380	
	Q&T*	540 (1000)		1030 (150)	910 (132)	17	57	315	
	Q&T*	650 (1200)		814 (118)	703 (102)	22	64	245	
	Normalized	870 (1600)		670 (97)	436 (63)	25	59	197	
	Annealed	865 (1585)		560 (81)	361 (52)	28	56	156	
	Q&T	205 (400)		1770 (257)	1640 (238)	8	38	510	
4140	Q&T	315 (600)		1550 (225)	1430 (208)	9	43	445	
	Q&T	425 (800)		1250 (181)	1140 (165)	13	49	370	
	Q&T	540 (1000)		951 (138)	834 (121)	18	58	285	
	Q&T	650 (1200)		758 (110)	655 (95)	22	63	230	
	Normalized	870 (1600)		1020 (148)	655 (95)	18	47	302	
	Annealed	815 (1500)		655 (95)	417 (61)	26	57	197	
	Q&T	315 (600)		1720 (250)	1590 (230)	10	40	486	
	Q&T	425 (800)		1470 (213)	1360 (198)	10	44	430	
4340	Q&T	540 (1000)		1170 (170)	1080 (156)	13	51	360	
	Q&T	650 (1200)		965 (140)	855 (124)	19	60	280	

\*Water-quenched

**Table A-22**

Results of Tensile Tests of Some Metals\*    Source: J. Datsko, "Solid Materials," chap. 32 in Joseph E. Shigley, Charles R. Mischke, and Thomas H. Brown, Jr. (eds.-in-chief), *Standard Handbook of Machine Design*, 3rd ed., McGraw-Hill, New York, 2004, pp. 32.49–32.52.

Number	Material	Condition	Strength (Tensile)					
			Yield $S_y$ , MPa (kpsi)	Ultimate $S_u$ , MPa (kpsi)	Fracture, $\sigma_f$ , MPa (kpsi)	Coefficient $\sigma_0$ , MPa (kpsi)	Strain Strength, Exponent $m$	Fracture Strain $\epsilon_f$
1018	Steel	Annealed	220 (32.0)	341 (49.5)	628 (91.1)†	620 (90.0)	0.25	1.05
1144	Steel	Annealed	358 (52.0)	646 (93.7)	898 (130)†	992 (144)	0.14	0.49
1212	Steel	HR	193 (28.0)	424 (61.5)	729 (106)†	758 (110)	0.24	0.85
1045	Steel	Q&T 600°F	1520 (220)	1580 (230)	2380 (345)	1880 (273)†	0.041	0.81
4142	Steel	Q&T 600°F	1720 (250)	1930 (210)	2340 (340)	1760 (255)†	0.048	0.43
303	Stainless steel	Annealed	241 (35.0)	601 (87.3)	1520 (221)†	1410 (205)	0.51	1.16
304	Stainless steel	Annealed	276 (40.0)	568 (82.4)	1600 (233)†	1270 (185)	0.45	1.67
2011	Aluminum alloy	T6	169 (24.5)	324 (47.0)	325 (47.2)†	620 (90)	0.28	0.10
2024	Aluminum alloy	T4	296 (43.0)	446 (64.8)	533 (77.3)†	689 (100)	0.15	0.18
7075	Aluminum alloy	T6	542 (78.6)	593 (86.0)	706 (102)†	882 (128)	0.13	0.18

\*Values from one or two heats and believed to be attainable using proper purchase specifications. The fracture strain may vary as much as 100 percent.

†Derived value.

**Table A-23**

Mean Monotonic and Cyclic Stress-Strain Properties of Selected Steels    *Source: ASM Metals Reference Book*, 2nd ed., American Society for Metals, Metals Park, Ohio, 1983, p. 217.

Grade (a)	Orientation (e)	Description (f)	Hardness HB	Tensile Strength $S_{ut}$		Reduction in Area %	True Strain at Fracture $\epsilon_f$	Modulus of Elasticity $E$		Fatigue Strength Coefficient $\sigma_f'$		Fatigue Strength Exponent $b$	Fatigue Ductility Coefficient $\epsilon_f'$	Fatigue Ductility Exponent $c$
				MPa	ksi			GPa	$10^6$ psi	MPa	ksi			
A538A (b)	L	STA	405	1515	220	67	1.10	185	27	1655	240	-0.065	0.30	-0.62
A538B (b)	L	STA	460	1860	270	56	0.82	185	27	2135	310	-0.071	0.80	-0.71
A538C (b)	L	STA	480	2000	290	55	0.81	180	26	2240	325	-0.07	0.60	-0.75
AM-350 (c)	L	HR, A		1315	191	52	0.74	195	28	2800	406	-0.14	0.33	-0.84
AM-350 (c)	L	CD	496	1905	276	20	0.23	180	26	2690	390	-0.102	0.10	-0.42
Gainex (c)	LT	HR sheet		530	77	58	0.86	200	29.2	805	117	-0.07	0.86	-0.65
Gainex (c)	L	HR sheet		510	74	64	1.02	200	29.2	805	117	-0.071	0.86	-0.68
H-11	L	Ausformed	660	2585	375	33	0.40	205	30	3170	460	-0.077	0.08	-0.74
RQC-100 (c)	LT	HR plate	290	940	136	43	0.56	205	30	1240	180	-0.07	0.66	-0.69
RQC-100 (c)	L	HR plate	290	930	135	67	1.02	205	30	1240	180	-0.07	0.66	-0.69
10B62	L	Q&T	430	1640	238	38	0.89	195	28	1780	258	-0.067	0.32	-0.56
1005-1009	LT	HR sheet	90	360	52	73	1.3	205	30	580	84	-0.09	0.15	-0.43
1005-1009	LT	CD sheet	125	470	68	66	1.09	205	30	515	75	-0.059	0.30	-0.51
1005-1009	L	CD sheet	125	415	60	64	1.02	200	29	540	78	-0.073	0.11	-0.41
1005-1009	L	HR sheet	90	345	50	80	1.6	200	29	640	93	-0.109	0.10	-0.39
1015	L	Normalized	80	415	60	68	1.14	205	30	825	120	-0.11	0.95	-0.64
1020	L	HR plate	108	440	64	62	0.96	205	29.5	895	130	-0.12	0.41	-0.51
1040	L	As forged	225	620	90	60	0.93	200	29	1540	223	-0.14	0.61	-0.57
1045	L	Q&T	225	725	105	65	1.04	200	29	1225	178	-0.095	1.00	-0.66
1045	L	Q&T	410	1450	210	51	0.72	200	29	1860	270	-0.073	0.60	-0.70
1045	L	Q&T	390	1345	195	59	0.89	205	30	1585	230	-0.074	0.45	-0.68
1045	L	Q&T	450	1585	230	55	0.81	205	30	1795	260	-0.07	0.35	-0.69
1045	L	Q&T	500	1825	265	51	0.71	205	30	2275	330	-0.08	0.25	-0.68
1045	L	Q&T	595	2240	325	41	0.52	205	30	2725	395	-0.081	0.07	-0.60
1144	L	CDSR	265	930	135	33	0.51	195	28.5	1000	145	-0.08	0.32	-0.58

1144	L	DAT	305	1035	150	25	0.29	200	28.8	1585	230	-0.09	0.27	-0.53
1541F	L	Q&T forging	290	950	138	49	0.68	205	29.9	1275	185	-0.076	0.68	-0.65
1541F	L	Q&T forging	260	890	129	60	0.93	205	29.9	1275	185	-0.071	0.93	-0.65
4130	L	Q&T	258	895	130	67	1.12	220	32	1275	185	-0.083	0.92	-0.63
4130	L	Q&T	365	1425	207	55	0.79	200	29	1695	246	-0.081	0.89	-0.69
4140	L	Q&T, DAT	310	1075	156	60	0.69	200	29.2	1825	265	-0.08	1.2	-0.59
4142	L	DAT	310	1060	154	29	0.35	200	29	1450	210	-0.10	0.22	-0.51
4142	L	DAT	335	1250	181	28	0.34	200	28.9	1250	181	-0.08	0.06	-0.62
4142	L	Q&T	380	1415	205	48	0.66	205	30	1825	265	-0.08	0.45	-0.75
4142	L	Q&T and deformed	400	1550	225	47	0.63	200	29	1895	275	-0.09	0.50	-0.75
4142	L	Q&T	450	1760	255	42	0.54	205	30	2000	290	-0.08	0.40	-0.73
4142	L	Q&T and deformed	475	2035	295	20	0.22	200	29	2070	300	-0.082	0.20	-0.77
4142	L	Q&T and deformed	450	1930	280	37	0.46	200	29	2105	305	-0.09	0.60	-0.76
4142	L	Q&T	475	1930	280	35	0.43	205	30	2170	315	-0.081	0.09	-0.61
4142	L	Q&T	560	2240	325	27	0.31	205	30	2655	385	-0.089	0.07	-0.76
4340	L	HR, A	243	825	120	43	0.57	195	28	1200	174	-0.095	0.45	-0.54
4340	L	Q&T	409	1470	213	38	0.48	200	29	2000	290	-0.091	0.48	-0.60
4340	L	Q&T	350	1240	180	57	0.84	195	28	1655	240	-0.076	0.73	-0.62
5160	L	Q&T	430	1670	242	42	0.87	195	28	1930	280	-0.071	0.40	-0.57
52100	L	SH, Q&T	518	2015	292	11	0.12	205	30	2585	375	-0.09	0.18	-0.56
9262	L	A	260	925	134	14	0.16	205	30	1040	151	-0.071	0.16	-0.47
9262	L	Q&T	280	1000	145	33	0.41	195	28	1220	177	-0.073	0.41	-0.60
9262	L	Q&T	410	565	227	32	0.38	200	29	1855	269	-0.057	0.38	-0.65
950C (d)	LT	HR plate	159	565	82	64	1.03	205	29.6	1170	170	-0.12	0.95	-0.61
950C (d)	L	HR bar	150	565	82	69	1.19	205	30	970	141	-0.11	0.85	-0.59
950X (d)	L	Plate channel	150	440	64	65	1.06	205	30	625	91	-0.075	0.35	-0.54
950X (d)	L	HR plate	156	530	77	72	1.24	205	29.5	1005	146	-0.10	0.85	-0.61
950X (d)	L	Plate channel	225	695	101	68	1.15	195	28.2	1055	153	-0.08	0.21	-0.53

Notes: (a) AISI/SAE grade, unless otherwise indicated. (b) ASTM designation. (c) Proprietary designation. (d) SAE HSLA grade. (e) Orientation of axis of specimen, relative to rolling direction; L is longitudinal (parallel to rolling direction); LT is long transverse (perpendicular to rolling direction). (f) STA, solution treated and aged; HR, hot rolled; CD, cold drawn; Q&T, quenched and tempered; CDSR, cold drawn strain relieved; DAT, drawn at temperature; A, annealed. From *ASM Metals Reference Book, 2nd edition*, 1983; ASM International, Materials Park, OH 44073-0002; table 217. Reprinted by permission of ASM International®, www.asminternational.org.

**Table A-24**

Mechanical Properties of Three Non-Steel Metals

(a) Typical Properties of Gray Cast Iron

[The American Society for Testing and Materials (ASTM) numbering system for gray cast iron is such that the numbers correspond to the *minimum tensile strength* in kpsi. Thus an ASTM No. 20 cast iron has a minimum tensile strength of 20 kpsi. Note particularly that the tabulations are *typical* of several heats.]

ASTM Number	Tensile Strength $S_{ut}$ , kpsi	Compressive Strength $S_{uc}$ , kpsi	Shear Modulus of Rupture $S_{sr}$ , kpsi	Modulus of Elasticity, Mpsi		Endurance Limit* $S_{er}$ , kpsi	Brinell Hardness $H_B$	Fatigue Stress-Concentration Factor $K_f$
20	22	83	26	9.6–14	3.9–5.6	10	156	1.00
25	26	97	32	11.5–14.8	4.6–6.0	11.5	174	1.05
30	31	109	40	13–16.4	5.2–6.6	14	201	1.10
35	36.5	124	48.5	14.5–17.2	5.8–6.9	16	212	1.15
40	42.5	140	57	16–20	6.4–7.8	18.5	235	1.25
50	52.5	164	73	18.8–22.8	7.2–8.0	21.5	262	1.35
60	62.5	187.5	88.5	20.4–23.5	7.8–8.5	24.5	302	1.50

\*Polished or machined specimens.

†The modulus of elasticity of cast iron in compression corresponds closely to the upper value in the range given for tension and is a more constant value than that for tension.

**Table A-24**Mechanical Properties of Three Non-Steel Metals (*Continued*)

## (b) Mechanical Properties of Some Aluminum Alloys

[These are typical properties for sizes of about  $\frac{1}{2}$  in; similar properties can be obtained by using proper purchase specifications. The values given for fatigue strength correspond to 50( $10^7$ ) cycles of completely reversed stress. All aluminum alloys do not have an endurance limit. Yield strengths were obtained by the 0.2 percent offset method.]

Aluminum Association Number	Temper	Yield, $S_y$ , MPa (kpsi)	Strength Tensile, $S_u$ , MPa (kpsi)	Fatigue, $S_f$ , MPa (kpsi)	Elongation in 2 in, %	Brinell Hardness $H_B$
Wrought:						
2017	O	70 (10)	179 (26)	90 (13)	22	45
2024	O	76 (11)	186 (27)	90 (13)	22	47
	T3	345 (50)	482 (70)	138 (20)	16	120
3003	H12	117 (17)	131 (19)	55 (8)	20	35
	H16	165 (24)	179 (26)	65 (9.5)	14	47
3004	H34	186 (27)	234 (34)	103 (15)	12	63
	H38	234 (34)	276 (40)	110 (16)	6	77
5052	H32	186 (27)	234 (34)	117 (17)	18	62
	H36	234 (34)	269 (39)	124 (18)	10	74
Cast:						
319.0*	T6	165 (24)	248 (36)	69 (10)	2.0	80
333.0†	T5	172 (25)	234 (34)	83 (12)	1.0	100
	T6	207 (30)	289 (42)	103 (15)	1.5	105
335.0*	T6	172 (25)	241 (35)	62 (9)	3.0	80
	T7	248 (36)	262 (38)	62 (9)	0.5	85

\*Sand casting.

†Permanent-mold casting.

## (c) Mechanical Properties of Some Titanium Alloys

Titanium Alloy	Condition	Yield, $S_y$ (0.2% offset) MPa (kpsi)	Strength Tensile, $S_u$ , MPa (kpsi)	Elongation in 2 in, %	Hardness (Brinell or Rockwell)
Ti-35A†	Annealed	210 (30)	275 (40)	30	135 HB
Ti-50A†	Annealed	310 (45)	380 (55)	25	215 HB
Ti-0.2 Pd	Annealed	280 (40)	340 (50)	28	200 HB
Ti-5 Al-2.5 Sn	Annealed	760 (110)	790 (115)	16	36 HRC
Ti-8 Al-1 Mo-1 V	Annealed	900 (130)	965 (140)	15	39 HRC
Ti-6 Al-6 V-2 Sn	Annealed	970 (140)	1030 (150)	14	38 HRC
Ti-6Al-4V	Annealed	830 (120)	900 (130)	14	36 HRC
Ti-13 V-11 Cr-3 Al	Sol. + aging	1207 (175)	1276 (185)	8	40 HRC

†Commercially pure alpha titanium.

**Table A-25**

Stochastic Yield and Ultimate Strengths for Selected Materials    *Source:* Data compiled from “Some Property Data and Corresponding Weibull Parameters for Stochastic Mechanical Design,” Trans. ASME Journal of Mechanical Design, vol. 114 (March 1992), pp. 29–34.

<b>Material</b>		$\mu_{Sut}$	$\hat{\sigma}_{Sut}$	$x_0$	$\theta$	$b$	$\mu_{Sy}$	$\hat{\sigma}_{Sy}$	$x_0$	$\theta$	$b$	$C_{Sut}$	$C_{Sy}$
1018	CD	87.6	5.74	30.8	90.1	12	78.4	5.90	56	80.6	4.29	0.0655	0.0753
1035	HR	86.2	3.92	72.6	87.5	3.86	49.6	3.81	39.5	50.8	2.88	0.0455	0.0768
1045	CD	117.7	7.13	90.2	120.5	4.38	95.5	6.59	82.1	97.2	2.14	0.0606	0.0690
1117	CD	83.1	5.25	73.0	84.4	2.01	81.4	4.71	72.4	82.6	2.00	0.0632	0.0579
1137	CD	106.5	6.15	96.2	107.7	1.72	98.1	4.24	92.2	98.7	1.41	0.0577	0.0432
12L14	CD	79.6	6.92	70.3	80.4	1.36	78.1	8.27	64.3	78.8	1.72	0.0869	0.1059
1038	HT bolts	133.4	3.38	122.3	134.6	3.64						0.0253	
ASTM40		44.5	4.34	27.7	46.2	4.38						0.0975	
35018	Malleable	53.3	1.59	48.7	53.8	3.18	38.5	1.42	34.7	39.0	2.93	0.0298	0.0369
32510	Malleable	53.4	2.68	44.7	54.3	3.61	34.9	1.47	30.1	35.5	3.67	0.0502	0.0421
Malleable	Pearlitic	93.9	3.83	80.1	95.3	4.04	60.2	2.78	50.2	61.2	4.02	0.0408	0.0462
604515	Nodular	64.8	3.77	53.7	66.1	3.23	49.0	4.20	33.8	50.5	4.06	0.0582	0.0857
100-70-04	Nodular	122.2	7.65	47.6	125.6	11.84	79.3	4.51	64.1	81.0	3.77	0.0626	0.0569
201SS	CD	195.9	7.76	180.7	197.9	2.06						0.0396	
301SS	CD	191.2	5.82	151.9	193.6	8.00	166.8	9.37	139.7	170.0	3.17	0.0304	0.0562
	A	105.0	5.68	92.3	106.6	2.38	46.8	4.70	26.3	48.7	4.99	0.0541	0.1004
304SS	A	85.0	4.14	66.6	86.6	5.11	37.9	3.76	30.2	38.9	2.17	0.0487	0.0992
310SS	A	84.8	4.23	71.6	86.3	3.45						0.0499	
403SS		105.3	3.09	95.7	106.4	3.44	78.5	3.91	64.8	79.9	3.93	0.0293	0.0498
17-7PSS		198.8	9.51	163.3	202.3	4.21	189.4	11.49	144.0	193.8	4.48	0.0478	0.0607
AM350SS	A	149.1	8.29	101.8	152.4	6.68	63.0	5.05	38.0	65.0	5.73	0.0556	0.0802
Ti-6AL-4V		175.4	7.91	141.8	178.5	4.85	163.7	9.03	101.5	167.4	8.18	0.0451	0.0552
2024	0	28.1	1.73	24.2	28.7	2.43						0.0616	
2024	T4	64.9	1.64	60.2	65.5	3.16	40.8	1.83	38.4	41.0	1.32	0.0253	0.0449
	T6	67.5	1.50	55.9	68.1	9.26	53.4	1.17	51.2	53.6	1.91	0.0222	0.0219
7075	T6 .025"	75.5	2.10	68.8	76.2	3.53	63.7	1.98	58.9	64.3	2.63	0.0278	0.0311

**Table A-26**

Stochastic Parameters for Finite Life Fatigue Tests in Selected Metals    Source: E. B. Haugen, *Probabilistic Mechanical Design*, Wiley, New York, 1980, Appendix 10-B.

Number	Condition	TS MPa (kpsi)	YS MPa (kpsi)	Distri- bution	Stress Cycles to Failure			
					10 <sup>4</sup>	10 <sup>5</sup>	10 <sup>6</sup>	10 <sup>7</sup>
1046	WQ&T, 1210°F	723 (105)	565 (82)	W	x <sub>0</sub>	544 (79)	462 (67)	391 (56.7)
					θ	594 (86.2)	503 (73.0)	425 (61.7)
					b	2.60	2.75	2.85
2340	OQ&T 1200°F	799 (116)	661 (96)	W	x <sub>0</sub>	579 (84)	510 (74)	420 (61)
					θ	699 (101.5)	588 (85.4)	496 (72.0)
					b	4.3	3.4	4.1
3140	OQ&T, 1300°F	744 (108)	599 (87)	W	x <sub>0</sub>	510 (74)	455 (66)	393 (57)
					θ	604 (87.7)	528 (76.7)	463 (67.2)
					b	5.2	5.0	5.5
2024 Aluminum	T-4	489 (71)	365 (53)	N	σ	26.3 (3.82)	21.4 (3.11)	17.4 (2.53)
					μ	143 (20.7)	116 (16.9)	95 (13.8)
Ti-6Al-4V	HT-46	1040 (151)	992 (144)	N	σ	39.6 (5.75)	38.1 (5.53)	36.6 (5.31)
					μ	712 (108)	684 (99.3)	657 (95.4)
								493 (71.6)

Statistical parameters from a large number of fatigue tests are listed. Weibull distribution is denoted W and the parameters are  $x_0$ , “guaranteed” fatigue strength;  $\theta$ , characteristic fatigue strength; and  $b$ , shape factor. Normal distribution is denoted N and the parameters are  $\mu$ , mean fatigue strength; and  $\sigma$ , standard deviation of the fatigue strength. The life is in stress-cycles-to-failure. TS = tensile strength, YS = yield strength. All testing by rotating-beam specimen.

**Table A-27**

Finite Life Fatigue Strengths of Selected Plain Carbon Steels    *Source:* Compiled from Table 4 in H. J. Grover, S. A. Gordon, and L. R. Jackson, *Fatigue of Metals and Structures*, Bureau of Naval Weapons Document NAVWEPS 00-25-534, 1960.

Material	Condition	BHN*	Tensile Strength ksi	Yield Strength ksi	RA*	Stress Cycles to Failure							
						10 <sup>4</sup>	4(10 <sup>4</sup> )	10 <sup>5</sup>	4(10 <sup>5</sup> )	10 <sup>6</sup>	4(10 <sup>6</sup> )	10 <sup>7</sup>	10 <sup>8</sup>
1020	Furnace cooled		58	30	0.63			37	34	30	28	25	
1030	Air-cooled	135	80	45	0.62		51	47	42	38	38	38	
1035	Normal	132	72	35	0.54			44	40	37	34	33	33
	WQT	209	103	87	0.65		80	72	65	60	57	57	57
1040	Forged	195	92	53	0.23				40	47	33	33	
1045	HR, N		107	63	0.49	80	70	56	47	47	47	47	
1050	N, AC	164	92	47	0.40	50	48	46	40	38	34	34	
	WQT												
	1200	196	97	70	0.58		60	57	52	50	50	50	50
.56 MN	N	193	98	47	0.42	61	55	51	47	43	41	41	41
	WQT	277	111	84	0.57	94	81	73	62	57	55	55	55
	1200												
1060	As Rec.	67 Rb	134	65	0.20	65	60	55	50	48	48	48	
1095		162	84	33	0.37	50	43	40	34	31	30	30	30
	OQT	227	115	65	0.40	77	68	64	57	56	56	56	56
	1200												
10120		224	117	59	0.12		60	56	51	50	50	50	
	OQT	369	180	130	0.15		102	95	91	91	91	91	
	860												

\*BHN = Brinell hardness number; RA = fractional reduction in area.

**Table A-28**

Decimal Equivalents of Wire and Sheet-Metal Gauges\* (All Sizes Are Given in Inches)

Name of Gauge:	American or Brown & Sharpe	Birmingham or Stubs Iron Wire Tubing, Ferrous Strip, Flat Wire, and Spring Steel	United States Standard <sup>†</sup> Ferrous Sheet and Plate, 480 lbf/ft <sup>2</sup>	Manufacturers Standard Ferrous Sheet	Steel Wire or Washburn & Moen Ferrous Wire Except Music Wire	Music Wire	Stubs Steel Wire	Twist Drill
Principal Use:	Nonferrous Sheet, Wire, and Rod						Steel Drill Rod	Twist Drills and Drill Steel
7/0			0.500		0.490			
6/0	0.580 0		0.468 75		0.461 5	0.004		
5/0	0.516 5		0.437 5		0.430 5	0.005		
4/0	0.460 0	0.454	0.406 25		0.393 8	0.006		
3/0	0.409 6	0.425	0.375		0.362 5	0.007		
2/0	0.364 8	0.380	0.343 75		0.331 0	0.008		
0	0.324 9	0.340	0.312 5		0.306 5	0.009		
1	0.289 3	0.300	0.281 25		0.283 0	0.010	0.227	0.228 0
2	0.257 6	0.284	0.265 625		0.262 5	0.011	0.219	0.221 0
3	0.229 4	0.259	0.25	0.239 1	0.243 7	0.012	0.212	0.213 0
4	0.204 3	0.238	0.234 375	0.224 2	0.225 3	0.013	0.207	0.209 0
5	0.181 9	0.220	0.218 75	0.209 2	0.207 0	0.014	0.204	0.205 5
6	0.162 0	0.203	0.203 125	0.194 3	0.192 0	0.016	0.201	0.204 0
7	0.144 3	0.180	0.187 5	0.179 3	0.177 0	0.018	0.199	0.201 0
8	0.128 5	0.165	0.171 875	0.164 4	0.162 0	0.020	0.197	0.199 0
9	0.114 4	0.148	0.156 25	0.149 5	0.148 3	0.022	0.194	0.196 0
10	0.101 9	0.134	0.140 625	0.134 5	0.135 0	0.024	0.191	0.193 5
11	0.090 74	0.120	0.125	0.119 6	0.120 5	0.026	0.188	0.191 0
12	0.080 81	0.109	0.109 357	0.104 6	0.105 5	0.029	0.185	0.189 0
13	0.071 96	0.095	0.093 75	0.089 7	0.091 5	0.031	0.182	0.185 0
14	0.064 08	0.083	0.078 125	0.074 7	0.080 0	0.033	0.180	0.182 0
15	0.057 07	0.072	0.070 312 5	0.067 3	0.072 0	0.035	0.178	0.180 0
16	0.050 82	0.065	0.062 5	0.059 8	0.062 5	0.037	0.175	0.177 0
17	0.045 26	0.058	0.056 25	0.053 8	0.054 0	0.039	0.172	0.173 0

(continued)

**Table A-28**Decimal Equivalents of Wire and Sheet-Metal Gauges\* (All Sizes Are Given in Inches) (*Continued*)

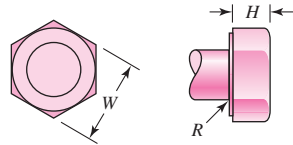
Name of Gauge:	American or Brown & Sharpe	Birmingham or Stubs Iron Wire	United States Standard <sup>†</sup>	Manufacturers Standard	Steel Wire or Washburn & Moen	Music Wire	Stubs Steel Wire	Twist Drill
Principal Use:	Nonferrous Sheet, Wire, and Rod	Tubing, Ferrous Strip, Flat Wire, and Spring Steel	Ferrous Sheet and Plate, 480 lbf/ft <sup>3</sup>	Ferrous Sheet	Ferrous Wire Except Music Wire	Music Wire	Steel Drill Rod	Twist Drills and Drill Steel
18	0.040 30	0.049	0.05	0.047 8	0.047 5	0.041	0.168	0.169 5
19	0.035 89	0.042	0.043 75	0.041 8	0.041 0	0.043	0.164	0.166 0
20	0.031 96	0.035	0.037 5	0.035 9	0.034 8	0.045	0.161	0.161 0
21	0.028 46	0.032	0.034 375	0.032 9	0.031 7	0.047	0.157	0.159 0
22	0.025 35	0.028	0.031 25	0.029 9	0.028 6	0.049	0.155	0.157 0
23	0.022 57	0.025	0.028 125	0.026 9	0.025 8	0.051	0.153	0.154 0
24	0.020 10	0.022	0.025	0.023 9	0.023 0	0.055	0.151	0.152 0
25	0.017 90	0.020	0.021 875	0.020 9	0.020 4	0.059	0.148	0.149 5
26	0.015 94	0.018	0.018 75	0.017 9	0.018 1	0.063	0.146	0.147 0
27	0.014 20	0.016	0.017 187 5	0.016 4	0.017 3	0.067	0.143	0.144 0
28	0.012 64	0.014	0.015 625	0.014 9	0.016 2	0.071	0.139	0.140 5
29	0.011 26	0.013	0.014 062 5	0.013 5	0.015 0	0.075	0.134	0.136 0
30	0.010 03	0.012	0.012 5	0.012 0	0.014 0	0.080	0.127	0.128 5
31	0.008 928	0.010	0.010 937 5	0.010 5	0.013 2	0.085	0.120	0.120 0
32	0.007 950	0.009	0.010 156 25	0.009 7	0.012 8	0.090	0.115	0.116 0
33	0.007 080	0.008	0.009 375	0.009 0	0.011 8	0.095	0.112	0.113 0
34	0.006 305	0.007	0.008 593 75	0.008 2	0.010 4		0.110	0.111 0
35	0.005 615	0.005	0.007 812 5	0.007 5	0.009 5		0.108	0.110 0
36	0.005 000	0.004	0.007 031 25	0.006 7	0.009 0		0.106	0.106 5
37	0.004 453		0.006 640 625	0.006 4	0.008 5		0.103	0.104 0
38	0.003 965		0.006 25	0.006 0	0.008 0		0.101	0.101 5
39	0.003 531				0.007 5		0.099	0.099 5
40	0.003 145				0.007 0		0.097	0.098 0

\*Specify sheet, wire, and plate by stating the gauge number, the gauge name, and the decimal equivalent in parentheses.

<sup>†</sup>Reflects present average and weights of sheet steel.

**Table A-29**

Dimensions of Square and Hexagonal Bolts



Nominal Size, in	Head Type											
	Square			Regular Hexagonal			Heavy Hexagonal			Structural Hexagonal		
	W	H	R <sub>min</sub>	W	H	R <sub>min</sub>	W	H	R <sub>min</sub>	W	H	R <sub>min</sub>
1/4	3/8	11/64	0.01	7/16	11/64					7/8	11/32	0.01
5/16	1/2	13/64	0.01	1/2	7/32					1 1/16	27/64	0.02
3/8	9/16	1/4	0.01	9/16	1/4					1 1/4	1/2	0.02
7/16	5/8	19/64	0.01	5/8	19/64					1 3/8	43/64	0.03
1/2	3/4	21/64	0.01	3/4	11/32					1 5/8	43/64	0.03
5/8	15/16	27/64	0.02	15/16	27/64					1 13/16	27/32	0.03
3/4	1 1/8	1/2	0.02	1 1/8	1/2					2	27/32	0.03
1	1 1/2	21/32	0.03	1 1/2	43/64					2	25/32	0.062
1 1/8	1 11/16	3/4	0.03	1 11/16	3/4					2 1/16	11/16	0.062
1 1/4	1 7/8	27/32	0.03	1 7/8	27/32					2 3/8	27/32	0.062
1 3/8	2 1/16	29/32	0.03	2 1/16	29/32					2 3/8	27/32	0.062
1 1/2	2 1/4	1	0.03	2 1/4	1					2 3/8	15/16	0.062
Nominal Size, mm												
M5	8	3.58	0.2	8	3.58	0.6						
M6		10	0.3		4.38							
M8		13	0.4		5.68							
M10		16	0.4		6.85							
M12		18	0.6		7.95					21	7.95	0.6
M14		21	0.6		9.25					24	9.25	0.6
M16		24	0.6		10.75					27	10.75	0.6
M20		30	0.8		13.40					34	13.40	0.8
M24		36	0.8		15.90					41	15.90	1.0
M30		46	1.0		19.75					50	19.75	1.2
M36		55	1.0		23.55					60	23.55	1.5

**Table A-30**

Dimensions of Hexagonal Cap Screws and Heavy Hexagonal Screws ( $W$ = Width across Flats; $H$ = Height of Head; See Figure in Table A-29)	<b>Nominal Size, in</b>	<b>Minimum Fillet Radius</b>	<b>Type of Screw</b>		
			<b>Cap W</b>	<b>Heavy W</b>	<b>Height H</b>
	$\frac{1}{4}$	0.015	$\frac{7}{16}$		$\frac{5}{32}$
	$\frac{5}{16}$	0.015	$\frac{1}{2}$		$\frac{13}{64}$
	$\frac{3}{8}$	0.015	$\frac{9}{16}$		$\frac{15}{64}$
	$\frac{7}{16}$	0.015	$\frac{5}{8}$		$\frac{9}{32}$
	$\frac{1}{2}$	0.015	$\frac{3}{4}$	$\frac{7}{8}$	$\frac{5}{16}$
	$\frac{5}{8}$	0.020	$\frac{15}{16}$	$1\frac{1}{16}$	$\frac{25}{64}$
	$\frac{3}{4}$	0.020	$1\frac{1}{8}$	$1\frac{1}{4}$	$\frac{15}{32}$
	$\frac{7}{8}$	0.040	$1\frac{5}{16}$	$1\frac{7}{16}$	$\frac{35}{64}$
	1	0.060	$1\frac{1}{2}$	$1\frac{1}{8}$	$\frac{39}{64}$
	$1\frac{1}{4}$	0.060	$1\frac{7}{8}$	2	$\frac{25}{32}$
	$1\frac{3}{8}$	0.060	$2\frac{1}{16}$	$2\frac{3}{16}$	$\frac{27}{32}$
	$1\frac{1}{2}$	0.060	$2\frac{1}{4}$	$2\frac{3}{8}$	$\frac{15}{16}$
<b>Nominal Size, mm</b>					
M5	0.2	8			3.65
M6	0.3	10			4.15
M8	0.4	13			5.50
M10	0.4	16			6.63
M12	0.6	18	21		7.76
M14	0.6	21	24		9.09
M16	0.6	24	27		10.32
M20	0.8	30	34		12.88
M24	0.8	36	41		15.44
M30	1.0	46	50		19.48
M36	1.0	55	60		23.38

**Table A-31**

Dimensions of  
Hexagonal Nuts

Nominal Size, in	Width <i>W</i>	Height <i>H</i>		
		Regular Hexagonal	Thick or Slotted	JAM
$\frac{1}{4}$	$\frac{7}{16}$	$\frac{7}{32}$	$\frac{9}{32}$	$\frac{5}{32}$
$\frac{5}{16}$	$\frac{1}{2}$	$\frac{17}{64}$	$\frac{21}{64}$	$\frac{3}{16}$
$\frac{3}{8}$	$\frac{9}{16}$	$\frac{21}{64}$	$\frac{13}{32}$	$\frac{7}{32}$
$\frac{7}{16}$	$\frac{11}{16}$	$\frac{3}{8}$	$\frac{29}{64}$	$\frac{1}{4}$
$\frac{1}{2}$	$\frac{3}{4}$	$\frac{7}{16}$	$\frac{9}{16}$	$\frac{5}{16}$
$\frac{9}{16}$	$\frac{7}{8}$	$\frac{31}{64}$	$\frac{39}{64}$	$\frac{5}{16}$
$\frac{5}{8}$	$\frac{15}{16}$	$\frac{35}{64}$	$\frac{23}{32}$	$\frac{3}{8}$
$\frac{3}{4}$	$1\frac{1}{8}$	$\frac{41}{64}$	$\frac{13}{16}$	$\frac{27}{64}$
$\frac{7}{8}$	$1\frac{5}{16}$	$\frac{3}{4}$	$\frac{29}{32}$	$\frac{31}{64}$
1	$1\frac{1}{2}$	$\frac{55}{64}$	1	$\frac{35}{64}$
$1\frac{1}{8}$	$1\frac{11}{16}$	$\frac{31}{32}$	$1\frac{5}{32}$	$\frac{39}{64}$
$1\frac{1}{4}$	$1\frac{7}{8}$	$1\frac{1}{16}$	$1\frac{1}{4}$	$\frac{23}{32}$
$1\frac{3}{8}$	$2\frac{1}{16}$	$1\frac{11}{64}$	$1\frac{3}{8}$	$\frac{25}{32}$
$1\frac{1}{2}$	$2\frac{1}{4}$	$1\frac{9}{32}$	$1\frac{1}{2}$	$\frac{27}{32}$
Nominal Size, mm				
M5	8	4.7	5.1	2.7
M6	10	5.2	5.7	3.2
M8	13	6.8	7.5	4.0
M10	16	8.4	9.3	5.0
M12	18	10.8	12.0	6.0
M14	21	12.8	14.1	7.0
M16	24	14.8	16.4	8.0
M20	30	18.0	20.3	10.0
M24	36	21.5	23.9	12.0
M30	46	25.6	28.6	15.0
M36	55	31.0	34.7	18.0

**Table A-32**

Basic Dimensions of American Standard Plain Washers (All Dimensions in Inches)	Fastener Size	Washer Size	Diameter		
			ID	OD	Thickness
	#6	0.138	0.156	0.375	0.049
	#8	0.164	0.188	0.438	0.049
	#10	0.190	0.219	0.500	0.049
	#12	0.216	0.250	0.562	0.065
	$\frac{1}{4}$ N	0.250	0.281	0.625	0.065
	$\frac{1}{4}$ W	0.250	0.312	0.734	0.065
	$\frac{5}{16}$ N	0.312	0.344	0.688	0.065
	$\frac{5}{16}$ W	0.312	0.375	0.875	0.083
	$\frac{3}{8}$ N	0.375	0.406	0.812	0.065
	$\frac{3}{8}$ W	0.375	0.438	1.000	0.083
	$\frac{7}{16}$ N	0.438	0.469	0.922	0.065
	$\frac{7}{16}$ W	0.438	0.500	1.250	0.083
	$\frac{1}{2}$ N	0.500	0.531	1.062	0.095
	$\frac{1}{2}$ W	0.500	0.562	1.375	0.109
	$\frac{9}{16}$ N	0.562	0.594	1.156	0.095
	$\frac{9}{16}$ W	0.562	0.625	1.469	0.109
	$\frac{5}{8}$ N	0.625	0.656	1.312	0.095
	$\frac{5}{8}$ W	0.625	0.688	1.750	0.134
	$\frac{3}{4}$ N	0.750	0.812	1.469	0.134
	$\frac{3}{4}$ W	0.750	0.812	2.000	0.148
	$\frac{7}{8}$ N	0.875	0.938	1.750	0.134
	$\frac{7}{8}$ W	0.875	0.938	2.250	0.165
	1 N	1.000	1.062	2.000	0.134
	1 W	1.000	1.062	2.500	0.165
	$1\frac{1}{8}$ N	1.125	1.250	2.250	0.134
	$1\frac{1}{8}$ W	1.125	1.250	2.750	0.165
	$1\frac{1}{4}$ N	1.250	1.375	2.500	0.165
	$1\frac{1}{4}$ W	1.250	1.375	3.000	0.165
	$1\frac{3}{8}$ N	1.375	1.500	2.750	0.165
	$1\frac{3}{8}$ W	1.375	1.500	3.250	0.180
	$1\frac{1}{2}$ N	1.500	1.625	3.000	0.165
	$1\frac{1}{2}$ W	1.500	1.625	3.500	0.180
	$1\frac{5}{8}$	1.625	1.750	3.750	0.180
	$1\frac{3}{4}$	1.750	1.875	4.000	0.180
	$1\frac{7}{8}$	1.875	2.000	4.250	0.180
	2	2.000	2.125	4.500	0.180
	$2\frac{1}{4}$	2.250	2.375	4.750	0.220
	$2\frac{1}{2}$	2.500	2.625	5.000	0.238
	$2\frac{3}{4}$	2.750	2.875	5.250	0.259
	3	3.000	3.125	5.500	0.284

N = narrow; W = wide; use W when not specified.

**Table A-33**

Dimensions of Metric Plain Washers (All Dimensions in Millimeters)

<b>Washer Size*</b>	<b>Minimum ID</b>	<b>Maximum OD</b>	<b>Maximum Thickness</b>	<b>Washer Size*</b>	<b>Minimum ID</b>	<b>Maximum OD</b>	<b>Maximum Thickness</b>
1.6 N	1.95	4.00	0.70	10 N	10.85	20.00	2.30
1.6 R	1.95	5.00	0.70	10 R	10.85	28.00	2.80
1.6 W	1.95	6.00	0.90	10 W	10.85	39.00	3.50
2 N	2.50	5.00	0.90	12 N	13.30	25.40	2.80
2 R	2.50	6.00	0.90	12 R	13.30	34.00	3.50
2 W	2.50	8.00	0.90	12 W	13.30	44.00	3.50
2.5 N	3.00	6.00	0.90	14 N	15.25	28.00	2.80
2.5 R	3.00	8.00	0.90	14 R	15.25	39.00	3.50
2.5 W	3.00	10.00	1.20	14 W	15.25	50.00	4.00
3 N	3.50	7.00	0.90	16 N	17.25	32.00	3.50
3 R	3.50	10.00	1.20	16 R	17.25	44.00	4.00
3 W	3.50	12.00	1.40	16 W	17.25	56.00	4.60
3.5 N	4.00	9.00	1.20	20 N	21.80	39.00	4.00
3.5 R	4.00	10.00	1.40	20 R	21.80	50.00	4.60
3.5 W	4.00	15.00	1.75	20 W	21.80	66.00	5.10
4 N	4.70	10.00	1.20	24 N	25.60	44.00	4.60
4 R	4.70	12.00	1.40	24 R	25.60	56.00	5.10
4 W	4.70	16.00	2.30	24 W	25.60	72.00	5.60
5 N	5.50	11.00	1.40	30 N	32.40	56.00	5.10
5 R	5.50	15.00	1.75	30 R	32.40	72.00	5.60
5 W	5.50	20.00	2.30	30 W	32.40	90.00	6.40
6 N	6.65	13.00	1.75	36 N	38.30	66.00	5.60
6 R	6.65	18.80	1.75	36 R	38.30	90.00	6.40
6 W	6.65	25.40	2.30	36 W	38.30	110.00	8.50
8 N	8.90	18.80	2.30				
8 R	8.90	25.40	2.30				
8 W	8.90	32.00	2.80				

N = narrow; R = regular; W = wide.

\*Same as screw or bolt size.

**Table A-34**

Values of  $\Gamma(n) = \int_0^\infty e^{-x} x^{n-1} dx$ ;  $\Gamma(n+1) = n\Gamma(n)$

## Gamma Function\*

*Source:* Reprinted with permission from William H. Beyer (ed.), *Handbook of Tables for Probability and Statistics*, 2nd ed., 1966. Copyright CRC Press, Boca Raton, Florida.

<b>n</b>	<b><math>\Gamma(n)</math></b>	<b>n</b>	<b><math>\Gamma(n)</math></b>	<b>n</b>	<b><math>\Gamma(n)</math></b>	<b>n</b>	<b><math>\Gamma(n)</math></b>
1.00	1.000 00	1.25	.906 40	1.50	.886 23	1.75	.919 06
1.01	.994 33	1.26	.904 40	1.51	.886 59	1.76	.921 37
1.02	.988 84	1.27	.902 50	1.52	.887 04	1.77	.923 76
1.03	.983 55	1.28	.900 72	1.53	.887 57	1.78	.926 23
1.04	.978 44	1.29	.899 04	1.54	.888 18	1.79	.928 77
1.05	.973 50	1.30	.897 47	1.55	.888 87	1.80	.931 38
1.06	.968 74	1.31	.896 00	1.56	.889 64	1.81	.934 08
1.07	.964 15	1.32	.894 64	1.57	.890 49	1.82	.936 85
1.08	.959 73	1.33	.893 38	1.58	.891 42	1.83	.939 69
1.09	.955 46	1.34	.892 22	1.59	.892 43	1.84	.942 61
1.10	.951 35	1.35	.891 15	1.60	.893 52	1.85	.945 61
1.11	.947 39	1.36	.890 18	1.61	.894 68	1.86	.948 69
1.12	.943 59	1.37	.889 31	1.62	.895 92	1.87	.951 84
1.13	.939 93	1.38	.888 54	1.63	.897 24	1.88	.955 07
1.14	.936 42	1.39	.887 85	1.64	.898 64	1.89	.958 38
1.15	.933 04	1.40	.887 26	1.65	.900 12	1.90	.961 77
1.16	.929 80	1.41	.886 76	1.66	.901 67	1.91	.965 23
1.17	.936 70	1.42	.886 36	1.67	.903 30	1.92	.968 78
1.18	.923 73	1.43	.886 04	1.68	.905 00	1.93	.972 40
1.19	.920 88	1.44	.885 80	1.69	.906 78	1.94	.976 10
1.20	.918 17	1.45	.885 65	1.70	.908 64	1.95	.979 88
1.21	.915 58	1.46	.885 60	1.71	.910 57	1.96	.983 74
1.22	.913 11	1.47	.885 63	1.72	.912 58	1.97	.987 68
1.23	.910 75	1.48	.885 75	1.73	.914 66	1.98	.991 71
1.24	.908 52	1.49	.885 95	1.74	.916 83	1.99	.995 81
						2.00	1.000 00

\*For large positive values of  $x$ ,  $\Gamma(x)$  approximates the asymptotic series

$$x^x e^{-x} \sqrt{\frac{2x}{x}} \left[ 1 + \frac{1}{12x} + \frac{1}{288x^2} - \frac{139}{51840x^3} - \frac{571}{2488320x^4} + \dots \right]$$

# B

## Appendix

### Answers to Selected Problems

#### B-1 Chapter 1

**1-8**  $P = 100$  units

**1-11** (a)  $e_1 = 0.005\ 751\ 311\ 1$ ,  $e_2 = 0.008\ 427\ 124\ 7$ ,  
 $e = 0.014\ 178\ 435\ 8$ , (b)  $e_1 = -0.004\ 248\ 688\ 9$ ,  
 $e_2 = -0.001\ 572\ 875\ 3$ ,  $e = -0.005\ 821\ 564\ 2$

**1-14** (a)  $w = 0.020 \pm 0.018$  in, (b)  $\bar{d} = 6.528$  in

**1-16**  $a = 1.569 \pm 0.016$  in

**1-17**  $D_o = 4.012 \pm 0.036$  in

**1-24** (a)  $\sigma = 1.90$  kpsi, (b)  $\sigma = 397$  psi, (c)  $y = 0.609$  in,  
(d)  $\theta = 4.95^\circ$

#### B-2 Chapter 2

**2-6**  $E = 30$  Mpsi,  $S_y = 45.5$  kpsi,  $S_{ut} = 85.5$  kpsi, area reduction = 45.8 percent

**2-9** (a) Before:  $S_y = 32$  kpsi,  $S_u = 49.5$  kpsi, After:  
 $S'_y = 61.8$  kpsi, 93% increase,  $S'_u = 61.9$  kpsi, 25%  
increase, (b) Before:  $S_u/S_y = 1.55$ , After:  $S'_u/S'_y = 1$

**2-15**  $\bar{S}_u = 117$  kpsi,  $s_{S_u} = 1.28$  kpsi

**2-17** (a)  $u_R \dot{=} 34.5$  in  $\cdot$  lbf/in $^3$ ,  
(b)  $u_T \dot{=} 66.7 (10^3)$  in  $\cdot$  lbf/in $^3$

**2-26** Aluminum alloys have greatest potential followed closely by high carbon heat-treated steel. Warrants further discussion.

**2-34** Steel, titanium, aluminum, and composites

#### B-3 Chapter 3

**3-1**  $R_B = 33.3$  lbf,  $R_O = 66.6$  lbf,  $R_C = 33.3$  lbf

**3-6**  $R_O = 740$  lbf,  $M_O = 8080$  lbf  $\cdot$  in

**3-14** (a)  $M_{\max} = 253$  lbf  $\cdot$  in, (b)  $a_{\min} = 2.07$  in,  
 $M_{\min} = 215$  lbf  $\cdot$  in

**3-15** (a)  $\sigma_1 = 22$  kpsi,  $\sigma_2 = -12$  kpsi,  $\sigma_3 = 0$  kpsi,  
 $\phi_p = 14.0^\circ$  cw,  $\tau_1 = 17$  kpsi,  $\sigma_{\text{ave}} = 5$  kpsi,  
 $\phi_s = 31.0^\circ$  ccw,  
(b)  $\sigma_1 = 18.6$  kpsi,  $\sigma_2 = 6.4$  kpsi,  $\sigma_3 = 0$  kpsi,  
 $\phi_p = 27.5^\circ$  ccw,  $\tau_1 = 6.10$  kpsi,  $\sigma_{\text{ave}} = 12.5$  kpsi,  
 $\phi_s = 17.5^\circ$  cw,

(c)  $\sigma_1 = 26.2$  kpsi,  $\sigma_2 = 7.78$  kpsi,  $\sigma_3 = 0$  kpsi,  
 $\phi_p = 69.7^\circ$  ccw,  $\tau_1 = 9.22$  kpsi,  $\sigma_{\text{ave}} = 17$  kpsi,  
 $\phi_s = 24.7^\circ$  ccw,

(d)  $\sigma_1 = 25.8$  kpsi,  $\sigma_2 = -15.8$  kpsi,  $\sigma_3 = 0$  kpsi,  
 $\phi_p = 72.4^\circ$  cw,  $\tau_1 = 20.8$  kpsi,  $\sigma_{\text{ave}} = 5$  kpsi,  
 $\phi_s = 27.4^\circ$  ccw

**3-20**  $\sigma_1 = 24.0$  kpsi,  $\sigma_2 = 0.819$  kpsi,  
 $\sigma_3 = -24.8$  kpsi,  $\tau_{\max} = 24.4$  kpsi

**3-23**  $\sigma = 34.0$  kpsi,  $\delta = 0.0679$  in,  $\epsilon_1 = 1.13(10^{-3})$ ,  
 $\epsilon_2 = -3.30(10^{-4})$ ,  $\Delta d = -2.48(10^{-4})$  in

**3-27**  $\delta = 5.9$  mm

**3-29**  $\sigma_x = 382$  MPa,  $\sigma_y = -37.4$  MPa

**3-35**  $\sigma_{\max} = 84.3$  MPa,  $\tau_{\max} = 5.63$  MPa

**3-40** (a)  $\sigma = 17.8$  kpsi,  $\tau = 3.4$  kpsi, (b)  $\sigma = 25.5$  kpsi,  
 $\tau = 3.4$  kpsi, (c)  $\sigma = 17.8$  kpsi,  $\tau = 3.4$  kpsi

**3-51** (a)  $T = 1318$  lbf  $\cdot$  in,  $\theta = 4.59^\circ$ ,  
(b)  $T = 1287$  lbf  $\cdot$  in,  $\theta = 4.37^\circ$

**3-53** (a)  $T_1 = 1.47$  N  $\cdot$  m,  $T_2 = 7.45$  N  $\cdot$  m,  
 $T_3 = 0$  N  $\cdot$  m,  $T = 8.92$  N  $\cdot$  m,  
(b)  $\theta_1 = 0.00348$  rad/mm

**3-59**  $H = 55.5$  kW

**3-66**  $d_c = 1.4$  in

**3-69** (a)  $T_1 = 2880$  N,  $T_2 = 432$  N, (b)  $R_O = 1794$  N,  
 $R_C = 3036$  N, (d)  $\sigma = 263$  MPa,  $\tau = 57.7$  MPa,  
(e)  $\sigma_1 = 276$  MPa,  $\sigma_2 = -12.1$  MPa,  $\tau_{\max} = 144$  MPa

**3-72** (a)  $F_B = 750$  lbf, (b)  $R_{Cy} = 183$  lbf,  $R_{Cz} = 861$  lbf,  
 $R_{Oy} = 209$  lbf,  $R_{Oz} = 259$  lbf, (d)  $\sigma = 35.2$  kpsi,  
 $\tau = 7.35$  kpsi, (e)  $\sigma_1 = 36.7$  kpsi,  $\sigma_2 = -1.47$  kpsi,  
 $\tau_{\max} = 19.1$  kpsi

**3-80** (a) Critical at the wall at top or bottom of rod.  
(b)  $\sigma_x = 16.3$  kpsi,  $\tau_{xz} = 5.09$  kpsi,  
(c)  $\sigma_1 = 17.8$  kpsi,  $\sigma_2 = -1.46$  kpsi,  
 $\tau_{\max} = 9.61$  kpsi

**3-84** (a) Critical at the top or bottom. (b)  $\sigma_x = 28.0$  kpsi,  
 $\tau_{xz} = 15.3$  kpsi, (c)  $\sigma_1 = 34.7$  kpsi,  $\sigma_2 = -6.72$  kpsi,  
 $\tau_{\max} = 20.7$  kpsi

**3-95**  $x_{\min} = 8.3$  mm

**3-97**  $x_{\max} = 1.9 \text{ kpsi}$

**3-100**  $p_o = 82.8 \text{ MPa}$

**3-104**  $\sigma_l = -18.6 \text{ psi}$ ,  $\sigma_t = 5710 \text{ psi}$ ,  $\sigma_r = -23.8 \text{ psi}$ ,  
 $\tau_{1/3} = 2870 \text{ psi}$ ,  $\tau_{1/2} = 2860 \text{ psi}$ ,  $\tau_{2/3} = 2.6 \text{ psi}$

**3-108**  $\tau_{\max} = 2.66 \text{ kpsi}$

**3-110**  $\delta_{\max} = 0.021 \text{ mm}$ ,  $\delta_{\min} = 0.0005 \text{ mm}$ ,  
 $p_{\max} = 65.2 \text{ MPa}$ ,  $p_{\min} = 1.55 \text{ MPa}$

**3-116**  $\delta = 0.001 \text{ in}$ ,  $p = 11.5 \text{ kpsi}$ ,  $(\sigma_t)_i = -11.5 \text{ kpsi}$ ,  
 $(\sigma_t)_o = 30.0 \text{ kpsi}$

**3-120**  $\sigma_i = 300 \text{ MPa}$ ,  $\sigma_o = -195 \text{ MPa}$

**3-126** (a)  $\sigma = \pm 8.02 \text{ kpsi}$ , (b)  $\sigma_i = -10.1 \text{ kpsi}$ ,  
 $\sigma_o = 6.62 \text{ kpsi}$ , (c)  $k_i = 1.255$ ,  $k_o = 0.825$

**3-129**  $\sigma_i = 182 \text{ MPa}$ ,  $\sigma_o = -47.8 \text{ MPa}$

**3-133**  $\sigma_{\max} = 353F^{1/3} \text{ MPa}$ ,  $\tau_{\max} = 106F^{1/3} \text{ MPa}$

**3-138**  $F = 117 \text{ lbf}$

**3-141**  $\sigma_x = -35.0 \text{ MPa}$ ,  $\sigma_y = -22.9 \text{ MPa}$ ,  
 $\sigma_z = -96.9 \text{ MPa}$ ,  $\tau_{\max} = 37.0 \text{ MPa}$

## B-4 Chapter 4

**4-3** (a)  $k = \frac{\pi d^4 G}{32} \left( \frac{1}{x} + \frac{1}{l-x} \right)$ ,

$$T_1 = 1500 \frac{l-x}{l}, T_2 = 1500 \frac{x}{l},$$

(b)  $k = 28.2 (10^3) \text{ lbf} \cdot \text{in}/\text{rad}$ ,  $T_1 = T_2 = 750 \text{ lbf} \cdot \text{in}$ ,  
 $\tau_{\max} = 30.6 \text{ kpsi}$

**4-7**  $\delta = 5.26 \text{ in}$ , % elongation due to weight = 3.22%

**4-10**  $y_{\max} = -25.4 \text{ mm}$ ,  $\sigma_{\max} = -163 \text{ MPa}$

**4-13**  $y_O = y_C = -3.72 \text{ mm}$ ,  $y|_{x=550\text{mm}} = 1.11 \text{ mm}$

**4-16**  $d_{\min} = 32.3 \text{ mm}$

**4-24**  $y_A = 7.99 \text{ mm}$ ,  $\theta_A = -0.0304 \text{ rad}$

**4-27**  $y_{Ay} = 0.0805 \text{ in}$ ,  $y_{Az} = -0.1169 \text{ in}$ ,  
 $\theta_{Ay} = -0.00144 \text{ rad}$ ,  $\theta_{Az} = -0.000861 \text{ rad}$

**4-30**  $\theta_{Oz} = 0.0131 \text{ rad}$ ,  $\theta_{Cz} = -0.0191 \text{ rad}$

**4-33**  $\theta_{Oy} = 0.0143 \text{ rad}$ ,  $\theta_{Oz} = 0.0118 \text{ rad}$ ,  
 $\theta_{Cy} = -0.0254 \text{ rad}$ ,  $\theta_{Cz} = -0.0151 \text{ rad}$

**4-36**  $d = 62.0 \text{ mm}$

**4-39**  $d = 2.88 \text{ in}$

**4-41**  $y = -0.1041 \text{ in}$

**4-43** Stepped bar:  $\theta = 0.026 \text{ rad}$ , simplified bar:  
 $\theta = 0.035 \text{ rad}$ , 34.6% difference,  $-0.848 \text{ in}$

**4-46**  $d = 38.1 \text{ mm}$

**4-51**  $y_B = -0.0155 \text{ in}$

**4-52**  $k = 8.10 \text{ N/mm}$

**4-69**  $\delta = 0.0102 \text{ in}$

**4-73** Stepped bar:  $\delta = 0.706 \text{ in}$ ,  
uniform bar:  $\delta = 0.848 \text{ in}$ , 20.1% difference

**4-76**  $\delta = 0.0338 \text{ mm}$

**4-78**  $\delta = 0.009 \text{ in}$

**4-81**  $\delta = 0.551 \text{ in}$

**4-85**  $\delta = 0.618 \text{ mm}$

**4-90** (a)  $\sigma_b = 48.8 \text{ kpsi}$ ,  $\sigma_c = -13.9 \text{ kpsi}$ ,  
(b)  $\sigma_b = 50.6 \text{ kpsi}$ ,  $\sigma_c = -12.1 \text{ kpsi}$

**4-92**  $R_B = 1.6 \text{ kN}$ ,  $R_O = 2.4 \text{ kN}$ ,  $\delta_A = 22.3 \text{ mm}$

**4-97**  $R_C = 1.33 \text{ kips}$ ,  $R_O = 4.67 \text{ kips}$ ,  
 $\delta_A = 0.0062 \text{ in}$ ,  $\sigma_{AB} = 14.7 \text{ kpsi}$

**4-101**  $\sigma_{BE} = 20.2 \text{ kpsi}$ ,  $\sigma_{DF} = 10.3 \text{ kpsi}$ ,  
 $y_B = -0.0255 \text{ in}$ ,  $y_C = -0.0865 \text{ in}$ ,  
 $y_D = -0.0129 \text{ in}$

**4-106** (a)  $t = 11 \text{ mm}$ , (b) No

**4-112**  $F_{\max} = 143.6 \text{ lbf}$ ,  $\delta_{\max} = 1.436 \text{ in}$

## B-5 Chapter 5

**5-1** (a) MSS:  $n = 3.5$ , DE:  $n = 3.5$ , (b) MSS:  $n = 3.5$ ,  
DE:  $n = 4.04$ , (c) MSS:  $n = 1.94$ , DE:  $n = 2.13$ ,  
(d) MSS:  $n = 3.07$ , DE:  $n = 3.21$ ,  
(e) MSS:  $n = 3.34$ , DE:  $n = 3.57$

**5-3** (a) MSS:  $n = 1.5$ , DE:  $n = 1.72$ , (b) MSS:  $n = 1.25$ ,  
DE:  $n = 1.44$ , (c) MSS:  $n = 1.33$ , DE:  $n = 1.42$ ,  
(d) MSS:  $n = 1.16$ , DE:  $n = 1.33$ ,  
(e) MSS:  $n = 0.96$ , DE:  $n = 1.06$

**5-7** (a)  $n = 3.03$

**5-12** (a)  $n = 2.40$ , (b)  $n = 2.22$ , (c)  $n = 2.19$ ,  
(d)  $n = 2.03$ , (e)  $n = 1.92$

**5-17** (a)  $n = 1.81$

**5-19** (a) BCM:  $n = 1.2$ , MM:  $n = 1.2$ ,  
(b) BCM:  $n = 1.5$ , MM:  $n = 2.0$ , (c) BCM:  $n = 1.18$ ,  
MM:  $n = 1.24$ , (d) BCM:  $n = 1.23$ , MM:  $n = 1.60$ ,  
(e) BCM:  $n = 2.57$ , MM:  $n = 2.57$

**5-24** (a) BCM:  $n = 3.63$ , MM:  $n = 3.63$

**5-29** (a)  $n = 1.54$

**5-34** (a)  $n = 1.54$

**5–40** MSS:  $n = 1.28$ , DE:  $n = 1.31$

**5–48** MSS:  $n = 12.5$ , DE:  $n = 10.1$

**5–53** MSS:  $n = 2.25$ , DE:  $n = 4.55$

**5–58** For yielding:  $p = 1.08$  kpsi,  
For rupture:  $p = 1.29$  kpsi

**5–63**  $d = 1.12$  in

**5–65** Model c:  $n = 1.80$ , Model d:  $n = 1.25$ ,  
Model e:  $n = 1.80$

**5–67**  $F_x = 2\pi f T/(0.2d)$

**5–68** (a)  $F_i = 16.7$  kN, (b)  $p_i = 111.3$  MPa,  
(c)  $\sigma_t = 185.5$  MPa,  $\sigma_r = -111.3$  MPa  
(d)  $\tau_{\max} = 148.4$  MPa,  $\sigma' = 259.7$  MPa,  
(e) MSS:  $n = 1.52$ , DE:  $n = 1.73$

**5–74**  $n_o = 2.58$ ,  $n_i = 2.38$

**5–76**  $n = 1.91$

**5–84** (a)  $F = 1140$  kN, (b)  $F = 329.4$  kN

**5–86**  $\sigma_{it} = N(-31\,000, 2899)$  psi,  
 $\sigma_{ot} = N(48\,760, 3445)$  psi

## B–6 Chapter 6

**6–1**  $S_e = 435$  MPa

**6–3**  $N = 116\,700$  cycles

**6–5**  $S_f = 117.0$  kpsi

**6–9**  $(S_f)_{ax} = 162 N^{-0.0851}$  kpsi for  $10^3 \leq N \leq 10^6$

**6–15**  $n_f = 1.42$ ,  $n_y = 1.51$

**6–17**  $n_f = 0.49$ ,  $N = 4600$  cycles

**6–20**  $n_y = 1.66$ , (a)  $n_f = 1.05$ , (b)  $n_f = 1.31$ ,  
(c)  $n_f = 1.31$

**6–24**  $n_y = 2.0$ , (a)  $n_f = 1.19$ , (b)  $n_f = 1.43$ , (c)  $n_f = 1.44$

**6–25**  $n_y = 3.3$ , using Goodman:  $n_f = 0.64$ ,  
 $N = 34\,000$  cycles

**6–28** (a)  $n_f = 0.94$ ,  $N = 637\,000$  cycles,  
(b)  $n_f = 1.16$  for infinite life

**6–30** The design is controlled by fatigue at the hole,  
 $n_f = 1.48$

**6–33** (a)  $T = 23.1$  lbf · in, (b)  $T = 28.3$  lbf · in,  
(c)  $n_y = 2.18$

**6–35**  $n_f = 1.21$ ,  $n_y = 1.43$

**6–38**  $n_f = 0.56$

**6–46**  $n_f = 5.45$

**6–47**  $n_f = 1.40$

**6–51**  $n_f = 0.72$ ,  $N = 7500$  cycles

**6–57**  $P = 4.12$  kips,  $n_y = 5.28$

**6–59** (a)  $n_2 = 7\,000$  cycles, (b)  $n_2 = 10\,000$  cycles

**6–66**  $R = 0.994$

**6–68**  $R = 0.824$

## B–7 Chapter 7

**7–1** (a) DE-Gerber:  $d = 25.85$  mm, (b) DE-Elliptic:  
 $d = 25.77$  mm, (c) DE-Soderberg:  $d = 27.70$  mm,  
(d) DE-Goodman:  $d = 27.27$  mm

**7–2** Using DE-Elliptic,  $d = 0.94$  in,  $D = 1.25$  in,  
 $r = 0.063$  in

**7–6** These answers are a partial assessment of potential failure. Deflections:  $\theta_O = 5.47(10)^{-4}$  rad,  
 $\theta_A = 7.09(10)^{-4}$  rad,  $\theta_B = 1.10(10)^{-3}$  rad. Compared to Table 7–2 recommendations,  $\theta_B$  is high for an uncrowned gear. Strength: Using DE-Elliptic at the shoulder at A,  $n_f = 3.91$

**7–18** (a) Fatigue strength using DE-Elliptic: Left keyway  $n_f = 3.5$ , right bearing shoulder  $n_f = 4.2$ , right keyway  $n_f = 2.7$ . Yielding: Left keyway  $n_y = 4.3$ , right keyway  $n_y = 2.7$ , (b) Deflection factors compared to minimum recommended in Table 7–2: Left bearing  $n = 3.5$ , right bearing  $n = 1.8$ , gear slope  $n = 1.6$

**7–28** (a)  $\omega = 883$  rad/s (b)  $d = 50$  mm  
(c)  $\omega = 1766$  rad/s (doubles)

**7–30** (b)  $\omega = 466$  rad/s = 4450 rev/min

**7–34**  $\frac{1}{4}$ -in square key,  $\frac{7}{8}$ -in long, AISI 1020 CD

**7–36**  $d_{\min} = 14.989$  mm,  $d_{\max} = 15.000$  mm,  
 $D_{\min} = 15.000$  mm,  $D_{\max} = 15.018$  mm

**7–42** (a)  $d_{\min} = 35.043$  mm,  $d_{\max} = 35.059$  mm,  
 $D_{\min} = 35.000$  mm,  $D_{\max} = 35.025$  mm,  
(b)  $p_{\min} = 35.1$  MPa,  $p_{\max} = 115$  MPa,  
(c) Shaft:  $n = 3.4$ , hub:  $n = 1.9$ ,  
(d) Assuming  $f = 0.3$ ,  $T = 1010$  N · m

## B–8 Chapter 8

**8–1** (a) Thread depth 2.5 mm, thread width 2.5 mm,  
 $d_m = 22.5$  mm,  $d_r = 20$  mm,  $l = p = 5$  mm

**8–4**  $T_R = 15.85$  N · m,  $T_L = 7.827$  N · m,  $e = 0.251$

**8–8**  $F = 182$  lbf

**8-11** (a)  $L = 45$  mm, (b)  $k_b = 874.6$  MN/m,  
(c)  $k_m = 3116.5$  MN/m

**8-14** (a)  $L = 3.5$  in, (b)  $k_b = 1.79$  Mlbf/in,  
(c)  $k_m = 7.67$  Mlbf/in

**8-19** (a)  $L = 60$  mm, (b)  $k_b = 292.1$  MN/m,  
(c)  $k_m = 692.5$  MN/m

**8-25** From Eqs. (8-20) and (8-22),  $k_m = 2762$  MN/m.  
From Eq. (8-23),  $k_m = 2843$  MN/m

**8-29** (a)  $n_p = 1.10$ , (b)  $n_L = 1.60$ , (c)  $n_0 = 1.20$

**8-33**  $L = 55$  mm,  $n_p = 1.30$ ,  $n_L = 11.77$ ,  $n_0 = 11.58$

**8-37**  $n_p = 1.30$ ,  $n_L = 12.53$ ,  $n_0 = 11.36$

**8-41** Bolt sizes of diameters 8, 10, 12, and 14 mm were evaluated and all were found acceptable. For  $d = 8$  mm,  $k_m = 926$  MN/m,  $L = 50$  mm,  $k_b = 233.9$  MN/m,  $C = 0.202$ ,  $N = 20$  bolts,  $F_i = 6.18$  kN,  $P = 2.71$  kN/bolt,  $n_p = 1.23$ ,  $n_L = 3.77$ ,  $n_0 = 2.86$

**8-46** (a)  $T = 823$  N · m, (b)  $n_p = 1.10$ ,  $n_L = 17.7$ ,  $n_0 = 57.7$

**8-51** (a) Goodman:  $n_f = 8.04$ , (b) Gerber:  $n_f = 12.1$ ,  
(c) ASME-elliptic:  $n_f = 10.4$

**8-55** Goodman:  $n_f = 12.7$

**8-60** (a)  $n_p = 1.16$ , (b)  $n_L = 2.96$ , (c)  $n_0 = 6.70$ ,  
(d)  $n_f = 4.56$

**8-63**  $n_p = 1.24$ ,  $n_L = 4.62$ ,  $n_0 = 5.39$ ,  $n_f = 4.75$

**8-67** Bolt shear,  $n = 2.30$ ; bolt bearing,  $n = 4.06$ ;  
member bearing,  $n = 1.31$ ; member tension,  $n = 3.68$

**8-70** Bolt shear,  $n = 1.70$ ; bolt bearing,  $n = 4.69$ ;  
member bearing,  $n = 2.68$ ; member tension,  $n = 6.68$

**8-75**  $F = 2.32$  kN based on channel bearing

**8-77** Bolt shear,  $n = 4.78$ ; bolt bearing,  $n = 10.55$ ;  
member bearing,  $n = 5.70$ ; member bending,  $n = 4.13$

## B-9 Chapter 9

**9-1**  $F = 49.5$  kN

**9-5**  $F = 51.0$  kN

**9-9**  $F = 31.1$  kN

**9-14**  $\tau = 22.6$  kpsi

**9-18** (a)  $F = 2.71$  kips, (b)  $F = 1.19$  kips

**9-22**  $F = 5.41$  kips

**9-26**  $F = 5.89$  kips

**9-29**  $F = 12.5$  kips

**9-31**  $F = 5.04$  kN

**9-34** All-around square, four beads each  $h = 6$  mm,  
75 mm long, Electrode E6010

**9-45**  $\tau_{\max} = 25.6$  kpsi

**9-47**  $\tau_{\max} = 45.3$  MPa

**9-48**  $n = 3.48$

**9-51**  $F = 61.2$  kN

## B-10 Chapter 10

**10-3** (a)  $L_0 = 162.8$  mm, (b)  $F_s = 167.9$  N,  
(c)  $k = 1.314$  N/mm, (d)  $(L_0)_{\text{cr}} = 149.9$  mm, spring  
needs to be supported

**10-5** (a)  $L_s = 2.6$  in, (b)  $F_s = 69.6$  lbf, (c)  $n_s = 1.78$

**10-7** (a)  $L_0 = 1.78$  in, (b)  $p = 0.223$  in, (c)  $F_s =$   
18.78 lbf, (d)  $k = 16.43$  lbf/in, (e)  $(L_0)_{\text{cr}} = 4.21$  in

**10-11** Spring is solid safe,  $n_s = 1.28$

**10-17** Spring is solid safe, but for  $n_s = 1.2$ ,  
 $L_0 \leq 66.7$  mm

**10-20** (a)  $N_a = 12$  turns,  $L_s = 1.755$  in,  $p = 0.396$  in,  
(b)  $k = 6.08$  lbf/in, (c)  $F_s = 18.2$  lbf, (d)  $\tau_s = 38.5$  kpsi

**10-23** With  $d = 2$  mm,  $L_0 = 48$  mm,  $k = 4.286$  N/mm,  
 $D = 13.25$  mm,  $N_a = 15.9$  coils,  $n_s = 2.63 > 1.2$ , ok.  
No other  $d$  works.

**10-28** (a)  $d = 0.2375$  in, (b)  $D = 1.663$  in, (c)  $k =$   
150 lbf/in, (d)  $N_t = 8.46$  turns, (e)  $L_0 = 3.70$  in

**10-30** Use A313 stainless wire,  $d = 0.0915$  in,  
OD = 0.971 in,  $N_t = 15.59$  turns,  $L_0 = 3.606$  in

**10-36** (a)  $L_0 = 16.12$  in, (b)  $\tau_i = 14.95$  kpsi,  
(c)  $k = 4.855$  lbf/in, (d)  $F = 85.8$  lbf, (e)  $y = 14.4$  in

**10-39**  $\Sigma = 31.3^\circ$  (see Fig. 10-9),  $F_{\max} = 87.3$  N

**10-42**  $k = EI\{4l^3 + 3R[2\pi l^2 + 4(\pi - 2)lR +$   
 $(3\pi - 8)R^2]\}^{-1}$ , (b)  $k = 3.02$  lbf/in, (c)  $F = 3.24$  lbf

## B-11 Chapter 11

**11-1**  $x_D = 525$ ,  $F_D = 3.0$  kN,  $C_{10} = 24.2$  kN,  
02-35 mm deep-groove ball bearing,  $R = 0.920$

**11-6**  $x_D = 456$ ,  $C_{10} = 145$  kN

**11-8**  $C_{10} = 20$  kN

**11-15**  $C_{10} = 26.1$  kN

**11-21** (a)  $F_e = 5.4$  kN, (b)  $\mathcal{L}_D = 430$  h

**11–24** 60 mm deep-groove

**11–27** (a)  $C_{10} = 12.8$  kips

**11–33**  $C_{10} = 5.7$  kN, 02–12 mm deep-groove ball bearing

**11–34**  $R_O = 112$  lbf,  $R_C = 298$  lbf, deep-groove  
02–17 mm at  $O$ , deep-groove 02–35 mm at  $C$

**11–38**  $I_2 = 0.267(10^6)$  rev

**11–43**  $F_{RA} = 35.4$  kN,  $F_{RB} = 17.0$  kN

## B–12 Chapter 12

**12–1**  $c_{\min} = 0.015$  mm,  $r = 12.5$  mm,  $r/c = 833$ ,  
 $N_j = 18.3$  r/s,  $S = 0.182$ ,  $h_0/c = 0.3$ ,  $rf/c = 5.4$ ,  
 $Q/(rcNl) = 5.1$ ,  $Q_s/Q = 0.81$ ,  $h_0 = 0.0045$  mm,  
 $H_{\text{loss}} = 11.2$  W,  $Q = 219$  mm $^3$ /s,  
 $Q_s = 177$  mm $^3$ /s

**12–3** SAE 10:  $h_0 = 0.000275$  in,  $p_{\max} = 847$  psi,  
 $c_{\min} = 0.0025$  in

**12–7**  $h_0 = 0.00069$  in,  $f = 0.00787$ ,  
 $Q = 0.0802$  in $^3$ /s

**12–9**  $h_0 = 0.011$  mm,  $H = 48.1$  W,  
 $Q = 1426$  mm $^3$ /s,  $Q_s = 1012$  mm $^3$ /s

**12–11**  $T_{\text{av}} = 154^\circ\text{F}$ ,  $h_0 = 0.00113$  in,  
 $H_{\text{loss}} = 0.0750$  Btu/s,  $Q_s = 0.0802$  in $^3$ /s

**12–20** Approx: 45.6 mPa · s, Fig. 12–13: 40 mPa · s

## B–13 Chapter 13

**13–1** 35 teeth, 3.25 in

**13–2** 400 rev/min,  $p = 3\pi$  mm,  $C = 112.5$  mm

**13–4**  $a = 0.3333$  in,  $b = 0.4167$  in,  $c = 0.0834$  in,  
 $p = 1.047$  in,  $t = 0.523$  in,  $d_1 = 7$  in,  $d_{1b} = 6.578$  in,  $d_2 = 9.333$  in,  $d_{2b} = 8.77$  in,  
 $p_b = 0.984$  in,  $m_c = 1.55$

**13–5**  $d_p = 2.333$  in,  $d_G = 5.333$  in,  $\gamma = 23.63^\circ$ ,  
 $\Gamma = 66.37^\circ$ ,  $A_0 = 2.910$  in,  $F = 0.873$  in

**13–10** (a) 13, (b) 15, 16, (c) 18

**13–12** 10:20 and higher

**13–15** (a)  $p_n = 3\pi$  mm,  $p_t = 10.40$  mm,  $p_x = 22.30$  mm, (b)  $m_t = 3.310$  mm,  $\phi_t = 21.88^\circ$ ,  
(c)  $d_p = 59.58$  mm,  $d_G = 105.92$  mm

**13–17**  $e = 4/51$ ,  $n_d = 47.06$  rev/min cw

**13–24**  $N_2 = N_4 = 15$  teeth,  $N_3 = N_5 = 44$  teeth

**13–29**  $n_A = 68.57$  rev/min cw

**13–36** (a)  $d_2 = d_4 = 2.5$  in,  $d_3 = d_5 = 7.33$  in,

(b)  $V_i = 1636$  ft/min,  $V_o = 558$  ft/min,  
 $W_{ti} = 504$  lbf,  $W_{ri} = 184$  lbf,  $W_i = 537$  lbf,  
 $W_{to} = 1478$  lbf,  $W_{ro} = 538$  lbf,  $W_o = 1573$  lbf,  
(d)  $T_i = 630$  lbf · in,  $T_o = 5420$  lbf · in

**13–38** (a)  $N_{p\min} = 15$  teeth, (b)  $P = 1.875$  teeth/in,  
(c)  $F_A = 311$  lbf,  $F_B = 777.6$  lbf

**13–41** (a)  $N_F = 30$  teeth,  $N_C = 15$  teeth,  
(b)  $P = 3$  teeth/in, (c)  $T = 900$  lbf · in,  
(d)  $W_r = 65.5$  lbf,  $W_t = 180$  lbf,  $W = 191.6$  lbf

**13–43**  $\mathbf{F}_A = 71.5 \mathbf{i} + 53.4 \mathbf{j} + 350.5 \mathbf{k}$  lbf,  
 $\mathbf{F}_B = -178.4 \mathbf{i} - 678.8 \mathbf{k}$  lbf

**13–50**  $\mathbf{F}_C = 1565 \mathbf{i} + 672 \mathbf{j}$  lbf,  
 $\mathbf{F}_D = 1610 \mathbf{i} - 425 \mathbf{j} + 154 \mathbf{k}$  lbf

## B–14 Chapter 14

**14–1**  $\sigma = 7.63$  kpsi

**14–4**  $\sigma = 32.6$  MPa

**14–7**  $F = 2.5$  in

**14–10**  $m = 2$  mm,  $F = 25$  mm

**14–14**  $\sigma_c = -617$  MPa

**14–17**  $W^t = 16\ 890$  N,  $H = 97.2$  kW  
(pinion bending);  $W^t = 3433$  N,  $H = 19.8$  kW  
(pinion and gear wear)

**14–18**  $W^t = 1283$  lbf,  $H = 32.3$  hp (pinion bending);  
 $W^t = 1510$  lbf,  $H = 38.0$  hp (gear bending);  
 $W^t = 265$  lbf,  $H = 6.67$  hp (pinion and gear wear)

**14–22**  $W^t = 775$  lbf,  $H = 19.5$  hp (pinion bending);  
 $W^t = 300$  lbf,  $H = 7.55$  hp (pinion wear), AGMA  
method accounts for more conditions

**14–24** Rating power =  $\min(157.5, 192.9, 53.0, 59.0) = 53$  hp

**14–28** Rating power =  $\min(270, 335, 240, 267) = 240$  hp

**14–34**  $H = 69.7$  hp

## B–15 Chapter 15

**15–1**  $W_P^t = 690$  lbf,  $H_1 = 16.4$  hp,  $W_G^t = 620$  lbf,  
 $H_2 = 14.8$  hp

**15–2**  $W_P^t = 464$  lbf,  $H_3 = 11.0$  hp,  $W_G^t = 531$  lbf,  
 $H_4 = 12.6$  hp

**15–8** Pinion core 300 Bhn, case, 373 Bhn; gear core  
339 Bhn, case, 345 Bhn

**15–9** All four  $W^t = 690 \text{ lbf}$

**15–11** Pinion core 180 Bhn, case, 266 Bhn; gear core, 180 Bhn, case, 266 Bhn

## B–16 Chapter 16

**16–1** (a) Right shoe:  $p_a = 711 \text{ kPa}$  cw rotation,

(b) Right shoe:  $T = 277.6 \text{ N} \cdot \text{m}$ ; left shoe:

$144.4 \text{ N} \cdot \text{m}$ ; total  $T = 422 \text{ N} \cdot \text{m}$ , (c) RH shoe:

$R^x = -1.01 \text{ kN}$ ,  $R^y = 3.94 \text{ kN}$ ,  $R = 4.06 \text{ kN}$ ,

LH shoe:  $R^x = 597 \text{ N}$ ,  $R^y = 793 \text{ N}$ ,  $R = 993 \text{ N}$

**16–3** LH shoe:  $T = 2.265 \text{ kip} \cdot \text{in}$ ,  $p_a = 133.1 \text{ psi}$ ,

RH shoe:  $T = 0.816 \text{ kip} \cdot \text{in}$ ,  $p_a = 47.93 \text{ psi}$ ,

$T_{\text{total}} = 3.09 \text{ kip} \cdot \text{in}$

**16–5**  $p_a = 27.4 \text{ psi}$ ,  $T = 348.7 \text{ lbf} \cdot \text{in}$

**16–8**  $a' = 1.209r$ ,  $a = 1.170r$

**16–10**  $P = 1.25 \text{ kips}$ ,  $T = 25.52 \text{ kip} \cdot \text{in}$

**16–14** (a)  $T = 8200 \text{ lbf} \cdot \text{in}$ ,  $P = 504 \text{ lbf}$ ,  $H = 26 \text{ hp}$ ,

(b)  $R = 901 \text{ lbf}$ , (c)  $p|_{\theta=0} = 70 \text{ psi}$ ,

$p|_{\theta=270^\circ} = 27.3 \text{ psi}$

**16–17** (a)  $F = 1885 \text{ lbf}$ ,  $T = 7125 \text{ lbf} \cdot \text{in}$ ,

(c) torque capacity exhibits a stationary point maximum

**16–18** (a)  $d^* = D/\sqrt{3}$ , (b)  $d^* = 3.75 \text{ in}$ ,  $T^* = 7173 \text{ lbf} \cdot \text{in}$ , (c)  $(d/D)^* = 1/\sqrt{3} = 0.577$

**16–19** (a) Uniform wear:  $p_a = 14.04 \text{ psi}$ ,  $F = 243 \text{ lbf}$ ,

(b) Uniform pressure:  $p_a = 13.42 \text{ psi}$ ,  $F = 242 \text{ lbf}$

**16–23**  $C_s = 0.08$ ,  $t = 143 \text{ mm}$

**16–26** (b)  $I_e = I_M + I_P + n^2 I_P + I_L/n^2$ ,

(c)  $I_e = 10 + 1 + 10^2(1) + 100/10^2 = 112$

**16–27** (c)  $n^* = 2.430$ ,  $m^* = 4.115$ , which are independent of  $I_L$

## B–17 Chapter 17

**17–1** (a)  $F_c = 0.913 \text{ lbf}$ ,  $F_i = 101.1 \text{ lbf}$ ,  $F_{1a} = 147 \text{ lbf}$ ,

$F_2 = 57 \text{ lbf}$ , (b)  $H_a = 2.5 \text{ hp}$ ,  $n_{fs} = 1.0$ ,

(c) 0.151 in

**17–3** A-3 polyamide belt,  $b = 6 \text{ in}$ ,  $F_c = 77.4 \text{ lbf}$ ,  $T = 10946 \text{ lbf} \cdot \text{in}$ ,  $F_i = 573.7 \text{ lbf}$ ,  $F_2 = 117.6 \text{ lbf}$ ,  $F_i = 268.3 \text{ lbf}$ ,  $\text{dip} = 0.562 \text{ in}$

**17–5** (a)  $T = 742.8 \text{ lbf} \cdot \text{in}$ ,  $F_i = 148.1 \text{ lbf}$ ,  
(b)  $b = 4.13 \text{ in}$ , (c)  $F_{1a} = 289.1 \text{ lbf}$ ,  $F_c = 17.7 \text{ lbf}$ ,  
 $F_i = 147.6 \text{ lbf}$ ,  $F_2 = 41.5 \text{ lbf}$ ,  $H = 20.6 \text{ hp}$ ,  
 $n_{fs} = 1.1$

**17–7**  $R^x = (F_1 + F_2)\{1 - 0.5[(D - d)/(2C)]^2\}$ ,  
 $R^y = (F_1 - F_2)(D - d)/(2C)$ . From Ex. 17–2,  
 $R^x = 1214.4 \text{ lbf}$ ,  $R^y = 34.6 \text{ lbf}$

**17–14** With  $d = 2 \text{ in}$ ,  $D = 4 \text{ in}$ , life of  $10^6$  passes,  
 $b = 4.5 \text{ in}$ ,  $n_{fs} = 1.05$

**17–17** Select one B90 belt

**17–20** Select nine C270 belts, life  $> 10^9$  passes,  
life  $> 150000 \text{ h}$

**17–24** (b)  $n_1 = 1227 \text{ rev/min}$ . Table 17–20 confirms this point occurs in the range  $1200 \pm 200 \text{ rev/min}$ ,  
(c) Eq. (17–40) applicable at speeds exceeding 1227 rev/min for No. 60 chain

**17–25** (a)  $H_a = 7.91 \text{ hp}$ ; (b)  $C = 18 \text{ in}$ ,  
(c)  $T = 1164 \text{ lbf} \cdot \text{in}$ ,  $F = 744 \text{ lbf}$

**17–27** Four-strand No. 60 chain,  $N_1 = 17 \text{ teeth}$ ,  
 $N_2 = 84 \text{ teeth}$ , rounded  $L/p = 134$ ,  $n_{fs} = 1.17$ , life  
 $15000 \text{ h}$  (pre-extreme)

## B–20 Chapter 20

**20–1**  $\bar{x} = 122.9 \text{ kilocycles}$ ,  $s_x = 30.3 \text{ kilocycles}$

**20–2**  $\bar{x} = 198.55 \text{ kpsi}$ ,  $s_x = 9.55 \text{ kpsi}$

**20–3**  $\bar{x} = 78.4 \text{ kpsi}$ ,  $s_x = 6.57 \text{ kpsi}$

**20–11** (a)  $\bar{F}_i = 5.979 \text{ lbf}$ ,  $s_{Fi} = 0.396 \text{ lbf}$ ,  
(b)  $\bar{k} = 9.766 \text{ lbf/in}$ ,  $s_k = 0.390 \text{ lbf/in}$

**20–19**  $L_{10} = 84.1 \text{ kcycles}$

**20–23**  $R = 0.987$

**20–25**  $x_{0.01} = 88.3 \text{ kpsi}$

**20–32** 78.1 kcycles, 82.7 kcycles

# Index

## A

Abrasion, 743  
Abrasive wear, 328  
Absolute safety, 12  
Absolute system of units, 21  
Absolute tolerance system, 21  
Absolute viscosity, 620  
Acme threads, 412  
Addendum, 676  
Addendum distances, 680  
Adhesive bonding  
    about, 498  
    adhesive types, 499–501  
    joint design, 504–506  
    stress distributions, 501–504  
Admiralty metal, 58  
AGMA equation factors  
    allowable bending stress  
        numbers, 747–749, 800  
    allowable contact stress, 750–752,  
        799–800  
    bending strength geometry factor,  
        751–754, 793–794  
    crowning factor for pitting, 793  
    dynamic factor, 756, 758, 791–792  
    elastic coefficient, 744, 756–757,  
        798–799  
    geometry factors, 751–756,  
        793–794  
    hardness-ratio factor, 761, 796  
    lengthwise curvature factor for  
        bending strength, 793  
    load-distribution factor, 759–760, 793  
    overload factor, 758, 791  
    pitting resistance geometry factor,  
        751, 754–756, 793  
    reliability factors, 763,  
        797–798  
    reversed loading, 800  
    rim-thickness factor, 764  
    safety factors, 765, 791

size factor, 759, 793  
stress-cycle factor, 762, 795–796  
surface condition factor, 758  
temperature factor, 764, 796  
AGMA gear method  
    bevel gears, 788, 801–802  
    helical gears, 745–750  
    spur gears, 745–750, 766–767  
    worm gears, 809  
AGMA transmission accuracy-level  
    number, 756  
Alignment, 607  
Allowance, 20  
Alloy cast irons, 55  
Alloying, 33  
Alloy steels  
    chromium, 52  
    manganese, 52  
    molybdenum, 53  
    nickel, 52  
    numbering system, 45  
    quenching, 50  
    silicon, 52  
    tempering, 50  
    tungsten, 53  
    vanadium, 53  
Alternating and midrange von Mises  
    stresses, 318, 367  
Alternating stresses, 266, 301  
Aluminum, 55–56  
Aluminum brass, 58  
Aluminum bronze, 58, 817  
American Bearing Manufacturers  
    Association (ABMA), 12  
    standard, 573  
American Gear Manufacturers  
    Association (AGMA), 12  
    approach, 734  
American Institute of Steel Construction  
    (AISC), 12  
    code, 489–490

American Iron and Steel Institute  
    (AISI), 12, 45  
American National (Unified) thread  
    standard, 410  
American Society for Testing and  
    Materials (ASTM), 12  
    numbering system, 46  
American Society of Mechanical  
    Engineers (ASME), 12, 620  
American Welding Society (AWS),  
    476–478  
American Welding Society (AWS), 12  
    code, 490  
Amplitude ratio, 302  
Anaerobic adhesives, 500  
Angle of action, 682  
Angle of approach, 682  
Angle of articulation, 908  
Angle of recess, 682  
Angle of twist, 101–102  
Angular-contact bearing, 572  
Angular-velocity ratios, 677, 683,  
    880, 882  
Annealing, 49  
Annealing effect, 44  
Antifriction bearing lubrication, 604  
Antifriction bearings, 570  
Arc of action, 684  
Arc of approach, 684  
Arc of recess, 684  
Area principal axes, 93  
Area reduction, 39  
Arithmetic mean, 980–984  
Arrow side (weld symbol), 477  
ASME-elliptic failure criteria, 305–306,  
    308, 338, 346, 369  
ASM Metals Handbook  
    (ASM), 269  
ASTM fastener specifications, 432  
Austenite, 50  
Average factor of safety, 249

Average film temperature, 645  
 Average life, 574  
 Average strain rate, 42  
 Average tangential stress, 114, 116  
 Axial clutches, 845  
 Axial fatigue, 332  
 Axial layout of components, 363  
 Axial load support, 363  
 Axial pitch, 692, 695  
 Axle, defined, 360

**B**

$B_{10}$  life, 574  
 Babbitt, 657  
 Backlash, 676  
 Back-to-back (DB) mounting, 606  
 Bainite, 50  
 Bairstow, I., 276  
 Ball bearings, 570  
 Ball bearings selection, 588–590  
 Band-type clutches and brakes, 844–845  
 Barth equation, 739  
 Base circles, 678, 680  
 Base pitch, 682  
 Basic dynamic load rating, 574  
 Basic load rating, 574  
 Basic size, 395  
 Basic static load rating, 580  
 Baushinger's theory, 276  
 Beach marks, 266  
 Beams  
     in bending, normal stresses, 89–94  
     in bending, shear stresses, 94–100  
     curved beams in bending, 118–122  
     deflection methods, 152–153  
     deflections by singularity functions, 156–162  
     deflections by superposition, 153–156  
     load and stress analysis, 75–76, 89–100  
     shear force and bending moments in, 75–76  
     shear stresses in bending, 93–94  
     shear stress in rectangular, 95  
 Bearing alloy characteristics, 657  
 Bearing characteristic number, 622  
 Bearing fatigue failure criteria, 573  
 Bearing film pressure, 625  
 Bearing housing heat dissipation, 645

Bearing life  
     life measure of an individual bearing, 573  
     recommendations for various classes of machinery, 583  
     reliability-life relationship, 570  
     rolling-contact bearings, 573–574  
 Bearing load life at rated reliability, 574–575  
 Bearings  
     boundary dimensions for, 580  
     direct mountings of, 591  
     indirect mountings of, 591  
     parts of, 570  
     reliability, 600–603  
     selection of, 936, 947  
     shields, 572  
     stress, 452  
     suppliers, 591  
     supports, 372  
     types, 570–573, 658–659  
 Belleville springs, 557  
 Belting equation, 887  
 Belts, 880–883  
     centrifugal tension in, 884  
     tension, 903  
 Bending factor, 794  
 Bending moment, 75  
 Bending strain energy, 163  
 Bergsträsser factor, 519  
 Beryllium bronze, 58  
 Bevel and worm gears  
     AGMA equation factors, 791–795  
     bevel gearing, general, 786–788  
     bevel-gear stresses and strengths, 788–791  
     Buckingham wear load, 820–821  
     designing a worm-gear mesh, 817–820  
     design of a straight-bevel gear mesh, 806–808  
     straight-bevel gear analysis, 803–805  
     worm-gear analysis, 813–816  
     worm gearing-AGMA equation, 809–812  
 Bevel gearing  
     force analysis, 709–712  
     general, 786–788  
 Bevel-gear mounting, 788  
 Bevel gears, 674  
     straight, 690–691  
     terminology of, 690  
     tooth forces, 709  
 Bevel-gear stresses and strengths, 788–791  
     bending stress, 791  
     fundamental contact stress equation, 788–790  
     permissible bending stress equation, 791  
     permissible contact stress number (strength) equation, 791  
 Bilateral tolerance, 19  
 Blanking, 49  
 Bolted and riveted joints loaded in shear, 451–459  
 Bolt elongation, 441  
 Bolt preload, 425  
 Bolts, loosening of, 448  
 Bolt spacing, 444  
 Bolt strength, 432–435  
 Bolt tension, 437–440  
 Bolt torque and bolt tension, 437–440  
 Bottom land, 676  
 Boundary conditions  
     axisymmetric beam and the bearing supports, 972  
     critical speeds, 383  
     finite-element analysis, 965–966  
     geometric, 151  
     long columns with central loading, 181  
     multipoint constraint equations, 966  
     simply supported beams, 152  
     superposition, 153  
 Boundary dimensions for bearings, 580  
 Boundary elements, 966  
 Boundary-lubricated bearings, 660–668  
     bushing wear, 663–666  
     linear sliding wear, 661–663  
     temperature rise, 666–668  
 Boundary lubrication, 619, 660–661  
 Boundary representative (B-rep) techniques, 963  
 Brake bands and flexible clutch, 844  
 Brake lining wear, 840  
 Brakes, operating mechanisms, 840  
 Brake shoes, self-deenergizing, 827

- Brass, 57  
 5 to 15 percent zinc, 57  
 20 to 36 percent zinc, 57–58  
 36 to 40 percent zinc, 58
- Breakeven points, 13–14
- Brinell hardness, 41, 761
- Brittle Coulomb-Mohr (BCM theory), 235–236
- Brittle fracture, 44
- Brittle materials, 33, 111  
 fatigue failure criteria, 314  
 maximum-normal-stress theory for, 235  
 meaning of, 238  
 modifications of the Mohr theory for, 235–237
- Smith-Dolan focus, 314
- Smith-Dolan fracture criteria for, 338–339
- Brittle metal behavior, 218
- Bronze, 57, 58
- Buckingham Lewis equation, 812
- Buckingham method, 848
- Buckingham wear equation, 821
- Buckingham wear load, 820–821
- Buckling, 149
- Burnishing, 690
- Bushed-pin bearings, 661
- Bushings, 618
- Bushing wear, 663–666
- Butt welds, 478–481
- C**
- Calculations and significant figures, 22–23
- Caliper brakes, 849
- Cams, 677
- Cap screws, 423
- Carbon content, 33
- Carburization, 51
- Cartesian stress components, 79–80
- Cartridge brass, 57
- Case hardening, 51
- Case study  
 bearing selection, 947–948  
 deflection check, 946–947  
 design for stress, 946  
 gear specification, 939–943
- key design, 948–949  
 problem specification, 934–935  
 shaft layout, 944–946  
 speed, torque, and gear ratios, 937–939
- Castigliano's theorem, 164–168, 169, 176, 553, 559
- Casting alloys, 56
- Casting materials  
 alloy cast irons, 55  
 cast steels, 55  
 ductile and nodular cast iron, 54  
 gray cast iron, 54  
 malleable cast iron, 55  
 white cast iron, 54–55
- Cast iron, 283
- Cast steels, 55
- Catalog load rating, 574
- Catastrophic failure, 190
- Catenary theory, 892
- Cementite, 54
- Center distance, 682–683
- Centipoise, 620
- Centrifugal castings, 47
- Centrifugal clutches, 832
- Centrifugal extrusions, 687
- Centrifugal force, 837
- Centrifugal tension in belt, 884
- Centroidal axis, 90, 119
- Cermet pads, 863
- Chain velocity, 909
- Charpy notched-bar test, 42
- Chevron lines, 267
- Chordal speed variation, 910
- Chromium, 52
- Circular (button or puck) pad caliper brake, 852–853
- Circular pitch, 675, 692
- Clamshell marks, 266
- Clearance, 19, 648–650, 676
- Clearance circle, 676
- Closed ends, 520
- Closed thin-walled tubes, 107–108
- Close running fit, 397
- Close-wound springs, 544
- Clutch capacity, 856
- Clutches  
 cone, 832  
 disk, 832  
 friction materials for, 864
- multiple-plate, 832
- operating mechanisms, 840
- types of, 832
- Clutches, brakes, couplings, and flywheels, 826–887  
 about, 827–831  
 band-type clutches and brakes, 844–845  
 cone clutches and brakes, 853–855  
 disk brakes, 849–853  
 energy considerations, 856–857  
 external contracting rim clutches and brakes, 840–844  
 flywheels, 866–871  
 frictional-contact axial clutches, 845–848  
 friction materials, 861–864  
 internal expanding rim clutches and brakes, 832–840  
 miscellaneous clutches and couplings, 864–865  
 temperature rise, 857–861
- Clutches and couplings, 864–865
- Codes, 12
- Coefficient of friction  
 of bearing, 625  
 elements affecting, 438  
 gears, general, 715–717  
 Petroff's equation, 638–639  
 of power screws, 421  
 variance of, 837
- Coefficient of speed fluctuation, 867
- Coefficient of variance (COV), 251, 982
- Coining, 49
- Cold drawing, 48
- Cold forming, 687
- Cold rolling, 48, 687
- Cold-work factor, 39
- Cold working, 38
- Cold-working processes, 48–49
- Columns  
 defined, 181  
 with eccentric loading, 184–188  
 Euler column formula, 181  
 intermediate-length, with central loading, 184  
 long, with central loading, 181–184  
 secant column formula, 186  
 unstable, 181

- Combinations of loading modes, 273, 317–321, 347  
 Combined radial and thrust loading, 579–584  
 Commercial bronze, 57  
 Commercial FEA packages, 954  
 Commercial seals, 607  
 Commercial vendor sources, 8–9  
 Companion distribution, 987  
 Completely reversed stress, 275, 285, 301, 317  
 Completely reversing simple loading, 344–346  
 Composite materials, 60  
 Compound gear ratio, 699  
 Compound reverted gear train, 701  
 Compression coil springs, 522  
 Compression members, general, 181  
 Compression springs, 520–521  
 Compressive stress, 79, 186, 190  
 Computational errors, 956  
 Computational tools, 8–9  
 Computer-aided design (CAD) software, 8  
 Computer-aided engineering (CAE), 9  
 Concept design, 6  
 Cone, 853  
 Cone angle, 853  
 Cone clutches, 832, 845, 853  
 Cone clutches and brakes, 853–855  
     uniform pressure, 855  
     uniform wear, 854–855  
 Conical springs, 558  
 Conjugate action, 677–678  
 Constant angular-velocity ratio, 906  
 Constant-force springs, 558  
 Constant-life curves, 303  
 Constructive solid geometry (CSG) techniques, 963  
 Contact adhesives, 500  
 Contact area, 691  
 Contact fatigue strength, 328  
 Contact-geometry factor, 794  
 Contact ratio, 684–685, 738  
 Contact strength, 328  
 Contact stresses, 122–126  
     cylindrical contact, 124–126  
     spherical contact, 123–124  
 Contact stress factor, 795  
 Contact-stress fatigue, AGMA strength, 762  
 Contact-stress fatigue failure, 762, 765  
 Continuous periodic load rotation, 586  
 Continuous random variable, 979  
 Continuous varying cyclic load, 587  
 Coordinate transformation equations, 86  
 Copper-base alloys  
     brass with 5 to 15 percent zinc, 57  
     brass with 20 to 36 percent zinc, 57–58  
     brass with 36 to 40 percent zinc, 58  
     bronze, 58  
 Correlation coefficient, 995  
 Corrosion, 294  
 Corrosion-resistant steels, 53  
 Cost estimates, 15  
 Coulomb-Mohr theory, 228–230, 255  
 Counter-rotating rotation, self-energization for, 842  
 Counting method for cycles, 322  
 Coupling clutches, 865  
 Crack extension, 278  
 Crack growth, 241, 279, 280–281  
 Crack modes, and stress intensity factor, 241–245  
 Cracks  
     crack stages, 266  
     cycles to failure at initial crack, 280  
     fatigue crack growth, 281  
     fatigue cracks, 267  
     fracture mechanism, 239  
     growth of, 267–268, 279  
     metal spraying and, 294  
     nucleation, 279  
     opening crack propagation mode, 241  
     quasi-static fracture, 240  
     quenching, 50  
     rotary fatigue, 327  
     sliding mode, 241  
     tearing mode, 241  
 Creep, 44  
 Critical buckling load, 969–971  
 Critical frequency of helical springs, 534–536  
 Critical load, 181  
 Critical locations, 366–379  
 Critical speeds, 383  
 Critical speeds for shafts, 383–388  
 Critical stress intensity factor, 245  
 Critical unit load, 182  
 Crowned pulleys, 880, 888–889  
 Crowning factor for pitting, 793  
 Crystal slip, 278  
 Cumulative density function (CDF), 979  
 Cumulative fatigue damage, 273, 321–327  
 Cumulative probability distribution, 979  
 Cups, 853  
 Current gauge length, 34  
 Curvature effect, 519–520  
 Curved beams in bending, 118–122  
 Curved beams in bending, alternative calculations, 120–122  
 Cycles, 280, 322  
 Cyclic frequency, 294  
 Cyclic plastic strains, 276  
 Cylindrical contact, 124–126  
 Cylindrical materials, 317  
 Cylindrical roller bearings selection, 588–590

## D

- Damping coefficients, 191  
 Dedendum, 676  
 Dedendum distances, 680  
 Definition of problem, 6  
 Deflection, 33  
     critical, 522  
     modes of, 156  
     and spring rate, 552–554  
     vs. strength, 66  
 Deflection and stiffness, 148–192  
     beam deflection methods, 152–153  
     beam deflections by singularity functions, 156–162  
     beam deflections by superposition, 153–156  
     Castigliano's theorem, 164–168  
     columns with eccentric loading, 184–188  
     compression members, general, 181  
     deflection due to bending, 150–152  
     deflection of curved members, 168–175  
     elastic stability, 190

- intermediate-length columns with central loading, 184
- long columns with central loading, 181–184
- shock and impact, 191–192
- spring rates, 148–149
- statically indeterminate problems, 175–181
- strain energy, 162–164
- struts or short compression members, 188–189
- tension, compression, and torsion, 149
- Deflection considerations, 379–383
- Deflection due to bending, 150–152
- Deflection of curved members, 168–175
- DE-ASME elliptic, 368–369
- DE-Gerber equation, 368–369
- DE-Goodman equation, 368–369
- DE-Soderberg, 368–369
- Degrees of freedom (dof's), 955
- Design, 4–5
- Design assessment for rolling-contact bearings, 599–603
- Design assessment for selected rolling-contact bearings, 599–603
- bearing reliability, 600–603
- matters of fit, 603
- Design categories, 216
- Design considerations, 8
- Design engineer's professional responsibilities, 10–11
- Design factors, 16
- and factor of safety, 17–18
- in fatigue, 342–343
- for static design, 282
- Design Manual for Cylindrical Wormgearing* (ANSI/AGMA), 810, 817
- Design of a gear mesh, 775–780
- gear bending, 776
- gear tooth bending, 779
- gear tooth wear, 779
- gear wear, 776
- pinion bending, 776
- pinion tooth bending, 778–779
- pinion tooth wear, 779
- pinion wear, 776
- rim, 780
- straight-bevel gear mesh, 806–808
- worm-gear mesh, 817–820
- Design requirements, 25
- Design sequence for power transmission, 935–936
- bearing selection, 936
- final analysis, 936
- force analysis, 935
- gear specification, 935
- key and retaining ring selection, 936
- power and torque requirements, 935
- shaft design for deflection, 936
- shaft design for stress (fatigue and static), 935
- shaft layout, 935
- shaft material selection, 935
- Design specifications, 25–26
- Design tools and resources, 8–10
- Design topic interdependencies, 23–24
- Deterministic failure curves for ductile materials, 338
- Deterministic quantity, 982
- Deviation, 395
- Diameter series, 580
- Diametral clearance, 19
- Diametral interferences, 399
- Diametral pitch, 676
- Die castings, 47
- Differential damage, 586
- Dimensionless multiple of rating life, 575
- Dimensions and tolerances, 19–21
- Dimension-series code, 580
- Dip, 892
- Directional characteristics, 293
- Direct load, 456
- Direct mountings of bearings, 591
- Direct shear, 89
- Discontinuities, 110, 267
- Discrete frequency histogram, 981
- Discrete random variable, 979
- Discretization errors, 956
- Disk brakes, 849
- circular (button or puck) pad caliper brake, 852–853
  - uniform pressure, 851–852
  - uniform wear, 850–851
- Disk clutches, 832, 845
- Displacement, 165
- Distance constraint, 701
- Distortion-energy (DE) failure theory, 221–227, 254–255, 368, 523
- Distribution curve
- lognormal, 576
  - Weibull, 576
- Double-enveloping worm gear sets, 675
- Double helical gear (herringbone), 691
- Double-lap joints, 501
- Double-row bearings, 572
- Double-threaded screw, 410
- Dowel pins, 391
- Dowling method for ductile materials, 302
- Drawing, 50
- Drive pins, 391
- Drum brake, 832
- Ductile and nodular cast iron, 54
- Ductile cast iron, 54
- Ductile materials, 33, 111, 317
- ASME-elliptic line for, 338
  - Coulomb-Mohr theory for, 228–230
  - deterministic failure curves for, 338
  - distortion-energy theory for, 221–227
  - Dowling method for, 302
  - maximum-shear-stress theory for, 219–221
  - static loading in, 218
- Ductile metal behavior, 218
- Ductility, 39
- Dunkerley's equation, 386
- Duplexing, 606
- Dynamic effects, 734–743
- Dynamic equivalent loads, 598
- Dynamic factor, 738, 756–758, 791–792
- Dynamic loading, 112
- Dynamic viscosity, 620
- Dyne, 620
- E**
- Eccentricity, 120, 625
- Eccentricity ratio, 186
- Economics, 12–15
- break-even points, 13–14
  - cost estimates, 15
  - large tolerances, 13
  - standard sizes, 13
- Effective arc, 883
- Effective coefficient of friction, 900
- Effective slenderness ratio, 522

- Effective stress, 222  
 Efficiency  
   belt drive gears, 883  
   defined, 716  
 Egs units (special names), 620  
 Eigenvalues, 971  
 Elastic coefficient, 744, 756  
 Elastic coefficient for pitting resistance, 798–799  
 Elastic creep, 883  
 Elastic deformation of power screws, 419  
 Elasticity, 148  
 Elastic limit, 33, 36  
 Elastic loading, 40  
 Elastic stability, 190  
 Elastic strain, 87–88  
 Elastic-strain line, 278  
 Elastrohydrodynamic lubrication (EHDL), 604, 619  
 Electrolytic plating, 294  
 Element geometries, 957–959  
 Element library, 957  
 Element loading, 964  
 Elimination approach, 961  
 Enclosures, 607–608  
 End-condition constant, 182, 522  
 Endurance limit, 272, 275, 282–283, 330–331  
 Endurance limit modifying factors  
   corrosion, 294  
   cyclic frequency, 294  
   electrolytic plating, 294  
   fretting corrosion, 294  
   loading factor, 290  
   Marin equation, 331–334  
   metal spraying, 294  
   miscellaneous-effects factor, 293–294  
   reliability factor, 292–293  
   rotating-beam specimen used, 286–294  
   size factor, 288–290  
   surface factor, 287–288  
   temperature factor, 290–292  
   types of, 272  
 Endurance strength Marin equation, 287  
 Energy considerations of clutches, brakes, couplings, and flywheels, 856–857  
 Energy-dissipation rate, 857  
 Energy method. *See* Castigliano's theorem  
 Engineering strengths, 35  
 Engineering stress, 34, 35  
 Engineering stress-strain diagrams, 34  
*Engineer's Creed* (National Society of Professional Engineers), 11  
 Engraver's brass, 57  
 Epicyclic gear trains, 703  
 Equation of motion of flywheel, 865  
 Equilibrium, 72  
 Equilibrium and free-body diagrams, 72–75  
 Equivalent bending load, 917, 922  
 Equivalent diameter, 289  
 Equivalent radial load, 579  
 Equivalent steady radial load, 584  
 Equivalent stress, 222  
 Equivalent von Mises stresses, 318  
 Euler column formula, 181  
 Euler columns, 183  
 Euler's equation for inertia, 869  
 Evaluation, 7  
 Expanding-ring clutches, 832  
 Extension springs, 542–550  
 External contracting rim clutches and brakes, 840–844  
 External loads, tension joints, 435–437  
 Extreme-pressure (EP) lubricants, 660  
 Extrusion, 48, 687
- F**
- Face, 83  
 Face-contact ratio, 695  
 Face load distribution factor, 759  
 Face-to-face mounting (DF), 606  
 Face width, 698  
 Factor of safety  
   average factor of safety, 249  
   and defects, 183  
   and design factor, 4, 17–18  
   fatigue, 446–447, 539, 922  
   MSS theory vs. DE theory, 183  
   in shear, 220  
   significance of, 46  
   static, 922  
 strength-to-stress ratio, 247  
 in wear, 776  
 of wire rope, 918, 920–921  
 Failure criteria, 306  
 Failures  
   of brittle materials summary, 238  
   defined, 214  
   of ductile materials summary, 231–234  
   Mohr theory of, 228  
 Failures resulting from static loading, 214–263  
 about, 214–215  
 Coulomb-Mohr theory for ductile materials, 228–230  
 distortion-energy theory for ductile materials, 221–227  
 failure of brittle materials summary, 238  
 failure of ductile materials summary, 231–234  
 failure theories, 219  
 introduction to fracture mechanics, 239–248  
 maximum-normal-stress theory for brittle materials, 235  
 maximum-shear-stress theory for ductile materials, 219–221  
 modifications of the Mohr theory for brittle materials, 235–237  
 selection of failure criteria, 238–239  
 static strength, 216–217  
 stochastic analysis, 248–254  
 stress concentration, 27–28  
 Failure theories, 219  
 Failure theory flowchart, 255  
 Failure zone, 342  
 Fastener specifications, 432  
 Fastener stiffness, 424–427  
 Fastening methods, 410  
 Fatigue axial loading, 432  
 Fatigue cracks  
   computer programs and growth, 281  
   formation and propagation, 267  
 Fatigue ductile coefficient, 277  
 Fatigue ductility exponent, 277  
 Fatigue factor of safety, 446–447, 539, 922

- Fatigue failure  
 appearance of, 266  
 approach in analysis and design,  
 267–271  
 from bending, 762  
 from contact-stress, 762  
 stages, 266–267  
 from variable loading, 54  
 of wire rope, 921
- Fatigue failure criteria  
 brittle materials, 314  
 fluctuating simple loading, 346  
 for fluctuating stress, 303–316  
 for modified Goodman line, 368
- Fatigue failure from variable loading  
 characterizing fluctuating stresses,  
 300–302  
 combinations of loading modes,  
 317–321  
 cumulative fatigue damage,  
 321–327  
 endurance limit, 282–283  
 endurance limit modifying factors,  
 286–294  
 fatigue failure criteria for fluctuating  
 stress, 303–316  
 fatigue-life methods, 273  
 fatigue strength, 283–286  
 introduction to fatigue in metals,  
 266–271  
 linear-elastic fracture mechanics  
 method, 278–282  
 road maps and important design  
 equations for the stress-life  
 method, 344–347  
 stochastic analysis, 330–344  
 strain-life method, 276–278  
 stress concentration and notch  
 sensitivity, 295–300  
 surface fatigue strength, 327–330  
 torsional fatigue strength under  
 fluctuating stresses, 317  
 varying, fluctuating stresses,  
 321–327
- Fatigue in metals, introduction,  
 266–271  
 combinations of loading  
 modes, 273  
 cumulative fatigue damage, 273
- endurance limit modifying  
 factors, 272  
 fatigue-life methods, 272  
 fatigue strength and the endurance  
 limit, 272  
 fluctuating stresses, 273  
 stress concentration and notch  
 sensitivity, 273  
 varying, fluctuating stresses, 273
- Fatigue-life methods, 272, 273
- Fatigue limit. *See also* endurance  
 limit  
 at high temperature, 291
- Fatigue loading, 496–497  
 of helical compression springs,  
 536–539  
 of tension joints, 444–451
- Fatigue of springs, 521
- Fatigue ratio, 330
- Fatigue strength, 274, 283–286  
 coefficients, 277  
 and endurance limit, 272  
 exponents, 278  
 helical coil torsion springs,  
 554–557  
 SAE approximation of, 284
- Fatigue-stress concentration factors,  
 295, 490, 752
- Fatigue-testing machine, 274
- Felt seals, 607
- Ferrite, 50
- Figure of merit  
 for belts, 894  
 for gears, 776, 780, 808  
 for springs, 528–529, 532, 540
- Fillers, 60
- Fillet radius of shoulders, 372
- Fillet welds, 478–481
- Filling notch, 572
- Film pressure, 641–642
- Final analysis, 936
- Finishing, 690
- Finite element (FE) programs, 175
- Finite element (term), 956
- Finite-element analysis (FEA), 218,  
 954–974  
 about, 954–955  
 boundary conditions, 965–966  
 critical buckling load, 969–971
- element geometries, 957–959  
 finite-element method,  
 955–957  
 finite-element solution process,  
 959–962  
 load application, 964–965  
 mesh generation, 962–964  
 modeling techniques, 966–969  
 thermal stresses, 969  
 vibration analysis, 971–972
- Finite-element method, 955–957
- Finite-element solution process,  
 959–962
- Finite life, 296
- Finite-life region, 275
- First-cycle localizing yielding, 318
- Fit, 603
- Fitted bearing, 625
- Flat-belt drives, 883–898
- Flat belts, 882
- Flat metal belts, 895–898
- Flat springs, 518
- Flexibility, 518
- Flexible clutch and brake bands, 844
- Flexible mechanical elements  
 belts, 880–883  
 flat- and round-belt drives,  
 883–898  
 flat metal belts, 895–898  
 flexible shafts, 924–925  
 roller chain, 907–915  
 timing belts, 906–907  
 V belts, 898–906  
 wire rope, 916–924
- Flexible shafts, 924–925
- Flexural endurance limit, 327
- Flexure formula, 94
- Floating caliper brakes, 849
- Fluctuating loads, 317
- Fluctuating simple loading,  
 346–347
- Fluctuating stresses, 266, 273  
 characterization of, 300–302  
 fatigue failure criteria for,  
 303–316  
 stochastic analysis, 338–342  
 torsional fatigue strength under, 317  
 varying, 321–327
- Fluid lubrication, 618

Flywheels, 866–871  
 equation of motion, 865  
 function of, 826  
 inertia, 868  
 work-input and output, 866–867

Force, 165

Force analysis, 935  
 bevel gearing, 709–712  
 helical gearing, 712–714  
 power transmission case study, 945  
 spur gearing, 705–706  
 worm gearing, 714–720

Force-contact ratio, 751

Forced-feed lubrication, 657

Force fit, 397

Forging, 48

Form cutters, 687

Forming, 49

Formulas for sections of curved beams, 121

Fracture mechanics  
 about, 239–240  
 crack modes and the stress intensity factor, 241–245  
 design equations, 256  
 fracture toughness, 245–248  
 quasi-static fracture, 240–241

Fracture toughness, 245–248

Free-body diagrams, 73

Free-cutting brass, 57

Free running fit, 397

Free-wheeling clutches, 865

Frequency function, 979

Frettage corrosion, 294

Frictional coefficients, 191

Frictional-contact axial clutches, 845–848  
 uniform pressure, 847–848  
 uniform wear, 846–847

Friction drives, 895

Friction materials  
 characteristics of, 861–862  
 for clutches, 864  
 clutches, brakes, couplings, and flywheels, 861–864

Friction variables, 638

Full bearing, 625

Full-film lubrication, 618

Functional products, 4

Fundamental contact stress equation, 788–790

Fundamental critical frequencies, 536

Fundamental deviation, 395–396

Fundamental division, 395

Fundamental frequencies, 535

Fundamentals, 678–684

**G**

Gamma function, 991, 1058

Gasketed joints, 444

Gauge length, 34

Gaussian (normal) distribution, 37, 985–986

Gear hobbing, 687

Gear mesh. *See also* design of a gear mesh  
 bevel and worm gears, 806–808, 817–820  
 design decisions for, 775–776

Gears, general, 674–732  
 AGMA factors, *See* AGMA equation factors  
 conjugate action, 677–678  
 contact ratio, 684–685  
 force analysis, bevel gearing, 709–712  
 force analysis, helical gearing, 712–714  
 force analysis, spur gearing, 705–706  
 force analysis, worm gearing, 714–720  
 fundamentals, 678–684  
 gear teeth formation, 687–690  
 gear trains, 698–705  
 interference, 685–687  
 involute properties, 678  
 nomenclature, 675–676  
 parallel helical gears, 691–695  
 straight bevel gears, 690–691  
 tooth systems, 696–698  
 types of gears, 674–675  
 worm gears, 695–696

Gear specification, 935, 936–937

Gear supports, shoulders at, 372

Gear teeth, 937  
 bending strength of, 739  
 maximum teeth on, 687

Gear teeth formation, 687–690  
 finishing, 690  
 hobbing, 689  
 milling, 688  
 shaping, 688–689

Gear tooth bending, 770, 773, 779

Gear tooth wear, 770, 773, 779

Gear trains, 698–705

Gear wear, 776, 808

Gear wear equations, 767

General three-dimensional stress, 86–87

Generating centers, 687

Generating line, 679, 682

Geometric stress-concentration factors, 111

Geometry factors, 751–756

Gerber fatigue failure criteria, 305–307, 342, 346, 368–369, 447

Gib-head key, 392

Gilding brass, 57

Goodman fatigue failure criteria, 305–307, 342, 346, 368–369, 447

Goodman line, 305

Government sources, 8–9

Gravity loading, 965

Gray cast iron, 54

Griffith, A. A., 240–241

Grinding, 690

Grip, 425, 437

Grooved pulleys, 880

Guest theory, 219

**H**

Hagen-Poiseulle law, 620

Hardness, 41–42

Hardness-ratio factor, 796, 797

Harmonic frequencies, 535

Harmonics, 383

Heading, 49

Heat dissipation of bearing housing, 645

Heat generation, 856

Heat generation rate, 646

Heat treatment, 33

Heat treatment of steel  
 annealing, 49  
 case hardening, 51  
 quenching, 50  
 tempering, 50–51

Helical coil torsion springs, 550–557  
 bending stress, 552  
 deflection and spring rate, 552–554  
 describing the end location, 551–552  
 fatigue strength, 554–557  
 static strength, 554

Helical compression springs  
design for fatigue loading, 539–542  
design for static service, 528–534  
fatigue loading of, 536–539  
Helical gearing force analysis, 712–714  
Helical gears, 674, 691  
parallel, 691–695  
Helical springs, 853  
critical frequency of, 534–536  
deflection, 520  
Helix angle, 692  
Hertzian endurance strength, 328  
Hertzian stresses, 122  
Hexagonal nuts, 423  
Hexagon-head cap screws, 423  
Hidden cycles, 321–322  
High-cycle fatigue, 273, 275  
High-leaded brass, 57  
High temperature, fatigue limit at, 291  
Hobbing, 689  
Holding power, 388  
Hole basis, 395  
Hook ends, 542  
Hooke's Law, 33, 87  
Hoop stress, 114  
Horizontal shear stress, 96  
Hot melts, 500  
Hot milling, 48  
Hot-working processes, 47–48  
Hydraulic clutches, 832  
Hydrodynamic lubrication, 618  
Hydrodynamic theory, 625–629  
Hydrostatic lubrication, 619  
Hyperbolic stress distribution, 119  
Hypoid gears, 674, 787

**I**  
Identification of knowns and unknowns, 10  
Identification of need, 5  
Idle arc, 884  
Idler pulleys, 880, 892  
Impact properties, 42–43  
Impact value, 42  
Important design equations  
Coulomb-Mohr theory, 255  
distortion-energy theory, 254–255  
failure theory flowchart, 255  
fracture mechanics, 256

lognormal-lognormal case, 256  
maximum shear theory, 254  
modified Mohr (plane stress), 255  
normal-normal case, 256  
stochastic analysis, 256  
Inch-pound-second system (ips), 21  
Indirect mountings of bearings, 591  
Influence coefficients, 384  
Initial crack, cycles to failure at, 280  
Initial belt tension, 885, 892  
Injection molding, 688  
In-line condition shafts, 702  
Interference, 20, 249, 397  
of gears, 685–687  
general, 253–254  
Intermediate-length columns with central loading, 184  
Internal expanding rim clutches and brakes, 832–840  
Internal friction theory, 228  
Internal gears, 682  
Internal shear force, 75  
Internal-shoe brake, 832  
International Committee of Weights and Measures (CIPM), 620  
International System of Units (SI), 22  
International tolerance grade numbers, 395  
Interpolation, 644–645  
Intersecting and offset-shaft bevel gearing, 788  
Invention of the concept, 6  
Investment casting, 47, 687  
Involute curve construction, 679  
Involute curves, 678  
Involute generating line, 678  
Involute helicoil, 691  
Involute profile, 677  
Involute properties, 678  
Isotropic materials, 60  
IT numbers, 396  
Izod notched-bar test, 42

**J**  
J. B. Johnson formula, 184  
Joints  
bolted and riveted, 455–459  
design, 504–506  
fastener stiffness, 424–427

gasketed, 444  
member, 427–432  
separation, 440–441  
shear, with eccentric loading, 455–459  
stiffness constant of, 436

Journal bearings  
loading on, 631  
lubrication for, 618

**K**  
Keys, 364  
design safety factors, 391  
and pins, 390–394  
and retaining ring selection, 936, 948–950  
Keyseats, 392  
Keyways and stress concentration, 372  
Kinematic viscosity, 620  
Kinetic energy, 856  
Kips, 21

**L**  
 $L_{10}$  life, 574  
Labyrinth seals, 607  
Laminates, 60  
Landgraf, R. W., 276  
Langer first-cycle yielding criteria, 306–308  
Lapping, 690  
Lap-shear joints, 501  
Large tolerances, 13  
Lead-bronze, 817  
Leakage. *See* side flow  
Length/diameter ratio, 664  
Lengthwise curvature factor for bending strength, 793  
Lewis bending equation, 734–743  
Lewis form factor, 737  
Libraries, 8–9  
Limits, 19  
Limits and fits, 395–400  
Linear damage hypothesis, 586  
Linear damage rule, 323  
Linear elastic fracture mechanics (LEFM), 239, 273, 278–282  
Linear regression, 994–997  
Linear sliding wear, 661–663

Linear spring, 148  
 Line elements, 957  
 Line of action, 677, 679, 682  
 Line of action and reaction, 73  
 Line of contact, 125  
 Load, life and reliability of bearings, 577–579  
 Load and stress analysis, 410  
     Cartesian stress components, 79–80  
     contact stresses, 122–126  
     curved beams in bending, 118–122  
     elastic strain, 87–88  
     equilibrium and free-body diagrams, 72–75  
     general three-dimensional stress, 86–87  
     Mohr's circle for plane stress, 80–86  
     normal stresses for beams in bending, 89–94  
     press and shrink fits, 115–117  
     shear force and bending moments in beams, 75–76  
     shear stresses for beams in bending, 94–100  
     singularity functions, 77–79  
     stress, 79  
     stress concentration, 110–113  
     stresses in pressurized cylinders, 113–115  
     stresses in rotating rings, 115–116  
     temperature effects, 117  
     torsion, 101–110  
     uniformly distributed stresses, 88–89  
 Load application, 964–965  
 Load application factors, 578  
 Load cycle factors, 762  
 Load-distribution factor, 759–760, 793  
 Load eccentricity, 504  
 Load factor, 440  
 Loading factor, 290  
 Loading modes, combination of, 347  
 Load intensity, 75  
 Load line, 221, 445  
 Loads and materials, 656–658  
 Load-sharing ratio, 752  
 Load-stress factor, 328  
 Load zone, 592  
 Local geometry, 360  
 Locational clearance fit, 397  
 Locational interference fit, 397

Logarithmic strain, 34  
 Lognormal distribution, 987–989  
 Lognormal distribution curve, 576  
 Lognormal-lognormal case, 250–251, 256  
 Long bar, 149  
 Long columns with central loading, 181–184  
 Long structural members in compression, 190  
 Loose running fit, 397  
 Loose-side tension, 884  
 Low-contact-ratio (LCR) helical gears, 752  
 Low-cycle fatigue, 273, 275  
 Lower deviation, 395–396  
 Lowest critical speed, 383  
 Low-leaded brass, 57  
 Lubricants  
     deterioration of, 631  
     flow of, 639–641  
     temperature rise, 642–644  
     velocity, 652  
 Lubrication  
     roller chain, 915  
     rolling-contact bearings, 603–604  
     selection, 657  
     viscosity, 632  
 Lubrication and journal bearings  
     bearing types, 658–659  
     boundary-lubricated bearings, 660–668  
     clearance, 648–650  
     design considerations, 629  
     hydrodynamic theory, 625–629  
     loads and materials, 656–658  
     Petroff's equation, 621–623  
     pressure-fed bearings, 650–656  
     relations of the variables, 631–645  
     stable lubrication, 623–624  
     steady-state conditions in self-contained bearings, 645–648  
     thick-film lubrication, 624–625  
     thrust bearings, 659–660  
     types of lubrication, 618–619  
     viscosity, 619–621  
 Lubrication types, 618–619  
 Lüder lines, 219  
 Lumped masses, Rayleigh's model for, 383

## M

Macaulay functions, 72, 76  
 Machine screws, 423  
 Magnesium, 56  
 Magnetic clutches, 832  
 Major diameter, 410  
 Malleable cast iron, 55  
 Manganese, 52  
 Manson-Coffin relationship, 278  
 Manson's approach, 325–326  
 Manual mesh generation, 962–963  
 Manufacturable products, 5  
 Margin of safety, defined, 249  
 Marin equation, 286–287  
 Marin factors, 287–294  
 Marin, Joseph, 231  
 Marin size factor, 759  
 Marketable products, 5  
 Martensite, 50, 283  
 Material efficiency coefficient, 65  
 Material index, 65  
 Materials  
     selection, 61–67  
     for shafts, 361  
     strength and stiffness, 32–36  
     worm gears, 817–820  
 Material selection charts, 61  
 Mating materials, 327  
 Matrix, 60  
 Maximum film pressure, 653  
 Maximum-normal-stress theory for brittle materials, 235  
 Maximum-shear-stress theory for ductile materials, 219–221  
 Maximum shear theory, 254  
 Maxwell's reciprocity theorem, 384  
 McKee abscissa, 623  
 Mean coil diameter, 518  
 Mean design failure and probability of failure, 338  
 Mean ultimate tensile strength, 331  
 Mechanical efficiency, 813  
 Mechanical engineering design, 5  
 Mechanical springs. *See* springs  
 Mechanics of power screws, 414–422  
 Median life, 574  
 Medium drive fit, 397  
 Member joints, 427–432  
 Mesh, 962

- Mesh generation, 962–964  
     manual mesh generation, 962–963  
     semiautomatic mesh generation, 963
- Mesh refinement, 962
- Metal-mold castings, 47
- Metal spraying, 293, 294
- Metric fastener specifications, 412, 432, 435
- Metric M and MJ profiles, 410
- Metric threads, 411
- Microdiscontinuity stress  
     concentration, 218
- Midspan compressive stress, 186
- Milling, 688
- Miner's rule, 322
- Minimum film thickness, 624, 625, 637–638
- Minimum film thickness curve, 650
- Minimum life, 574
- Minimum proof load, 432
- Minimum proof strength, 432
- Minimum tensile strength, 282, 432
- Minor diameter, 410
- Misalignment, 572
- Miscellaneous-effects factor, 293–294
- Miscellaneous springs, 558–560
- Mixed-film lubrication, 660
- Model analysis, 971, 972
- Modeling techniques, 966–969
- Moderate applications, 740
- Modern Steels and Their Properties Handbook* (Bethlehem Steel), 52
- Modes of deflection, 156
- Modifications of the Mohr theory for brittle materials  
     brittle-Coulomb-Mohr, 235–236  
     modified Mohr, 235–237
- Modified Goodman criteria, 370
- Modified Goodman diagrams, 303–304
- Modified Goodman fatigue failure criteria, 305–307, 342, 346, 368–369, 447
- Modified Goodman line, 306
- Modified Mohr theory, 235–237, 255
- Modified Neuber equation, 335
- Module, 676
- Modulus of elasticity, 33, 87  
     of rope in wire rope, 916  
     and slenderness ratio, 182
- Modulus of resilience, 36
- Modulus of rigidity, 35, 88
- Modulus of roughness, 36
- Modulus of rupture, 35
- Mohr's circle diagram, 82
- Mohr's circle for plane stress, 80–86
- Mohr's circle shear convention, 82–84
- Mohr theory of failure, 228
- Molded-woven-asbestos lining, 863
- Molded-woven-asbestos pads, 863
- Molybdenum, 53
- Moment connection, 482
- Moment load, 456
- Moments, 76
- Monte Carlo computer simulation, 21
- Moperay, 223
- Mounting and enclosure  
     alignment, 607  
     enclosures, 607–608  
     preload, 607  
     rolling-contact bearings, 604–608
- Multiple-plate clutches, 832
- Multiple-threaded product, 410
- Multiple-thread worms, 813
- Multiplication method, 52
- Multipoint constraint equations, 966
- Muntz metal, 58
- N**
- N (factor of safety), 46
- Natural frequencies, 535
- Naval brass, 58
- Needle bearings, 573
- Neuber constant, 296
- Neuber equation, 296
- Neutral axis, 89
- Neutral plane, 90
- Newtonian fluids, 620
- Newtonian heat transfer equation, 858–859
- Newton's cooling model, 858
- Newton's equation for viscous flow, 651
- Newton's third law, 73
- Newton's viscous effect, 619
- Nickel, 52
- Nickel-bronze, 817
- Nodes, 955
- Noise, vibration and harshness (NVH), 499
- Nomenclature of gears, 675–676
- Nominal mean stress method, 302
- Nominal size, 19
- Nominal strengths, 35
- Nominal stresses, 35, 111
- Noncircular cross sections, 92
- Nonferrous metals  
     aluminum, 55–56  
     copper-base alloys, 57  
     magnesium, 56  
     titanium, 57
- Noninvolute flank, 685
- Nonlinear softening spring, 149
- Nonlinear stiffening spring, 148
- Normal circular pitch, 692
- Normal coupling equation, 250
- Normal diametral pitch, 692
- Normal distribution, 37, 985–986
- Normalizing, 49
- Normal-normal case, 249–250, 256
- Normal stress, 79
- Normal stresses for beams in bending  
     beams with asymmetrical, 93–94  
     load and stress analysis, 89–94  
     two-plane bending, 92
- Normal tooth force components, 712
- Notch-free materials, 317
- Notch sensitivity  
     defined, 295  
     and stress concentration, 295–300, 334–335, 338
- Notch sensitivity equations, 296
- Notch summary, 43
- Numbering systems, 45–46
- Number of cycles vs. stress reversals, 277
- Nuts  
     grades of, 433  
     reuse of, 423
- O**
- Octahedral-shear-stress theory, 223–224
- Offset method, 33
- Oiles bearings, 661
- Oiliness agents, 660
- Oilite bearings, 661
- Oil outlet temperature, 632
- Opening crack propagation mode, 241
- Open thin-walled sections, 109–110

Optimization, 7  
 Original area, 35  
 Other side (weld symbol), 477  
 Output power of worm gears, 814  
 Overconstrained systems, 175  
 Overload factors, 758, 765, 791, 792  
 Overload release clutches, 864  
 Overrunning clutch, 865

**P**

Palmgren linear damage rule, 327  
 Palmgren-Miner cycle-ratio summation rule, 322  
 Parabolic formula, 184  
 Parallel-axis theorem, 91, 483  
 Parallel helical gears, 691–695  
 Parent distribution, 987  
 Paris equation, 280  
 Partial bearing, 625  
 Partitioning approach, 961  
 Pattern of variation, 978  
 Pearlite, 54  
 Pedestal bearings, 645  
 Peel stresses, 504  
 Performance factors, 630  
 Permanent joint design  
     adhesive bonding, 498–506  
     butt and fillet welds, 478–481  
     fatigue loading, 496–497  
     references, 507  
     resistance welding, 498  
     static loading, 492–495  
     welded joints, strength of, 489–491  
     welded joints in torsion, stresses in, 482–486  
     welding symbols, 476–478  
 Permanent-mold castings, 687  
 Permissible bending stress equation, 791  
 Permissible contact stress number (strength) equation, 791  
 Peterson, R. E., 218  
 Petroff's equation, 621–623  
 Phases and interactions of the design process, 5–8  
 Phosphor bronze, 57, 58  
 Photoelastic analysis, 480  
 Piecewise continuous cycle, 585  
 Pillow-block bearings, 645  
 Pinion, 675, 682

Pinion bending, 776, 808  
 Pinion teeth, smallest number of, 687  
 Pinion tooth bending, 770, 772–773, 778–779  
 Pinion tooth wear, 770, 773, 779  
 Pinion wear, 776, 808  
 Pins, 364  
 Pitch, 410  
 Pitch circles, 675, 677  
 Pitch cones, 690  
 Pitch diameters, 675, 679  
 Pitch length, 900  
 Pitch-line velocity, 679, 707, 792  
 Pitch point, 677, 679  
 Pitch radius, 677  
 Pitting, 743  
 Pitting failure, 327  
 Pitting resistance  
     geometry factor, 754, 793  
     stress-cycle factor for, 795  
 Plain ends, 520  
 Plane of analysis, 220  
 Plane slider bearing, 626  
 Plane strain fracture toughness, 245  
 Plane stress, 80, 220, 254  
 Plane-stress transformation equations, 80  
 Planetary gear trains, 703  
 Planet carrier gears, 703  
 Planet gears, 703  
 Plastics, 58–59  
 Plastic-strain line, 278  
 Pneumatic clutches, 832  
 Point of contact, 678  
 Poise, 620  
 Poisson's ratio, 88  
 Polished materials, 317  
 Polymeric adhesives, 498  
 Population, 980  
 Positioning drives, 895  
 Positive-contact clutches, 864  
 Positive lubrication, 657  
 Potential energy, 162  
 Pound-force, 21  
 Powder-metallurgy bushings, 657  
 Powder-metallurgy process, 47, 687  
 Power and speed relationship, 707  
 Power and torque requirements, 935, 936  
 Power in equals power out  
     concept, 936  
 Power ratings, 900  
 Power screws, 414  
     coefficient of friction of, 421  
     elastic deformation of, 419  
     mechanics of, 414–422  
 Power takeoff (PTO), 365  
 Power transmission case study  
     about, 934  
     bearing selection, 947–948  
     deflection check, 946–947  
     design for stress, 946  
     design sequence for power transmission, 935–936  
     force analysis, 945  
     gear specification, 936–937, 939–943  
     key and retaining ring selection, 948–950  
     key design, 948–949  
     power and torque requirements, 936  
     problem specification, 934–935  
     shaft design for deflection, 946  
     shaft design for stress, 946  
     shaft layout, 943  
     shaft material selection, 945  
     speed, torque, and gear ratios, 937–939  
 Power transmission case study  
     specifications  
     design requirements, 25  
     design specifications, 25–26  
 Preload, 435, 442  
 Preloading, 607  
 Presentation, 7  
 Presetting process, 521  
 Press and shrink fits, 115–117  
 Press fits, 365  
 Pressure angle, 679  
 Pressure-cone method for stiffness calculations, 428  
 Pressure-fed bearings, 650–656  
 Pressure line, 679, 682  
 Pressure-sensitive adhesives, 500  
 Pretension, 425  
 Primary shear, 456, 482  
 Principal directions, 81  
 Principal distribution, 987  
 Principal shear stresses, 87  
 Principal straight-bevel gear bending equations, 801  
 Principal straight-bevel gearwear equations, 801

- Principal stresses, 81, 254  
 Probability density, 37  
 Probability density function (PDF), 37, 979, 989  
 Probability distributions  
   cumulative, 979  
   Gaussian (normal) distribution, 985–986  
   linear regression, 994–997  
   lognormal distribution, 987–989  
   propagation of error, 992–994  
   uniform distribution, 989–990  
   Weibull distribution, 990–992  
 Probability function, 979, 991  
 Probability of failure  
   and mean design failure, 338  
   reliability and, 18  
 Problem analysis, 11  
 Problem definition, 6, 10  
 Professional societies, 8–9  
 Proof load, 432  
 Proof strength, 432  
 Propagation of dispersion, 19  
 Propagation of error, 19, 992–994  
 Propagation of uncertainty, 19  
 Proportional limit, 33  
 Pulley correction factor, 887  
 Punch presses, 869  
 Pure, defined, 88  
 Pure compression, 88  
 Pure rolling, 715  
 Pure shear, 88  
 Pure sliding, 715  
 Pure tension, 88
- Q**  
 Quality numbers, 756  
 Quasi-static fracture, 240–241  
 Quench-hardenability, 53  
 Quenching, 50
- R**  
 Rack, 682  
 Radial clearance, 19, 624  
 Radial clearance ratio, 622  
 Rain-flow counting techniques, 322  
 Random experiments, 978  
 Random variables, 978–980, 982  
 Rate of shear, 620  
 Rating life, 574, 575  
 Rayleigh's model for lumped masses, 383  
 Rectangular beam, shear stress in, 95  
 Red brass, 57  
 Redundant systems, 175  
 Regression, 994  
 Relations of the variables  
   coefficient of friction, 638–639  
   film pressure, 641–642  
   interpolation, 644–645  
   iteration technique, 631–632  
   lubricant flow, 639–641  
   lubricant temperature rise, 642–644  
   minimum film thickness, 637–638  
   viscosity charts, 632–638  
 Relatively brittle condition, 240  
 Relative velocity, 716  
 Reliability, 4, 18–19, 249, 990  
 Reliability factors, 292–293, 763–764, 797–798  
 Reliability goal, 579  
 Reliability-life relationship, 570  
 Reliability method of design, 18  
 Reliability versus life, 576–577  
 Reliable products, 5  
 Repeated stresses, 266  
 Residual stresses, 293  
 Residual stress methods, 302  
 Resilience, 36  
 Resistance welding, 498  
 Resultant forces, 456  
 Retaining rings, 394–395  
 Retaining ring selection, 949  
 Reversed loading, 800  
 Reversing pulley, 880  
 Reyn (ips viscosity unit), 620  
 Reynolds equation for one-dimensional flow, 629  
 Right-hand rule  
   for gears, 698, 718  
   threaded fasteners, 410  
   for vectors, 101  
 Rigid elements, 966  
 Rim, 780  
 Rim-thickness factor, 764–765  
 Ring gears, 682, 703  
 Rivet joints, 453  
 Road maps
- for bending fatigue failure, 765  
 for contact-stress fatigue failure, 765  
 Roadmaps  
   of gear bending equations, 766  
   of gear wear equations, 767  
   of principal straight-bevel gear bending equations, 801  
   of principal straight-bevel gearwear equations, 801  
 for straight-bevel gear bending, 800  
 for straight-bevel gearwear relations, 767  
 for straight-bevel gear wear relations, 800  
 Road maps and important design  
   equations for the stress-life method  
   combination of loading modes, 347  
   completely reversing simple loading, 344–346  
   fluctuating simple loading, 346–347  
 Roark's formulas, 153  
 Rockwell hardness, 41, 761  
 Rolled threads, 444  
 Roller chain, 907–915  
 Roller chain lubrication, 915  
 Rolling bearings, 570  
 Rolling-contact bearings, 570  
   ball bearings selection, 588–590  
   bearing life, 573–574  
   bearing load life at rated reliability, 574–575  
   bearing survival, 576–577  
   bearing types, 570–573  
   combined radial and thrust loading, 579–584  
   cylindrical roller bearings selection, 588–590  
   design assessment for, 599–603  
   lubrication, 603–604  
   mounting and enclosure, 604–608  
   relating load, life and reliability, 577–579  
   reliability versus life, 576–577  
   tapered roller bearings selection, 590–599  
   variable loading, 584–588  
 Roll threading, 49  
 Root diameter, 410  
 Rope in wire rope, 916  
 Rotary fatigue, 327

Rotating-beam machine, 274  
 Rotating-beam specimens, 282  
 Rotating-beam test, 274  
 Rotational degrees of freedom, 955  
 Rotation factor, 580  
 Roughness, 36  
 Round-belt drives, 883–898  
 Running fits, 648

**S**

SAE approximation of fatigue strength, 284  
 SAE fastener specifications, 432  
 Safety, 765  
 Safety and product liability, 4, 15  
 Safety factors  
     AGMA equation factors, 791  
     in key design, 391  
 Saint Venant's principle, 964–965  
 Sample, 980–981  
 Sample mean, 980  
 Sample space, 978  
 Sample standard deviation, 981  
 Sample variance, 980  
 Sand casting, 46, 687  
 Saybolt Universal Viscosimeter, 620  
 Saybolt universal viscosity (SUV)  
     seconds, 620  
 Scoring, 743  
 Screws, self-locking, 416  
 Seam welding, 498  
 Secant column formula, 186  
 Second-area moments, 93  
 Secondary shear, 456, 482  
 Section median line, 108  
 Section modulus, 90  
 Seireg curve, 655  
 Selection of failure criteria, 238–239  
 Self-acting phenomena, 829  
 Self-aligning bearings, 572, 580, 607  
 Self-deenergizing brake shoe, 827  
 Self-energization for counter-rotating rotation, 842  
 Self-energizing design, 849  
 Self-energizing shoes, 840  
 Self-locking phenomena, 829  
 Self-locking screws, 416  
 Semiautomatic mesh generation, 963  
 Separators, 571  
 Set removal process, 521

Setscrews, 364, 388–390  
 Shaft basis, 396  
 Shaft components, miscellaneous  
     keys and pins, 390–394  
     retaining rings, 394–395  
     setscrews, 388–390  
 Shaft design for deflection, 936, 946  
 Shaft design for stress  
     critical locations, 366–379  
     fatigue and static, 935  
     power transmission case study, 946  
     shaft stresses, 367–372  
     stress-concentration estimation, 372–378  
 Shaft layout, 361–366, 935  
     assembly and disassembly, 365–366  
     axial layout of components, 363  
     axial load support, 363  
     case study gear specification, 944–946  
     power transmission case study, 943  
     torque transmission provision, 363–365  
 Shaft materials, 360–361  
 Shaft material selection, 935, 945  
 Shafts, defined, 360  
 Shafts and shaft components  
     about, 360  
     critical speeds for shafts, 383–388  
     deflection considerations, 379–383  
     limits and fits, 395–400  
     shaft components, miscellaneous, 388–395  
     shaft design for stress, 366–379  
     shaft layout, 361–366  
     shaft materials, 360–361  
     Shaft shoulders, 605  
     Shaft stresses, 367–372  
     Shallow drawing, 49  
     Shaping, 688–689  
     Shear, yield strength in, 220  
     Shear energy theory, 223  
     Shear force, 76  
     Shear force and bending moments in beams, 75–76  
     Shear-lag model, 501  
     Shear loading, strain energy due to, 163  
     Shear loading failure, 452–453  
     Shear modulus, 35  
 Shear modulus of elasticity, 88  
 Shear-stress correction factor, 519  
 Shear stresses  
     beams in bending, 94–100  
     rectangular beams, 95  
 Shear yield strength, 225  
 Sheave diameters, 899–900  
 Sheaves, 880  
 Shell molding, 47, 687  
 Shock, 191  
 Shock and impact, 191–192  
 Short compression members, 188–189  
 Shot peening, 536  
 Shoulders  
     at bearing supports, 372  
     fillet radius of, 372  
     at gear supports, 372  
 Shrink fits, 365  
 Side flow, 632, 639, 653  
 Significant angular speed, 630  
 Silicon, 52  
 Silicon bronze, 58, 817  
 Simple, defined, 88  
 Sines failure criterion of torsional fatigue, 536, 539  
 Single-enveloping worm gear sets, 675  
 Single-lap joints, 501  
 Single-row bearings, 572  
 Single stress, 222  
 Singularity functions, 72, 76, 77–79  
 Sintered-metal pads, 863  
 Size factor, 288–290, 759  
 Size factor for bending, 793  
 Size factor for pitting resistance, 793  
 Sleeves, 618  
 Slenderness ratio, 182  
 Sliding bearings design decisions, 629  
 Sliding fits, 396, 397  
 Sliding velocity, 716  
 Slip lines, 219–220  
 Slug, 21  
 Smith-Dolan focus, 314  
 Smith-Dolan fracture criteria, 338–339  
 Snug-tight condition, 437  
 Society of Automotive Engineers (SAE), 12, 45  
 Socket setscrews, 388  
 Soderberg criteria, 369  
 Soderberg fatigue failure criteria, 346

- Soderberg line, 305  
 Software, 8–9  
 Solid circular cross sections, 92  
 Solid elements, 957  
 Solid-film lubricants, 619  
 Solution processing technique, 10  
 Sommerfield number, 622, 630, 637–642  
 Special-purpose elements, 957  
 Specification-grade bolts, 432  
 Specific modulus, 63  
 Specific stiffness, 63  
 Specific strength, 66  
 Speed ratio, 754  
 Spherical ball bearings, 607  
 Spherical contact, 123–124  
 Spherical-roller thrust bearings, 573  
 Spiral angle, 786  
 Spiral bevel gears, 674, 786  
 Spiroid gearing, 787  
 Splines, 365  
 Spot welding, 498  
 Spring, 148  
 Spring ends, 520  
 Spring index, 519  
 Spring materials, 523–528  
 Spring rates, 148–149, 425, 552–554.  
*See also* stiffness  
 Springs, 518–560  
     Belleville springs, 557  
     compression springs, 520–521  
     critical frequency of helical springs, 534–536  
     curvature effect, 519–520  
     extension springs, 542–550  
     fatigue loading of helical compression springs, 536–539  
     fatigue of, 521  
     helical coil torsion springs, 550–557  
     helical compression spring design for fatigue loading, 539–542  
     helical compression spring design for static service, 528–534  
     helical springs, deflection of, 520  
     with hook ends, 542, 549  
     miscellaneous springs, 558–560  
     spring materials, 523–528  
     stability, 522–523  
     stresses in helical springs, 518–519  
 Spring surge, 534  
 Spring types, 518  
 Sprockets, 880  
 Spur and helical gears  
     AGMA stress equations, 745–746  
     design of a gear mesh, 775–780  
     geometry factors, 751–756  
     Lewis bending equation, 734–743  
     surface durability, 743–745  
     symbols, 735–736  
 Spur gearing force analysis, 705–706  
 Spur gears  
     described, 674  
     minimum teeth on, 685  
     tooth systems, 696  
 Spur pinion, 685  
 Squared ends, 520  
 Square-jaw clutches, 864  
 Square keys, 391  
 Square threads, 412  
 Stability in springs, 522–523  
 Stable lubrication, 623–624  
 Stage I fatigue, 278  
 Stage II fatigue, 278  
 Stage III fatigue, 279  
 Stamping, 49  
 Standard deviation, 980–984  
*Standard Handbook of Machine Design*  
     (Shigley, Mischke and Brown, eds.), 51, 52  
 Standards, 12  
 Standards and codes, 12  
 Standard sizes, 13  
 Statically indeterminate problems, 175–181  
 Statically loaded tension joint with preload, 440–444  
 Static conditions, 266  
 Static design, 282  
 Static equilibrium, 72  
 Static factor of safety, 922  
 Static load, 42  
 Static loading, 111, 218, 492–495  
 Static loads, defined, 214  
 Static strength, 216–217, 554  
 Static stress, 301  
 Statistical considerations  
     arithmetic mean, variance and standard deviation, 980–984  
     probability distributions, 985–992  
     random variables, 978–980  
 Statistical significance of material properties, 36–38  
 Statistical tolerance system, 21  
 Steady equivalent load, 587  
 Steady-state conditions in self-contained bearings, 645–648  
 Steady stress, 301  
 Steel castings, 46  
 Steels  
     hardness and strengths, 41  
     temperature effects on static properties of, 43  
 Stiffness  
     of bolts in clamped zone, 425  
     pressure-cone method for calculation, 428  
 Stiffness constant, 427, 436  
 Stochastic analysis  
     about, 248–249  
     design factor in fatigue, 342–344  
     endurance limit, 330–331  
     endurance limit modifying factors, 331–334  
     fluctuating stresses, 338–342  
     important design equations, 254–256  
     interference, general, 253–254  
     lognormal-lognormal case, 250–251  
     normal-normal case, 249–250  
     stress concentration and notch sensitivity, 334–335, 338  
 Stochastic variables, 978, 982  
 Stokes, 620  
 Straight-bevel gear analysis, 803–805  
 Straight-bevel gear bending, 800  
 Straight bevel gears, 690–691  
 Straight-bevel gearwear relations, 767  
 Straight-bevel gear wear relations, 800  
 Straight-tooth bevel gears, 674  
 Strain concentration factors, 278  
 Strain energy, 162–164  
     of bending, 163  
     due to shear loading, 163  
     of torsion, 162  
 Strain hardened material, 39  
 Strain hardening, 44  
 Strain-life method, 273, 276–278  
 Strain strengthening, 217

- Strength, 34  
 and cold work, 38–41  
 defined, 214  
 vs. deflection, 66  
 property defined, 15  
 Strength life diagram, 272  
 Strength-to-stress ratio, 247  
 Stress, 34, 79  
 in helical springs, 518–519  
 in pressurized cylinders, 113–115  
 property defined, 16  
 in rotating rings, 115–116  
 and strength, 15–16  
 in thin-walled vessels, 114–115  
 and torque capacity in interference fits, 398–400  
 Stress components, 80  
 Stress concentration, 27–28, 110–113  
 FEA analysis, 963  
 and keyways, 373  
 and notch sensitivity, 273, 295–300, 334–335, 338  
 of threaded fasteners, 422–424  
 Stress-concentration effect, 452  
 Stress-concentration estimation, 372–378  
 Stress-concentration factors, 217, 218, 240, 295, 753  
 Stress-cycle factors, 762–763, 774  
 of bending strength, 795  
 for bending strength, 795–796  
 for pitting resistance, 795  
 Stress distributions, 501–504  
 Stress intensity factor, 242  
 and crack modes, 241–245  
 Stress intensity modification factor, 243  
 Stress-life method, 273, 344–347  
 Stress raisers, 110  
 Stress ratio, 302  
 Stress relieving, 50  
 Stress reversals vs. number of cycles, 277  
 Stress-strain diagram, 33  
 Stress values, 36  
 Stress yield envelope, 220  
 Structural adhesives, 499–500  
 Structural instabilities (buckling), 190  
 Struts or short compression members, 188–189  
 Studs, 425
- Subsidiary distribution, 987  
 Suddenly applied loading, 191–192  
 Sun gears, 703  
 Superposition, 153  
 Surface compression stress, 744  
 Surface condition factor, 758  
 Surface durability, 743–745  
 Surface elements, 957  
 Surface endurance shear, 327  
 Surface endurance strength, 328  
 Surface factor, 287–288  
 Surface fatigue strength, 327–330  
 Surface-strength geometry factor, 754–756  
 Synthesis, 6, 7
- T**
- Tandem (DT) mounting, 606  
 Tangential shear stress, 79  
 Tangential stress, 114  
 Tape drives, 895  
 Tapered fits, 365  
 Tapered roller bearings, 573  
 components of, 591  
 selection, 590–599  
 Tearing mode, 241  
 Technical societies/organizations, 12  
 Temperature  
 average film, 645  
 high, fatigue limit at, 291  
 oil outlet, 632  
 Temperature effects, 43–45  
 load and stress analysis, 117  
 on static properties of steels, 43  
 Temperature factor  
 AGMA equation factors, 796  
 endurance limit modifying factors, 290–292  
 geometry factors, 764  
 Temperature rise  
 boundary-lubricated bearings, 666–668  
 clutches, brakes, couplings, and flywheels, 857–861  
 lubricants, 642–644  
 pressure fed bearings, 650  
 Temper carbon, 55  
 Tempered martensite, 50  
 Tempering, 50–51
- Tensile strength, 33  
 Tensile strength correlation method, 330  
 Tensile-stress area, 411  
 Tension, compression, and torsion, 149  
 Tension joints  
 external load, 435–437  
 fatigue loading of, 444–451  
 statically loaded, with preload, 440–444  
 Tension pulley, 880  
 Tension tests, 36  
 Tension-test specimen, 32  
 Testing statistics, 539  
 Theoretical stress-concentration factors, 111  
 Thermal loading, 965  
 Thermal stresses, 117, 969  
 Thermoplastics, 58, 59  
 Thermosets, 58, 59  
 Thick-film lubrication, 624–625  
 Thin-film lubrication, 660. *See also* boundary lubrication  
 Thin structural members in compression, 190  
 Thin-walled vessels, 114–115  
 Threaded fasteners, 422–424  
 Thread series, 411  
 Thread standards and definitions, 410–414  
 Three-dimensional state of stress, 220  
 Three-parameter Weibull distribution, 990  
 Throat design, 631  
 Thrust bearings, 659–660  
 Tight-side tension, 884  
 Timing belts, 882, 906–907  
 Timing drives, 895  
 Timken bearings, 595, 597  
 Tin bronzes, 57, 817  
 Titanium, 57  
 Tolerance, 19, 395  
 Tolerance position letters, 396  
 Toothed wheels, 880  
 Tooth force, 712  
 Tooth systems, 696–698  
 Tooth thickness, 675, 681  
 Top land, 676  
 Torque, 102  
 Torque coefficient, 438

- Torque transmission provision, 363–365  
 Torque-twist diagram, 35  
 Torque vector, 101  
 Torsion, 101–110  
     closed thin-walled tubes, 107–108  
     fluctuating stresses, 347  
     open thin-walled sections, 109–110  
     strain energy of, 162  
 Torsional fatigue, 536  
 Torsional fatigue strength under fluctuating stresses, 317  
 Torsional stress, 545  
 Torsional yield strength, 523  
 Torsion springs, 550  
 Torsion stress, 367  
 Total film pressure, 653  
 Total-strain amplitude, 278  
 Total tooth force components, 712  
 Train value, 699  
 Translational degrees of freedom, 955  
 Transmission accuracy numbers, 792  
 Transmission error, 756  
 Transmitted load, 706  
 Transverse circular pitch, 692, 695  
 Transverse shear stress, 95, 97–98  
 Tresca theory, 219  
 Triple-threaded screw, 410  
 True strain, 34, 39  
 True stress, 34  
 True stress-strain diagrams, 34  
 Trumpler's design criteria for journal bearings, 630–631  
 Tungsten, 53  
 Turbines and brake bands, 844  
 Turn-the-nut method, 437  
 Two-dimensional principal stresses, 254  
 Two-parameter Weibull distribution, 991  
 Two-parameter Weibull model, 597  
 Two-plane bending, 92  
 Two-way (reversed) loading, 751
- U**  
 Ultimate strength, 33  
 Ultimate tensile strength of wire rope, 919–920  
 Unbraced parts, 190  
 Uncertainty, 16–17
- Uncorrected torsional stress, 545  
 Undamaged material, 323  
 Undercutting, 685  
 Unified Numbering System for Metals and Alloys (UNS), 45  
 Uniform distribution, 989–990  
 Uniformly distributed stresses, 88–89  
 Uniform pressure  
     cone clutches and brakes, 855  
     disk brakes, 851–852  
     frictional-contact axial clutches, 847–848  
 Uniform-section cantilever springs, 558–559  
 Uniform wear  
     cone clutches and brakes, 854–855  
     disk brakes, 850–851  
     frictional-contact axial clutches, 846–847  
 Unilateral tolerance, 19  
 Unit loads, 656  
 Units, 21–22  
 Unit second polar moment of area, 483  
 UNR thread series, 411  
 Unstable columns, 181  
 Unstable equilibrium, 182  
 Unstable lubrication, 623  
 Unstressed cross-sectional area, 35  
 UN thread series, 411  
 Upper deviation, 395–396  
 Usable products, 5  
 U.S. customary foot-pound-second system (fps), 21
- V**  
 Vanadium, 53  
 Variable loading, 584–588  
 Variable-speed drives, 882  
 Variable stresses, 266  
 Variance, 980–984  
 Variate, 982  
 Varying, fluctuating stresses, 273, 321–327  
 V belts, 882, 898–906  
 Velocity factor, 738, 739  
 Velocity gradient, 620  
 V-groove weld, 478  
 Vibration analysis, 971–972
- Virgin material, 323  
 Virtual number of teeth, 691, 693  
 Viscosity, 619–621, 632  
 Viscosity charts, 632–638  
 Volute springs, 558  
 von Mises, Richard, 223  
 von Mises-Hencky theory, 223  
 von Mises maximum stress vs. yield strength, 370  
 von Mises stress, 224
- W**  
 Wahl factor, 519  
 Washers, 422, 429, 433  
 Wear, 743  
 Wear factor. *See also* load-stress factor  
 Wear factor of safety, 776  
 Wear failure, 328  
 Weibull distribution, 570, 990–992  
     three-parameter, 990  
     two-parameter, 991  
 Weibull distribution curve, 576  
 Weibull parameters, 578  
     three-parameter, 990  
     two-parameter, 991  
 Weld bonding, 505  
 Welded joints  
     strength, 489–491  
     stress in torsion, 482–486  
 Welding symbols, 476–478  
 Welds, torsion of, 482  
 White cast iron, 54–55  
 Whole depth, 676  
 Width of space, 675  
 Width series, 580  
 Wire diameter, 518  
 Wire rope, 916–924  
     factor of safety, 918, 920–921  
     fatigue failure of, 921  
     long lay, 916  
     regular lay, 916  
     tension, 917  
     ultimate tensile strength of, 919–920  
 Wire springs, 518  
 Woodruff key, 392  
 Worm axis direction, 715

Worm gearing  
AGMA equation, 809–812  
cooling, 813  
force analysis, 714–720  
Worm gears, 675, 695–696  
analysis, 813–816  
coefficient of friction, 717  
materials, 817–820  
output power, 814  
Worms, 675

Woven-asbestos lining, 863  
Woven cotton lining, 863  
Wrought alloys, 56

**Y**  
Yellow brass, 57  
Yield point, 33, 36  
Yield strength, 35, 40  
    in shear, 220  
    vs. von Mises maximum stress, 370

Yield stress, 33  
Young's modulus of elasticity,  
    65, 87

**Z**  
Zerol bevel gear, 786  
Zero shear stress, 81  
Zimmerli data, 539

**Part 1 Properties of Sections** $A$  = area $G$  = location of centroid

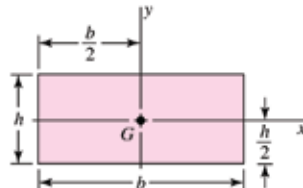
$$I_x = \int x^2 dA = \text{second moment of area about } x \text{ axis}$$

$$I_{xy} = \int xy dA = \text{mixed moment of area about } x \text{ and } y \text{ axes}$$

$$J_G = \int r^2 dA = \int (x^2 + y^2) dA = I_x + I_y \\ = \text{second polar moment of area about axis through } G$$

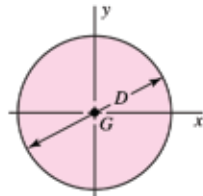
$$k_x^2 = I_x/A = \text{squared radius of gyration about } x \text{ axis}$$


---

**Rectangle**

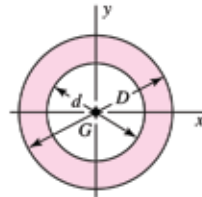
$$A = bh \quad I_x = \frac{bh^3}{12} \quad I_y = \frac{b^3h}{12} \quad I_{xy} = 0$$


---

**Circle**

$$A = \frac{\pi D^2}{4} \quad I_x = I_y = \frac{\pi D^4}{64} \quad I_{xy} = 0$$


---

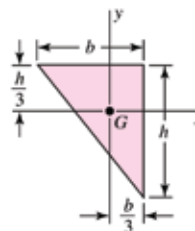
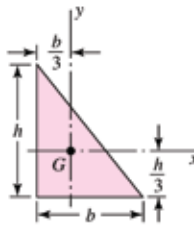
**Hollow circle**

$$A = \frac{\pi}{4}(D^2 - d^2) \quad I_x = I_y = \frac{\pi}{64}(D^4 - d^4) \quad I_{xy} = 0$$


---

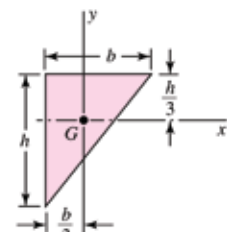
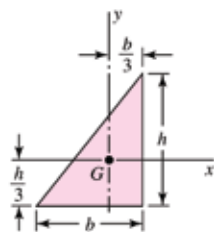
Geometric Properties  
(Continued)

Right triangles



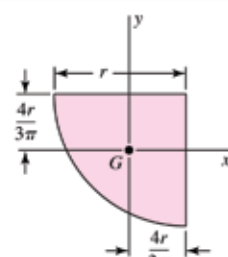
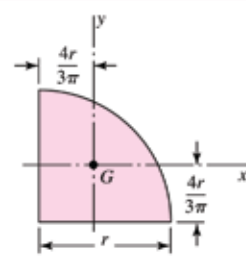
$$A = \frac{bh}{2} \quad I_x = \frac{bh^3}{36} \quad I_y = \frac{b^3h}{36} \quad I_{xy} = \frac{-b^2h^2}{72}$$

Right triangles



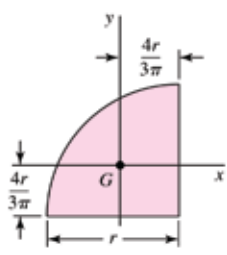
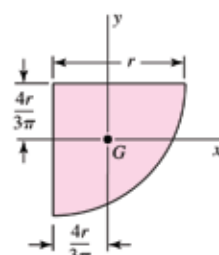
$$A = \frac{bh}{2} \quad I_x = \frac{bh^3}{36} \quad I_y = \frac{b^3h}{36} \quad I_{xy} = \frac{b^2h^2}{72}$$

Quarter-circles



$$A = \frac{\pi r^2}{4} \quad I_x = I_y = r^4 \left( \frac{\pi}{16} - \frac{4}{9\pi} \right) \quad I_{xy} = r^4 \left( \frac{1}{8} - \frac{4}{9\pi} \right)$$

Quarter-circles



$$A = \frac{\pi r^2}{4} \quad I_x = I_y = r^4 \left( \frac{\pi}{16} - \frac{4}{9\pi} \right) \quad I_{xy} = r^4 \left( \frac{4}{9\pi} - \frac{1}{8} \right)$$